OPEN ACCESS

University of BRISTOL

This electronic thesis or dissertation has been downloaded from the University of Bristol Research Portal, http://research-information.bristol.ac.uk

Author:
Mortimer, James E

Title:
The Photochemistry of Conjugated Enolates

General rights
Access to the thesis is subject to the Creative Commons Attribution - NonCommercial-No Derivatives 4.0 International Public License. A copy of this may be found at https://creativecommons.org/licenses/by-nc-nd/4.0/legalcode This license sets out your rights and the restrictions that apply to your access to the thesis so it is important you read this before proceeding.

Take down policy
Some pages of this thesis may have been removed for copyright restrictions prior to having it been deposited on the University of Bristol Research Portal. However, if you have discovered material within the thesis that you consider to be unlawful e.g. breaches of copyright (either yours or that of a third party) or any other law, including but not limited to those relating to patent, trademark, confidentiality, data protection, obscenity, defamation, libel, then please contact collections-metadata@bristol.ac.uk and include the following information in your message:

•Your contact details
•Bibliographic details for the item, including a URL
•An outline nature of the complaint

Your claim will be investigated and, where appropriate, the item in question will be removed from public view as soon as possible.

The Photochemical Reactivity of Conjugated Enolates

James Edward Mortimer

Supervised by Prof. Jonathan Clayden and Prof. Andrew Orr-Ewing

A dissertation submitted to the University of Bristol in accordance with the requirements for award of the degree of Doctor of Philosophy in the Faculty of Science

School of Chemistry

September 2024

Word Count: 80,796

Author’s Declaration

I declare that the work in this dissertation was carried out in accordance with the requirements of the University’s Regulations and Code of Practice for Research Degree Programmes and that it has not been submitted for any other academic award. Except where indicated by specific reference in the text, the work is the candidate’s own work. Work done in collaboration with, or with the assistance of, others, is indicated as such. Any views expressed in the dissertation are those of the author.

Signed: James Mortimer

Date: 14/09/2024

Abstract

This thesis investigates the novel photochemical reactivity of conjugated enolates, transforming their conventional role as thermally reactive intermediates into photochemically active species that enable a range of unique synthetic transformations. Utilising chromoselective irradiation, we discovered a variety of unprecedented enolate-based reactions that broaden the synthetic toolkit available for organic chemists. The Clayden group have previously discovered that performing a benzylic deprotonation on a benzyl benzamide with a chiral base led to a spontaneous dearomatising ring-closure, forming a conjugated enolate *in situ*. Chromoselective irradiation of this enolate led to an unprecedented enantioselective transformation, giving a cycloheptatriene with excellent enantioselectivity.[1]

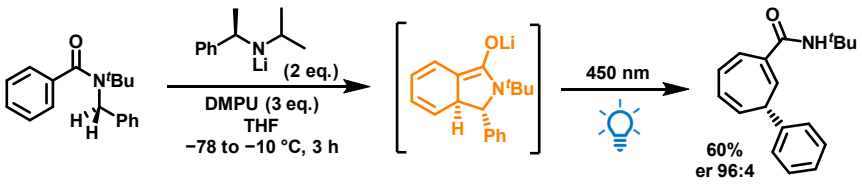

Leveraging this foundation, we explored the photochemical behaviour of acyclic *N*-benzyl amide trienolates. Through selective irradiation, these trienolates undergo radical-driven benzyl migrations, resulting in multiple regioisomers. This photochemical migration demonstrates the opportunities to diversify enolate photochemistry, highlighting the potential for new avenues towards the synthesis of complex molecular architectures through controlled photochemical transformations.

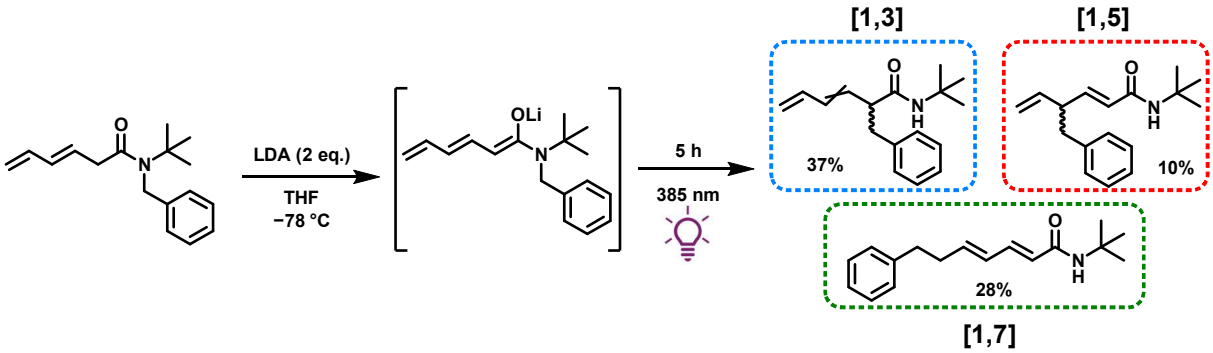

This thesis also explores the photochemical ring-contraction and migration of both five- and six-membered lactam enolates, revealing efficient pathways for synthesising highly substituted cyclopropanes and cyclobutanes under mild irradiation conditions. Although trienolates and monoenolates showed some reactivity, dienolates were found to afford the highest yield for photochemical products, with the cleanest reaction profile under mild conditions.

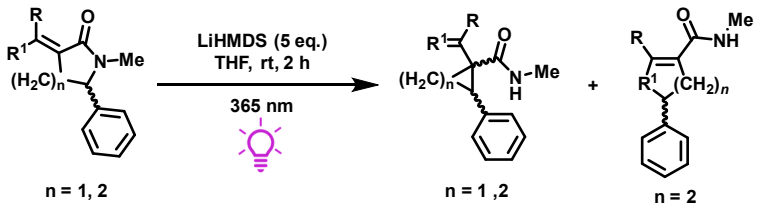

The photochemical ring-contraction of five-membered lactam dienolates resulted in high yields and diastereoselectivity from fine tuning of lactam substrate.

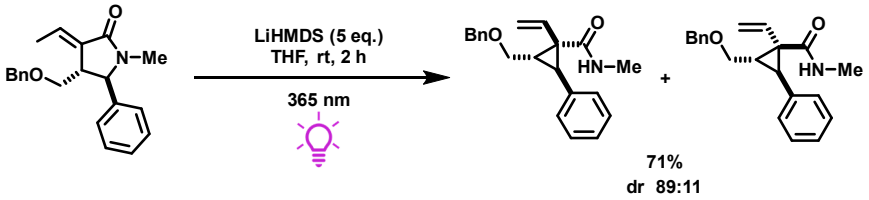

The development of these ring-contraction reactions provides new methodologies for the construction of strained, valuable ring systems, offering potential applications in pharmaceutical synthesis due to their conformational rigidity and biological relevance.

When the chromophore in a lactam system is positioned internally, the photochemistry shifts from a ring-contraction process to an electrocyclic ring-opening reaction. In this study, irradiation of an enolate generated from a six-membered lactam bearing an internal diene chromophore led to the successful formation of four distinct ring-opened stereoisomers, again showing versatility in the methods by which enolates react photochemically.

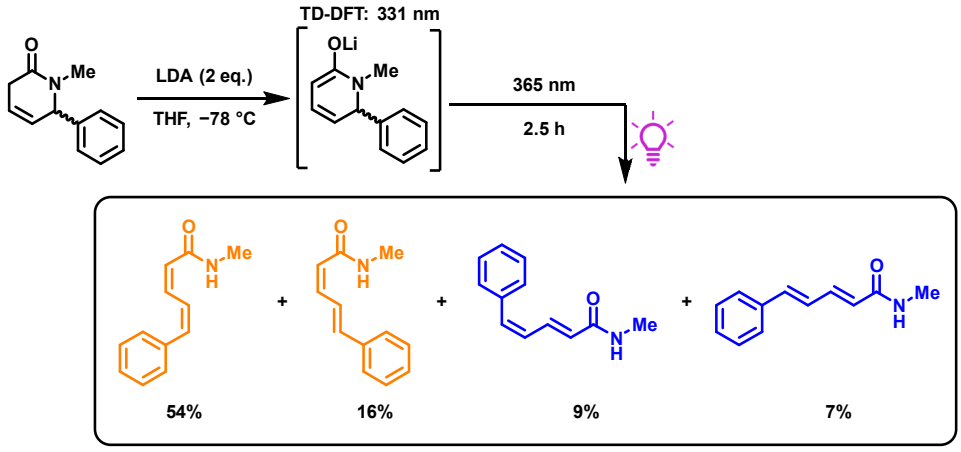

In addition to the photochemistry on lactam-based enolates, preliminary investigations into the potential photochemistry of quinoline-based and pyrrole-based enolates have been initiated. Although successful photoreactivity has not yet been achieved, the insights gained from other enolate systems offer a foundational understanding that could allow for unique reactivity through the irradiation of these unconventional enolates in future studies.

Overall, this thesis expands the understanding of enolate chemistry by exploiting their intrinsic chromophore, presenting a range of innovative photochemical transformations. These findings open up new pathways for the synthesis of complex molecular architectures and lay a foundation for future developments in utilising enolates as versatile, photochemically active intermediates in synthetic chemistry. The novel methodologies developed here not only offer alternative synthetic routes but also demonstrate the potential for control over selectivity and further exploration of photochemical reactivities, setting the stage for groundbreaking applications in complex molecule synthesis.

Contents

Acknowledgements

This has been an incredible ride and I have so many people to thank. I won't be able to thank everyone here but I will do my best!

The greatest thanks and appreciation go to Professor Jonathan Clayden for being an excellent PhD mentor, supporting and guiding me through this long journey. I think I am a much better chemist at the end of this PhD and I have you to thank! Thanks for allowing us to have fun and enjoy learning chemistry in the process.

Mom and family, I wouldn't be here without your support over the years. Thanks for always pushing me towards the next step and encouraging me to grasp every opportunity, your support is invaluable. I hope along the way I have done you proud and exceeded expectations!

Sammy – You are such an incredible guy, and bring me so much joy. I'm sad I only met you towards the end of this PhD. You have been an incredible support to me over the past year and made the end of this PhD so much more fun, I'm forever grateful.

Thanks to all my housemates. Malcolm you have been there with me since the very first day and I never thought we would get along as we have, your humour really made my bad days feel so insignificant. I am not sure I could have finished without you. Stay in touch big man. Kat – you are a huge inspiration. I only wish I could be as funny as you one day! Keep on being yourself and shutting up the naysayers. Olivia you are such a camp queen. I will miss all our deep conversations and us always being brutally honest with each other. I knew I could always rely on you and I didn't show my appreciation enough to you for that. Izzie, you were always up for a laugh and thanks for always being able to deal with the debates and being able to settle things when the house got tense! I will miss your insights, even when we disagreed. Alex you are such a calming presence, and I am thrilled you became a part of our family. You always put me at ease when things were tough, thanks le grande. Patrick thanks for entertaining me with politics and introducing me to activities I would have never done on my own, it has been a pleasure annoying you every day, I am really grateful for our friendship – make sure you come visit me in the states!

I have had the best lab group to work alongside for the past three years and I am so grateful to all of you. My MSci students Will and Callum, thanks for being great students and allowing me to have some fun while teaching along the way. Xiyue, Patrick, Ben and Marc for being really great CDT project rotation students to me, you made teaching enjoyable and I gained great friendships with you in the process. Katie – I am so glad we started at the same time to keep each other going, it's been great fun and thanks for being there for me and letting me be myself. Mehul – you were a great mentor to me in the lab and always made the lab fun with your games, thanks for keeping me inspired! Theo, my partner in crime – I will miss you debating me every day and driving me mad in the lab. And of course, our weekly Wetherspoons trips! Helge – One of the funniest people I know, thanks for all the stories and your guidance with securing my postdoc, we missed you a lot when you left. Ömer – I appreciate all the German words you taught me (even if they were stupid ones), for letting me test your perfumes and thanks for always being a friendly face in the group. Michael – Thanks for keeping me entertained in the lab and being really supportive with my work and postdoc position! It has been great getting to know you, thanks for enriching my life and for the burgers and pizzas. Maria – I have had a great four years since meeting you, thanks for being a support from day one and putting up with sharing a fumehood next to me (it's lovely and clean now at least!). Lucia – Thanks for all your help and teaching me about Italian culture, I still can't agree that American pizza is worse than Italian but I loved our spirited discussions. Matthew – for teaching me chess and being a fellow photochemist in the group, we miss you! Marc – a ray of joy in the group! I am glad you joined us and I know you will keep everyone's energy up over the next three years, I always had a great laugh with you. Will – I am so pleased you are carrying on the project, it couldn't be in safer hands. You are so talented and I was very lucky that you were my first full student – good luck with the photochemistry, you will smash it! Others I miss and will miss too including Nick, Branca, Nathan (le minet), Connie (we always look back fondly on our karaoke duet), Rajendra, Steve, Ellie, Mark, Matej and Jordan and more that I can't fit in here.

As for my CDT cohort, Grace for being a good laugh and another fellow photochemist, thanks for keeping us sane. Kaiman – one of my gym pals, I will miss overloading you with my stupidity at 6:30am. Sarah – you kept me sane in the covid year, thanks for being the support I needed. Josie – as radiant as your hair colour, thanks for always being up for a laugh with

me. Emma – you made my thesis writing a lot more fun, thanks for being a good friend through the whole PhD. Dylan – thanks for providing us with a constant reminder of the curiosities of Boron and for our adventures to GSK for the symposium.

I could not forget about Herlinda, thanks for brightening my day whenever I see you and always being a ray of sunshine. Thanks for being a huge support at all my talks.

Himali and Erzebet and all the technical staff at the department – thanks for always being a support to all of us carrying out research. A special thanks to Paul and Debbie for always being helpful with NMR support.

Sbu, Krissy and the rest of the TECS management team – thanks for being a support to all of us in the CDT and allowing me to act as the student rep during my PhD.

My assessors Prof. Varinder Aggarwal and Dr. Giacomo Crisenza – I appreciate getting the opportunity to get to share my research with you and thanks for taking the time to go through my thesis.

All machine learning data provided here was generously provided by Ben Honore in the group of Craig Butts, to whom I am incredibly thankful and grateful.

So many more people deserve a mention. It takes a whole team to create a successful PhD experience, and I am incredibly fortunate at the team that I had. I really couldn't have made it through without everyone mentioned here. I will miss them greatly.

Stereochemistry Notation

To indicate the presence of racemic mixtures, bold or hashed straight bonds are used. These bonds indicate relative stereochemistry and not absolute.

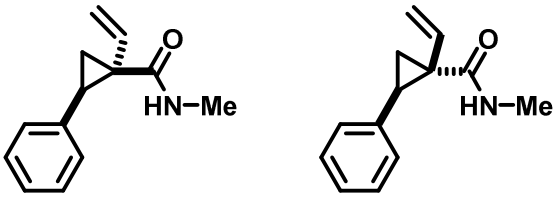

Absolute stereochemistry is defined by bold wedged and hashed wedged bonds.

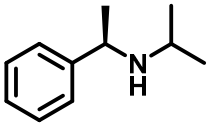

Abbreviations

λ_{max} – Maximum Wavelength of Absorption

acac – Acetylacetonate

aug-cc-pVDZ – Augmented Correlation-Consistent Polarised Valence Double-Zeta

B3LYP – Becke, 3-parameter, Lee–Yang–Parr

BARF – Tetrakis[3,5-bis(trifluoromethyl)phenyl]borate

Boc – *tert*-Butyloxycarbonyl

Bpy – 2,2'-Bipyridine

CAM – Coulomb-Attenuating Method

CASSCF – Complete Active Space Self-Consistent Field

DCC – *N*,*N*'-Dicyclohexylcarbodiimide

DCE – 1,2-Dichloroethane

DFT – Density Functional Theory

DIPA – Diisopropylamine

DIPEA – *N*,*N*-Diisopropylethylamine

DMAP – 4-Dimethylaminopyridine

DMF – Dimethylformamide

DMPU – *N*,*N*'-Dimethylpropyleneurea

DMSO – Dimethyl Sulfoxide

dr – Diastereomeric Ratio

eq. – Equivalents

er – Enantiomeric Ratio

EI – Electron Ionisation

ESI – Electrospray Ionisation

GCMS – Gas Chromatography – Mass Spectrometry

HATU – 1-[Bis(dimethylamino)methylene]-1H-1,2,3-triazolo[4,5-b]pyridinium 3-oxide hexafluorophosphate (Hexafluorophosphate Azabenzotriazole Tetramethyl Uronium)

HFIP – Hexafluoroisopropanol

HMDS – Hexamethyldisilazane

HMPA – Hexamethylphosphoramide

HOMO – Highest Occupied Molecular Orbital

HPLC – High-Performance Liquid Chromatography

HRMS – High-Resolution Mass Spectrometry

IR – Infrared

ISC – Intersystem Crossing

LDA – Lithium Diisopropylamide

LED – Light-Emitting Diode

LUMO – Lowest Unoccupied Molecular Orbital

MP – Melting Point

MW – Microwave

NMR – Nuclear Magnetic Resonance

NOE – Nuclear Overhauser Effect

PC – Photocatalyst

PCM – Polarisable Continuum Model

ppm – Parts per million

quant. – Quantitative

RASPT2 – Restricted Active Space Second-Order Perturbation Theory

SOMO – Singly Occupied Molecular Orbital

S_x – Electronic State (Excited when $x > 0$)

TD – Time-Dependent

TEMPO – (2,2,6,6-Tetramethylpiperidin-1-yl)oxyl or (2,2,6,6-tetramethylpiperidin-1-yl)oxidanyl

TFA – Trifluoroacetic Acid

THF – Tetrahydrofuran

TLC – Thin-Layer Chromatography

TMP – 2,2,6,6-Tetramethylpiperidine

Tf – Triflate

Ts – Tosyl

TX – Thioxanthone

UV – Ultraviolet

Vis – Visible

Introduction

1.0. Enolates

Enolates are highly reactive intermediates in organic chemistry, typically formed by deprotonation at the α-position relative to a carbonyl group in ketones, aldehydes, or esters (Scheme 1). The enolate negative charge is delocalised (such as on deprotonation of acetone (**1**)) between the oxygen atom of the carbonyl in **2** and the α-carbon atom in **3**, conferring both nucleophilic and basic properties at these sites. However, reactivity predominantly occurs at the carbon terminus, since this pathway facilitates the reformation of the carbonyl double bond, which has a higher bond dissociation energy (~760 kJ/mol) compared to a carbon-carbon double bond (~614 kJ/mol).[2] Additionally, carbon-based reactivity is often favoured due to the stronger interaction of the enolate oxygen with the counter-ion, such as lithium in the case presented in Scheme 1. This preferential binding can influence the regioselectivity and overall reactivity of enolates in synthetic applications.[3]

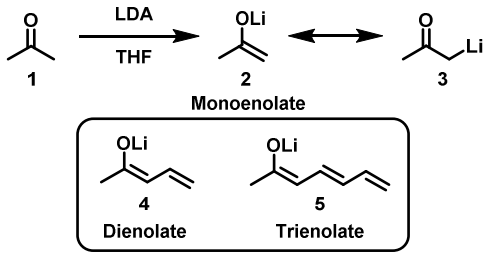

*Scheme 1: The formation of enolate **2** from acetone (**1**) and its resonance form **3**, along with examples of a di- and trienolate **4** and **5**.*

While monoenolates—enolates with only one double bond and no extended conjugation—are the most commonly utilised type of enolate in synthetic chemistry, dienolates such as **4** and trienolates such as **5** also hold significant synthetic value. The increased conjugation of higher enolates such as dienolates or trienolates reduces the energy of the chromophore, resulting in a bathochromatic-shifted absorption in the electromagnetic spectrum, allowing these species to absorb longer wavelengths of light. This property enhances their utility in photochemical applications, where selective excitation with visible-light can be achieved, broadening the scope of enolate reactivity in complex synthetic transformations.

One of the most common uses of enolates involves participation in nucleophilic addition or substitution reactions, such as alkylation and acylation processes. An example of a nucleophilic substitution alkylation reaction involving an enolate is shown in Scheme 2. Ethyl acetoacetate **6** is first

deprotonated under basic conditions, forming enolate **7**, which subsequently reacts with an electrophile (methyl iodide in this instance) to give **8**. This method is highly valuable for introducing alkyl or acyl groups adjacent to carbonyls that have an enolisable position.

Enolates also play a crucial role in the formation of 1,5-dicarbonyl compounds through Michael addition processes, where they add to α,β-unsaturated carbonyl compounds. As illustrated in Scheme 2, deprotonation of diethyl malonate **9** generates desired enolate **10**, which then reacts with methyl vinyl ketone (**11**) in a Michael addition to yield 1,5-dicarbonyl **12**. These 1,5-dicarbonyl compounds are significant and versatile intermediates in synthetic chemistry.

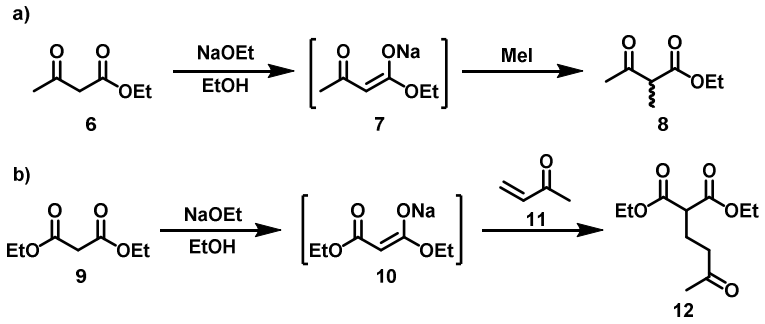

*Scheme 2: a) The alkylation of ethyl acetoacetate (**6**) with MeI via enolate **7**. b) The Michael addition reaction of diethyl malonate (**9**) with methyl vinyl ketone (**11**) via enolate **10** to give **12**.*

Of particular importance to the synthesis of valuable photoreactive compounds is the use of enolates in aldol addition reactions. In this process, an enolate reacts with a neutral carbonyl compound in the presence of an acid or base catalyst to form a β-hydroxy carbonyl compound. A representative example of this reaction is the aldol addition of enolate **14** derived from acetaldehyde (**13**) into acetaldehyde (**13**) in its keto-form, yielding β-hydroxy aldehyde **15** (Scheme 3). This product can subsequently undergo a heat-promoted condensation step, resulting in the formation of crotonaldehyde (**16**).

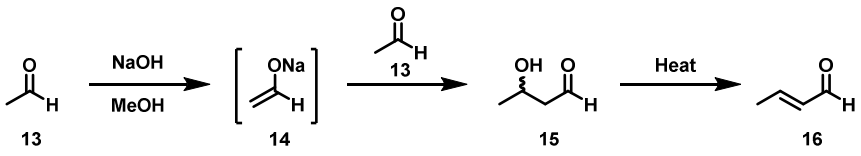

*Scheme 3: Aldol addition and condensation of acetaldehyde (**13**) under basic conditions via enolate **14**.*

All of these conventional enolate reactions in synthetic chemistry involve enolates acting as nucleophilic substrates under thermal, rather than photochemical, conditions. While enolate nucleophilicity is highly valuable in synthesis, the scope of enolate reactivity could be broadened by

exploring their potential as photoreactive species. Given that enolates possess a double bond, there is the possibility for direct irradiation, potentially leading to subsequent photochemical reactivity. This approach would reimagine enolates as photochemically active intermediates, significantly expanding the scope of their synthetic applications.

1.1. The Evolution of Photochemistry

Photochemistry, a branch of chemistry concerned with the absorption or emission of light, has increasingly been employed to provide the necessary energy for driving chemical reactions. This often enables unique reactivities that are not accessible through thermal means. While sunlight is nature's original photochemical initiator—exemplified by processes such as photosynthesis—its direct application in academic and industrial chemistry has been limited.[4,5] This is due to challenges in achieving high and consistent intensities of sunlight, and the polychromatic nature of sunlight, complicating chromoselective transformations, where selective irradiation at specific wavelengths is desired.[6] The Sun's emission spectrum roughly corresponds to a black body at 5800 K, with peak irradiation near 500 nm and a broad emission range extending up to 880 nm, contributing to these limitations.[7]

Early pioneers of photochemical transformations leveraged sunlight-rich environments to supply the necessary energy for their reactions. The first documented example of a sunlight-mediated photochemical synthesis was reported by Carl Fritzsche in 1867 (Scheme 4). In this pioneering work, Fritzsche observed the photodimerisation of anthracene (**17**) via a photochemical [4+4] cycloaddition, resulting in the formation of dimeric product **18**.[8]

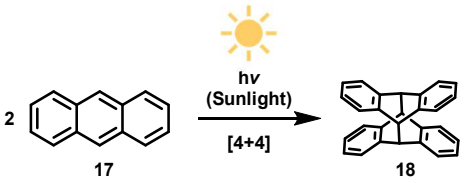

*Scheme 4: The dimerisation of anthracene (**17**) to give **18** founded by Carl Fritzsche in 1867 using sunlight.*[8]

Giacomo Ciamician, an Italian chemist often regarded as the "father of modern photochemistry", discovered a sunlight-mediated photocoupling of benzophenone (**19**) in 1900 (Scheme 5).[9] This reaction utilised sunlight to excite the carbonyl group of benzophenone (**19**), leading to intermolecular coupling, affording dimer **20**.

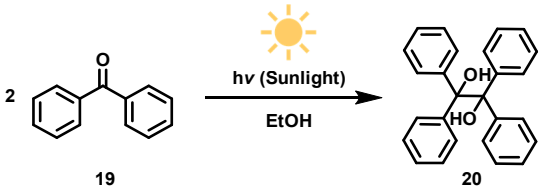

*Scheme 5: The photocoupling of benzophenone (**19**) achieved by Giacomo Ciamician by employing sunlight, affording **20**.*[9]

However, the reliance on sunlight posed significant challenges due to its inconsistent availability and variable intensity, often resulting in reaction times that extended over several weeks to achieve the desired product.[10]

A more recent example of sunlight-initiated photochemistry is the photooxygenation of 1,5-dihydroxynaphthalene (**21**), reported by Oelgemöller *et al*. (Scheme 6).[11] This approach exemplifies green photochemistry, utilising a non-hazardous solvent, an organic sensitiser, oxygen, and direct sunlight. The reaction was efficiently conducted in a flow system with continuous sunlight irradiation, which initially excited the photocatalyst, facilitating the subsequent oxygenation. This method achieved high yields of up to 80% for the synthesis of 5-hydroxy-1,4-naphthoquinone (**22**), without the need for an external LED light source.

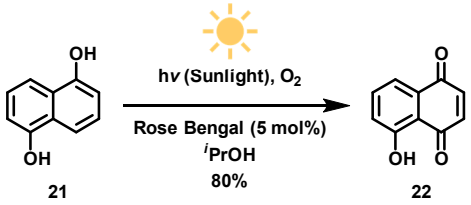

*Scheme 6: Photooxygenation of 1,5-dihydroxynapthalene (**21**) investigated in 2006 by Oelgemöller.* [11]

Flow chemistry has emerged as a major driving force in photochemical advancements over the past 20 years, including reactions mediated by sunlight.[6,12,13] In flow systems, the shorter path length of light reaching the photochemical reagent in solution allows for lower light intensity requirement to achieve sufficient excitation and reactivity compared to batch processes.

An example of this is demonstrated in the work by Silva *et al.*, where a flow solar cell, known as the "sunflow" reactor, was employed to transform azosulfones such as **23** into building blocks for sp^2–sp^2 cross-coupling processes (Scheme 7).[12] This approach eliminates the need for metals, utilising sunlight as a green energy source to produce useful building blocks **24** with yields of up to 82%.

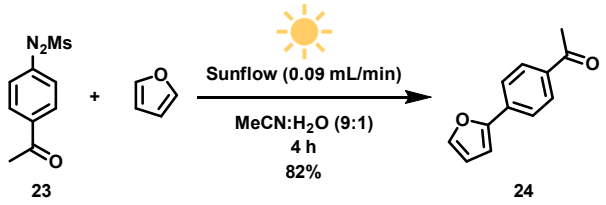

*Scheme 7: The flow photochemistry of azosulfones such as **23**, giving metal-free arylation.* [12]

Since the advent of organic photochemistry, extensive research has focused on the wavelength dependence of light in photosensitive reactions, leading to a deeper understanding of the importance of chromoselective irradiation.[14–16] Hence, commercial lamps have been developed to serve as irradiation media. Among traditional options, mercury, halogen and tungsten-based lamps have been widely used in organic photochemistry for over thirty years.[17,18] Although these lamps are high-powered (typically around 125 W), they possess spectrally diverse emission spectra, making them inefficient for chromoselective irradiation. Furthermore, the high power output of these lamps generates significant heat, which complicates the study of thermally unstable, photochemically active intermediates. Additionally, in the event of a halogen or mercury lamp breakage, toxic gas or mercury vapour could be released, posing significant health hazards through inhalation or dermal exposure.

Fortunately, energy-efficient LEDs have become commercially available and widely accessible over the past two decades. These LEDs help overcome the challenges associated with mercury, halogen and tungsten lamps, enabling the selective initiation of organic photochemical reactions with minimal unwanted heat irradiation.[19,20] In addition to allowing for chromoselective irradiation, LEDs offer a consistent and reliable energy source.[21] These LEDs also present a reduced chemical risk during operation, since they do not contain highly toxic vapours, unlike mercury or halogen lamps.

This development has also enabled the investigation of thermally unstable, photochemically active intermediates, which forms the basis of this thesis.[1] Although these LEDs typically operate at lower power than mercury and tungsten lamps (usually between 4–40 W), they can be precisely focussed onto the reaction vessel either through specific LED design or by using an attached collimator lens. This ensures that the light intensity at the target vessel or reaction site is sufficient to efficiently initiate photochemical processes.

The use of LEDs with reaction temperature control is demonstrated by Svejstrup *et al.*, where energy-efficient LEDs were employed in a photoredox-mediated α-functionalisation of various amines (Scheme 8).[22] For instance, tertiary amine **25** was subjected to a Giese addition with methyl vinyl ketone (**11**), yielding α-functionalised **26**. The mechanism of this reaction involves the initial

photoexcitation of a ruthenium photocatalyst, followed by electron transfer from tertiary amine **25** to the catalyst. Subsequent proton loss from radical cation **27** generates α-amino radical **28**, which undergoes a Michael addition to methyl vinyl ketone (**11**), producing intermediate **29**. A final regenerative electron transfer from the photocatalyst, along with proton quenching, yields α-functionalised amine **26**. By utilising light sources that minimise unwanted heat emission, the authors were able to investigate the effects of temperature and light intensity on the reaction, a study that would have been challenging with traditional lamps. Research of this type encourages the consideration of thermally unstable enolates as potential photoreactive species with thermally controlled LED irradiation.

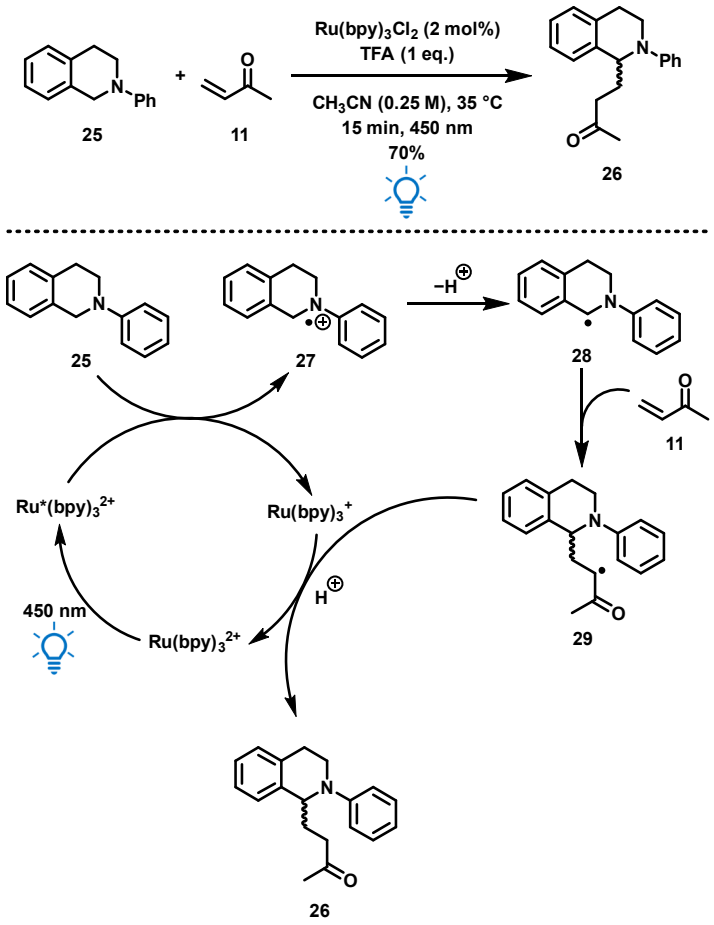

*Scheme 8: The photoredox-mediated α-functionalisation of tertiary amine **25** using LED irradiation and various temperatures.*[22,23]

While the detailed physical theory of photochemistry extends beyond the scope of this thesis, a brief overview of fundamental photochemical principles and their mechanisms is essential. This foundational understanding will provide context for how enolates may be engaging in photochemical reactions following LED irradiation.

1.2. Theory of Photochemistry

The general photochemical processes that many molecules can undergo are best illustrated using a Jablonski diagram (Figure 1), which outlines the initiation of these processes as the absorption of a photon by a molecule.[24] Upon absorption, the molecule transitions from its ground electronic singlet state (S_0) to an electronically excited singlet state (S_1), accompanied by excitation to a higher vibrational energy level. This excess vibrational energy is typically dissipated through a process known as vibrational relaxation, which results in the molecule reaching the ground vibrational state of the electronically excited singlet state S_1. From this excited state, the molecule can undergo various photophysical processes, such as internal conversion or fluorescence, to return to the ground electronic state S_0.[25]

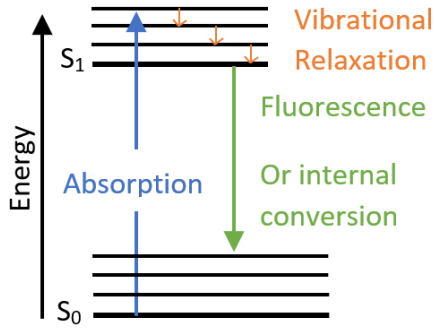

Figure 1: A Jablonski diagram indicating photophysical processes which molecules undertake following photochemical excitation.

The relaxation of an excited molecule to the ground electronic state can occur via intermolecular energy transfer, in which the energy is transferred to an acceptor molecule, provided that the energy gap for relaxation corresponds to an available excitation in the acceptor.[26] A notable example of such intermolecular energy transfer from photochemical excitation is the triplet energy transfer process reported by Oddy *et al.* (Scheme 9).[27] In this process, thioxanthones (TX) are excited to a singlet excited state upon visible-light irradiation, followed by intersystem crossing to the corresponding triplet thioxanthone excited state. The energy of this triplet state closely matches that of aryl amide **30**, enabling the transfer of triplet energy, thereby generating the triplet excited state of target compound **31**. This excited state facilitates the appropriate orbital overlap required for a 6π-electrocyclisation, yielding **32** and subsequently **33**, which ultimately achieves a formal $C(sp^2)$-$C(sp^3)$ bond formation through a photochemical intermolecular energy transfer.

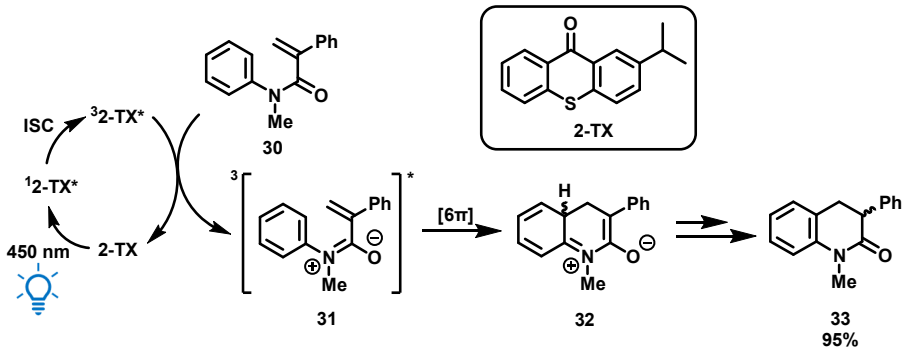

*Scheme 9: The proposed mechanism for triplet energy transfer from thioxanthone (**2-TX**) to unsaturated phenyl amide **30** to afford a fused ring structure in **33**.* [27]

In cases where a suitable acceptor molecule is unavailable, the energy from an excited species may instead be dissipated to the surroundings, either as light (e.g., through fluorescence) or as heat (e.g., through internal conversion).

Excitation of an electron to higher-energy orbitals can lead to entirely new and distinct reactivity for a molecule. When an electron in a HOMO in a molecule is excited, a SOMO (singly occupied molecular orbital) is created. This SOMO exhibits different electronic characteristics compared to the ground-state HOMO, thus offering new possibilities for reactivity. In the case of enolates, the formation of a SOMO during photochemical irradiation could explain their unique reactivity, which contrasts sharply with their behaviour under thermal conditions.

1.3. Enolate Formation by Dearomatising Cyclisation

While most enolate formation reactions involve simple deprotonation adjacent to a carbonyl, the Clayden group has extensively studied the formation of enolates through a dearomatising cyclisation reaction. This reactivity was first discovered by the group in the late 1990s when, during an attempt to ortho-lithiate benzyl naphthamide **34**, serendipitous *in situ* transient enolate **36** was formed via dearomatisation of the naphthyl ring, affording tricyclic amide **37** on aqueous quench (Scheme 10).[28,29] The cyclisation process begins with an unexpected benzylic lithiation **35**, followed by dearomatisation upon warming in the presence of HMPA or DMPU. The addition of complexing agent HMPA or DMPU improved the yields of dearomatised products due to the activation of organolithium **35** presumably via the weakening of the C-Li bond.[30] This lithiation-dearomatisation reaction has demonstrated

significant versatility, extending to both heteroaromatic species and simple aromatic rings, including pyridines, quinolines, and pyrroles.[29,31–34]

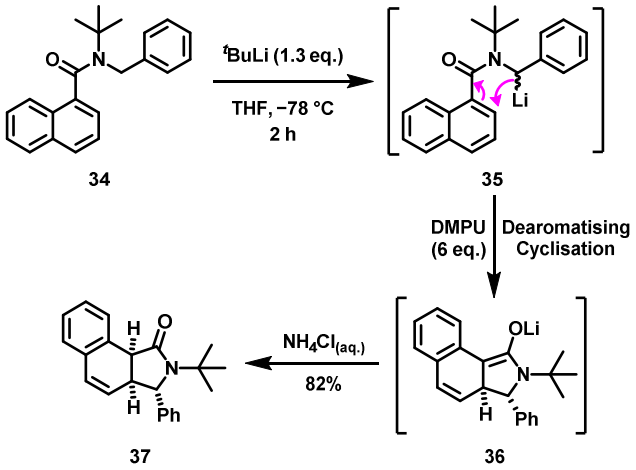

*Scheme 10: The dearomatising cyclisation of benzyl napthamide **34** to form **37** via transient enolate **36**.*[30]

Moreover, benzyl organolithium intermediate **35** exhibits sufficient configurational stability over the timescale of the dearomatising step, allowing for enantioselective transformations at a stereogenic centre (Scheme 11).[28,35] Enolate **39**, formed through addition into the aromatic ring in α-methyl benzyl naphthamide **38**, can be quenched to yield tricyclic amide **40** with selective protonation on the "outside" *exo*-face of the sterically bulky rings, affording an enantiomeric ratio of greater than 99:1. The stereochemistry of the resulting product is therefore directly influenced by the chirality of the starting amide. This enolate formation preserves the stereochemical integrity of the stereogenic centres, making it a valuable method for synthesising complex, stereochemically-rich molecules from chiral starting materials.

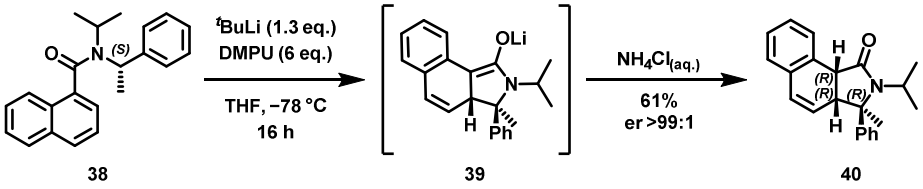

*Scheme 11: The diastereoselective dearomatising cyclisation of naphthyl amide **38** via enolate **39**, giving enantiopure **40**.*[28]

This dearomatisation step is facilitated by the conjugated amide carbonyl, which enables a plausible electrocyclic ring-closing step. Evidence for this mechanism was provided by conducting the cyclisation with oxazolidine **41** (Scheme 12).[36] If the mechanism of the ring-closure were ionic in nature, oxazolidine **41** would be expected to react via the more thermodynamically stable *trans*- tricyclic

enolate **43**, via benzylic organolithium **42** through a Baldwin-disfavoured 5-*endo-trig* cyclisation, affording tricyclic **44** on aqueous quench. However, the reaction yielded the less stable *cis*-compound **46** via intermediate **45**, indicating a 6π disrotatory thermal electrocyclic ring-closing process. This stereochemical outcome is consistent with the Woodward–Hoffmann rules, supporting a concerted, disrotatory mechanism rather than an ionic pathway which would have predominantly produced *trans*-isomer **44**.

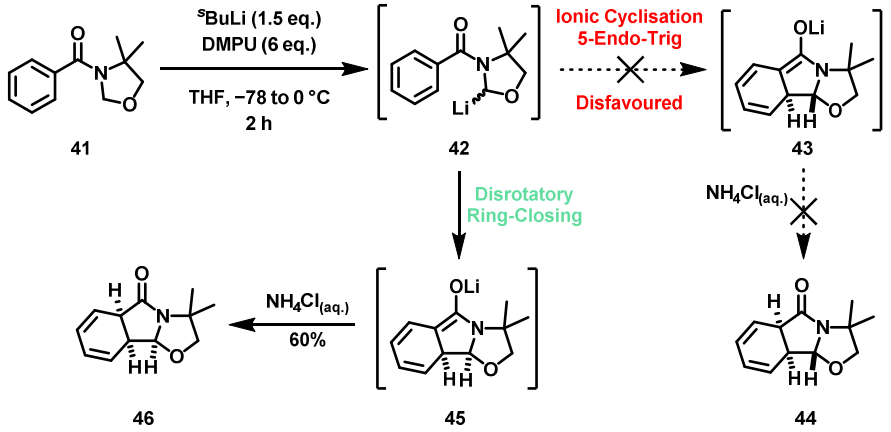

*Scheme 12: The electrocyclic ring closure investigated for oxazolidine **41**, indicating that the mechanism is electrocyclic, rather than ionic, based on the product stereochemistry.* [36]

A disrotatory thermal electrocyclic ring-closure would also account for the correct relative stereochemistry observed when treating achiral benzamides such as **47** with base, resulting in the phenyl group being positioned on the *exo*-face of the bicyclic ring system in **48** (Scheme 13).[29,37]

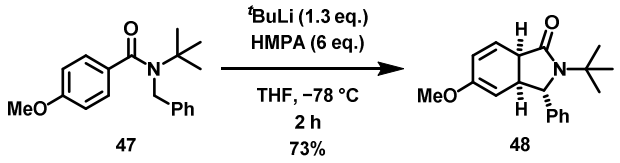

*Scheme 13: The dearomatising cyclisation of benzylbenzamide **47** to give the phenyl group* exo *to the fused ring system in **48**.* [37]

Recent work in the Clayden group has shown that asymmetric cyclisation on an achiral benzamide substrate such as **47** can be achieved through deprotonation with a chiral lithium base such as **49** (similar in reactivity to LDA). This leads to the isolation of isoindolone **48** with an enantiomeric ratio of >99:1 following recrystallisation (Scheme 14).[35] While previous studies with chiral substituents such as **38** had their stereochemistry dictated by the starting material, the use of a chiral base allows the

stereochemical outcome to be governed by an external chiral source, thereby offering increased flexibility in the selection of starting substrates.

The origin of this stereoselectivity could arise from either a stereoselective deprotonation followed by a stereospecific cyclisation, or from a stereoselective cyclisation of a racemic organolithium intermediate in the presence of protonated **49** as a chiral inductor. To determine the operating mechanism for selectivity, benzyl amide **47** was deprotonated with ^{t}BuLi to form racemic organolithium **50**. In one experiment, protonated **51** was added and the cyclisation proceeded, yielding isoindolone **48** with a poor er of 55:45, indicating that **51** does not significantly influence stereoselectivity when starting with a racemic organolithium.

In a second experiment, racemic organolithium **50** was deuterated to form **52**. Subsequent deprotonation with chiral base **49** and cyclisation resulted in expected isoindolone **53** without enantioselectivity and with greater than 99% deuteration. This finding suggests that the deprotonation step has a large primary kinetic isotope effect, completely nullifying the base's enantioselectivity. Therefore, the enantioselective step must involve the deprotonation itself, as it is subject to the primary kinetic isotope effect, confirming that this step is intrinsically enantioselective.

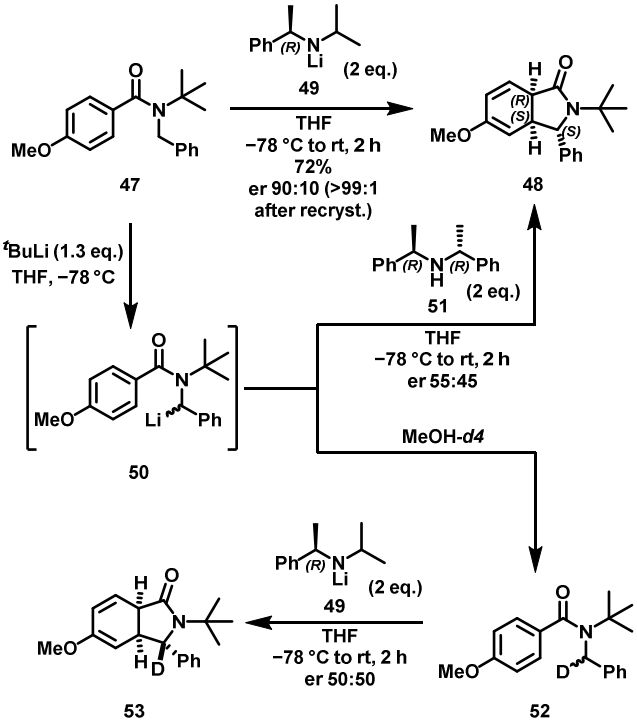

*Scheme 14: The asymmetric deprotonation and dearomatising cyclisation of benzyl benzamide **47**, along with reactions carried out to probe the mechanism of stereoselectivity of the process.*[35]

The enolates generated from dearomatising cyclisation possess three conjugated double bonds, classifying them as trienolates. This extended conjugation results in a chromophore with a bathochromatic-shifted absorption maxima λ_{max}, indicating absorbance at longer wavelengths and lower energies compared to less conjugated enolates.

The previous discussion on benzylic lithiation/cyclisation focused exclusively on anionic cyclisations and thermal reactivity, without involving photochemical processes. However, the distinct colour and absorbance properties of these trienolates led previous members of the Clayden group to explore their potential for photochemical reactivity. By generating trienolates *in situ* and exposing them to irradiation, the Clayden group sought to comprehensively investigate their photochemical behaviour and unlock new pathways for their reactivity.

If successful photochemical transformations could be initiated from these trienolates, it would be essential to further examine the potential for these enolates to be formed stereoselectively and to yield photochemical products with enantioenrichment. This approach not only broadens the scope of enolate photochemistry but also paves the way for the synthesis of enantioenriched compounds through photochemical pathways.

1.4. Photochemistry of Enolates and Related Compounds

There are few reported examples of the photochemical reactivity of enolates or closely related compounds, such as enols, in the literature. Most of the documented cases date back to the 1960s and 1970s, when photochemistry was still in its infancy and energy-efficient, chromoselective light sources were not commercially available. In 1964, Yogev *et al.* reported the photochemical rearrangement of enol acetates such as **54** to β-diketones such as **55** (Scheme 15).[38] Although not involving enolates directly, the photochemistry of vinyl ethers suggests that enolates might exhibit analogous reactivity upon irradiation. The proposed mechanism for the formation of **55** involves the photochemical excitation of the enol functionality in **54** to give diradical **56**, leading to radical cleavage of the oxygen-acetyl bond and formation of acetyl and ketone radicals (**57** and **58**). Recombination of these radicals yields β-diketone product **55**.

The authors describe this as an intramolecular process which is potentially influenced by a solvent cage effect. The complexity of this type of transformation is further exemplified by the photoreactivity of 2-methylcyclohexenyl acetate **59**, which resulted in a mixture of products, all obtained in low yields. Although the desired rearrangement product **61** was successfully isolated, side products such as 2-

methylcyclohexanone **60** and a radical dimerisation product **62** were also formed. This outcome indicates a lack of selectivity for the targeted synthetic pathway for some substrates, highlighting the challenges in controlling photochemical reactivity under these conditions. The photochemical acetyl enol rearrangement was further applied to steroid **63**, achieving the highest reported yield for this photochemistry, affording diketone product **64** in 37% yield.

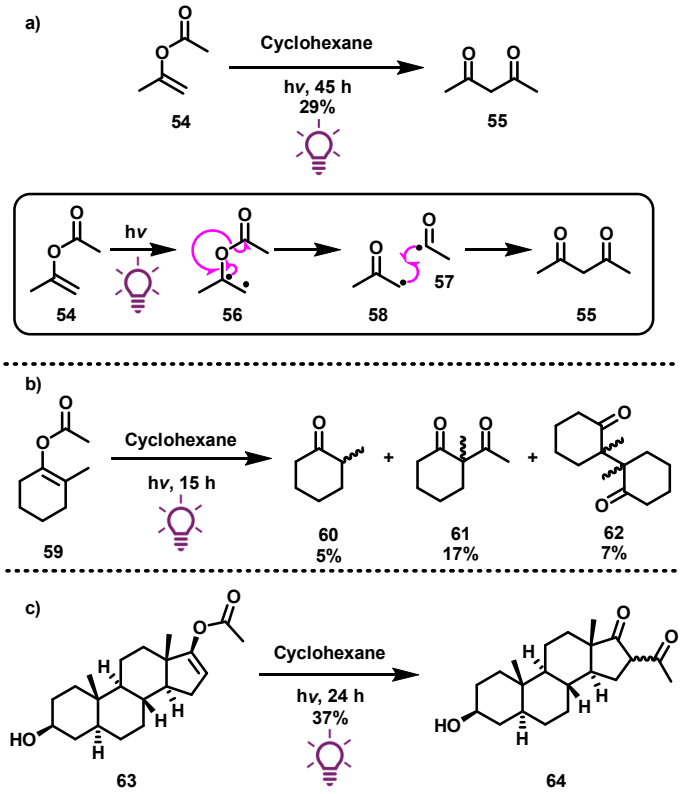

*Scheme 15: a) The photochemical enol rearrangement to give diketone **55** from **54** and the proposed mechanism for its formation. b) With cyclohexyl acetyl enol **59**, multiple products are formed. c) The process also works on steroid scaffolds such as **63**.*[38]

Overall, this transformation suffered from generally low yields, with considerable amounts of unreacted starting material. The low yields obtained may be attributed to the use of a low-pressure mercury lamp, which likely lacked chromoselectivity and generated excess heat, potentially leading to the decomposition of intermediate radical species. The authors further proposed that diketone products, such as **55**, **61** and **64**, have a significantly higher ultraviolet absorption efficiency compared to the starting enol acetates **54**, **59** and **63**. This suggests that the reaction conversion may have stalled due to the diketone products absorbing a disproportionate amount of the incident light, effectively acting as a light filter and inhibiting further reaction progress. Furthermore, the study focused exclusively on enol acetates, suggesting that the applicability of this photochemical process may be

restricted to such species. This limitation highlights the need for further exploration of substrate scope to determine whether similar photoreactivity could be achieved with other enolate or enol derivatives.

While the photochemistry of enol acetates by Yogev *et al.* led to the formation of 1,3-diketones, the well-established de Mayo reaction (from 1971) utilises an enol (typically derived from a 1,3-diketone) and an alkene in a photochemical [2+2] cycloaddition.[39] This reaction results in the formation of a cyclobutane, which subsequently undergoes a retro-aldol reaction to yield a 1,5-diketone. An illustrative example of this photochemical transformation is presented by Minter *et al.* (Scheme 16).[40] Here, the irradiation of a 1,3-diketone (which exists in solution as an equilibrium mixture of diketone **65** and enol **66**) with a mercury lamp facilitates an intramolecular [2+2] cycloaddition, producing cyclobutane intermediate **67**. This unstable intermediate undergoes a retro Diels-Alder reaction to generate 1,5-diketone **68**, forming a fused 6,6,5-ring system with a notable yield of 70%. The diketone product **68** was further converted to a Galanthan derivative—a class of natural products known for their neuroprotective properties.[41]

The proposed mechanism for the photochemical step in the de Mayo reaction begins with the excitation of enol **66**, followed by intersystem crossing to yield triplet enol species **69**.[42] This excited triplet state then engages in a stepwise [2+2] cycloaddition with the alkenyl group to give **70**. A spin inversion facilitates the formation of the desired radical pairing in **71**, culminating in the formation of cyclobutane intermediate **67**.

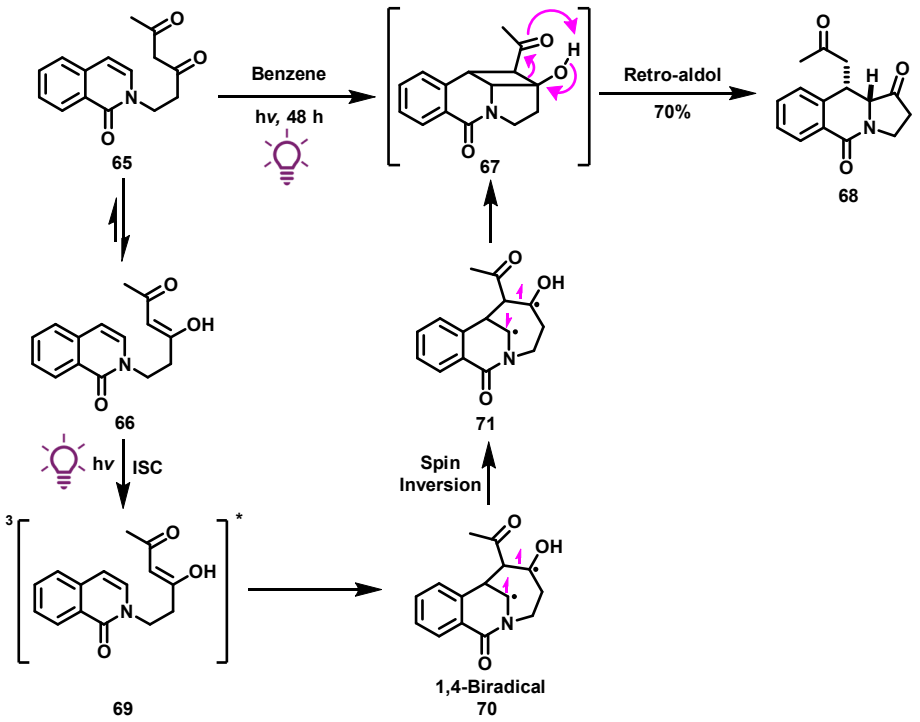

*Scheme 16: An example of the de Mayo reaction, towards Galanthan derivatives.[40] The proposed mechanism for formation of cyclobutane intermediate **67** is shown.*

Since the enol form exists only in small proportions in solution, the reaction is promoted both by the hydrogen bonding present in the enol, as seen in 1,3-diketones, and by the photochemical step that drives the formation of the cyclobutane intermediate, thereby shifting the diketone/enol tautomerisation towards the enol. This essentially exemplifies how photochemistry can drive an equilibrium process towards complete conversion. While the example discussed here utilised a potentially toxic mercury lamp, modern implementations of the de Mayo reaction have employed safer, contemporary LEDs. However, the use of potentially harmful UV light is still necessary for the excitation of the enol, unless a visible-light absorbing photocatalyst is incorporated into the reaction (as in a photoredox process).[43,44] Although extensively studied in the literature, the de Mayo reaction remains a process that involves the irradiation of enol species rather than their related enolates. Nonetheless, there are clear parallels between enolate photochemistry and the de Mayo reaction, which are explored in greater detail later in Section 5.1.

Regarding direct enolate photochemistry, there are very few reported examples, many of which originate from the Clayden group. However, an early instance of direct enolate photochemistry was documented in 1970 by Van Tamelen *et al.*, who described the photochemical isomerisation of sodium enolate **73** from 3-pentanone (**72**) using a Hanovia quartz (medium-pressure mercury) lamp (Scheme 17).[45] This process resulted in the formation of *cis*- and *trans*-epoxides **74** and **75** with yields of 2% and 0.2%, respectively, after eight hours of irradiation. Hanovia quartz lamps are particularly advantageous for precise photochemistry due to their superior UV intensity compared to halogen, tungsten or other mercury lamps, facilitating more efficient and controlled photochemical reactions. While this study provides preliminary evidence of the potential for enolates to undergo photochemical transformations, the low yields of the target epoxides and the complex mixture of by-products reported highlight significant limitations and the need for further optimisation in harnessing enolate photochemistry effectively.

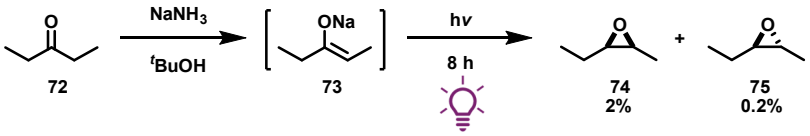

*Scheme 17: The photoisomerisation on enolate **73**, giving* cis- *and* trans-*epoxides **74** and **75**.*[45]

Additionally, this photoisomerisation exploited the inherent chromophore within monoenolate **73**, which absorbs photons in the ultraviolet region. By increasing the degree of conjugation, as would be the case in the progression to dienolates or trienolates, the absorption could be shifted bathochromically, enabling chromoselective irradiation. This is particularly advantageous when

targeting molecules with diverse unsaturated functionalities and therefore UV-absorbing characteristics.

Conjugated enolates, such as trienolates, are often visibly coloured species, yet the photochemistry of these systems remains largely underexplored. In trienolate systems, the presence of a visible-light absorbing chromophore, typically associated with a π-π* transition, offers significant potential to drive photochemical, chromoselective transformations.

Previous work from the Clayden group in 2003 led to the development of a unique, transition-metal-free, and operationally straightforward method for the photochemical one-carbon ring expansion of *N*-benzyl benzamides such as **76** (Scheme 18).[46] This approach exploited the orange colour and trienolate chromophore in **77** formed *in situ* via a dearomatising cyclisation. Upon formation of enolate **77** and irradiation with a tungsten lamp, a benzylic shift occured via which was assumed to be a [1,3]-sigmatropic rearrangement to form norcaradiene **78**. A subsequent [1,5]-sigmatropic shift led to a "walked" norcaradiene **79**, which underwent thermal electrocyclic ring-opening to afford cycloheptatriene **80**.

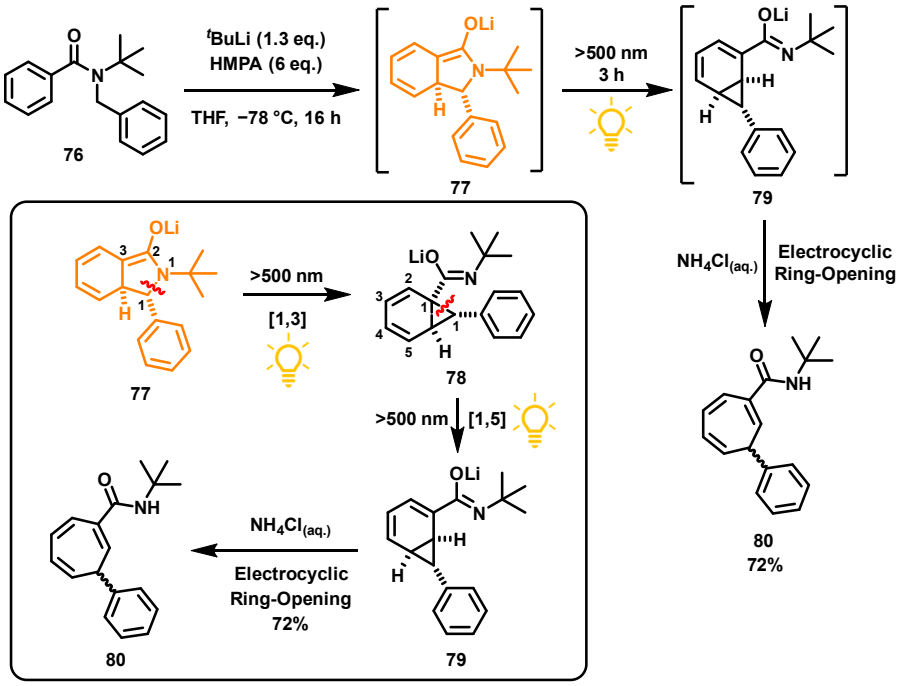

Scheme 18: The photochemical ring-expansion of N*-benzyl benzamide **76** from irradiation of enolate **77** including the mechanism from enolate **77** through norcaradienes **78** and **79** to cycloheptatriene **80**.*[46]

Additionally, reacting related benzamides with LDA or ^{t}BuLi and photochemically irradiating their respective enolates resulted in the formation of one of four product classes (A, B, C and D), depending on the substitution pattern on the expanding ring (Scheme 19). Compounds derived from classes A

and B arise via what was presumed to be a [1,3]-sigmatropic shift to form a norcaradiene (Class A), followed by a disrotatory electrocyclic ring-opening to produce a cycloheptatriene (Class B), effectively inserting a benzyl group adjacent to the carboxamide functionality. Alternatively, compounds of class C and D are believed to form from initially a [1,3]- and then a [1,5]-sigmatropic shift to give a "walked" norcaradiene (Class C), followed by electrocyclic ring-opening to yield a "walked" cycloheptatriene (Class D).

Substrates with *ortho*-substitution on the aromatic ring tended to favour the formation of [1,3]-norcaradiene products (Class A) or their ring-opened equivalents (Class B), due to increased conjugation and enhanced stability these substituents provide to the diene motif in the [1,3]-norcaradiene or cycloheptatriene. Consequently, the norcaradiene does not always undergo rearrangement to [1,5]-products (Class C and D) in these cases. In contrast, *para*-substitution in the starting amides predominantly yields "walked" [1,5]-norcaradienes (Class C) due to conjugative stabilisation between the *para*-substituted functionality and the amide carbonyl, which subsequently ring-open to form cycloheptatrienes of Class D in some cases. Substrates with *meta*-substituents can undergo ring expansion; however, they typically do not favour a particular product class due to their weaker conjugative stabilisation effects. For instance, a single methoxy group substituted at the *meta*-position in the expanding ring results in Class D cycloheptatriene **81**.

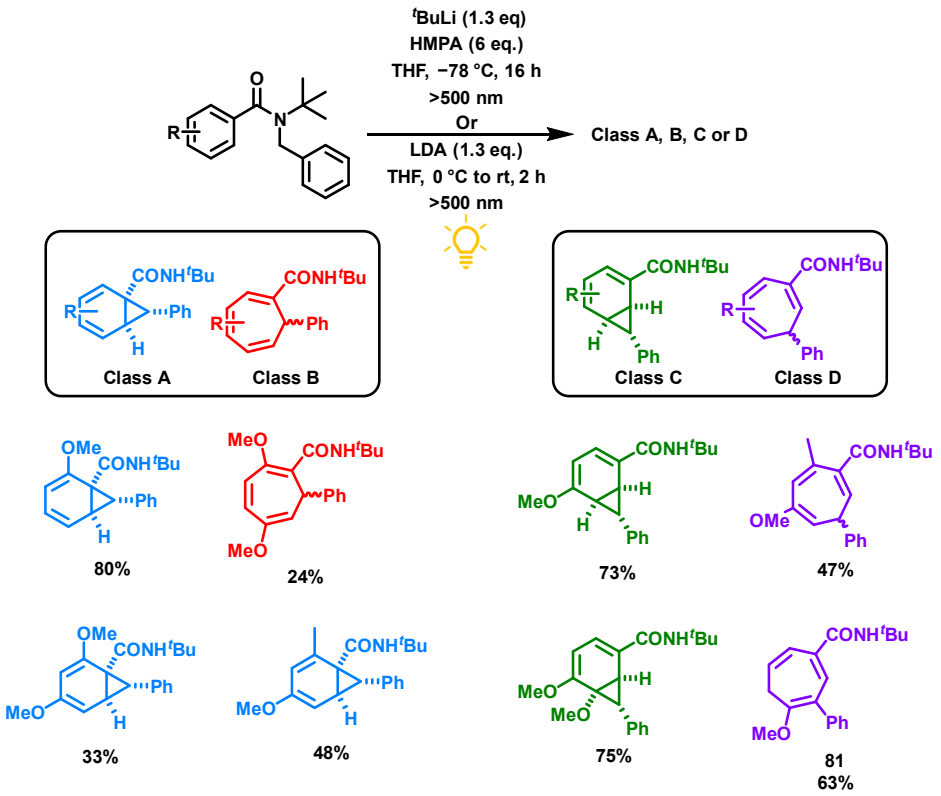

Scheme 19: Photochemical migration and ring-expansion of N*-benzyl benzamides to give one of four possible classes of products. Reaction quench was carried out with either* $NH_4Cl_{(aq.)}$ *or* $HCl_{(aq.)}$*.* [46]

In addition to synthesising stable norcaradienes through photochemical irradiation, the potential for initiating rearrangements with stereocontrol was explored. This was achieved by deprotonating chiral, enantiopure α-methyl benzamide **82**, followed by stereospecific cyclisation with retention of stereochemistry at the migrating position. For example, irradiation of methoxy-substituted enolate **83** led to the formation of norcaradiene **84** with an excellent enantiomeric ratio of 99:1 (Scheme 20).[18] The enhanced stability of the diene, due to conjugation between both the amide and methoxy groups, allowed for facile isolation of norcaradiene **84** in excellent yield. This high stereoselectivity confirms that stereochemical integrity is preserved during photochemical irradiation and benzylic migration, highlighting the potential for stereoselective enolate photochemistry in future studies.

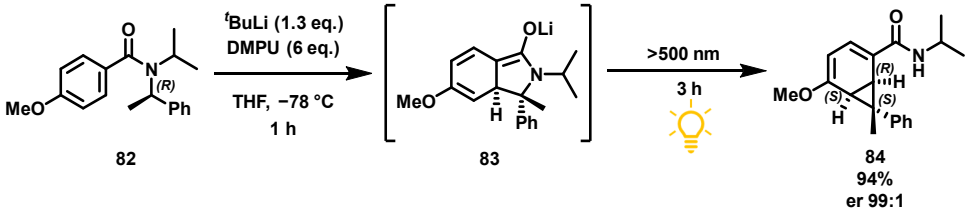

*Scheme 20: The irradiation of enolate **83** from enantiopure benzyl amide **82** to give "walked" norcaradiene **84**.[46]*

Although the visible-light photochemistry of trienolates was initially explored by the Clayden group in the early 2000s, these species proved too thermally unstable to be effectively studied to a greater extent using the energy-inefficient, heat-emitting halogen, mercury or tungsten lamps that were prevalent for photochemical applications at that time.[46] Fortunately, the recent advent of accessible, energy-efficient, and wavelength-selective LEDs has expanded the scope of photochemical investigations. The minimisation of unwanted thermal exposure with these modern light sources allows for easier exploration of new photochemical reactivity of thermally unstable, coloured species in solution. Cyclisation of benzamide **76** using chiral lithium amide base **49** goes via intermediate **85** to yield a photochemically active, stereochemically-enriched trienolate **77** (Scheme 21).

Previous members of the Clayden group have performed photochemistry on enantioenriched trienolate **77** using an energy-efficient Kessil® Blue LED, leading to the formation of the expected photochemical product. This enantioselective transformation typically afforded cycloheptatrienes such as **80** with high enantioselectivity (up to er 99:1), demonstrating that asymmetric deprotonation can impart stereoselectivity that persists through to the final reaction product. This pathway represents a unique transformation from a simple achiral starting material to a highly enantioenriched cycloheptatriene, achieved solely through irradiation of a transient coloured enolate.

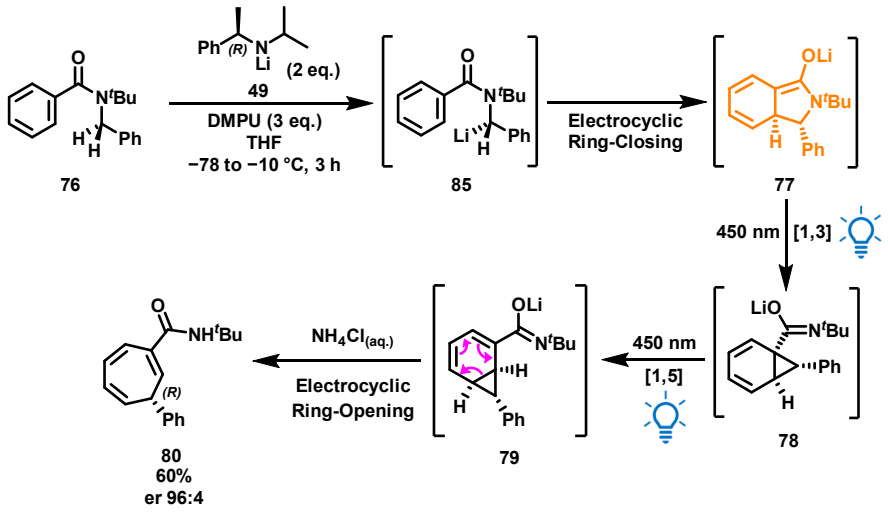

*Scheme 21: The asymmetric photochemical transformation on benzyl benzamide **76** explored by the Clayden group using chiral lithium base **49** to initiate stereoselectivity.*[1]

The asymmetric deprotonation, cyclisation, and rearrangement of derivatives of **76** accommodated various substitution patterns on the expanding ring, including methyl and methoxy groups. However, more electron-rich substituents generally reduced the enantioselectivity of the migration. This is likely due to the fact that an electron-rich expanding ring slows down the dearomatising cyclisation, allowing more time for chiral organolithium **85** to undergo racemisation rather than proceeding directly in the desired cyclisation. Pleasingly, electronic and structural variations on the migrating ring were well tolerated, with substrates such as 4-methylnaphthyl, pyridinyl, and anisole derivatives successfully participating in the transformation.

To summarise, the chromophore of enolates has rarely been leveraged for photochemical transformations. Historically, such reactions were constrained by thermally inefficient and potentially toxic and harmful light sources. However, the advent of modern, energy-efficient LEDs has enabled the facilitation of new and improved transformations involving thermally unstable intermediates such as enolates. Previous members of the Clayden group have demonstrated this by irradiating bicyclic trienolates such as **77**, triggering a sequence of photochemical and thermal steps, to afford cycloheptatrienes such as **80**. This process was eventually rendered enantioselective when using chiral base **49** for initial benzylic deprotonation. Despite this intriguing reaction pathway, our initial understanding of the requirements for successful enolate photochemistry was limited. Gaining this foundational knowledge could open opportunities to broaden the scope of enolate photochemistry, potentially leading to diverse reaction products and expanding its synthetic utility. This represents a significantly underexplored area of photochemical research, likely due to the strong scientific bias toward utilising enolates as nucleophilic reagents. This focus may have hindered creative exploration

of their chromophore as a photoreactive motif, limiting advancements in their photochemical applications until now.

1.5. Project Aims

This project commenced with a restricted understanding of the limitations and capabilities of enolates to participate in unique and useful photochemical transformations. Our objectives, therefore, were driven by a desire to deepen our understanding of these photochemical processes and to leverage that knowledge to expand enolate photoreactivity for preparative synthesis.

The aims can be categorised into three main objectives, as detailed below.

1. The initial goal was to elucidate the structural and electronic requirements necessary for enolates to engage in photochemical reactions. This involved investigating the underlying mechanisms by which enolates react under irradiation, alongside a study of skeletal modifications of enolate **77** to identify which alterations could be made while still preserving photoreactivity.

2. The next objective was to apply our understanding of the structural requirements necessary for photoreactivity to develop new, synthetically valuable photochemical transformations. This approach has the potential to broaden the scope of enolate photochemistry and enables a focussed effort on realising transformations that may be challenging to accomplish using conventional methods.

3. Finally, we aimed to revisit dearomatising cyclisations, which have been extensively studied within the Clayden group. Given that these cyclisations occur on various aromatic motifs, such as pyridines and pyrroles, we sought to leverage the intermediate enolates formed during these processes for photochemical rearrangements. This approach could lead to the formation of unusual and potentially unique molecular scaffolds.

With these aims, we sought to reimagine enolates not only as thermal nucleophilic reagents, but as photochemically active species capable of producing synthetically valuable materials through direct irradiation under mild conditions. This approach eliminates the need for external photocatalysts, toxic or expensive heavy metals, and relies solely on a mild light source provided by energy-efficient LEDs.

Computational Predictions for Electronic Spectra

2.0. Time-Dependent Density Functional Theory

To thoroughly investigate the photochemical properties of reactive enolate intermediates, time-dependent density functional theory (TDDFT) calculations were performed using the CAM-B3LYP functional combined with the 6-31+G(d,p) basis set. TDDFT is a valuable computational approach that models the behaviour of excited states under time-dependent external influences, such as electromagnetic radiation.[47] This allows for the prediction of photochemical absorption characteristics, such as UV-Vis spectra, which are crucial for understanding the photophysics and photochemistry of enolates.

The choice of the CAM-B3LYP/6-31+G(d,p) combination is well-regarded in computational photochemistry due to its balance between computational efficiency and accuracy. It is particularly suitable for studying excited states, charge transfer processes, and electronic transitions in organic and conjugated systems.[48] While more extensive basis sets, such as aug-cc-pVDZ, may offer enhanced accuracy, they significantly increase computational costs, making them less practical for larger systems or broader studies.[49]

For this project, solvent effects were included in the computational model using a polarisable continuum model (PCM), specifically parameterised for tetrahydrofuran (THF). This addition enhances the accuracy of the predictions by accounting for solvent interactions that can influence electronic properties. However, while TDDFT is a robust tool for such predictions, it does have limitations, particularly for systems with considerable electron correlation or those involving higher-energy transitions or potential diradical states.[50] In these cases, more sophisticated multireference methods, such as Complete Active Space Self-Consistent Field (CASSCF) or Restricted Active Space Perturbation Theory (RASPT2), may provide more precise results.[51]

The computational results, including UV-Vis absorption predictions and molecular orbital diagrams, offer valuable insights into the structural and electronic characteristics critical for achieving visible-light absorption in enolates. These results help clarify the nature of the molecular orbitals involved, the types of electronic transitions, and the excitation modes that govern the photochemical behaviour of these species.

Throughout this thesis, TDDFT predictions for enolates are integrated and discussed in relevant sections, highlighting their role in understanding the photophysical properties of the compounds studied. Although computational models inherently come with limitations and potential inaccuracies, they provide valuable approximations that are generally well-suited for most substrates examined in this research. Notably, TDDFT calculations often tend to underestimate the UV-Vis absorption maxima (λ_{max}) of the studied enolates by varying amounts, with their discrepancies detailed in Table 1. These discrepancies are discussed on an individual basis in relevant sections of this body of work. The underestimation of λ_{max} values by TDDFT is often attributed to its handling of electron correlation effects and the functional's limitations in accurately capturing long-range charge transfer states.[52] Further refinement using range-separated hybrid functionals could potentially mitigate these deviations.

Table 1: Relevant enolates discussed in this thesis, with their calculated and experimental λ_{max} value where possible.

Enolate	λ_{max} Experimental / nm	λ_{max} Calculated (TDDFT) / nm	Difference in λ_{max} / nm
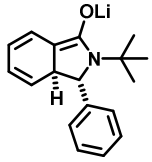	448	421	27
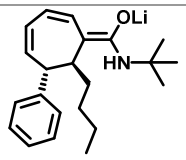	554	396	158
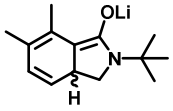	525/570	428	97 or 142
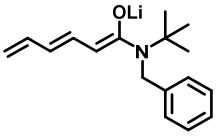	350-390	365	<25
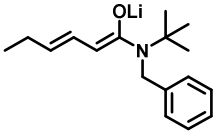	<350	316	<34
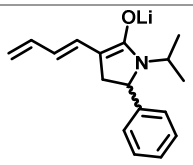	-	367	-

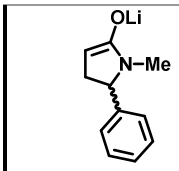	-	320	-
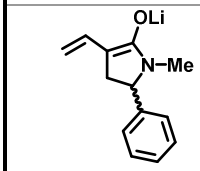	-	340	-
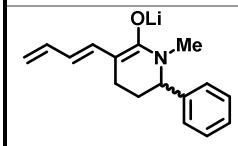	-	367	-
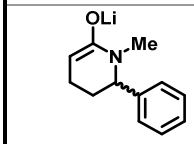	-	335	-
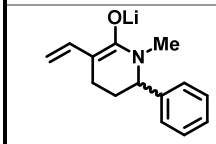	-	346	-
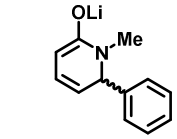	-	331	-
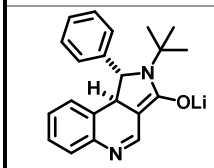	-	372	-
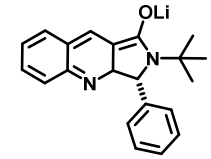	523	478	45
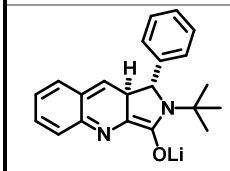	561/615	558	3 or 57
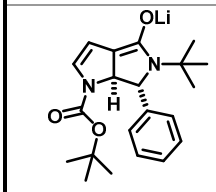	-	339	-

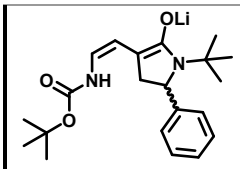	-	342	-

2.1. UV-Vis Spectra and Calculations for Enolate 77

Upon performing computational geometry optimisation followed by a TDDFT calculation on enolate **77**, the predicted λ_{max} was found to be 421 nm, closely aligning with the experimentally measured value of 448 nm. This strong correlation demonstrates the high predictive accuracy of these computational methods for certain substrates. As illustrated in Figure 2, overlaying the Kessil® Blue LED emission spectra with the UV-Vis spectra of enolate **77** reveals a significant overlap between the enolate's absorbance and the LED's emission wavelengths. This overlap provides a clear rationale for the efficient facilitation of photochemical reactions involving enolate **77** by blue light irradiation.

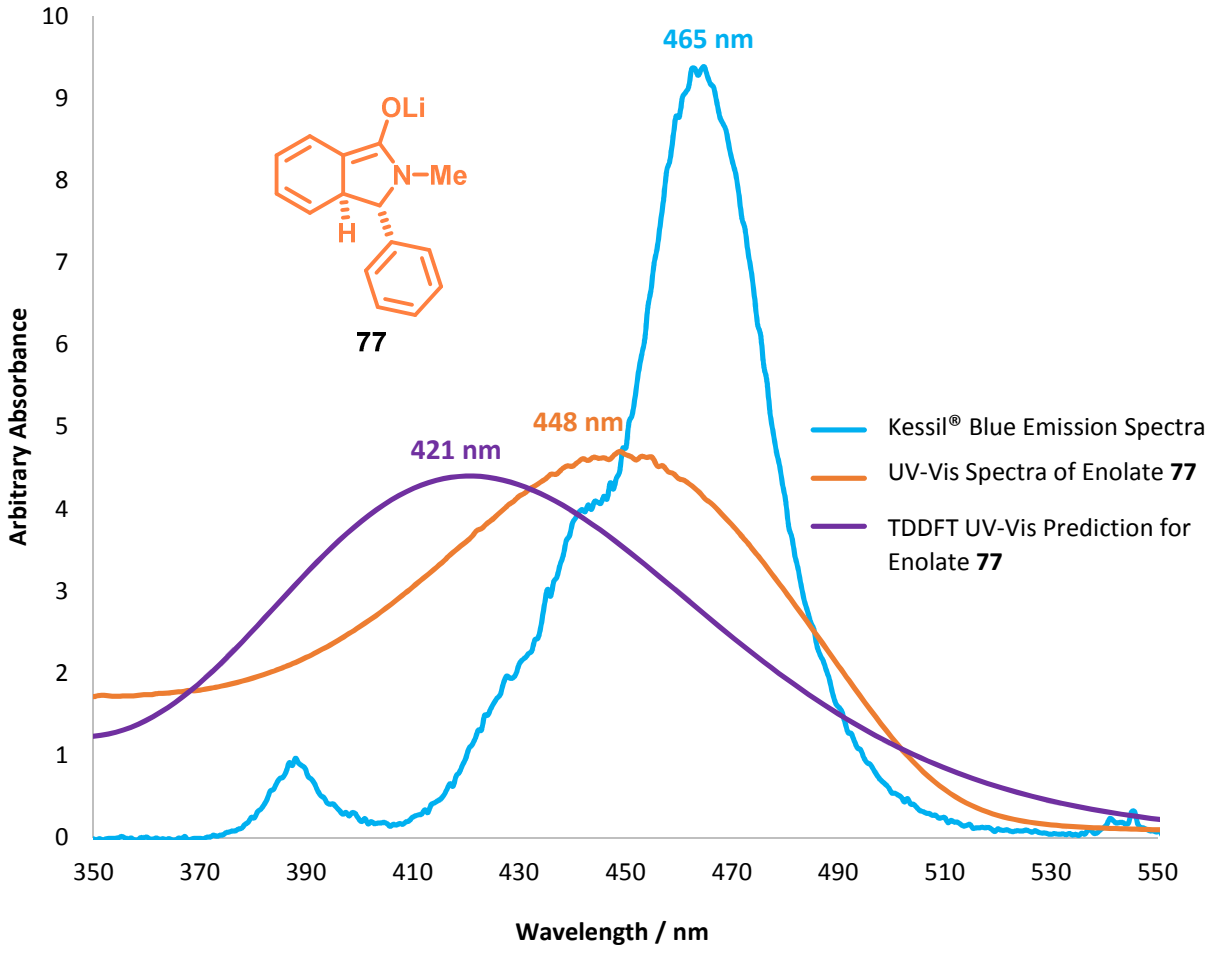

*Figure 2: The predicted and calculated UV-Vis spectra of enolate **77** along with the emission spectra of the Kessil® Blue LED used for photochemistry.*

2.2. Understanding the Excited State of Enolate 77

TDDFT calculations also yield molecular orbital predictions, which were utilised to characterise the excitation likely responsible for the photochemistry of enolate **77**. As illustrated in Figure 3, The HOMO-LUMO transition in enolate **77**, characterised by significant π-π* interactions, suggests that electron density redistribution primarily occurs across the conjugated system upon excitation. This redistribution may facilitate specific bond rearrangements or photochemical reactions, as observed experimentally. This supports the conclusion that the observed photochemistry is driven by a π-π* excitation within the trienolate system, corresponding to the absorption of photons at a wavelength of ~448 nm.

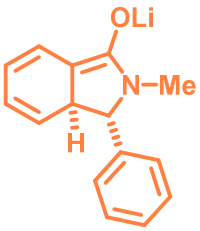

77

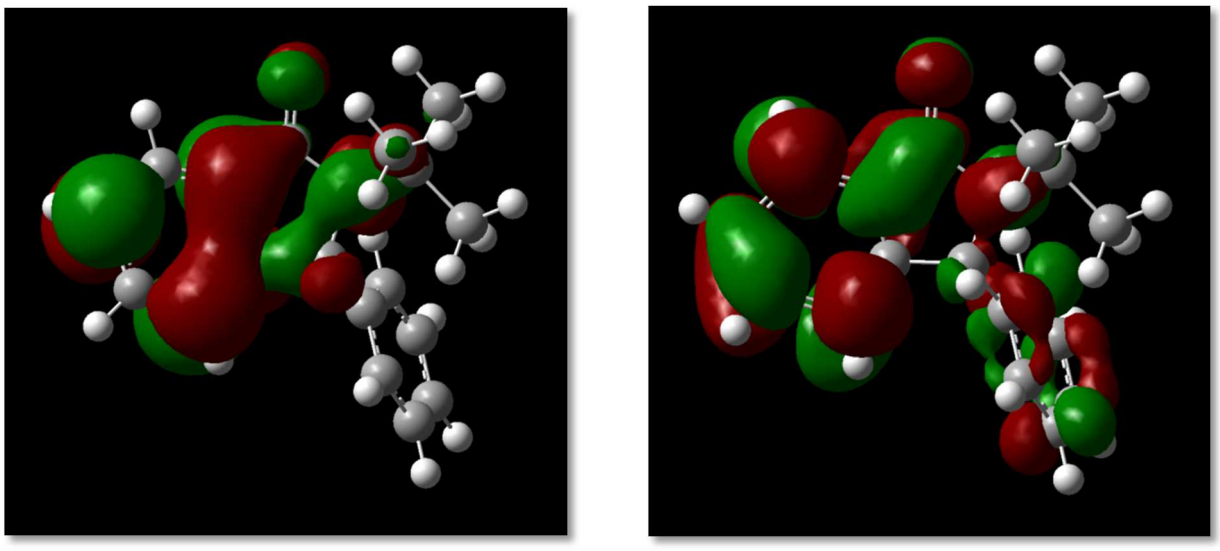

*Figure 3: The calculated HOMO (left) and the calculated LUMO (right) for enolate **77**, modelled as the naked anion.*

Time-resolved infrared (TRIR) spectroscopy could provide further confirmation that the proposed excitation is indeed responsible for the observed photochemical behaviour. This technique involves exciting the compound at a specific wavelength and measuring changes in infrared stretching frequencies upon excitation.[53] This approach would be particularly valuable for studying enolate **77**, where a π-π* transition is hypothesised. Observing the elongation and weakening of carbon-carbon

double bonds in a transient IR study would offer compelling evidence that the S_0-S_1 excitation underlies the observed photochemical transformation.

The photophysics of enolate **77** can be further investigated by determining the lifetime of the excited state generated upon irradiation, using transient UV-Vis spectroscopy. In transient UV-Vis spectroscopy, a pulse laser would irradiate the enolate at its absorption wavelength, promoting a fraction of the photochemically active molecules into an excited state. A weak probe pulse is then sent through the sample after a controlled delay relative to the laser pulse. By calculating a difference absorption spectrum from these readings, the lifetime of the excited state can be determined.[54,55] The delay between the laser and probe pulses is systematically varied, and the experiment is repeated to measure absorbance differences over different time intervals.

Transient absorption spectroscopy can also be performed in a variable wavelength mode, where the excitation occurs as before, but changes in absorption across various wavelengths are detected. This approach could be valuable for identifying intermediates in the photochemistry of enolate **77**, such as norcaradienes **78** and **79**, which would exhibit different absorption wavelengths compared to the parent enolate. The identification of such transient species is enabled by the pulsed lasers used in this technique, which can probe transformations on timescales as short as 10^{-16} seconds.[56] These transient spectroscopy methods, both IR and UV-Vis, could be pursued in future studies as an extension of this work.

Exploring Alternative Cyclic Trienolates for Photoreactivity

Building on the photochemical studies of trienolate **77**, it was hypothesised that synthesising structurally related cyclic trienolates could yield similar UV-Visible absorbances, thereby enabling the exploration of analogous photochemical processes using visible-light irradiation. We designed new substrates with structural modifications to the amide framework of enolate **77** to identify features that optimise visible-light absorption and photoreactivity (Figure 4). These modifications include using the photochemical product of enolate **77** (cycloheptatriene **80**) to create a new trienolate **86**, removing the aromatic ring from the benzylic position as in compound **87**, and substituting the amide functionality with an ester as in **88**.

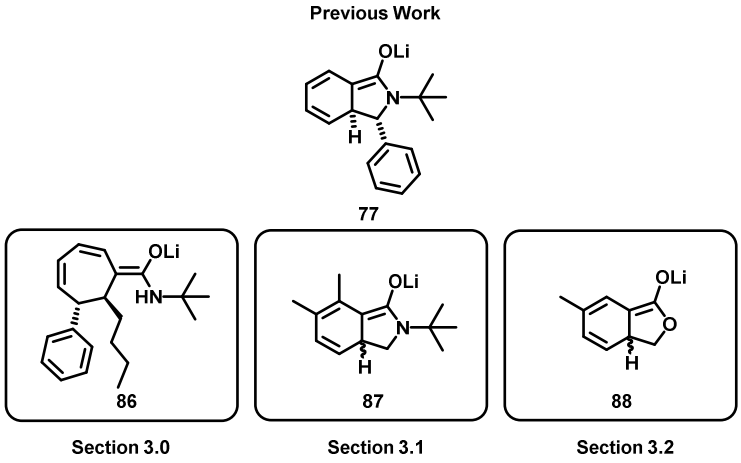

*Figure 4: The three cyclic trienolates studied in this report, **86**, **87** and **88**, based on the original trienolate **77**.*

3.0. Cycloheptatrienolate

The photochemical study of trienolate **77** revealed the generation of cycloheptatriene **80** via a migration and rearrangement cascade. Despite having a conjugated system of three double bonds, cycloheptatriene **80** does not absorb in the visible region of the electromagnetic spectrum. However, generating an enolate from this system could allow photochemical reactivity under visible-light irradiation.

Previous work demonstrated that the intermediate lithiated cycloheptatrienolate **89** could be successfully methylated by quenching with iodomethane to give **90** (Scheme 22).[1] The cycloheptatriene could subsequently be racemised via deprotonation at the benzylic position using

LDA, forming an enolate, as confirmed by methylation α- to the carbonyl, giving **91**. This suggests that enolates can indeed be formed on such substrates, presenting opportunities for further visible-light photochemical exploration. The specific enolate resulting from the deprotonation of **90** has not yet been studied photochemically and could be a focus for future research, beyond this thesis.

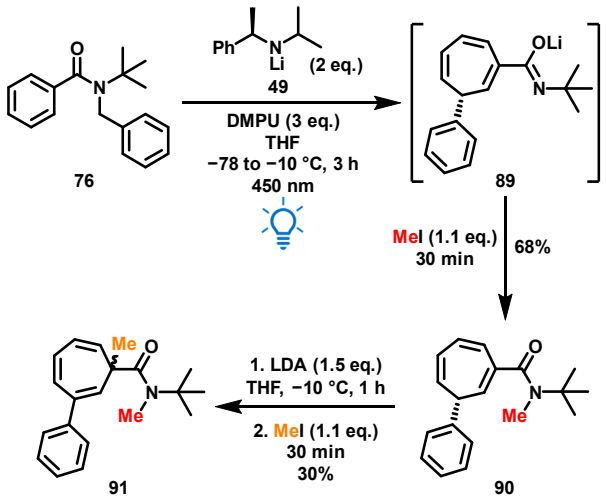

*Scheme 22: Photochemistry to afford lithiated cycloheptatriene **80,** followed by methylation at nitrogen **90** and methylation α- to the carbonyl from enolate formation to give **91**.*

The formation of an alternative, unexpected enolate on cycloheptatriene **80** was discovered serendipitously. When a sample of cycloheptatriene **80** was placed in a quartz cuvette and treated with an excess of ^{n}BuLi, a deep purple colour immediately developed, and a UV-Vis spectrum of the mixture showed a clear peak with λ_{max} = 554 nm. Initially, it was anticipated that the base would deprotonate the amide nitrogen. However, it was determined that ^{n}BuLi acted as a nucleophile, adding to one of the triene double bonds via a conjugate addition to give enolate **86** (Scheme 23). The regioselectivity of this addition was influenced by coordination to the carbonyl and the potential for conjugation into the carbonyl of the amide group in **80**. This reaction produced a trienolate with a significant visible-light absorbance.

TDDFT predictions for enolate **86** estimated an absorbance with λ_{max} = 396 nm, highlighting a substantial discrepancy between the predicted and observed absorbance. Upon aqueous quench of this trienolate, cycloheptadiene **92** was formed diastereoselectively (with only one isomer observed by NMR), suggesting a stereoselective addition of the butyl chain opposite to the bulky phenyl ring. The stereochemical arrangement was confirmed by a 1D NOE experiment, which revealed a cross-peak between the proton adjacent to the amide carbonyl and the newly introduced butyl chain.

Quenching intermediate trienolate **86** with iodomethane resulted in regioselective methylation at the γ-position relative to the carbonyl to give **93**, again with only one diastereomer observed by NMR. This selectivity is likely attributed to reduced steric hindrance at this site compared to the α-position. The methyl group also added to trienolate **86** on the face opposite the phenyl ring, consistent with the relative stereochemistry observed on formation of **92**. This was confirmed by a distinct NOE interaction between the proton adjacent to the methyl group and the protons on the phenyl ring, as well as the proton adjacent to the butyl chain. This outcome demonstrates a remarkable degree of both regio- and stereoselectivity for these stereochemically-rich products, with no alternative diastereomers detected upon isolation.

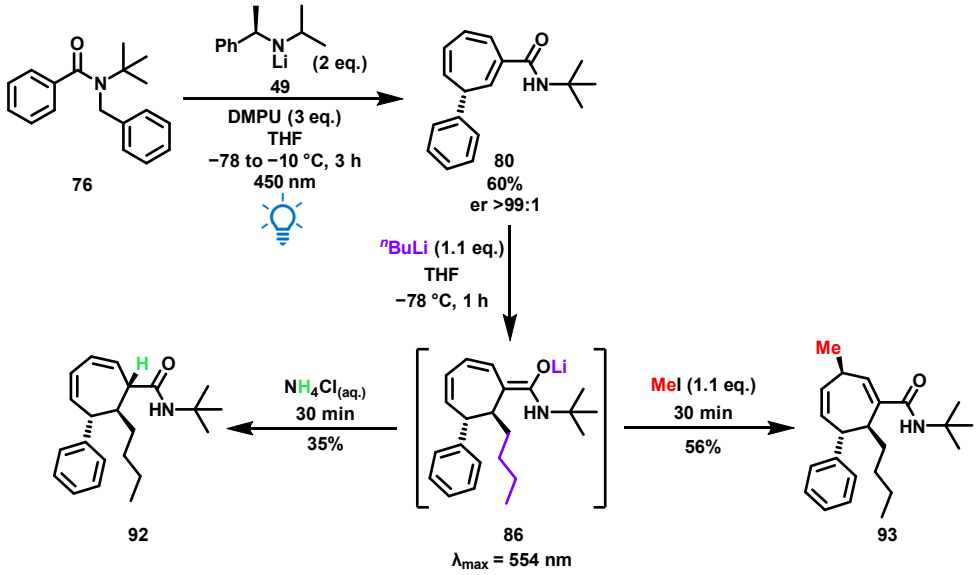

*Scheme 23: The formation of trienolate **86** by conjugate addition with ⁿBuLi, followed by the results on quench.*

The formation of trienolate **86** suggests the potential for the addition of multiple nucleophiles to the triene motif via conjugate addition, indicating that similar trienolates could be generated by simply varying the nucleophile or base used. Irradiation of trienolate **86** at 554 nm has not resulted in observable photochemical reactions, potentially due to the absence of a carbon group on the nitrogen that can facilitate migration across the enolate framework. Future investigations should explore modifications, such as introducing a benzyl group to the amide nitrogen, which could enable successful migration and reactivity upon irradiation (Scheme 24). Irradiation of the enolate derived from *N*-benzyl cycloheptatrienamide **94** could lead to benzyl-migration products **95**, **96**, and **97**, assuming sigmatropic-type rearrangements of the benzyl group across the seven-membered ring.

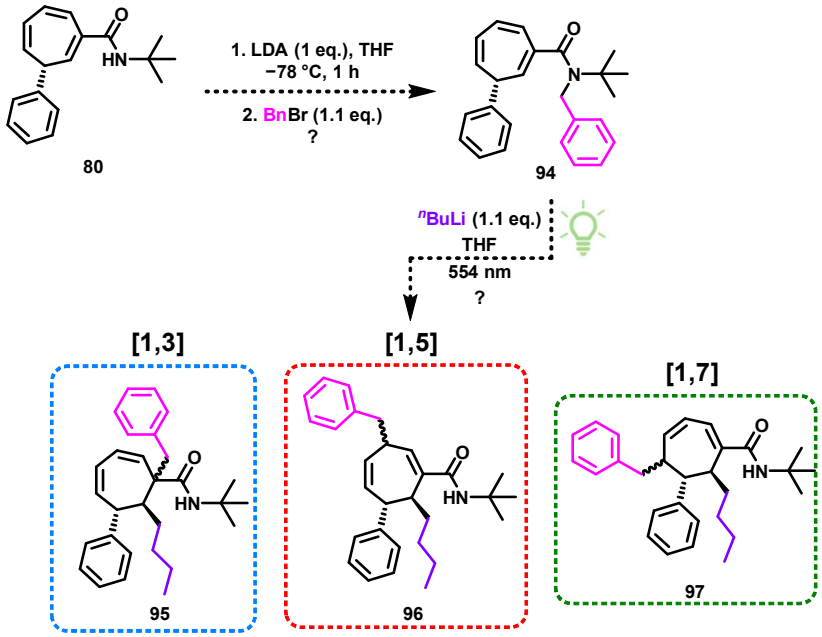

*Scheme 24: The planned potential pathway towards benzylated amide **94**, giving rise to the possible photochemical migration of a benzyl group across the respective trienolate photochemically, potentially affording **95**, **96** and **97**.*

3.1. Bicyclic Lactam Trienolate

So far, we have only demonstrated photochemical reactivity with bicyclic trienolates featuring a migrating benzyl group. We aimed to investigate whether a bicyclic trienolate lacking a benzylic group, such as enolate **98**, could still undergo analogous reactivity, provided that the structural core of the molecule remains similar to the previously reported bicyclic trienolate **77** (Figure 5). However, synthesising compounds with a dienyl bicyclic motif comprising a six- and five-membered fused ring has proven to be particularly challenging, with few examples reported in the literature. The most straightforward approach to synthesise a conjugated diene in a bicyclic system could involve the dearomatising cyclisation reaction developed by the Clayden group.[35] This method, however, necessitates a stabilised lithium intermediate, such as benzylic organolithium **99**, to achieve successful deprotonation prior to cyclisation. Therefore, dearomatising cyclisation from unstabilised organolithium **100** is unlikely to occur. To synthesise a bicyclic diene devoid of an aromatic group, an alternative pathway that bypasses the need for anionic cyclisation must be explored.

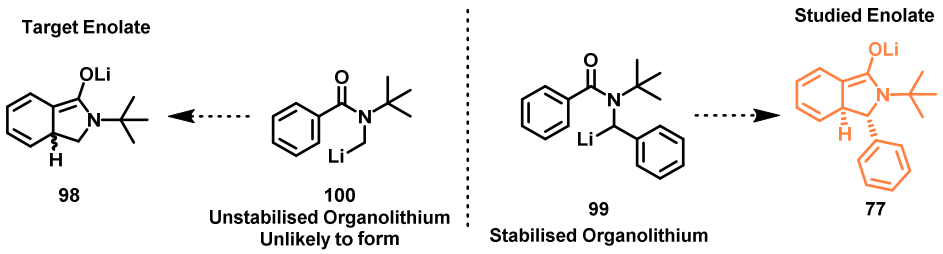

*Figure 5: A comparison between the stabilised organolithium **99** used in dearomatising cyclisation and the unstabilised organolithium **100** which is unlikely to form and therefore unlikely to undergo a cyclisation step to give enolate **98**.*

To achieve cyclisation, we employed an intramolecular Diels-Alder reaction with tethered diene and dienophile groups. Reductive amination of *tert*-butylamine (**101**) with hexa-2,4-dienal (**102**) yielded secondary dienamine **103** (Scheme 25). The use of hexa-2,4-dienal (**102**), instead of the preferred (*E*)-penta-2,4-dienal, introducing an additional methyl group on the product's bicyclic structure, is due to the former's commercial availability. Amine **103** was subsequently subjected to amide coupling conditions with propiolic acid (**104**) to position the dienophile moiety appropriately within the molecular framework for the planned intramolecular Diels-Alder reaction. However, no desired product **105** was obtained in acceptable yields, and a mixture of unknown by-products were formed when employing coupling reagents such as HATU, DCC, or Mukaiyama-type reagents.

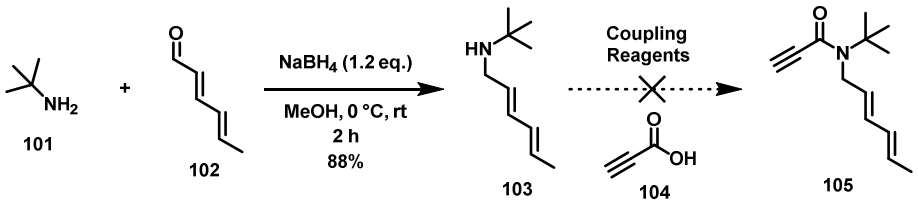

*Scheme 25: The synthesis of amine **103** and an attempted amide coupling to **105**.*

Based on literature reports involving similar alkyne substrates, it is believed that the electrophilic nature of the alkyne bond in propiolic acid (**104**) facilitates competitive aza-conjugate addition of amine **103** to the triple bond, subsequently leading to various rearrangement products.[57,58] Furthermore, amines have been shown to act as polymerisation catalysts in the presence of propiolic esters. This phenomenon was documented by McCulloch and McInnes, who reported that, in the presence of water, betaine **108** was the major product formed in the reaction between ethyl propiolate (**106**) and triethylamine (**107**) (Scheme 26).[58]

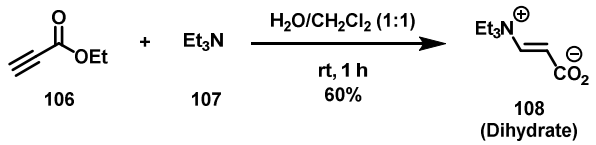

*Scheme 26: The reported formation of betaine **108** as a major product from reaction of ethyl propiolate (**106**) and triethylamine (**107**).*[54]

To prevent conjugate addition, we increased steric hindrance by using a bulkier alkyne, but-2-ynoic acid (**109**), in the coupling reaction. This strategy, using HATU as the coupling reagent, yielded desired amide **110** in 20% yield (Scheme 27). Although this modification adds two methyl groups to the product, it was deemed acceptable given the expected minimal impact on its photoreactive properties.

The amide positions the diene and alkyne in close proximity, facilitating an intramolecular Diels-Alder reaction that forms the bicyclic ring system in a 65% yield. The resulting bicyclic amide **111** was obtained as a single diastereomer, with its stereochemistry assigned by analogy to its lactone equivalent in literature.[59]

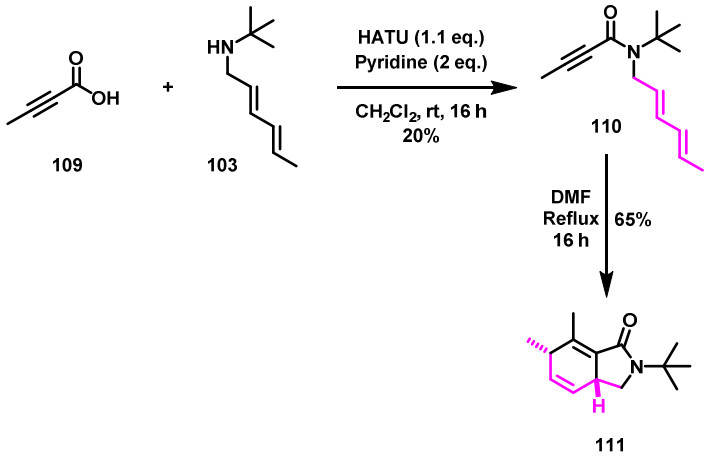

*Scheme 27: The modified synthetic route through alkynyl amide **110** in an intramolecular Diels-Alder reaction towards dienyl amide **111**.*

Although the synthesis of unsaturated bicycle **111** was successful under these conditions, it was observed that oxidation occurred upon exposure to air, resulting in the formation of aromatic bicyclic amide **112** over several days (Scheme 28). The instability of this cyclic diene towards oxidation may explain the scarcity of reported syntheses for such substrates in the literature.

When a mixture of the inseparable dienamide **111** and aromatic amide **112** in a 75:25 ratio was treated with LDA for deprotonation, a deep-red coloured mixture was produced. This mixture exhibited two distinct UV-Vis absorption peaks at a λ_{max} of 525 nm and 570 nm, suggesting the presence of two

chromophore-containing species. It was hypothesised that desired enolate **87** was generated in solution from dienamide **111**, alongside a possible tetraenolate **113** formed via lateral deprotonation of aromatic amide **112** by LDA. This indicates that the methyl group originating from but-2-ynoic acid (**109**) may play a role in promoting dearomatisation and enolate formation on aromatic amide **112** under the basic conditions. Notably, this represents the first and only instance of a potential tetraenolate within this body of work.

TDDFT calculations for desired trienolate **87** predicted a λ_{max} of 428 nm. If the actual trienolate absorbance corresponds to either 525 or 570 nm, the prediction appears to have considerably underpredicted the bathochromatic absorbance shift when compared to bicyclic trienolate **77**.

The formation of enolates **87** and **113** was confirmed by NMR analysis, where deuteration of the basic mixture resulted in laterally-deuterated compound **113**, indicating lateral lithiation and subsequent enolate formation. The presence of trienolate **87** derived from dienyl amide **111** was also verified by deuteration, which produced monocyclic amide **115**. In this process, aromatisation occurred upon deuterium quenching, involving the cleavage of a C-C bond and the opening of the five-membered ring—essentially the reverse of the dearomatising cyclisation reaction previously reported by the Clayden group.[36]

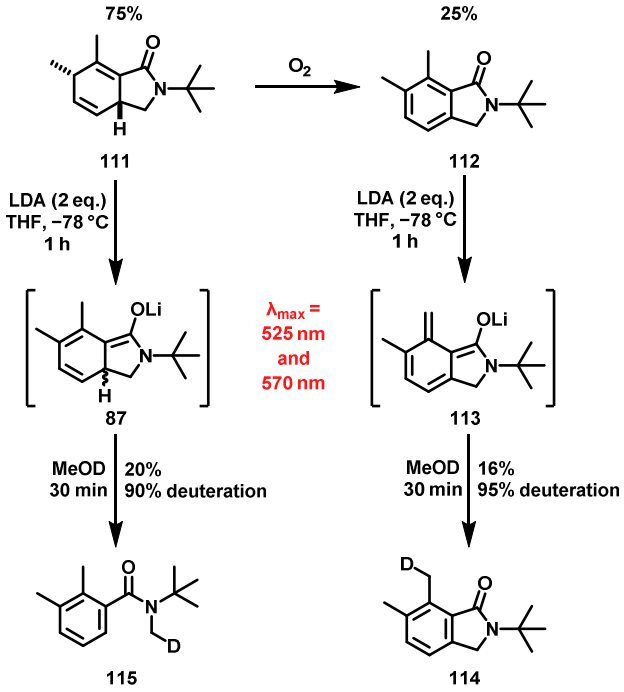

*Scheme 28: The deprotonation of amide **111** to give trienolate **87**, along with its aromatic equivalent **112** undergoing lateral lithiation to form a potential tetraenolate **113** and their products from quench, **114** and **115**.*

Due to the inherent stability challenges associated with bicycle **111**, further investigation into the photoreactivity of this trienolate was postponed in favour of exploring other substrates with potentially greater air stability, such as those incorporating a lactone instead of an amide as the structural core.

3.2. Bicyclic Lactone Trienolate

A similar strategy to the one described in Section 3.1 was used to synthesise bicyclic ester **118**. Starting from hexa-2,4-dienal (**102**), the aldehyde was reduced to sorbic alcohol (**116**) using sodium borohydride, achieving a high yield (Scheme 29). Subsequent esterification of the alcohol with propiolic acid (**104**), mediated by DCC and DMAP, afforded unsaturated ester **117** in 58% yield.

This ester then participated in an intramolecular Diels-Alder reaction, yielding the desired dienyl ester **118** with high diastereoselectivity (only a single diastereomer was observed), in moderate yield. It is noteworthy that, in this synthesis, the coupling step proceeded successfully without the need to increase the bulk of the alkyne coupling partner. This is likely due to the reduced nucleophilicity of sorbic alcohol (**116**) compared to amine **103**, resulting in a diminished propensity for nucleophilic addition to the alkyne.

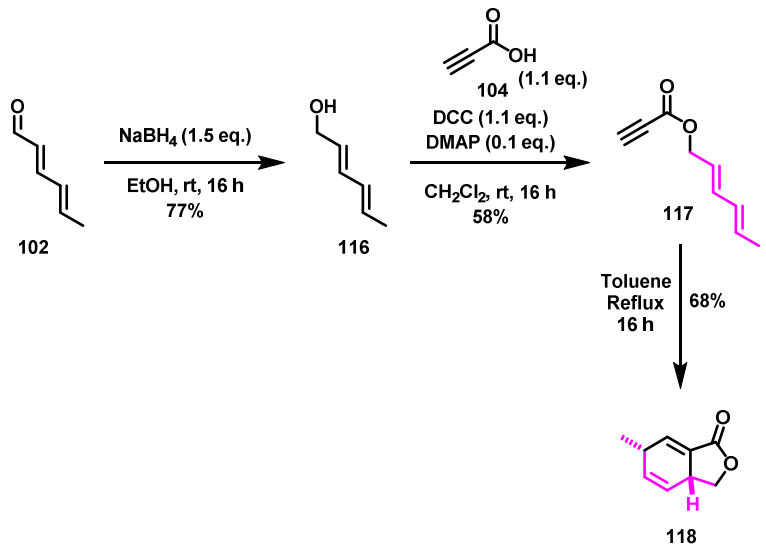

*Scheme 29: The synthesis of dienyl ester **118**, utilising an intramolecular Diels-Alder process.*

Despite the modifications, aromatisation still occurred when this substrate was exposed to aerobic conditions, albeit at a seemingly slower rate than with amide **111**. When a mixture of ester **118** and

its aromatic counterpart (in a 90:10 ratio respectively) was treated with LDA, an orange solution formed, giving a λ_{max} of 394 nm, which is close to the TDDFT-predicted value of 414 nm for the trienolate of **118**. However, it remains unclear if this absorbance is attributable to the expected enolate, as the subsequent quench yielded numerous unidentifiable compounds, suggesting substrate degradation during the deprotonation process or upon quenching. The instability of these substrates under basic and aerobic conditions led us to discontinue this line of investigation, shifting focus to more promising and stable alternatives. Future studies could revisit these substrates with modified conditions to enhance stability.

Photochemical Migrations of Acyclic *N*-Benzyl Amide Enolates

Our comprehensive investigations into the photochemistry of bicyclic trienolate **77** have elucidated its ring expansion under irradiation at 450 nm. Building on this foundational understanding, we sought to explore structural modifications to the enolate core to determine whether similar photochemical transformations could be achieved with alternative frameworks. This study aimed to assess the role of the bicyclic system in enhancing visible-light absorbance and promoting photochemical activity. One particularly intriguing modification involved the removal of the cyclic backbone that previously enforced a rigid structure on the enolate (Figure 6). If the cyclic framework is not crucial for maintaining the spatial proximity needed for photochemical migration, this could broaden the scope of photochemical transformations, allowing for a more flexible and unconstrained conjugated system to provide photoreactivity. This consideration prompted us to investigate the photochemistry of acyclic amide enolates such as *N*-benzyl amide trienolate **119**. Our initial objective was to measure the UV-Vis absorbance of these enolates to evaluate their potential for chromoselective irradiation and subsequent photochemical reactivity. In considering possible reaction pathways, parallels can be drawn with [1,3], [1,5] and [1,7]-type rearrangements, which would involve the migration of a substituent from nitrogen to carbon along the enolate framework in *N*-benzyl amide trienolate **119**.

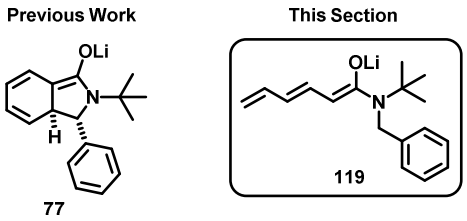

*Figure 6: Acyclic enolate **119** investigated in this section, removing the cyclic structure of bicyclic enolate **77**.*

4.0. Synthesis of Acyclic *N*-Benzyl Amide Trienolate Precursors

To maintain structural similarity to the bicyclic enolate **77** while eliminating the fused cyclic structure, dienamide **123** was synthesised (Scheme 30). This amide was obtained via an amide coupling reaction between sorbic acid (**122**) and *N*-*tert*-butyl benzylamine (**121**) using HATU, affording the desired product in 13% yield. *N*-*tert*-Butyl benzylamine (**121**) was synthesised through reductive amination of *tert*-butylamine (**101**) and benzaldehyde (**120**), achieving a yield of 92%.

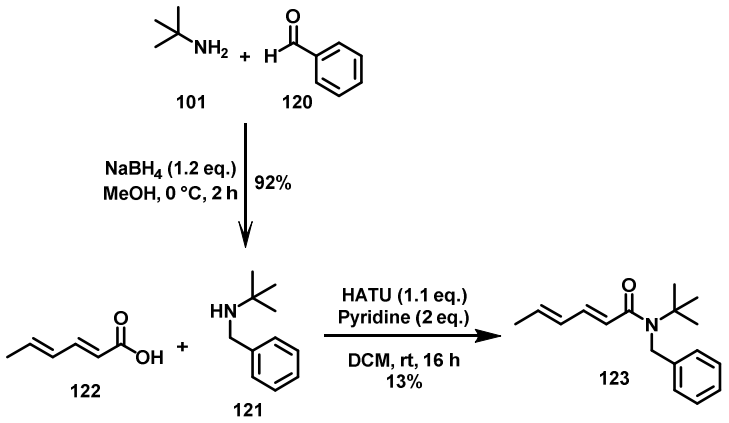

*Scheme 30: Synthesis of dienylamide **123** from sorbic acid (**122**) and* tert*-butyl benzylamine (**121**) from reductive amination of benzaldehyde (**120**) with* tert*-butylamine (**101**).*

With dienamide **123** in hand, the next step was to determine the UV-Vis absorbance of the corresponding trienolate upon treatment with LDA. However, treatment with LDA did not yield the desired enolate; instead, an unanticipated aza-Michael conjugate addition was observed, with LDA acting as a nucleophile attacking the double bond conjugated to the amide carbonyl (**124** via **LDA-123**; Scheme 31). This reaction likely arises from a conformational coordination between the lithiated base and the carbonyl group, directing nucleophilic attack to the β-position. Furthermore, it is plausible that the terminal carbon of the amide lacks the kinetic acidity required to overcome the electronic preference for conjugate addition. The low yield observed during formation of amide **123** could also be partially attributed to an aza-Michael addition involving *N-tert*-butyl benzylamine (**121**).

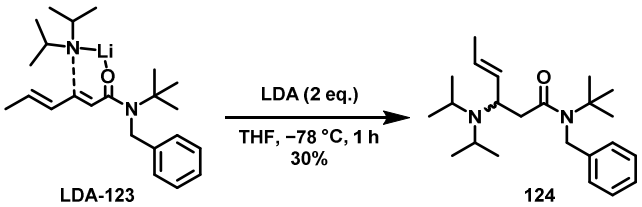

*Scheme 31: The effect of adding LDA to amide **123**, giving a conjugate addition likely directed by the carbonyl.*

A similar conjugate addition was observed when using ^{n}BuLi, as confirmed by deuteration at the electrophilic β-position, which resulted in the selective formation of a monoenolate. Although the use of bulkier lithiated bases, such as LiTMP or LiHMDS, could potentially minimise this side reaction, we chose to pursue a more streamlined strategy. These considerations led us to investigate alternative reaction substrates that avoid the risk of conjugate addition entirely, providing a more generalisable approach to enolate generation for diverse substrates.

Consequently, we utilised a reported isomerisation of sorbic acid (**122**) using LDA at −78 °C to obtain terminal alkenyl acid **125** (Scheme 32).[60] Notably, the carboxylate generated during deprotonation clearly disfavours conjugate addition of LDA, as evidenced by the quantitative yield for formation of isomerised acid **125**. This acid was then coupled with *N*-*tert*-butylbenzylamine (**121**) using HATU as a coupling agent, affording amide **126** in 40% yield.

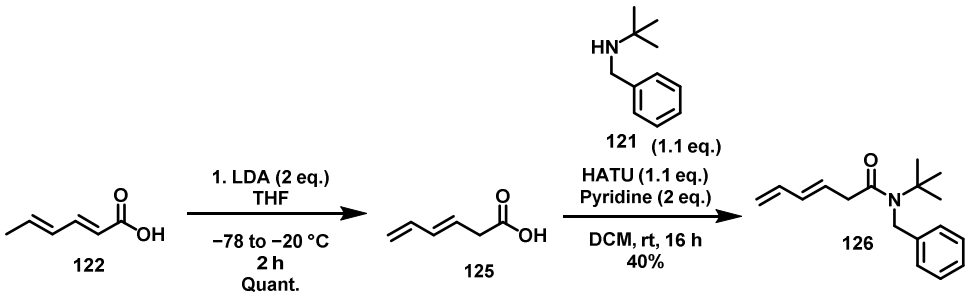

*Scheme 32: The isomerisation of sorbic acid to give **125** followed by coupling to amine **121** to give unconjugated amide **126**.*

Upon treatment of amide **126** with LDA, desired trienolate **119** was successfully generated, as confirmed by deuteration at the α-position relative to the carbonyl to afford **127** (Scheme 33). The resulting enolate solution exhibited a striking green colour, indicative of visible-light absorption. UV-Vis analysis showed a broad absorbance with a maximum wavelength (λ_{max}) ranging between 350 nm and 390 nm.

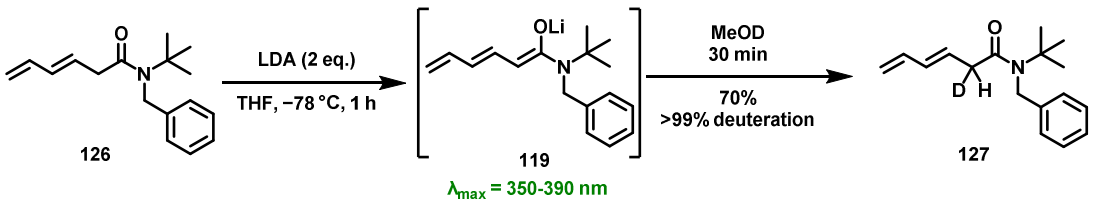

*Scheme 33: Formation of trienolate **118** from amide **126** followed by quench to confirm its formation (**127**).*

This absorption data allows for a meaningful comparison between the well-characterised, photochemically active trienolate **77** and acyclic *N*-benzyl amide trienolate **119**. The observed decrease in λ_{max} by approximately 60-100 nm indicates that the removal of the cyclic structure in the enolate raises the energy of the π-π* transition, resulting in a hypsochromic shift. This shift suggests a more flexible enolate geometry in the acyclic system, which could influence the efficiency of subsequent photochemical migrations. Therefore, we next explored how such geometric flexibility affects the photochemical reactivity of acyclic enolate systems.

4.1. Acyclic *N*-Benzyl Amide Trienolate Photochemistry

Irradiation of enolate **119** formed from dienyl amide **126** at 385 nm for five hours at −78 °C resulted in the green mixture transitioning to an orange solution, which exhibited visible fluorescence under the irradiation conditions. Isolation after an aqueous quench resulted in a mixture of three regioisomeric compounds: the [1,3] (***E/Z*-128**), [1,5] (**129**), and [1,7] (**130**)-benzylic migration products, with approximate NMR yields of 37%, 10%, and 28%, respectively (Scheme 34). Notably, no additional products were isolated from this reaction. The observed mass loss is likely due to polymerisation of the enolate or its intermediates during the photochemical process. Polymerisation is a recurrent issue in enolate photochemistry and competes with the desired photochemical benzyl migration in amide trienolates.

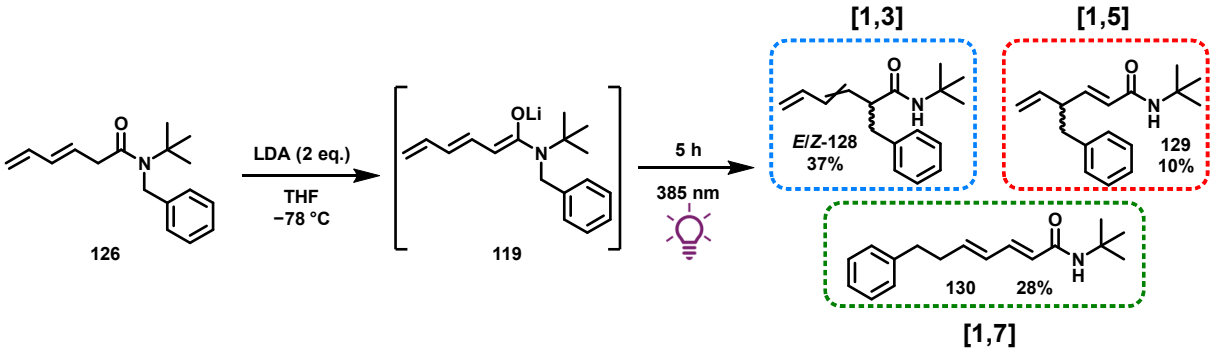

*Scheme 34: Photochemical migration of a benzyl group in enolate **119** to give a mixture of three regioisomers. The yields reported are NMR yields.*

Repeating the deprotonation step under identical conditions, but without irradiation, resulted in the recovery of starting amide **126**, confirming the photochemical nature of the migration. Given that the enolate functionality serves as the chromophore responsible for visible-light absorption, it is likely that varying the substituents on nitrogen would not significantly alter the maximum wavelength of absorbance for the enolate. This flexibility could facilitate a variety of transformations without requiring UV-Vis spectroscopy to determine the absorbance characteristics of each enolate.

Although this specific transformation may have limited synthetic value, the potential to extend the reaction to a broader range of migrating groups could yield a more reliable and predictable process, enhancing its synthetic utility. For instance, if the migration of a chiral α-methyl benzyl group could be achieved stereoselectively, it would allow for the installation of a chiral functional group at a position that would otherwise be challenging to access without the use of chiral auxiliaries or extensive molecular modifications.

4.2. Attempted Asymmetric Benzylic Migration Across an Amide Trienolate

With the understanding that a benzyl group may be necessary for photochemical transformation, we explored the potential of incorporating a chiral benzylic group to facilitate asymmetric migration. Alkenyl amide **132** was synthesised by coupling isomerised sorbic acid **125** with *S*-α-isopropyl-α-methyl benzylamine (**131**), which is the enantiomer of chiral base **49** used in our previously reported photochemical studies, affording desired chiral amide **132** in 53% yield (Scheme 35). When this amide was treated with LDA under the same conditions as amide **126**, a dark green solution formed, as expected. Irradiation of the resulting enolate at 385 nm produced a mixture of [1,3] (***E/Z*-133**), [1,5] (**134**), and [1,7] (**135**)-migration products. The [1,3]-products ***E/Z*-133** were obtained as an inseparable mixture of *E*/*Z* isomers and diastereomers, with an isolated yield of 21%. The [1,5]- and [1,7]-migration products, **134** and **135**, were isolated in yields of 10% (as a diastereomeric mixture) and 20% (as an enantiomeric mixture), respectively. Racemisation occurred during the reaction, leading to a diastereomeric ratio of 26:19:26:29 for the [1,5]-migration product mixture **134** and an enantiomeric ratio of 50:50 for the [1,7]-migration product **135**.

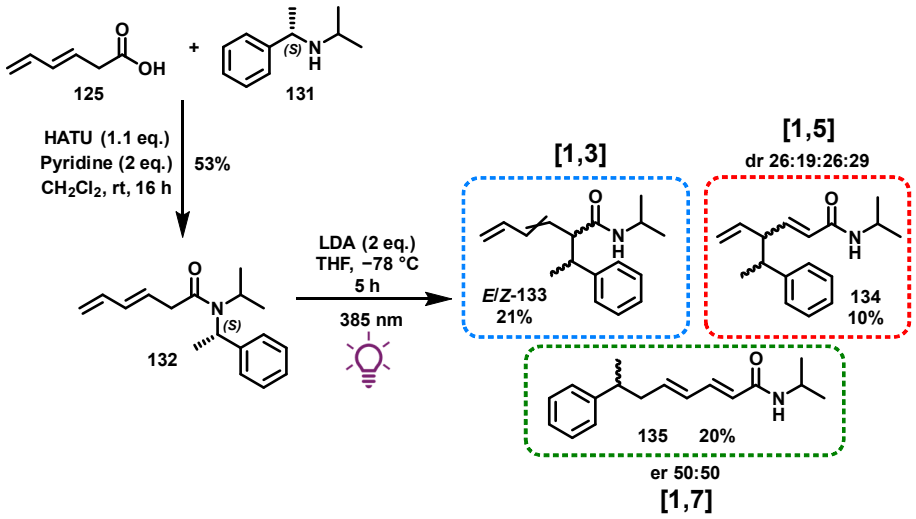

*Scheme 35: Photochemical migration of a chiral benzylamine group in **132** to give a mixture of products, including diastereomers.*

The observed racemisation is likely attributable to the formation of a stabilised benzylic radical following irradiation and excitation (from **136**; Scheme 36). This radical could then recombine with the chromophore in **137**, resulting in the formation of the migration products. However, competitive benzylic deprotonation under the basic conditions of the rearrangement could also play a role in the racemisation process (**138** to **139**). The deprotonated benzyl species may undergo inversion and racemisation, leading to racemic migration products. Furthermore, this potential benzylic

deprotonation could occur in the photochemical products, contributing to racemisation of the substrates after migration.

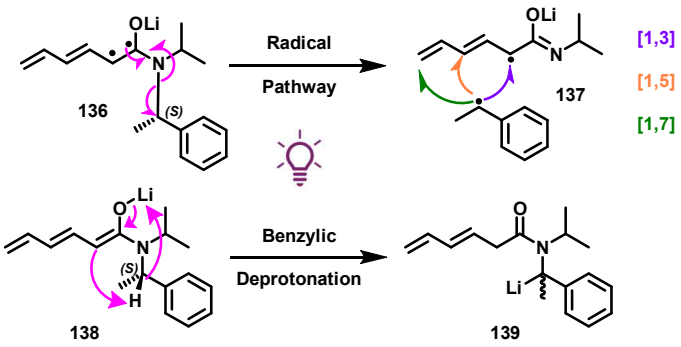

Scheme 36: The two main possible pathways for the photochemistry discussed. Benzylic deprotonation may also be occurring on the photochemical products as well as the starting enolate.

The migration in Scheme 35 also suggests that photochemical migrations of this type do not require substantial steric bulk on the nitrogen, such as that provided by a *tert*-butyl group. Given that the migration of an α-methyl benzyl group in **132** utilised an isopropyl group on nitrogen, the reaction may be compatible with a broader range of alkyl or even unsaturated groups on the amide.

4.3. Benzylic Migration: Radical or Sigmatropic?

4.3.0. Evidence for a Sigmatropic Process

Due to the observed racemisation of the chiral group in dienyl amide **132** during enolate formation and photochemical migration, the focus of this work shifted towards experiments aimed at elucidating whether the reaction mechanism is radical or pericyclic in nature. Experiments were designed to determine the presence of a benzylic radical during the transformation. The first study involved an attempt to trap the potential benzylic radical *in situ* by performing photochemical irradiation of enolate **119** in the presence of two equivalents of TEMPO. The addition of TEMPO, a known radical scavenger, did not inhibit the aryl migration of enolate **119**, suggesting that the reaction mechanism may not involve a free radical intermediate. In a radical pathway, TEMPO would typically trap any radical species, preventing the formation of migration products and potentially resulting in a TEMPO-bound intermediate. The absence of such products and the continued formation of aryl migration products implies a non-radical pathway. However, the potential influence of a solvent shell effect, which could keep reactive radicals in close proximity to their origin molecules and thereby avoid TEMPO trapping, could not be completely ruled out without further research.

To further investigate the photochemical behaviour of acyclic benzylic amide trienolates, a cross-over experiment was conducted using two previously discussed acyclic amides, **126** and **132**. When an equimolar mixture of these amides was subjected to deprotonation and irradiation, two possible outcomes were considered. The first, consistent with an intramolecular sigmatropic rearrangement, would yield products with the same mass as the starting materials, indicating no intermixing of the benzylic groups (Scheme 37). The second, indicative of a radical mechanism, would involve intermolecular reactivity of the benzylic group of one enolate with the conjugated system of the other, resulting in products with different masses. Analysis of the crude mixture by GC-MS revealed multiple clear peaks with an *m/z* of 257, which aligns with the expected outcome for a non-radical, intramolecular sigmatropic process. Notably, no peaks corresponding to benzylic intermolecular cross-over products were detected, further supporting a sigmatropic mechanism. As with the addition of TEMPO, the absence of observed intermolecular reactivity could, however, be attributed to the presence of a solvent shell or cage effect. This effect would promote intramolecular recombination over intermolecular reactions, making recombination within the same molecule more favourable than interactions between different molecules.

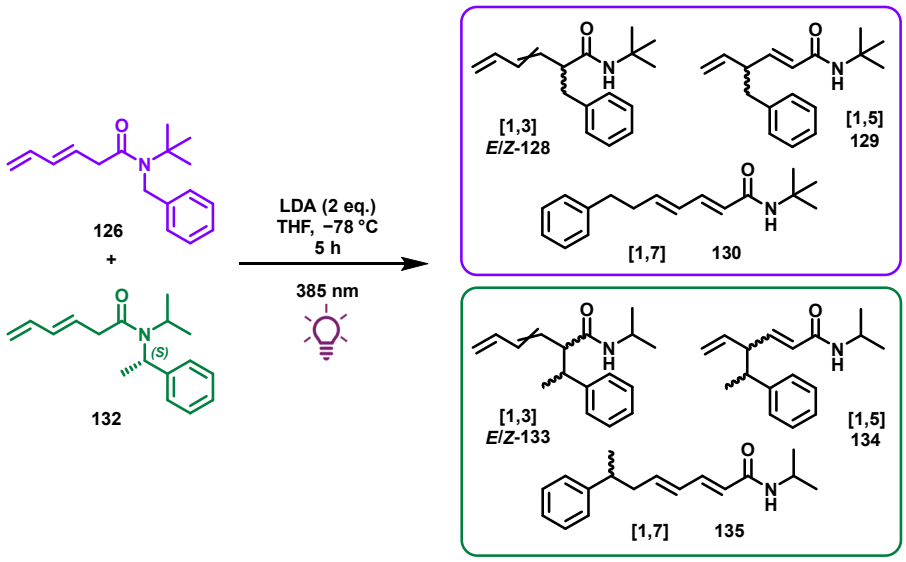

*Scheme 37: The crossover experiment carried out with amides **126** and **132**, with GCMS confirming no products being formed with expected masses from a crossover reaction.*

To further explore the mechanism of this photochemistry, an experiment was conducted using a cyclopropyl benzyl group in amide **145** as the migrating moiety. If a benzylic radical is generated during the process, it could induce the opening of the strained cyclopropyl ring, leading to the formation of an internal propenyl benzyl radical. Radical ring-opening of simple cyclopropyl rings is one of the fastest unimolecular reactions, with a rate constant of 6.1×10^8 s^{-1} at 353 K, making it a valuable

indicator of the nature of this photochemical process.[61] However, in this context, the radical formed from a retro 3-*exo*-*trig* reaction (**141**) is likely *less* stable than the benzyl radical generated via photochemical cleavage (**140**), suggesting that ring-opening might not occur even if a radical is formed adjacent to the cyclopropyl group (Scheme 38).

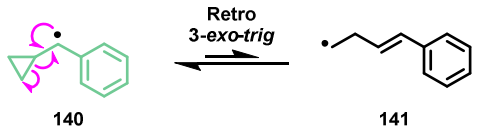

*Scheme 38: The theorised intramolecular radical ring-opening of **140** during photochemical migration.*

The reaction of cyclopropyl phenyl ketone (**142**) with isopropylamine via reductive amination afforded the desired amine **143** in 88% yield. Subsequent coupling with isomerised sorbic chloride **144** produced the desired cyclopropyl benzyl amide **145** in 42% yield (Scheme 39).

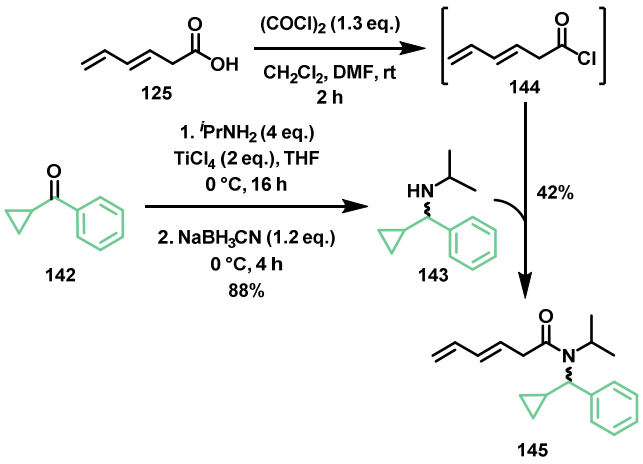

*Scheme 39: Formation of a cyclopropyl benzyl amide **145** through reductive amination onto cyclopropyl ketone (**142**) followed by addition-elimination with isomerised sorbic chloride **144**.*

Photochemical irradiation of the enolate of amide **145** demonstrated that the reaction proceeded as standard, with the cyclopropyl benzyl group migrating successfully across the chromophore (Scheme 40). This resulted in the formation of ***E*/*Z*-146** in an 8% isolated yield, **147** in a 9% yield, and **148** in a 21% yield. Notably, the regioselectivity of this reaction appears to favour [1,7] product **148**, which may be attributed to the increased steric hindrance of the cyclopropyl ring. This steric effect likely promotes the formation of the product with the least steric congestion in this case.

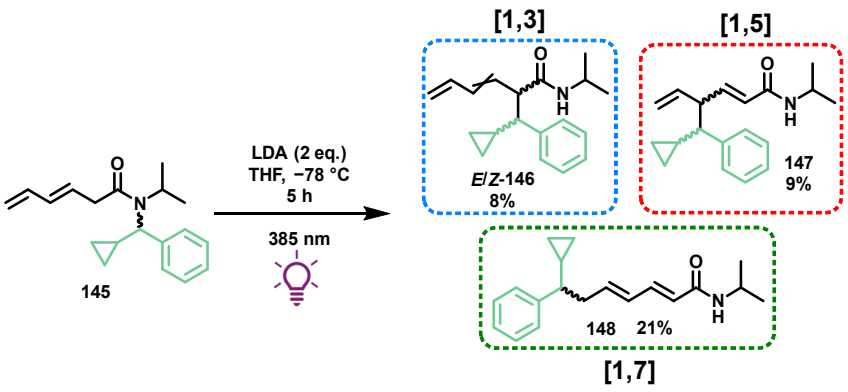

*Scheme 40: The migration of a cyclopropyl benzyl group in **145**, without ring-opening of the cyclopropyl moiety.*

In addition to the intramolecular radical-trapping experiment, another study investigated the potential for a 5-*exo-trig* cyclisation to form a five-membered ring (Scheme 41). However, similar to with cyclopropyl radical **140**, the initial benzylic radical **149** in this process is likely more stabilised than the resulting ring-closed radical **150**, potentially making cyclisation less favourable.

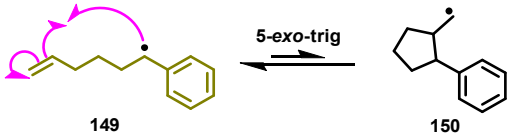

*Scheme 41: The theorised intramolecular 5-exo-trig cyclisation of radical **149** during photochemical migration.*

Amide **155** was synthesised via a nucleophilic addition-elimination reaction of pent-4-en-1-yl-magnesium bromide (**151**) with benzoyl chloride (**152**), affording corresponding ketone **153** in 73% yield (Scheme 42). The ketone was subsequently subjected to reductive amination with isopropylamine, producing amine **154** in good yield. This was followed by coupling with isomerised sorbic chloride **144**, yielding dienyl amide **155** in 17%.

Photochemical irradiation on the enolate of amide **155** resulted in the formation of the seven migration products (**156, 157 and 158**), including diastereomers, without any evidence of radical ring-closure. Consistent with other bulky substituents, the major regioisomer observed was the [1,7]-migration product (**158**). In addition, the [1,3]-migration products **156** were present as their *E*-isomer without any observable *Z*-isomer present. This most likely arises from the bulky migrating group enhancing preference for the *E*-isomer in **156**.

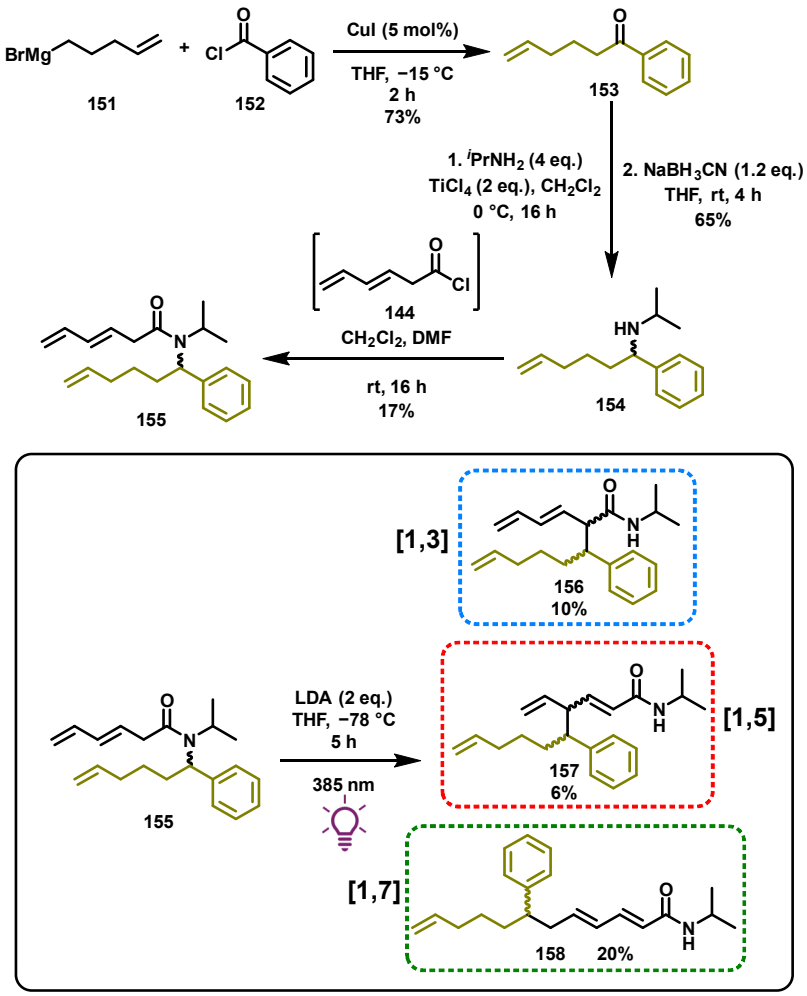

*Scheme 42: The synthesis of amide **155** and its photochemistry, showing that radical ring-closure did not occur.*

4.3.1. Evidence for a Radical Process

Thus far, this chemistry has focused on the migration of radical-stabilising benzylic groups. If the process were sigmatropic in nature, one might expect a non-radical stabilising substituent to migrate across the chromophore in a similar manner. To test this hypothesis, we investigated the photochemical behaviour of methyl- and isopropyl-capped amides **159** and **160**, synthesised using the same approach as amide **126** (Scheme 43). When these amides were independently subjected to deprotonation and irradiation at 385 nm, no photochemical reaction was observed. The product mixtures contained only the starting amide **159** or **160** and their *E*/*Z* stereoisomer.

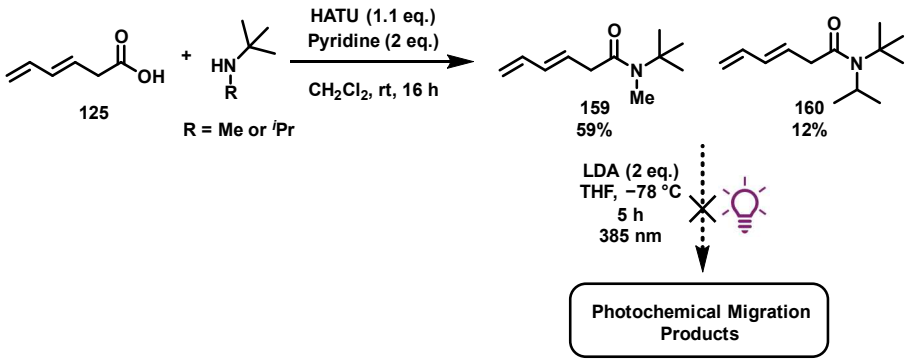

*Scheme 43: The synthesis of amides **159** and **160**, without a benzyl group. Migration of these* N*-centred groups was not observed on irradiation of the enolates of **159** and **160**.*

Similarly, a non-alkyl substituent was synthesised for investigation. *N*-Isopropyl-*N*-phenylhexa-3,5-dienamide **162** was prepared via *in situ* formation of sorbic chloride **144**, followed by reaction with *N*-isopropylaniline **161**, yielding the desired aryl-capped amide product **162** in moderate yield (Scheme 44). When amide **162** was subjected to the standard deprotonation and irradiation conditions, it again showed no desired photochemical reactivity and only starting material and its stereoisomer remained.

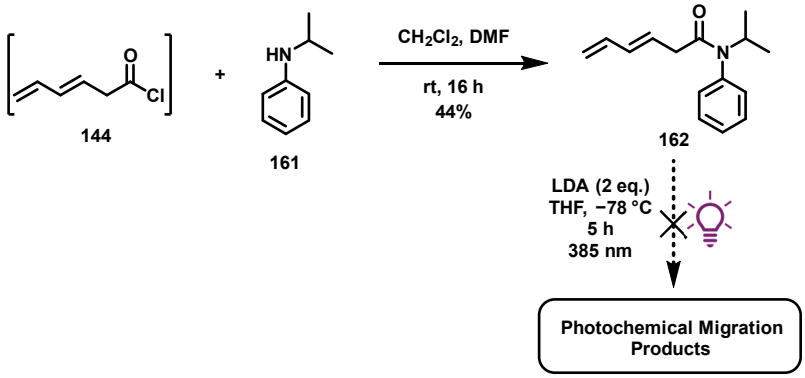

Scheme 44: Formation of N*-isopropyl-*N*-phenylhexa-3,5-dienamide **162** from* in situ *formation of sorbic chloride **144**, and then subjection to the standard photochemical conditions.*

The lack of photochemical reactivity observed with this substrate likely arises from the absence of a radical-stabilising group on the migrating substituent, suggesting that a potential migrating radical cannot form without sufficient stabilisation. Notably, TDDFT calculations for these proposed alkyl-migrating enolates are similar to those for benzyl or allyl groups, indicating that the chosen irradiation wavelength should still be optimal for inducing migration.

To ascertain whether the racemisation observed on substrate **132** is a result of benzylic radical formation or deprotonation-induced racemisation, we commenced the synthesis of substrate **168** (Scheme 45). If a radical is not involved, the quaternary centre in amide **168** could migrate

stereospecifically without undergoing rapid inversion and racemisation. The procedure began with the nucleophilic addition of chiral amine **H-49** to 4-chlorophenyl isocyanate (**163**), affording urea **164** in 81% yield. The free nitrogen was subsequently methylated using sodium hydride and methyl iodide, resulting in protected urea **165** in quantitative yield. Subjecting this urea to asymmetric aryl migration with ^{s}BuLi generated a new quaternary stereogenic centre in **166** in 53% yield, with an enantiomeric ratio of 75:25.[62] Urea hydrolysis of **166** then afforded amine **167** in 73% yield.

Numerous attempts to couple amine **167** with acid **125**, employing reagents such as HATU, DCC, DIC, and oxalyl chloride, were unsuccessful, predominantly recovering starting amine **167**. This outcome may be attributed to the steric hindrance of the bulky amine, rendering it reluctant to coupling. Consequently, an alternative strategy was pursued to synthesise a quaternary migrating group without two adjacent phenyl groups.

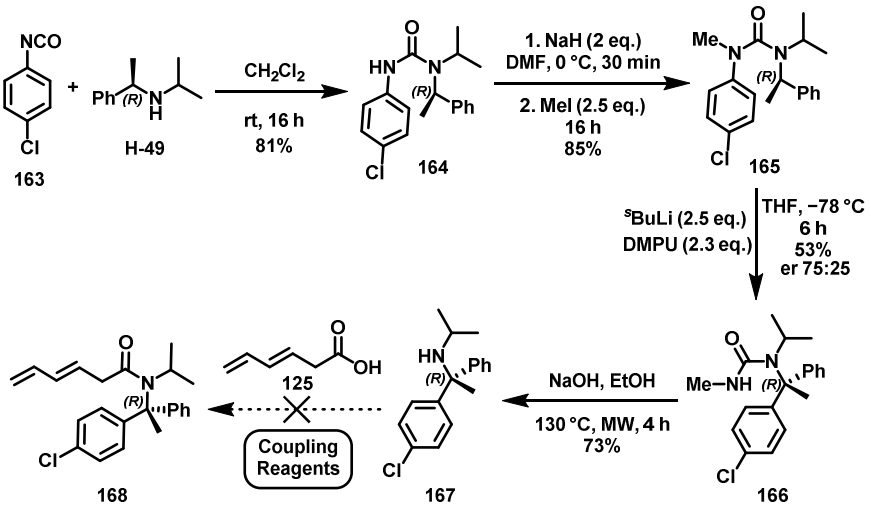

*Scheme 45: The route towards tetrasubstituted chiral amide **168** using asymmetric aryl migration chemistry developed in the Clayden group [62]*

The synthetic route to such a substrate began with the formation of Ellman imine **171** through the condensation of acetophenone (**169**) with (*S*)-*tert*-butanesulfinamide (**170**) in the presence of Ti(O^{i}Pr)$_4$ (Scheme 46). Subsequent diastereoselective addition of ^{n}BuLi to imine **171** afforded **172** as a single diastereomer, as confirmed by NMR analysis. According to literature precedent, the major stereoisomer formed from nucleophilic addition is expected to possess *R*-stereochemistry at the quaternary centre.[63,64] The sulfinyl auxiliary was then cleaved using HCl in dioxane to yield primary amine **173**, followed by installation of the isopropyl group via reductive amination, resulting in **174** in 73% yield. The final synthetic step involved a HATU-mediated coupling reaction to install the chromophore. This step, typically characterised by low yield, resulted in a final enantiomeric ratio of 95:5 for amide **175**.

The photochemical reaction on the enolate of amide **175** was carried out with limited success. Unlike previous examples, the resulting product mixture was messy and complex; however, some of the [1,7]-migration product **176** was successfully isolated. This substrate was found to have racemised during migration (with an enantiomeric ratio of 51:49), further supporting the involvement of a benzylic radical as an intermediate in this photochemical process.

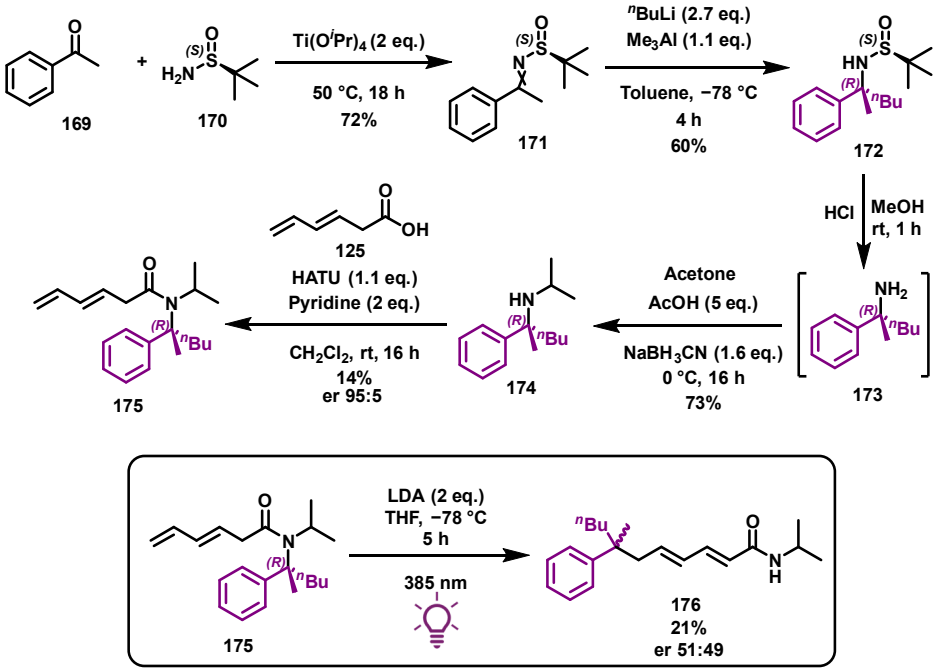

*Scheme 46: The Ellman auxiliary route towards the quaternary migrating group in **175**, and photochemistry on its enolate.*

Additional evidence supporting a radical mechanism was obtained by investigating the migration of a benzylic cyclopropyl group in amide **181**, which would produce a stabilised radical upon ring-opening (Scheme 47). The lack of observable ring-opening during the migration of the benzyl cyclopropyl group in amide **145** may be attributed to the stabilisation of the initial benzylic radical, whereas the product radical formed by ring-opening lacks such stabilisation (i.e. has no adjacent benzylic group). This experiment aimed to determine whether this factor accounts for the absence of ring-opening in the cyclopropyl dienyl amide **145**, assuming the mechanism is indeed radical-based.

The synthesis of amide **181** commenced with the cyclopropanation of *trans*-chalcone (**177**) using trimethylsulfoxonium iodide (**178**), yielding the *trans*-stereoisomer of **179** stereospecifically in moderate yield.[65] Subsequent reductive amination with isopropylamine and $TiCl_4$ afforded amine **180** as a mixture of two pairs of diastereomers (with a diastereomeric ratio of 58:42) in high yield. A final HATU coupling reaction with isomerised sorbic acid **125** yielded the desired amide **181**, again as a pair of diastereomers with a diastereomeric ratio of 50:50 after purification. Due to the inability to achieve

chromatographic separation of these diastereomers, the mixture was used in the photochemical step without achieving diastereopurity. Upon performing the photochemical reaction under standard conditions, notable colour changes were observed, with the mixture transitioning from dark green to dark sapphire blue, indicating enolate reactivity. The resulting reaction mixture was complex, as expected from a diastereomerically diverse starting material, but a significant major product was identified. Isolation of this compound revealed that the cyclopropyl ring in **181** had undergone ring-opening (**182** to **183**), before radical recombination occurred between alkenyl substituent **183** and enolate chromophore **184** via a [1,7]-type migration to afford **185**. This provides compelling evidence for the presence of a radical intermediate in this photochemical process. Thus, based on the balance of available evidence, it is likely that the enolate photochemistry discussed thus far proceeds through a radical-based pathway following excitation.

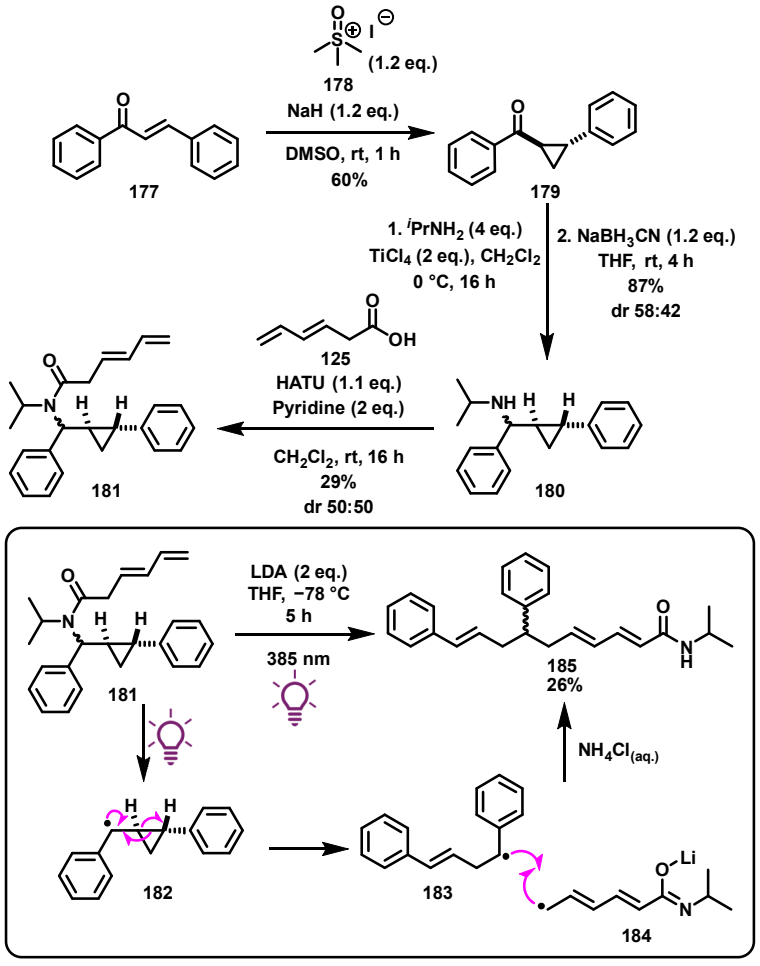

*Scheme 47: The synthesis of cyclopropyl benzyl amide **181** and the ring-opening photochemistry that followed.*

4.3.2. Summary of Mechanistic Studies

While evidence has been gathered which supports both a sigmatropic and radical mechanism, the cumulative analysis indicates a greater likelihood that this photochemical transformation proceeds via a radical pathway. Notably, the racemisation of a quaternary migrating centre in amide **132** and the ring-opening observed in the cyclopropyl benzyl substrate **181** provide strong evidence for the involvement of a benzylic radical intermediate.

The evidence previously favouring a concerted sigmatropic pathway can be rationalised by invoking a solvent cage or shell as part of the mechanism. The absence of TEMPO trapping and the lack of substrate cross-over during photochemical reactivity on the enolates of both amides **126** and **132** could be explained by the benzyl radical being retained in proximity to the molecule from which it was cleaved, within a solvent shell. This close association would promote intramolecular recombination before any intermolecular processes could occur. Furthermore, the lack of substrate cross-over could be attributed to the relatively low competitiveness of cross-over reactions compared to unwanted radical polymerisation or radical recombination following benzylic cleavage.

The absence of intramolecular ring-opening or cyclisation from the intermediate radical in the cases of amides **145** and **155** can be explained by considering the relative stability of the product radicals (from ring-closing or opening, **141** and **150**) compared to the benzylic radicals initially formed (**140** and **149**) (Scheme 48). If the newly formed radical would be less stable than the starting radical, intramolecular ring-opening or ring-closing transformations are unlikely to occur to any significant extent before radical recombination, resulting in the expected photochemical products.

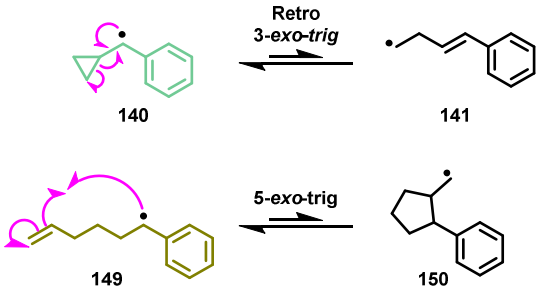

*Scheme 48: The theorised intramolecular radical reactions not observed during photochemical migration, likely due to enhanced stability of starting radicals **140** and **149**.*

4.4. Scope of *N*-Protecting Group

When the Clayden group first reported the formation of cycloheptatrienes from benzyl benzamides, the only substituents on nitrogen that facilitated this transformation were *tert*-butyl and isopropyl groups. This specificity arises from the conformational requirement for the organolithium intermediate, formed upon deprotonation, to be positioned at an optimal angle to attack the aromatic ring during the cyclisation step. Less sterically bulky substituents on nitrogen significantly reduce the efficiency of this step, likely due to an inability to maintain the necessary alignment for effective intramolecular attack.[30]

In the photochemical studies of acyclic *N*-benzyl amide trienolates, these substrates do not require a cyclisation step prior to photochemical activation. Consequently, it may be possible to modify the non-migrating substituent on the amidyl nitrogen without influencing the reaction outcome. To investigate this, a series of substrates with varying nitrogen substituents were synthesised using standard HATU coupling conditions, or oxalyl chloride in the case of *N*-allyl-*N*-benzyl amide **186**, yielding the desired amides **186**, **187** and **188** in moderate yields (Scheme 49).

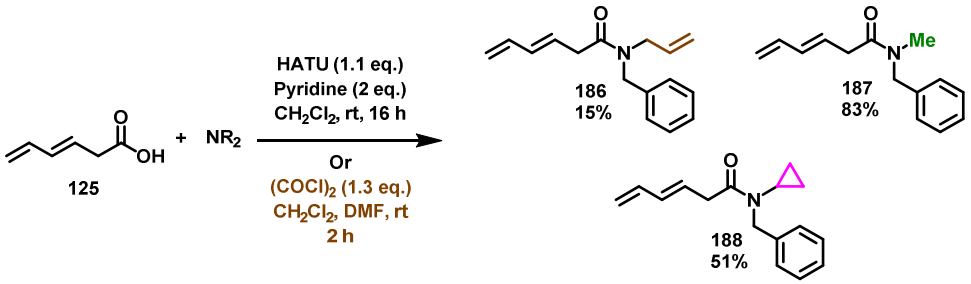

*Scheme 49: The synthesis of amides **186**, **187** and **188** with varying nitrogen capping groups.*

Photochemical benzyl migration was subsequently conducted on substrates bearing various nitrogen capping groups, and all afforded the expected regioisomeric products, demonstrating that the group on nitrogen has minimal influence on the reaction outcome (Table 2). Substituents such as *tert*-butyl (**126**), isopropyl (**132**), allyl (**186**), methyl (**187**), and cyclopropyl (**188**) all facilitated successful migration, resulting in secondary amides with the non-benzyl group preserved. In the case of *N*-allyl-*N*-benzyl amide **186**, some allyl migration was observed in the crude NMR spectra, but the benzyl migration products were the predominant species and the only ones isolated and characterised in this study. The only substrate that exhibited incomplete conversion was amide **187**, bearing a methyl protecting group. This may be attributed to a conformational effect, where the methyl group induces a twist in the amide that hinders complete benzylic cleavage, leaving some starting material unreacted.

In all cases, the [1,5]-migration product was the minor regioisomer, likely due to reduced electron density localisation at this position within the chromophore. Notably, substrate **188**, capped with a cyclopropyl group, provided higher yields potentially due to a conformational effect where the cyclopropyl group biases the amide into a geometry that promotes radical cleavage and subsequent radical recombination. However, the overall yields from the photochemical migrations were still lower than desired, likely due to polymerisation of intermediate radicals during the reaction, as suggested by the broad signals observed in the NMR spectra of crude mixtures. Despite these limitations, it is promising that all protecting groups enabled successful photochemical benzylic migration.

Table 2: The photochemical benzylic migration of various amides with different non-migrating nitrogen groups, and the isolated yields for each regioisomer of migration product.

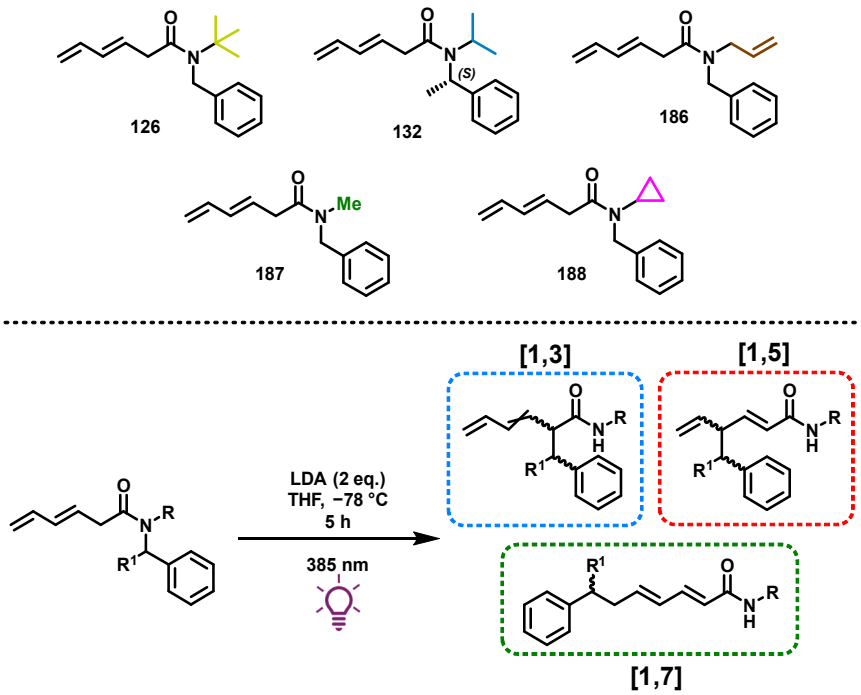

Amide	Starting Material	*Z*-Starting Material	[1,3]-Products	[1,5]-Products	[1,7]-Products
126	-	-	30%	8%	16%
132	-	-	21%	10%	20%
186*	-	-	16%	6%	14%
187	9%	6%	13%	10%	13%
188	-	-	27%	16%	43%

*Allyl, rather than benzylic, migration was also observed, but could not be quantified due to difficulty in purification of the allyl migration isomers. Allyl migration products were only present in minute quantities.

4.5. Scope of Migrating Group

Given that migrating groups which provided no photoreactivity were covered in the mechanistic study in Section 4.3, this section focuses on those that demonstrated successful reactivity. Our investigations indicate that any group can be transferred across the amide via photochemical migration, provided the migrating substituent can stabilise a radical.

We therefore aimed to investigate the tolerance of the photochemistry to variations in radical-stabilising groups for migration. As a result, amine **189**, bearing a diaryl substituent, was synthesised from benzophenone (**19**) through a reductive amination step, followed by conversion to diaryl amide **190** via an oxalyl chloride coupling, giving a yield of 36% (Scheme 50). Meanwhile, allyl amide **192** was prepared directly from *N*-allyl-*N*-*tert*-butylamine (**191**) using oxalyl chloride in 24% yield.

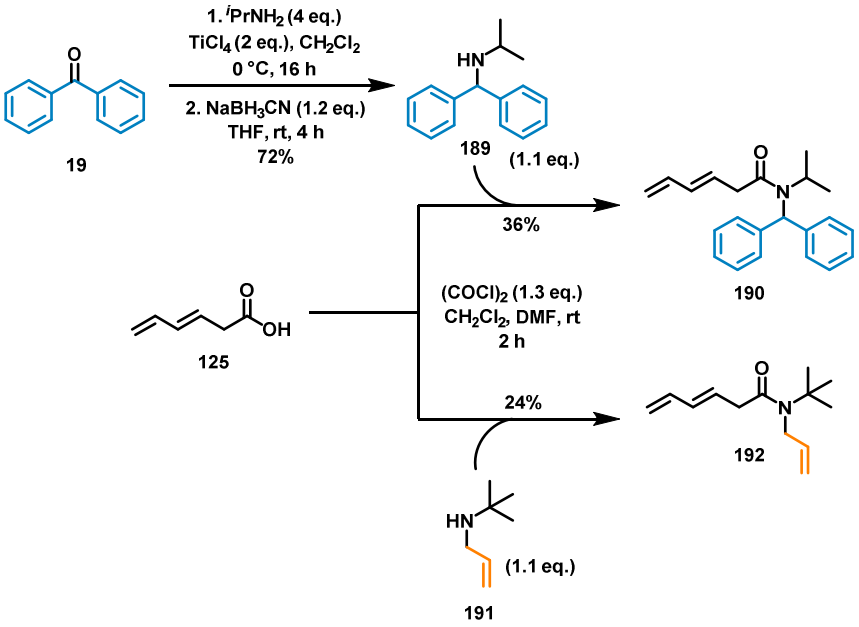

*Scheme 50: The synthesis of diaryl amide **190** from amine **189** and the formation of allyl amide **192**.*

Applying the standard photochemical conditions to dienyl amides **145**, **155**, **175**, **190** and **192**, independently, resulted in the formation of the three photochemical products listed in Table 3. All substrates underwent successful migration, albeit with varying efficiencies. Bulkier migrating groups demonstrated a stronger preference for the formation of the [1,7]-regioisomer over the [1,3]- and [1,5]-isomers. Consistent with prior observations, the [1,5]-regioisomer was typically the minor product. Notably, the migration of an allyl group across the trienolate of amide **192** under photochemical irradiation represents the first instance of a non-benzyl group migrating across the

enolate chromophore in this photochemical system. This result underscores the versatility of the process, with the likelihood of successful migration aligning well with the mechanistic insights previously established.

Table 3: The photochemical benzylic migration of various amides with different migrating groups and the isolated yields for each regioisomer of migration product.

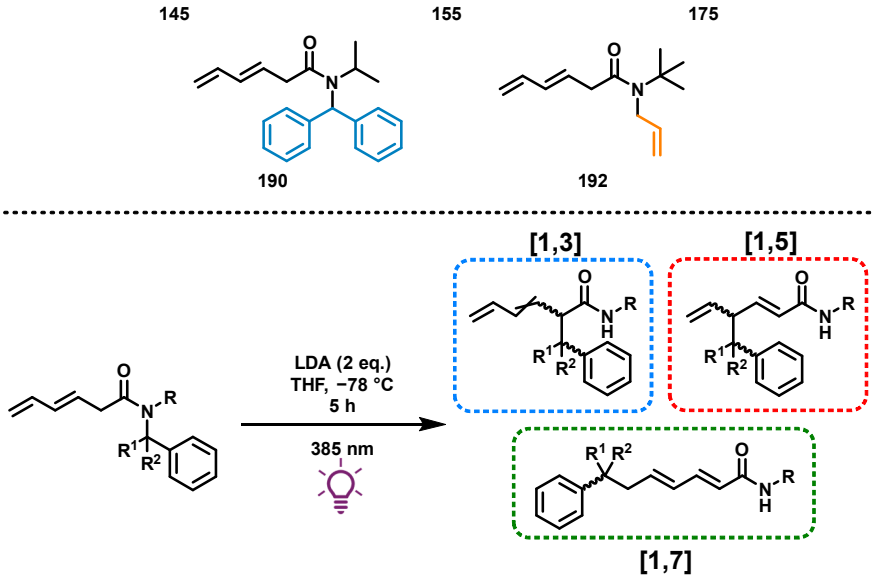

Amide	Starting Material	*Z*-Starting Material	[1,3]-Products	[1,5]-Products	[1,7]-Products
145	-	-	8%	9%	21%
155	-	-	10%	6%	20%
175	-	-	Messy and Complex		21%
190	-	-	7%	29%	
192	-	-	14%	6%	9%

4.6. Benzylic Migration Across an Ester Trienolate

An additional example of photochemical benzylic migration is illustrated by the reaction of conjugated ester **194** under the previously established conditions (Scheme 51). Ester **194** was synthesised via the coupling of isomerised sorbic acid **125** with benzyl alcohol (**193**) in 92% yield. Despite lower yields and a more complex impurity profile, the anticipated photochemical transformation on the trienolate of ester **194** successfully yielded acids ***E/Z*-195**, **196**, and **197**. This reaction marks the first instance of using an ester, rather than an amide, in the photochemistry of lithiated enolates. The [1,3]-product ***E/Z*-195** was isolated in 10% yield, while a chromatographically inseparable mixture of the [1,5]- and [1,7]-migration products was obtained, with the [1,5]-regioisomer **196** being obtained in a 5% yield and the [1,7]-isomer **197** in an 8% yield.

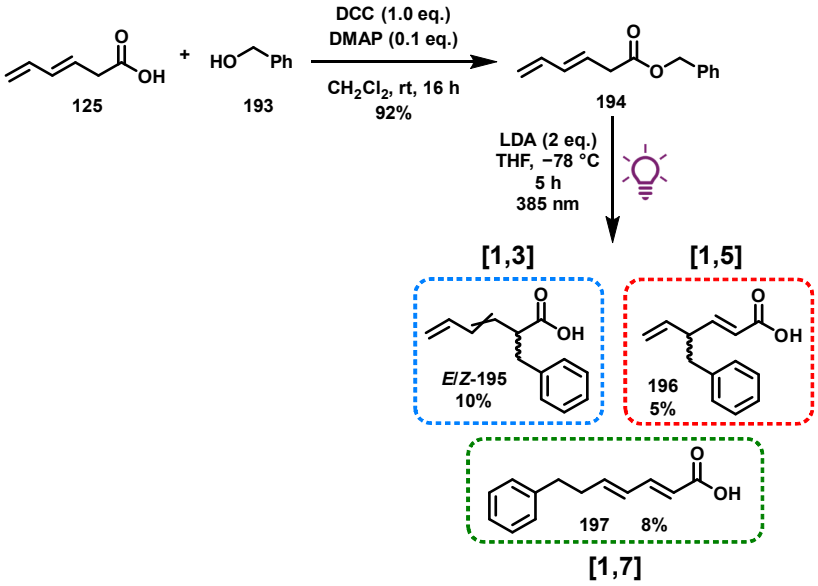

*Scheme 51: The synthesis of benzyl ester **194** followed by photochemical migration across the trienolate.*

4.7. Ring-Expansion by Photochemical Migration

Having established the scope of benzylic migration across an acyclic amide trienolate, we shifted our focus towards leveraging this process for a more distinct and synthetically challenging transformation: a photochemical ring-expansion. We hypothesised that this methodology could be utilised to expand smaller rings into medium-sized ones. To explore this concept, pyrrolidinyl amide **198**, pyrrolo amide **199**, and tetrahydroisoquinoline **200** were synthesised via HATU-mediated coupling, each in high yield (Scheme 52).

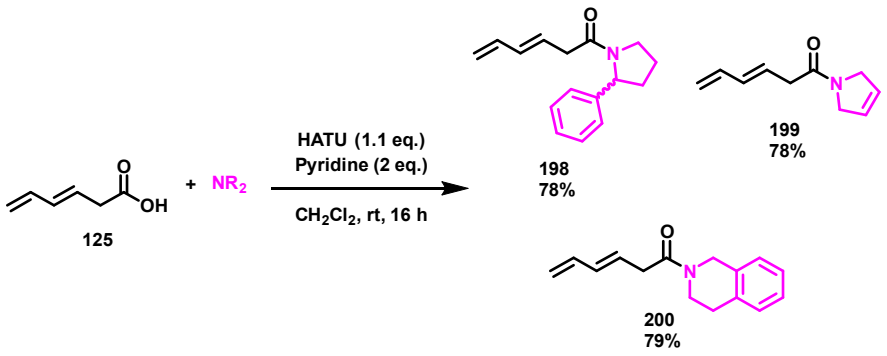

*Scheme 52: The synthesis of pyrrolidinyl amide **198**, pyrrolo amide **199** and tetrahydroisoquinoline **200**.*

Drawing a parallel to the previously discussed benzylic migration across a trienolate, one could anticipate the formation of a benzylic radical adjacent to nitrogen in these enolates (**203** via **202** from trienolate **201**; Scheme 53). This radical could theoretically recombine with the enolate chromophore via a [1,3], [1,5], or [1,7]-recombination, leading to a ring expansion of n+2, n+4, or n+6, where n represents the number of atoms in the original ring. However, the n+6 ([1,7]) migration is likely the least favourable pathway, as it would require the benzylic radical to span the entire molecule, thereby introducing significant strain. Consequently, the most probable outcome of successful photochemical transformation is the n+2 ([1,3])-migration as in secondary ring-expanded amide **204**.

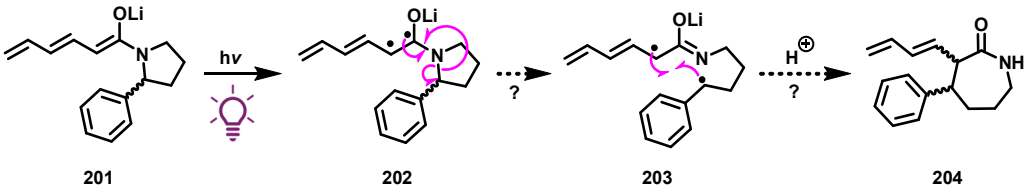

*Scheme 53: The planned mechanism for photochemical ring-expansion of pyrrolidinyl amide trienolate **201**.*

However, irradiation of the trienolates derived from cyclic amides **198**, **199**, and **200** independently at 385 nm did not yield any ring-expansion products. Instead, the crude reaction mixtures consisted only of the starting material and its *Z*-isomer in varying ratios. Initially, this was thought to be due to a conformational twist in these substrates, potentially shifting the enolate's λ_{max} outside the LED emission range. While UV-Vis spectra could not be recorded due to the low stability of these enolates, TDDFT calculations suggested minimal deviation from the λ_{max} of 365 nm reported for acyclic *N*-benzyl amide trienolate **119**. Moreover, the isomerisation observed across all three substrates suggests that the photochemistry was sufficiently exciting the chromophore, generating a diradical along the enolate's conjugated system and resulting in double bond isomerisation upon reformation.

The reason for the lack of successful photochemistry in these cases remains unclear but could be attributed to the benzyl radical recombining with the amide nitrogen atom (via a 5-*exo-trig* as in **203** to **201** and **206** to **205** or a 6-*exo-trig* cyclisation as in **208** to **207**) more rapidly than undergoing the desired ring-expansion process (Scheme 54).[66]

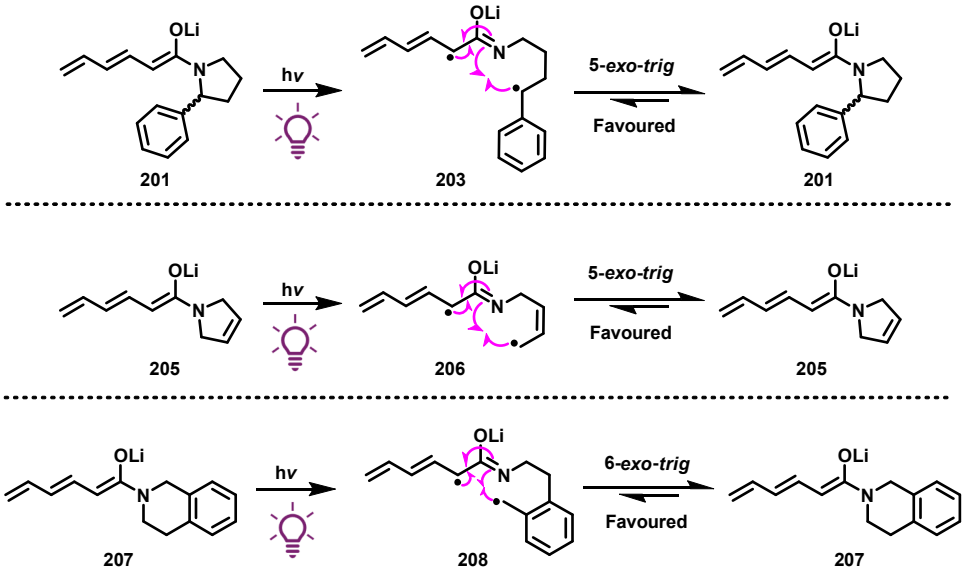

*Scheme 54: The respective cyclisations of photochemical diradical intermediates **203**, **206** and **208**, reforming starting material, with no desired ring-expansion occurring.[66]*

4.8. Acyclic *N*-Benzyl Amide Dienolates

Building upon the photochemistry of trienolate **119**, we investigated reducing the conjugation level within the enolate chromophore to attempt photochemical benzylic migration without the possibility for a [1,7]-transfer. To achieve this, amide **210** was synthesised through a HATU-mediated coupling reaction between trans-2-hexenoic acid (**209**) and amine **121**, yielding 22% of the desired amide (Scheme 55). However, upon treatment with LDA or ^{n}BuLi, it was observed that the base once again engaged in an undesired aza-Michael addition (**211**) on amide **210**, mirroring the reactivity previously seen with diene **123**.

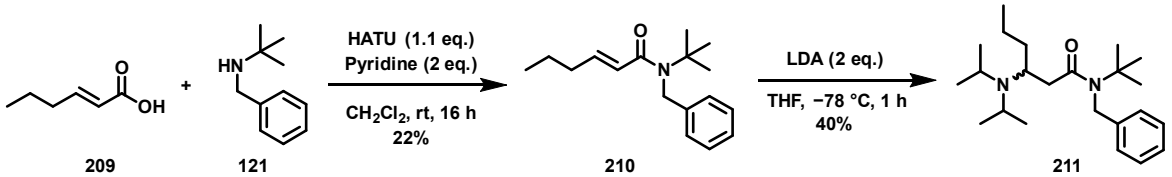

*Scheme 55: The synthesis of conjugated alkenylamide **210** followed by conjugate addition that was observed with LDA to give **211**.*

To address this issue, an isomerised variant of amide **210** was synthesised from trans-3-hexenoic acid (**212**) and amine **121**, resulting in a 26% yield of amide **213** (Scheme 56). This modified alkenyl amide successfully formed the desired enolate upon treatment with LDA, as confirmed by α-deuteration following quenching with deuterated methanol, affording **214**.

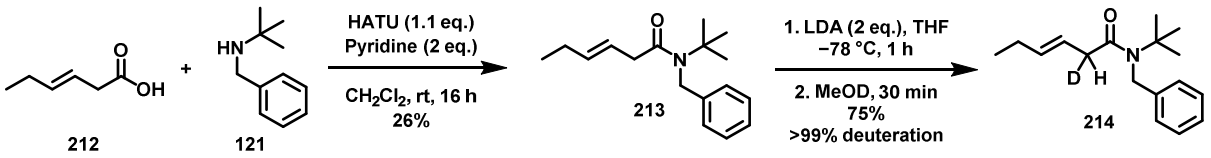

*Scheme 56: Synthesis of unconjugated amide **213** followed by enolate formation and quench at the α-position as in **214**.*

When unconjugated amide **213** was treated with LDA, the resulting colourless solution indicated minimal visible-light absorbance by the corresponding enolate. UV-Vis spectroscopy revealed no peaks in the visible region, confirming that the enolate chromophore in this molecule absorbs below 350 nm. The precise absorbance could not be determined due to interference from UV-absorbing functionalities within the sample mixture or the formation of higher-energy excited states, which dominated the UV-Vis spectra at wavelengths below 350 nm. TDDFT calculations predicted a λ_{max} of 316 nm for this enolate, aligning well with the anticipated absorbance region observed in the UV-Vis spectra.

This absorbance data provided a useful indication that reducing the level of conjugation in this acyclic system from a trienolate to a dienolate decreases the λ_{max} by approximately 50 nm. Although photochemical migration might be feasible with this enolate, the requirement for high-energy irradiation poses limitations on chromoselectivity and has an increased safety risks due to the requirement for UV LEDs. Consequently, further investigations on this enolate were not pursued, allowing focus on other branches of enolate photochemistry that exploit visible-light absorbances.

4.9. Summary of Acyclic Trienolate Photochemistry

This section presents the discovery of a novel transformation involving the photochemical migration of a benzyl group from the amide nitrogen to the enolate chromophore in an acyclic *N*-benzyl amide trienolate upon irradiation. The key findings of this study are as follows:

- Acyclic benzyl amide trienolate **119** shows visible-light absorption within the range of 350-390 nm and irradiation at 385 nm results in the formation of three distinct regioisomeric photochemical products (***E/Z*-128**, **129** and **130**; Scheme 57).

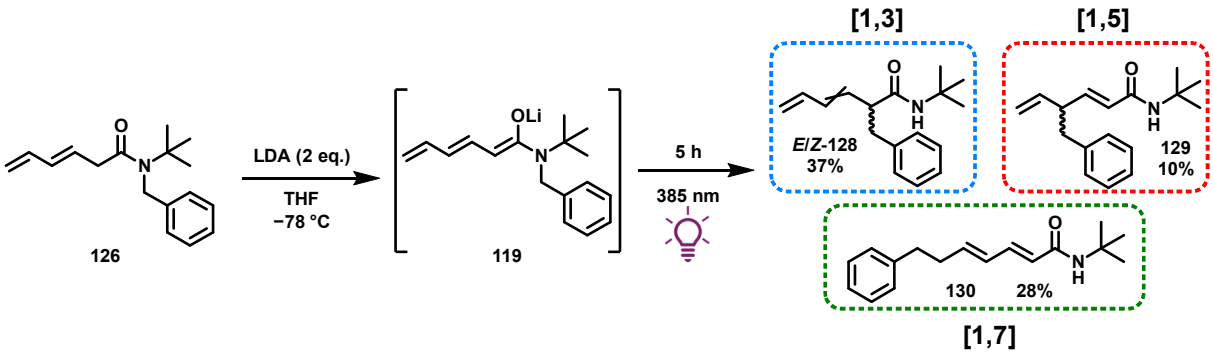

*Scheme 57: Photochemical migration of a benzyl group in enolate (**119**) to give a mixture of three regioisomers. The yields reported are NMR yields.*

- A chiral migrating group, as in amide **132**, undergoes racemisation during the transformation.
- The photochemistry is successful only when there is a radical-stabilising group on the migrating atom.
- The non-migrating group on the amide nitrogen has minimal impact on the success of migration.
- The mechanism for the photochemical migration is likely radical in nature and evidence suggesting otherwise can be rationalised by considering factors such as radical stability during reactivity or the influence of a solvent cage effect, which favours intramolecular over intermolecular recombination.
- Key evidence supporting a radical mechanism includes the observed ring-opening of the benzyl phenyl cyclopropyl group in amide **181** upon photochemical irradiation, followed by radical recombination to form **185** (Scheme 58).

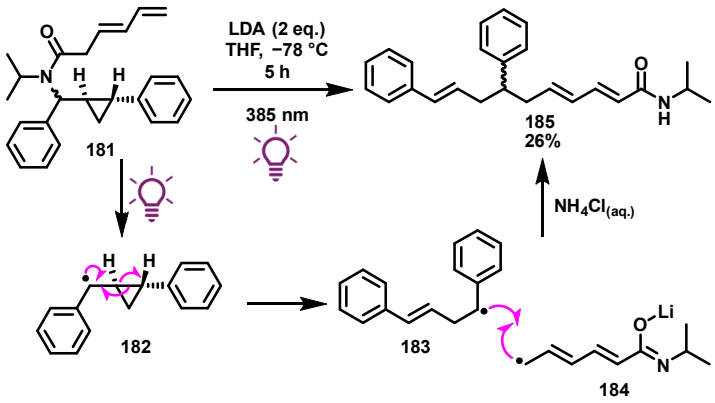

*Scheme 58: The ring-opening photochemistry on benzyl phenyl cyclopropyl amide **181** to afford **185**.*

- This photochemical process was extended to ester **194**; however, the resultant product mixtures were more complex and exhibited lower yields compared to amides.
- Attempts at utilising this transformation to provide a ring-expansion methodology has been unsuccessful, presumably due to preferential cyclisation which returns starting amides **198**, **199** and **200** (Scheme 59). These undesired cyclisations are favoured according to Baldwin's rules.[66]

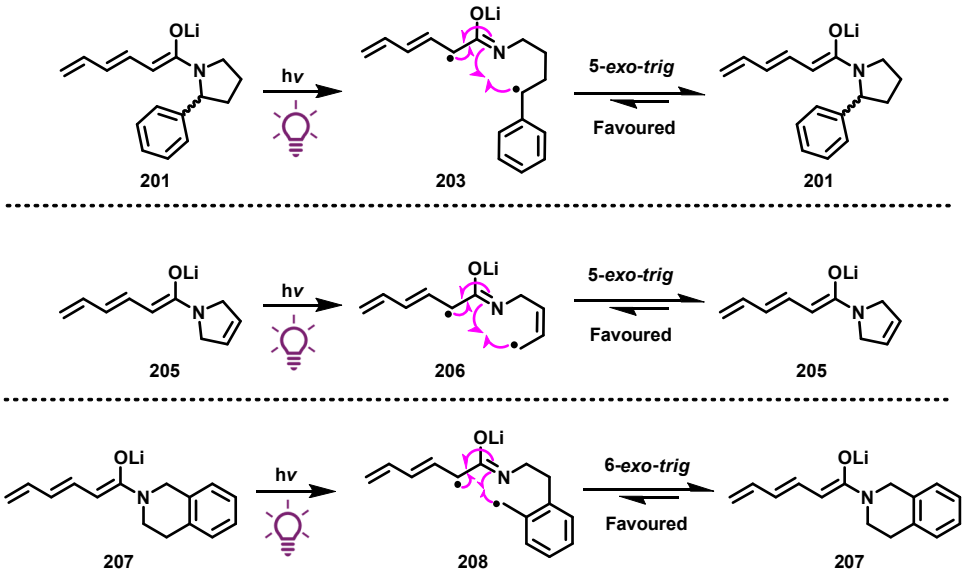

*Scheme 59: The respective cyclisations of photochemical diradical intermediates **203**, **206** and **208**, reforming starting material, with no desired ring-expansion occurring.[66]*

- Acyclic dienolates, such as those derived from alkenyl amide **213** in this study demonstrated high-energy absorbances, making chromoselective irradiation impractical. Consequently, they were not further investigated.

Photochemistry on Lactam-Based Enolates

Building upon the successful benzylic migration observed in the acyclic *N*-benzyl amide trienolate system, we aimed to leverage the underlying mechanism to achieve a distinctive ring-contraction reaction. While in Section 4 the N–C bond cleavage led to the proposed formation of a benzylic radical that migrated through space, our current objective was to retain the benzylic radical within the same molecular framework after its generation. This approach would allow for the radical to recombine intramolecularly, resulting in the formation of a smaller carbon-based ring, contracted by two atoms relative to the original. For this transformation, it is crucial that one of the double bonds in the chromophore is integrated into the cyclic lactam prior to irradiation (Scheme 60). If this process proceeds as anticipated, the enolate of a five-membered lactam, such as **215**, would undergo ring contraction to yield cyclopropyl amide **217** via the diradical intermediate **216**. This transformation would be remarkable, considering it would be achieved from relatively simple starting materials under conditions limited to deprotonation and irradiation.

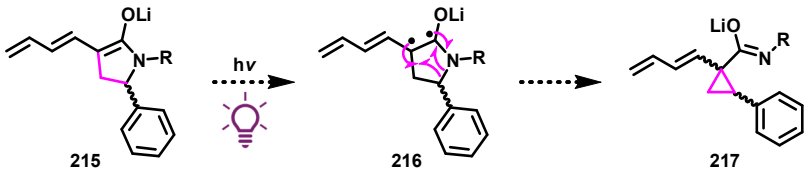

*Scheme 60: The potential mechanism for a photochemical ring-contraction process on trienolate **215**.*

5.0. Cyclopropanes and Their Syntheses

The cyclopropane motif holds substantial significance in drug discovery and development, being the 10th most commonly observed ring system in small-molecule drug targets. Its prevalence is attributed to its ability to enhance potency, provide conformational stability, and improve pharmacokinetics and solubility properties to drug targets.[67–69] Furthermore, cyclopropanes are frequently found in various biologically active natural products.[70] Some examples of cyclopropyl-containing drug targets include GT2331 (**218**) which acts as a histamine antagonist, Pevonedistat (**219**) which is being studied for treatment of leukaemia, UPF-648 (**220**) for the inhibition of the kynurenine pathway and GPR88 (**221**) which has showed promise as a treatment for neurological conditions (Figure 7).[71–74] Note that these examples also contain conjugation, such as unsaturation or a carbonylic group, attached to the cyclopropyl ring, which are similar in structure to potential products from ring-contraction of lactam enolates proposed here.

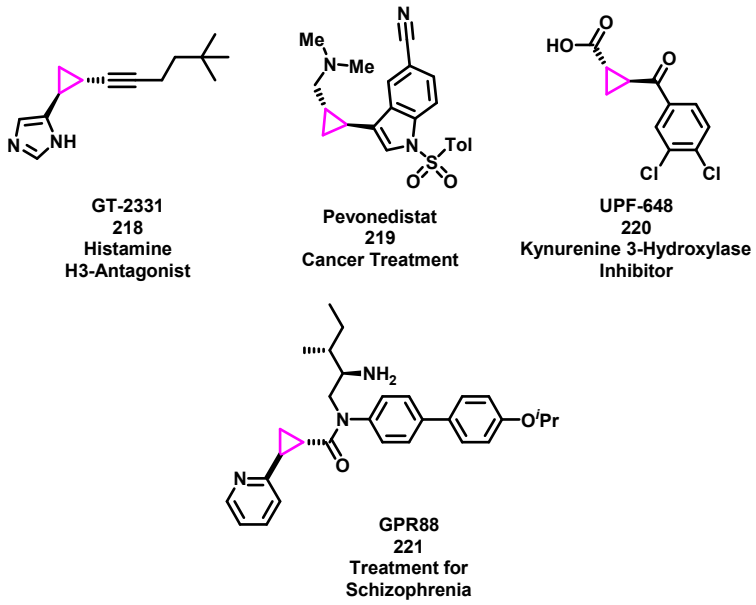

*Figure 7: Examples of substituted cyclopropanes **218-221** in pharmaceutical targets.*[71–74]

Substituted cyclopropanes exhibit a well-defined three-dimensional shape, conformational rigidity, and electronic properties that lie between those of an alkene and a geminal dimethyl group.[75] The theory of σ-aromaticity, which describes the partial delocalisation of the six electrons across the three C–C σ-bonds of the cyclopropane ring, provides insight into the stability and reactivity of these motifs.[76] The distinctive orbital overlap in these structures is frequently referred to as "banana bonds".

These characteristics render cyclopropyl rings as strained and highly reactive motifs, often capable of functioning similarly to π-donors. For instance, Richmond *et al.* have demonstrated the ring-opening hydroarylation of monosubstituted cyclopropanes, such as those bearing an aryl group in **223** to afford **224** (Scheme 61).[77] In this transformation, the cyclopropane ring undergoes an S_N1-type mechanism initiated by acid-induced ring-opening (**226** via **225**), followed by nucleophilic attack by aryl rings **222** to afford diphenyl **224**. This reaction exemplifies the alkene-like electronic properties of cyclopropanes and the strain-release that frequently drives the reactivity of these small rings.

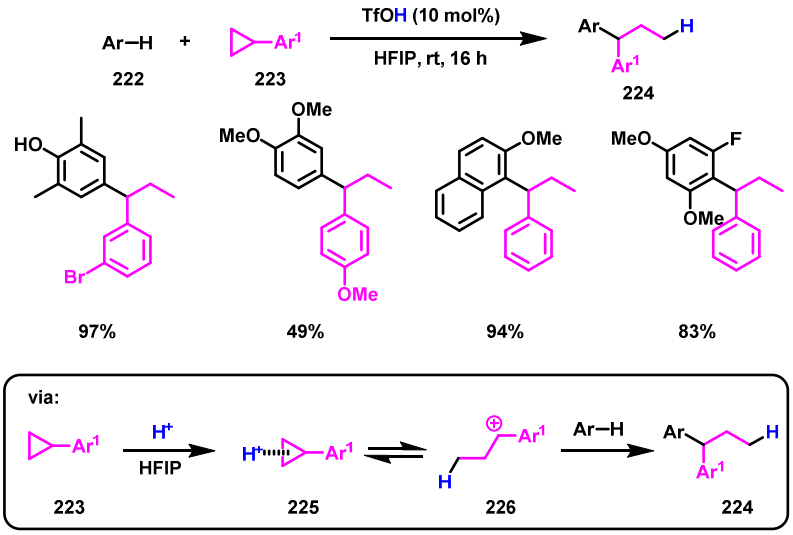

Scheme 61: Hydroarylation of cyclopropanes using acid, showing a few select examples and the proposed mechanism.[77]

The high synthetic utility of such small rings has spurred extensive interest in their synthesis over an extended period. Consequently, various cyclopropanation methods are reported in the literature, with numerous reviews covering these strategies.[78,79] Many of these methods involve the use of expensive or toxic metals, require harsh reaction conditions, proceed via ylide and Lewis acid chemistry, or necessitate electron-deficient alkenes, such as those employed in the Corey-Chaykovsky reaction.[78,80,81] Several examples of synthetic methods for cyclopropanation are illustrated in Scheme 62.

One such method of cyclopropanation is the gold(I)-catalysed oxidative cyclisation used in the total synthesis of (-)-nardoarisolone B.[81] This process involves an external oxidant and proceeds via a reactive gold carbene intermediate generated *in situ* from **227**, affording tricyclic cyclopropane **228**. While this method avoids the need for starting materials containing diazo groups—a common requirement in many substituted cyclopropane syntheses—it is not without its drawbacks, particularly in terms of cost. Moving away from gold catalysis, cyclopropanations can also be achieved through the enantioselective reactivity of unsaturated keto esters **229** and diazoacetates **230** using a Lewis acid catalyst, resulting in remarkably high stereoselectivity for the formation of **231**.[80] However, this approach relies on indium, which poses challenges related to heavy metal availability and cost.

A more environmentally benign approach involves the photochemical generation of a free carbene from diazoacetate **232**, which subsequently adds to allylic alcohol **233**, followed by cyclisation to give **234**. This method's advantage lies in its avoidance of metal catalysts or external oxidants, making it a notable improvement in cyclopropane synthesis. However, it still requires access to suitable starting

diazoacetates, which are often highly toxic and potentially explosive. Thus, a mild synthetic route that circumvents the need for such hazardous reagents is highly desirable.

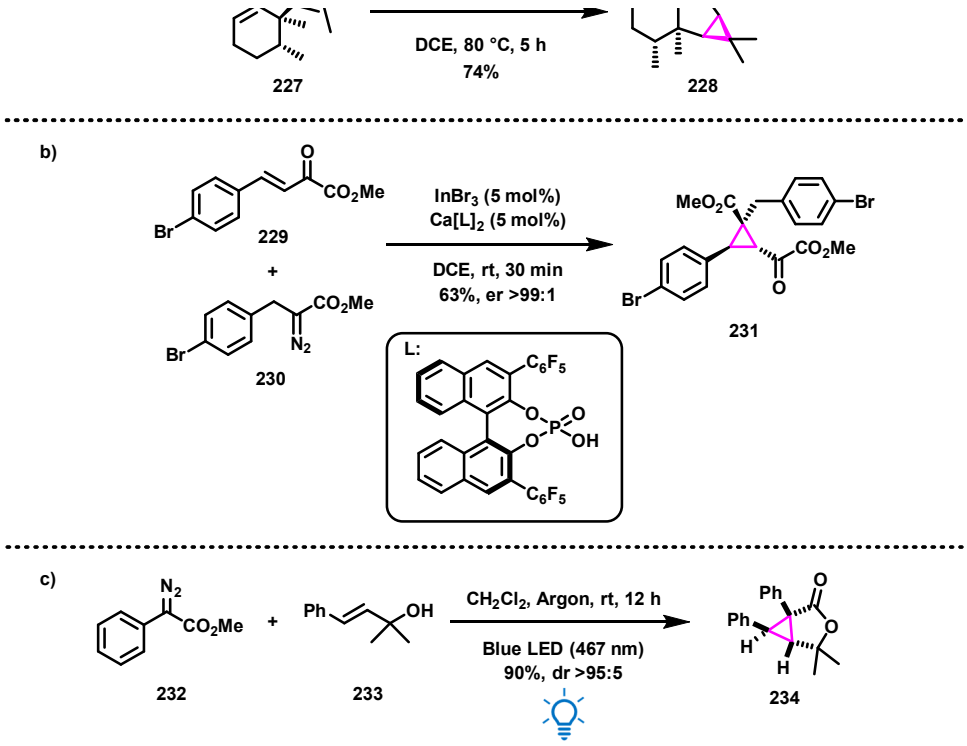

*Scheme 62: a) The gold-catalysed oxidative cyclopropanation to form **228**.[81] Oxidant = 3,5-Dichloropyridine N-oxide. b) The Lewis-acid-mediated stereoselective synthesis of highly substituted cyclopropane **231** from diazoacetate **230** and unsaturated ester **229**.[80] c) Photochemical cyclopropanation through a free carbene, addition and cyclisation to yield **234**.[82]*

We therefore aimed to explore our photochemical strategy, which does not require toxic or expensive starting materials, as a valuable addition to the current methodologies for cyclopropane formation. Previous work by Faye Knowles in the Clayden group in 2005 reported preliminary investigations into the photochemical ring-contraction of lactam enolates.[18] These studies demonstrated that five-membered lactams, bearing electron-rich aromatics at the migration position and protected with either a BOC or benzyl group on the nitrogen, could undergo ring contraction under photochemical irradiation in the absence of an extended chromophore (such as the formation of **236** from **235**; Scheme 63). The highest yield obtained from such a ring contraction was 34% on synthesising **238** from **237**, and the best diastereoselectivity achieved was a 75:25 mixture of *trans*:*cis* isomers. These modest outcomes clearly indicate the potential for optimisation and provide a strong rationale for revisiting and refining this photochemical transformation.

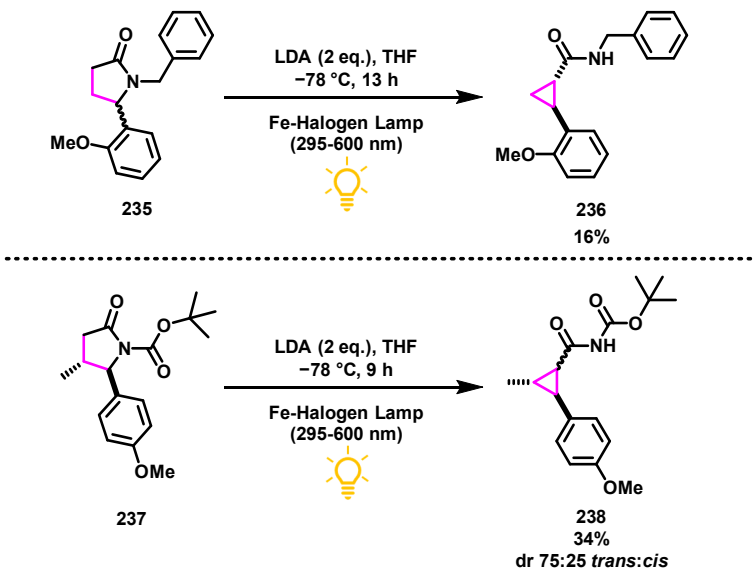

Scheme 63: The photochemical ring-contraction explored using an iron-halogen lamp by Faye Knowles.[18]

During the period in which this research was conducted, modern LEDs were not yet commercially available, and instead, heat-inefficient halogen lamps were employed. These lamps presented challenges due to their broad emission spectra, which made chromoselective irradiation difficult, and provided significant heat emission, which often led to the degradation of enolates and resulted in complex mixtures and low yields of the desired photochemical ring-contraction products. The use of an extended chromophore attached to the lactam also proved unsuccessful, likely due to the degradation of enolate or intermediates in the photochemical pathway.

However, with the advent of more energy-efficient LEDs and an enhanced understanding of the requirements for achieving successful photochemical reactivity, there is now an opportunity to revisit and expand this photochemical methodology. This could allow for a broader range of photochemical migrations with improved diastereoselectivity. To maintain as much similarity as possible to the acyclic *N*-benzyl amide trienolate system, the initial substrate chosen for photochemical investigation was a five-membered lactam trienolate with a phenyl group adjacent to nitrogen. To further ensure consistency with initial photochemical ring-expansion studies performed at the turn of the century, either a *tert*-butyl (^{t}Bu) or isopropyl (^{i}Pr) protecting group on nitrogen was initially planned to be employed.

5.1. Five-Membered Lactam and Lactone Trienolate Ring-Contraction

Interestingly, there is limited literature on the synthesis of simple lactam rings with a phenyl group adjacent to the amide nitrogen. Most examples of substituted lactams describe an ester functional group at this position (often derived from amino acids) or a phenyl ring at the beta position relative to the nitrogen atom.[83–85] There are instances of forming five-membered lactams with nitrogen protecting groups of lower steric bulk (as discussed later), but far fewer examples where bulkier groups such as *tert*-butyl or isopropyl are used on the nitrogen. Therefore, we developed our own synthetic route to these types of lactams. From these lactams, a chromophore can be introduced using aldol chemistry, which could potentially allow for photochemistry similar to that observed in the acyclic systems.

The synthesis of a conjugated lactam bearing *tert*-butyl or isopropyl capping groups began with the methyl esterification of readily available 3-benzoylpropionic acid (**239**), yielding methyl ester **240** in a high yield (Scheme 64). This was followed by reductive amination with *tert*-butyl amine or isopropylamine in the presence of $TiCl_4$ to give amine **242** via intermediate imine **241**. Although various reducing agents and conditions were explored for this step, it was found that isolating the stable imine formed from the condensation of the amine and ketone before subsequent reduction provided the best results. This reaction consistently yielded high results across different substrates, highlighting the effectiveness of $TiCl_4$ as a Lewis acid and directing group.

Following the formation of amine **242**, an intramolecular cyclisation was performed using an excess of DMAP in refluxing DMF over three days to yield lactam **243** in moderate yield. It is important to note that this cyclisation step does not proceed to completion when a *tert*-butyl group is on the nitrogen, presenting a limitation to this route in that case. However, when using an isopropyl group on the nitrogen, desired lactam **243** was obtained in a higher yield (74%), suggesting that the less bulky the nitrogen substituent, the higher the yield of the cyclisation product. This observation aligns with literature findings, which report that similar substrates preferentially cyclise with less bulky nitrogen capping groups.[86] Since it has been demonstrated that the acyclic *N*-benzyl amide photochemical migration is effective with this nitrogen group (Section 4), it was anticipated that this less bulky substituent could facilitate successful photochemistry while increasing the yield of the intramolecular cyclisation.

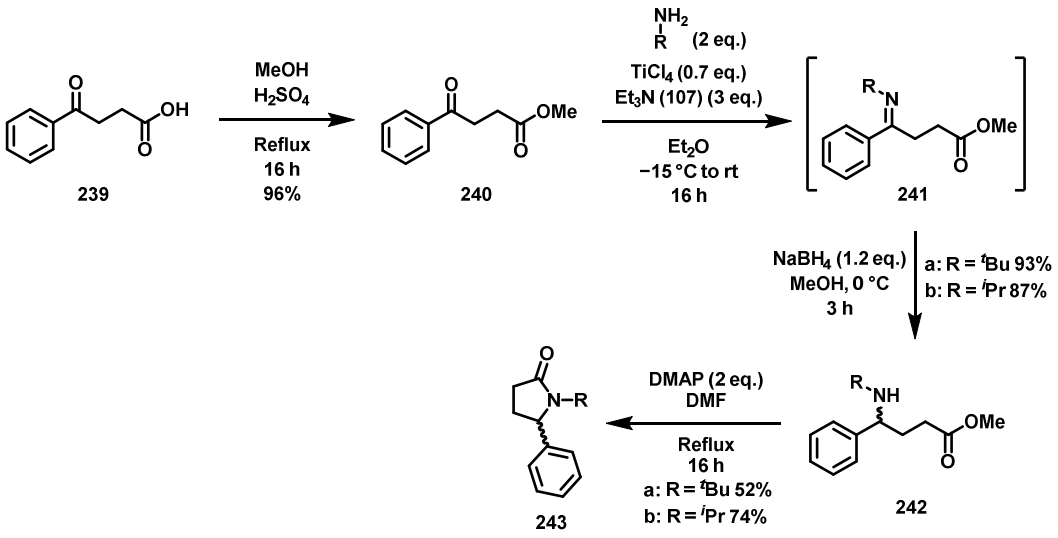

*Scheme 64: The synthesis of benzyl lactam **243** through amine formation and cyclisation.*

The isopropyl-capped lactam **243** was therefore chosen for subsequent reactions. The chromophore was introduced through an aldol addition with crotonaldehyde (**16**) (Scheme 65). A copper- and DCC-mediated elimination then produced a complex mixture of conjugated lactam stereoisomers.[87] Two isomers were isolated and characterised from this mixture: the *Z*,*E*-isomer **245** and the structural isomer **246**, in which the double bonds had shifted to form a terminal diene. The installation of the diene chromophore was low-yielding and difficult to analyse and purify, likely due to the polymerisation of intermediate alcohols or product dienes, and the inherent complexity of the final product mixture with multiple isomers present. This complexity is unavoidable with this particular chromophore, necessitating the consideration of alternative chromophores for the ring-contraction of lactams, as discussed later in this section.

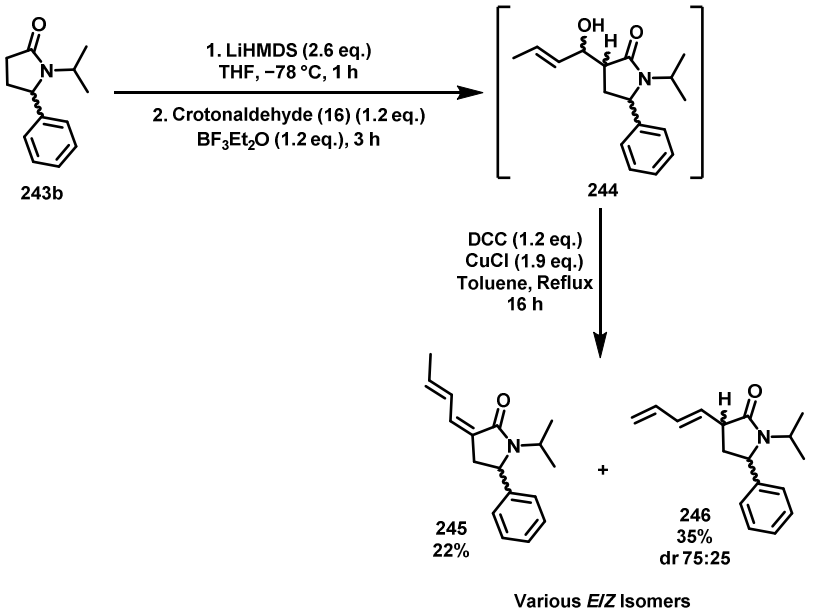

*Scheme 65: The installation of a diene chromophore onto lactam **243**.*

With conjugated lactam **245** available, photochemical experiments were conducted. TDDFT calculations predicted a λ_{max} for the lactam trienolate of **245** very similar to that of the acyclic amide enolates (367 nm compared to 365 nm for acyclic trienolate **119**), hence the same LED (385 nm) was used for irradiation. In all cases of lactam enolate photochemistry discussed here, the enolates are too unstable to record a UV-Vis spectrum due to their sensitivity to elevated temperatures and air exposure.

To avoid unwanted conjugate addition to the chromophore that might occur with less sterically hindered bases, a large excess of LiHMDS, a weaker and sterically bulky base, was employed in the lactam enolate photochemistry. LiHMDS may also facilitate the formation of an enolate mixture under equilibrium conditions, which is then driven to completion by photochemical reactivity. This is analogous to the de Mayo reaction, where an enol in equilibrium is driven to form a 1,5-diketone under photochemical conditions (Section 1.4). Using a large excess of LiHMDS may be shifting the equilibrium towards the enolate form, away from the starting lactam.

Upon irradiation of the enolate formed from the deprotonation of the *Z,E*-isomer of conjugated lactam **245**, a complex mixture of products was generated, complicating purification (Scheme 66). However, a diastereomeric mixture of desired cyclopropyl products **247** were successfully isolated.

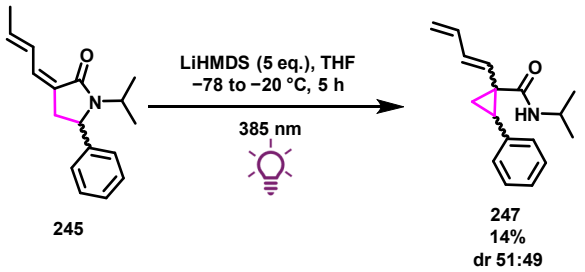

*Scheme 66: The photochemistry on the dienolate of lactam **245**, giving ring-contraction to **247**.*

This result demonstrates the potential of applying our acyclic photochemistry strategy to a cyclic ring-contraction via deprotonation and irradiation, albeit with low yields most likely arising from polymerisation of intermediates or starting diene/enolate.

Building on the ring-contraction photochemistry of the five-membered ring, a logical next step was to attempt a similar contraction on a lactone precursor. Desired lactone **248** was synthesised via a reductive method reported by Clerici et al., using acidic $TiCl_3$ and ammonia with 3-benzoylpropionic acid (**239**) (Scheme 67).[88] This approach yielded lactone **248** in high yield, which was then functionalised to install the target diene chromophore, producing compounds **250** and **251** via **249**.

However, NOE data was inconclusive for isomer stereochemical determination, preventing definitive structural assignment. Aside from indicating that each isomer contained a trans double bond, NMR analysis could not provide full stereochemical details. Although it is not vital to determine stereochemistry of starting dienyl substrates in this study (since they all form the same enolate on deprotonation), these substrates may give insight into the ability for machine learning methods to accurately predict alkene isomers from NMR data. Consequently, a machine learning algorithm was employed to predict NMR spectra for the two possible dienyl lactones. Using the IMPRESSION tool, developed by members of the Butts group in Bristol, chemical shifts were predicted for the alkene region in both the *Z*,*E* and *E*,*E* isomers of the lactone products **250** and **251**.[89]

The results were compelling: the alkene signals for both isolated compounds matched one of the predicted spectra with high accuracy, enabling assignment of the isolated isomers. The first isolated isomer was identified as the *Z*,*E* isomer **250** with an 11% yield, while the second was determined to be the *E*,*E* isomer **251** with a 19% yield. As shown in Figure 8, the NMR shifts of unknown isomer 1 closely matched the predicted data for *Z*,*E* isomer **250**, whereas those of unknown isomer 2 aligned with the predicted data for *E*,*E* isomer **251**.

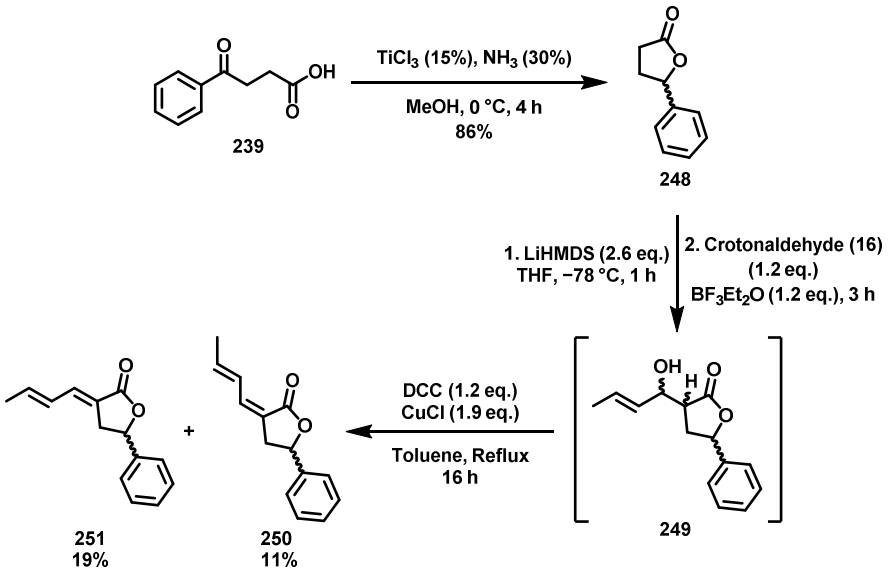

*Scheme 67: The synthesis of lactones **250** and **251**.*

With the stereochemistry confirmed, photochemical experiments were conducted on the *E*,*E* isomer **251** using the same conditions as for the earlier lactam ring-contraction. The reaction proceeded remarkably cleanly, yielding a single compound. However, this was not the expected ring-contraction product. Instead, mass spectrometry data (*m*/*z* = 540) suggested an intermolecular addition reaction had occurred between two lactone molecules. The exact structure of this product could not be elucidated from the NMR and other spectroscopic data.

The formation of this compound was also observed in the absence of light, indicating that it likely arises from a simple nucleophilic addition of an enolate to a neutral lactone, resulting in ring opening. Neither direct addition of the substrate to the base nor slow addition via a syringe pump altered this reactivity. In all cases, the only product obtained was the potential intermolecular addition compound. Consequently, further photochemical studies on the lactone system were discontinued.

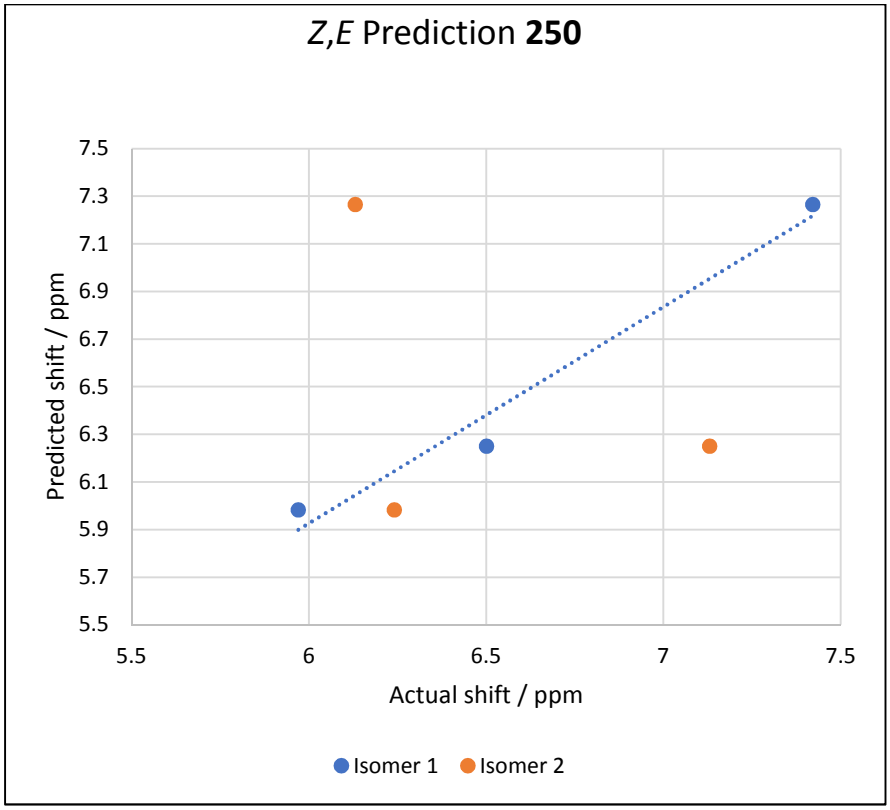

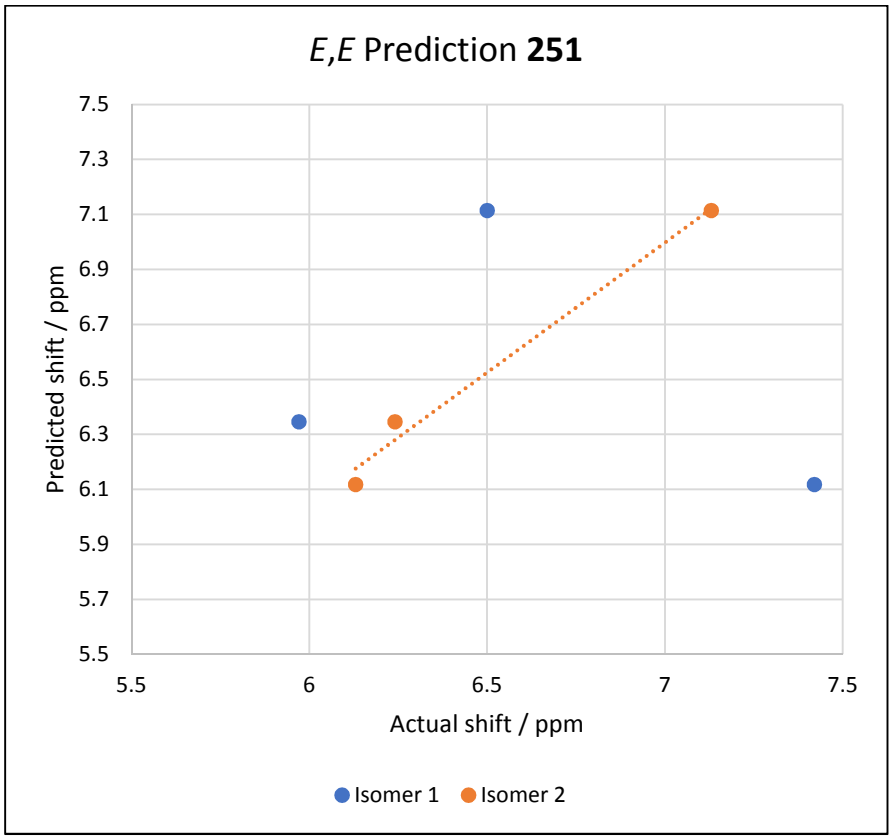

*Figure 8: The Machine Learning data for the alkene region of lactone isomers **250** and **251**, with a clear agreement between "Isomer 1" and the E/Z prediction, and between "Isomer 2" and the E/E prediction.*

5.2. Five-Membered Lactam Monoenolate Ring-Contraction

Until now, we have demonstrated enolate photochemistry primarily with enolates containing extended chromophores, such as trienolates. Given our successful ring contraction of a five-membered lactam trienolate, we sought to explore the limitations of this technique. In this section, we present the ring contraction of a mono-enolate lacking an extended chromophore.

To simplify the synthesis of starting materials, we used a modified, microwave-assisted procedure by Li *et al.*,[90] where formamide derivatives react with keto-acids such as **239** in a single step under microwave irradiation and pressure (Scheme 68). Although this method has been reported for various substrates, it had not yet been applied to obtain lactam **254** from *N*-methyl formamide **255**. This modification required harsher temperatures and longer reaction times compared to those reported, but it successfully produced target lactam **254** from 4-oxo-4-phenylbutanoic acid (**239**) in good yield in a single step. As discussed in Section 4, the choice of nitrogen protecting group had minimal impact on the success of the photochemistry. Therefore, methyl was chosen over bulkier groups, since it can be directly introduced during this cyclisation.

The proposed mechanism for lactam formation involves the equilibration of *N*-methyl formamide **255** with water to generate methylamine **256** and formic acid **257**. Methylamine **256** then reacts with keto acid **239** to form imine **252**, which is subsequently reduced by formic acid **257**. Finally, spontaneous cyclisation of secondary amine **253** under pressure yields lactam **254**.

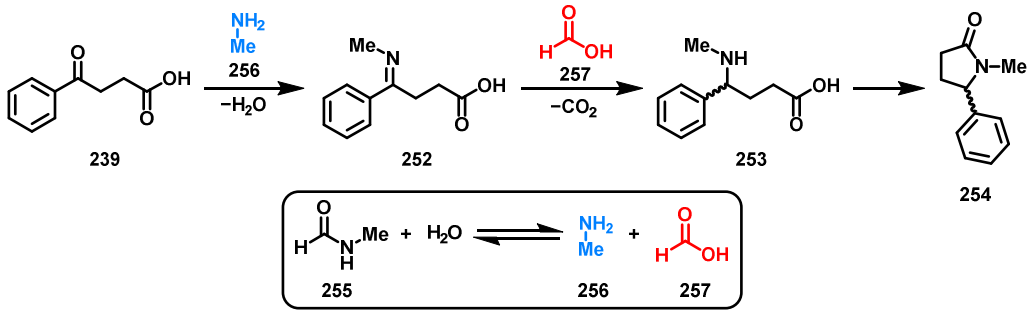

*Scheme 68: The proposed mechanism for the formation of lactam **254** from oxo acid **239** under pressure and microwave irradiation.*

The TDDFT prediction for the monoenolate of lactam **254** indicated a λ_{max} of approximately 320 nm yet was too unstable to allow for the recording of a UV-Vis spectra. Therefore, LEDs emitting at 340 nm or 365 nm were chosen for irradiation. With benzylic lactam **254** synthesised, deprotonation to form a monoenolate followed by irradiation at 340 nm was performed. This reaction yielded two

diastereomers of a di-substituted ring-contracted cyclopropane but left a substantial amount of unreacted starting material.

Using a more powerful and longer wavelength 365 nm LED (2000 mW compared to 69.2 mW for the 340 nm LED) increased the consumption of the starting material, resulting in a total yield of 25% for the formation of **258** and **259** via **261**, with a slight preference for *trans*-diastereomer **258** (Scheme 69). However, approximately 25% of the starting material still remained unreacted. Extending the reaction time did not improve the conversion, consistently leaving about the same proportion of starting material in the mixture.

The lower reactivity of this monoenolate compared to its trienolate counterpart could be attributed to the stability of the diradicals formed upon irradiation. In a monoenolate, diradical **260** is less stabilised due to the lack of an extended chromophore, which would otherwise allow for delocalisation of the radicals along the chromophore chain. Furthermore, the absence of an external chromophore chain in **254** likely results in a diminished Thorpe-Ingold effect on the contraction of the monoenolate of lactam **254** compared to the trienolate contraction on lactam **245**, lowering the success of ring-contraction. A further reason for the lack of complete conversion to ring-contracted product could be that photochemical products **258** and **259** absorb efficiently around the same wavelength as the monoenolate of **254**, effectively acting as a light filter, reducing the amount of light reaching the monoenolate as the reaction progresses.

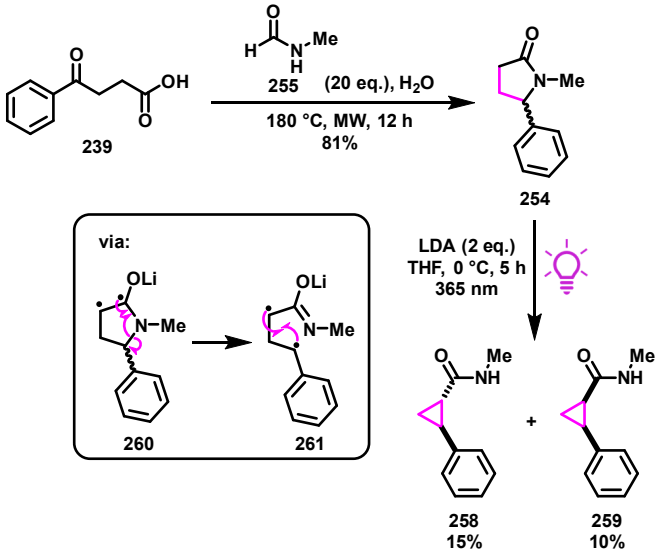

*Scheme 69: The synthesis of benzylic lactam **254** and its respective enolates' photochemistry to give **258** and **259**.*

This was an exciting development in our research, demonstrating that enolates can undergo significant photochemical rearrangements without needing an extended chromophore or specific protecting groups, such as those employed by Faye Knowles from the Clayden group at the turn of the century. However, the incomplete consumption of starting material indicates that photochemical reactivity is less favourable for a monoenolate compared to a trienolate.

5.3. Five-Membered Lactam Dienolate Ring-Contraction

We have observed that the ring contraction on a trienolate derived from lactam **245** proceeded with complete conversion but yielded a complex array of products, likely due to intermediate polymerisation, resulting in low overall yields. In contrast, a monoenolate derived from **254** underwent a cleaner transformation with a simpler product profile but without complete conversion of the starting material being achieved. The next logical step was to investigate the photochemistry of a dienolate lactam, which we hypothesised could offer a balance between these extremes, achieving complete conversion of the starting material while reducing the complexity of the product mixture and minimising unwanted polymerisation.

Using the same lactam precursor as in the monoenolate ring-contraction (**254**), an aldol addition to acetaldehyde (**13**) followed by DCC- and copper-mediated elimination produced two stereoisomers of alkenyl lactam (**262** and **263**) in good overall yield (Scheme 70). Although the dienolate derived from each stereoisomer is identical, *trans*-isomer **262** was selected since it was isolated as the major isomer of alkenyl lactam. The corresponding enolate from **262** had a TDDFT-predicted λ_{max} of 340 nm but was again too unstable for UV-Vis spectroscopic analysis.

Given that alkenyl lactam **262** contains a double bond in conjugation with the lactam carbonyl, LiHMDS was again employed as the base to prevent aza-Michael addition, which could occur with less sterically hindered bases like LDA. Upon forming the dienolate and irradiating at 365 nm, the expected ring contraction proceeded to **264** via **266** and **265** with a surprisingly high yield for such a unique and challenging transformation, though with poor diastereoselectivity. Both diastereomers in **264** were isolated together due to difficulties in chromatographic purification, as was the case for all lactam ring-contraction reactions discussed in this section, unless otherwise noted. NOE analysis identified the major diastereomer as having a *trans*-relationship between the phenyl ring and the alkenyl substituent.

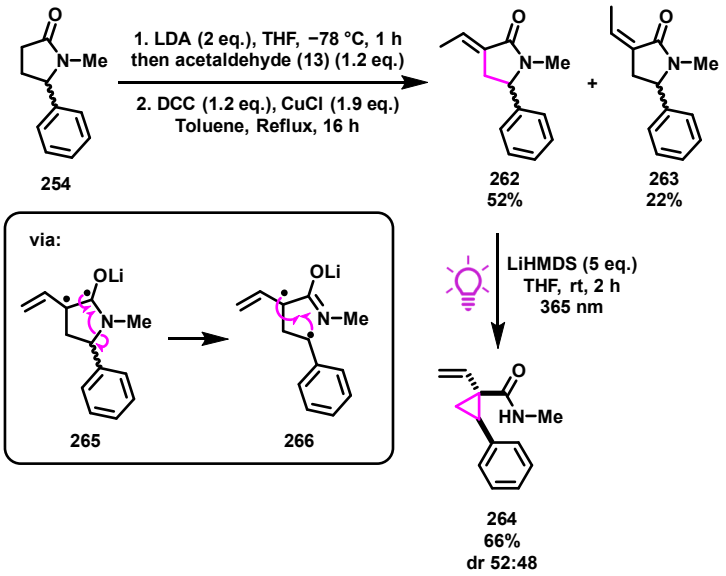

*Scheme 70: The synthesis of alkenyl lactams **262** and **263**, and the photochemical ring-contraction on the enolate of **262**.*

Unlike the five-membered lactam trienolate and monoenolate equivalents, which require lower temperatures to prevent degradation and extended reaction times for complete conversion, the ring-contraction on the dienolate of lactam **262** proceeded efficiently at room temperature and was complete within two hours. These mild conditions and high yield make this substrate an excellent candidate for exploring enolate photochemistry in flow.

5.3.0. Flow Photochemistry

Flow chemistry has gained significant traction in the literature over the past twenty years, offering the potential for faster, safer reactions with rapid scalability (Figure 9).[91–93] In 2019, IUPAC recognised flow chemistry as one of the top emerging technologies in chemistry.[94] The ability to perform reactions at dilute concentrations in flow systems is particularly advantageous for photochemical applications. According to the Beer-Lambert law, irradiating a dilute solution of a photoreactive substrate requires a lower rate of light absorption to initiate reactivity.[95] Combined with the capability of continuously feeding reagents through a flow photochemical reactor, this can lead to improved product yields. The increasing availability of affordable LEDs, polymer capillaries, and pump equipment suitable for flow further supports the development of innovative methods for photochemical synthesis in this field.[96]

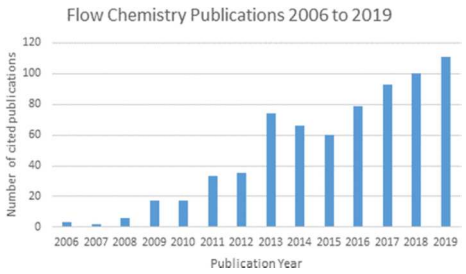

Figure 9: Publications detailing flow chemistry from 2006 to 2019. Figure taken from Baumann et al.[93]

Although the alkylation of enolates has been successfully performed in flow at room temperature by other groups (Scheme 71), achieving alkylation of **265** with allyl iodide (**266**) to afford **267**, the photochemistry of these species has not yet been explored in flow.[97,98]

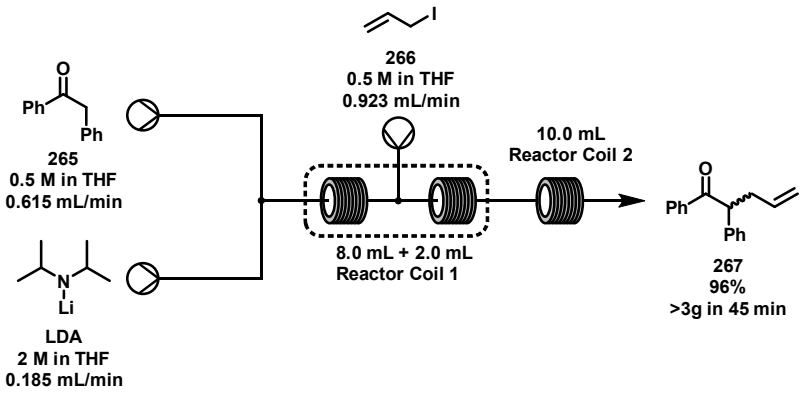

*Scheme 71: The alkylation in flow of **265** with allyl iodide (**266**) to give **267** reported in literature.*[98]

Many enolates require low temperatures for both their formation and reactivity, complicating their integration into a flow setup without significant equipment modifications, which increase cost and processing time. Consequently, only the room-temperature flow photochemistry on the dienolate of lactam **262** was investigated as part of an initial study.

In collaboration with William Terry-Wright from the Clayden group, a flow cell was developed that allowed for irradiation at 365 nm without significant heat transfer to the generated enolate. Using the setup shown in Figure 10 and the reaction described in Table 4, a substrate solution (5 mg/mL) was mixed with LiHMDS (directly from the bottle at 1 mol/dm^3) via a Vapourtec peristaltic pump in a Teflon T-junction under inert conditions. This mixture then passed through the flow reactor, which was equipped with a 365 nm LED strip, before being dispensed into a beaker containing ammonium chloride solution to quench the reaction.

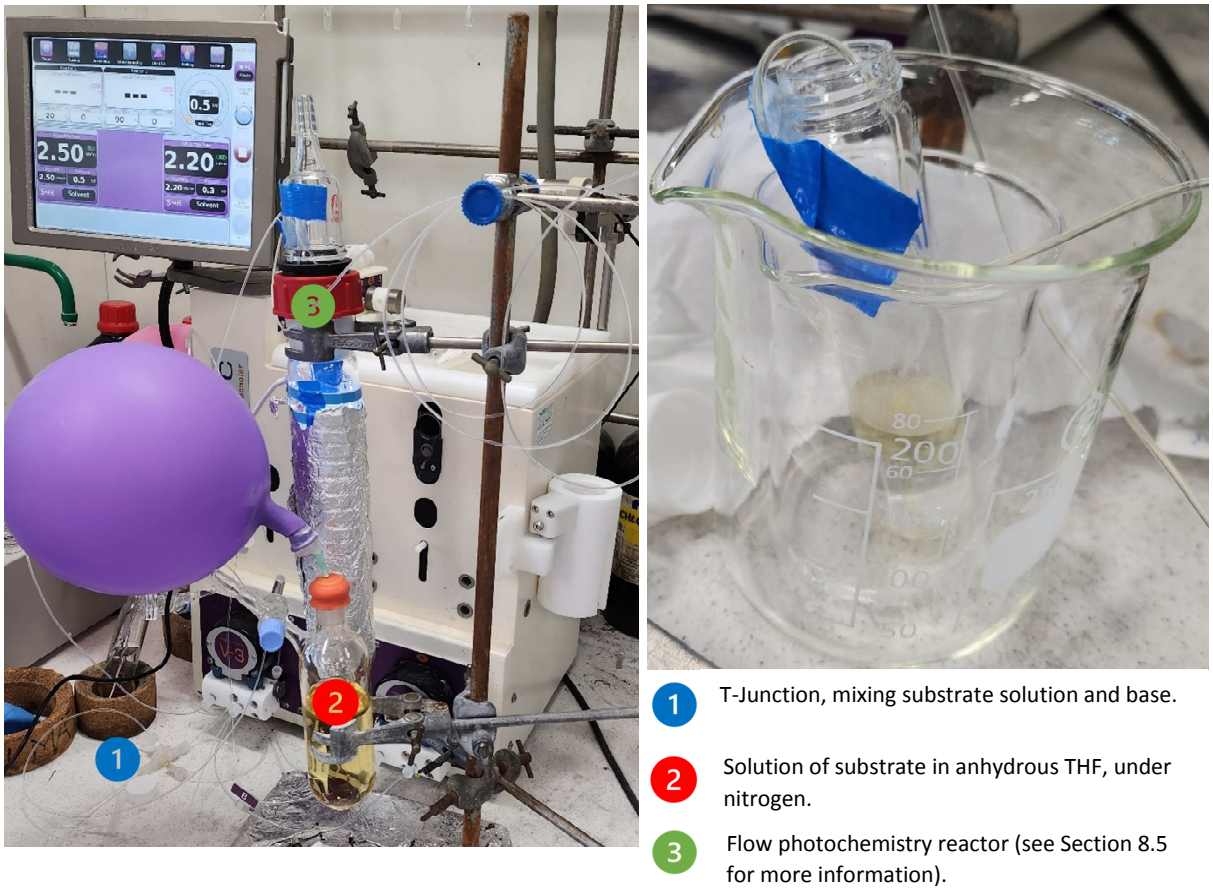

Figure 10: The flow photochemistry setup used and the tubing flowing into the quench solution (right).

For the purposes of this study, irradiation was performed at three different substrate flow rates (1, 0.5, and 0.25 mL/min) sequentially, and product yields were determined by quantitative NMR. It is important to note that while the substrate flow rate was varied, the flow rate of LiHMDS (0.12 mL/min) remained constant due to limitations in the flow pump's ability to accurately deliver the base at lower rates.

Consequently, at a substrate flow rate of 1 mL/min, LiHMDS was added at approximately 5 equivalents relative to the starting material. At a substrate flow rate of 0.5 mL/min, LiHMDS was supplied at 10 equivalents, and at 0.25 mL/min, an excess of 20 equivalents was provided. Thus, decreasing the substrate flow rate had two effects: it increased the residence time of the enolate in the flow photochemical reactor and provided a greater excess of base to drive the conversion to enolate. For future studies, a more dilute LiHMDS solution could be prepared to maintain consistent base equivalency. However, for this initial study, this adjustment was not deemed critical. In each experiment, collection was stopped after 75 mg of substrate had passed through the system, which corresponded to 15 minutes for a 1 mL/min flow rate, 30 minutes for 0.5 mL/min, and 1 hour for 0.25 mL/min.

*Table 4: The reaction scheme for the three flow photochemical studies carried out, with the NMR yields (using 3,4,5-trichloropyridine as internal standard) of remaining starting material **262** and the two diastereomers of photochemical products reported (**264**).*

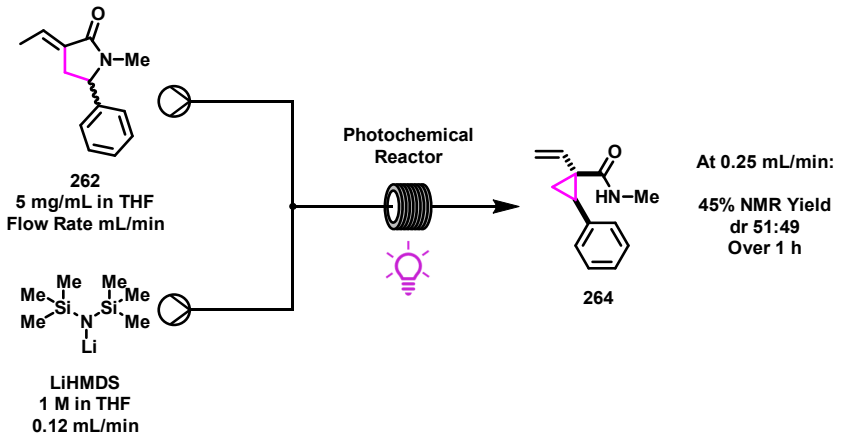

Flow Rate / mL/min	Time / min	LiHMDS Equivalents	Starting Material 262	Major Diastereomer in 264	Minor Diastereomer in 264
1.00	15	5	23%	11%	10%
0.50	30	10	24%	20%	20%
0.25	60	20	15%	23%	22%

As shown in Table 4, at a flow rate of 1 mL/min (5 eq. LiHMDS), approximately 21% of the ring-contracted products **264** were obtained, with a significant amount of unreacted starting material remaining. Encouragingly, reducing the flow rate improved conversion and increased the NMR yields of the product isomers, giving 40% of ring-contraction products **264** with a flow rate of 0.5 mL/min and a 45% yield of **264** with a flow rate of 0.25 mL/min. Since the equivalent batch reaction requires two hours for complete enolate conversion, it is unsurprising that longer retention times enhance conversion. However, it is important to note that this improvement may also be attributed to the higher base equivalency at lower flow rates.

Initially, it was a concern that longer retention times might reduce product yield due to potential thermal degradation of the enolate from unwanted LED heat irradiation within the flow reactor. However, this issue was not observed in this study, which is a promising outcome.

Achieving a 45% NMR yield of photochemical products **264** from the first attempt at flow photochemistry with these unstable intermediates is a positive result. This demonstrates that the developed photochemistry may be well-suited for flow and high-throughput chemistry methodologies.

Future work should focus on optimising this reaction in flow, aiming for complete conversion and dissecting the independent effects of flow rate and base equivalency on the reaction's success. Following this, additional substrates that react effectively at room temperature in batch could be explored in flow systems. The LED strip used in this study was accessible and affordable (£13 for two metres) but not particularly intense or powerful. Future studies might consider incorporating a different LED strip in the flow reactor to assess the impact of a more powerful or different wavelength light source.

5.3.1. Migrating Group Alterations

Our study on acyclic *N*-benzyl amide trienolates (Section 4) revealed that the migrating group during photochemical irradiation must possess radical-stabilising properties. This insight allows us to focus on other aryl groups that could potentially migrate during a ring-contraction of lactam dienolates, with the aim of improving yield and diastereoselectivity. To maintain consistency in the synthetic pathway for these lactams, we utilised the same microwave-mediated process for their formation. Thus, the various migrating groups were incorporated into the starting keto acids used in the microwave lactam synthesis. Although the availability of specific keto acids posed some limitations, their affordability (less than £4 per gram) made this pathway desirable for introducing the migrating group into the lactam.

Three substrates were initially selected to investigate the effects of a range of electronic properties and structures of the migrating group on ring contraction (Scheme 72). These included an inductively electron-deficient aryl ring (bearing a *para*-chloro substituent (**268**)), an electron-rich aryl ring (with a *para*-methoxy substituent (**269**)), and 2-thiophene (**270**) as an alternative aromatic migrating group. The synthesis of lactams with these groups α- to nitrogen was successfully achieved under microwave irradiation and pressure, giving **271**, **272** and **273** in moderate to good yield. Additionally, the installation of the alkenyl chromophore occurred as expected in all cases, yielding a mixture of *cis*- and *trans*-alkenes. This therefore afforded alkenyl lactams **274** and **277** with a *para*-chloro substituent, **275** and **278** with a *para*-methoxy substituent and **276** and **279** with a thiophene substituent.

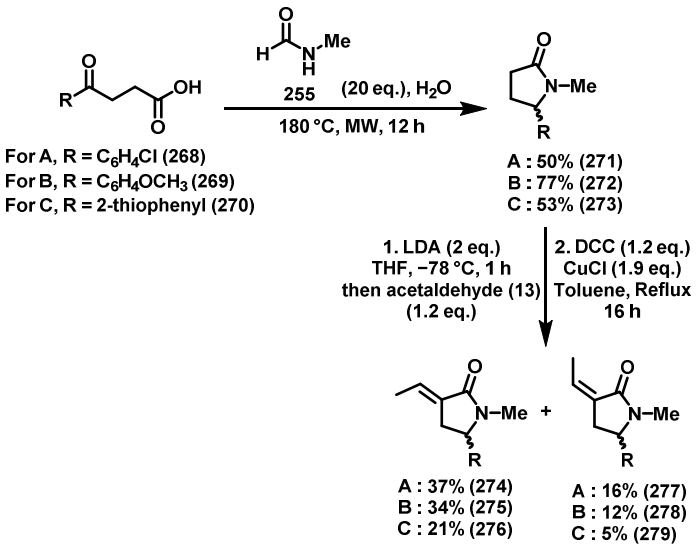

Scheme 72: The synthesis of dienyl lactams bearing various migrating groups.

For substrate **274**, bearing a *para*-chloro group on the aromatic ring, deprotonation followed by irradiation resulted only in a polymerised crude mixture, with no desired product **280** observed (Scheme 73). The exact cause is unclear, but it is possible that abstraction of a chloride radical is occurring under these conditions, leading to radicals prone to polymerisation.

When performing dienolate photochemistry at 365 nm with an electron-donating methoxy group on the migrating ring (**275**), the ring contraction proceeded as expected at room temperature, giving **281** but with poor diastereoselectivity, similar to previous observations. When shifting from a benzyl-based scaffold to a heteroaromatic one, such as 2-thiophene **276**, the ring contraction displayed similar selectivity for the major diastereomer. However, only one diastereomer was isolated after purification, with a yield of 35% for **282**. This is the only instance in this section where ring-contraction products were not isolated as a mixture of diastereomers, likely due to the instability of the minor diastereomer of the substituted cyclopropyl ring on silica.

To address the absence of the desired ring contraction on the dienolate of *para*-chloro benzyl lactam **274**, we hypothesised that replacing the chloride substituent with a fluoride might decrease the likelihood of radical dehalogenation, given the increased strength of a C-F bond compared to a C-Cl bond.[99]

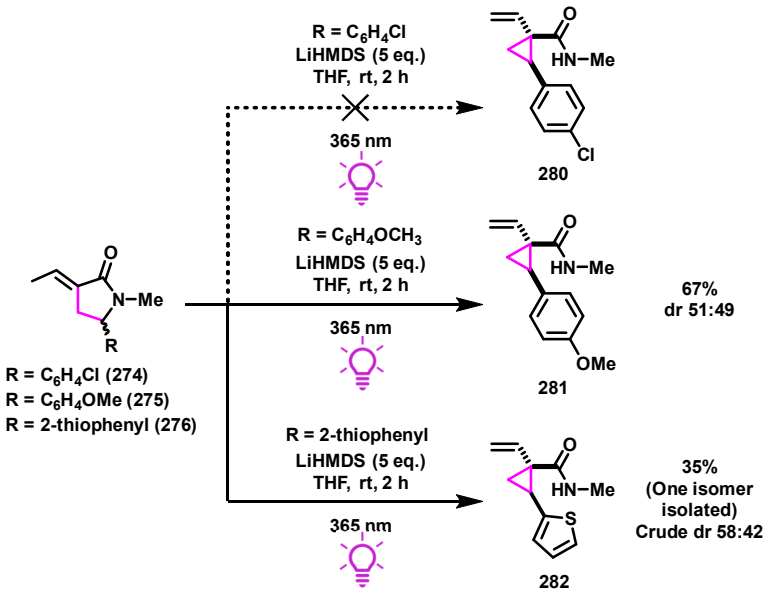

Scheme 73: The photochemical ring-contraction on dienolates of lactams bearing various migrating groups.

Para-fluoro benzyl lactam **286** was synthesised to achieve an electron-deficient ring contraction without polymerisation of the intermediates (Scheme 74). Attempts to directly form tertiary lactam **286** using *N*-methyl formamide **255** under microwave irradiation resulted in poor yields and significant degradation. Consequently, the microwave-mediated cyclisation was performed using formamide **284**, affording secondary lactam **285** in 49% yield. This secondary lactam was then methylated in high yield to give **286**, followed by the installation of the chromophore as previously detailed, producing compounds **287** and **288**.

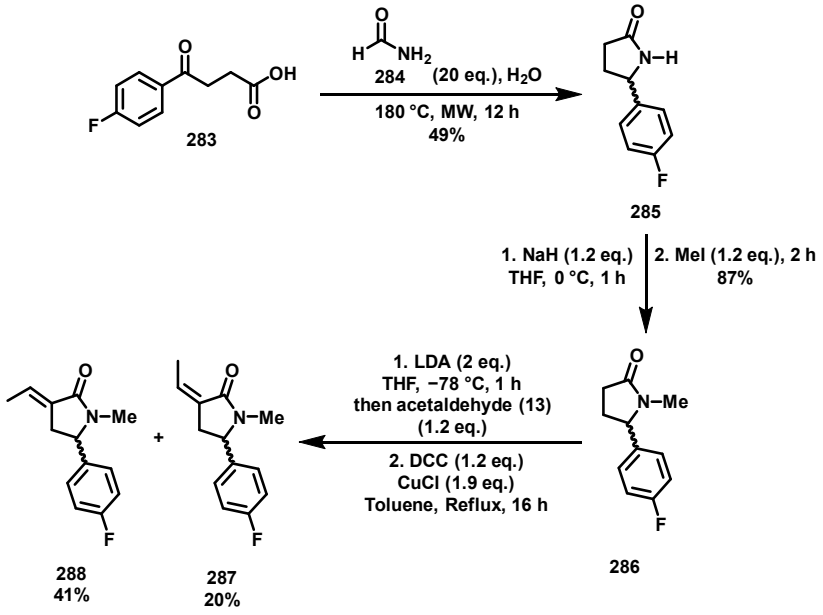

Scheme 74: The synthesis of para*-fluoro alkenyl lactams **287** and **288**.*

Deprotonation of *trans*-alkenyl lactam **288**, bearing a *para*-fluoro substituent on the migrating group, generated the photoreactive enolate. Irradiation at 365 nm resulted in the formation of the ring-contracted product diastereomers **289** with a 45% yield and a diastereoselectivity of 52:48 (Scheme 75).

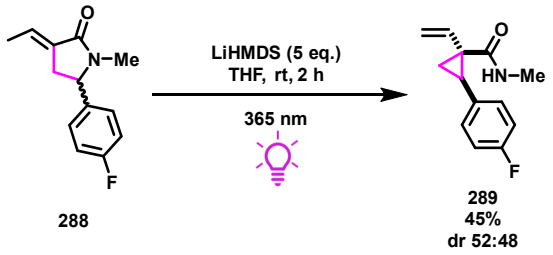

Scheme 75: The photochemical ring-contraction on the enolate of para*-fluoro benzyl alkenyl lactam* ***288****.*

This result clearly demonstrates that the migrating group can be varied with relative ease, without concern for aryl electronic effects, as long as the intermediate radicals are not prone to dehalogenation or rapid polymerisation. However, the diastereoselectivity remains poor, indicating that the selectivity during radical recombination is minimally influenced by the nature of the migrating group.

5.3.2. Steric Bulk Alterations on the Chromophore

The formation of substituted cyclopropane ring-contraction products involves radical recombination between a benzylic radical and a radical adjacent to the light-absorbing chromophore. Given the chromophore's proximity to the recombination site, increasing the steric bulk of the chromophore was considered as a strategy to improve diastereoselectivity during contraction.

The simplest modification involved replacing the acetaldehyde (**13**)-derived chromophore with one derived from acetone (**1**), adding an extra methyl group to increase steric bulk and potentially enhance diastereoselectivity (Scheme 76). Aldol addition onto lactam **254** followed by elimination yielded two structural isomers of the desired alkenyl lactam (**290** and **291**) in good overall yield. Although both isomers were suitable for the ring-contraction reaction, major isomer **290** (with the double bond conjugated with the amide) was selectively deprotonated and irradiated, producing the expected ring-contraction products **292** with a diastereoselectivity of 58:42. While this was an improvement over many previously explored substrates, it still represents only a modest enhancement.

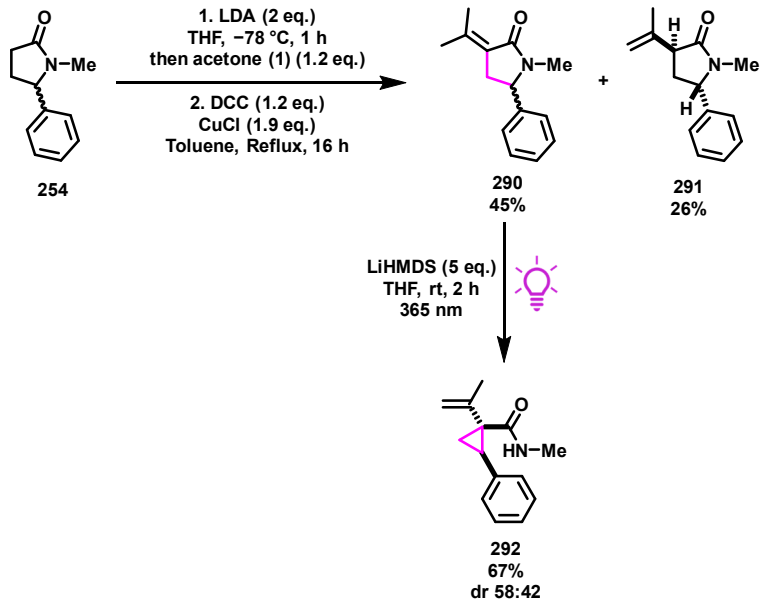

*Scheme 76: The synthesis of acetone-derived alkenyl lactams **290** and **291**, and the photochemistry on the enolate of **290**.*

A further increase in steric hindrance around the chromophore was achieved by introducing a *tert*-butyl group at one end of the molecule (Scheme 77). The synthesis of lactams **293** and **294** from **254** proceeded in good yield, with the bulkier group favouring the formation of *trans*-alkenyl lactam **293** more than with a less sterically hindered group. However, deprotonation of **293** followed by irradiation did not yield expected products **295** and instead returned just starting lactam **293**. Deuteration experiments revealed that the intended enolate was not forming under standard conditions, likely due to the steric bulk around the deprotonation site. This steric hindrance seemingly prevented the bulky LiHMDS base from effectively accessing the enolisable proton, rendering the desired enolate kinetically inaccessible.

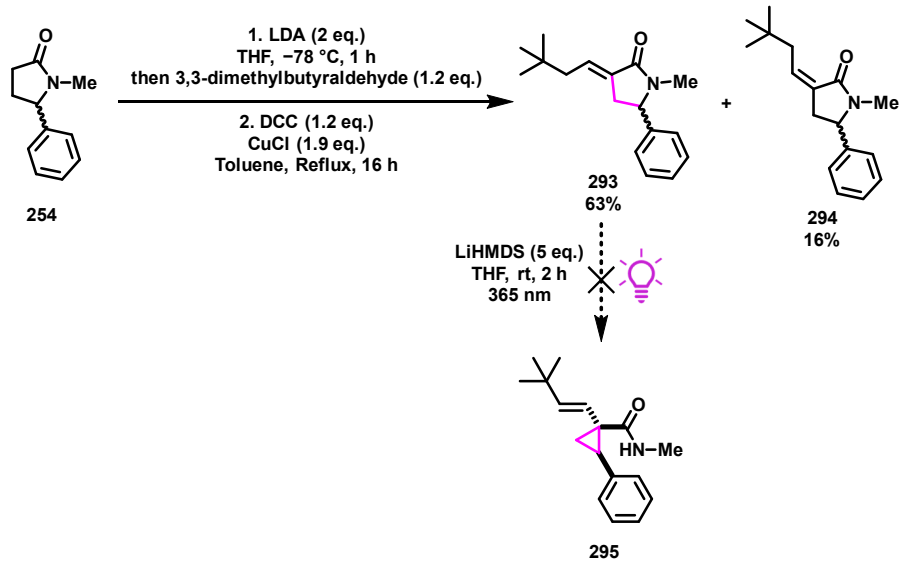

*Scheme 77: The synthesis of dimethylbutyrate alkenyl lactam **293** and **294** and the photochemistry attempted on the enolate of **293**.*

This finding prompted us to investigate enolate formation at a position shielded by two methyl groups instead of a *tert*-butyl group (Scheme 78). Using isobutyraldehyde as the aldehyde component in an aldol addition with lactam **254**, followed by elimination, selectively afforded *trans*-alkenyl lactam **296** in 56% yield. However, upon deprotonation and irradiation, no reactivity was observed towards **297**. This lack of reactivity can again be attributed to the steric hindrance around the deprotonation site.

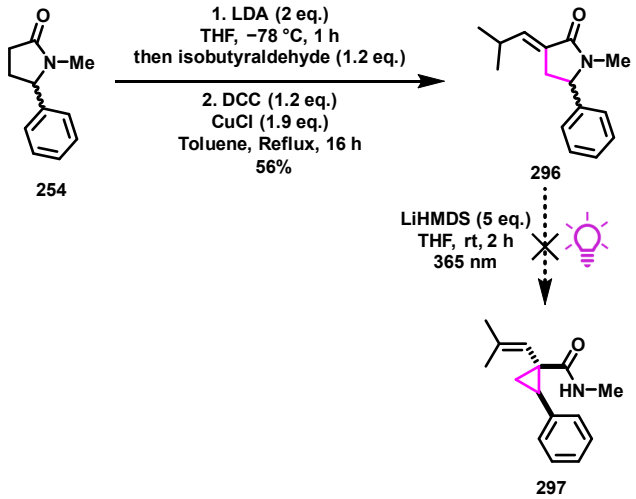

*Scheme 78: The synthesis of isobutyl alkenyl lactam **296** and the attempted photochemistry on its enolate.*

Although deprotonation at these sites was unachievable under standard conditions, we hypothesised that using a structural isomer of **296** with the chromophore's alkene positioned adjacent to the steric bulk, as in **298**, could provide access to the desired enolate (Figure 11). In this configuration, the deprotonation site required for forming the dienolate is less sterically hindered and should therefore have higher kinetic acidity, favouring deprotonation.

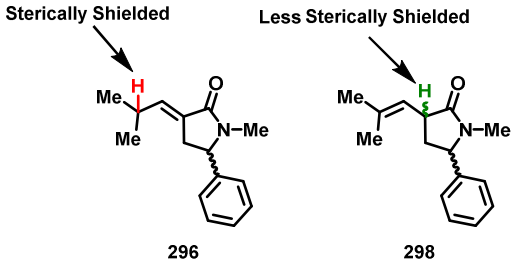

*Figure 11: The two isomers **296** and **298** which, on deprotonation, give rise to the desired dienolate.*

In order to synthesise desired isomer **298**, lactam **254** was deprotonated before addition of 3-bromo-2-methylpropene (**299**) as an electrophile (Scheme 79). This afforded two diastereomers of unconjugated lactam **300** and **301** in 25% and 19% yield respectively. *Trans*-isomer **300** was then subjected to isomerisation by addition of tosylic acid and heating for four hours to yield an internal alkenyl lactam with *trans*-configuration (**302**) in 55% yield. This product has a relatively accessible acidic proton suitable for deprotonation.

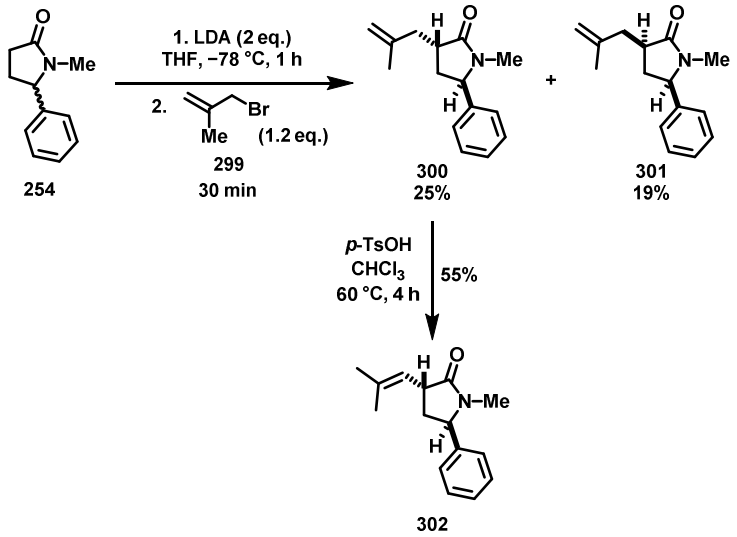

*Scheme 79: The nucleophilic addition on 3-bromo-2-methylpropene (**299**), followed by alkene isomerisation of **300** to **302**.*

Deprotonation at the accessible reactive site in lactam **302**, followed by irradiation, resulted in the desired ring contraction with a 63% yield for **297** and a modest diastereoselectivity of 57:43 (Scheme 80).

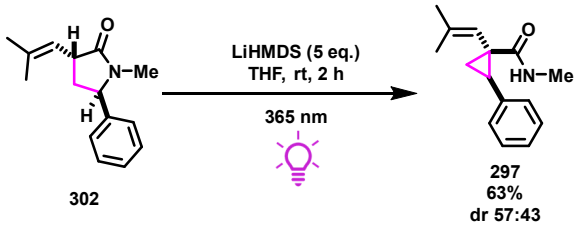

*Scheme 80: The photochemical reactivity on the enolate of alkenyl lactam **302** to give only a modest diastereoselectivity in ring-contracted products **297**.*

The chromophore modifications discussed so far have only achieved mild improvements in diastereoselectivity. As a final approach to enhance diastereoselectivity by increasing chromophore bulk in the ring-contraction process, a cyclohexene group was proposed as the alkene functionality to introduce steric hindrance on both sides of the double bond.

Desired substrate **304** was synthesised via aldol addition of the enolate of **254** onto cyclohexanone, followed by an elimination step to afford **303** (Scheme 81). Complete elimination of the alcohol intermediate in this step was not achieved, even with extended reaction times. However, deprotonation of the partially eliminated material induced isomerisation, shifting the alkene into the cyclohexyl ring, affording **304** as a single diastereomer in this case following protonation on the least hindered face of the lactam. This shift allowed for easier purification of the unreacted alcohol and positioned the deprotonation site at a less hindered position, α to the carbonyl, enhancing accessibility and reactivity.

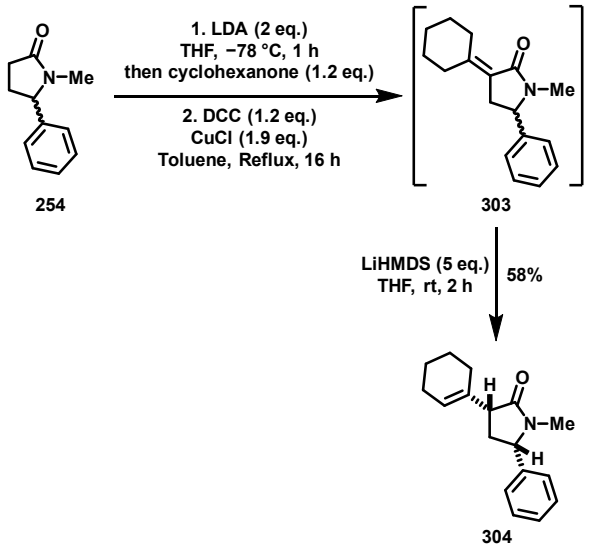

*Scheme 81: The synthesis of cyclohexenyl lactam **304**, following elimination and isomerisation.*

Photochemistry on the enolate of **304** yielded the substituted cyclopropane isomers **305** in 60% yield, with a similar diastereoselectivity to that reported previously (Scheme 82). The inability of chromophore modifications to achieve diastereoselectivity beyond 58:42 suggests that the chromophore has minimal influence on selectivity during radical recombination in the reaction.

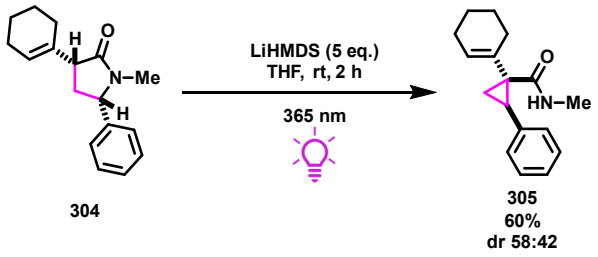

*Scheme 82: Photochemical ring-contraction of a lactam bearing a cyclohexene group (**304**).*

5.3.3. Other Alterations

Two main structural modifications that were further explored for enhancing five-membered lactam dienolate ring contraction was alteration of the nitrogen capping group and the currently unsubstituted position in the lactam ring. Introducing a bulkier group on the nitrogen, such as with a chiral motif, was hypothesised to allow for an increase in diastereoselectivity during the cyclopropane-forming step.

This was investigated by introducing a chiral α-methyl benzyl group, which might induce selectivity by partially blocking one face of the forming cyclopropane. Additionally, the presence of an enantiopure

capping group would result in four diastereomers of the product, allowing for the study of selectivity among all four.

Desired lactam **312** was initially synthesised following a procedure by Butters *et al.*,[100] where *R*-α-methylbenzylamine (**306**) was refluxed in toluene with succinic anhydride (**307**), followed by a brief reflux in acetic anhydride to give **308** in 72% yield (Scheme 83). Imide **308** was then treated with super hydride to selectively reduce one carbonyl to an alcohol, affording **309**. This intermediate was reacted directly with benzene and triflic acid, substituting the alcohol for a benzyl group via an *N*-acyliminum ion, yielding benzylic lactam **310** with some diastereoselectivity (68:32) but in low yield, using a modified procedure by Zhang *et al.*[101] Aldol addition and elimination to install the chromophore yielded the expected mixture of products. The *cis*-isomer mixture **311** had a diastereomeric ratio of 63:37, while the *trans*-isomer mixture **312** had a ratio of 60:40. The diastereomeric ratios at this stage are not indicative of the expected selectivity in the ring-contraction step, as one of the stereogenic centres undergoes reaction via a benzylic radical, likely scrambling the stereochemistry at that position, while the chiral capping group remains unchanged.

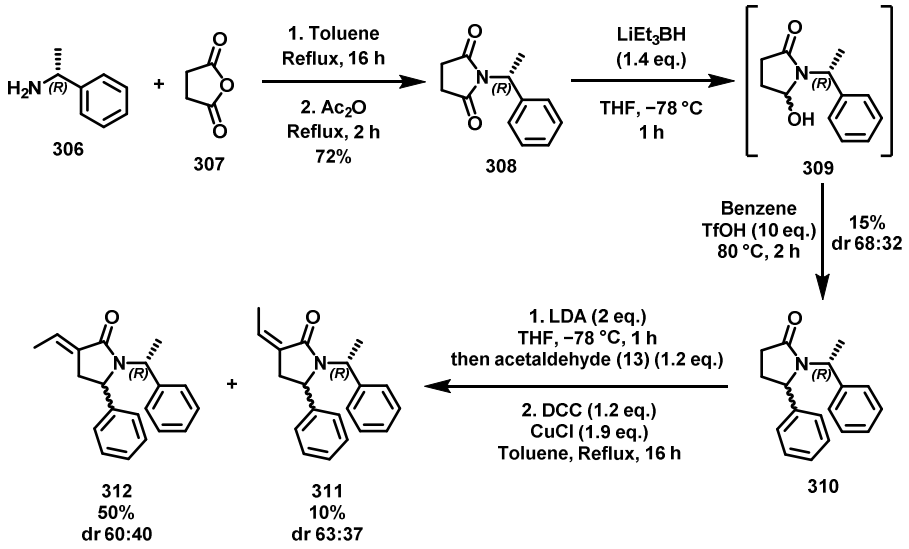

*Scheme 83: The synthesis of a diastereomeric mix of alkenyl lactams **311** and **312** bearing a chiral* N*-capping group.*[100,101]

Deprotonation of the diastereomeric mixture of *trans*-alkenyl lactam **312**, followed by irradiation at 365 nm, produced four diastereomers of ring-contracted products **313**, **314**, **315** and **316** in a 60% yield, with an approximate diastereomeric ratio of 36:27:19:18, isolated as a mixture of all isomers (Scheme 84). NOE analysis identified the two major diastereomers as the *S*,*R* and *R*,*S* isomers (**313** and **314**), where the terminal alkene is positioned *trans* to the migrating benzyl substituent. This outcome may seem unexpected given the bulk of the chiral capping group. However, it can be explained by

considering this group as being held away from the radical recombination site during product formation. If rotation around the nitrogen-carbon bond of the capping group occurs faster than the photochemical reaction, the bulkier aryl group could rotate away from the recombination centre, resulting in low selectivity between diastereomers. The absolute stereochemistry could not be easily assigned to each diastereomer, so the results are reported as pairs.

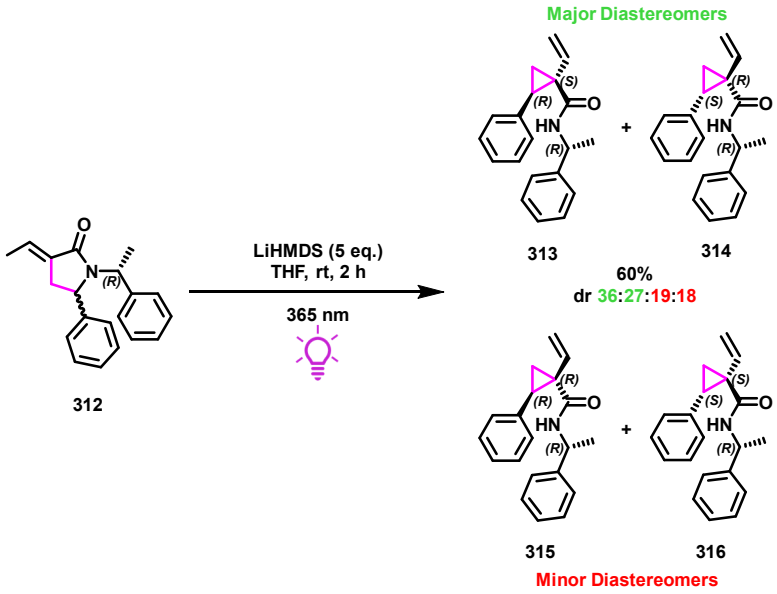

*Scheme 84: The photochemical ring-contraction of the enolate of alkenyl lactam **312**, bearing a chiral capping group, giving four diastereomers of ring-contraction product **313**, **314**, **315** and **316**.*

Although the selectivity of this methodology remained poor with substrate **312**, it demonstrates the versatility of the overall photochemistry, showing that a more complex capping group on nitrogen can be used without compromising the reaction's success.

As a final study to improve the selectivity of lactam dienolate ring contraction, we increased substitution on the lactam ring (Figure 12). By substituting at the 4-position in the ring, and increasing steric bulk around the lactam as in **317**, we aimed to promote ring contraction with greater stereoselectivity.

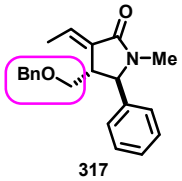

*Figure 12: Alkenyl lactam **317**, bearing ether substitution at the 4-position.*

We began the synthesis of lactam **317** with a literature procedure by Piwowarczyk *et al*.[102] which introduced a carboxylic acid at the desired position for substitution in the lactam ring (Scheme 85). This was achieved by refluxing *N*-methyl-1-phenylmethanimine (**318**) and succinic anhydride (**307**) in toluene overnight, yielding the lactam core with selective *trans*-stereochemistry in **319**. The carboxylic acid was then esterified and reduced to produce primary alcohol **320**, primed for protection, in 87% yield. While various protecting groups could be explored for their effect on ring-contraction diastereoselectivity, a benzyl group was chosen due to its steric bulk and likely stability under basic conditions. Deprotonation of the alcohol and subsequent protection with benzyl bromide afforded benzylic ether **321** in 72% yield. Aldol addition with acetaldehyde (**13**), followed by elimination, yielded two isomers of alkenyl lactam **317** and **322**.

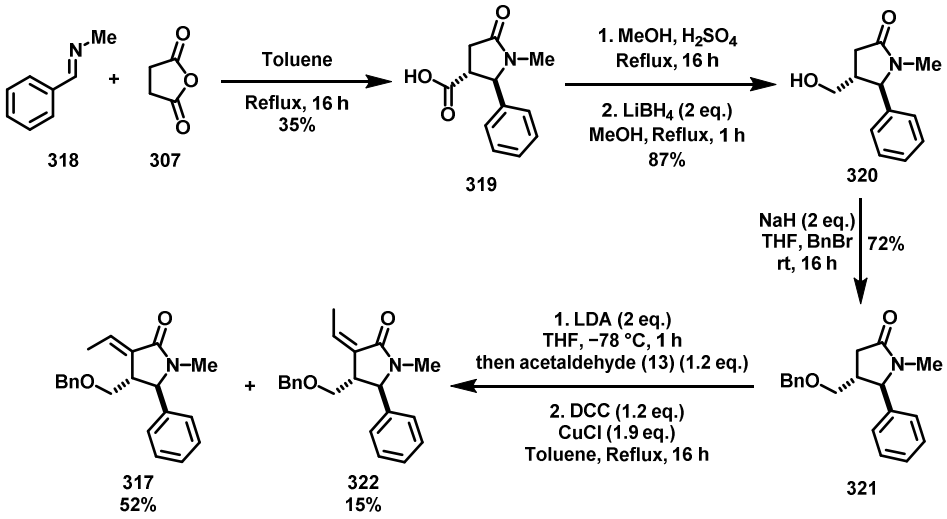

*Scheme 85: The synthesis of benzylic ether-substituted alkenyl lactams **317** and **322**.*

Trans-isomer **317** was subsequently deprotonated and irradiated, affording highly substituted cyclopropanes **323** and **324** (Scheme 86). Notably, this ring contraction achieved a diastereoselectivity of 89:11, for **323** and **324** respectively, and a high yield of 71%. This remarkable transformation, which generates a stereochemically-rich, substituted cyclopropane, highlights the potential of meticulously designed lactam substrates for synthesising complex and potentially valuable products via ring contraction.

In major diastereomer **323**, the alkenyl group is positioned *trans*- to the benzylic ether and *cis*- to the aryl ring at the opposing cyclopropane position. This suggests a preference for the alkenyl group to adopt a position opposite the benzylic ether, likely due to steric or electronic interactions that favour such an arrangement within the cyclopropyl ring. Consistently, the benzylic ether and phenyl groups are *trans*- to each other in both observed diastereomers **323** and **324**, with no evidence of

cyclopropanes where these substituents bear a *cis*- relationship. Furthermore, the high yield observed may be attributed to the Thorpe-Ingold effect, where increased substitution at the starting lactam enhances the ring-closing reaction.[103]

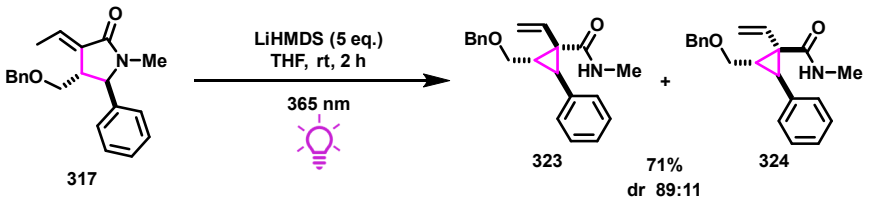

*Scheme 86: The photochemical ring-contraction on the enolate of substituted lactam **317**, giving a high diastereoselectivity for cyclopropane products **323** and **324**.*

Future studies on five-membered lactam ring contractions will focus on varying the alcohol protecting group on lactam **320** and examining its influence on the photochemical reaction outcomes. This will help ascertain the extent to which the choice of protecting group affects the reaction's efficiency and selectivity. Additionally, efforts will be made to introduce alternative functional groups in place of the alcohol moiety in **320**, potentially replacing the alcohol with a phenyl or alkyl group. It is hypothesised that incorporating a group with greater steric bulk directly attached to the cyclopropane ring could potentially enhance both diastereoselectivity and overall contraction yields.

5.4. Six-Membered Lactam Trienolate Ring-Contraction

Building on the photochemistry of five-membered lactam ring contractions, it was anticipated that a similar approach could be applied to six-membered lactams, potentially enabling ring contraction to form cyclobutane derivatives. Cyclobutane rings are of significant interest in pharmaceuticals, where their conformational rigidity contributes to enhanced biological activity across a wide pharmacological spectrum, including treatments for cancer and autoimmune diseases.[104] This rigidity often plays a crucial role in promoting desired biological interactions. Notable examples of pharmaceutical agents featuring cyclobutanes include Miransertib (**325**), a treatment for tumours, substituted indole cyclobutene **326**, which is being investigated as a potential treatment for schizophrenia and BMS-814580 (**327**), an anti-obesity agent (Figure 13).[105–107]

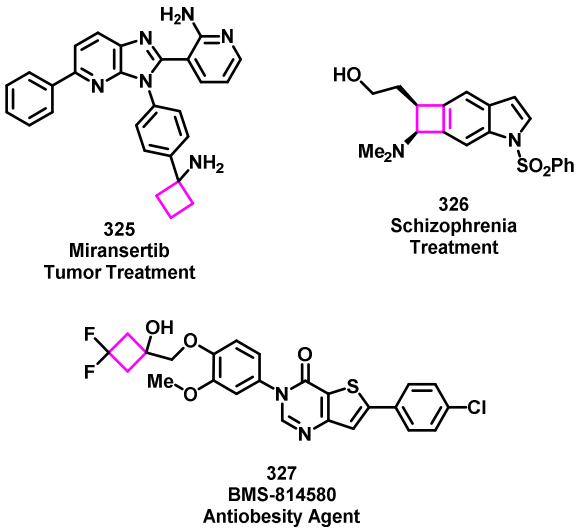

*Figure 13: Some examples of pharmaceutical targets containing a cyclobutane ring (**325**, **326** and **327**).*[105–107]

The construction of cyclobutane rings presents significant challenges in synthetic chemistry due to their highly strained ring systems. While synthetic methodologies for creating these motifs are rapidly advancing, the ability to efficiently generate cyclobutene frameworks in a diverse and straightforward manner remains highly valuable.[108] We hypothesised that our simple starting materials, combined with subsequent deprotonation and irradiation steps, could facilitate the direct formation of four-membered rings from six-membered rings via a unique and operationally simple ring-contraction process.

Our investigation into this approach began with the incorporation of a diene chromophore into six-membered lactam **329** (Scheme 87). The synthesis of lactam **329** was performed following the procedure described in Section 5.2, employing microwave-mediated cyclisation of 5-oxo-5-phenylpentanoic acid (**328**) with *N*-methyl formamide (**255**) to establish the lactam core in **329** in a high yield.

Aldol condensation with crotonaldehyde (**16**), as previously described, resulted in a characteristically complex mixture of regio- and stereoisomers of the dienyl lactam through **330** as an intermediate. On purification, the *Z*,*E*-isomer of dienyl lactam **331** was obtained in 12% yield, while the *E*,*E*-isomer **332** was isolated in 33% yield.

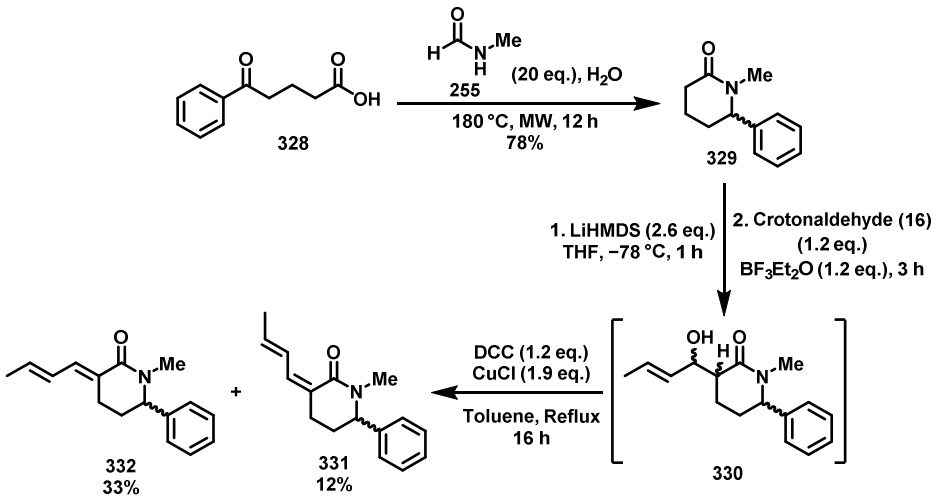

*Scheme 87: The synthesis of six-membered lactam isomers **331** and **332**.*

Computational predictions indicated a λ_{max} of 367 nm for trienolate **335**, derived from **332**, closely matching the predicted value for the trienolate of the five-membered ring analogue **245**. As with the five-membered analogues, trienolate **335** was again too unstable for spectroscopic analysis. Upon deprotonation of lactam **332** with LiHMDS, followed by irradiation at 385 nm, two photochemical products were obtained (Scheme 88). The first product was a diastereomeric mixture of cyclobutane **333**, formed through the expected photochemical ring contraction in a 14% yield, with a diastereoselectivity of approximately 80:20 for the isomer bearing a *cis*-relationship between the migrating aryl ring and dienyl functionality. Interestingly, this stereochemical arrangement is opposite to that observed in the major diastereomers isolated from ring-contraction of a five-membered ring to various cyclopropanes. In this case, only the major diastereomers of the ring-contraction product could be isolated in pure form. The second product, cyclohexene **334**, resulting from a photochemical migration or "ring-swing", was obtained in a 17% yield with a diastereoselectivity of approximately 66:33. This transformation is quite unusual, converting a lactam into a different six-membered ring through simple deprotonation and irradiation. We believe this "ring-swing" occurs from irradiation of trienolate **335** to give **336** which may undergo radical addition to the middle of the trienolate chromophore, affording **334**. Unfortunately, due to substrate polymerisation and a complex reaction mixture, NOESY experiments to determine the relative stereochemistry of the major diastereomer were inconclusive but **334** is expected to bear a *trans*-relationship between the vinyl group and migrating aromatic ring to reduce steric hindrance.

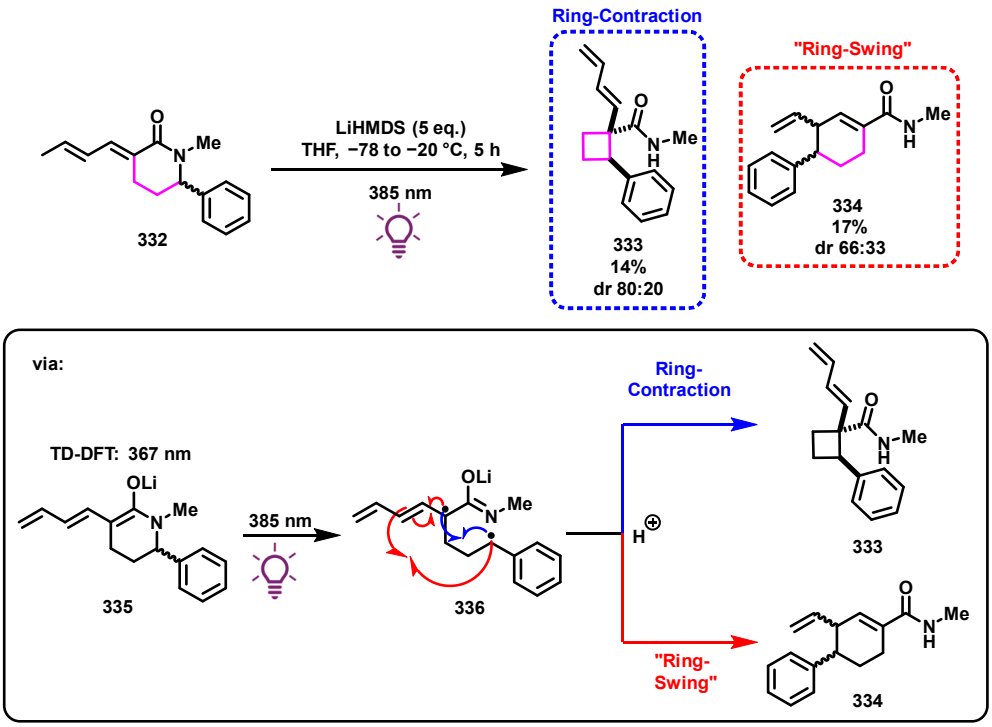

*Scheme 88: The photochemistry of trienolate **335**, derived from lactam **332**, giving ring-contraction and migration, with the mechanism for formation of both products **333** and **334** shown.*

The disappointing yields obtained for **333** and **334** may be attributed to unoptimised reaction conditions or potentially polymerisation occurring during the reaction. We aimed to address these issues by exploring the migration of different substituents and altering the attached chromophore, similar to the approach taken with the five-membered lactam ring-contraction photochemistry.

While photochemical reactivity on enolate **335** involves the migration of a benzyl group, we hypothesised that the photochemical process could also facilitate the migration of a vinyl substituent. Previous work on the acyclic *N*-benzyl amide trienolate system demonstrated that an allyl group could undergo migration, albeit with lower yields than with a benzyl group.

To investigate this possibility, allyl lactam **342** was synthesised by an initial reduction and sulfonylation of glutarimide (**337**) with sodium borohydride and sodium benzenesulfinate to afford sulfonyl lactam **338** in good yield (Scheme 89). Subsequently, vinylmagnesium bromide was used for a nucleophilic attack at the sulfinyl centre, followed by methylation of the nitrogen to afford **340** from **339** in high yield. Finally, the chromophore was installed using the same aldol addition and elimination process, which, as expected, resulted in a low yield of **342** through **341** (11%) due to the formation of a mixture of stereoisomers.

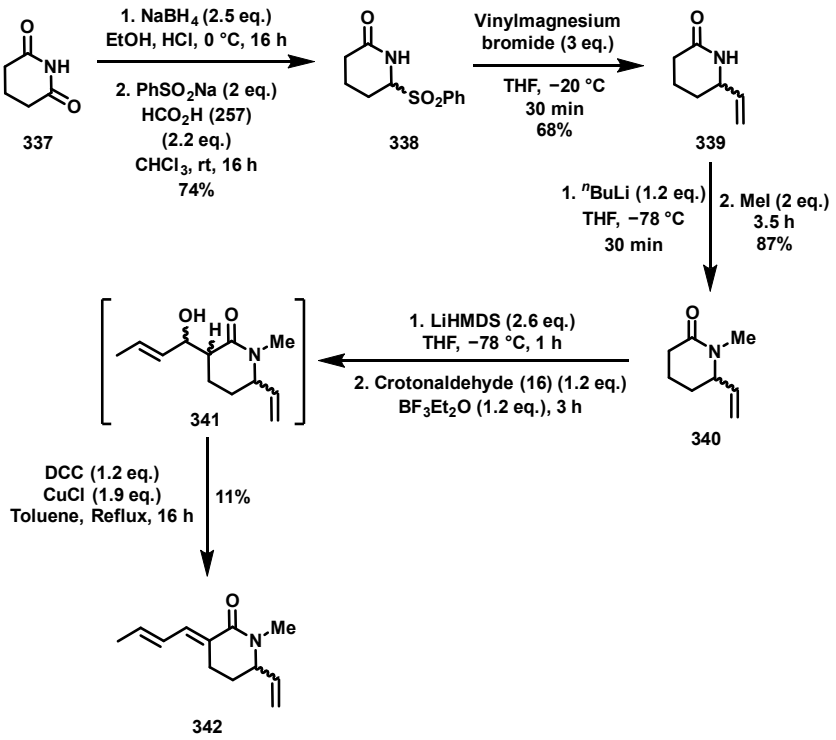

*Scheme 89: The synthesis of vinylic lactam **342** from glutarimide **337**.*

Deprotonation and irradiation of allyl lactam **342** at 385 nm yielded expected cyclobutene **343**, albeit in a low yield, with only one diastereomer observed. Notably, a significant proportion (39%) of the reaction produced the regioisomeric "ring-swing" migration product **344** (Scheme 90).

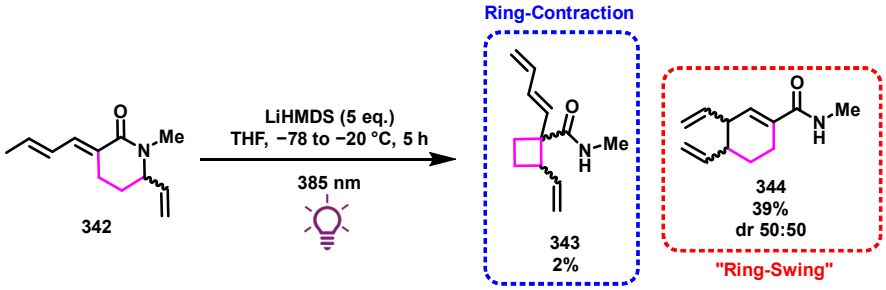

*Scheme 90: Photochemistry on the enolate of six-membered lactam **342**, migrating a vinyl group.*

This moderate yield is higher than previously observed in the ring-contraction photochemistry of benzyl lactam trienolate **335** and contrasts with photochemical benzylic migrations reported in Section 4, where allyl groups performed worse than benzylic ones. The high regioselectivity is also intriguing, since regioselectivity in the photochemistry on trienolate **335** was minimal between the two types of products formed. This suggests a possible conformational preference of the ring-opened diradical intermediate, positioning the radical allyl substituent closer to the centre of the

chromophore, thereby favouring the formation of the "ring-swing" product. The observed regioselectivity could also be partially attributed to the limited stability of the vinyl cyclobutane products under photochemical conditions.

The two alkenyl groups in compound **344** appear to be well-aligned for a [3,3]-sigmatropic, or Cope, rearrangement to afford **345**. However, when a diastereomeric mixture of di-alkenyl amide **344** was subjected to microwave irradiation at 200 °C for two hours, no rearrangement was observed, and only starting material **344** was recovered (Scheme 91). Computational energy predictions, comparing the ground-state energies of *cis*-alkenyl amide **344** with the ground-state energy of the potential sigmatropic rearrangement product **345**, indicated that the anticipated product is approximately 61 kJ/mol less stable than the starting material. This reduced stability likely explains the absence of rearrangement under these harsh conditions.

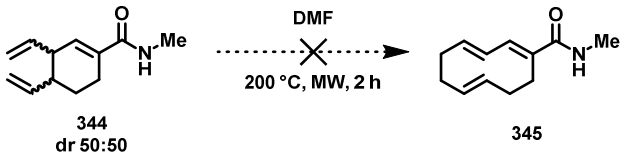

*Scheme 91: The attempted [3,3]-sigmatropic rearrangement on **344**, with the expectation to form **345**.*

5.5. Six-Membered Lactam Monoenolate Ring-Contraction

Inspired by the observed photochemical reactivity of a five-membered monoenolate from **254**, which produced a cyclopropyl ring bearing only an amide and a phenyl group, we hypothesised that a similar approach could be applied to synthesise four-membered rings (**346** from **329**) without the need for an extended chromophore (Scheme 92).

The enolate of lactam **329** yielded a TDDFT-predicted λ_{max} of 335 nm, but due to the instability of the enolate to temperature and air, a clear UV-Vis trace could not be obtained. Consequently, irradiation at both 340 nm and 365 nm was independently attempted, but no reactivity was observed. Varying conditions including temperature (−78 °C to room temperature), base equivalents (1 to 10 eq.), reaction time (1 to 24 h), and LED wavelength (340 and 365 nm)—all resulted in the recovery of only starting material **329**. This suggests that six-membered lactam monoenolates are less prone to photochemical ring contraction compared to five-membered lactam monoenolates.

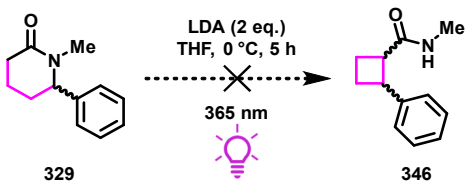

*Scheme 92: The attempted ring-contraction of a six-membered ring through the monoenolate of lactam **329**.*

This difference in reactivity can be attributed to the fact that five-membered lactam monoenolate **347** would need to undergo a 5-*endo-trig* cyclisation from **261** to regenerate the starting material after a radical-initiated benzylic cleavage—a process disfavoured by Baldwin's rules (Scheme 93).[66] As a result, the reformation of lactam monoenolate **347** is disfavoured, making the benzylic radical available to participate in a ring-contraction process. This is in contrast to a six-membered monoenolate, which would require a favoured 6-*endo-trig* cyclisation to reform its starting enolate. Baldwins rules may also explain why irradiation of five-membered lactam dienolate **348** does not yield any "ring-swing" product, **349** from **266**, since such a rearrangement would require a disfavoured 5-*endo-trig* cyclisation. In contrast, for six-membered trienolate **335**, a 6-*endo-trig* cyclisation is both rapid and spontaneous, to give **350** via **336**, since it is favoured by Baldwin's rules.[66]

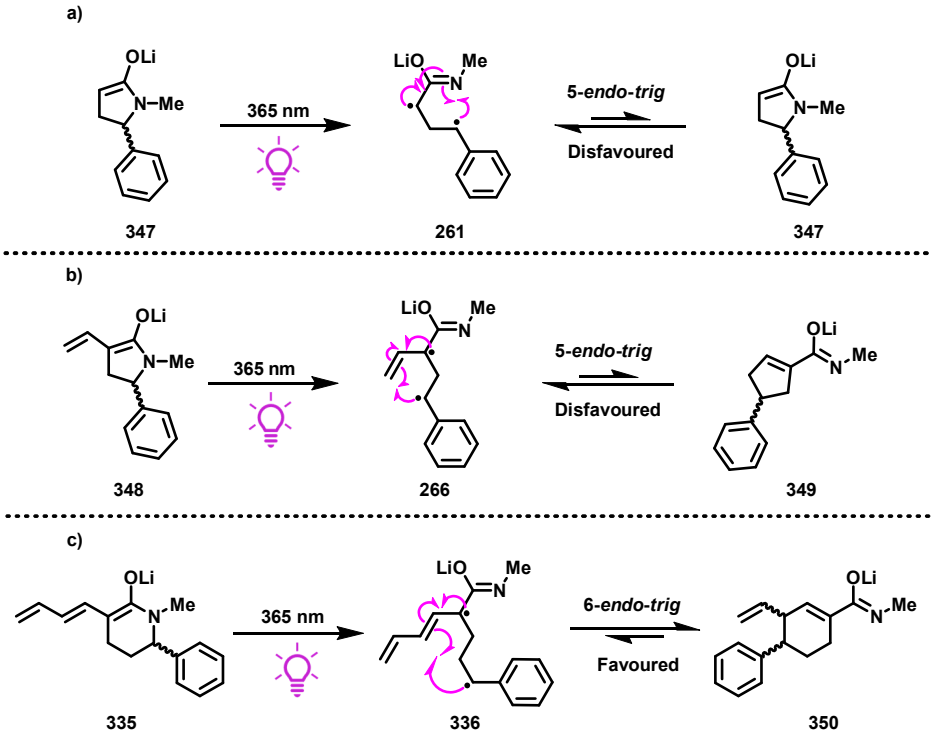

Scheme 93: a) The disfavoured 5-endo-trig *cyclisation to reform 5-membered lactam monoenolate **347**. b) The disfavoured* 5-endo-trig *cyclisation which would give "ring-swing" product **349** via diradical **266** from 5-membered lactam dienolate **348**. C) The favoured* 6-endo-trig *cyclisation to give "ring-swing" migration product **350** via **336** from six-membered lactam trienolate **335**.*

The photochemical inactivity of six-membered monoenolates may also result from the lack of a Thorpe-Ingold effect, which is strengthened by the presence of an additional chromophore in trienolates, thereby favouring ring contraction. This effect likely induces a sterically favoured conformation that facilitates ring contraction and "ring-swing" rather than the reformation of the starting material. However, this hypothesis requires further investigation to confirm its validity.

5.6. Six-Membered Lactam Dienolate Ring-Contraction

Given the lack of photoreactivity of the monoenolate of six-membered lactam **329** compared to the successful reactivity of trienolate **335**, we sought to determine whether a dienolate such as **355** would exhibit the desired reactivity (Scheme 94). To explore this, alkenyl lactams **351** and **352** were synthesised via aldol addition and elimination on lactam **329**, following the established procedure. This resulted in the *cis*- and *trans*-isomers of the desired conjugated lactam **351** and **352**, in yields of 21% and 46%, respectively.

TDDFT analysis of dienolate **355**, derived from lactam **351** predicted a λ_{max} of 346 nm, closely matching the value calculated for the five-membered equivalent, yet a clear UV-Vis trace could not be obtained as per other examples of lactam-based enolates. With the chromophore installed, deprotonation with LiHMDS followed by irradiation at 365 nm for two hours afforded expected ring-contraction products **353** in 30% yield, via enolate **355** and diradical **356**, with high diastereoselectivity (83:17) for the isomer bearing a *cis*- relationship between the aryl ring and alkene. Interestingly, this stereochemical outcome is opposite to that observed with five-membered lactam dienolates, where the aryl ring and alkene were *cis*- in the major diastereomer of cyclopropyl product. Additionally, the "ring-swing" product **354** was isolated in 21% yield.

The higher yields obtained for dienolate ring-contraction, compared to mono- and trienolates, support the idea that dienolates provide greater radical stability due to resonance conjugation, without excessive conjugation that would promote undesirable polymerisation of radical intermediates, such as that observed with their trienolate equivalents.

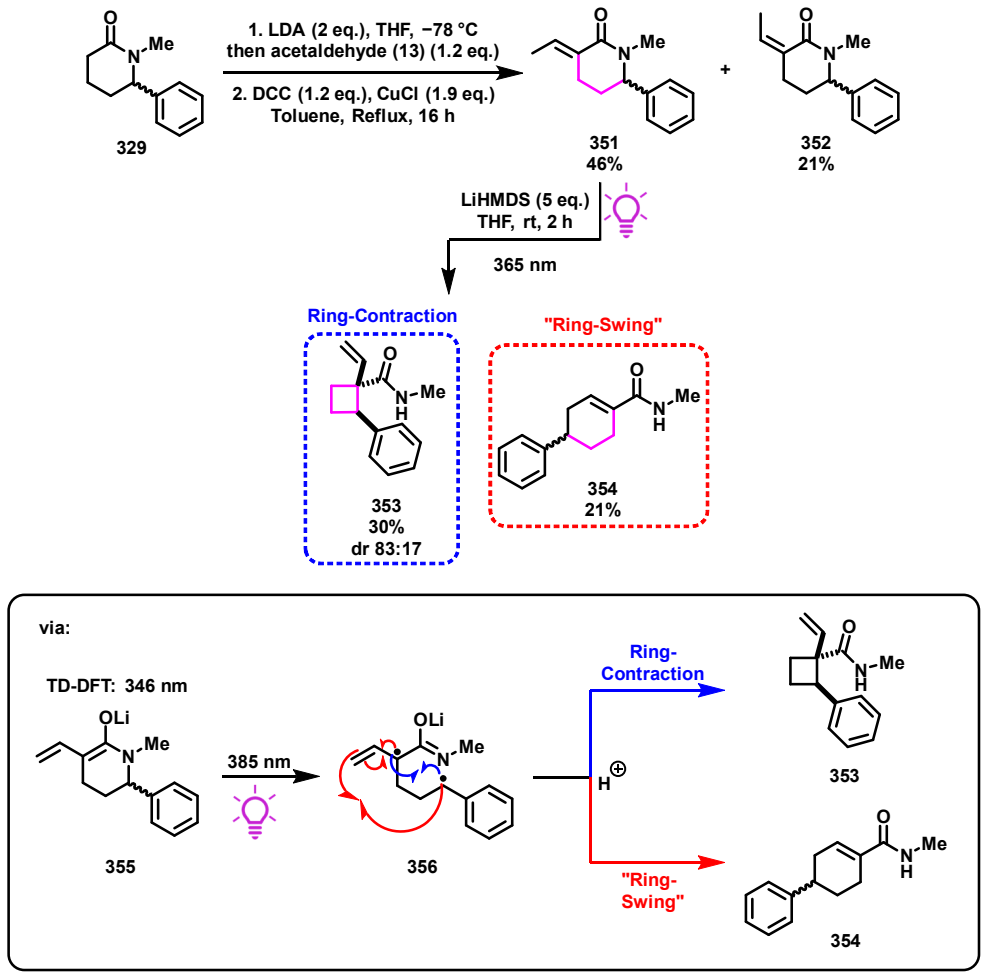

*Scheme 94: The synthesis of alkenyl lactams **351** and **352** followed by the photochemistry on the respective enolate of **351**.*

Unfortunately, optimisation attempts to improve the overall yield or selectivity for the ring-contraction products **353** were unsuccessful. Varying temperature (−78 °C to rt), base equivalents (1 to 10 eq.), base type (LiHMDS, KHMDS, LiOtBu), reaction time (1 to 5 hours), reaction concentration (50 mM to 500 mM), and solvent (THF, MeCN, CH_2Cl_2, Et_2O) resulted in no improvement. Yields and product selectivity remained consistent across all conditions, suggesting that polymerisation is competitive with the desired photochemistry and occurs rapidly, irrespective of the reaction conditions. Notably, this ring-contraction occurred successfully following enolate formation by KHMDS and irradiation. Although the photochemistry on the corresponding potassium enolate provided poorer yields at room temperature over two hours (20% for **353** and 10% for **354**), it is pleasing that enolate photochemistry is shown to not be limited to just lithium-based enolates. Due to the failure to increase yields from this study, the standard mild conditions used for the ring contraction of five-membered lactam dienolates (Section 5.3) were adopted as the standard protocol, as shown in Scheme 94.

While it was encouraging to observe ring contraction to cyclobutanes from six-membered lactams bearing di- and trienolate motifs, the lower yields compared to the five-membered dienolate ring contractions indicate that further exploration of cyclobutane formation via photochemistry was deprioritised in favour of expanding the scope of five-membered ring contractions.

5.7. Enol Ethers as Alternatives to Enolates for Photochemical Reactivity

All cases of enolate photochemistry carried out in this project have involved the direct irradiation of an enolate species, rather than the use of enolate equivalents such as enol ethers. Direct enolate photochemistry ensures that the starting material does not absorb within the irradiation window, while the enolate, with its extended conjugation, selectively absorbs visible light within the range of the irradiation source. This minimises the risk of unwanted photochemical processes and ensures that only the target species is excited during irradiation.

Nonetheless, the potential to carry out the ring-contraction photochemistry discussed in Section 5 using an enolate equivalent as the photoreactive species, is an intriguing possibility. This would broaden the scope of reactivity beyond enolates that absorb visible-light.

Silyl enol ethers, similar to enamines, are electron-rich alkenes due to the conjugation of a heteroatom with their double bond. This conjugation often results in a longer wavelength absorbance in the electromagnetic spectrum compared to their alkenyl equivalents.[109] Additionally, silyl enol ethers generally exhibit greater stability than enolates, which are typically unstable at room temperature and in the presence of air.[110] Therefore, we considered silyl enol ethers to be a promising alternative to enolates, potentially overcoming the issues of enolate instability that may be limiting the yields of some photochemical processes.

The ability to isolate silyl enol ethers such as **357** prior to simply dissolving and irradiating them to initiate photochemistry to afford cyclopropanes **258** and **259** is particularly advantageous, as it eliminates the need for *in situ* deprotonation before irradiation (Scheme 95). This stability may enable successful photochemical reactivity at room temperature—conditions that have not been feasible with some of the more unstable enolate substrates discussed in Sections 4 and 5.

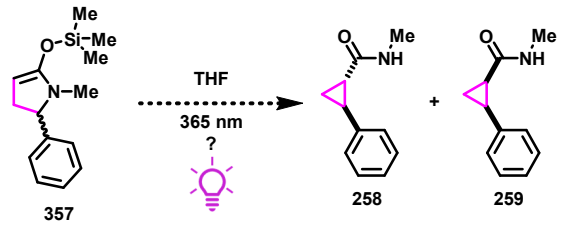

*Scheme 95: The potential ring-contraction of a lactam silyl enol ether **357**.*

While this approach appears operationally simple and promising, there are few examples of silyl enol ether formations involving amides. This scarcity is primarily due to the increased propensity for C-silylation over the desired O-silylation, since the nitrogen atom in an amide enolate enhances electron density and nucleophilicity at the enolate carbon.

Despite this challenge, we attempted to isolate some O-silylated enol ethers based on a literature study by Woodbury *et al*.[111] In their report, various amides were silylated with TMSCl and TBSCl, resulting in different ratios of C- and O-silylation (Scheme 96). The authors highlighted that the amide structure significantly influenced silylation selectivity. For instance, silylation of *N*,*N*-dimethylacetamide **358** produced a 93:7 ratio of C- to O-silylated products **359** and **360**, whereas silylation of *N*,*N*-dimethylbutyramide **361** yielded almost exclusively the O-silylated product **363**, rather than C-silylated **362**. Furthermore, upon heating, O-silylated enol ethers often isomerised to the more thermodynamically stable C-silylated products within a short time frame (less than one hour). This underscores the difficulties in isolating O-silylated enol ethers derived from certain amides and the potential challenges associated with their storage over time.

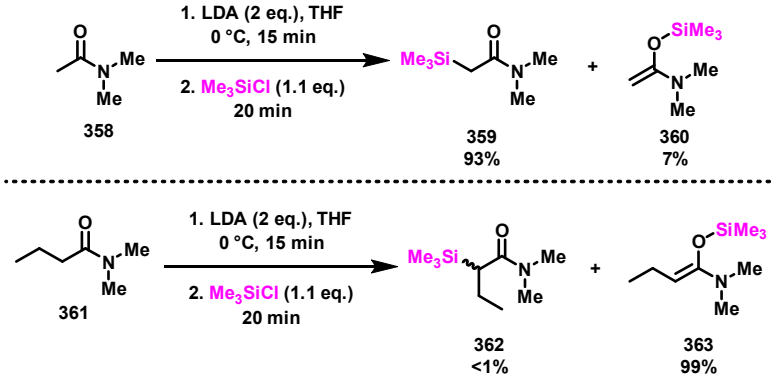

*Scheme 96: The reported O- and C-silylation of amides **358** and **361**, showing their significantly different ratios of the two product-types.*[111]

Despite these challenges, we aimed to silylate five-membered lactam **254**, which lacks an extended chromophore, at oxygen to obtain a stable O-silyl enol ether suitable for photochemical ring

contraction. Silylation was attempted using LDA and TMSCl, but this resulted in the formation of two diastereomers of the C-silylated product **364** (Scheme 97). Unfortunately, no O-silylated product was detected.

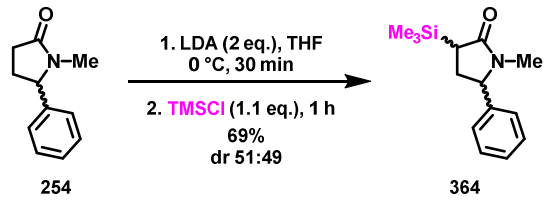

*Scheme 97: The silylation of lactam **254**, giving a mixture of diastereomers of C-silylated product **364**.*

This result suggests that the enolate of lactam **254** has a strong preference for C-silylation with TMSCl, making it unsuitable for a study on the photochemistry of silyl enol ethers. Consequently, we attempted to silylate the enolate of *N*-benzyl amide **126** that was extensively investigated in Section 4 for its photochemistry. However, deprotonation with LDA followed by silylation with TMSCl or TBDMSCl resulted in a complex mixture, with no distinct silylation products, such as enol ether **365**, identifiable (Scheme 98). This complexity may arise from the extended chromophore, which allows silylation at multiple positions along the enolate chain, leading to a mixture of various silylation products.

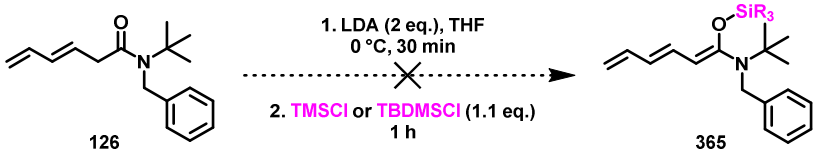

*Scheme 98: The attempted silylation of acyclic dienyl amide **126**, giving a complex crude mixture with undeterminable products.*

Due to the challenges associated with selective O-silylation of certain amides and the difficulties encountered in silylating two key structures in our photochemistry studies, this line of research was set aside. Future investigations could explore the formation of silyl enol ethers on a broader range of substrates, as well as the use of alternative silylating agents which have the potential to favour O-silylation.

5.8. Electrocyclic Ring-Opening of Lactam Dienolates

The ring-contraction photochemistry explored thus far has relied on an alkenyl group external to the lactam ring to provide the extended chromophore necessary for the desired photochemical reactivity. A logical extension of this approach is to investigate the potential for photochemical rearrangement of a dienolate lactam such as **367** from **366**, where both double bonds are contained within a six-membered ring (Scheme 99). This configuration should allow for absorption at an appropriate wavelength, while potentially enabling the formation of cyclobutenes such as **368** through radical recombination.

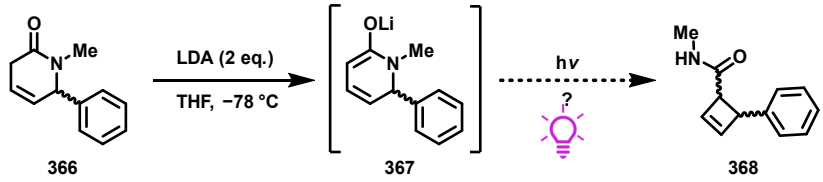

*Scheme 99: The planned photochemical ring-contraction to give cyclobutene **368** from an internal dienolate **367**.*

Cyclobutenes are highly sought-after intermediates in synthetic chemistry due to their pronounced chemical reactivity, which stems from their considerable ring strain. This strain renders cyclobutenes prone to ring-opening metathesis and electrocyclic ring-opening reactions, subsequently generating dienes that can participate in further downstream transformations.[112] Despite their synthetic utility, the preparation of cyclobutene motifs is relatively underexplored, primarily due to their inherent instability. Traditional synthetic routes typically involve [2+2] cycloaddition reactions between alkynes such as **369** and alkenes such as cyclohexene (**370**) to afford, in this case, bicyclic cyclobutene **371** (Scheme 100), which, although straightforward in execution, generally necessitate the use of heavy, precious metal catalysts.[113–115]

An alternative strategy for cyclobutene synthesis involves the migratory insertion of aryl halides such as **372** into cyclobutane-bearing metal carbenes derived from **373**, affording substituted cyclobutene **374**.[116,117] However, this method also requires transition metal catalysts, thereby imposing similar limitations related to cost, toxicity, and environmental impact. Given these constraints, there is considerable interest in developing a transition-metal-free methodology for cyclobutene formation. A protocol relying solely on a mild base and photoinduced ring contraction would present a significant advancement, providing a more sustainable and operationally simple approach to accessing these strained, yet versatile, synthetic intermediates.

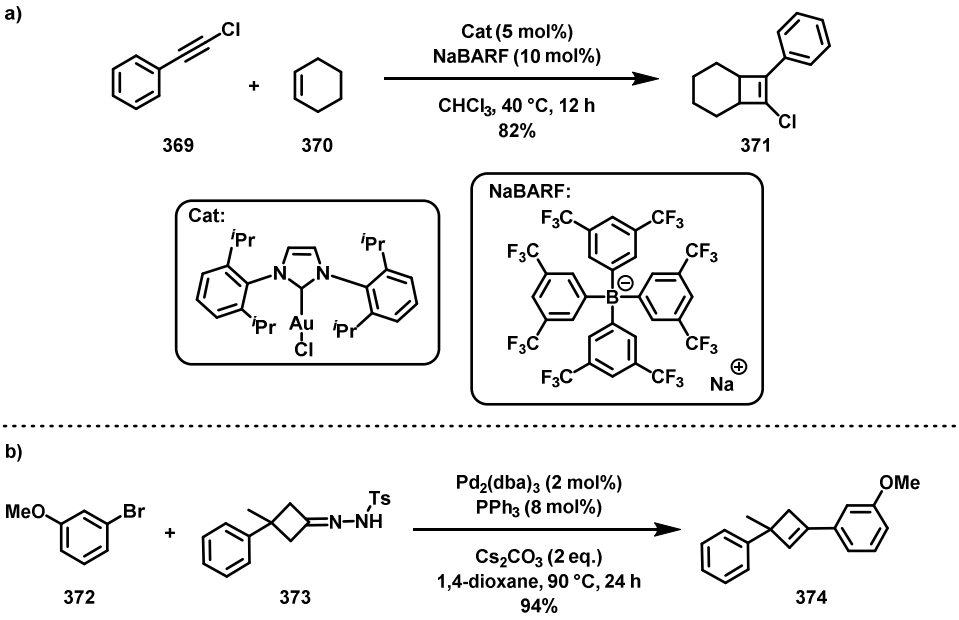

*Scheme 100: Examples of the synthesis of cyclobutenes in literature by a) [2+2] cycloaddition to give **371.** b) Carbene formation and insertion/elimination to give **374**.*[115,116]

Regrettably, there are limited synthetic methodologies available to access the desired six-membered lactam bearing an internal chromophore (**366**). The most straightforward approach to synthesising target alkenyl lactam **366** involves selective iron-mediated Grignard addition of phenyl magnesium bromide (**376**) to *N*-methyl-2-pyridone (**375**), as reported by Huang *et al*. (Scheme 101).[118] However, the scope for expanding substrate synthesis is constrained by the limited availability of specific 2-pyridone starting materials.

The resultant pyridone **366** features a double bond adjacent to the benzylic group, which is advantageous for our study since it mitigates the risk of undesired nucleophilic addition onto a conjugated double bond via an aza-Michael addition pathway. The corresponding enolate **367**, with a TDDFT-calculated λ_{max} of 331 nm, was subjected to irradiation at 340 nm, resulting in a mixture of four stereoisomers of ring-opened product (**377**, **378**, **379** and **380**). Irradiation at this wavelength, however, did not drive the reaction to completion. On switching to irradiation with a 365 nm LED, complete conversion was achieved in under three hours. UV-Vis analysis may indicate that the absorbance of **367** better matches the 365 nm LED, but a clear spectra could not be recorded for this enolate, again due to instability.

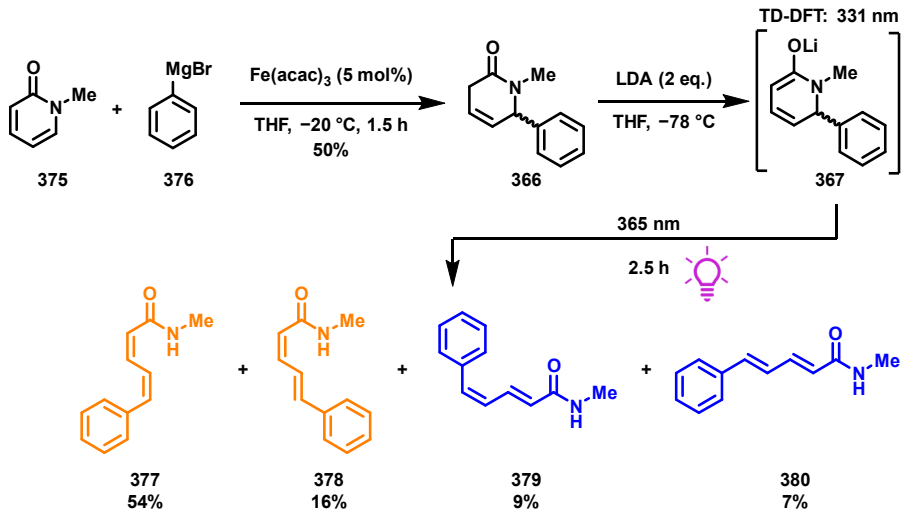

*Scheme 101: The synthesis of alkenyl lactam **366** bearing an internal chromophore and the subsequent photochemistry on enolate **367**.[118] Orange - formed directly on irradiation. Blue - formed on product isomerisation.*

While a non-concerted, radical pathway could theoretically facilitate this transformation, the high yields observed suggest a concerted mechanism in which undesired polymerisation is not a competitive pathway. We therefore hypothesise that this transformation proceeds via a photochemically-driven electrocyclic conrotatory ring-opening mechanism (Scheme 102).

The *Z*,*Z* and *Z*,*E* isomers of ring-opened diene (**377** and **378**, orange) are likely formed directly via a 6π-conrotatory electrocyclic ring-opening, whereas the *E*,*Z* and *E*,*E* isomers (**379** and **380**, blue) are generated through photochemical isomerisation of the initial product mixture. This isomerisation was validated by irradiating a mixture of *Z*,*Z* and *Z*,*E* isomers **377** and **378** at 365 nm, which resulted in partial conversion to *E*,*Z* and *E*,*E* isomers **379** and **380**, as anticipated.

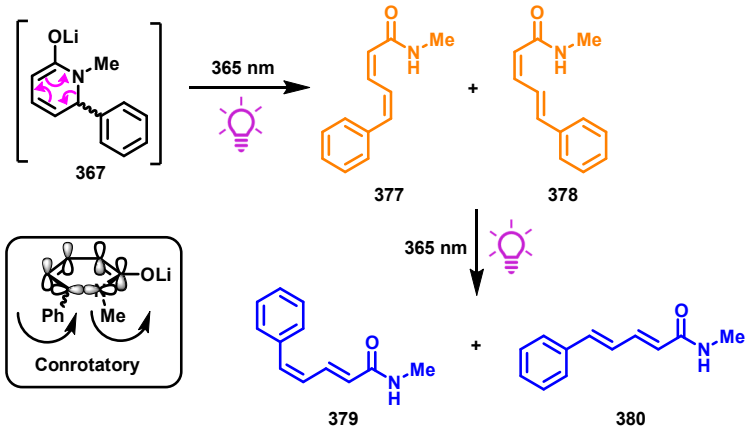

*Scheme 102: A possible electrocyclic ring-opening mechanism for ring-opening of dienolate **367**, followed by photochemical isomerisation of product isomers **377** and **378**.*

With this novel enolate reactivity established, we sought to investigate lactam analogue **381**, bearing a vinyl group in place of a benzyl, to determine whether this reactivity is a generalisable process or specific to substrate **366** (Scheme 103). Following a protocol by Sośnicki *et al*., we performed a regioselective addition of a vinyl "ate" complex to *N*-methyl-2-pyridone (**375**), successfully installing a vinyl group adjacent to nitrogen in **381** in 65% yield.[119] Lactam **381** was then subjected to deprotonation and irradiation, affording three isomers of ring-opened product **383**, **384** and **385**, once again in high overall yield.

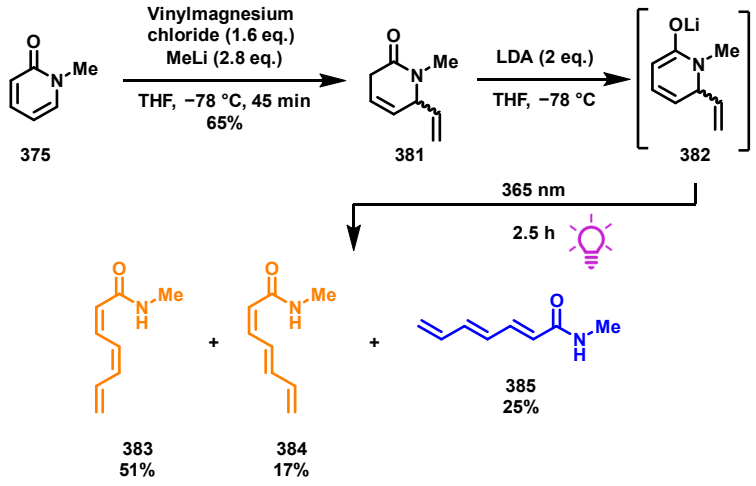

*Scheme 103: The synthesis of lactam **381** bearing a vinyl group adjacent to nitrogen, followed by the photochemical ring-opening of enolate **382**.*

Notably, this reaction did not yield any detectable amounts of the *E*,*Z* isomer that was observed when a phenyl group was positioned adjacent to nitrogen in **366**. This outcome is likely due to a thermodynamic preference for the formation of *E*,*E* isomer **385** during isomerisation, since in this case rotation around a bulky phenyl group is not required to achieve the energetically favoured *E*,*E*-product isomer.

The consistently high yields observed in these reactions further demonstrate the potential versatility of this process. If the mechanism is indeed concerted and does not proceed via a radical intermediate, then the identity of the substituent adjacent to nitrogen should have minimal impact on the reaction outcome. The ability to achieve ring-opening of the six-membered ring, irrespective of the substituent adjacent to nitrogen, would suggest a highly adaptable process. However, the limited availability of suitable starting materials, coupled with the fact that the photochemical products are not of significant synthetic interest, led to the decision not to pursue this study further.

Future work could involve exploring alternative synthetic routes to access the required unsaturated lactams, followed by screening the photoreactivity of a broader range of substrates with varying substituents within the ring to produce ring-opened products.

5.9. Summary of Lactam-Based Photochemistry

Our exploration of enolate photochemistry has been expanded by incorporating one or more enolate double bonds within a lactam ring system. This approach has enabled a range of transformations contingent on the nature of the chromophore and ring size, leading to some of the highest yields and most compelling outcomes reported in the field of enolate photochemistry. Below is a summary of the key results and insights derived from our investigations into lactam-based photochemical processes.

Five-Membered Lactams

- Trienolate **386**, derived from five-membered lactam **245** was ring-contracted with 385 nm irradiation, albeit in a poor yield and with a very complex reaction profile, most likely due to polymerisation of intermediate radicals (Scheme 104).

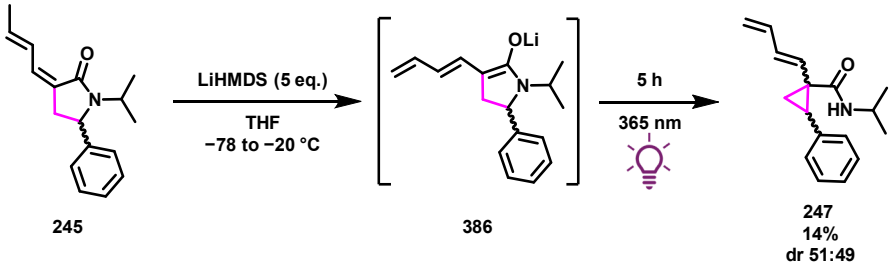

*Scheme 104: The photochemistry on trienolate **386**, derived from lactam **245**, giving ring-contraction to **247**.*

- Ring-contraction was also possible on monoenolate **347** (derived from lactam **254**) at 365 nm with no extended conjugation to afford **258** and **259**, albeit with persistent starting material **254** (Scheme 105).

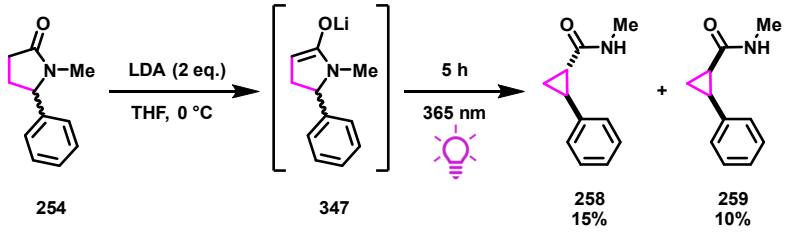

*Scheme 105: The five-membered lactam monoenolate ring-contraction on **347** to afford two diastereomers of ring-contraction product **258** and **259**.*

- Upon irradiation at 365 nm, dienolate **348**, derived from alkenyl lactam **262** underwent the anticipated ring-contraction, producing a near-equimolar mixture of diastereomers with a commendable yield of 66% for **264** (Scheme 106). The mild and operationally straightforward reaction conditions facilitated the successful implementation of this photochemical transformation in a continuous flow system.

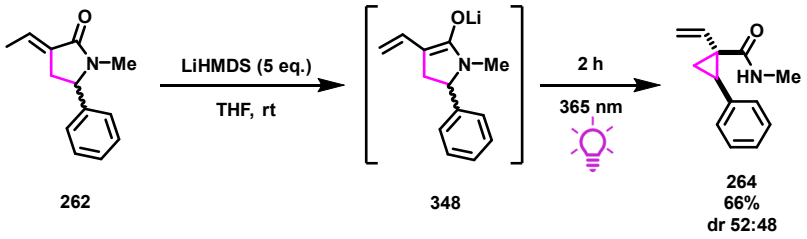

*Scheme 106: Ring-contraction on dienolate **348**, derived from five-membered lactam **262**, giving **264** as a diastereomeric mixture.*

- Dienolate ring-contraction was effective with various migrating groups, including a thiophene moiety in **276**. However, the potential for radical dehalogenation prevented the formation of any product when using a *para*-chloro phenyl migrating group as in **274**.
- Increasing steric bulk around the chromophore resulted in only modest improvements in diastereoselectivity (up to 58:42). In contrast, introducing substituents within the lactam ring enhanced both the yield (71%) of cyclopropyl product **323** and the diastereomeric ratio between **323** and **324** (89:11) (Scheme 107).

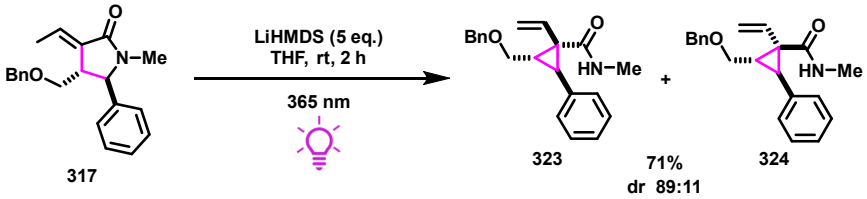

*Scheme 107: The ring-contraction on the dienolate of five-membered lactam **317**, which bears substitution in the lactam ring, offering a good yield and high diastereoselectivity for **323**.*

Six-Membered Lactams

- Irradiation of trienolate **335**, derived from six-membered lactam **332** at 385 nm induced ring contraction to **333**, and resulted in the formation of "ring-swing" product **334** due to radical recombination along the chromophoric chain (Scheme 108).

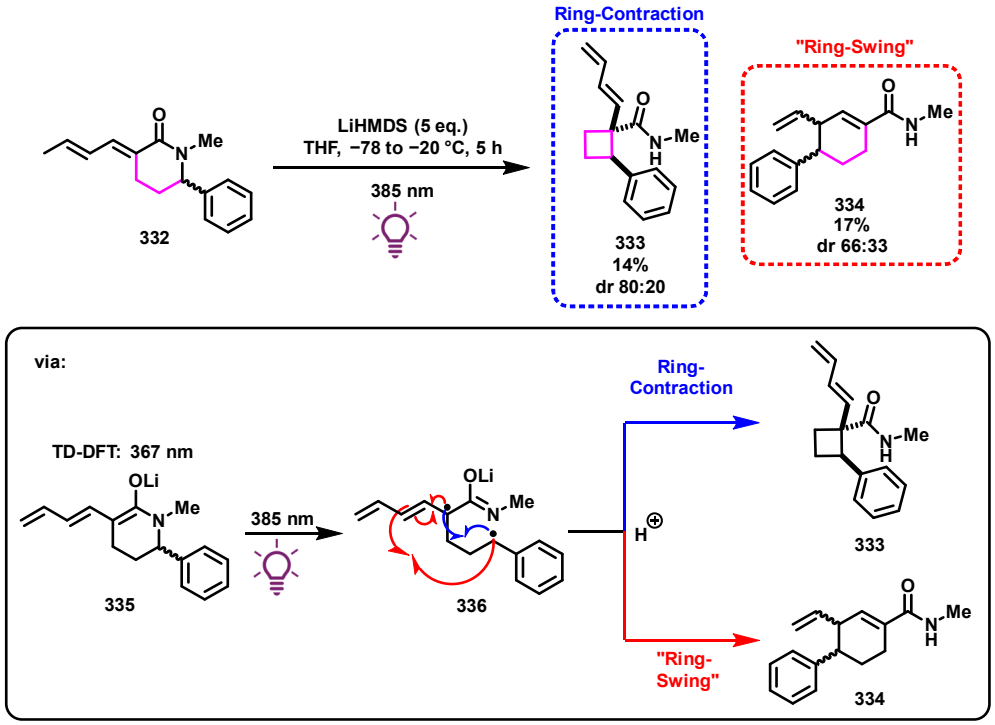

*Scheme 108: The photochemistry of trienolate **335**, giving ring-contraction and migration, with the mechanism for formation of both products **333** and **334** shown.*

- The related six-membered lactam monoenolate did not undergo ring contraction upon irradiation at either 340 nm or 365 nm.
- Irradiation of dienolate **355**, derived from alkenyl lactam **351** at 365 nm afforded ring-contracted cyclobutanes **353** in 30% yield with high diastereoselectivity (83:17), alongside a "ring-swing" product **354** in 21% yield (Scheme 109). While this represents an improvement over the six-membered trienolate photoreactivity, it remains inferior to five-membered lactam ring-contractions, which demonstrated superior yields and a cleaner reaction profile.

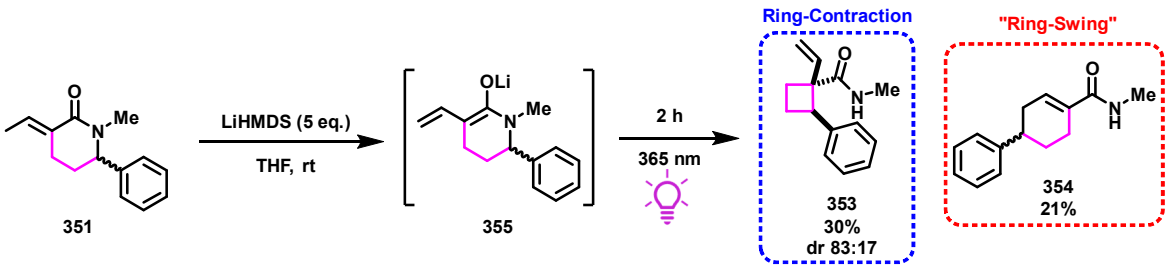

*Scheme 109: Ring-contraction and migration on dienolate **355**, derived from alkenyl lactam **351**, giving cyclobutanes **353** with good diastereoselectivity and **354** as the "ring-swing" product.*

A summary of the photochemical prowess of the key enolates discussed in this Section is displayed in Table 5.

Ring-Contraction Summary

Table 5: Key enolates studied for their ring-contraction in this section, and their photochemical output.

Enolate	λ_{max} Calculated (TDDFT) / nm	Ring-Contraction Yield	"Ring-Swing" Yield	Notes
	367 (Irradiation at 385 nm)	14% (dr 51:49)	-	Complex reaction profile.
	320 (Irradiation at 365 nm)	25% (dr 60:40)	-	Recovered starting material **254** (25%).
	340 (Irradiation at 365 nm)	66% (dr 52:48)	-	Mild reaction conditions (rt for 2 hours).
	See dienolate **348**	71% (dr 89:11)	-	Improved yield and diastereoselectivity from **348**.

	367 (Irradiation at 385 nm)	14% (dr 80:20)	17% (dr 66:33)	Complex reaction profile.
	See trienolate **335**	2% (Only 1 diastereomer isolated)	39% (dr 50:50)	Greater regioselectivity for the "ring-swing" product.
	335	-	-	No reactivity, recovered starting material **329**.
	346 (Irradiation at 365 nm)	30% (dr 83:17)	21%	Mild reaction conditions (rt for 2 hours).

- Formation of enolate **367**, featuring a purely internal chromophore within a lactam ring, results in an electrocyclic ring-opening, yielding a range of diene products (**377**, **378**, **379** and **380**) with an aryl group adjacent to the lactam nitrogen (Scheme 110) and a series of triene products (with a vinyl group adjacent to lactam nitrogen).

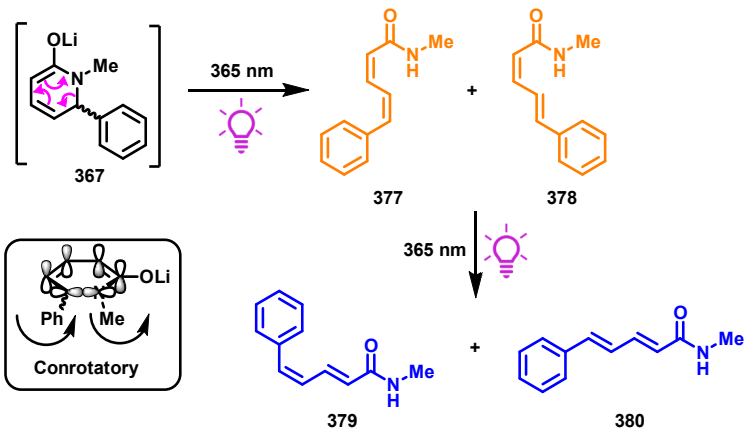

*Scheme 110: A possible electrocyclic ring-opening mechanism for ring-opening of dienolate **367**, followed by photochemical isomerisation of product isomers **377** and **378**.*

- This reaction potentially offers significant versatility, as it likely does not proceed via a radical mechanism and is therefore not constrained by the limitations governing radical enolate

photochemistry. This implies that any substituent could be positioned adjacent to the nitrogen, followed by subsequent enolate ring-opening, provided suitable starting materials or synthetic routes for their preparation are available.

Although lactam-based photochemistry has predominantly focused on five- and six-membered rings, the potential for ring contraction of a seven-membered lactam enolate warrants consideration. However, the synthesis of such lactams is scarcely documented in the literature, highlighting the need for further studies to develop robust synthetic methodologies for these seven-membered systems. Should a seven-membered lactam dienolate undergo photochemical reaction, it is anticipated that ring contraction could yield a five-membered ring, potentially accompanied by a "ring-swing" product.

Photochemistry of Enolates Formed by the Dearomatisation of Pyridine Derivatives

6.0. Dearomatising Cyclisation on Pyridines

In Section 1.3, dearomatising cyclisations on aromatic systems were discussed, which proceed via a conjugated enolate intermediate before quenching to yield either a tetrahydroisoindolone or its rearomatised counterpart.[30] While the previously described systems have demonstrated the remarkable dearomatisation of phenyl-based scaffolds, this reaction is not confined to aromatic systems of this type. In 2005, the Clayden group expanded this concept to include the intramolecular dearomatisation of pyridinyl-derived aromatics, such as *N*-benzyl-nicotinamides, isonicotinamides, and picolinamides.[34]

For example, in the case of isonicotinamide derivative **387**, the addition of various electrophiles to the reaction mixture resulted in the formation of a spirocyclic β-lactam **389** via intermediate **388**. This transformation occurs due to the conjugation of the π-system onto the pyridinyl nitrogen, which becomes positively charged upon reaction with an electrophile (Scheme 111). In contrast, quenching with ammonium chloride led exclusively to the expected cyclisation product **391** via enolate intermediate **390**.

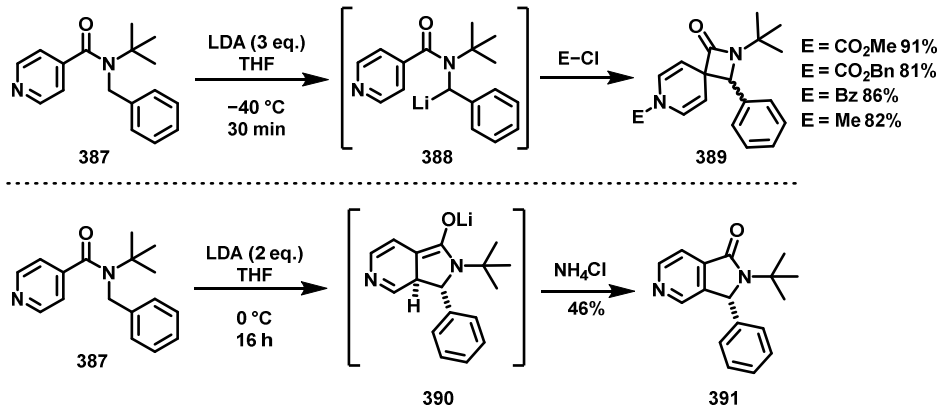

*Scheme 111: The cyclisation on pyridine **387**, with different products based on electrophilic attack.* [34]

The other two pyridine-based benzyl amides, the nicotinamide and picolinamide equivalent, when subjected to basic conditions, consistently reacted through a conjugated enolate intermediate to yield a rearomatised bicyclic lactam, similar to benzyl bezamides. However, the dearomatisation of these

pyridine-based precursors required more forcing conditions, including higher temperatures and extended reaction times, to achieve high conversion to the bicyclic products.

While this reaction is synthetically valuable on its own, the ability to form a bicyclic dearomatised analogue—by circumventing the rearomatisation step after cyclisation—could provide greater synthetic utility. This analogue could allow for further functionalisation and reactivity via a diene (or enone) motif. To investigate this potential, methoxy-isonicotinamide **392** was subjected to dearomatisation by previous members of the Clayden group, resulting in the formation of dearomatised enolate **393**, which subsequently hydrolysed upon purification to yield bicyclic lactone **394** (Scheme 112). The introduction of the methoxy group disfavourably influenced the rearomatisation step by stabilising a canonical form where a carbonyl replaces the methoxy substituent.

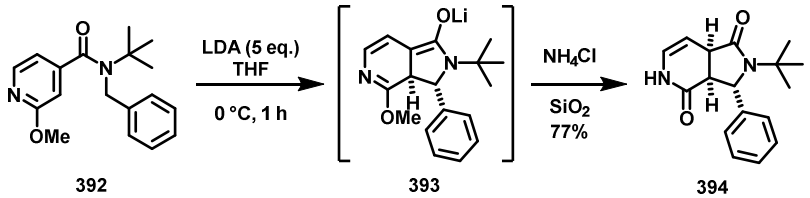

*Scheme 112: Cyclisation on methoxy pyridine **392**, avoiding product rearomatisation.*

6.0. Photochemical Azepine Synthesis from Pyridines

The dearomatisation observed in pyridinyl amides is of particular interest, primarily due to the conjugated enolate intermediates formed during the reaction. These enolates bear a close structural resemblance to benzyl benzamide enolates, which the Clayden group has extensively studied for their photochemical reactivity. Consequently, we hypothesised that irradiating these pyridinyl enolates could produce analogous reactivity, potentially leading to the formation of seven-membered nitrogen-containing rings, such as azepines. Azepines are well-established pharmacophores, particularly noted for their therapeutic applications in treating depressive disorders, certain types of cancer, and microbial infections.[120–126] For example, Carbamazepine (**395**) acts as a treatment for epilepsy, Imipramine (**396**) behaves as a treatment for depression, and azepine **397**, bearing two ester groups on the ring, operates as an anti-microbial (Figure 14).[124–126]

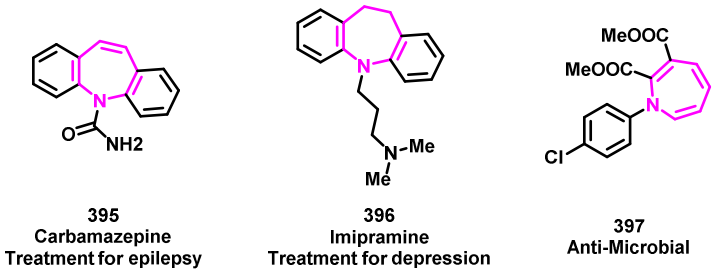

395
Carbamazepine
Treatment for epilepsy

396
Imipramine
Treatment for depression

397
Anti-Microbial

Figure 14: Examples of azepine-based drug targets and their applications.[124–126]

Although azepines are prevalent in medicinal chemistry, the methodologies for their synthesis remain relatively limited. Most synthetic routes require starting materials containing a nitrogen group, such as an azide, strategically positioned on an aromatic ring. Azepines can then be synthesised via various methods, including photochemical ring-expansion, nitrene insertion, or Michael addition-cyclisation cascades.[127–130]

For instance, the mechanism of a photochemical ring-expansion to produce azepines is illustrated in Scheme 113. Here, electron-deficient aryl azide **398** is irradiated with light to generate triplet nitrene **399**, which reacts through benzazirine intermediate **400** in resonance with ketenimine **401**. This ketenimine is then converted to substituted azepine **402** upon reaction with a nucleophile.[127] Another example involves the insertion of a nitrene derived from tolyl sulphonyl azide (**403**) into benzene under pressure to afford tolyl azepine **404**.[129] Alternatively, azepine derivatives can be synthesised via an intramolecular Michael addition cascade of tertiary enamide **405**. This process begins with aldol condensation of the aldehyde functionality in **405** with the enolate of **406**, followed by cyclisation with aluminium trichloride, yielding desired substituted azepine derivative **407** in good yield.[130] However, these synthetic methods often require hazardous reagents (e.g., azides), highly electron-deficient starting materials, or extreme conditions such as high temperatures and pressures.

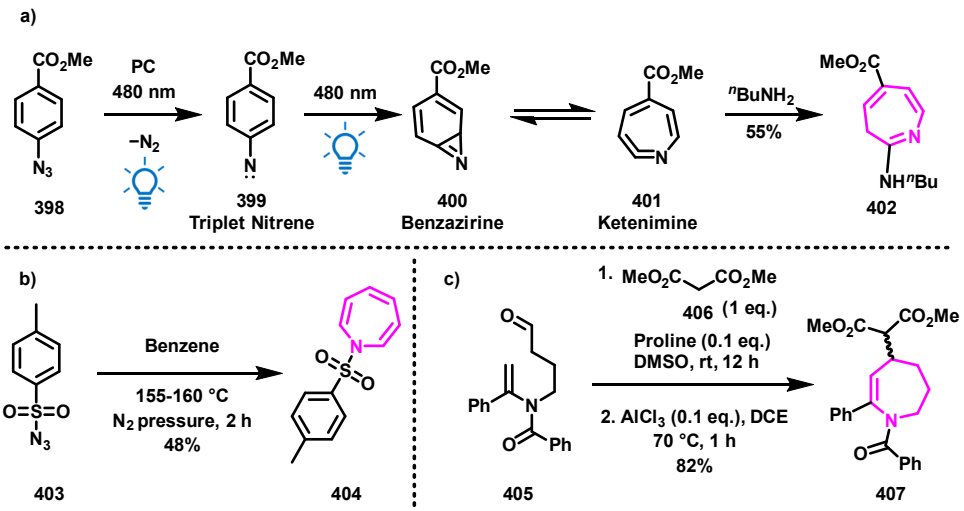

*Scheme 113: a) The mechanism for photochemical nitrene insertion into an electron-deficient aromatic ring to afford azepine **402**.[127] PC = Photocatalyst. b) Sulfonyl nitrene into benzene under pressure to give **404**.[129] c) Aldol condensation followed by a Michael addition-cascade on enamide **405** to afford azepine derivative **407**.[130]*

Consequently, the synthesis of azepines from a pyridinyl amide enolate via deprotonation followed by photochemical irradiation emerged as an appealing target for applying our photochemical methods to. This approach was explored by William Terry-Wright during his MSci project within the Clayden group, under my supervision.[131] In his study, Terry-Wright generated enolates from *N*-benzyl-nicotinamide (**408**), isonicotinamide (**390**), and picolinamide (**409**) and recorded their UV-Vis spectra (Figure 15). The observed λ_{max} values for these enolates were 390, 440, and 462 nm, respectively, which aligned reasonably well with TDDFT predictions of 370, 415 and 430 nm, despite a consistent underestimation of the λ_{max} by 20-35 nm. As a result, azepine synthesis from a simple pyridinyl amide, utilising deprotonation and irradiation, appeared to be an attractive target to apply our photochemical methods to.

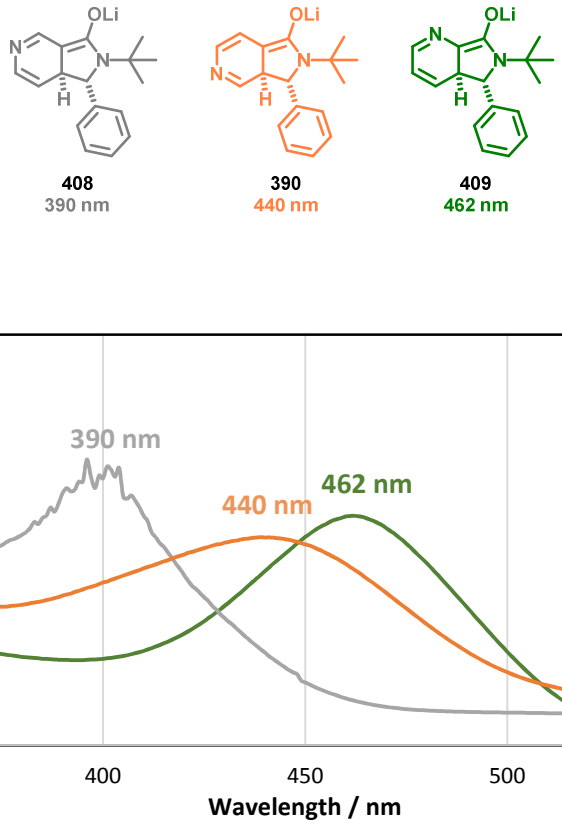

*Figure 15: The experimental UV-Vis spectra of enolates **408**, **390** and **409**, recorded by William Terry-Wright.*[131]

Irradiation of nicotinamide enolate **408** at 385 nm did not alter the outcome of the cyclisation reaction compared to the process conducted in the absence of light, resulting in the formation of the dearomatised bicyclic compound. This outcome can be rationalised by considering the excitation of the chromophore as a π-π* transition, leading to diradical intermediate **410** (Scheme 114). One of these radicals may localise on the nitrogen atom within the dearomatised ring as in **411**. Such localisation stabilises the radical on the nitrogen, potentially preventing the desired bond cleavage needed for the ring-opening step that forms an azepine.

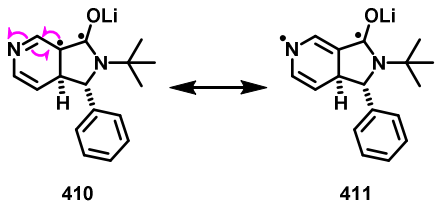

*Scheme 114: Radical delocalisation onto nitrogen in **410** to **411**, meaning desired ring-breakage doesn't occur.*[131]

Irradiation of picolinamide enolate **390** and isonicotinamide enolate **409** at 448 nm over several hours did not result in the formation of azepines. Instead, these photochemical reactions produced a higher

proportion of the starting amide relative to the rearomatised bicyclic product. This suggests that irradiation generated expected diradical intermediate such as **412**, which subsequently fragmented to expel a benzyl radical as in **413** (Scheme 115). The benzyl radical can then be quenched, regenerating the starting pyridinyl amide. While this outcome demonstrates bond cleavage via *in-situ* enolate photochemistry, it does not achieve the specific bond dissociation needed to form an azepine.

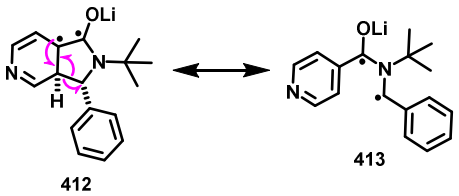

*Scheme 115: Undesired photochemical bond breakage observed on irradiation of enolate **390** via diradical **412** to **413**.*[131]

Although the rearomatisation energy of pyridine is lower than that of benzene,[132] we have observed that tetrahydroindolones formed via dearomatising cyclisation from benzyl benzamides are bench-stable, whereas pyridinyl bicyclic lactams readily undergo rearomatisation during workup and column chromatography.[124] This suggests that the photochemical rearomatisation to regenerate the starting material likely results from the inherent tendency of these dearomatised intermediates to rearomatise.

To overcome this undesired photochemistry, William Terry-Wright utilised ortho-methoxy nicotinamide **392** under the same photochemical conditions. Since bicyclic lactam **394** derived from this methoxy-substituted nicotinamide is resistant to rearomatisation, it was hypothesised that the diradical formed upon irradiation of the corresponding enolate might facilitate the desired bond cleavage, rather than the bond cleavage leading to rearomatisation and recovery of the starting material.

The enolate generated from methoxy nicotinamide **392** exhibited a λ_{max} of 403 nm. Upon irradiation at 405 nm, an inseparable mixture of two regioisomeric azepines (**414** and **415**) was formed (Scheme 116). The major regioisomer (**414**, orange) forms via cyclisation adjacent to the methoxy substituent, followed by irradiation to give **417** via **416**, before radical recombination to produce norcaradiene intermediate **418**, which then undergoes an electrocyclic ring-opening to afford **414**. The minor regioisomer (**415**, green) arises from cyclisation on the opposite side of the molecule, away from the methoxy substituent. The enolate from this pathway undergoes diradical formation upon irradiation, giving **420** via **419** followed by recombination to norcaradiene **421** and a final electrocyclic ring-opening step to afford azepine **415**.

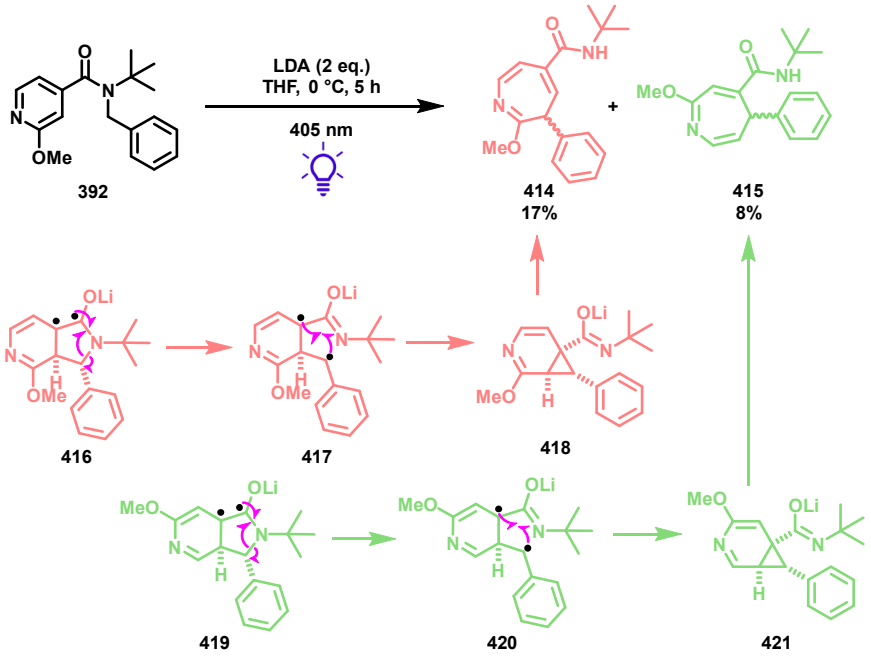

*Scheme 116: The formation of two regioisomeric azepines from targeted irradiation of the enolate of cyclised methoxy nicotinamide **392**, carried out by William Terry-Wright.*[131]

Although the yields of this photochemical reaction have yet to be fully optimised, these results provide a compelling insight into the potential versatility of enolate photochemistry. Beyond the pyridine-based enolate generated through dearomatising cyclisation, MSci student Callum Trent, under my supervision, discovered that the nucleophilic addition of ^{n}BuLi to 2-methoxynicotinamide **422** yielded trienolate **423** (Scheme 117). Upon irradiation, this trienolate underwent a diastereoselective migration of the benzyl group, through **424** followed by radical recombination of **425** and benzyl radical **426**, exclusively forming the *trans*-diastereomer of **427** adjacent to the amide functionality.[133] While the reaction yield remains low, it represents an intriguing example of benzylic migration through space facilitated by enolate formation and subsequent irradiation. However, in this instance, no azepine formation was observed from irradiation of enolate **423**.

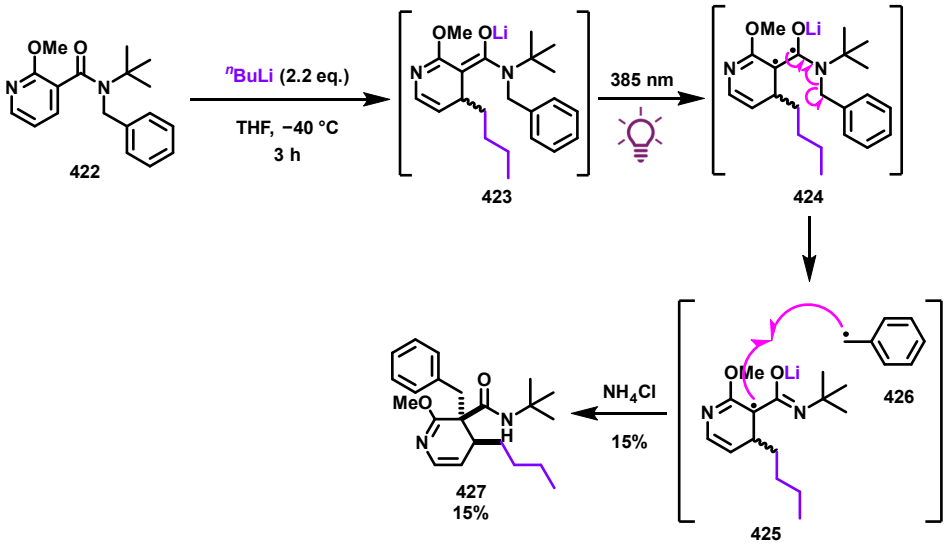

*Scheme 117: The nucleophilic addition of ^{n}BuLi into methoxynicotinamide **422** followed by the proposed mechanism of irradiation and diastereoselective photochemical benzylic migration to give **427**.*[133]

6.1. Quinoline Dearomatisation

In 2005, the Clayden group extended their investigation of the dearomatising cyclisation of pyridinyl amides to quinolines, demonstrating that an analogous reaction is feasible.[34] The cyclisation of quinoline-3-carboxamide **428** proceeded rapidly at −40 °C, leading to the formation of pyrroloquinoline **430** via intermediate enolate **429** (Scheme 118). This transformation was achieved by quenching with ammonium chloride (NH_4Cl), followed by oxidation and aromatisation during the workup and purification. Alternatively, when enolate **429** was quenched with methyl chloroformate, the reaction resulted in substitution at the nitrogen of the quinoline, forming carbamate derivative **431**.

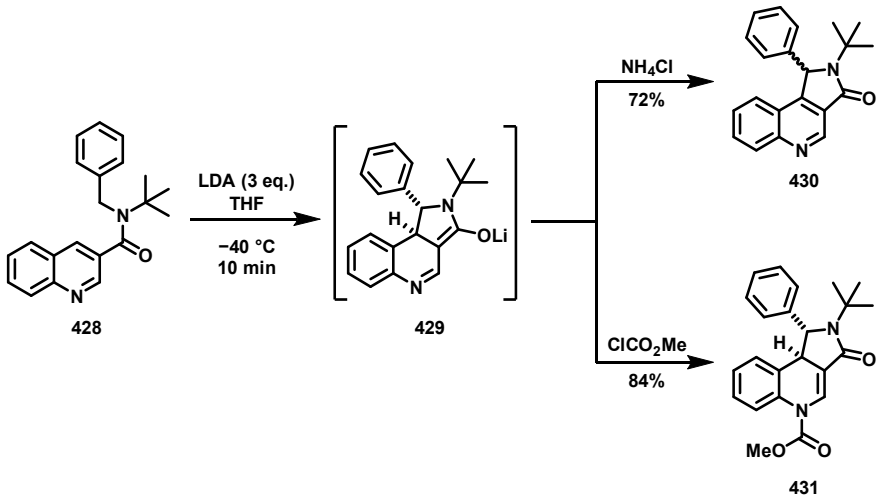

*Scheme 118: The cyclisation of 3-quinoline amide **428**.*[34]

When the reaction was applied to quinoline-4-carboxamide **432** under conditions of higher temperature and extended reaction time, a diastereoselective cyclisation occurred, resulting in the formation of spirocyclic dihydroquinoline **434** via intermediate **433** (Scheme 119). Notably, this cyclisation does not proceed through an enolate intermediate, distinguishing it from other related transformations. In contrast, the cyclisation of quinoline-2-carboxamide **435** generated a highly conjugated enolate **436**, which, upon workup, underwent rearomatisation to produce quinolopyrrolone **437**.

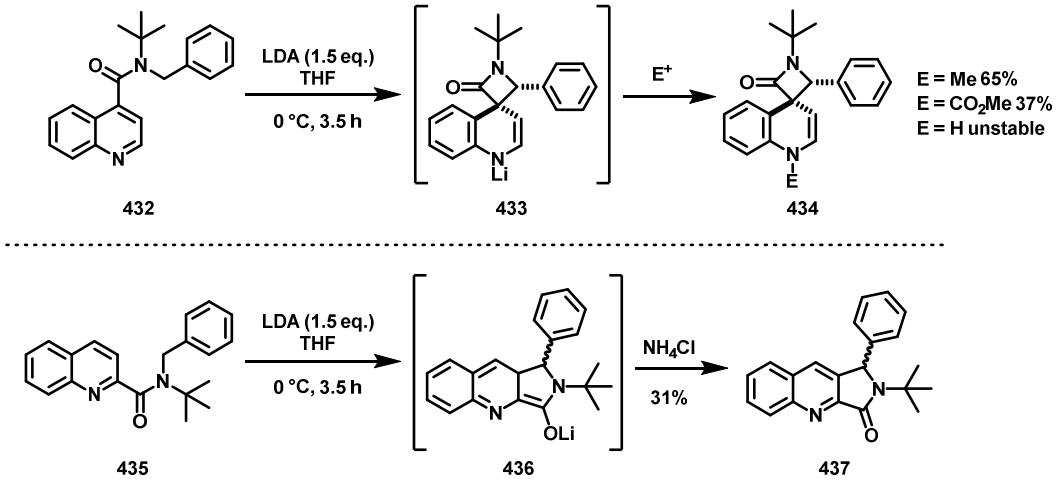

*Scheme 119: The reported cyclisation of 4-quinoline carboxamide **432** and 2-quinoline carboxamide **435**.*[34]

This section investigates the photoreactivity of conjugated enolates generated from the dearomatising cyclisation of 2- and 3-quinoline carboxamides **428** and **435**. Initially, the dearomatisation reaction was carried out for each enolate to confirm that it could be reliably reproduced, successfully forming the desired enolate. Chromoselective irradiation could then be performed on the chromophore of interest. We anticipated that this process could lead to the formation of benzazepines through a reaction cascade previously detailed by the Clayden group (Section 1.4).

Benzazepines, much like azepines, are present in various pharmaceutical treatments, including those for neurodegenerative diseases, allergic reactions, and cancers, and face similar synthetic challenges as azepines.[134] Notable examples include Fedovapagon **438**, a benzazepine-based treatment for nocturia (frequent night-time urination), and Benzazepril **439**, a medication used to manage hypertension (Scheme 120). Developing a method to synthesise benzazepines from commercially available quinoline starting materials through a straightforward deprotonation and irradiation procedure could significantly improve existing synthetic approaches. For instance, irradiation of enolate **429**, derived from the dearomatising cyclisation of quinoline-3-carboxamide **428**, was

envisioned to yield benzazepines such as **441** via an electrocyclic ring-opening of the photochemically-derived norcaradiene **440**.

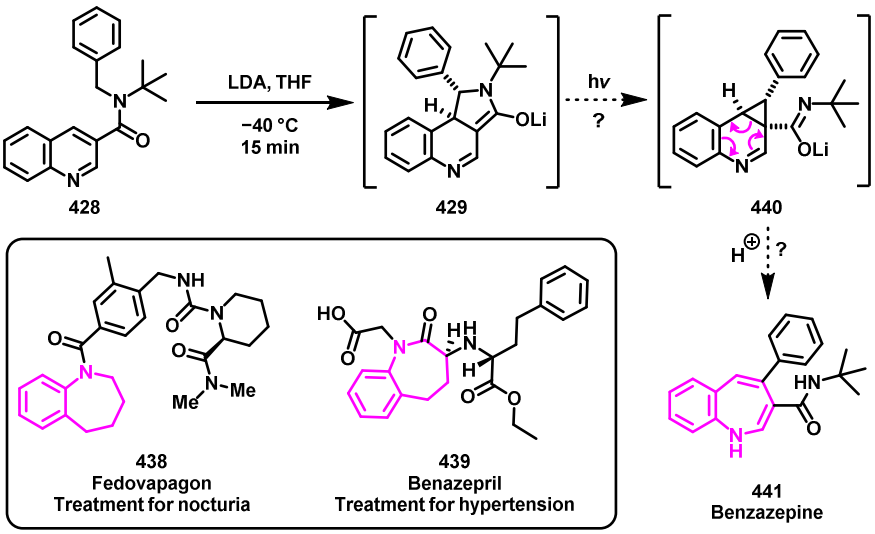

*Scheme 120: The planned photochemical ring-expansion of quinoline-based enolate **428** to benzazepine **441**. Some known pharmaceutical treatments based on benzazepines are shown.*[135,136]

6.2. 3-Quinoline Carboxamide Cyclisation

Initially, the dearomatisation of 3-quinoline carboxamide **428** was investigated, since this substrate provided the highest yield for the cyclised product (74%) in the published literature.[34] Upon addition of the substrate to a solution of lithium diisopropylamide (LDA), the reaction mixture rapidly developed a vivid, deep purple colour, indicating the rapid formation of the enolate and its strong absorption of visible-light.

After 15 minutes, the reaction was quenched, followed by purification, which yielded an inseparable mixture of two compounds (Scheme 121). The major product was dearomatised dihydroquinoline **443**, while the minor product was its rearomatised counterpart **444**, formed via enolate **442**.

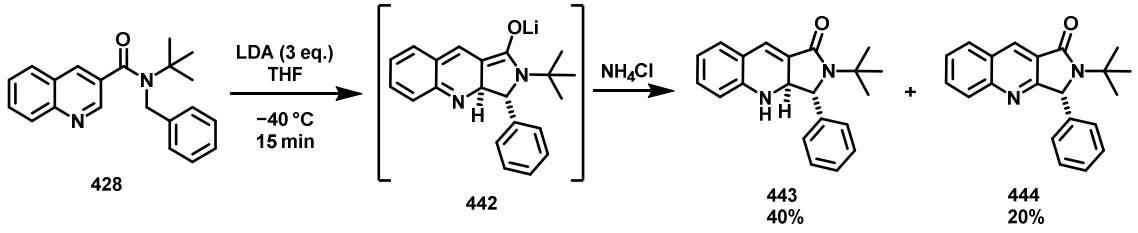

*Scheme 121: Observed cyclisation of 3-quinoline carboxamide **428**, giving cyclisation at an unexpected position.*

It was also found that leaving dihydroquinoline **443** in a solution of ethyl acetate (EtOAc) overnight led to its complete conversion to quinolopyrrolone **444**. Although rearomatised product **444** was initially thought to have the structure reported by the Clayden group (**430**), single-crystal X-ray crystallography confirmed that the organolithium attack had occurred adjacent to the nitrogen atom, rather than at the 4-position as previously described by the Clayden group (Scheme 122).[34]

The observed preference for attack adjacent to the nitrogen in quinoline **428** can be attributed to the increased electrophilicity and reduced steric hindrance at the carbon next to the nitrogen. After confirming the correct product and, consequently, the enolate intermediate by which it is formed (**442**), a UV-Vis spectrum was recorded, revealing a distinct λ_{max} of 523 nm. The TDDFT prediction slightly underestimated this value, giving a λ_{max} of 478 nm. The enolate formed by an attack at the 4-position of quinoline (**429**) has a TDDFT-predicted λ_{max} of 372 nm. This significant discrepancy between the recorded enolate absorbance and the predicted value for the 4-position attack provides additional evidence that the enolate formed in this cyclisation indeed arises from an attack at the 2-position rather than the 4-position.

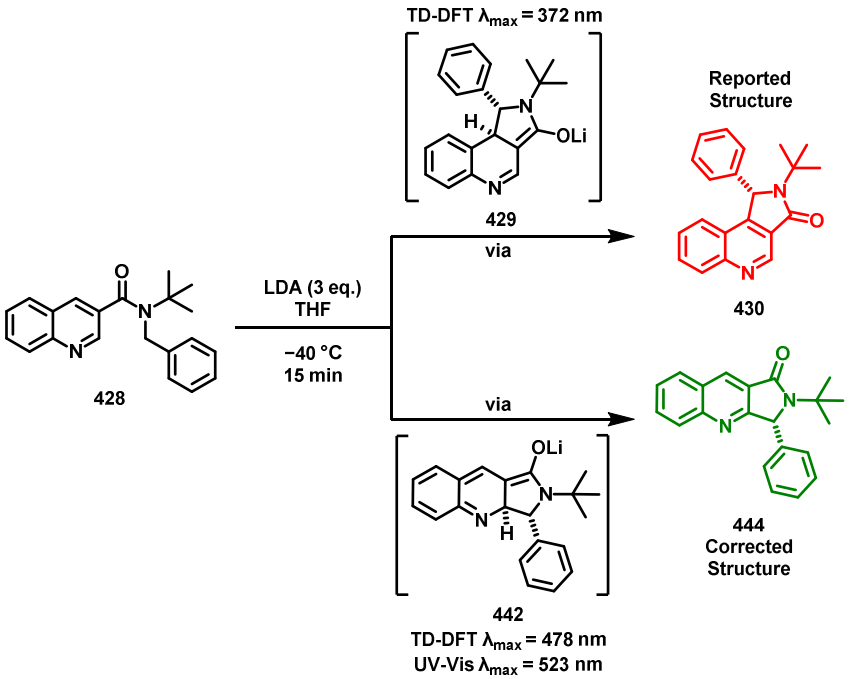

*Scheme 122: The comparison between reported structure for 3-quinoline cyclisation product **430** from literature and the corrected structure **444** determined here.[34] The λ_{max} values of each respective enolate are reported.*

With the optimal irradiation wavelength determined, the next step was to investigate the effect of light on enolate **442**. However, irradiation of the mixture at 530 nm for three hours at −40 °C resulted in no observable change, with the product mixture still predominantly consisting of the dearomatised dihydroquinoline **443** and its rearomatised equivalent **444**.

This outcome aligns closely with the work of William Terry-Wright in the Clayden group on pyridinyl enolates, where irradiation of nicotinamide enolate **390** similarly resulted in no reactivity, likely due to radical localisation onto the nitrogen atom.[131] In the present case, upon irradiation of enolate **442**, one of the radicals formed may localise on the nitrogen, leading to a more stable diradical intermediate **446** via **445** (Scheme 123). This additional stability may reduce the likelihood of radical recombination, thereby hindering the formation of the norcaradiene-type structure required for the synthesis of the desired benzazepine.

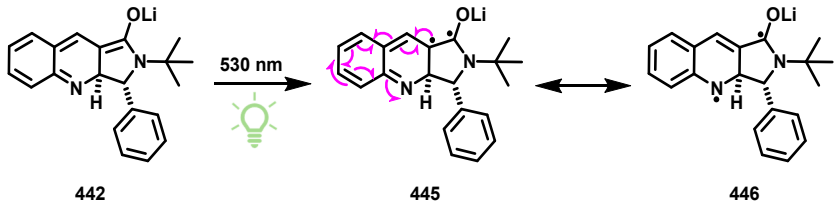

*Scheme 123: Photochemical di-radical formation on **442** to give **445** followed by delocalisation onto nitrogen (**446**), giving rearomatisation of the quinoline ring.*

Future research on the cyclisation and photochemistry of 3-quinoline carboxamides could focus on increasing substitution around the aromatic system. This strategy might reduce electron localisation on the nitrogen, and, provided that the substitution does not hinder cyclisation, facilitate benzazepine formation upon cyclisation and subsequent irradiation. For instance, introducing a methoxy group on the aromatic ring could be a promising modification. This substitution could disfavour rearomatisation of the quinoline ring, thereby promoting the desired photochemical bond cleavage, as demonstrated in the pyridine ring-expansion studies conducted by William Terry-Wright and Callum Trent.[131,133]

Based on the lack of photoreactivity of 3-quinoline-based enolate **442**, it was proposed that the enolate derived from cyclised 2-quinoline carboxamide **436** could exhibit desired photoreactivity, since the enolate diradical formed upon irradiation would not be able to localise on the nitrogen atom.

6.3. 2-Quinoline Carboxamide Cyclisation

The dearomatising cyclisation of 2-quinoline carboxamide **435** was conducted at 0 °C overnight, yielding tricyclic quinoline **437** in 23%, though with a complex reaction profile (Scheme 124). When the cyclisation was attempted at a lower temperature of −78 °C, only a single compound was isolated: β-lactam **447** via **448**. This spirocyclic compound has not been previously reported and seems to suggest, once again, a preference for the benzyl organolithium to attack the electrophilic position adjacent to quinoline nitrogen, consistent with the cyclisation observed for 3-quinoline carboxamide **428**.

Unfortunately, it was not possible to obtain a crystal structure for spiro amide **447** due to the degradation of the crystal into a black goo, indicating instability of this cyclisation product over a few days. Moreover, the stereochemistry of **447** has not yet been confirmed, but only a single diastereomer was observed upon formation at −78 °C.

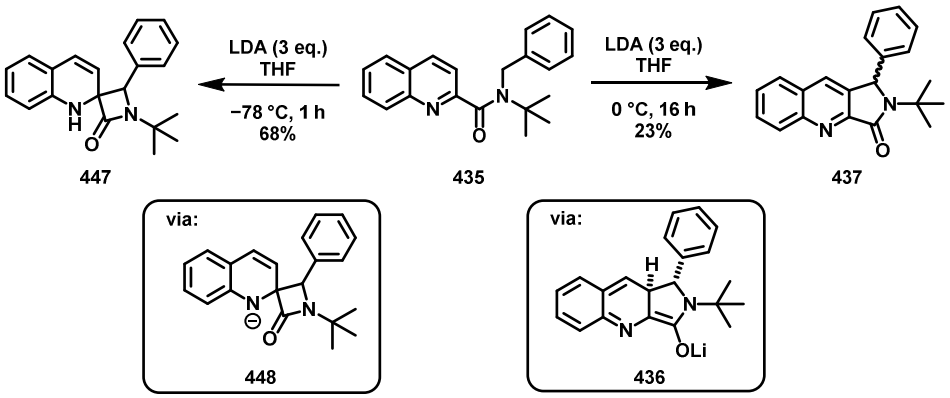

*Scheme 124: The cyclisation carried out on 2-quinoline carboxamide **435**, including the formation of a single diastereomer of β-lactam **447**.*

Attempts to alter the reaction conditions to favour the formation of desired enolate **436** were unsuccessful. The addition of DMPU only contributed to an increasingly complex mixture of products. It is evident that the desired cyclisation is unfavourable for this substrate, meaning photochemistry on enolate **436** would be, to a large extent, unyielding.

Despite the complexity associated with the cyclisation, a UV-Vis study was conducted to investigate whether two distinct peaks corresponding to the two main isolated compounds could be detected. When 2-quinoline carboxamide **435** was treated with base at −40 °C, the UV-Vis spectrum showed at least two broad peaks, with λ_{max} values recorded at 561 nm and 615 nm. When the same sample was examined at −78 °C, the longer-wavelength peak (615 nm) became more pronounced. However, its

intensity gradually decreased when the sample was re-analysed at room temperature. This suggests that the longer wavelength peak may correspond to spiro lactam anion **448**, which forms selectively at −78 °C, although this cannot be definitively confirmed. Forming spiro-carboxamide anion **448** at −78 °C and then warming to −40 °C still predominantly yielded spiro-cyclisation product **447**, indicating that spiro-carboxamide anion **448** is not a precursor to desired cyclisation product **437**. The TDDFT prediction for the enolate **436** yielded a calculated λ_{max} of 558 nm, which aligns closely with the lower of the two experimentally observed values.

Due to the complex array of products formed during cyclisation, further work on 2-quinoline carboxamide **435** was discontinued. Future research will likely focus on the dearomatising cyclisation of 3-quinoline carboxamides, which provides higher selectivity for the desired cyclisation, although achieving the desired photochemistry remains a challenge.

Pyrrole Dearomatisation and Photochemistry

7.0. Dearomative Cyclisation and Fragmentation of DEB-Protected Pyrroles

Thus far in this thesis, the dearomatising cyclisation of a range of aromatic and heteroaromatic substrates has been discussed, including benzyl benzamides, pyridinyl amides, and quinolines. In this section, the focus will shift to the dearomatising cyclisation of pyrrole-based amides, discussing their potential use in photochemical transformations analogous to those previously described.

In 2004, the Clayden group reported the dearomatising cyclisation of pyrrole carboxamide **449** (Scheme 125).[137] Notably, unlike the simpler formation of bicyclic fused systems observed with other (hetero)aromatic molecules, the pyrrole substrate underwent a complex cascade of mechanistic steps that resulted in the formation of an unsaturated lactam, with the pyrrole ring undergoing fragmentation. The reaction initiated with the deprotonation of benzyl amide **449** using LDA, and resultant organolithium **450** subsequently cyclised onto the pyrrole ring to form dienolate **451** *in situ* (red, Scheme 125). This intermediate is highly unstable due to the extensive unsaturation within the small, fused ring system and hence undergoes electron delocalisation, leading to the expulsion of the nitrogen atom (originally part of the pyrrole ring) in what is likely an electrocyclic ring-opening process, thereby alleviating ring strain and generating intermediates **452** and **453**. Upon aqueous quenching, lactam **454** was obtained in 81% yield. Similarly, the conjugated enolate intermediate **453** could be quenched with D_2O, resulting in deuteration adjacent to the phenyl ring in **455** with a 48% yield, and it could also undergo α-alkylation with allyl bromide to afford **456** in 50% yield.

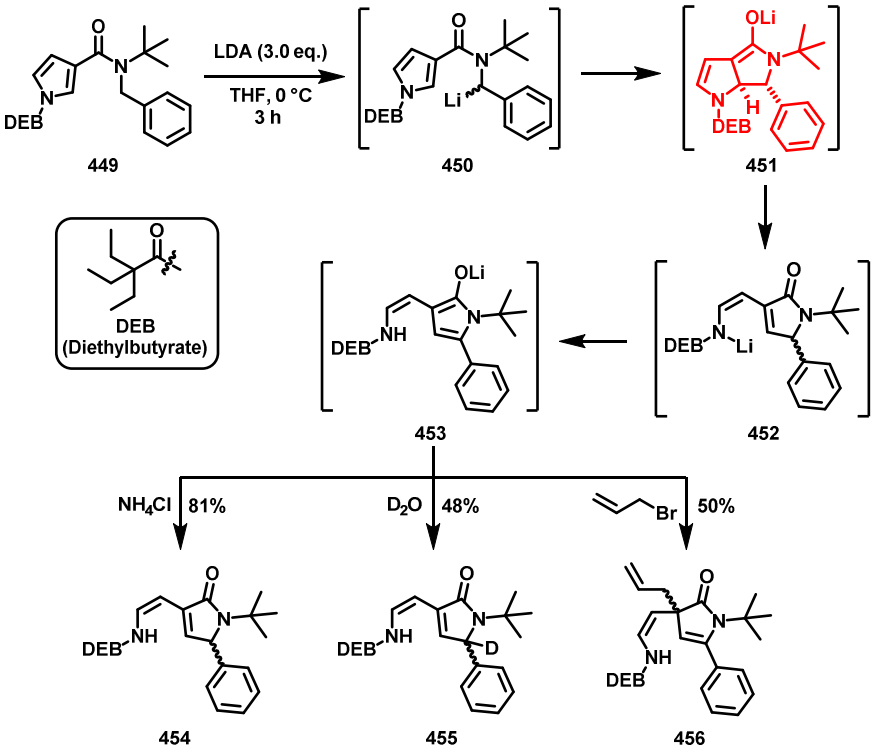

*Scheme 125: Pyrrole cyclisation on **449** followed by differing electrophilic quench. DEB = diethylbutyrate.*

This reaction demonstrated notable versatility, achieving a high yield in the dearomatising cyclisation of indole **457** to produce **458** (Scheme 126). Additionally, it displayed enantiospecificity in the cyclisation of the preformed chiral substrate **459**, resulting in the enantioenriched product **460**.

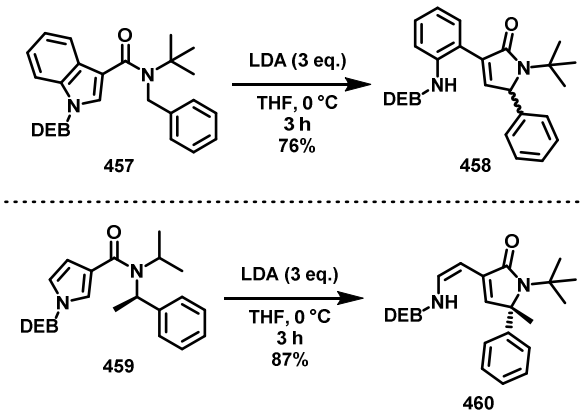

*Scheme 126: The cyclisation and fragmentation observed on lithiating benzyl indole **457** and chiral benzyl pyrrolo amide **459**.*

In this study, conducted by Rachel Turnbull and colleagues in the Clayden group, it was determined that DEB (diethylbenzyl) served as the most effective protecting group for the dearomatising cyclisation.[32] DEB provided an optimal balance of electron deficiency and steric bulk, facilitating

addition into the pyrrole ring. When BOC (*tert*-butoxycarbonyl) was employed as the protecting group, it was observed that LDA merely deprotected the BOC group during the dearomatisation step, resulting in the formation of deprotected pyrrole. Conversely, when a methyl group was present on the nitrogen, no reaction occurred, underscoring the necessity for an electron-deficient group on the pyrrole to enable the nucleophilic attack by the benzylic organolithium.

To evaluate the potential application of this work in our photochemical studies, we first needed to replicate the dearomatisation reaction to ensure its reproducibility. Following this, two possible enolates were identified for potential irradiation:

1. Enolate **451**, formed directly from the cyclisation process (Scheme 127).
2. Enolate **462**, potentially generated by adding a hydride (or other reducing/nucleophilic agent) to lactam **454** (Scheme 128).

In the first scenario, a UV-Vis study to determine the enolate's absorbance would be impractical due to the cascade of reactions occurring within the flask, rendering direct analysis of the enolate's chromophore unfeasible. As a result, reliance would have to be placed on TDDFT predictions to guide the irradiation process. If photochemistry on this enolate proves successful, it could lead to the formation of a strained cyclopropyl group attached to the pyrrole ring such as **461**, or potentially a ring-opened analogue resulting from a cascade mechanism akin to the dearomatising cyclisation observed in pyrrole species.

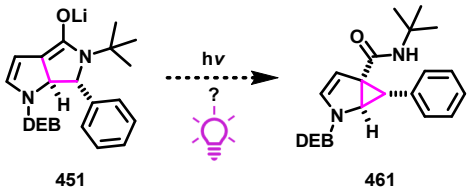

*Scheme 127: Potential irradiation of pyrrole-based enolate **451**, giving a cyclopropyl ring in **461**.*

In the second scenario, obtaining a UV-Vis spectrum of the enolate of interest may be feasible. However, this would depend on the nucleophilic attack occurring at the desired position, as in **454** to **462** as anticipated, without undesired deprotonation of the N-H functional group. Upon irradiation of this enolate at the appropriate wavelength, a di-radical recombination might be expected to yield a cyclopropyl group such as in **463**, akin to the ring-contraction process discussed earlier in this thesis (Section 5).

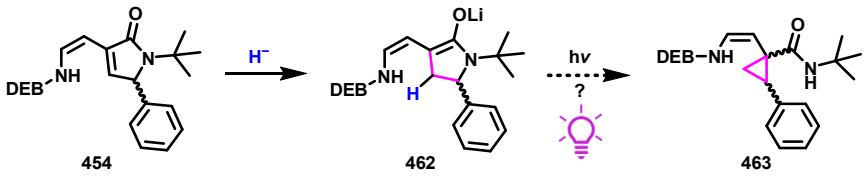

*Scheme 128: Potential hydride addition to **454**, giving an enolate which may then ring-contract photochemically to **463** via **462**.*

However, the chromophore in dienolate **462** differs from any others that have previously demonstrated successful ring-contraction photochemistry in our work, and the presence of a nitrogen atom within the chromophore may modify or even negate the expected photochemical reactivity. These two potential enolates warrant systematic investigation, and ongoing work within the Clayden group is focused on such studies.

7.1. Dearomative Cyclisation of BOC-Protected Benzylic Pyrrole

Although the dearomatisation of BOC-protected pyrrole **464** reportedly results in deprotected pyrrole, we sought to revisit this reaction to verify these findings. The DEB protecting group used in the 2004 study by the Clayden group requires multiple synthetic steps, making it preferable to explore alternative protecting groups. Before detailing the synthesis of such substrates, the TDDFT predictions for the two possible enolates of interest will be discussed.

Enolate **465**, generated from the direct dearomatisation of the pyrrole ring in **464** has a predicted λ_{max} of 339 nm (Scheme 129). Similarly, the second enolate **467**, formed via hydride addition to unsaturated lactam **466**, has a comparable TDDFT-predicted λ_{max} of 342 nm. If these enolates can be formed cleanly and efficiently, irradiation at 340 nm or 365 nm will be pursued.

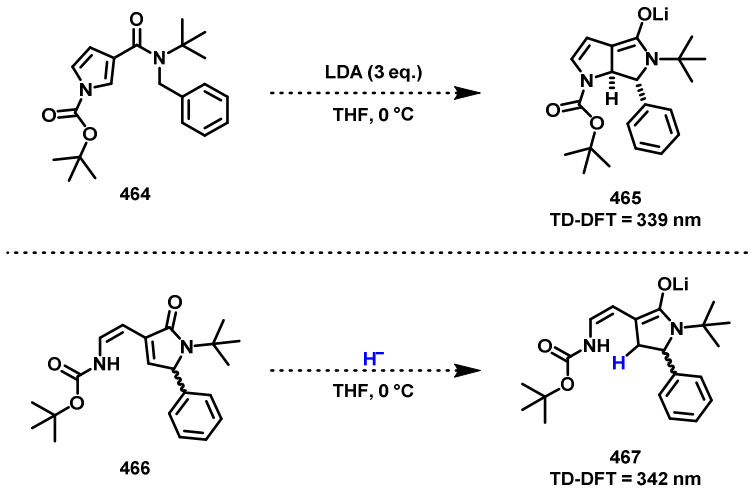

*Scheme 129: The planned formation of enolates **465** and **467** from BOC-protected pyrrole amides **464** and **466**.*

For the synthesis of protected pyrrole **464**, the initial coupling of *N*-tert-butyl-*N*-benzylamine (**121**) with acryloyl chloride (**468**) yielded unsaturated amide **469** in high yield (Scheme 130). Subsequently, the pyrrole scaffold was introduced using TOSMIC (**470**), affording intermediate **471**. The pyrrole was then protected with di-*tert*-butyl dicarbonate under mild conditions, resulting in the formation of pyrrolo amide **464** in high yield.

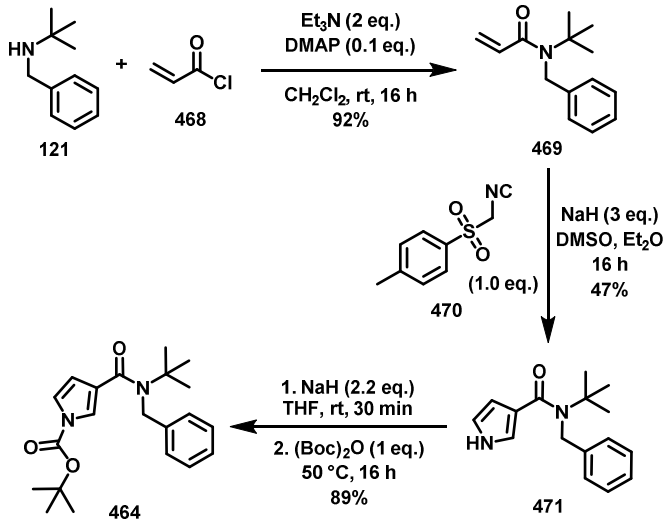

*Scheme 130: Synthesis of BOC-protected carboxy pyrrole **464**.*

With pyrrolo amide **464** in hand, its dearomatising cyclisation was attempted. Initial investigations indicated that cyclisation was proceeding as desired, evidenced by the formation of a yellow-orange coloured enolate, yielding unsaturated lactam **466** in 29%, with the only other observed compound being the starting material (Scheme 131). This result is promising and contradicts prior reports that

suggested BOC-protected pyrrole **464** would lead only to deprotected starting material under basic conditions.

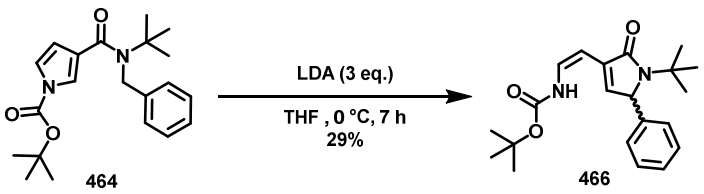

*Scheme 131: Observed, but unreproducible cyclisation and fragmentation seen on lithiating pyrrole **464**, giving **466**.*

However, attempts to increase the isolated yield of lactam **466** revealed that the dearomatisation result was irreproducible. Using identical methods and scales, some reactions yielded only product **466** and starting amide **464**, while others resulted in a mixture of deprotected pyrrole **471** and starting material **464**. This inconsistency posed a significant challenge to our goal of studying the corresponding enolate(s) from this reaction, as it was not possible to reliably confirm the presence of the desired enolate in the reaction mixture. It was therefore reasoned that the reproducibility of the dearomatisation process could potentially be improved by employing an alternative protecting group.

7.2. Pyrrole Protecting Groups

Although the DEB protecting group has been reported to facilitate the desired cyclisation in good yield and could potentially allow access to the desired enolate for study, its synthesis involves multiple steps and poses challenges in purification due to volatile intermediates. Consequently, alternative protecting groups have been explored by master's student Callum Trent in the Clayden group, including phthalimide and 2-mesitylenesulfonyl.[133] However, attempts to install these protecting groups on pyrrolo amide **471** were unsuccessful, with the protection step yielding only starting material.

Encouragingly, protection of **471** with a tosyl group proceeded as intended, providing a good yield for the formation of **472** (Scheme 132). Subsequent deprotonation at the benzylic position in **472** initiated the desired cyclisation, followed by the reaction cascade described earlier, affording expected cyclised product **473** in 24% yield. However, Callum Trent again found that this cyclisation proved to be irreproducible, with some attempts yielding cyclised product **473**, while others resulted in only starting material **472** and some deprotected pyrrole **471**. This inconsistency prevents reliable

photochemical studies of this substrate, leaving us without a clear understanding of whether photochemical irradiation could lead to interesting reactivity in these pyrrole systems.

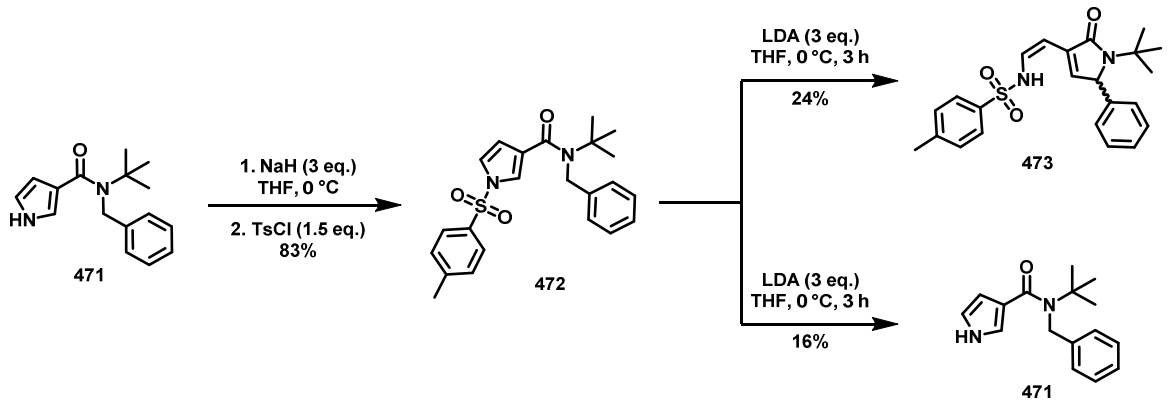

*Scheme 132: The synthesis of tosyl protected pyrrolo amide **472** and dearomative cyclisation and fragmentation observed on **472** to give **473** irreproducibly, with deprotected pyrrole **471** often formed instead, carried out by Callum Trent.*[133]

Future work could involve a more comprehensive investigation into protecting groups that provide an optimal balance of electron deficiency and steric bulk to enable successful cyclisation and enolate formation. Once a reliable and reproducible cyclisation protocol is established, photochemical studies could be conducted with the aim of identifying novel bicyclic products generated upon irradiation.

Summary

Enolates have traditionally been employed as thermal nucleophilic reagents, typically reacting with electrophiles to introduce functionality adjacent to carbonyl groups. However, their inherent chromophore, which has been infrequently harnessed photochemically, presents new chemical opportunities. We have now demonstrated that enolates can serve as photochemical reagents, rather than thermal ones, enabling mechanistically intriguing yet operationally straightforward transformations.

We have previously illustrated that enolate species can engage in a unique ring-expansion process following photochemical excitation of their intrinsic chromophores (Section 1). This excitation has previously been employed to expand an aromatic ring into a cycloheptatriene (**76** to **80**) following a dearomatising cyclisation and subsequent irradiation (Scheme 133).[1,46] While various bicyclic trienolates have exhibited similar reactivity, it remained unclear at the start of this project whether this chemistry could tolerate alterations to the structural core of the enolate or modifications to the level of conjugation within the chromophore.

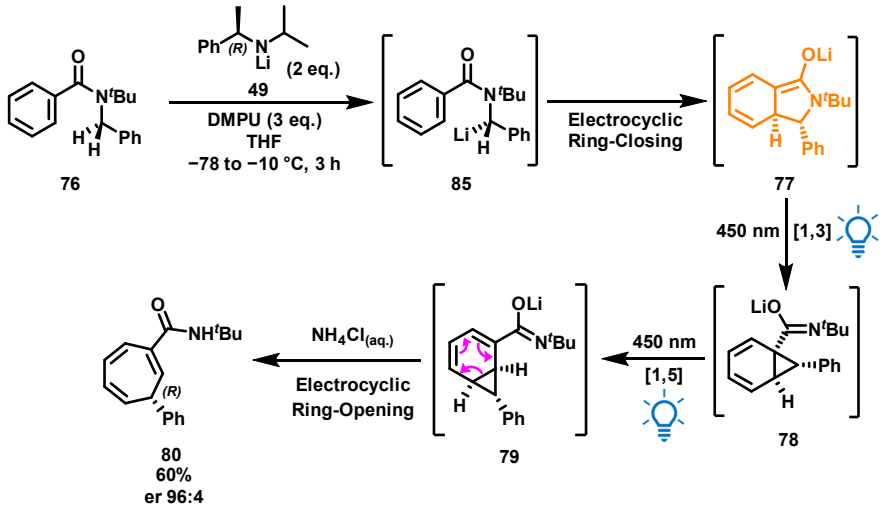

*Scheme 133: The asymmetric photochemical transformation on benzyl benzamide **76** explored by the Clayden group using chiral lithium base **49** to initiate stereoselectivity.*[1]

In Section 3, several modifications were explored in an effort to generate photoreactive cyclic trienolates with varying structural integrity compared to bicyclic trienolate **77**. However, these altered substrates either exhibited no photoreactivity or were prone to air-induced aromatisation, ultimately making them unsuitable for our intended photochemical investigations.

We have demonstrated In Section 4 that acyclic *N*-benzyl amides containing a diene moiety can be deprotonated (to give trienolates such as **119**) and subjected to chromoselective irradiation, resulting in a mixture of regioisomers (such as ***E*/*Z*-128**, **129** and **130**) produced via benzylic migration through a nitrogen-to-carbon shift (Scheme 134). This reactivity suggests that the bicyclic structure present in enolate **77** is not essential for initiating analogous, yet distinct, photochemical transformations.

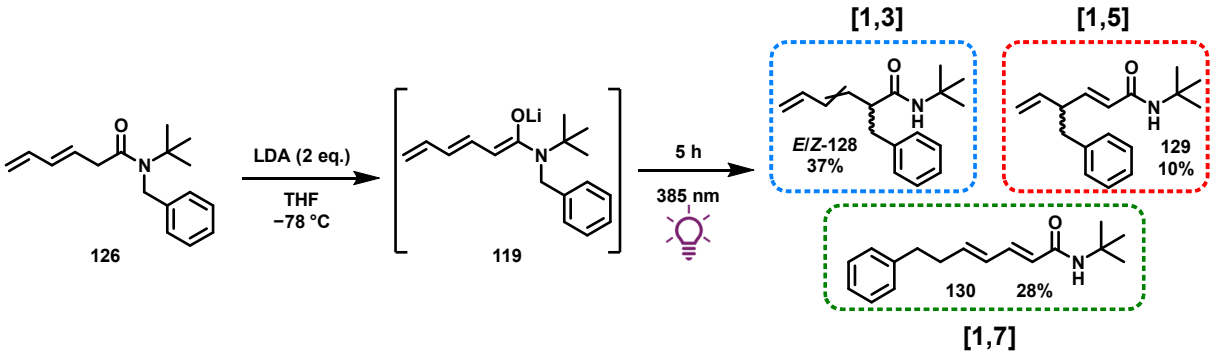

*Scheme 134: Photochemical migration of a benzyl group in enolate **119** to give a mixture of three regioisomeric products.*

The mechanism of this photochemical migration was investigated, revealing that the reaction likely proceeds via a benzylic radical intermediate (such as **182** from **181**) which subsequently recombines with the trienolate chain (such as **183** with **184**) at various positions, resulting in [1,3], [1,5], and [1,7]-migrations (Scheme 135). Notably, the reaction was largely unaffected by variations in the nitrogen protecting group and exhibited successful migration of a range of substituents, provided that the migrating group adjacent to the amide nitrogen contained a radical-stabilising feature. While regioselectivity was often poor, the [1,5]-regioisomer consistently appeared as the minor product. Moreover, the presence of larger, bulkier migrating groups favoured the formation of the [1,7]-regioisomer (such as **185**), enhancing the selectivity towards this pathway.

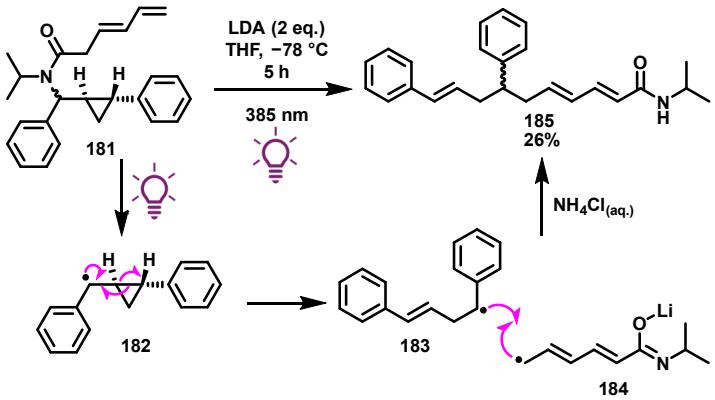

*Scheme 135: The ring-opening photochemistry on benzyl phenyl cyclopropyl amide **181**, presumably through benzylic radical **182**.*

With a clear understanding of the requirements for successful enolate photochemistry, we shifted our focus towards utilising enolate photochemistry to achieve synthetically valuable ring-contractions, discussed in Section 5. This was accomplished by positioning one of the enolate double bonds within a lactam ring such as in **348** from **262**, allowing for the formation of a benzylic radical upon enolate irradiation, followed by intramolecular radical recombination to yield a cyclopropyl ring as in **264** (Scheme 136).

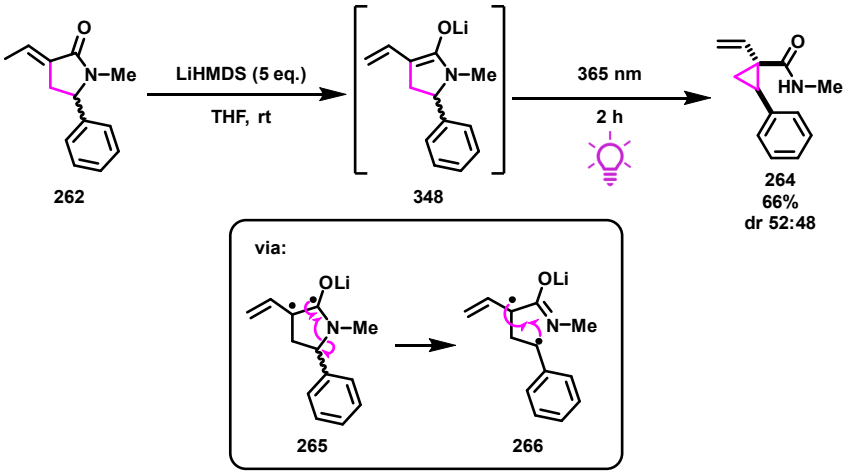

*Scheme 136: The photochemical ring-contraction of lactam dienolate **348** to **264** and the proposed mechanism by which it occurs.*

This method offered reactivity across lactam trienolates, dienolates, and monoenolates of five-membered rings. Notably, dienolates such as **348** provided the highest yields for ring contraction, compared to mono- or trienolates and reacted under mild conditions, involving two hours of irradiation at 365 nm at room temperature.

Furthermore, photochemical ring-contraction of preformed enolate **348** was successfully performed in flow, yielding 45% from an initial study. This represents an exciting proof of concept, demonstrating that enolate photochemistry can be adapted to flow conditions.

Although the yield for the ring-contraction of dienolate **348** was promising for such a synthetically valuable transformation, the limited diastereoselectivity of ring-contracted **264** initially posed a significant challenge. Modifications to the migrating group, the steric bulk surrounding the lactam chromophore, and alterations to the nitrogen protecting group all resulted in minimal improvements in selectivity. However, introducing substitution at the unfunctionalised 4-position of the lactam significantly enhanced diastereoselectivity, achieving a diastereomeric ratio of 89:11 for substituted cyclopropanes **323**:**324** from the dienolate of **317** (Scheme 137). Future work will focus on replacing

the benzylic ether with alternative substituents of varying steric bulk to investigate the sensitivity of diastereoselectivity to the size of the 4-substituent on the five-membered ring.

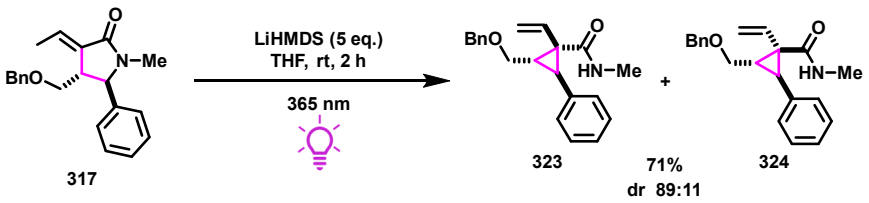

*Scheme 137: The ring-contraction on the dienolate of five-membered lactam **317**, which bears substitution in the lactam ring, offering a good yield and high diastereoselectivity for **323**.*

Ring-contraction of a six-membered ring to form a cyclobutane (as in **353**) was also achievable upon irradiation of either a dienolate (as in **355** formed from **351**) or a trienolate (Scheme 138). In addition to the anticipated ring-contraction product, this process yielded a "ring-swing" product (such as **354**), arising from the formation of a benzylic radical followed by intramolecular recombination at the conjugated chromophore chain.

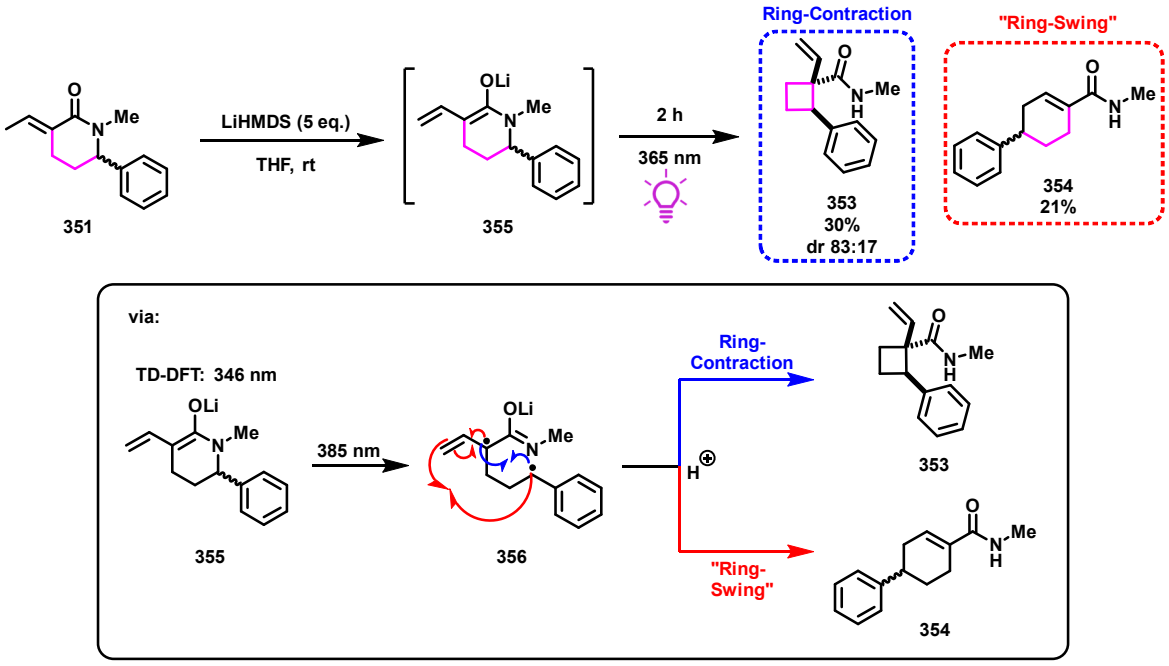

*Scheme 138: The photochemical ring-contraction to give **353** and "ring-swing" to afford **354** on six-membered dienolate **355**, derived from lactam **351** including the mechanism for their formation.*

While the processes described thus far are believed to proceed through radical-based pathways, we have identified that ring-opening of a six-membered lactam bearing an internal dienolate chromophore (such as **367**) can occur, most likely via an electrocyclic ring-opening mechanism

(Scheme 139). This afforded regioisomeric alkenyl chains (**377** and **378**), which, on isomerisation, gave **379** and **380**.

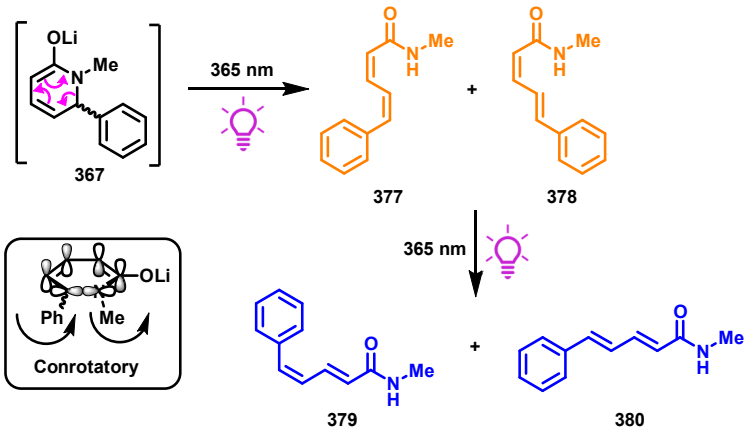

*Scheme 139: A possible electrocyclic ring-opening mechanism for ring-opening of dienolate **367**, followed by photochemical isomerisation of product isomers **377** and **378**.*

This indicates that enolate photochemistry exhibits significant versatility, with the capacity to proceed through multiple mechanistic pathways. This high-yielding reaction type (giving up to 93% yield) has the potential to be further expanded by exploring the ring-opening of lactams bearing substituents other than benzyl or vinyl groups adjacent to nitrogen, which could afford a diverse array of dienes with broad applicability.

Although not yet achieved, we aim to form pharmaceutically relevant benzazepines via quinoline dearomatisation followed by photochemical irradiation (Section 6). This would likely be dependent on having appropriate substitution around the quinoline ring, dissuading electron localisation onto the nitrogen atom. Thus far, irradiation has not successfully yielded benzazepines, likely due to radical stabilisation on nitrogen (such as from **442** to **445** and **446**) which favours rearomatisation and benzylic cleavage rather than the desired product formation (Scheme 140).

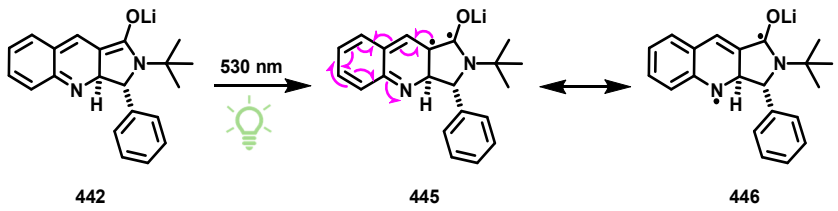

*Scheme 140: Photochemical di-radical formation on **442** to give **445** followed by delocalisation onto nitrogen (**446**), giving rearomatisation of the quinoline ring.*

Section 7 detailed the established dearomatisation of benzyl pyrrole carboxamide **449** under basic conditions, proceeding via dienolate **451**. If dienolate **451** could be generated cleanly *in situ* without the occurrence of undesirable side reactions, subsequent irradiation may yield unique molecular scaffolds such as **461**, as illustrated in Scheme 141. Currently, identifying the optimal protecting group remains a challenge, as deprotection of pyrrole nitrogen under basic conditions has been observed with various motifs.

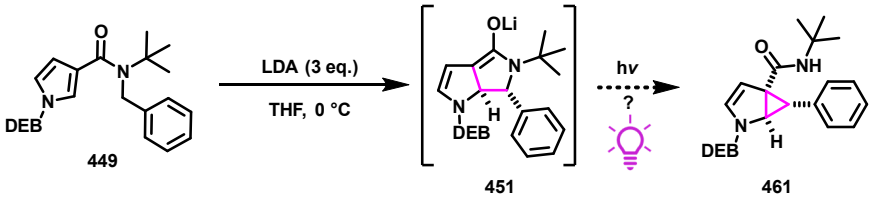

*Scheme 141: Potential irradiation of pyrrole-based enolate **451**, derived from **449**, giving a cyclopropyl ring in **461**.*

In summary, by leveraging chromoselective irradiation, a variety of unprecedented enolate-based reactions have been uncovered and developed. The research showcases innovative methods such as photochemical migrations and ring-contraction of lactam enolates, revealing new pathways to synthesise substituted cyclopropanes and cyclobutanes under mild conditions. This work not only broadens the scope of enolate chemistry but also opens up new opportunities for developing complex molecular architectures with potential applications in pharmaceuticals. The methodologies developed in this thesis promise exciting prospects for the future of synthetic enolate photochemistry, offering a foundation for further exploration of the chemical space.

Future Work

Building on the findings of this thesis, the next steps for advancing enolate photochemistry involve exploring new substrates, refining reaction conditions, and expanding the applications of this reactivity in complex molecular synthesis. Some potential future directions include:

1. **Expanding Substrate Scope**

Future studies should investigate enolate photochemistry using a broader range of substrates, including those with non-benzyl or non-vinyl groups adjacent to nitrogen. This could reveal additional pathways for ring-opening reactions and increase the variety of accessible diene products.

Exploring other heteroaromatic systems, such as quinolines and pyrroles, could provide insight into the broader applicability of these photochemical transformations. Tailoring substitutions to minimise electron localisation on nitrogen may enable the formation of new pharmaceutically relevant compounds, like benzazepines.

2. **Enhancing Regioselectivity and Diastereoselectivity**

Addressing the challenge of limited regio- and diastereoselectivity remains a key area for improvement. Future work could involve systematic modification of substituents on the enolate and migrating groups, particularly focusing on steric and electronic effects to optimise selective pathways.

We propose that introducing a bulky substituent directly attached to a five-membered lactam ring, adjacent to the migrating group (such as in **474**), could enhance both yield and diastereoselectivity for ring-contracted products (such as **475** over **476**) (Scheme 142).

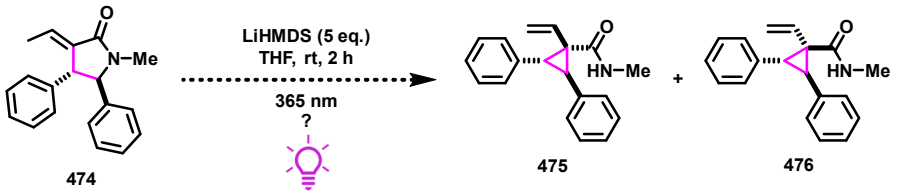

*Scheme 142: The proposed ring-contraction on di-phenyl substituted lactam **474** to give **475** and **476**, which we believe will offer high selectivity.*

Investigating the influence of different reaction parameters, such as solvent and temperature, on the outcome of enolate photochemical reactivity may further refine control over product distributions.

3. **Integration with Flow Chemistry**

The preliminary success of transferring enolate photochemistry into flow systems opens up a promising avenue for scalability and continuous processing. Future studies should aim to optimise flow conditions, such as flow rates, light intensity, and reaction times, to enhance yields and streamline the photochemical processes.

The most robust and well-studied enolate photochemical reactions will be prioritised for flow chemistry, particularly those requiring the mildest conditions for effective reactivity. As such, the focus will likely be on five-membered lactam dienolate ring-contractions, given that these transformations reliably provide consistent yields at room temperature within two hours, using a mild base.

Development of specialised flow reactors capable of precise temperature control may mitigate the challenges associated with the thermal instability of certain enolate intermediates.

4. **Computational Modelling and Mechanistic Studies**

Continued use of computational tools, like time-dependent density functional theory (TDDFT), will be essential in predicting and rationalising the reactivity of new enolate systems. Expanding computational studies to incorporate dynamic simulations could offer deeper mechanistic insights and inform experimental design by providing detailed information on the progression of enolate photochemistry. These simulations could enable the visualisation of molecular motions, reaction pathways, and intermediate states, offering a more comprehensive understanding of the underlying photochemical processes.

Detailed mechanistic investigations, possibly involving time-resolved spectroscopic techniques such as UV-Vis or IR, could elucidate intermediate species and transition states, offering a clearer understanding of the photochemical pathways.

5. **Application to Complex Synthesis**

The potential of enolate photochemistry to facilitate complex molecular transformations suggests its utility in the synthesis of natural products, pharmaceuticals, and other high-value compounds. Future

research should focus on applying these photochemical methods to the construction of complex architectures, highlighting the practical advantages of this approach. However, a specific synthetic target has not yet been identified.

The work presented here serves as a foundational platform for future research in enolate photochemistry, offering insights into the structural and electronic prerequisites required to achieve the desired reactivity. With further development, we believe that these photochemical processes may hold potential for future industrial applications.

Limitations

While numerous promising and intriguing future directions exist, it is essential to evaluate them in the context of potential limitations associated with enolate photochemistry, which are summarised as follows:

1. **Thermal Instability of Enolates**: Some of the enolates studied are thermally unstable, which complicates their handling and limits their desired reactivity under standard conditions.

2. **Limited Scope of Substrates**: The photochemical transformations largely rely on specific substrate types (e.g., benzylbenzamides). A broader range of substrates is needed to generalise the applicability of the photochemical methods.

3. **Mechanistic Ambiguities**: While evidence has been gathered that points towards a radical photochemical mechanism, mechanistic pathways for some transformations remain speculative. Further experiments, such as transient spectroscopic studies, could provide more definitive mechanistic insights.

4. **Reaction Yield and Selectivity**: Several transformations yield complex mixtures with moderate regioselectivity, which could limit their synthetic utility. Further optimisation is needed to enhance selectivity and yield. Additionally, the yield is often compromised by what we believe to be the polymerisation of radical intermediates during the reaction process. However, this issue can be paritally mitigated by reducing the extent of chromophoric conjugation, which appears to diminish the propensity for polymerisation.

5. **Flow Chemistry Challenges**: The adaptation of enolate photochemistry to flow systems is still in its infancy, with challenges such as cooling and maintaining stability under continuous flow conditions. More robust solutions and apparatus improvements are needed for future research into photochemical reactions in flow using thermally-unstable intermediates.

The Use of Technology in this Project

As part of the Technology Enhanced Chemical Synthesis (TECS) CDT, we have incorporated various technological innovations into our research in chemistry. Notably, the deployment of modern LEDs and advanced photochemical equipment has been crucial to the progress of this photochemistry project. Towards the conclusion of the study, we successfully conducted enolate photochemistry in a flow system, utilising a custom-built photoreactor integrated with a Vapourtec pump setup. It is important to again highlight that flow chemistry presents specific challenges for enolate photochemistry, particularly because the available flow equipment typically operates at room temperature and lacks effective methods for cooling the flow tubing during reactions. While this limitation is manageable for enolates reactive at ambient conditions, it poses a significant constraint that must be addressed in future research to fully exploit this technology. Recent advancements in photochemical flow setups, such as the PhotoCube by ThalesNano®, offer the capability to select various wavelengths for photochemical irradiation, enhancing the flexibility of these systems.

Although not conducted directly by myself, design of experiment (DoE) optimisation studies were undertaken by MSci students William Terry-Wright and Callum Trent, under my supervision, using specialised software. These studies aimed to optimise the yield of azepines synthesised through photochemical irradiation of enolate intermediates, focusing on fine-tuning reaction conditions to maximise efficiency and product yield.

Throughout this project, additional technological resources were employed, including automated purification systems and modern microwave reactors. These technologies have proven to be highly effective in advancing the project's objectives, particularly by streamlining the synthesis and purification of challenging substrates such as in the formation of lactams **254** and **329** (Scheme 143), thus enhancing overall efficiency and productivity in experimental workflows.

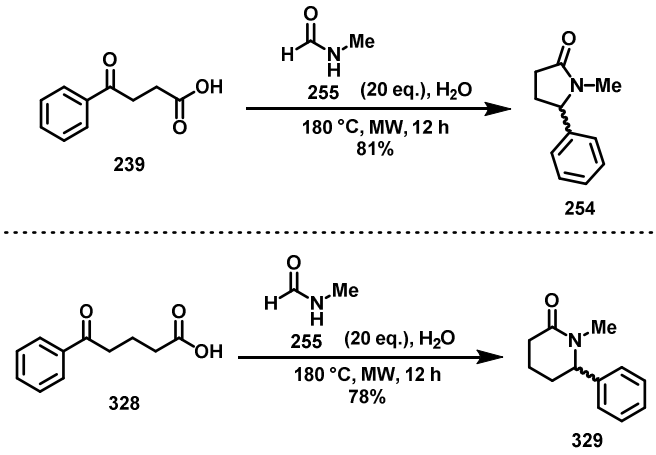

*Scheme 143: Microwave-mediated lactam formation reactions, giving us starting scaffolds for lactam ring-contractions (**254** and **329**).*

Computational predictions have been extensively employed in this project to estimate the λ_{max} values for key enolates, providing crucial insights into their photochemical behaviour. Additionally, a machine learning algorithm was utilised to predict the NMR shifts of diene stereoisomers, aiding in the structural characterisation of reaction products. This computational data was generously provided by Ben Honore and Malcolm George from Craig Butts' group (University of Bristol).

Experimental

8.0. Materials and Solvents

All starting materials were obtained from commercial suppliers unless otherwise stated. Anhydrous solvents were dried on an Anhydrous Engineering alumina column before being stored in an atmosphere of nitrogen. Deuterated solvents such as chloroform-*d* and DMSO-d_6 were used directly as purchased.

8.1. Methods and Instrumentation

For all reactions employed, where an anhydrous solvent was used, inert conditions were employed using standard Schlenk line techniques under an atmosphere of nitrogen using oven-dried glassware. Where thin layer chromatography (TLC) was employed to monitor reaction progress, Merck TLC silica gel 60 F_{254} plates were used and were visualised using UV light (254 nm), often with staining either in prepared solutions of $KMnO_4$ (general) or I_2 (diene or trienes). Normal phase flash column chromatography was carried out using a Biotage® Isolera Four system using Biotage® Sfär Duo pre-packed silica gel columns, with solvent systems specified.

NMR: ^{1}H NMR spectra were measured at 400 MHz on a Bruker Avance 400, Varian 400-MR, Jeol ECZ400 or Jeol ECS400. The corresponding ^{13}C frequencies are 101 MHz and 126 MHz. ^{19}F Spectra was measured at 377 MHz. 1D and 2D NOE Spectra were recorded on a Jeol Varian 500 MHz spectrometer, with 8 scans and a mixing time of 0.8 s. All ^{13}C and ^{19}F spectra are recorded with proton-decoupling ({^{1}H}). NMR samples were analysed as solutions with solvents specified below and, unless otherwise stated, at 298 K.

Chemical shifts (^{1}H and ^{13}C) are reported in parts per million (ppm) relative to residual solvent (chloroform-*d* δ_H 7.26 and δ_C 77.2; DMSO-d_6 δ_H 2.50 and δ_C 39.5), quoted to the nearest 0.01 ppm and 0.1 ppm respectively. ^{19}F Chemical shifts are reported in parts per million (ppm), quoted to the nearest 0.1 ppm, relative to hexafluorobenzene (−164.9 ppm). Coupling constants (*J*) are reported to the nearest 0.1 Hz (^{1}H NMR) and multiplicities are defined as: s (singlet), d (doublet), t (triplet), q (quartet), quint (quintet), sept (septet), m (multiplet) and combinations thereof. Assignments are stated

throughout. However, some assignments are not possible where considerable overlap of spectral peaks exist (mainly with aromatic signals). Where NMR yields are reported, the standard used was 3,4,5-trichloropyridine.

HRMS: High resolution mass spectra were recorded on a Bruker Daltronics MicrOTOF 2 mass spectrometer (ESI). Where a mixture of diastereomers was present, LC-MS or GC-MS was utilised to provide individual masses for isomers.

Melting Points: Melting points are expressed in °C and were measured on a Stuart SMP30 melting point apparatus and are uncorrected.

High Performance Liquid Chromatography: Enantiomeric ratios were determined by HPLC analysis on Agilent 1100 series or Agilent Technologies 1260 Infinity with UV detection at 280, 254, 230 and 210 nm.

IR: IR spectra were recorded on a Perkin Elmer (Spectrum One) FT-IR spectrometer (ATR sampling accessory). Only strong and selected absorbance's (expressed in cm^{-1}) are reported.

UV-Vis: UV-visible spectra were recorded on an Agilent Cary Series 300 UV-Vis spectrophotometer using a baseline correction for the solvent used in the sample.

Cryostat: All low temperature reactions (below 0 °C) were carried out using either a Huber TC100E or a Thermo Scientific EK90 Immersion Cooler using a solvent bath of methanol unless otherwise stated.

Polarimeter: $[\alpha]_D$ values were recorded on an ADP220 polarimeter using the solvent specified as a background corrector.

Microwave: A Biotage® Initiator$^+$ microwave system was used for microwave reactions using a sealed tube, with pre-stirring of the mixture for 30 seconds, unless otherwise stated.

8.2. UV-Visible Spectroscopy Measurements

To an oven-dried 5 mm cuvette was attached a septum secured with Parafilm® (Figure 16). The cuvette was swing-purged using a Schlenk line and put under an atmosphere of nitrogen. The cuvette was placed in an ice bath. In the ice bath, a solution of enolate (formed from the corresponding amide and deprotonation with two equivalents of LDA) in anhydrous THF was added by syringe. The cuvette was kept in an ice bath until running the spectrum.

A blank sample containing anhydrous THF was ran before UV-vis measurements.

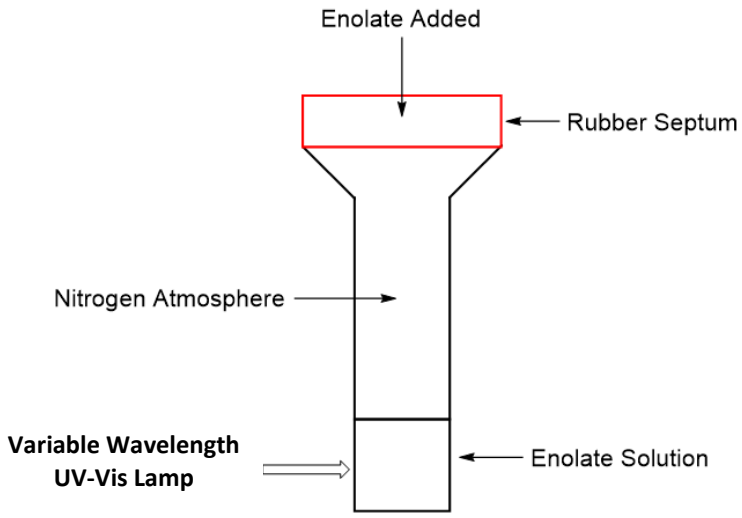

Figure 16: The method for recording UV-Vis spectra of enolates, indicating the air-free nature required.

8.3. Time-Dependent Density Functional Theory Calculations

Computational characterisations of the ground- and excited-state properties of the enolate were performed using Gaussian 16 software.[138] The ground electronic state geometry of the enolate was computed using density functional theory (DFT). The B3LYP functional was used with the 6-31+G(d,p) basis set. Solvent effects for THF were included by implicit simulation of solvation as a conductor-like polarisable continuum medium. Vertical transition energies, oscillator strengths and excitation amplitudes were computed using time-dependent density functional theory (TDDFT) using the Coulomb attenuated variant of the B3LYP functional (CAM-B3LYP). CAM-B3LYP was used with the 6-31+G(d,p) basis set and conductor-like continuum simulation of THF as solvent. Note that all reported TDDFT prediction values are for the anion of the respective enolate (without the lithium counterion) unless otherwise stated.

8.4. Photochemistry Reaction Setup

The Cryostat was attached to a Dewer containing methanol with a temperature probe in the solution adjacent to the reaction flask (Figure 17). The LED was clamped above the mixture, giving a clear line of consistent irradiation onto the mixture. If the glassware of the reaction becomes cloudy with condensation, methanol was ran down the sides to clear it, allowing for better light penetration. The reaction was carried out with consistent flow of nitrogen through a needle and septum.

Figure 17: The setup for photochemical irradiation.

The LED is powered by either a Thorlabs T-Cube™ LED driver or a Thorlabs DC4100 four-channel LED driver (Figure 18) at the maximum LED current, where possible. The Thorlabs LEDs were used with an attached aspheric condenser lens (Ø 25 mm, coated for 350-700 nm).

Figure 18: The two drivers used for controlling and powering the LED system.

8.5. Flow Photochemistry Setup

The flow photoreactor was constructed by William Terry-Wright in the Clayden group.

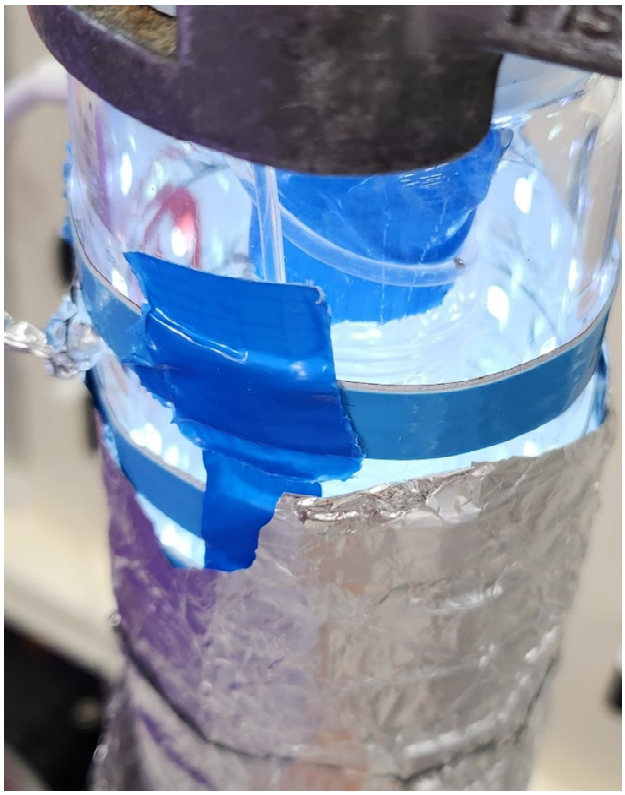

Figure 19: The flow photoreactor, showing inner flow tubing and the LED strip secured on the outside.

The flow reactor utilised coiled PFA tubing (1 mm × 1.6 mm) around a nitrogen cold-trap (Figure 19). The LED strip (λ_{max} 373 nm, Figure 20) was secured to the outside of the trap, to give sufficient distance to avoid heat transfer to substrate.

The LED strip was purchased from AliExpress and is rated at 8.64 W/m with a 12 V attached power supply.

Tin foil was wrapped around the LED strip to improve reflectivity of irradiation onto reactant.

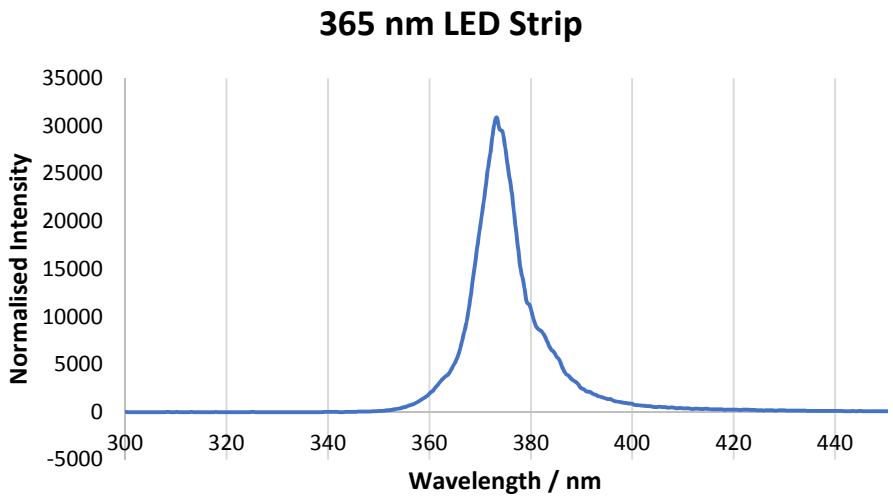

Figure 20: The LED emission spectra for the LED strip used in the flow photochemistry.

The reagents were mixed and pumped using a commercially available Vapourtec V-3 peristaltic pump (R-series) through a Teflon T-mixer.

The flow system (Figure 21) was primed initially by flowing anhydrous THF through the lines. Following from this, the substrate in THF was mixed with the basic LiHMDS (1 M in THF) solution in the T-junction. This enolate solution then flows through the flow photoreactor before being quenched into aqueous ammonium chloride. After one minute of this solution flowing out into the quench, the output tubing was placed into a new quench mixture and the stopwatch started to ensure the desired amount of substrate (75 mg) has flowed through the system (15 mins for 1 mL/min, 30 mins for 0.5 mL/min and 60 mins for 0.25 mL/min).

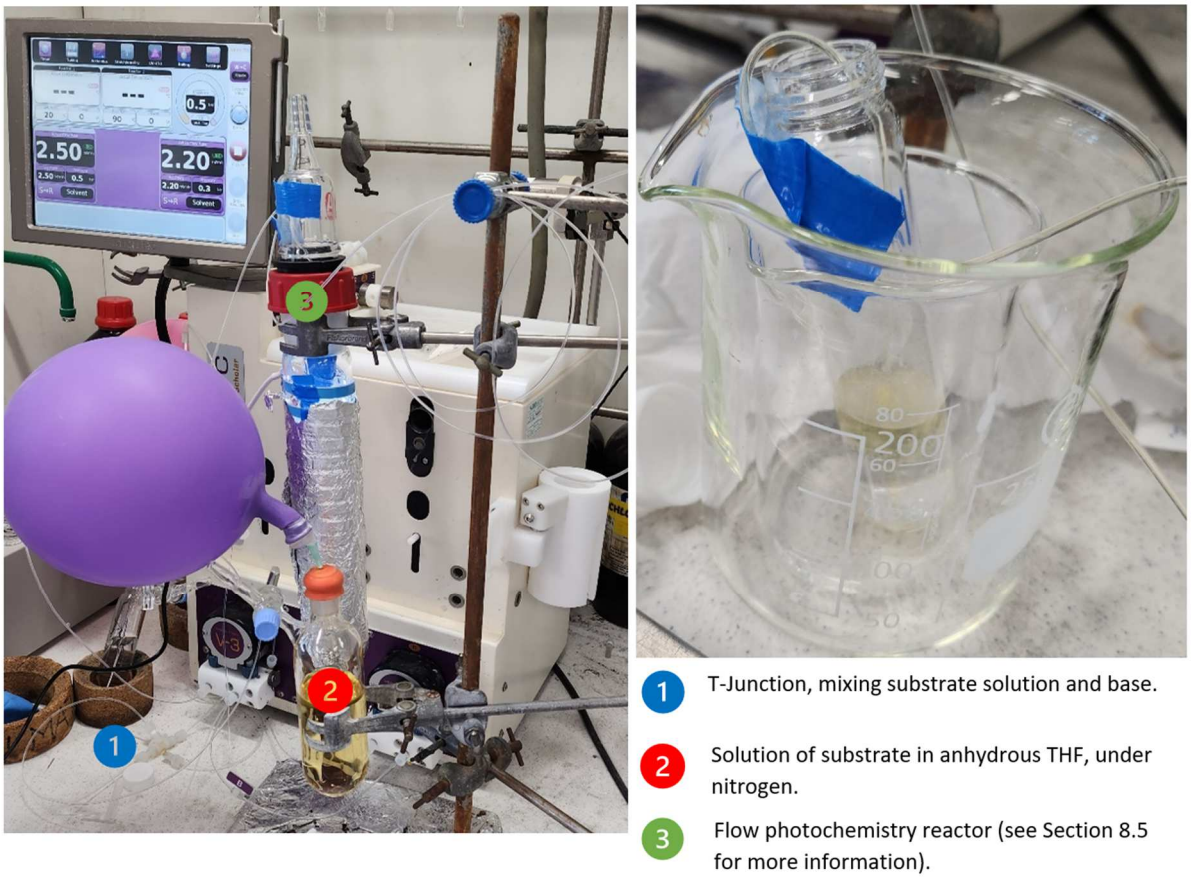

Figure 21: The flow photochemistry setup used for enolate reactivity (left) and the tubing flowing into the quench solution (right).

For each experiment, the substrate was extracted with EtOAc as in the batch equivalent, before the NMR yields determined using 3,4,5-trichloropyridine as internal standard.

8.6. LED Emission Data

The LED emission data was obtained in collaboration with the group of Andrew Orr-Ewing where possible. Otherwise, the data provided here is from the LED supplier.

Kessil® A160WE Tuna Blue: Blue-coloured LED with spectral tuning, shifting measured maximum emission (shown below). The "blue-end" consists of λ_{max} 465 nm (Figure 22) whereas the "white-end" consists of a greater proportion of emission at 441 nm (Figure 23). When irradiation at 450 nm is reported in this thesis, the "blue-end" was utilised. This LED has a 40 W rating with an attached power supply.

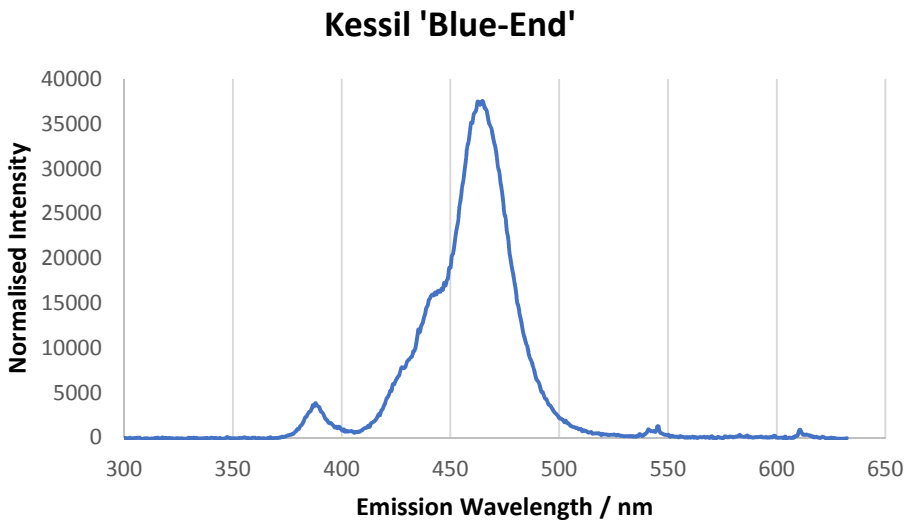

Figure 22: Kessil Tuna Blue LED recorded emission spectra for the "blue end" of the spectral options for this LED.

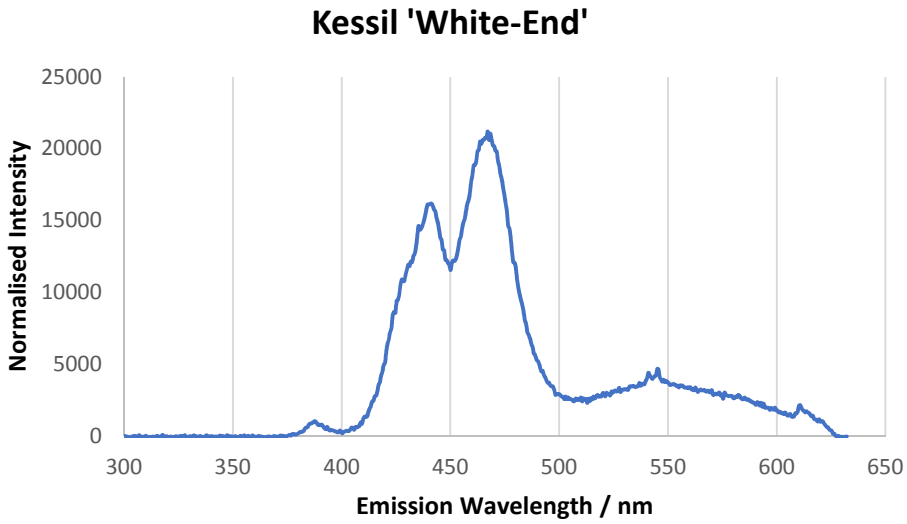

Figure 23: Kessil Tuna Blue LED recorded emission spectra for the "white end" of the spectral options for this LED.

Thorlabs M365LP1: Mounted LED (UV-colour, 365 nm) with a power rating of 6.80 W. Measured emission spectra of this LED is shown below, with a λ_{max} of 367 nm (Figure 24).

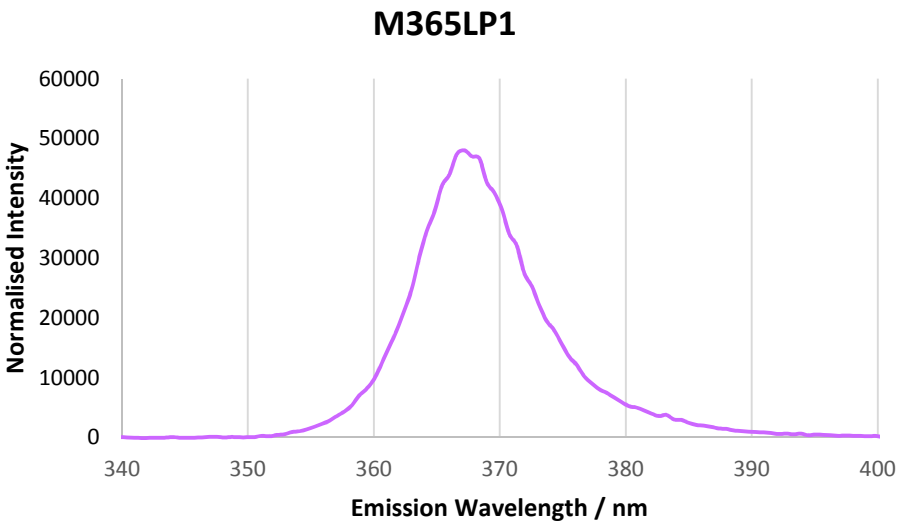

Figure 24: The recorded emission spectra for the Thorlabs M365LP1 LED.

Thorlabs M385LP1: Mounted LED (UV-colour, 385 nm) with a power rating of 6.63 W. Measured emission spectra of this LED is shown below, with a λ_{max} of 383 nm (Figure 25).

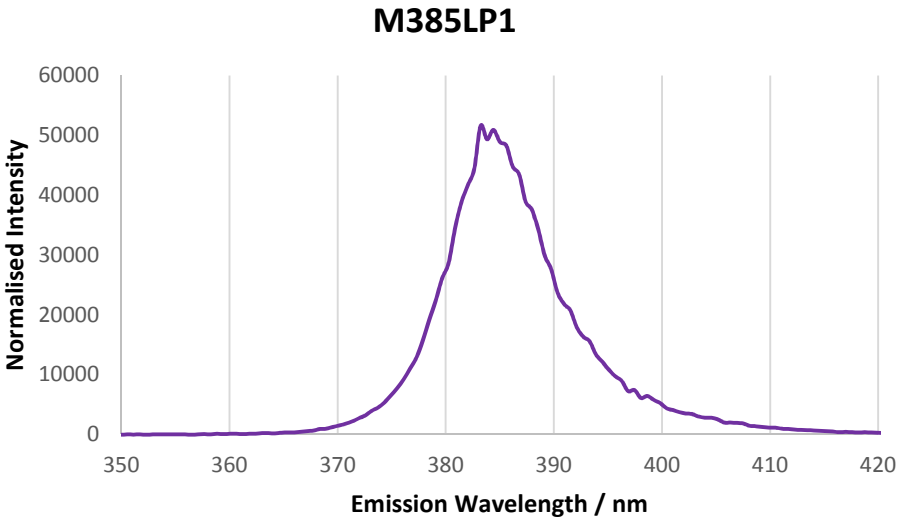

Figure 25: The recorded emission spectra for the Thorlabs M385LP1 LED.

Thorlabs M530L4: Mounted LED (green colour, 530 nm) with a power rating of 4.3 W. Emission spectra has not been recorded for this LED but is available from Thorlabs (Figure 26).[139]

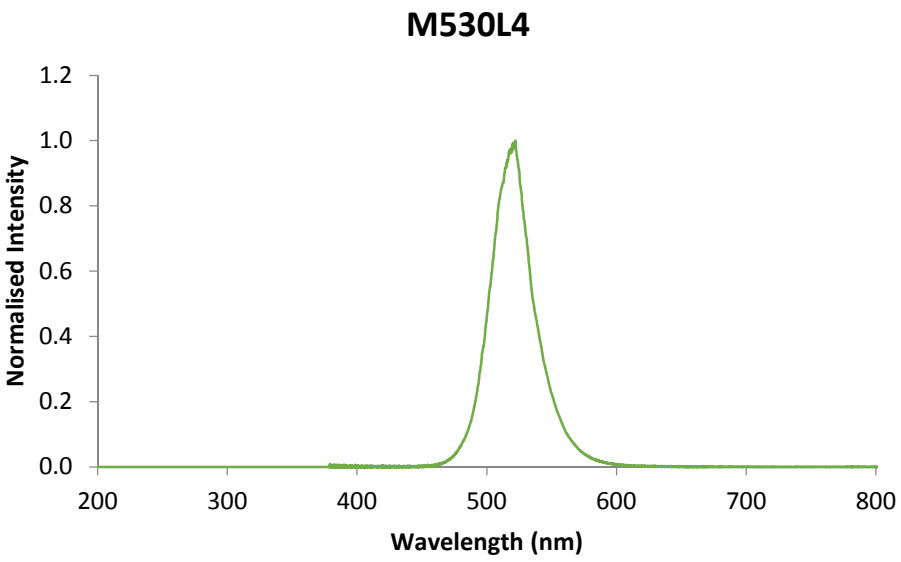

Figure 26: Emission spectra for the Thorlabs M530L4 LED. Data provided by Thorlabs.[139]

Thorlabs MINTL5: Mounted LED (mint green colour, 554 nm) with a power rating of 4.3 W. Emission spectra has not yet been recorded for this LED but is available from Thorlabs (Figure 27).

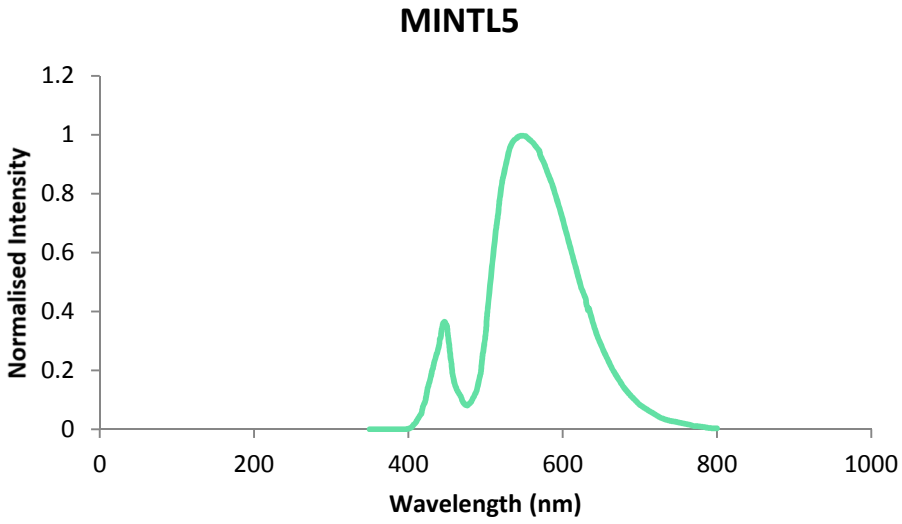

Figure 27: Emission spectra for the Thorlabs MINTL5 LED. Data provided by Thorlabs.[140]

8.7. General Procedures

General Procedure 1a: Amide Coupling Using HATU

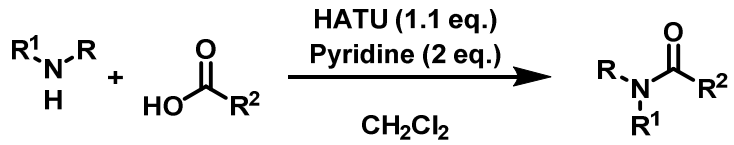

The corresponding carboxylic acid (1.0 eq.) was dissolved in CH_2Cl_2 (0.5 M) along with HATU (1.1 eq.) before addition of the respective amine (1.1 eq.). The mixture was stirred for 5 minutes before addition of pyridine (2.0 eq.) and the mixture was stirred at rt for 16 h. Saturated $NaHCO_{3(aq.)}$ (60 mL) was added and the layers separated. The aqueous layer was extracted with CH_2Cl_2 (2 × 40 mL) before the combined organics were washed with brine (60 mL), dried over $MgSO_4$, filtered and concentrated *in vacuo*. Purification by flash column chromatography afforded the amide product.

General Procedure 1b: Amide Coupling Using Oxalyl Chloride

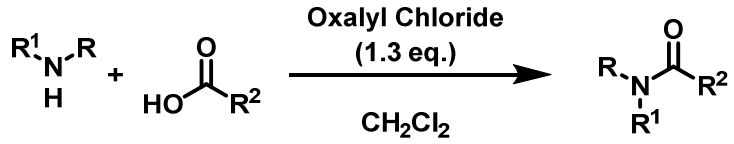

The corresponding acid (1.0 eq.) was dissolved in CH_2Cl_2 (0.5 M) before addition of a few drops of DMF. Oxalyl chloride (1.3 eq., 2 M in CH_2Cl_2) was added slowly to give an orange solution before being left to stir for 2 h. Excess volatiles were removed *in vacuo* before again dissolving the residue in CH_2Cl_2 (1 M) and the respective amine (1.1 eq.) was added slowly. The mixture was left to stir for 16 h before addition of water (20 mL) and the layers separated. The aqueous layer was washed with CH_2Cl_2 (3 × 30 mL) before the combined organics were washed with saturated $NaHCO_{3(aq.)}$ (2 × 20 mL). The organics were dried over $MgSO_4$, filtered and concentrated *in vacuo*. Purification by flash column chromatography afforded the amide product.

General Procedure 2: Photochemistry on Acyclic Enolates Using LDA

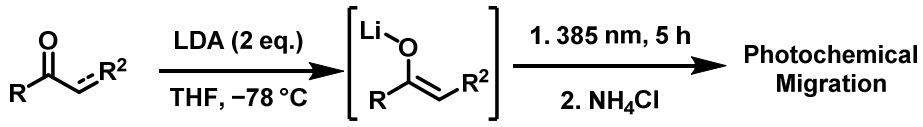

DIPA (2.0 eq.) was dissolved in anhydrous THF (5 mL) before dropwise addition of ^{n}BuLi (2.1 eq., 2.5 M in hexanes) at −78 °C. A solution of amide (1.0 eq.) in anhydrous THF (0.5 M) was added to the basic solution at −78 °C to give a coloured enolate solution. Irradiation was started at 385 nm (Thorlabs M385LP1) for 5 h before quenching with saturated $NH_4Cl_{(aq.)}$ (10 mL). The layers were separated at room temperature before the aqueous layer was extracted with EtOAc (3 × 10 mL) and the combined organics were washed with brine (10 mL), dried over Na_2SO_4, filtered and concentrated *in vacuo*. Purification by flash column chromatography afforded the respective photochemical products.

General Procedure 3: Lactam Cyclisation under Microwave Conditions

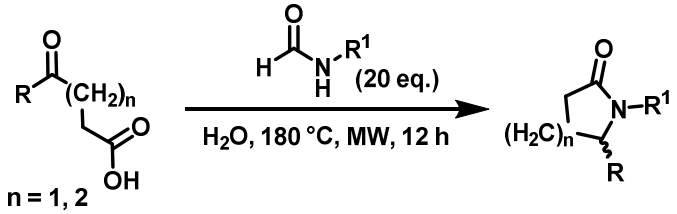

Synthesised according to a modified procedure by Li *et al*.[90]

To a 10-20 mL microwave vial was added the corresponding keto acid (1.0 eq.), H_2O (2 mL) and respective formamide (20.0 eq.). A small amount of H_2O (1 mL) was used to wash the walls of the vial before the vial was placed under microwave conditions (30 s pre-stirring, 180 °C, 12 h, high absorption setting). After cooling to rt, H_2O (10 mL) was added and the aqueous layer extracted with CH_2Cl_2 (3 × 10 mL) before the combined organics washed with brine (10 mL), dried over $MgSO_4$, filtered and concentrated *in vacuo*. Purification by flash column chromatography afforded the lactam product.

General Procedure 4a: Aldol Condensation for Dienyl Lactams

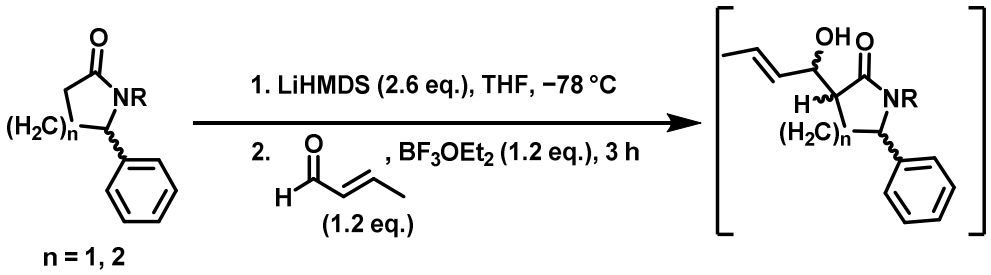

The respective lactam (1.0 eq.) was dissolved in anhydrous THF (0.25 M) before slow addition of LiHMDS (2.6 eq., 1 M in THF) at −78 °C. After stirring at this temperature for 1 h, a solution of crotonaldehyde (**16**) (1.2 eq.), BF_3OEt_2 (1.2 eq.) and anhydrous THF (15 mL) was added slowly at −78 °C. The mixture was left to stir for 3 h at this temperature before being quenched with saturated $NH_4Cl_{(aq.)}$ (30 mL) and water (30 mL). The aqueous layer was extracted with EtOAc (3 × 40 mL) before the combined organics were washed with water (2 × 30 mL), brine (2 × 30 mL), dried over $MgSO_4$, filtered and concentrated *in vacuo*. The crude mixture was used as a mixture of diastereomers in the next step without further purification.

General Procedure 4b: Aldol Condensation/Electrophilic Addition for Alkenyl Lactams

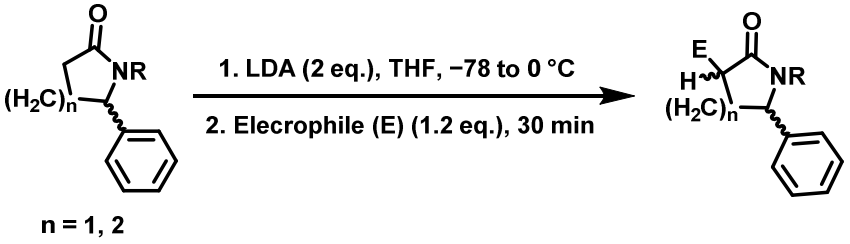

To an oven-dried flask was added anhydrous THF (10 mL), DIPA (2.0 eq.) and ^{n}BuLi (2.1 eq., 2.5 M in hexanes) at −78 °C. The base solution was transferred to an ice bath for 30 minutes before cooling again to −78 °C. A solution of lactam (1.0 eq.) was dissolved in anhydrous THF (0.25 M) before transferring the lactam solution to base solution at −78 °C. The mixture was transferred to an ice bath for 1 h before again being cooled to −78 °C. Electrophile (1.2 eq.) was added slowly at this temperature before again being transferred to an ice bath for 30 minutes. The reaction was quenched with saturated $NH_4Cl_{(aq.)}$ (30 mL) and water (30 mL). The aqueous layer was extracted with EtOAc (3 × 40 mL) before the combined organics were washed with brine (30 mL), dried over $MgSO_4$, filtered and

concentrated *in vacuo*. The crude mixture was used as a mixture of diastereomers in the next step without further purification.

General Procedure 5: Elimination of Alcoxy Lactams to Alkenyl Lactams

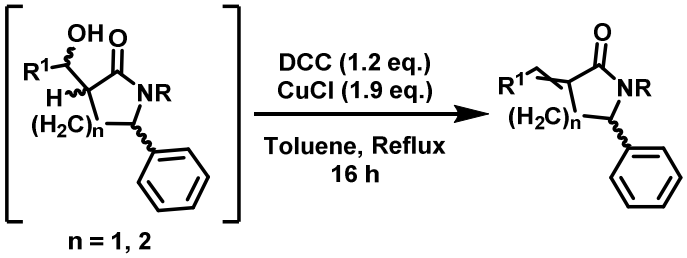

Synthetic procedure adapted from Santos *et al*.[87]

To an oven-dried flask was added a solution of α-alcoxy lactam (1.0 eq.) in anhydrous toluene (0.4 M) before addition of DCC (1.2 eq.) and CuCl (1.9 eq.). The mixture was heated to reflux for 16 h before slow addition of 30% $NH_{3(aq.)}$ (30 mL). The aqueous layer was extracted with EtOAc (5 × 30 mL) before the combined organics organics were washed with brine (2 × 50 mL), dried over $MgSO_4$, filtered and concentrated *in vacuo*. Purification by flash column chromatography afforded the product as a mixture of isomers.

General Procedure 6a: Photochemical Ring-Contraction of Lactam Trienolates

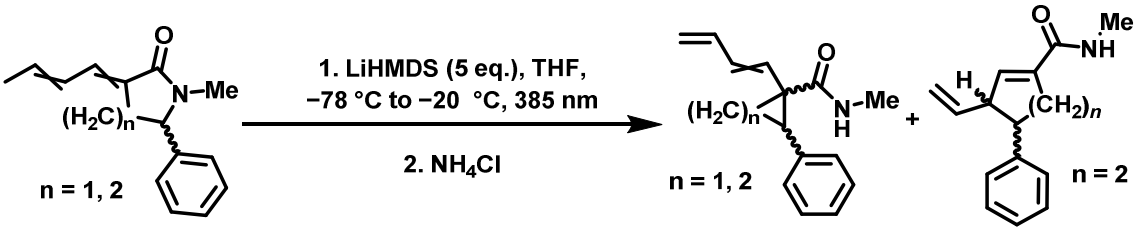

The respective lactam (1.0 eq.) was dissolved in anhydrous THF (0.05 M) before slow addition of LiHMDS (5.0 eq., 1 M in THF) at −78 °C with irradiation at 385 nm (Thorlabs M385LP1). After 1 h at this temperature, the mixture was allowed to slowly warm to −20 °C. After 5 h of total irradiation, the mixture was quenched with saturated $NH_4Cl_{(aq.)}$ (10 mL) before the aqueous layer was extracted with EtOAc (3 × 10 mL). The combined organics were washed with brine (10 mL) before being dried over Na_2SO_4, filtered and concentrated *in vacuo*. Purification by flash column chromatography gave the photochemical products. When n = 1, only the 1,3 ring-contraction product is seen (left product above). When n = 2, both photochemical products (1,3 and 1,5), shown above, were isolated.

General Procedure 6b: Photochemical Ring-Contraction of Lactam Dienolates

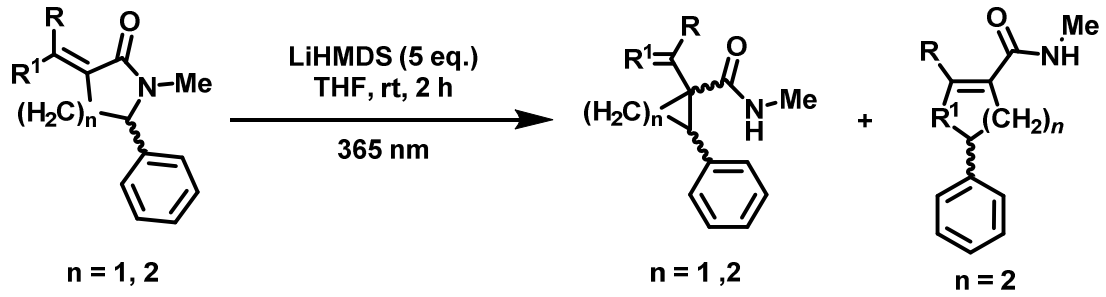

The respective alkenyl lactam (1.0 eq.) was dissolved in anhydrous THF (0.05 M) before slow addition of LiHMDS (5.0 eq.) at rt with constant 365 nm LED irradiation (Thorlabs M365LP1). After 2 h irradiation time, the reaction was quenched with saturated $NH_4Cl_{(aq.)}$ (10 mL) and H_2O (10 mL) and the mixture was extracted with EtOAc (3 × 10 mL) before organics washed with brine (10 mL), dried over Na_2SO_4, filtered and concentrated *in vacuo*. Purification by flash column chromatography afforded the final product(s).

General Procedure 6c: Photochemical Ring-Contraction of Lactam Monoenolates

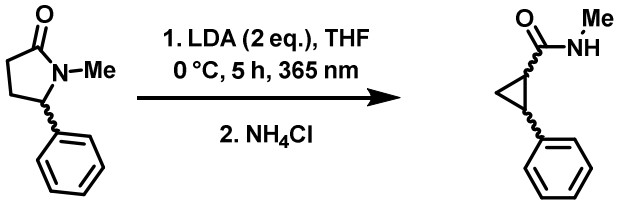

DIPA (2.0 eq.) was dissolved in anhydrous THF (5 mL) before dropwise addition of ^{n}BuLi (2.1 eq., 2.5 M in hexanes) at −20 °C. A solution of amide (1.0 eq.) in anhydrous THF (0.5 M) was added to the basic solution at −20 °C to give a coloured enolate solution. Irradiation was started at 365 nm (Thorlabs M365LP1) for 5 h before quenching with saturated $NH_4Cl_{(aq.)}$ (10 mL). The layers were separated at rt before the aqueous layer was extracted with EtOAc (3 × 10 mL) and the combined organics were washed with brine (10 mL), dried over Na_2SO_4, filtered and concentrated *in vacuo*. Purification by flash column chromatography afforded the respective photochemical product(s).

8.8. Experimental Procedures

Note that atomic numberings in experimental procedures are for assignments and don't always match systematic naming.

Where diastereomers are present, NOE analysis was used for isomer determination, where possible. Select and important NOE correlations are shown in this section, to illustrate the expected and common correlations.

Section 1 Experimental

(R)-N-(1-Phenylethyl)propan-2-amine (49)

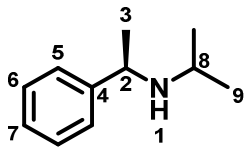

Synthesised according to the procedure by Saunthwal *et al.*[1]

A solution of (*R*)-phenylethylamine (**306**) (10.58 mL, 83.00 mmol, 1.0 eq.) in acetone (300 mL) was refluxed for 16 h before solvent was removed *in vacuo*. The residue was dissolved in MeOH (350 mL) and $NaBH_4$ (3.77 g, 99.60 mmol, 1.2 eq.) was added portion-wise in an ice bath. The mixture was allowed to stir for 6 h before solvent was evaporated *in vacuo*. Water (30 mL) was added followed by CH_2Cl_2 (30 mL) and the layers separated. The aqueous layer was further extracted with CH_2Cl_2 (2 × 30 mL) before the combined organics were washed with brine (30 mL), dried over $MgSO_4$, filtered and concentrated *in vacuo*. Purification by flash column chromatography (20% EtOAc / petroleum ether) afforded the title amine as a colourless oil (12.01 g, 73.62 mmol, 74%).

^{1}H NMR (400 MHz, Chloroform-*d*): δ 7.31-7.23 (4H, m, H5, H6), 7.21-7.17 (1H, m, H7), 3.85 (1H, q, *J* = 6.6 Hz, H2), 2.60 (1H, sept, *J* = 6.3 Hz, H8), 1.31 (3H, d, *J* = 6.6 Hz, H3), 1.00 (3H, d, *J* = 6.3 Hz, H9), 0.96 (3H, d, *J* = 6.3 Hz, H9).

^{13}C NMR (101 MHz, Chloroform-*d*): δ 146.2 (C4), 128.5 (C6), 126.8 (C7), 126.5 (C5), 54.4 (C2), 45.6 (C8), 25.0 (C3), 24.1 (C9), 21.9 (C9).

$[\alpha]_D^{24}$: +100 (*c* 1, $CHCl_3$).

Data consistent with literature.[1,141]

N-Benzyl-2-methylpropan-2-amine (121)

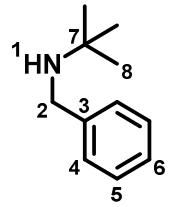

Synthesised according to the procedure by Saunthwal *et al.*[1]

tert-Butylamine (**101**) (21.01 mL, 0.20 mol, 1.0 eq.) and benzaldehyde (**120**) (20.32 mL, 0.20 mol, 1.0 eq.) were dissolved in MeOH (500 mL) and the resulting solution was stirred for 4 h at rt. $NaBH_4$ (9.08 g, 0.24 mol, 1.2 eq.) was added portion-wise in an ice bath and the mixture stirred for 15 min before being allowed to warm to rt. After 2 h, solvent was removed *in vacuo* before addition of water (300 mL) and CH_2Cl_2 (200 mL), and the layers separated. The aqueous layer was further extracted with CH_2Cl_2 (2 × 100 mL), and the combined organics were washed with brine (60 mL), dried over $MgSO_4$, filtered and concentrated *in vacuo* to give the title compound as a yellow oil (31.00 g, 0.19 mol, 92%) which was used without further purification.

^{1}H NMR (400 MHz, Chloroform-*d*): δ 7.41-7.32 (4H, m, H4, H5), 7.29-7.24 (1H, m, H6), 3.78 (2H, s, H2), 1.23 (9H, s, H8).

^{13}C NMR (101 MHz, Chloroform-*d*): δ 141.5 (C3), 128.4 (C4), 128.2 (C5), 125.6 (C6), 51.5 (C7), 46.7 (C2), 29.1 (C8).

Data consistent with literature.[142]

N-Benzyl-*N*-(tert-butyl) benzamide (76)

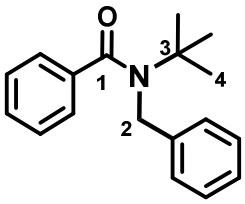

Synthesised according to the procedure by Clayden *et al.*[1]

Benzoyl chloride (**152**) (17.40 mL, 0.15 mol, 1.0 eq.) was added dropwise to a solution of *N*-benzyl-2-methylpropan-2-amine (**121**) (24.50 g, 0.15 mol, 1.0 eq.) and Et_3N (**107**) (32.00 mL, 0.23 mol, 1.5 eq.) in CH_2Cl_2 (200 mL) in an ice bath. The mixture was allowed to warm to rt for 16 h before being

quenched with water (100 mL) and the aqueous phase extracted with CH_2Cl_2 (3 × 30 mL). The combined organics were washed with brine (30 mL), dried over $MgSO_4$, filtered and concentrated *in vacuo*. Purification by flash column chromatography (5-10% EtOAc / petroleum ether) afforded the title compound as a white crystalline solid (25.11 g, 93.99 mmol, 65%).

^{1}H NMR (400 MHz, Chloroform-*d*): δ 7.38-7.34 (2H, m, Ar), 7.30-7.23 (5H, m, Ar), 7.22-7.17 (3H, m, Ar), 4.57 (2H, s, H2), 1.47 (9H, s, H4).

^{13}C NMR (101 MHz, Chloroform-*d*): δ 174.0 (C1), 140.1 (Ar), 139.4 (Ar), 129.1 (Ar), 128.6 (Ar), 128.5 (Ar), 127.1 (Ar), 126.4 (Ar), 126.3 (Ar), 58.2 (C3), 51.7 (C2), 28.9 (C4).

Data consistent with literature.[143]

(3*S*,3a*S*,7a*R*)-2-(*tert*-Butyl)-3-phenyl-2,3,3a,7a-tetrahydro-1*H*-isoindol-1-one

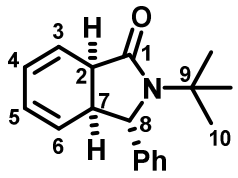

To a solution of *N*-benzyl-*N*-(tert-butyl) benzamide (**76**) (1.00 g, 3.74 mmol, 1.0 eq.) in anhydrous THF (40 mL) was added LDA (1.20 mL, 11.22 mmol, 3.0 eq., 2 M in THF) dropwise at −10 °C followed by DMPU (1.35 mL, 11.22 mmol, 3.0 eq.). The dark-brown/red coloured solution was held at −10 °C for 5 h before further addition of DMPU (1.35 mL, 11.22 mmol, 3.0 eq.) and the mixture stirred at −10 °C for 16 h. The mixture was allowed to warm to rt before addition of saturated $NH_4Cl_{(aq.)}$ (50 mL) and the layers separated. The aqueous layer was extracted with EtOAc (3 × 50 mL) before the combined organics were washed with brine (50 mL), dried over Na_2SO_4, filtered and concentrated *in vacuo*. Purification by flash column chromatography (5-10% EtOAc / petroleum ether) afforded the title compound as a white solid (0.82 g, 3.07 mmol, 82%).

^{1}H NMR (400 MHz, Chloroform-*d*): δ 7.31-7.24 (2H, m, Ar), 7.23-7.16 (3H, m, Ar), 5.88-5.84 (2H, m, H4, H5), 5.82-5.73 (1H, m, H3), 5.59-5.55 (1H, m, H6), 4.62 (1H, d, *J* = 2.2 Hz, H8), 3.36 (1H, dd, *J* = 11.1, 6.2 Hz, H2), 2.87 (1H, ddd, *J* = 11.1, 6.2, 2.2 Hz, H7), 1.26 (9H, s, H10).

^{13}C NMR (101 MHz, Chloroform-*d*): δ 175.5 (C1), 144.1 (Ar), 129.1 (Ar), 127.7 (Ar), 126.6 (C6), 125.4 (Ar), 124.4 (C5), 123.5 (C4), 122.8 (C3), 69.7 (C8), 55.5 (C9), 43.2 (C7), 40.4 (C2), 28.2 (C10).

HRMS (ESI$^+$) *m/z* calculated for $C_{18}H_{22}NO$ $[M+H]^+$ 268.1696, found 268.1699.

MP: 127-128 °C

IR: ν_{max} = 2969 (C-H), 1663 (C=O), 1493 (C=C), 1455, 1395, 1213, 1087 cm^{-1}.

$[\alpha]_D^{23}$**:** -7 (*c* 1, $CHCl_3$).

(*R*)-*N*-(*tert*-Butyl)-3-phenylcyclohepta-1,4,6-triene-1-carboxamide (80)

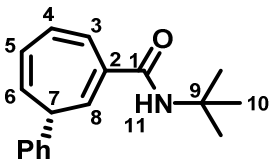

Synthesised according to the procedure by Saunthwal *et al*.[1]

To a solution of *(R)-N*-(1-phenylethyl)propan-2-amine (**H-49**) (0.14 mL, 0.75 mmol, 2.0 eq.) in anhydrous THF (5 mL) at −78 °C was added ^{n}BuLi (0.44 mL, 1.11 mmol, 3.0 eq., 2.5 M in hexanes) dropwise. The mixture was allowed to warm to rt over 15 minutes to give a clear yellow/orange solution. This was then cooled down again to −78 °C before slow addition of *N*-benzyl-*N*-(tert-butyl) benzamide (**76**) (100 mg, 0.37 mmol, 1.0 eq.) in anhydrous THF (0.5 mL). After 30 minutes at −78 °C the temperature was allowed to increase to −10 °C. After 1 hour of the warming process, DMPU (0.13 mL, 1.12 mmol, 3.0 eq.) was added before irradiation was initiated using the Kessil® Tuna Blue 40 W LED. After 3 h of irradiation, the reaction was quenched with saturated $NH_4Cl_{(aq.)}$ (10 mL) before the layers were separated at rt. The aqueous phase was extracted with EtOAc (3 × 10 mL) before the combined organics were washed with brine (10 mL), dried over Na_2SO_4, filtered and concentrated *in vacuo*. Purification by flash column chromatography (10% EtOAc / petroleum ether) afforded the title compound as a colourless oil (60 mg, 0.22 mmol, 60%).

^{1}H NMR (400 MHz, Chloroform-*d*): δ 7.38-7.36 (3H, m, Ar), 7.31-7.27 (2H, m, Ar), 7.08 (1H, d, *J* = 10.9 Hz, H3), 6.85 (1H, dd, *J* = 10.9, 5.7 Hz, H4), 6.26 (1H, ddd, *J* = 9.3, 5.7, 1.6 Hz, H5), 5.94 (1H, d, *J* = 5.6 Hz, H8), 5.54 (1H, br s, H11), 5.50 (1H, ddq, *J* = 9.3, 5.6, 0.8 Hz, H6), 2.74 (1H, td, *J* = 5.6, 1.6 Hz, H7), 1.37 (9H, s, H10).

^{13}C NMR (101 MHz, Chloroform-*d*): δ 167.1 (C1), 143.0 (Ar), 133.6 (C2), 132.3 (C3), 128.9 (C8), 128.2 (C4), 127.7 (Ar), 127.1 (Ar), 126.5 (C5), 125.7 (C6), 125.3 (Ar), 51.6 (C9), 44.7 (C7), 28.9 (C10).

$[\alpha]_D^{21}$**:** +11 (*c* 1, $CHCl_3$).

Data consistent with literature.[1]

Section 3 Experimental

(1*S*,6*R*,7*S*)-*N*-(*tert*-Butyl)-7-butyl-6-phenylcyclohepta-2,4-diene-1-carboxamide (92)

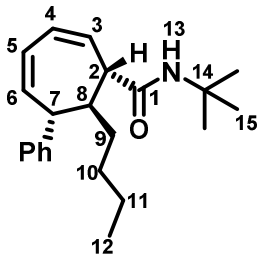

To a solution of (*R*)-*N*-(*tert*-butyl)-3-phenylcyclohepta-1,4,6-triene-1-carboxamide (**80**) (100 mg, 0.37 mmol, 1.0 eq.) in dry THF (10 mL) was added ^{n}BuLi (0.30 mL, 0.74 mmol, 2.0 eq., 2.5 M in hexanes) dropwise at −78 °C to give a dark-purple coloured solution. The mixture was left to stir at −78 °C for 1 h before being quenched with saturated $NH_4Cl_{(aq.)}$ (10 mL). After warming to rt, the layers were separated before the aqueous layer was extracted with EtOAc (3 × 10 mL). The combined organics were washed with brine (10 mL), dried over Na_2SO_4, filtered and concentrated *in vacuo*. Purification by flash column chromatography (5-10% EtOAc / petroleum ether) afforded the title compound as a white solid (42 mg, 0.13 mmol, 35%).

^{1}H NMR (400 MHz, Chloroform-*d*): δ 7.30-7.14 (5H, m, Ar), 6.17 (1H, dd, *J* = 11.0, 4.8 Hz, H4), 6.09 (1H, dd, *J* = 11.0, 7.0 Hz, H3), 5.98 (1H, dd, *J* = 11.1, 6.1 Hz, H6), 5.91 (1H, dd, *J* = 11.1, 4.8 Hz, H5), 5.45 (1H, br s, H13), 3.44 (1H, dd, *J* = 8.6, 6.1 Hz, H7), 3.33-3.28 (1H, m, H8), 2.99 (1H, dd, *J* = 7.0, 4.8 Hz, H2), 1.44-1.23 (6H, m, H9, H10, H11), 1.19 (9H, s, H15), 0.78 (3H, t, *J* = 7.1 Hz, H12).

^{13}C NMR (101 MHz, Chloroform-*d*): δ 171.9 (C1), 139.7 (C6), 132.2 (C3), 130.2 (C4), 129.0 (Ar), 129.0 (Ar), 128.4 (Ar), 126.3 (Ar), 126.0 (C5), 54.4 (C8), 51.1 (C7), 50.9 (C2), 48.6 (C14), 33.4 (C9), 29.1 (C10), 28.7 (C15), 22.9 (C11), 14.1 (C12).

HRMS (ESI^{+}) *m/z* calculated for $C_{22}H_{32}NO$ $[M+H]^{+}$ 326.2478, found 326.2476.

IR: ν_{max} = 3311 (N-H), 2962 (C-H), 2929 (C-H), 2858 (C-H), 1661 (C=O), 1642 (C=C), 1540 (C=C), 1453, 1260, 1090, 1019.

$[\boldsymbol{\alpha}]_{\boldsymbol{D}}^{\boldsymbol{24}}$**:** −8 (*c* 1, $CHCl_3$).

1D NOESY for this isomer:

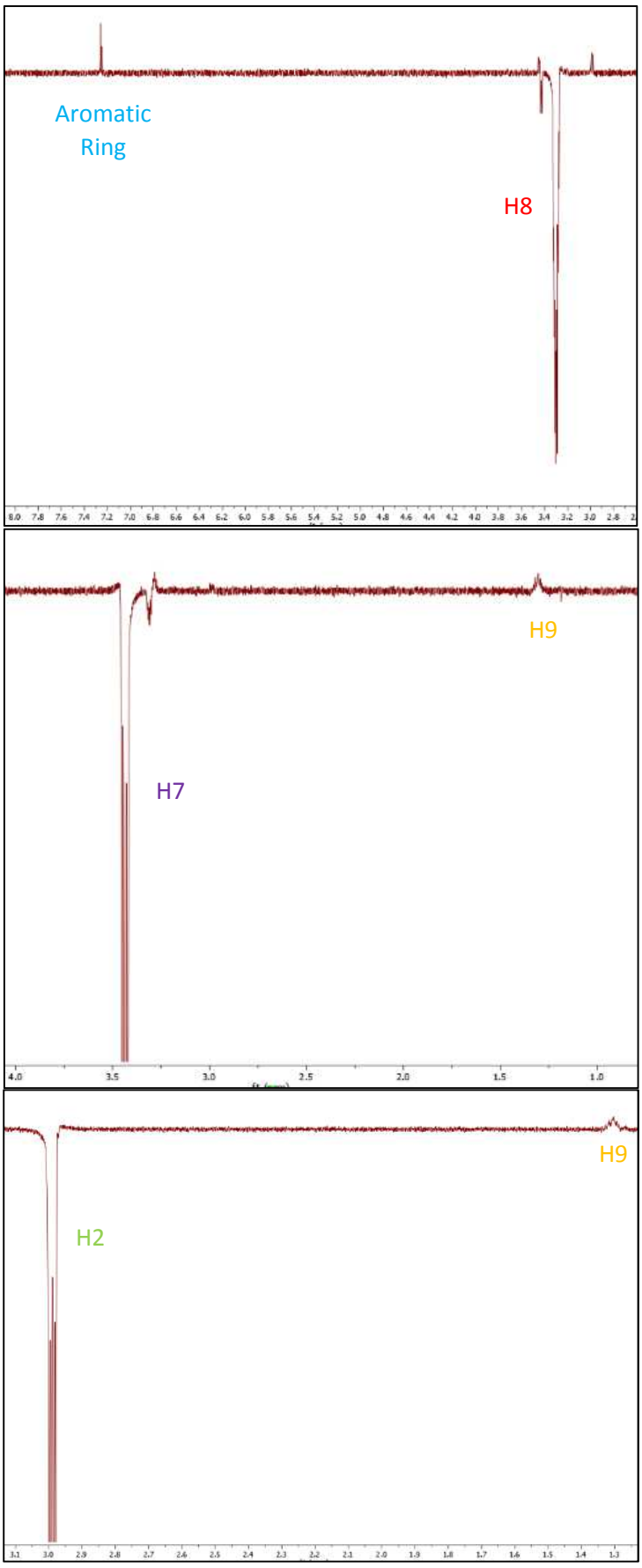

The tentative stereochemical assignment arises from weak 1D NOESY couplings between H8 and the aromatic ring, between H7 and H9 and between H2 and H9.

*Figure 28: 1D NOESY data for **92**, indicating the stereochemical arrangement detailed.*

(3*R*,6*R*,7*S*)-*N*-(*tert*-Butyl)-7-butyl-3-methyl-6-phenylcyclohepta-1,4-diene-1-carboxamide (93)

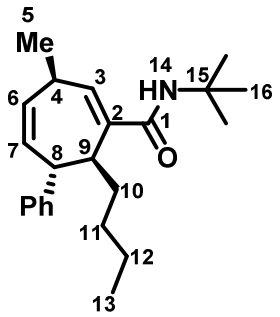

To a solution of (*R*)-*N*-(*tert*-butyl)-3-phenylcyclohepta-1,4,6-triene-1-carboxamide (**80**) (100 mg, 0.37 mmol, 1.0 eq.) in dry THF (10 mL) was added ^{n}BuLi (0.30 mL, 0.74 mmol, 2.0 eq., 2.5 M in hexanes) dropwise at −78 °C to give a dark-purple coloured solution. The mixture was left to stir at −78 °C for 1 h before being quenched with MeI (0.05 mL, 0.74 mmol, 2.0 eq.). After warming to rt, the layers were separated before the aqueous layer was extracted with EtOAc (3 × 10 mL). The combined organics were washed with brine (10 mL), dried over Na_2SO_4, filtered and concentrated *in vacuo*. Purification by flash column chromatography (5-10% EtOAc / petroleum ether) afforded the title compound as a colourless oil (71 mg, 0.21 mmol, 56%).

^{1}H NMR (400 MHz, Chloroform-*d*): δ 7.31-7.17 (5H, m, Ar), 5.96 (1H, d, *J* = 6.7 Hz, H3), 5.73-5.58 (2H, m, H6, H7), 4.52 (1H, br s, H14), 3.74 (1H, dd, *J* = 6.8, 5.3 Hz, H8), 3.24-3.16 (1H, m, H4), 2.79 (1H, td, *J* = 7.4, 5.3 Hz, H9), 1.83-1.73 (2H, m, H10), 1.63-1.49 (2H, m, H11), 1.41-1.35 (2H, m, H12), 1.11 (9H, s, H16), 0.92-0.89 (6H, m, H5, H13).

^{13}C NMR (101 MHz, Chloroform-*d*): δ 171.6 (C1), 144.1 (Ar), 141.2 (C2), 134.9 (C3), 134.3 (C6), 128.5 (Ar), 128.3 (Ar), 126.8 (C7), 126.3 (Ar), 51.2 (C15), 48.2 (C9), 47.3 (C8), 36.6 (C4), 36.2 (C10), 36.0 (C11), 30.1 (C12), 28.5 (C16), 22.7 (C5), 14.1 (C13).

HRMS (ESI^{+}) *m/z* calculated for $C_{23}H_{34}NO$ $[M+H]^{+}$ 340.2635, found 340.2639.

IR: ν_{max} = 3359 (N-H), 2959 (C-H), 2871 (C-H), 1649 (C=O), 1621 (C=C), 1525 (C=C), 1453, 1365, 1219.

$[\boldsymbol{\alpha}]_{\boldsymbol{D}}^{\mathbf{24}}$**:** −19 (*c* 1, $CHCl_3$).

1D NOESY for this isomer:

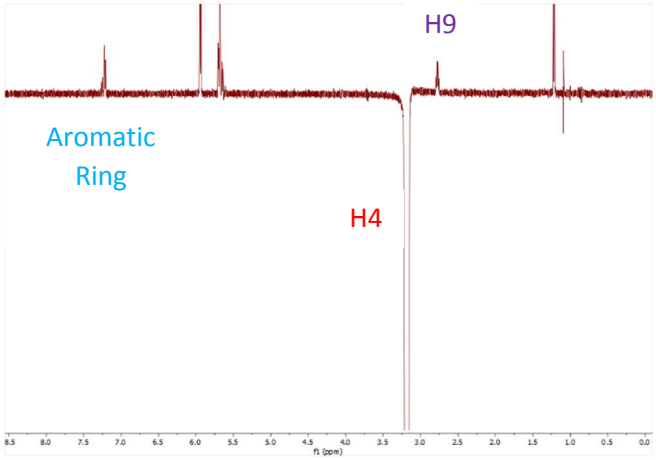

The tentative stereochemical assignment arises from weak 1D NOESY coupling between H4 and the aromatic ring and between H4 and H9.

*Figure 29: 1D NOESY data for **93**, indicating the stereochemical arrangement detailed.*

(2*E*,4*E*)-*N*-(*tert*-Butyl)hexa-2,4-dien-1-amine (103)

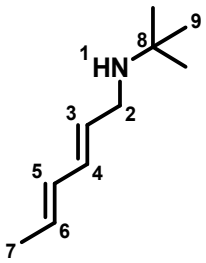

To a stirred solution of (2*E*,4*E*)-hexa-2,4-dienal (**102**) (7.34 mL, 68.36 mmol, 1.0 eq.) in MeOH (200 mL) was added *tert*-butylamine (**101**) (7.18 mL, 68.36 mmol, 1 eq.). After 2 h, $NaBH_4$ (3.10 g, 82.04 mmol, 1.2 eq.) was added portion-wise in an ice bath. The mixture was allowed to stir at rt for 16 h before solvent was removed *in vacuo*. Water (100mL) was added and the aqueous layer was extracted with CH_2Cl_2 (3 × 30 mL) before the combined organics were washed with brine (60 mL), dried over $MgSO_4$, filtered and concentrated *in vacuo*. This afforded a yellow oil which was used without further purification (9.20 g, 60.07 mmol, 88%).

^{1}H NMR (400 MHz, Chloroform-*d*): δ 6.13-5.97 (2H, m, H4, H5), 5.66-5.56 (2H, m, H3, H6), 3.18 (2H, d, *J* = 6.9 Hz, H2), 1.71 (3H, d, *J* = 6.9 Hz, H7), 1.09 (9H, s, H9).

^{13}C NMR (101 MHz, Chloroform-*d*): δ 131.4 (C4), 131.3 (C5), 130.3 (C3), 128.5 (C6), 50.5 (C8), 44.9 (C2), 29.2 (C9), 18.1 (C7).

HRMS (APCI$^+$) *m/z* calculated for $C_{10}H_{20}N$ $[M+H]^+$ 154.1590, found 154.1590.

IR: ν_{max} = 3019 (N-H), 2962 (C-H), 2914 (C-H), 1441 (C=C), 1361 (C=C), 1231, 986, 706 cm^{-1}.

(*N*)-(*tert*-Butyl)-*N*-((2*E*,4*E*)-hexa-2,4-dien-1-yl)but-2-ynamide (110)

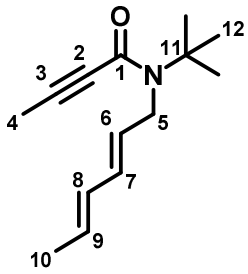

The title compound was synthesised according to General Procedure 1a using 2-butynoic acid (**109**) (1.00 g, 11.89 mmol, 1.0 eq.) and (2*E*,4*E*)-*N*-(*tert*-butyl)hexa-2,4-dien-1-amine (**103**) (2.00 g, 13.08 mmol, 1.1 eq.). Purification by flash column chromatography (5-10% EtOAc / petroleum ether) afforded the amide as an orange oil (0.52 g, 2.38 mmol, 20%).

^{1}H NMR (400 MHz, Chloroform-*d*): δ 6.12-5.94 (2H, m, H7, H8), 5.69-5.58 (1H, m, H6), 5.54-5.46 (1H, m, H9), 4.26 (2H, d, *J* = 5.8 Hz, H5), 1.91 (3H, s, H4), 1.72 (3H, d, *J* = 6.9 Hz, H10), 1.39 (9H, s, H12).

^{13}C NMR (101 MHz, Chloroform-*d*): δ 157.9 (C1), 131.9 (C7), 130.4 (C8), 129.3 (C6), 128.0 (C9), 87.5 (C3), 74.3 (C2), 57.5 (C11), 48.9 (C5), 28.5 (C12), 18.1 (C10), 4.0 (C4).

HRMS (ESI^+) *m/z* calculated for $C_{14}H_{22}NO$ $[M+H]^+$ 220.1696, found 220.1689.

IR: ν_{max} = 2968 (C-H), 2951 (C-H), 1689 (C=O), 1666 (C=C), 1631 (C=C), 1386, 1228, 1196.

(6*S*)-2-(*tert*-Butyl)-6,7-dimethyl-2,3,3a,6-tetrahydro-1*H*-isoindol-1-one (111)

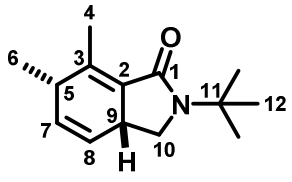

A solution of (*N*)-(*tert*-butyl)-*N*-((2*E*,4*E*)-hexa-2,4-dien-1-yl)but-2-ynamide (**110**) (0.40 g, 1.83 mmol, 1.0 eq.) in DMF (10 mL) was heated to reflux for 16 h. Water was added (25 mL) before the aqueous layer was extracted with CH_2Cl_2 (3 × 30 mL). The combined organics were washed with brine (2 x 60 mL) before being dried over $MgSO_4$, filtered and concentrated *in vacuo*. Purification by flash column chromatography (5-10% EtOAc / petroleum ether) afforded the title compound as a yellow oil (0.26

mmol, 65%). The product stereochemistry is tentatively assigned based on analogy to literature reporting on lactone analogue **118**.[59]

^{1}H NMR (400 MHz, Chloroform-*d*): δ 5.70 (1H, ddd, *J* = 9.6, 2.9, 1.8 Hz, H7), 5.61 (1H, ddd, 9.6, 2.8, 2.0 Hz, H8), 3.60 (1H, t, *J* = 8.5 Hz, H10), 3.16-3.06 (1H, m, H9), 2.92 (1H, dd, *J* = 9.5, 8.5 Hz, H10), 2.83-2.72 (1H, m, H5), 2.19 (3H, dd, *J* = 2.5, 1.3 Hz, H4), 1.40 (9H, s, H12), 1.20 (3H, d, *J* = 7.6 Hz, H6).

^{13}C NMR (101 MHz, Chloroform-*d*): δ 169.4 (C1), 133.9 (C8), 132.1 (C3), 124.1 (C7), 119.3 (C2), 54.1 (C11), 48.3 (C10), 36.7 (C5), 36.1 (C9), 27.9 (C12), 18.7 (C6), 13.7 (C4).

HRMS (ESI$^+$) *m/z* calculated for $C_{14}H_{22}NO$ $[M+H]^+$ 220.1696, found 220.1685.

IR: ν_{max} = 2971 (C-H), 2928 (C-H), 1704 (C=O), 1666 (C=C), 1454, 1363, 1205.

$[\boldsymbol{\alpha}]_{\boldsymbol{D}}^{\boldsymbol{24}}$**:** +3 (*c* 1, $CHCl_3$).

(2*E*,4*E*)-Hexa-2,4-dien-1-ol (116)

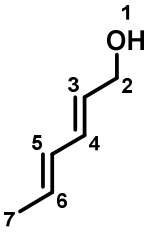

Synthesised according to the procedure by Pini *et al.*[144]

To a stirred solution of (2*E*,4*E*)-hexa-2,4-dienal (**102**) (6.82 mL, 63.46 mmol, 1.0 eq.) in EtOH (100 mL) was added a solution of $NaBH_4$ (3.60 g, 95.18 mmol, 1.5 eq.) in EtOH (25 mL) portion-wise. The mixture was left to stir at rt for 16 h before the solvent was removed *in vacuo*. Water (60 mL) was added and the aqueous layer was extracted with Et_2O (3 × 30 mL). The combined organics were washed with brine (60 mL), dried over Na_2SO_4, filtered and concentrated *in vacuo*. Purification by flash column chromatography (10-20% EtOAc / petroleum ether) afforded the title compound as a colourless oil (4.80 g, 48.91 mmol, 77%).

^{1}H NMR (400 MHz, Chloroform-*d*): δ 6.16 (1H, dd, *J* = 15.2, 10.6 Hz, H4), 6.05-5.97 (1H, m, H5), 5.71-5.61 (2H, m, H3 and H6), 4.12 (2H, d, *J* = 5.2 Hz, H2), 1.74 (3H, d, *J* = 6.7 Hz, H7).

^{13}C NMR (101 MHz, Chloroform-*d*): δ 131.8 (C4), 130.9 (C5), 129.9 (C3), 129.4 (C6), 63.4 (C2), 18.1 (C7).

Data consistent with literature.[144,145]

(2*E*,4*E*)-Hexa-2,4-dien-1-yl propiolate (117)

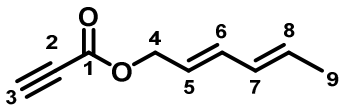

Synthesised according to the procedure by Saito *et al.*[59]

To a solution of (2*E*,4*E*)-hexa-2,4-dien-1-ol (**116**) (1.00 g, 10.20 mmol, 1.0 eq.) in CH_2Cl_2 (10 mL) was added propiolic acid (**104**) (0.68 mL, 11.00 mmol, 1.1 eq.). A solution of DCC (2.30 g, 11.15 mmol, 1.1 eq.) and DMAP (0.12 g, 1.00 mmol, 0.1 eq.) in CH_2Cl_2 (10 mL) was added to the reaction flask slowly to give a black mixture. This mixture was left to stir for 16 h before being filtered through a pad of celite, washing through with Et_2O. Purification by flash column chromatography (0-5% EtOAc / petroleum ether) afforded the title compound as a colourless oil (0.89 g, 5.92 mmol, 58%).

^{1}H NMR (400 MHz, Chloroform-*d*): δ 6.27 (1H, dd, *J* = 15.2, 10.6 Hz, H6), 6.08-5.99 (1H, m, H7), 5.82-5.70 (1H, m, H8), 5.60 (1H, dt, *J* = 15.2, 7.5 Hz, H5), 4.67 (2H, d, *J* = 7.5 Hz, H4), 2.88 (1H, s, H3), 1.76 (3H, d, *J* = 6.9 Hz, H9).

^{13}C NMR (101 MHz, Chloroform-*d*): δ 152.6 (C1), 135.9 (C6), 132.2 (C8), 130.3 (C7), 122.2 (C5), 74.8 (C3), 74.7 (C2), 67.2 (C4), 16.8 (C9).

Data consistent with literature.[59,146]

(6*S*)-6-Methyl-3a,6-dihydroisobenzofuran-1(3*H*)-one (118)

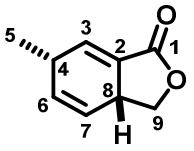

A solution of (6*S*)-6-methyl-3a,6-dihydroisobenzofuran-1(3*H*)-one (**117**) (0.74 g, 4.93 mmol, 1.0 eq.) in toluene (27 mL) was heated to reflux for 16 h. Water (30 mL) was added and the aqueous layer was extracted with EtOAc (3 × 25 mL) before the combined organics were washed with brine (30 mL), dried over $MgSO_4$, filtered and concentrated *in vacuo*. Purification by flash column chromatography (10% EtOAc / petroleum ether) afforded the title compound as a yellow oil (0.50 g, 3.35 mmol, 68%).

^{1}H NMR (400 MHz, Chloroform-*d*): δ 6.67-6.65 (1H, m, H3), 5.75 (1H, ddd, *J* = 9.7, 2.4, 1.8 Hz, H6), 5.71 (1H, m, H7), 4.62 (1H, ddd, *J* = 9.4, 8.2, 0.5 Hz, H9), 3.81 (1H, dd, *J* = 10.3, 8.1 Hz, H9), 3.53-3.44 (1H, m, H8), 3.05-2.95 (1H, m, H4), 1.24 (3H, d, *J* = 7.6 Hz, H5).

^{13}C NMR (101 MHz, Chloroform-*d*): δ 165.6 (C1), 138.8 (C3), 133.3 (C7), 128.5 (C2), 121.9 (C6), 70.8 (C9), 37.1 (C8), 33.0 (C4), 20.1 (C5).

$[\boldsymbol{\alpha}]_{\boldsymbol{D}}^{\mathbf{24}}$**:** −4 (*c* 1, $CHCl_3$).

Data consistent with literature.[59]

Section 4 Experimental

(2*E*,4*E*)-*N*-Benzyl-*N*-(*tert*-butyl)hexa-2,4-dienamide (123)

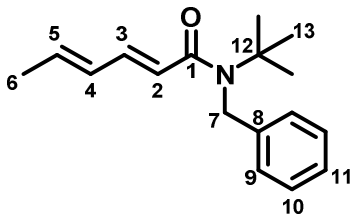

The title compound was synthesised according to General Procedure 1a using 2*E*,4*E*-hexadienoic acid (**122**) (1.00 g, 8.92 mmol, 1.0 eq.) and *N*-benzyl-2-methylpropan-2-amine (**121**) (1.60 g, 9.81 mmol, 1.1 eq.). Purification by flash column chromatography (10% EtOAc / petroleum ether) afforded the amide as a white solid (0.30 g, 1.16 mmol, 13%).

^{1}H NMR (400 MHz, Chloroform-*d*): δ 7.38-7.33 (2H, m, H10), 7.28-7.21 (4H, m, H3, H9, H11), 6.06-5.97 (3H, m, H2, H4, H5), 4.62 (2H, s, H7), 1.77 (3H, d, *J* = 5.4 Hz, H6), 1.44 (9H, s, H13).

^{13}C NMR (101 MHz, Chloroform-*d*): δ 169.4 (C1), 142.7 (C3), 140.0 (C8), 137.1 (C5), 130.4 (C4), 128.9 (C10), 127.1 (C11), 125.9 (C9), 122.3 (C2), 57.8 (C12), 49.1 (C7), 28.8 (C13), 18.6 (C6).

HRMS (ESI$^+$) *m/z* calculated for $C_{17}H_{24}NO$ $[M+H]^+$ 258.1852, found 258.1848.

MP: 95-96 °C.

IR: ν_{max} = 2984 (C-H), 1656 (C=O), 1630 (C=C), 1601 (C=C), 1495, 1393, 1354, 1193, 1006 cm^{-1}.

(*E*)-Hexa-3,5-dienoic acid (125)

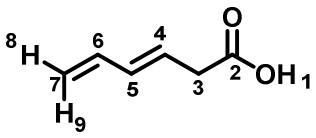

Synthesised according to the procedure by Ballester *et al.*[60]

To a solution of DIPA (7.50 mL, 53.55 mmol, 2.0 eq.) in anhydrous THF (15 mL) was added ^{n}BuLi (22.50 mL, 56.22 mmol, 2.1 eq., 2.5 M in hexanes) at −78 °C. A solution of 2*E*,4*E*-hexadienoic acid (**122**) (3.00 g, 26.77 mmol, 1.0 eq.) in anhydrous THF (30 mL) was added to the base solution to give an orange cloudy mixture at −78 °C. The solution was allowed to warm to −20 °C gradually for 2.5 h before being quenched with saturated $NH_4Cl_{(aq.)}$ (50 mL). The layers were separated before the aqueous layer was acidified using $HCl_{(aq.)}$ (3 M) until pH 2 and extracted with EtOAc (3 × 40 mL). The combined organics were dried over $MgSO_4$ before being filtered and concentrated *in vacuo* to give an orange oil as the title compound (6.88 g, 26.77 mmol, quant.).

^{1}H NMR (400 MHz, Chloroform-*d*): δ 9.43 (1H, br s, H1), 6.33 (1H, dt, *J* = 17.1, 10.1 Hz, H6), 6.15 (1H, dd, *J* = 15.2, 10.1 Hz, H5), 5.77 (1H, dt, *J* = 15.2, 7.5 Hz, H4), 5.17 (1H, dd, *J* = 17.1, 1.1 Hz, H9), 5.07 (1H, dd, *J* = 10.1, 1.1 Hz, H8), 3.15 (2H, d, *J* = 7.5 Hz, H3).

^{13}C NMR (101 MHz, Chloroform-*d*): δ 177.7 (C2), 137.2 (C6), 133.8 (C5), 127.1 (C4), 116.9 (C7), 40.9 (C3).

HRMS (ESI^-) *m/z* calculated for $C_6H_7O_2$ $[M-H]^-$ 111.0446, found 111.0451.

IR: ν_{max} = 3087 (O-H), 3021 (C-H), 2974 (C-H), 1704 (C=O), 1652 (C=C), 1604 (C=C), 1410, 1273, 1219, 1002 cm^{-1}.

(*E*)-*N*-Benzyl-*N*-(*tert*-butyl)hexa-3,5-dienamide (126)

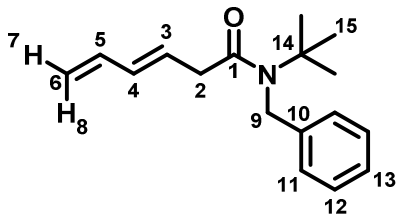

The title compound was synthesised according to General Procedure 1a using (*E*)-hexa-3,5-dienoic acid (**125**) (2.00 g, 17.83 mmol, 1.0 eq.) and *N*-benzyl-2-methylpropan-2-amine (**121**) (3.20 g, 19.61 mmol, 1.1 eq.). Purification by flash column chromatography (10% EtOAc / petroleum ether) afforded the amide as a white solid (1.83 g, 7.13 mmol, 40%).

^{1}H NMR (400 MHz, Chloroform-*d*): δ 7.36 (2H, t, *J* = 6.9 Hz, H12), 7.28-7.19 (3H, m, H11, H13), 6.33 (1H, dt, *J* = 17.0, 10.4 Hz, H5), 6.00 (1H, dd, *J* = 15.5, 10.4 Hz, H4), 5.86 (1H, dt, *J* = 15.5, 6.6 Hz, H3),

5.09 (1H, dd, *J* = 17.0, 0.8 Hz, H7), 5.00 (1H, dd, *J* = 10.4, 0.8 Hz, H8), 4.58 (2H, s, H9), 3.10 (2H, d, *J* = 6.6 Hz, H2), 1.43 (9H, s, H15).

^{13}C NMR (101 MHz, Chloroform-*d*): δ 174.5 (C1), 140.3 (C10), 136.8 (C5), 134.7 (C4), 129.3 (C12), 128.3 (C13), 126.6 (C3), 125.6 (C11), 116.3 (C6), 58.1 (C14), 49.2 (C9), 39.3 (C2), 27.2 (C15).

HRMS (ESI$^+$) *m/z* calculated for $C_{17}H_{24}NO$ $[M+H]^+$ 258.1852, found 258.1846.

MP: 49-50 °C.

IR: ν_{max} = 2967 (C-H), 1630 (C=O), 1603 (C=C), 1395, 1359, 1192, 703 cm^{-1}.

2-Benzyl-*N*-(*tert*-butyl)hexa-3,5-dienamide (*E*/*Z*-128), (*E*)-4-Benzyl-*N*-(*tert*-butyl)hexa-2,5-dienamide (129) and (2*E*,4*E*)-*N*-(*tert*-Butyl)-7-phenylhepta-2,4-dienamide (130)

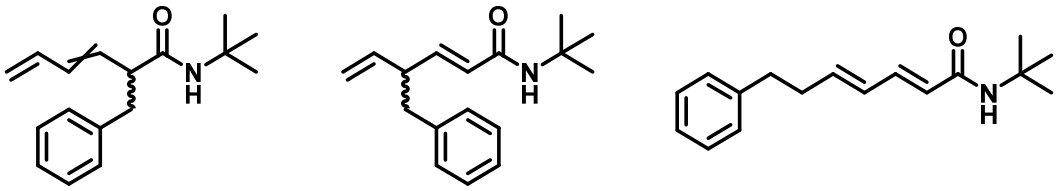

The title compounds were synthesised according to General Procedure 2 using (*E*)-*N*-benzyl-*N*-(*tert*-butyl)hexa-3,5-dienamide (**126**) (100 mg, 0.39 mmol, 1.0 eq.). Purification by flash column chromatography (5-10% EtOAc / petroleum ether) afforded the various migration products.

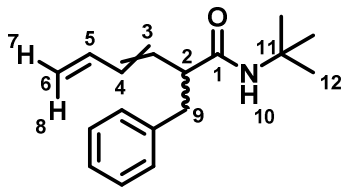

[1,3]-Isomers *E*/*Z*-128: Yellow solid (30 mg, 0.12 mmol, 30%). Isolated as a mixture of *E*- and *Z*- isomers, in a ratio of 55:45 respectively and an NMR yield of 37%. Assignments *E*- and *Z*- in the assignments below relate to the stereoisomer of the molecule, and not the individual atom discussed.

^{1}H NMR (400 MHz, Chloroform-*d*): δ 7.29-7.24 (4H, m, Ar), 7.22-7.17 (6H, m, Ar), 6.46 (1H, dt, *J* = 16.9, 10.0 Hz, *Z*-H5), 6.32 (1H, dt, *J* = 16.9, 10.2 Hz, *E*-H5), 6.15-6.05 (2H, m, *E*-H4, *Z*-H4), 5.78 (1H, dd, *J* = 15.2, 8.8 Hz, *E*-H3), 5.55 (1H, t, *J* = 9.8 Hz, *Z*-H3), 5.27-5.05 (6H, m, *E*-H10, *Z*-H10, *E*-H7, *Z*-H7, *E*-H8, *Z*-H8), 3.42 (1H, dt, *J* = 9.8, 7.0 Hz, *Z*-H2), 3.15 (2H, 2 x dd, *J* = 13.6, 7.2 Hz and 10.8, 7.1 Hz, *E*-H9, *Z*-H9),

2.94 (1H, dt, *J* = 8.8, 7.1 Hz, *E*-H2), 2.80 (2H, 2 x dd, *J* = 13.3, 7.3 and 10.5, 7.3 Hz, *E*-H9, *Z*-H9), 1.25 (9H, s, *Z*-H12), 1.23 (9H, s, *E*-H12).

^{13}C NMR (101 MHz, Chloroform-*d*): δ 171.8 (*E*-C1), 171.6 (*Z*-C1), 139.5 (Ar), 139.4 (Ar), 136.6 (*E*-C5), 133.2 (*Z*-C4), 132.8 (*E*-C3) , 131.7 (*E*-C4), 131.4 (*Z*-C5), 130.2 (*Z*-C3), 131.0 (Ar), 130.9 (Ar), 129.5 (Ar), 129.4 (Ar), 128.4 (Ar), 126.4 (Ar), 119.6 (*E*/*Z*-C6), 117.1 (*E*/*Z*-C6), 53.4 (*E*-C2), 50.8 (*E*-C11), 50.8 (*Z*-C11), 48.7 (*Z*-C2), 39.1 (E/Z-C9), 38.5 (*E*/*Z*-C9), 28.8 (*E*/*Z*-C12), 28.7 (*E*/*Z*-C12).

HRMS (ESI$^+$) *m/z* calculated for $C_{17}H_{24}NO$ $[M+H]^+$ 258.1858, found 258.1853.

MP: 94-95 °C.

IR: ν_{max} = 3291 (N-H), 2966 (C-H), 2924 (C-H), 1648 (C=O), 1635 (C=C), 1480, 1324, 1202.

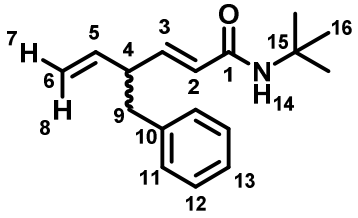

[1,5]-Isomers 129: Colourless oil (8 mg, 0.03 mmol, 8%) with an NMR yield of 10%.

^{1}H NMR (400 MHz, Chloroform-*d*): δ 7.29-7.24 (2H, m, H12), 7.20-7.12 (3H, m, H11, H13), 6.77 (1H, dd, *J* = 15.2, 7.2 Hz, H3), 5.73 (1H, ddd, *J* = 17.2, 10.3, 7.6 Hz, H5), 5.61 (1H, dd, *J* = 15.2, 1.3 Hz, H2), 5.24 (1H, br s, H14), 5.03 (1H, dd, *J* = 10.3, 2.1 Hz, H7), 4.97 (1H, dd, *J* = 17.2, 2.1 Hz, H8), 3.16-3.08 (1H, m, H4), 2.81 (1H, dd, *J* = 13.5, 7.0 Hz, H9), 2.75 (1H, dd, *J* = 13.6, 7.7 Hz, H9), 1.36 (9H, s, H16).

^{13}C NMR (101 MHz, Chloroform-*d*): δ 171.2 (C1), 144.8 (C3), 139.3 (C10), 138.9 (C5), 129.4 (C11), 128.3 (C12), 126.3 (C13), 124.3 (C2), 115.6 (C6), 51.4 (C15), 47.9 (C4), 41.0 (C9), 29.0 (C16).

HRMS (ESI$^+$) *m/z* calculated for $C_{17}H_{24}NO$ $[M+H]^+$ 258.1858, found 258.1860.

IR: ν_{max} = 3302 (N-H), 2968 (C-H), 1663 (C=O), 1627 (C=C), 1538, 1453, 1365, 1221.

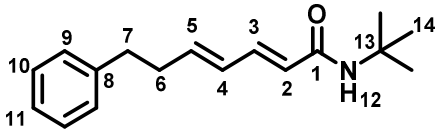

[1,7]-Isomer 130: White crystalline solid (16 mg, 0.06 mmol, 16%) with an NMR yield of 28%.

^{1}H NMR (400 MHz, Chloroform-*d*): δ 7.28-7.24 (2H, m, H10), 7.19-7.13 (3H, m, H9, H11), 7.10 (1H, dd, *J* = 15.0, 9.9 Hz, H3), 6.14-6.00 (2H, m, H4, H5), 5.66 (1H, d, *J* = 15.0 Hz, H2), 5.31 (1H, br s, H12), 2.71 (2H, t, *J* = 7.2 Hz, H7), 2.44 (2H, dt, *J* = 9.3, 7.2 Hz, H6), 1.36 (9H, s, H14).

^{13}C NMR (101 MHz, Chloroform-*d*): δ 166.8 (C1), 142.9 (C5), 141.4 (C8), 139.8 (C3), 130.5 (C4), 128.9 (C9), 128.5 (C10), 125.3 (C11), 123.0 (C2), 52.4 (C13), 35.3 (C7), 34.8 (C6), 28.9 (C14).

HRMS (ESI$^+$) *m/z* calculated for $C_{17}H_{24}NO$ $[M+H]^+$ 258.1858, found 258.1860.

MP: 127-128 °C.

IR: ν_{max} = 3262 (N-H), 2968 (C=O), 1654 (C=O), 1628 (C=C), 1611 (C=C), 1553, 1364, 1228, 1033.

(*S,E*)-*N*-Isopropyl-*N*-(1-phenylethyl)hexa-3,5-dienamide (132)

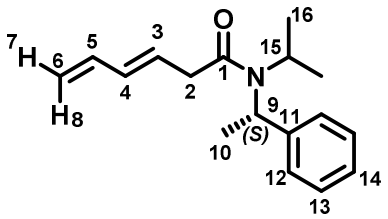

The title compound was synthesised according to General Procedure 1a using (*E*)-hexa-3,5-dienoic acid (**125**) (2.00 g, 17.83 mmol, 1.0 eq.) and (*S*)-*N*-(1-phenylethyl)propan-2-amine (**131**) (3.56 mL, 19.61 mmol, 1.1 eq.). Purification by flash column chromatography (5-10% EtOAc / petroleum ether) afforded the amide as a colourless oil (2.43 g, 9.45 mmol, 53%). Broad NMR peaks noted due to rotameric structure.

^{1}H NMR (400 MHz, Chloroform-*d*): δ 7.37-7.18 (5H, m, H12-H14), 6.33 (1H, dt, *J* = 17.1, 10.6 Hz, H5), 6.16-5.98 (1H, m, H4), 5.88 (1H, dt, *J* = 15.3, 6.7 Hz, H3), 5.10 (1H, d, *J* = 17.1 Hz, H8), 5.00 (1H, d, *J* = 10.6 Hz, H7), 4.99-4.93 (1H, m, H9), 3.86 (0.33H, br s, H15), 3.49 (0.66H, br s, H15), 3.19 (2H, d, *J* = 6.7 Hz, H2), 1.62 (3H, d, *J* = 6.7 Hz, H10), 1.33 (3H, d, *J* = 7.3 Hz, H16), 1.05 (3H, d, *J* = 7.3 Hz, H16).

^{13}C NMR (101 MHz, Chloroform-*d*): δ 171.1 (C1), 140.6 (C11), 136.8 (C5), 133.7 (C4), 129.3 (C3), 128.9 (C13), 127.9 (C12), 127.1 (C14), 115.9 (C6), 54.2 (C9), 47.6 (C15), 40.8 (C2), 21.0 (C10), 20.0 (C16), 18.2 (C16).

HRMS (ESI$^+$) *m/z* calculated for $C_{17}H_{24}NO$ $[M+H]^+$ 258.1858, found 258.1853.

IR: ν_{max} = 2971 (C-H), 1935 (C-H), 1632 (C=O), 1601 (C=C), 1439, 1329, 1116, 1004.

$[\boldsymbol{\alpha}]_{\boldsymbol{D}}^{\boldsymbol{24}}$**:** −68 (*c* 1, $CHCl_3$).

N-(Isopropyl)-2-(1-phenylethyl)hexa-3,5-dienamide (*E*/*Z*-133), *N*-(Isopropyl)-4-(1-phenylethyl)hexa-2,5-dienamide (134) and (2*E*,4*E*)-*N*-(Isopropyl)-7-phenylocta-2,4-dienamide (135)

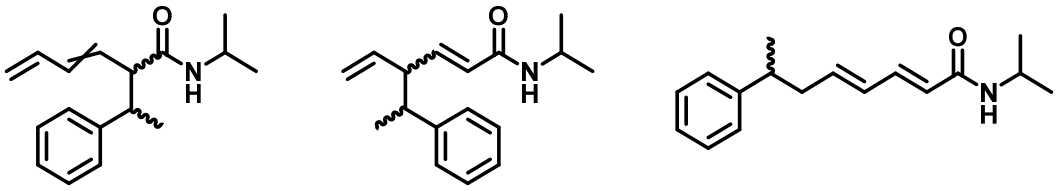

The title compounds were synthesised according to General Procedure 2 using (*S,E*)-*N*-Isopropyl-*N*-(1-phenylethyl)hexa-3,5-dienamide (**132**) (100 mg, 0.39 mmol, 1.0 eq.). Purification by flash column chromatography (5-20% EtOAc / petroleum ether) afforded the various migration products.

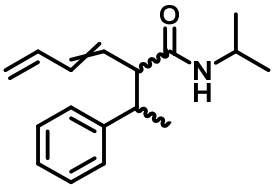

[1,3]-Isomers *E*/*Z*-133: Colourless oil (21 mg, 0.08 mmol, 21%). Isolated as a complex mixture of *E*- and *Z*- isomers and diastereomers. Assignments and NMR yield determination was not possible here due to the complexity of the resulting mixture. However, note that 12 doublets are seen as expected for the methyl/isopropyl groups for a mixture of four stereoisomers.

^{1}H NMR (400 MHz, Chloroform-*d*): δ 7.29-7.13 (m), 6.58 (dt, *J* = 10.2, 1.1 Hz), 6.53 (dt, *J* = 10.2, 1.0 Hz), 6.39 (dt, *J* = 10.4, 0.7 Hz), 6.34 (dt, *J* = 10.2, 0.5 Hz), 6.25-6.15 (m), 6.12 (ddd, *J* = 15.3, 10.5, 0.7 Hz), 6.03 (td, *J* = 11.1, 0.8 Hz), 5.94-5.82 (m), 5.65 (t, *J* = 10.5 Hz), 5.54 (ddd, *J* = 15.3, 9.1, 0.5 Hz), 5.30-4.81 (m), 4.11-4.02 (m), 3.84-3.72 (m), 3.41-3.12 (m), 2.88 (td, *J* = 9.7, 0.7 Hz), 2.72 (t, *J* = 9.7 Hz), 1.32 (d, *J* = 7.0 Hz), 1.30 (d, *J* = 7.1 Hz), 1.24 (d, *J* = 6.8 Hz), 1.23 (d, *J* = 7.2 Hz), 1.11 (d, *J* = 6.7 Hz), 1.09 (d, *J* = 6.6 Hz), 1.08 (d, *J* = 6.6 Hz), 1.04 (d, *J* = 6.5 Hz), 0.95 (d, *J* = 6.5 Hz), 0.94 (d, *J* = 6.6 Hz), 0.67 (d, *J* = 6.6 Hz), 0.62 (d, *J* = 6.6 Hz).

^{13}C NMR (101 MHz, Chloroform-*d*): δ 171.8, 171.6, 171.5, 171.3, 145.0, 144.9, 143.8, 143.3, 136.7, 136.6, 134.1, 133.9, 132.4, 132.3, 132.0, 131.8, 131.5, 131.0, 129.3, 128.5, 128.4, 128.3, 128.3, 128.1, 128.1, 127.6, 127.6, 127.6, 126.5, 126.5, 119.5, 119.3, 116.9, 60.3, 58.2, 54.4, 53.0, 42.4, 42.3, 42.3, 42.1, 41.5, 41.1, 41.0, 22.9, 22.8, 22.6, 22.6, 22.4, 19.6, 19.6, 19.5, 19.5, 19.4, 19.4, 19.2, 19.0, 19.0, 18.9, 18.6.

HRMS (ESI^{+}) *m/z* calculated for $C_{17}H_{24}NO$ $[M+H]^{+}$ 258.1858, found 258.1853.

IR: ν_{max} = 3290 (N-H), 2969 (C-H), 1634 (C=O), 1544, 1453, 1366, 1003.

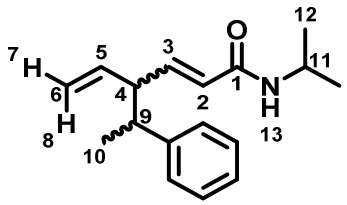

[1,5]-Isomers 134: Colourless oil (10 mg, 0.04 mmol, 10%) with an NMR yield of 13%. Isolated as a mixture of diastereomers with a dr of 50 : 50 for D1:D2 where D1 and D2 refer to the diastereomer of product. The stereoisomer ratio was determined as 26 : 19 : 26 : 29 using a chiral HPLC Registech® Whelk column with hexane:isopropanol (90:10) as eluent with retention time (min) 10.54 : 13.47 : 14.38 : 15.40.

^{1}H NMR (400 MHz, Chloroform-*d*): δ 7.30-7.24 (4H, m, Ar), 7.20-7.12 (6H, m, Ar), 6.81 (1H, dd, *J* = 15.1, 7.5 Hz, H3 D1), 6.67 (1H, dd, *J* = 15.4, 7.5 Hz, H3 D2), 5.72 (1H, td, *J* = 17.1, 10.1 Hz, H5 D1), 5.67 (1H, dd, *J* = 15.1, 1.2 Hz, H2 D1), 5.61 (1H, td, *J* = 17.5, 10.1 Hz, H5 D2), 5.54 (1H, dd, *J* = 15.4, 1.4 Hz, H2 D2), 5.37-5.27 (1H, br d, *J* = 7.6 Hz, H13 D1/D2), 5.17 (1H, br d, *J* = 7.6 Hz, H13 D1/D2), 5.10 (1H, dd, *J* = 10.1, 1.1 Hz, H7 D1), 5.01 (1H, dd, *J* = 17.1, 1.1 Hz, H8 D1), 4.94 (1H, dd, *J* = 10.1, 1.6 Hz, H7 D2), 4.89 (1H, dd, *J* = 17.5, 1.6 Hz, H8 D2), 4.19-4.03 (2H, m, H11 D1, H11 D2), 3.04-2.96 (2H, m, H4 D1, H4 D2), 2.88-2.80 (2H, m, H9 D1, H9 D2), 1.26 (3H, d, *J* = 7.1 Hz, H10 D1/D2), 1.25 (3H, d, *J* = 7.2 Hz, H10 D1/D2), 1.17 (3H, d, *J* = 6.6 Hz, H12 D1/D2), 1.16 (3H, d, *J* = 6.6 Hz, H12 D1/D2), 1.12 (3H, d, *J* = 6.6 Hz, H12 D1/D2), 1.11 (3H, d, *J* = 6.6 Hz, H12 D1/D2).

^{13}C NMR (101 MHz, Chloroform-*d*): δ 164.9 (C1 D1), 164.8 (C1 D2), 145.1 (C3 D2), 144.6 (C3 D1), 138.2 (C5 D2), 137.9 (C5 D1), 128.5 (Ar), 128.4 (Ar), 128.3 (Ar), 128.0 (Ar), 128.0 (Ar), 127.0 (Ar), 126.4 (Ar), 126.4 (Ar), 125.0 (C2 D1), 124.6 (C2 D2), 117.1 (C6 D1), 116.5 (C6 D2), 53.7 (C4 D1), 52.6 (C4 D2), 44.1 (C9 D2), 44.0 (C9 D1), 41.5 (C11 D1/D2), 41.4 (C11 D1/D2), 23.0 (C12 D1/D2), 22.9 (C12 D1/D2), 22.8 (C12 D1/D2), 22.8 (C12 D1/D2), 19.5 (C10 D1/D2), 19.2 (C10 D1/D2).

HRMS (ESI^{+}) *m/z* calculated for $C_{17}H_{24}NO$ $[M+H]^{+}$ 258.1858, found 258.1861.

IR: ν_{max} = 3272 (N-H), 2970 (C-H), 2925 (C-H), 1662 (C=O), 1623 (C=C), 1453, 1364, 1033.

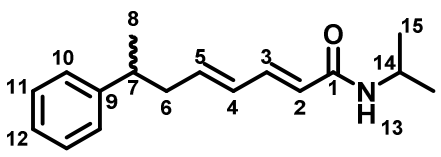

[1,7]-Isomers 135: Colourless oil (20 mg, 0.08 mmol, 20%) with an NMR yield of 27%. Isolated as a racemate, with a stereoisomer ratio determined as 50:50, using a chiral HPLC Chiralcel® OJ column with hexane:isopropanol (93:7) as eluent with retention time (min) 11.26 : 12.75.

^{1}H NMR (400 MHz, Chloroform-*d*): δ 7.31-7.26 (2H, m, H11), 7.20-7.15 (3H, m, H10, H12), 7.11 (1H, dd, *J* = 15.0, 10.4 Hz, H3), 6.08 (1H, dd, *J* = 15.0, 10.4 Hz, H4), 5.94 (1H, td, *J* = 15.0, 7.4 Hz, H5), 5.69 (1H, d, *J* = 15.0 Hz, H2), 5.40 (1H, br d, *J* = 7.3 Hz, H13), 4.19-4.09 (1H, m, H14), 2.86-2.78 (1H, m, H7), 2.50-2.32 (2H, m, H6), 1.25 (3H, d, *J* = 7.1 Hz, H8), 1.16 (6H, d, *J* = 6.6 Hz, H15).

^{13}C NMR (101 MHz, Chloroform-*d*): δ 167.2 (C1), 147.0 (C9), 141.0 (C5), 140.9 (C3), 129.8 (C4), 128.5 (C10), 127.0 (C11), 126.3 (C12), 122.5 (C2), 41.9 (C6), 41.5 (C10), 39.9 (C7), 23.3 (C11), 21.6 (C8).

HRMS (ESI^{+}) *m/z* calculated for $C_{17}H_{24}NO$ $[M+H]^{+}$ 258.1858, found 258.1861.

IR: ν_{max} = 3280 (N-H), 2968 (C-H), 2923 (C-H), 1654 (C=O), 1627 (C=C), 1539, 1453, 1003.

N-(Cyclopropyl(phenyl)methyl)propan-2-amine (143)

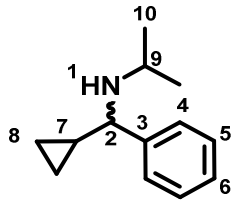

To a solution of cyclopropyl phenyl ketone (**142**) (2.10 mL, 15.20 mmol, 1.0 eq.) in anhydrous CH_2Cl_2 (50 mL) was added isopropylamine (5.20 mL, 60.80 mmol, 4.0 eq.). In an ice bath, $TiCl_4$ (18.00 mL, 18.10 mmol, 2.0 eq., 1 M in CH_2Cl_2) was added slowly and the mixture stirred for 16 h at rt. A solution of $NaBH_3CN$ (1.13 g, 18.24 mmol, 1.2 eq.) in anhydrous THF (10 mL) was added and the mixture left to stir for 4 h. The reaction was quenched with $NaOH_{(aq.)}$ (50 mL, 1 M) before the aqueous layer was extracted with CH_2Cl_2 (3 × 30 mL). The combined organics were washed with brine (60 mL), dried over Na_2SO_4, filtered and concentrated *in vacuo*. Purification by flash column chromatography (20-30% EtOAc / petroleum ether) afforded the title compound as an orange oil (2.50 g, 13.38 mmol, 88%).

^{1}H NMR (400 MHz, Chloroform-*d*): δ 7.28-7.24 (4H, m, H4, H5), 7.21-7.16 (1H, m, H6), 2.89 (1H, d, *J* = 8.7 Hz, H2), 2.58 (1H, sept, *J* = 6.3 Hz, H9), 1.04-0.95 (1H, m, H7), 0.94 (6H, d, *J* = 6.3 Hz, H10), 0.57-0.51 (1H, m, H8), 0.35-0.29 (1H, m, H8), 0.24-0.15 (2H, m, H8).

^{13}C NMR (101 MHz, Chloroform-*d*): δ 144.6 (C3), 128.3 (C4), 127.3 (C5), 126.9 (C6), 65.6 (C2), 45.7 (C9), 24.3 (C10), 22.3 (C10), 19.6 (C7), 5.0 (C8), 2.9 (C8).

HRMS (ESI$^+$) *m/z* calculated for $C_{13}H_{20}N$ $[M+H]^+$ 190.1590, found 190.1590.

IR: ν_{max} = 3330 (N-H), 2979 (C-H), 1465 (C=C), 1452.

(*E*)-*N*-(Cyclopropyl(phenyl)methyl)-*N*-isopropylhexa-3,5-dienamide (145)

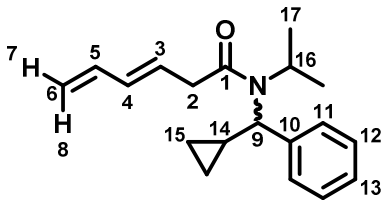

The title compound was synthesised according to General Procedure 1b using (*E*)-hexa-3,5-dienoic acid (**125**) (0.60 g, 5.35 mmol, 1.0 eq.) and *N*-(cyclopropyl(phenyl)methyl)propan-2-amine (**143**) (1.01 g, 5.89 mmol, 1.1 eq.). Purification by flash column chromatography (0-10% EtOAc / petroleum ether) afforded the amide as a yellow oil (0.64 g, 2.02 mmol, 42%). Broad NMR peaks noted due to rotameric structure.

^{1}H NMR (400 MHz, Chloroform-*d*, 50 °C): δ 7.52-7.18 (5H, m, H11-H13), 6.42-6.30 (1H, ddd, *J* = 17.8, 9.6, 7.0 Hz, H5), 6.25-6.02 (1H, br m, H4), 5.99-5.88 (1H, br m, H3), 5.12 (1H, br d, *J* = 17.8 Hz, H8), 5.03 (1H, d, *J* = 9.6 Hz, H7), 3.97 (1H, br d, *J* = 9.6 Hz, H9), 3.43-3.12 (3H, br m, H2, H16), 1.44 (3H, br d, *J* = 6.2 Hz, H17), 1.18 (3H, br d, *J* = 6.2 Hz, H17), 1.10-1.06 (1H, br m, H14), 0.98 (1H, br m, H15), 0.70 (1H, br m, H15), 0.51-0.35 (2H, br m, H15).

^{13}C NMR (101 MHz, Chloroform-*d*): δ 170.5 (C1), 140.0 (C10), 136.7 (C5), 133.7 (C4), 128.5 (C11), 128.2 (C3), 127.7 (C12), 127.5 (C13), 116.5 (C6), 65.8 (C9), 49.1 (C16), 39.4 (C2), 20.8 (C17), 20.2 (C17), 13.9 (C14), 7.5 (C15), 4.5 (C15).

HRMS (ESI$^+$) *m/z* calculated for $C_{19}H_{26}NO$ $[M+H]^+$ 284.2009, found 284.2016.

IR: ν_{max} = 2980 (C-H), 2971 (C-H), 1719 (C=O), 1621 (C=C), 1446 (C=C), 1361, 1139.

2-(Cyclopropyl(phenyl)methyl)-*N*-isopropylhexa-3,5-dienamide (*E*/*Z*-146), 4-(Cyclopropyl(phenyl)methyl)-*N*-isopropylhexa-2,5-dienamide (147) and (2*E*,4*E*)-7-Cyclopropyl-*N*-isopropyl-7-phenylhepta-2,4-dienamide (148)

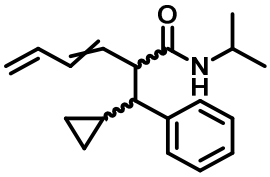
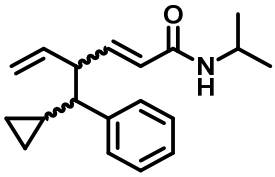
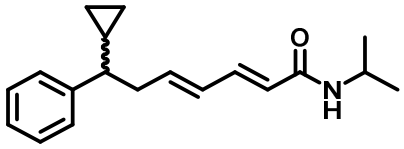

The title compounds were synthesised according to General Procedure 2 using (*E*)-*N*-(cyclopropyl(phenyl)methyl)-*N*-isopropylhexa-3,5-dienamide (**145**) (100 mg, 0.35 mmol, 1.0 eq.). Purification by flash column chromatography (5-30% EtOAc / petroleum ether) afforded the various migration products.

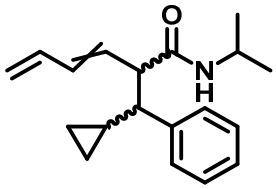

[1,3]-Isomers *E*/*Z*-146: Colourless oil (8 mg, 0.03 mmol, 8%). Isolated as a mixture of *E*- and *Z*- isomers and diastereomers. Assignments were not possible here due to the complexity of the resulting mixture. However, note that 8 doublets are seen as expected for the isopropyl groups for a mixture of four stereoisomers. Not all carbon signals observed due to overlap and weak spectra.

^{1}H NMR (400 MHz, Chloroform-*d*): δ 7.30-7.14 (m), 6.57 (dtd, *J* = 16.4, 10.5, 0.9 Hz), 6.38 (dtd, *J* = 16.5, 10.7, 1.1 Hz), 6.27-6.10 (m), 6.04-5.92 (4 x d), 5.74 (t, *J* = 10.6 Hz), 5.56 (dd, *J* = 9.7 Hz), 5.37 (t, *J* = 10.2 Hz), 5.30-4.98 (8 x d), 4.04 (sept, *J* = 6.3 Hz), 3.88-3.75 (m), 3.66 (ddd, *J* = 10.3, 6.2, 0.9 Hz), 3.52 (ddd, *J* = 10.8, 8.2, 0.9 Hz), 3.14 (ddd, *J* = 9.5, 6.9, 0.6 Hz), 3.00 (t, *J* = 9.3 Hz), 2.58 (dd, *J* = 10.7, 6.1 Hz), 2.49 (dd, *J* = 10.4, 7.1 Hz), 2.45 (dd, *J* = 10.2, 8.2 Hz), 2.38 (t, *J* = 9.9 Hz), 1.10 (d, *J* = 6.6 Hz), 1.07 (d, *J* = 6.7 Hz), 1.05 (d, *J* = 6.6 Hz), 1.01 (d, *J* = 6.6 Hz), 0.98 (d, *J* = 6.8 Hz), 0.97 (d, *J* = 6.4 Hz), 0.75 (d, *J* = 6.6 Hz), 0.68 (d, *J* = 6.6 Hz), 0.63-0.56 (m), 0.48-0.27 (m), 0.11-0.03 (m), 0.01-0.00 (m).

^{13}C NMR (101 MHz, Chloroform-*d*): δ 171.4, 143.3, 138.7, 136.6, 134.6, 133.5, 132.2, 130.2, 128.7, 128.4, 128.1, 128.0, 126.5, 125.6, 117.5, 116.4, 59.9, 58.2, 53.2, 52.6, 44.0, 40.6, 23.3, 23.3, 22.8, 21.7, 15.5, 14.9, 8.2, 6.6, 4.1, 2.8.

HRMS (ESI^{+}) *m/z* calculated for $C_{19}H_{26}NO$ $[M+H]^{+}$ 284.2009, found 284.2010.

IR: ν_{max} = 3425 (N-H), 2980 (C-H), 2888 (C-H), 1633 (C=O), 1630 (C=C), 1381, 1251, 1152.

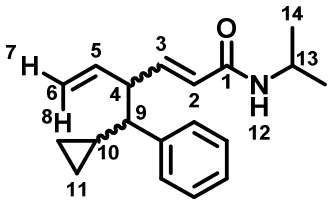

[1,5]-Isomers 147: Colourless oil (9 mg, 0.03 mmol, 9%). Isolated as a mixture of diastereomers with a dr of 52:48 for D1:D2 where D1 and D2 refer to the diastereomer of product.

^{1}H NMR (400 MHz, Chloroform-*d*): δ 7.32-7.13 (10H, m), 6.91 (1H, dd, *J* = 15.1, 8.0 Hz, H3 D1), 6.79 (1H, dd, *J* = 16.0, 8.4 Hz, H3 D2), 5.84-5.68 (2H, m, H5 D1, H5 D2), 5.65 (1H, dd, *J* = 15.1, 1.2 Hz, H2 D1), 5.60 (1H, dd, *J* = 16.0, 1.0 Hz, H2 D2), 5.06 (1H, dd, *J* = 10.2, 1.2 Hz, H7 D1/D2), 5.02 (1H, dd, *J* = 10.5, 1.1 Hz, H7 D1/D2), 5.00-4.94 (2H, m, H8 D1, H8 D2), 4.20-4.06 (2H, m, H13 D1, H13 D2), 3.30-3.22 (2H, m, H4 D1, H4 D2), 2.00-1.90 (2H, m, H9 D1, H9 D2), 1.16 (3H, d, *J* = 6.5 Hz, H14 D1/D2), 1.16 (3H, d, *J* = 6.7 Hz, H14 D1/D2), 1.15-1.12 (2H, 2 × d, *J* = 6.6 Hz, H14 D1, H14 D2), 1.14-1.07 (2H, m, H10 D1, H10 D2), 0.71-0.62 (2H, m, H11 D1/D2), 0.44-0.36 (2H, m, H11 D1/D2), 0.30-0.22 (2H, m, H11 D1/D2), 0.03-0.00 (2H, m, H11 D1/D2).

^{13}C NMR (101 MHz, Chloroform-*d*): δ 164.9 (C1 D1), 164.8 (C1 D2), 145.0 (C3 D1), 144.4 (C3 D2), 143.0 (Ar), 142.9 (Ar), 138.4 (C5 D1/D2), 137.9 (C5 D1/D2), 128.6 (Ar), 128.4 (Ar), 128.2 (Ar), 128.1 (Ar), 126.5 (Ar), 126.4 (Ar), 124.6 (C2 D2), 124.4 (C2 D1), 116.6 (C6 D1/D2), 116.3 (C6 D1/D2), 55.9 (C9 D1/D2), 55.7 (C9 D1/D2), 53.1 (C4 D1/D2), 53.2 (C4 D1/D2), 41.4 (C13 D1/D2), 41.3 (C13 D1/D2), 23.0 (C14 D1/D2), 22.9 (C14 D1/D2), 14.7 (C10 D1/D2), 14.6 (C10 D1/D2), 7.3 (C11 D1/D2), 7.2 (C11 D1/D2), 4.0 (C11 D1/D2), 3.8 (C11 D1/D2).

HRMS (ESI^{+}) *m/z* calculated for $C_{19}H_{26}NO$ $[M+H]^{+}$ 284.2009, found 284.2010.

IR: ν_{max} = 3275 (N-H), 2979 (C-H), 2971 (C-H), 1662 (C=O), 1622 (C=C), 1542, 1383, 1129.

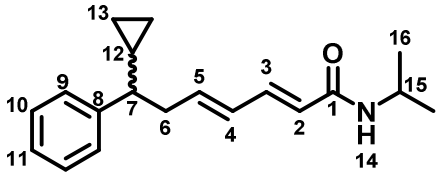

[1,7]-Isomers 148: Colourless oil (21 mg, 0.07 mmol, 21%).

^{1}H NMR (400 MHz, Chloroform-*d*): δ 7.36-7.22 (5H, m, H9-H11), 7.15 (1H, dd, *J* = 15.6, 10.9 Hz, H3), 6.17-5.99 (2H, m, H4, H5), 5.73 (1H, d, *J* = 15.6 Hz, H2), 5.45 (1H, br s, H14), 4.20 (1H, sept, *J* = 6.9 Hz, H15), 2.73-2.58 (2H, m, H6), 1.97 (1H, td, *J* = 8.5, 7.1 Hz, H7), 1.22 (6H, d, *J* = 6.9 Hz, H16), 1.12-1.02

(1H, m, H12), 0.71-0.63 (1H, m, H13), 0.50-0.43 (1H, m, H13), 0.31-0.25 (1H, m, H13), 0.18-0.11 (1H, m, H13).

^{13}C NMR (101 MHz, Chloroform-*d*): δ 165.6 (C1), 145.5 (C8), 141.4 (C3), 140.9 (C4), 129.5 (C5), 128.4 (C9), 127.2 (C10), 126.3 (C11), 122.4 (C2), 51.1 (C7), 41.5 (C15), 40.5 (C6), 23.3 (C16), 23.2 (C16), 16.5 (C12), 5.9 (C13), 4.0 (C13).

HRMS (ESI^+) *m/z* calculated for $C_{19}H_{26}NO$ $[M+H]^+$ 284.2009, found 284.2010.

IR: ν_{max} = 3293 (N-H), 2980 (C-H), 2971 (C-H), 1651 (C=O), 1626 (C=C), 1538, 1453.

1-Phenylhex-5-en-1-one (153)

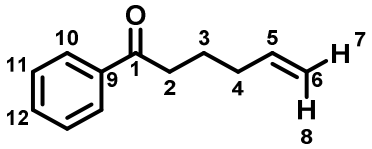

To a solution of benzoyl chloride (**152**) (0.83 mL, 7.14 mmol, 1.0 eq.) in anhydrous THF (10 mL) was added copper(I) iodide (70 mg, 0.37 mmol, 5 mol%). The suspension was cooled in an NaCl/ice/water bath to −15 °C and a solution of pent-4-en-1-ylmagnesium bromide (**151**) prepared from 5-bromo-1-pentene (0.84 mL, 7.14 mmol, 1.0 eq.) and magnesium turnings (0.18 g, 7.28 mmol, 1.02 eq.) in anhydrous THF (10 mL) was added dropwise and the mixture left to stir for 1 h in the ice-salt bath. After warming to rt, the reaction was stirred for a further 2 h before solvent was removed *in vacuo*. To this mixture, $HCl_{(aq.)}$ (20 mL, 1 M) and CH_2Cl_2 (30 mL) were added, and the layers separated. The organics were washed with saturated $NaHCO_{3(aq.)}$ (30 mL) before being dried over Na_2SO_4, filtered and concentrated *in vacuo*. Purification by flash column chromatography (0-5% EtOAc / petroleum ether) afforded the title compound as a colourless oil (0.90 g, 5.21 mmol, 73%).

^{1}H NMR (400 MHz, Chloroform-*d*): δ 7.97 (2H, dd, *J* = 7.1, 1.6 Hz, H10), 7.56 (1H, tt, *J* = 7.5, 1.6 Hz, H12), 7.46 (2H, dd, *J* = 7.5, 7.1 Hz, H11), 5.84 (1H, ddt, *J* = 16.9, 10.4, 6.9 Hz, H5), 5.06 (1H, dq, *J* = 16.9, 1.7 Hz, H8), 5.01 (1H, dq, *J* = 10.4, 1.7 Hz, H7), 2.99 (2H, t, *J* = 7.1 Hz, H2), 2.18 (2H, dt, *J* = 7.1, 6.9 Hz, H4), 1.87 (2H, quint, *J* = 7.1 Hz, H3).

^{13}C NMR (101 MHz, Chloroform-*d*): δ 200.3 (C1), 138.1 (C5), 137.2 (C9), 133.0 (C12), 128.6 (C11), 128.1 (C10), 115.4 (C6), 38.5 (C2), 32.0 (C4), 23.4 (C3).

Data consistent with literature.[147]

N-Isopropyl-1-phenylhex-5-en-1-amine (154)

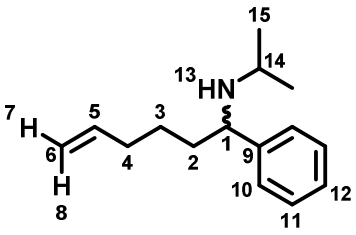

To a solution of 1-phenylhex-5-en-1-one (**153**) (1.20 g, 6.89 mmol, 1.0 eq.) in anhydrous CH_2Cl_2 (30 mL) was added isopropylamine (2.40 mL, 27.93 mmol, 4.0 eq.) and $TiCl_4$ (8.30 mL, 8.30 mmol, 1.2 eq., 1 M in CH_2Cl_2) in an ice bath. The mixture was allowed to stir at rt for 16 h before a solution of $NaBH_3CN$ (0.52 g, 8.27 mmol, 1.2 eq.) in anhydrous THF (10 mL) was added and the mixture left to stir for 4 h. The reaction was quenched with $NaOH_{(aq.)}$ (50 mL, 1 M) and the aqueous layer was extracted with CH_2Cl_2 (3 × 30 mL). The combined organics were washed with $NaOH_{(aq.)}$ (50 mL, 1 M), brine (60 mL), dried over $MgSO_4$, filtered and concentrated *in vacuo*. Purification by flash column chromatography (0-3% MeOH / CH_2Cl_2) afforded the title compound as an orange oil (0.97 g, 4.48 mmol, 65%).

^{1}H NMR (400 MHz, Chloroform-*d*): δ 7.36-7.21 (5H, m, H10-H12), 5.75 (1H, ddt, *J* = 17.1, 10.1, 7.6 Hz, H5), 4.97 (1H, dd, *J* = 17.1, 2.1 Hz, H8), 4.92 (1H, dd, *J* = 10.1, 2.1 Hz, H7), 4.46 (1H, br s, H13), 3.69 (1H, dd, *J* = 8.2, 6.1 Hz, H1), 2.60 (1H, sept, *J* = 6.5 Hz, H14), 2.03 (2H, t, *J* = 7.6 Hz, H4), 1.78-1.69 (1H, m, H2), 1.66-1.56 (1H, m, H2), 1.42-1.33 (1H, m, H3), 1.27-1.19 (1H, m, H3), 1.02 (3H, d, *J* = 6.5 Hz, H15), 0.98 (3H, d, *J* = 6.5 Hz, H15).

^{13}C NMR (101 MHz, Chloroform-*d*): δ 144.8 (C9), 138.8 (C5), 128.4 (C10), 127.2 (C11), 126.9 (C12), 114.6 (C6), 60.3 (C1), 45.5 (C14), 38.2 (C2), 33.8 (C4), 25.8 (C3), 22.1 (C15), 21.5 (C15).

HRMS (ESI^+) *m/z* calculated for $C_{15}H_{24}N$ $[M+H]^+$ 218.1903, found 218.1895.

IR: ν_{max} = 3252 (N-H), 2980 (C-H), 2931 (C-H), 1463 (C=C), 1378, 1165, 1071.

(*E*)-*N*-Isopropyl-*N*-(1-phenylhex-5-en-1-yl)hexa-3,5-dienamide (155)

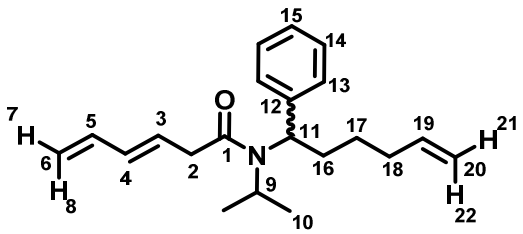

The title compound was synthesised according to General Procedure 1b using (*E*)-hexa-3,5-dienoic acid (**125**) (0.30 g, 2.68 mmol, 1.0 eq.) and *N*-isopropyl-1-phenylhex-5-en-1-amine (**154**) (0.49 g, 2.95 mmol, 1.0 eq.). Purification by flash column chromatography (0-1% MeOH / CH_2Cl_2) afforded the amide as a yellow oil (0.12 g, 0.41 mmol, 17%). Broad NMR peaks noted due to rotameric structure.

^{1}H NMR (400 MHz, Chloroform-*d*): δ 7.42-7.18 (5H, br m, H13-H15), 6.37 (1H, dt, *J* = 17.2, 10.5 Hz, H5), 6.14 (1H, dd, *J* = 15.1, 10.5 Hz, H4), 5.99-5.88 (1H, br m, H3), 5.79 (1H, ddt, *J* = 17.1, 10.3, 6.7 Hz, H19), 5.13 (1H, d, *J* = 17.2 Hz, H8), 5.02 (1H, d, *J* = 10.5 Hz, H7), 5.00-4.91 (2H, br m, H21, H22), 4.88-4.75 (1H, br m, H11), 3.39-3.12 (3H, br m, H2, H9), 2.21-2.06 (2H, br m, H18), 2.06-1.81 (2H, br m, H16), 1.62-1.41 (2H, br m, H17), 1.41-1.28 (3H, br m, H10), 0.92 (3H, br d, *J* = 6.1 Hz, H10).

^{13}C NMR (101 MHz, Chloroform-*d*): δ 170.2 (C1), 139.2 (C12), 137.9 (C19), 136.7 (C5), 133.7 (C4), 128.5 (C13), 128.2 (C14), 127.9 (C15), 127.8 (C3), 116.4 (C6), 115.4 (C20), 60.2 (C11), 47.9 (C9), 39.5 (C2), 33.8 (C18), 30.7 (C16), 26.2 (C17), 20.6 (C10), 19.8 (C10).

HRMS (ESI^+) *m/z* calculated for $C_{21}H_{30}NO$ $[M+H]^+$ 312.2322, found 312.2333.

IR: ν_{max} = 2980 (C-H), 2888 (C-H), 1620 (C=O and C=C broad), 1382, 1251, 1152.

2-(Buta-1,3-dien-1-yl)-*N*-isopropyl-3-phenyloct-7-enamide (156), *N*-isopropyl-5-phenyl-4-vinyldeca-2,9-dienamide (157) and (2*E*,4*E*)-*N*-isopropyl-7-phenyldodeca-2,4,11-trienamide (158)

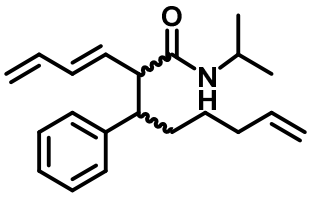
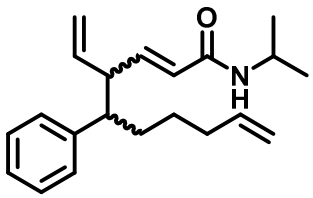
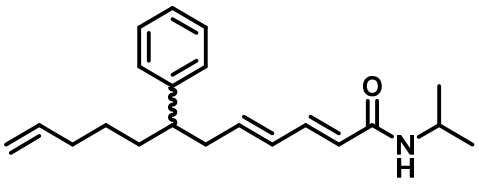

The title compounds were synthesised according to General Procedure 2 using (*E*)-*N*-isopropyl-*N*-(1-phenylhex-5-en-1-yl)hexa-3,5-dienamide (**155**) (100 mg, 0.32 mmol, 1.0 eq.). Purification by flash column chromatography (5-10% EtOAc / petroleum ether) afforded the various migration products.

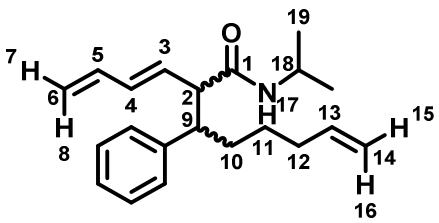

[1,3]-Isomers 156: Colourless oil (10 mg, 0.03 mmol, 10%). Isolated as a mixture of diastereomers with a dr of 64:36 for D1:D2 where D1 and D2 refer to the diastereomer of product.

^{1}H NMR (400 MHz, Chloroform-*d*): δ 7.28-7.08 (10H, m, Ar), 6.55 (1H, dt, *J* = 17.0, 10.5 Hz, H5 D1), 6.37 (1H, dt, *J* = 17.2, 10.2 Hz, H5 D2), 6.25-6.07 (2H, m, H4 D1, H4 D2), 5.93-5.81 (2H, m, H13 D1), 5.75-5.61 (2H, m, H13 D2, H3 D1), 5.49 (1H, dd, *J* = 15.3, 9.2 Hz, H3 D2), 5.28 (1H, dd, *J* = 17.0, 2.1 Hz, 1H, H8 D1), 5.17 (1H, dd, *J* = 17.2, 1.6 Hz, H8 D2), 5.07 (1H, dd, *J* = 10.2, 1.6 Hz, H7 D2), 5.00 (1H, dd, *J* = 10.5, 2.1 Hz, H7 D1), 4.96-4.84 (4H, m, H15 D1, H15 D2, H16 D1, H16 D2), 4.78 (1H, br s, H17 D1), 4.72 (1H, s, H17 D2), 4.05 (1H, sept, *J* = 6.5 Hz, H18 D1), 3.72 (1H, sept, *J* = 6.5 Hz, H18 D2), 3.42 (1H, dd, *J* = 10.2, 7.9 Hz, H2 D1), 3.25 (1H, t, *J* = 9.2 Hz, H2 D2), 3.19-3.12 (1H, m, H9 D1), 3.03-2.94 (1H, m, H9 D2), 2.92 (1H, t, *J* = 9.3 Hz, H12 D1), 2.74 (1H, t, *J* = 10.1 Hz, H12 D2), 2.04-1.85 (4H, m, H11 D1, H11 D2), 1.80-1.59 (4H, m, H10 D1, H10 D2), 1.12 (3H, d, *J* = 6.5 Hz, H19 D2), 1.09 (3H, d, *J* = 6.5 Hz, H19 D1), 1.05 (3H, d, *J* = 6.5 Hz, H19 D2), 1.00 (3H, d, *J* = 6.5 Hz, H19 D1).

^{13}C NMR (101 MHz, Chloroform-*d*): δ 171.8 (C1 D1), 171.5 (C1 D2), 143.0 (Ar), 141.7 (Ar), 138.8 (C13 D2), 136.8 (C5 D2), 136.6 (C5 D1), 134.2 (C13 D1), 134.0 (C4 D1), 132.2 (C4 D2), 130.8 (C3 D2), 129.6 (Ar), 128.9 (Ar), 128.5 (Ar), 128.4 (Ar), 128.3 (Ar), 126.5 (Ar), 119.3 (C6 D1), 116.9 (C6 D2), 114.6 (C14 D1), 114.5 (C14 D2), 59.0 (C12 D2), 57.5 (C9 D2), 54.0 (C2 D2), 48.4 (C9 D1), 48.2 (C12 D1), 48.2 (C2 D2), 41.5 (C18 D1), 41.0 (C18 D2), 40.9 (C2 D1), 33.8 (C11 D2), 33.7 (C11 D1), 33.0 (C10 D2), 32.4 (C10 D1), 22.91 (C19 D1), 22.8 (C19 D2), 22.6 (C19 D1), 22.4 (C19 D2).

HRMS (ESI$^+$) *m/z* calculated for $C_{21}H_{30}NO$ $[M+H]^+$ 312.2322, found 312.2313.

IR: ν_{max} = 3657 (N-H), 2980 (C-H), 1631 (C=O), 1600 (C=C), 1381 (C=C), 1151, 953.

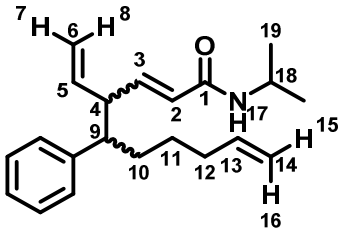

[1,5]-Isomers 157: Colourless oil (6 mg, 0.02 mmol, 6%). Isolated as a mixture of diastereomers with a dr of 52:48 for D1:D2 where D1 and D2 refer to the diastereomer of product.

^{1}H NMR (400 MHz, Chloroform-*d*): δ 7.36-7.06 (10H, m, Ar), 6.80 (1H, dd, *J* = 16.1, 8.4 Hz, H3 D1), 6.63 (1H, dd, *J* = 15.5, 8.3 Hz, H3 D2), 5.75-5.62 (4H, m, H2 D1, H13 D1, H13 D2, H5 D1/D2), 5.60-5.48 (2H, m, H2 D2, H5 D1/D2), 5.24 (2H, br d, *J* = 7.7 Hz, H17 D1, H17 D2), 5.10 (1H, dd, *J* = 10.5, 1.4 Hz, H7 D1/D2), 5.02 (1H, d, *J* = 17.5 Hz, H8 D1/D2), 4.95-4.84 (6H, m, H7 D1/D2, H8 D1/D2, H15 D1, H15 D2, H16 D1, H16 D2), 4.15 (1H, sept, *J* = 7.6 Hz, H18 D1), 4.07 (1H, sept, *J* = 7.5 Hz, H18 D2), 3.06-2.98 (2H,

m, H4 D1, H4 D2), 2.68-2.60 (2H, m, H9 D1, H9 D2), 2.06-1.87 (4H, H12 D1, H12 D2), 1.81-1.68 (2H, m, H11 D1/D2), 1.65-1.52 (2H, m, H11 D1/D2), 1.19-1.15 (10H, m, H10 D1, H10 D2, H19 D1/D2), 1.12 (6H, *J* = 7.6 Hz, H19 D1/D2).

^{13}C NMR (101 MHz, Chloroform-*d*): δ 164.9 (C1 D1), 164.8 (C1 D2), 145.0 (C3 D1), 144.5 (C3 D2), 142.5 (Ar), 142.4 (Ar), 138.8 (C2 D1), 138.4 (C13 D1, C13 D2), 138.1 (C2 D2), 128.7 (Ar), 128.7 (Ar), 128.4 (Ar), 128.3 (Ar), 126.5 (Ar), 126.5 (Ar), 124.9 (C5 D1), 124.6 (C5 D2), 116.9 (C6 D1), 116.4 (C6 D2), 114.6 (C14 D1/D2), 114.54 (C14 D1/D2), 53.1 (C4 D1/D2), 52.8 (C4 D1/D2), 50.2 (C9 D1, C9 D2), 41.5 (C18 D1/D2), 41.4 (C18 D1/D2), 33.8 (C12 D1/D2), 33.7 (C12 D1/D2), 33.0 (C11 D1/D2), 32.7 (C11 D1/D2), 27.0 (C10 D1/D2), 26.9 (C10 D1/D2), 23.0 (C19 D1/D2), 22.9 (C19 D1/D2), 22.8 (C19 D1/D2), 22.8 (C19 D1/D2).

HRMS (ESI$^+$) *m/z* calculated for $C_{21}H_{30}NO$ $[M+H]^+$ 312.2322, 312.2314.

IR: ν_{max} = 3273 (N-H), 2979 (C-H), 2930 (C-H), 1662 (C=O), 1622 (C=C), 1544 (C=C), 1453 (C=C), 1260.

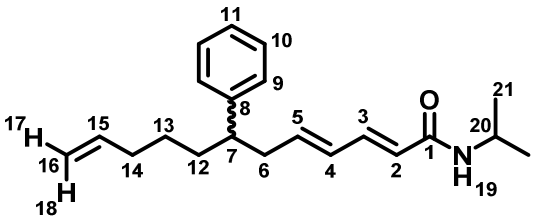

[1,7]-Isomers 158: Colourless oil (20 mg, 0.06 mmol, 20%).

^{1}H NMR (400 MHz, Chloroform-*d*): δ 7.23-7.03 (5H, m, H9-H11), 7.00 (1H, dd, *J* = 15.0, 10.8 Hz, H3), 5.97 (1H, d, *J* = 15.0, 10.8 Hz, H4), 5.82 (1H, dt, *J* = 15.0, 7.5 Hz, H5), 5.65 (1H, ddt, *J* = 16.9, 10.3, 6.7 Hz, H15), 5.58 (1H, d, *J* = 15.0 Hz, H2), 5.27 (1H, br s, H19), 4.87 (1H, dd, *J* = 16.9, 1.8 Hz, H18), 4.83 (1H, dd, *J* = 10.3, 1.8 Hz, H17), 4.07 (1H, sept, *J* = 6.6 Hz, H20), 2.60-2.51 (1H, m, H7), 2.40-2.96 (2H, m, H6), 1.99-1.83 (2H, m, H14), 1.65-1.46 (2H, m, H12), 1.23-1.12 (2H, m, H13), 1.08 (6H, d, *J* = 6.6 Hz, H21).

^{13}C NMR (101 MHz, Chloroform-*d*): δ 165.5 (C1), 144.8 (C8), 140.9 (C5), 140.8 (C3), 138.3 (C11), 130.4 (C4), 128.5 (C9), 127.1 (C10), 125.9 (C11), 122.5 (C2), 114.6 (C16), 46.0 (C7), 41.5 (C20), 40.6 (C6), 35.5 (C12), 33.8 (C14), 26.9 (C13), 23.0 (C21), 22.9 (C21).

HRMS (ESI$^+$) *m/z* calculated for $C_{21}H_{30}NO$ $[M+H]^+$ 312.2322, 312.2313.

IR: ν_{max} = 3286 (N-H), 2980 (C-H), 2929 (C-H), 1711 (C=O), 1638 (C=C), 1539 (C=C), 1453, 1383.

(*E*)-*N*-(*tert*-Butyl)-*N*-methylhexa-3,5-dienamide (159)

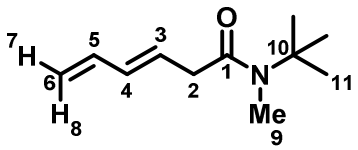

The title compound was synthesised according to General Procedure 1a using (*E*)-hexa-3,5-dienoic acid (**125**) (1.00 g, 8.92 mmol, 1.0 eq.) and *N*-*tert*-butylmethylamine (1.18 mL, 9.81 mmol, 1.1 eq.). Purification by flash column chromatography (5-10% EtOAc / petroleum ether) afforded the amide as a colourless oil (0.95 g, 5.26 mmol, 59%).

^{1}H NMR (400 MHz, Chloroform-*d*): δ 6.33 (1H, dt, *J* = 17.0, 10.1 Hz, H5), 6.07 (1H, dd, *J* = 15.4, 10.1 Hz, H4), 5.82 (1H, dt, *J* = 15.4, 7.4 Hz, H3), 5.09 (1H, dd, *J* = 17.0, 1.7 Hz, H8), 4.99 (1H, dd, *J* = 10.1, 1.7 Hz, H7), 3.12 (1H, d, *J* = 7.4 Hz, H2), 2.87 (3H, s, H9), 1.38 (9H, s, H11).

^{13}C NMR (101 MHz, Chloroform-*d*): δ 172.6 (C1), 136.9 (C5), 132.3 (C4), 128.1 (C3), 116.1 (C6), 56.3 (C10), 42.3 (C2), 32.3 (C9), 28.3 (C11).

HRMS (ESI^{+}) *m/z* calculated for $C_{11}H_{20}NO$ $[M+H]^{+}$ 182.1545, found 182.1548.

IR: ν_{max} = 2964 (C-H), 2924 (C-H), 1636 (C=O and C=C), 1379, 1364, 1212, 1107, 1004 cm^{-1}.

(*E*)-*N*-(*tert*-Butyl)-*N*-isopropylhexa-3,5-dienamide (160)

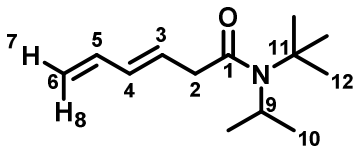

The title compound was synthesised according to General Procedure 1a using (*E*)-hexa-3,5-dienoic acid (**125**) (1.00 g, 8.92 mmol, 1.0 eq.) and *N*-*tert*-butylisopropylamine (1.55 mL, 9.81 mmol, 1.1 eq.). Purification by flash column chromatography (5-10% EtOAc / petroleum ether) afforded the amide as a colourless oil (0.22 g, 1.07 mmol, 12%).

^{1}H NMR (400 MHz, Chloroform-*d*): δ 6.29 (1H, dt, *J* = 17.0, 10.2 Hz, H5), 6.07 (1H, dd, *J* = 15.4, 10.2 Hz, H4), 5.83 (1H, dt, *J* = 15.4, 7.0 Hz, H3), 5.07 (1H, dd, *J* = 17.0, 1.7 Hz, H8), 4.95 (1H, dd, *J* = 10.2, 1.7 Hz, H7), 3.91 (1H, sept, *J* = 7.1 Hz, H9), 3.14 (2H, d, *J* = 7.0 Hz, H2), 1.93 (9H, s, H12), 1.33 (6H, d, *J* = 7.1 Hz, H10).

^{13}C NMR (101 MHz, Chloroform-*d*): δ 177.2 (C1), 137.1 (C5), 133.7 (C4), 128.1 (C3), 118.1 (C6), 47.0 (C9), 46.0 (C11), 42.3 (C2), 30.4 (C12), 27.3 (C10).

HRMS (ESI$^+$) *m/z* calculated for $C_{13}H_{24}NO$ $[M+H]^+$ 210.1858, found 258.1857.

IR: ν_{max} = 2972 (C-H), 2960 (C-H), 1622 (C=O), 1567 (C=C), 1382, 1370, 1176, 1003 cm^{-1}.

(*E*)-*N*-Isopropyl-*N*-phenylhexa-3,5-dienamide (162)

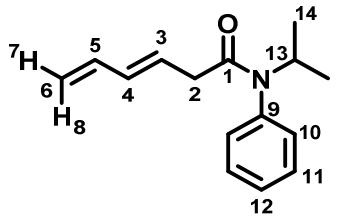

The title compound was synthesised according to General Procedure 1b using (*E*)-hexa-3,5-dienoic acid (**125**) (1.00 g, 8.92 mmol, 1.0 eq.) and *N*-isopropylaniline (**161**) (1.21 mL, 9.81 mmol, 1.1 eq.). Purification by flash column chromatography (0-5% EtOAc / petroleum ether) to afford the amide as a yellow oil (0.89 g, 3.92 mmol, 44%).

^{1}H NMR (400 MHz, Chloroform-*d*): δ 7.43-7.35 (3H, m, H10, H12), 7.09-7.06 (2H, m, H11), 6.26 (1H, dt, *J* = 17.0, 9.9 Hz, H5), 5.85-5.70 (2H, m, H3, H4), 5.02 (1H, dd, *J* = 17.0, 1.1 Hz, H8), 5.00-4.93 (1H, m, H13), 4.93 (1H, dd, *J* = 9.9, 1.1 Hz, H7), 2.73 (2H, d, *J* = 6.5 Hz, H2), 1.02 (6H, d, *J* = 6.8 Hz, H14).

^{13}C NMR (101 MHz, Chloroform-*d*): δ 170.2 (C1), 140.5 (C9), 136.8 (C5), 133.5 (C4), 131.0 (C10), 129.2 (C12), 128.4 (C11), 127.9 (C3), 116.9 (C6), 45.7 (C13), 39.1 (C2), 21.0 (C14).

HRMS (ESI$^+$) *m/z* calculated for $C_{15}H_{20}NO$ $[M+H]^+$ 230.1539, found 230.1542.

IR: ν_{max} = 2973 (C-H), 1645 (C=O), 1592 (C=C), 1494 (C=C), 1391, 1118, 703 cm^{-1}.

(*R*)-3-(4-Chlorophenyl)-1-isopropyl-1-(1-phenylethyl)urea (164)

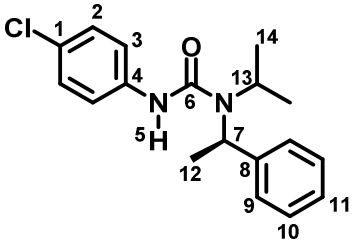

To a solution of 4-chlorophenyl isocyanate (**163**) (2.00 g, 13.07 mmol, 1.0 eq.) in anhydrous CH_2Cl_2 (50 mL) was added *(R)-N*-(1-phenylethyl)propan-2-amine (**H-49**) (2.61 mL, 14.37 mmol, 1.1 eq.). The mixture was stirred for 16 h before solvent was removed *in vacuo*. Purification by flash column chromatography (10% EtOAc / petroleum ether) afforded the title compound as a white solid (3.34 g, 10.57 mmol, 81%).

^{1}H NMR (400 MHz, Chloroform-*d*): δ 7.49-7.33 (5H, m, H9-H11), 7.12 (2H, d, *J* = 9.2 Hz, H2), 6.97 (2H, d, *J* = 9.2 Hz, H3), 6.02 (1H, br s, H5), 4.91 (1H, q, *J* = 7.4 Hz, H13), 4.61 (1H, sept, *J* = 7.2 Hz, H7), 1.74 (3H, d, *J* = 7.4 Hz, H14), 1.35 (3H, d, *J* = 7.2 Hz, H12), 1.27 (3H, d, *J* = 7.4 Hz, H14).

^{13}C NMR (101 MHz, Chloroform-*d*): δ 155.4 (C6), 141.5 (C8), 131.3 (C4), 129.3 (C1), 128.7 (C2), 128.1 (C9), 127.5 (C11), 126.8 (C10), 120.6 (C3), 50.5 (C13), 46.9 (C7), 21.7 (C14), 21.3 (C14), 18.4 (C12).

HRMS (ESI^+) *m/z* calculated for $C_{18}H_{22}ClN_2O$ $[M+H]^+$ 317.1415, found 317.1425.

MP: 117-118 °C.

IR: ν_{max} = 3403 (N-H), 2991 (C-H), 1651 (C=O), 1590 (C=C), 1494 (C=C), 1415, 1233.

(*R*)-1-(4-Chlorophenyl)-3-isopropyl-1-methyl-3-(1-phenylethyl)urea (165)

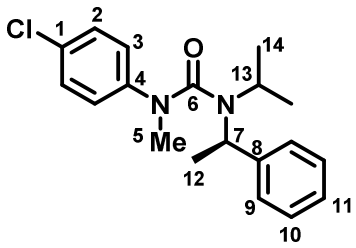

To a solution of (*R*)-3-(4-chlorophenyl)-1-isopropyl-1-(1-phenylethyl)urea (**164**) (2.00 g, 6.33 mmol, 1.0 eq.) in anhydrous DMF (35 mL) was added NaH (0.51 g, 12.66 mmol, 2.0 eq., 60% in mineral oil). After 30 minutes, MeI (1.00 mL, 15.83 mmol, 2.5 eq.) was added, and the reaction left to stir for 16 h. Water (30 mL) was added, and the aqueous layer extracted with Et_2O (5 × 30 mL) before the combined organics were dried over Na_2SO_4, filtered and concentrated *in vacuo*. Purification by flash column chromatography (10% EtOAc / petroleum ether) afforded the title compound as a colourless oil (1.78 g, 5.38 mmol, 85%).

^{1}H NMR (400 MHz, Chloroform-*d*): δ 7.33-7.22 (7H, m, H2, H9-H11), 6.95 (2H, d, *J* = 9.1 Hz, H3), 4.82 (1H, q, *J* = 7.3 Hz, H7), 3.48 (1H, sept, *J* = 7.5 Hz, H13), 3.07 (3H, s, H5), 1.33 (3H, d, *J* = 7.5 Hz, H14), 1.26 (3H, d, *J* = 7.5 Hz, H14), 0.87 (3H, d, *J* = 7.3 Hz, H12).

^{13}C NMR (101 MHz, Chloroform-*d*): δ 162.6 (C6), 146.7 (C4), 140.8 (C8), 130.1 (C1), 129.6 (C9), 128.2 (C2), 127.7 (C11), 127.3 (C10), 125.8 (C3), 54.8 (C13), 48.3 (C7), 39.8 (C5), 21.1 (C14), 20.7 (C14), 16.6 (C12).

HRMS (ESI$^+$) *m/z* calculated for $C_{19}H_{24}ClN_2O$ $[M+H]^+$ 331.1572, found 331.1581.

IR: ν_{max} = 2970 (C-H), 1650 (C=O and C=C broad), 1491, 1314, 1094.

(*R*)-1-(1-(4-Chlorophenyl)-1-phenylethyl)-1-isopropyl-3-methylurea (166)

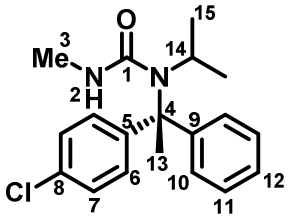

A solution of (*R*)-1-(4-chlorophenyl)-3-isopropyl-1-methyl-3-(1-phenylethyl)urea (**165**) (0.70 g, 2.12 mmol, 1.0 eq.) in anhydrous THF (20 mL) was cooled to −78 °C before addition of DMPU (0.59 mL, 4.88 mmol, 2.3 eq.) and ^{s}BuLi (3.80 mL, 5.30 mmol, 2.5 eq., 1.4 M in cyclohexane). After 6 h stirring at −78 °C, the reaction was quenched with saturated $NH_4Cl_{(aq.)}$ (30 mL) and water (20 mL). The aqueous layer was extracted with Et_2O (3 × 30 mL) before combined organics were washed with brine (60 mL), dried over Na_2SO_4, filtered and concentrated *in vacuo*. Purification by flash column chromatography (10-20% EtOAc / petroleum ether) afforded the title compound as a yellow solid (0.37 g, 1.12 mmol, 53%). The enantiomeric ratio determined as 75:25, through the use of a chiral HPLC Registech® Whelk column with hexane:isopropanol (85:15) as eluent with retention time (min) 11.19 : 13.45.

^{1}H NMR (400 MHz, Chloroform-*d*): δ 7.34-7.18 (9H, m, H6, H7, H10-H12), 3.95 (1H, br d, *J* = 5.7 Hz, H2), 3.39 (1H, sept, *J* = 7.3 Hz, H14), 2.41 (3H, d, *J* = 5.7 Hz, H3), 2.08 (3H, s, H13), 1.41 (3H, d, *J* = 7.3 Hz, H15), 1.39 (3H, d, *J* = 7.3 Hz, H15).

^{13}C NMR (101 MHz, Chloroform-*d*): δ 160.0 (C1), 145.7 (C9), 144.8 (C5), 132.8 (C8), 128.7 (C6), 128.6 (C7), 128.5 (C10), 127.3 (C12), 127.0 (C11), 68.3 (C4), 49.1 (C14), 29.4 (C13), 27.0 (C3), 22.9 (C15), 22.7 (C15).

HRMS (APCI$^+$) *m/z* calculated for $C_{19}H_{24}ClN_2O$ $[M+H]^+$ 331.1572, found 331.1581.

IR: ν_{max} = 3355 (N-H), 2979 (C-H), 1632 (C=O and C=C broad), 1512 (C=C), 1489, 1261, 1092.

(*R*)-*N*-(1-(4-Chlorophenyl)-1-phenylethyl)propan-2-amine (167)

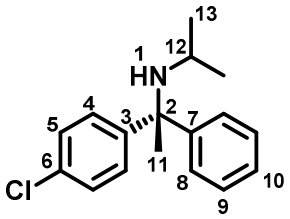

To a solution of (*R*)-1-(1-(4-chlorophenyl)-1-phenylethyl)-1-isopropyl-3-methylurea (**166**) (0.29 g, 0.88 mmol, 1.0 eq.) in EtOH (5 mL) was mixed with $NaOH_{(aq.)}$ (5 mL, 2 M) and subjected to microwave irradiation (30 s pre-stirring, 130 °C, 4 h, high absorption setting) before addition of EtOAc (40 mL). The aqueous layer was extracted with EtOAc (3 × 30 mL) before combined organics washed with brine (60 mL), dried over $MgSO_4$, filtered and concentrated *in vacuo*. Purification by flash column chromatography (5% EtOAc / petroleum ether) afforded the title compound as a colourless oil (0.17 g, 0.64 mmol, 73%).

^{1}H NMR (400 MHz, Chloroform-*d*): δ 7.26-7.09 (9H, m, H4, H5, H8-H10), 2.61 (1H, sept, *J* = 6.3 Hz, H12), 1.68 (3H, s, H11), 1.38 (1H, br s, H1), 0.85 (3H, d, *J* = 6.3 Hz, H13), 0.84 (3H, d, *J* = 6.3 Hz, H13).

^{13}C NMR (101 MHz, Chloroform-*d*): δ 148.9 (C3), 148.3 (C7), 132.1 (C6), 128.8 (C4), 128.1 (C5), 128.0 (C8), 127.2 (C10), 126.6 (C9), 62.9 (C2), 43.9 (C12), 28.9 (C11), 26.2 (C13), 26.1 (C13).

HRMS (nanospray$^+$) *m/z* calculated for $C_{17}H_{21}NCl$ $[M+H]^+$ 274.1363, found 274.1366.

IR: ν_{max} = 3659 (N-H), 2980 (C-H), 1487 (C=C), 1379, 1225.

(*S*,*E*)-2-Methyl-*N*-(1-phenylethylidene)propane-2-sulfinamide (171)

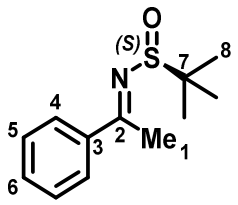

Synthesised according to the procedure by Cogan *et al.*[64]

To a solution of $Ti(O^iPr)_4$ (1.24 mL, 8.34 mmol, 2.0 eq.) was added acetophenone (**169**) (0.49 mL, 4.20 mmol, 1.0 eq.) and (*S*)-*tert*-butanesulfinamide (**170**) (0.53 g, 4.40 mmol, 1.1 eq.) and the solution heated to 50 °C for 18 h. To this mixture was added THF (30 mL) along with brine (30 mL) to precipitate the insoluble salts. The solids were removed by filtration through celite before the aqueous layer was

extracted with EtOAc (3 × 30 mL). The combined organics were washed with water (2 × 30 mL), brine (30 mL), dried over Na_2SO_4, filtered and concentrated *in vacuo*. Purification was carried out through a silica plug, eluting with 20% EtOAc / petroleum ether to give the title compound as an *E*/*Z* mixture (51:49) as a yellow liquid (0.67 g, 3.02 mmol, 72%). Assignments *E*- and *Z*- in the assignments below relate to the stereoisomer of the molecule, and not the individual atom discussed.

^{1}H NMR (400 MHz, Chloroform-*d*): δ 7.97 (2H, d, *J* = 7.0 Hz, *Z*-H4), 7.90 (2H, d, *J* = 7.1 Hz, *E*-H4), 7.52-7.46 (2H, *E*-H6, *Z*-H6), 7.46-7.40 (4H, m, *E*-H5, *Z*-H5), 2.78 (3H, s, *E*-H1), 2.61 (3H, s, *Z*-H1), 1.44 (9H, s, *Z*-H8), 1.34 (9H, s, *E*-H8).

^{13}C NMR (101 MHz, Chloroform-*d*): δ 176.5 (*E*/*Z*-C2), 176.4 (*E*/*Z*-C2), 138.9 (*E*-C3), 137.2 (*Z*-C3), 133.2 (*E*-C6), 131.8 (*Z*-C6), 128.6 (*E*-C5), 128.5 (*Z*-C5), 128.4 (*Z*-C4), 127.3 (*E*-C4), 57.5 (*E*/*Z*-C7), 57.5 (*E*/*Z*-C7), 30.4 (*Z*-C8), 27.2 (*Z*-C1), 22.6 (*E*-C8), 19.9 (*E*-C1).

Data consistent with literature.[64]

(*S*)-2-Methyl-*N*-((*R*)-2-phenylhexan-2-yl)propane-2-sulfinamide (172)

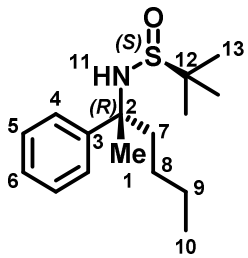

Synthesised according to the procedure by Ellman *et al.*[64]

To a solution of (*S*,*E*)-2-methyl-*N*-(1-phenylethylidene)propane-2-sulfinamide (**171**) (0.60 g, 2.69 mmol, 1.0 eq.) in anhydrous toluene (10 mL) was added Me_3Al (0.28 mL, 2.96 mmol, 1.1 eq.) slowly at −78 °C. At this temperature, the sulfinyl compound was added dropwise to a solution of ^{n}BuLi (2.90 mL, 7.25 mmol, 2.7 eq., 2.5 M in hexanes) in anhydrous toluene (5 mL) to give a thick orange slurry (rapid stirring required for mobilisation). After 4 h at −78 °C, Na_2SO_4 was added slowly until effervescence ceased. The aqueous layer was extracted with EtOAc (3 × 20 mL) before the combined organics were washed with water (30 mL), brine (30 mL), dried over $MgSO_4$, filtered and concentrated *in vacuo*. Purification by flash column chromatography (0-20% EtOAc / petroleum ether) afforded the title compound as a colourless oil (1.61 mmol, 60%). Only one diastereomer was observed in this reaction.

^{1}H NMR (400 MHz, Chloroform-*d*): δ 7.37 (2H, d, *J* = 7.6 Hz, H4), 7.29 (2H, t, *J* = 7.6 Hz, H5), 7.19 (1H, t, *J* = 7.6 Hz, H6), 3.47 (1H, br s, H11), 2.00-1.91 (1H, m, H7), 1.90-1.80 (1H, m, H7), 1.68 (3H, s, H1), 1.27-1.19 (2H, m, H9), 1.17 (9H, s, H13), 1.12-1.00 (2H, m, H8), 0.79 (3H, t, *J* = 7.3 Hz, H10).

^{13}C NMR (101 MHz, Chloroform-*d*): δ 145.3 (C3), 128.2 (C5), 126.8 (C6), 126.3 (C4), 60.9 (C2), 55.9 (C12), 44.1 (C7), 28.2 (C1), 26.2 (C8), 22.8 (C9), 22.7 (C13), 13.9 (C10).

$[\alpha]_D^{24}$**:** −0.14 (*c* 1, $CHCl_3$).

Data consistent with literature.[64]

(*R*)-*N*-Isopropyl-2-phenylhexan-2-amine (174)

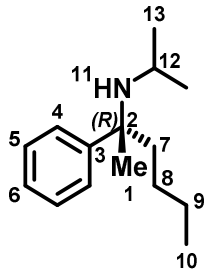

To a solution of (*S*)-2-methyl-*N*-((*R*)-2-phenylhexan-2-yl)propane-2-sulfinamide (**172**) (1.20 g, 4.27 mmol, 1.0 eq.) in MeOH (10 mL) before slow addition of HCl (4.25 mL, 17.01 mmol, 4.0 eq., 4 M in dioxane). After 1 h, solvent was removed *in vacuo* before the orange oil was dissolved in acetone (**1**) (10 mL) and Et_3N (**107**) (9.00 mL, 64.57 mmol, 15.0 eq.) was added. After 1 h, solvent was again removed *in vacuo* before water (50 mL) was added and the aqueous layer was extracted with CH_2Cl_2 (3 × 30 mL). The combined organics were washed with water (50 mL), brine (50 mL), dried over $MgSO_4$, filtered and concentrated *in vacuo* to give (*R*)-*N*-isopropyl-2-phenylhexan-2-amine (**173**) as an orange liquid which was used without further purification in the next step.

A solution of $NaBH_3CN$ (0.26 g, 6.87 mmol, 1.6 eq.), AcOH (1.22 mL, 21.35 mmol, 5.0 eq.) and anhydrous CH_2Cl_2 (20 mL) was prepared in an ice bath and allowed to stir for 1 h at this temperature before the mixture was allowed to warm to rt. A solution of (*R*)-*N*-isopropyl-2-phenylhexan-2-amine (**173**) (0.76 g, 4.27 mmol, 1.0 eq.) in anhydrous CH_2Cl_2 (20 mL) was added with AcOH (0.41 mL, 7.11 mmol, 1.7 eq.) and the mixture left to stir for 10 min. Acetone (6.90 mL, 93.94 mmol, 22.0 eq.) was added slowly, and the mixture left to stir for 16 h. Solvent was removed *in vacuo* before addition of saturated $NaHCO_{3(aq.)}$ (30 mL) and the aqueous layer extracted with EtOAc (3 × 30 mL). The combined organics were washed with brine (30 mL), dried over $MgSO_4$, filtered and concentrated *in vacuo* to give an orange liquid (0.68 g, 3.12 mmol, 73%) which was used without further purification.

^{1}H NMR (400 MHz, Chloroform-*d*): δ 7.39-7.33 (2H, m, H4), 7.24 (2H, t, *J* = 7.6 Hz, H5), 7.13 (1H, t, *J* = 7.6 Hz, H6), 2.60 (1H, sept, *J* = 6.5 Hz, H12), 1.74-1.56 (2H, m, H7), 1.44 (3H, s, H1), 1.20-1.02 (3H, m, H8, H9), 0.94 (3H, d, *J* = 6.5 Hz, H13), 0.85-0.80 (1H, m, H8), 0.78 (3H, d, *J* = 6.5 Hz, H13), 0.74 (3H, t, *J* = 6.9 Hz, H10).

^{13}C NMR (101 MHz, Chloroform-*d*): δ 140.2 (C3), 128.0 (C5), 126.7 (C4), 126.3 (C6), 59.6 (C2), 44.1 (C7), 44.0 (C12), 26.5 (C8), 26.1 (C13), 25.4 (C13), 24.9 (C1), 23.3 (C9), 14.1 (C10).

HRMS (ESI$^+$) *m/z* calculated for $C_{15}H_{26}N$ $[M+H]^+$ 219.2013, found 219.2024.

IR: ν_{max} = 3214 (N-H), 2875 (C-H), 1463 (C=C), 1382, 1145.

(*R*,*E*)-*N*-Isopropyl-*N*-(2-phenylhexan-2-yl)hexa-3,5-dienamide (175)

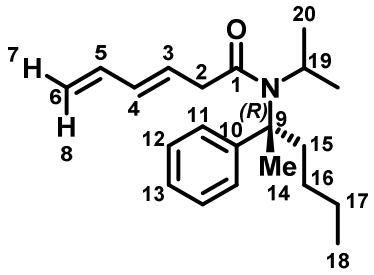

The title compound was synthesised according to General Procedure 1a using (*E*)-hexa-3,5-dienoic acid (**125**) (240 mg, 2.14 mmol, 1.0 eq.) and (*R*)-*N*-isopropyl-2-phenylhexan-2-amine (**174**) (520 mg, 2.35 mmol, 1.1 eq.). Purification by flash column chromatography (0-5% EtOAc / petroleum ether) afforded the amide as a colourless oil (94 mg, 0.30 mmol, 14%). Broad NMR peaks noted due to rotameric structure. The enantiomeric ratio was determined as 95:5, through the use of a chiral HPLC Registech® Chiralpak IA column with hexane:isopropanol (95:5) as eluent with retention time (min) 14.83 : 18.00.

^{1}H NMR (400 MHz, Chloroform-*d*): δ 7.38-7.34 (2H, m, H11), 7.29-7.22 (2H, m, H12), 7.19-7.12 (1H, m, H13), 6.32 (1H, dt, *J* = 16.6, 10.8 Hz, H5), 6.17 (1H, dd, *J* = 16.1, 10.8 Hz, H4), 5.82-5.70 (1H, m, H3), 5.16 (1H, d, *J* = 16.6 Hz, H8), 5.05 (1H, d, *J* = 10.8 Hz, H7), 2.97 (2H, d, *J* = 7.3 Hz, H2), 2.60 (1H, sept, *J* = 6.4 Hz, H19), 2.02-1.92 (1H, m, H15), 1.86-1.74 (1H, m, H15), 1.67 (3H, s, H14), 1.65-1.59 (2H, m, H16), 1.25-1.15 (2H, m, H17), 0.95 (3H, d, *J* = 6.4 Hz, H20), 0.81-0.75 (6H, m, H18, H20).

^{13}C NMR (101 MHz, Chloroform-*d*): δ 169.5 (C1), 145.8 (C10), 136.4 (C5), 135.5 (C4), 128.4 (C11), 126.9 (C3), 126.6 (C12), 126.1 (C13), 117.4 (C6), 58.9 (C9), 44.3 (C16), 43.7 (C19), 41.8 (C15), 41.5 (C2), 26.3 (C20), 25.7 (C14), 25.6 (C20), 23.0 (C17), 14.09 (C18).

HRMS (ESI$^+$) *m/z* calculated for $C_{21}H_{32}NO$ $[M+H]^+$ 314.2483, found 314.2479.

IR: ν_{max} = 2884 (C-H), 1654 (C=O), 1474 (C=C), 1372, 1145.

(2*E*,4*E*)-*N*-Isopropyl-7-methyl-7-phenylundeca-2,4-dienamide (176)

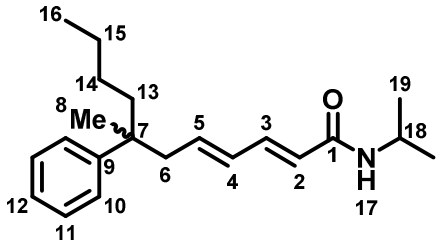

The title compounds were synthesised according to General Procedure 2 using (R,E)-*N*-isopropyl-*N*-(2-phenylhexan-2-yl)hexa-3,5-dienamide (**175**) (60 mg, 0.19 mmol, 1.0 eq.). Purification by flash column chromatography (0-30% EtOAc / petroleum ether) afforded the migration product as a colourless oil (12 mg, 0.04 mmol, 21%). Note that this reaction gave an uncharacteristically complex array of compounds. The enantiomeric ratio determined as 51:49, through the use of a chiral HPLC Registech® Whelk column with hexane:isopropanol (85:15) as eluent with retention time (min) 12.19 : 16.09.

^{1}H NMR (400 MHz, Chloroform-*d*): δ 7.41 (2H, d, *J* = 7.8 Hz, H10), 7.34-7.28 (2H, m, H11), 7.23-7.17 (1H, m, H12), 7.12 (1H, dd, *J* = 15.1, 10.5 Hz, H3), 6.13 (1H, dd, *J* = 14.5, 10.5 Hz, H4), 6.02-5.92 (1H, m, H5), 5.81 (1H, d, *J* = 15.1 Hz, H2), 5.68 (1H, br s, H17), 2.64 (1H, sept, *J* = 6.6 Hz, H18), 2.29-2.24 (2H, m, H6), 2.14-2.05 (1H, m, H13), 1.94-1.83 (1H, m, H13), 1.72-1.59 (2H, m, H14), 1.49 (3H, s, H8), 1.25-1.14 (2H, m, H15), 0.99 (3H, d, *J* = 6.6 Hz, H19), 0.86-0.81 (6H, m, H16, H19).

^{13}C NMR (101 MHz, Chloroform-*d*): δ 165.2 (C1), 146.1 (C9), 141.2 (C5), 141.0 (C3), 129.2 (C4), 128.4 (C11), 127.9 (C10), 126.7 (C12), 123.1 (C2), 59.1 (C7), 44.4 (C14), 43.8 (C18), 42.1 (C13), 32.3 (C6), 26.5 (C15), 26.3 (C19), 25.7 (C19), 25.2 (C8), 14.1 (C16).

HRMS (ESI$^+$) *m/z* calculated for $C_{21}H_{32}NO$ $[M+H]^+$ 314.2483, found 313.2480.

IR: ν_{max} = 3325 (N-H), 2882 (C-H), 2756 (C-H), 1640 (C=O), 1444 (C=C), 1312.

Phenyl((1*R*,2*R*)-2-phenylcyclopropyl)methanone (179)

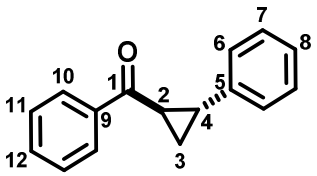

Synthesised according to the procedure by Ciaccio *et al.* in a modified Corey-Chaykovsky reaction.[148]

To a slurry of NaH (0.69 g, 17.30 mmol, 1.2 eq., 60% in mineral oil) in anhydrous DMSO (15 mL) was added trimethylsulfoxonium iodide (**178**) (3.81 g, 17.30 mmol, 1.2 eq.) and the mixture left to stir for 1 h. A solution of trans-chalcone (**177**) (3.00 g, 14.42 mmol, 1.0 eq.) in anhydrous DMSO (28 mL) was added slowly to give a clear, orange solution. The mixture was left to stir for 16 h before addition of brine (50 mL). The aqueous layer was extracted with Et_2O (3 × 30 mL) before the combined organics were washed with water (2 × 50 mL), brine (50 mL), dried over $MgSO_4$, filtered and concentrated *in vacuo*. Purification by flash column chromatography (0-5% EtOAc / petroleum ether) afforded a peach-coloured solid (1.92 g, 8.65 mmol, 60%).

^{1}H NMR (400 MHz, Chloroform-*d*): δ 8.03-7.97 (2H, m, H10), 7.56 (1H, tt, *J* = 7.4, 1.3 Hz, H12), 7.49-7.44 (2H, m, H11), 7.35-7.29 (2H, m, H6), 7.24 (1H, tt, *J* = 7.2, 1.3 Hz, H7), 7.21-7.17 (2H, m, H8), 2.91 (1H, ddd, *J* = 9.3, 5.3, 4.1 Hz, H2), 2.71 (1H, ddd, *J* = 10.6, 6.7, 4.1 Hz, H4), 1.94 (1H, ddd, *J* = 9.5, 5.3, 4.1 Hz, H3), 1.56 (1H, ddd, *J* = 10.6, 6.7, 4.1 Hz, H3).

^{13}C NMR (101 MHz, Chloroform-*d*): δ 198.7 (C1), 140.6 (C9), 137.9 (C5), 133.0 (C10), 128.7 (C12), 128.6 (C11), 128.3 (C6), 126.7 (C7), 126.4 (C8), 30.1 (C4), 29.4 (C2), 19.4 (C3).

Data consistent with literature.[148]

X-Ray Crystallography confirming relative stereochemistry:

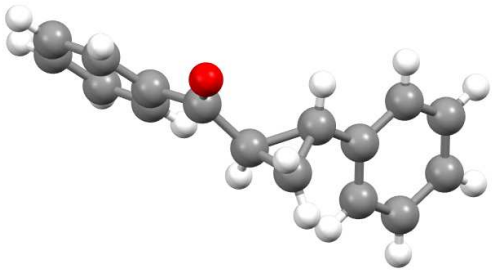

Empirical formula	$C_{16}H_{14}O$
Formula weight	222.27
Temperature/K	100(2)
Crystal system	orthorhombic
Space group	$P2_12_12_1$
a/Å	5.9851(2)
b/Å	8.5508(3)
c/Å	23.3489(8)
α/°	90
β/°	90
γ/°	90
Volume/Å^3	1194.94(7)
Z	4
ρ_{calc}g/cm^3	1.236
μ/mm^{-1}	0.586
F(000)	472.0
Crystal size/mm^3	0.35 × 0.287 × 0.147
Radiation	CuKα (λ = 1.54178)
2Θ range for data collection/°	7.572 to 144.972
Index ranges	-7 ≤ h ≤ 7, -10 ≤ k ≤ 10, -28 ≤ l ≤ 28
Reflections collected	15872
Independent reflections	2373 [R_{int} = 0.0555, R_{sigma} = 0.0342]
Data/restraints/parameters	2373/0/155
Goodness-of-fit on F^2	1.093
Final R indexes [I>=2σ (I)]	R_1 = 0.0418, wR_2 = 0.1107
Final R indexes [all data]	R_1 = 0.0430, wR_2 = 0.1116
Largest diff. peak/hole / e Å^{-3}	0.28/-0.26
Flack parameter	0.2(5)

N-(Phenyl((1*R*,2*R*)-2-phenylcyclopropyl)methyl)propan-2-amine (180)

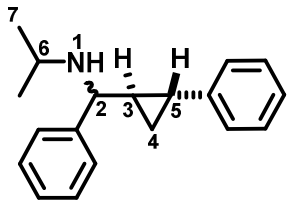

To a solution of phenyl((1*R*,2*R*)-2-phenylcyclopropyl)methanone (**179**) (1.20 g, 5.40 mmol, 1.0 eq.) in anhydrous CH_2Cl_2 (25 mL) was added isopropylamine (1.86 mL, 21.61 mmol, 4.0 eq.). In an ice bath, $TiCl_4$ (10.81 mL, 10.81 mmol, 2.0 eq., 1 M in CH_2Cl_2) was added slowly and the mixture stirred for 16 h at rt. A solution of $NaBH_3CN$ (0.41 g, 6.48 mmol, 1.2 eq.) in anhydrous THF (10 mL) was added and the mixture left to stir for 4 h. The reaction was quenched with $NaOH_{(aq.)}$ (40 mL, 1 M) before the aqueous layer was extracted with CH_2Cl_2 (3 × 30 mL). The combined organics were washed with water (30 mL), brine (40 mL), dried over Na_2SO_4, filtered and concentrated *in vacuo* to afford an orange oil (1.25 g, 4.70 mmol, 87%) as a mixture of 2 diastereomers (dr 58:42). This was used without further purification in the next step.

^{1}H NMR (400 MHz, Chloroform-*d*): δ 7.40-7.04 (18H, m, Ar), 6.91 (2H, d, *J* = 7.4 Hz, Ar), 4.15 (2H, br s, H1 D1, H1 D2), 3.32 (1H, d, *J* = 5.0 Hz, H2 D1), 3.30 (1H, d, *J* = 4.6 Hz, H2 D2), 2.78-2.67 (2H, m, H6 D1, H6 D2), 1.90-1.83 (2H, m, H5 D1, H5 D2), 1.50-1.38 (2H, m, H3 D1, H3 D2), 1.08-1.00 (13H, m, H7 D1, H7 D2, H4 D1/D2), 1.00-0.92 (2H, m, H4 D1/D2), 0.87-0.81 (1H, m, H4 D1/D2).

^{13}C NMR (101 MHz, Chloroform-*d*): δ 144.1 (Ar), 144.0 (Ar), 143.0 (Ar), 142.7 (Ar), 128.5 (Ar), 128.5 (Ar), 128.4 (Ar), 128.3 (Ar), 127.4 (Ar), 127.2 (Ar), 127.2 (Ar), 127.1 (Ar), 126.3 (Ar), 125.9 (Ar), 125.6 (Ar), 125.5 (Ar), 68.1 (C2 D1), 64.9 (C2 D2), 45.8 (C6 D1), 45.7 (C6 D2), 31.0 (C3 D2), 30.4 (C3 D1), 24.3 (C7 D1), 24.1 (C7 D2), 23.6 (C5 D1), 22.6 (C7 D1), 22.4 (C7 D2), 21.2 (C5 D2), 15.3 (C4 D2), 14.0 (C4 D1).

HRMS (ESI$^+$) *m/z* calculated for $C_{19}H_{24}N$ $[M+H]^+$ 266.1903, found 266.1906.

IR: ν_{max} = 3658 (N-H), 2979 (C-H), 2970 (C-H), 1496 (C=C), 1364, 1088.

(*E*)-*N*-Isopropyl-*N*-(phenyl((1*R*,2*R*)-2-phenylcyclopropyl)methyl)hexa-3,5-dienamide (181)

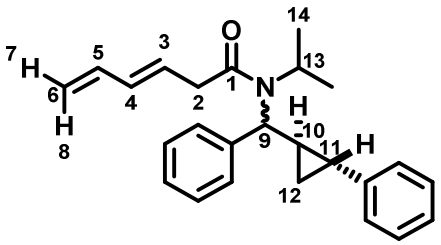

The title compound was synthesised according to General Procedure 1a using (*E*)-hexa-3,5-dienoic acid (**125**) (0.40 g, 3.57 mmol, 1.0 eq.) and *N*-(phenyl((1*R*,2*R*)-2-phenylcyclopropyl)methyl)propan-2-amine (**180**) (1.04 g, 3.93 mmol, 1.1 eq.). Purification by flash column chromatography (0-20% EtOAc / petroleum ether) afforded the amide as a colourless oil (0.37 g, 1.04 mmol, 29%) as a mixture of two diastereomers (dr 50:50). D1 and D2 refer to the diastereomer of product. Broad NMR peaks noted due to rotameric structure.

^{1}H NMR (400 MHz, Chloroform-*d*): δ 7.49-6.88 (20H, m, Ar), 6.28 (2H, dt, *J* = 17.1, 10.8 Hz, H5 D1, H5 D2), 6.17-5.94 (2H, br m, H4 D1, H4 D2), 5.94-5.81 (2H, m, H3 D1, H3 D2), 5.05 (2H, dd, *J* = 17.1, 4.4 Hz, H8 D1, H8 D2), 4.95 (2H, d, *J* = 10.4 Hz, H7 D1, H7 D2), 4.26-4.06 (1H, br m, H9 D1), 3.41-3.23 (1H, br m, H13 D1), 3.23-3.09 (5H, m, H2 D1, H2 D2, H9 D2), 2.60 (1H, sept, *J* = 6.1 Hz, H13 D2), 1.97 (1H, br s, H11 D1), 1.83 (1H, br s, H11 D2), 1.77-1.70 (2H, m, H10 D1, H10 D2), 1.37-1.28 (1H, m, H12 D1/D2), 1.11-1.00 (7H, br m, H12 D1/D2, H14 D1), 0.92 (3H, d, *J* = 6.1 Hz, H14 D2), 0.90 (3H, d, *J* = 6.1 Hz, H14 D2), 0.83 (1H, dt, *J* = 8.9, 5.4 Hz, H12 D1/D2), 0.71 (1H, dt, *J* = 8.6 Hz, H12 D1/D2).

^{13}C NMR (101 MHz, Chloroform-*d*): δ 171.6 (C1 D1), 170.4 (C1 D2), 143.9 (Ar), 142.9 (Ar), 136.7 (C5 D1, C5 D2), 133.7 (C4 D1, C4 D2), 128.5 (Ar), 128.3 (C3 D1, C3 D2), 128.3 (Ar), 128.2 (Ar), 127.7 (Ar), 127.3 (Ar), 127.0 (Ar), 125.8 (Ar), 125.6 (Ar), 125.5 (Ar), 116.6 (C6 D1, C6 D2), 65.8 (C9 D1), 64.8 (C9 D2), 49.1 (C13 D1), 45.7 (C13 D2), 39.5 (C2 D1, C2 D2), 31.8 (C12 D1/D2), 25.5 (C11 D2), 24.0 (C14 D2), 23.5 (C10 D1/D2), 22.6 (C14 D2), 22.5 (C11 D1), 20.2 (C12 D1/D2, C14 D1), 18.6 (C12 D1/D2), 15.0 (C12 D1/D2, C14 D1), 14.2 (C12 D1/D2), 13.8 (C12 D1/D2).

HRMS (ESI^{+}) *m/z* calculated for $C_{25}H_{30}NO$ $[M+H]^{+}$ 360.2322, found 360.2325.

IR: ν_{max} = 3027 (C-H), 2930 (C-H), 1630 (C=O), 1602 (C=C), 1496, 1356, 1185.

(2*E*,4*E*,9*E*)-*N*-Isopropyl-7,10-diphenyldeca-2,4,9-trienamide (185)

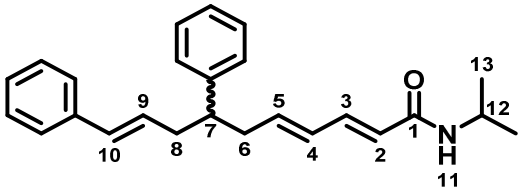

The title compounds were synthesised according to General Procedure 2 using (*E*)-*N*-isopropyl-*N*-(phenyl((1*R*,2*R*)-2-phenylcyclopropyl)methyl)hexa-3,5-dienamide (**181**) (150 mg, 0.19 mmol, 1.0 eq.). Purification by flash column chromatography (0-30% EtOAc / petroleum ether) afforded the migration product as a colourless oil (18 mg, 0.05 mmol, 26%).

^{1}H NMR (400 MHz, Chloroform-*d*): δ 7.20-7.05 (10H, m, Ar), 7.00 (1H, dd, *J* = 14.9, 10.4 Hz, H3), 6.27 (1H, dt, *J* = 15.8, 1.3 Hz, H10), 6.03-5.91 (2H, m, H5, H9), 5.88-5.77 (1H, m, H4), 5.59 (1H, d, *J* = 14.9 Hz, H2), 5.33 (1H, br s, H11), 4.06 (1H, sept, *J* = 7.1 Hz, H12), 2.74 (1H, quint, *J* = 6.7 Hz, H7), 2.60-2.33 (4H, m, H6, H8), 1.07 (6H, d, *J* = 7.1 Hz, H13).

^{13}C NMR (101 MHz, Chloroform-*d*): δ 165.5 (C1), 144.1 (Ar), 140.7 (C3), 140.3 (C4), 137.7 (Ar), 131.8 (C10), 130.0 (C5), 128.6 (Ar), 128.5 (Ar), 128.4 (C9), 127.7 (Ar), 127.1 (Ar), 126.5 (Ar), 126.1 (Ar), 122.7 (C2), 46.0 (C7), 41.5 (C12), 39.7 (C6), 39.4 (C8), 22.9 (C13), 22.8 (C13).

HRMS (ESI^{+}) *m/z* calculated for $C_{25}H_{30}NO$ $[M+H]^{+}$ 360.2322, found 360.2323.

IR: ν_{max} = 3281 (N-H), 2929 (C-H), 1651 (C=O), 1627 (C=C), 1496 (C=C), 1385, 1130.

(*E*)-*N*-Allyl-*N*-benzylhexa-3,5-dienamide (186)

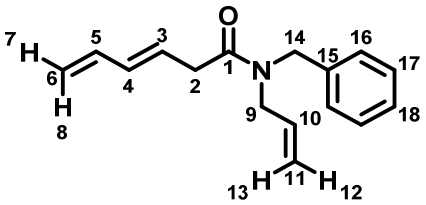

The title compound was synthesised according to General Procedure 1b using (*E*)-hexa-3,5-dienoic acid (**125**) (0.50 g, 4.46 mmol, 1.0 eq.) and *N*-benzylprop-2-en-1-amine (0.59 g, 4.91 mmol, 1.1 eq.). Purification by flash column chromatography (0-1% MeOH / CH_2Cl_2) afforded the amide as a yellow oil (0.16 g, 0.61 mmol, 15%). Broad NMR peaks and ^{13}C signal doubling noted due to rotameric structure.

^{1}H NMR (400 MHz, Chloroform-*d*): δ 7.36-7.10 (5H, m, H16-H18), 6.30 (1H, ddd, *J* = 17.0, 10.2, 10.0 Hz, H5), 6.09 (1H, dd, *J* = 15.7, 10.0 Hz, H4), 5.90-5.78 (1H, m, H3), 5.77-5.64 (1H, m, H10), 5.19 (1H, dd, *J*

= 10.4, 1.4 Hz, H12), 5.14-4.96 (3H, m, H7, H8, H13), 4.55 (1.2H, s, H14), 4.47 (0.8H, s, H14), 3.97 (0.8H, d, *J* = 6.5 Hz, H9), 3.79 (1.2H, d, *J* = 6.5 Hz, H9), 3.17 (2H, t, *J* = 7.1 Hz, H2).

^{13}C NMR (101 MHz, Chloroform-*d*): δ 171.2 (C1), 171.1 (C1), 137.4 (C15), 137.4 (C15) 136.5 (C5), 136.5 (C5), 136.4 (C16), 136.3 (C16), 133.7 (C4), 133.6 (C4) 132.8 (C10), 132.5 (C10), 128.9 (C18), 128.5 (C18), 128.2 (C17), 127.5 (C17), 127.2 (C3), 127.0 (C3), 117.6 (C6), 116.9 (C11), 116.5 (C6), 116.4 (C11), 50.1 (C14), 49.1 (C9), 48.2 (C9), 48.0 (C14), 37.3 (C2), 37.1 (C2).

HRMS (ESI$^+$) *m/z* calculated for $C_{16}H_{20}NO$ $[M+H]^+$ 242.1539, found 242.1533.

IR: ν_{max} = 2958 (C-H), 2927 (C-H),M 2860 (C-H), 1732 (C=O), 1622 (C=C), 1451 (C=C), 1166.

N-Allyl-2-benzylhexa-3,5-dienamide, (*E*)-*N*-Allyl-4-benzylhexa-2,5-dienamide and (2*E*,4*E*)-*N*-Allyl-7-phenylhepta-2,4-dienamide

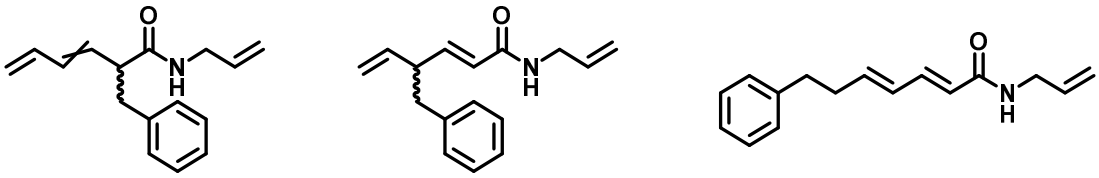

The title compounds were synthesised according to General Procedure 2 using (*E*)-*N*-allyl-*N*-benzylhexa-3,5-dienamide (**186**) (100 mg, 0.42 mmol, 1.0 eq.). Purification by flash column chromatography (0-20% EtOAc / petroleum ether) afforded the various migration products.

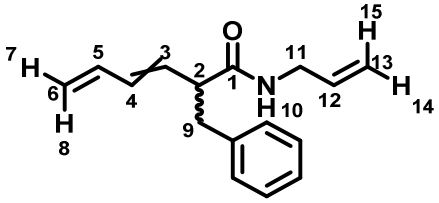

[1,3]-Isomers: Colourless oil (16 mg, 0.07 mmol, 16%). Isolated as a mixture of *E*- and *Z*- isomers, in a ratio of 67:33 respectively. Assignments *E*- and *Z*- in the assignments below relate to the stereoisomer of the molecule, and not the individual atom discussed. Not all aromatic signals seen in the ^{13}C NMR, likely due to overlap.

^{1}H NMR (400 MHz, Chloroform-*d*): δ 7.32-7.09 (10H, m, Ar), 6.45 (1H, dtd, *J* = 16.6, 10.1, 1.0 Hz, *Z*-H5), 6.30 (1H, dtd, *J* = 17.0, 9.8, 1.0 Hz, *E*-H5), 6.17-6.05 (2H, m, *E*-H4, *Z*-H4), 5.77 (1H, dd, *J* = 15.2, 8.8 Hz, *E*-H3), 5.73-5.64 (2H, m, *E*-H12, *Z*-H12), 5.53 (1H, t, *J* = 10.4 Hz, *Z*-H3), 5.46 (2H, br s, *E*-H10, *Z*-H10), 5.25 (1H, dd, *J* = 16.6, 1.6 Hz, *Z*-H8), 5.19-5.12 (2H, m, *E*-H8, *Z*-H7), 5.09-5.05 (1H, dd, *J* = 9.8, 1.6 Hz, *E*-

H7), 5.04-4.95 (4H, m, *E*-H14, *Z*-H14, *E*-H15, *Z*-H15), 3.87-3.74 (4H, m, *E*-H11, *Z*-H11), 3.59-3.51 (1H, m, *Z*-H2), 3.27-3.15 (2H, m, *E*-H9, *Z*-H9), 3.08 (1H, q, *J* = 7.2 Hz, *E*-H2), 2.88-2.81 (2H, m, *E*-H9, *Z*-H9).

^{13}C NMR (101 MHz, Chloroform-*d*): δ 172.5 (*E*-C1), 172.3 (*Z*-C1), 139.3 (Ar), 139.2 (Ar), 136.4 (*Z*-C5), 134.1 (*E*-C5), 133.9 (*E*-C4), 132.3 (*Z*-C4), 132.0 (*E*-C12), 131.2 (*Z*-C12), 129.5 (*Z*-C3), 129.3 (*E*-C3), 128.5 (Ar), 126.5 (Ar), 120.0 (*Z*-C6), 117.6 (*E*-C6), 116.4 (*E*-C13), 116.3 (*Z*-C13), 53.2 (*E*-C2), 48.0 (*Z*-C2), 42.0 (*E*-C11), 41.9 (*Z*-C11), 38.8 (*E*-C9), 38.8 (*Z*-C9).

HRMS (ESI$^+$) *m/z* calculated for $C_{16}H_{20}NO$ $[M+H]^+$ 242.1539, found 242.1532.

IR: ν_{max} = 3288 (N-H), 2922 (C-H), 2853 (C-H), 1638 (C=O), 1532 (C=C), 1258, 1029.

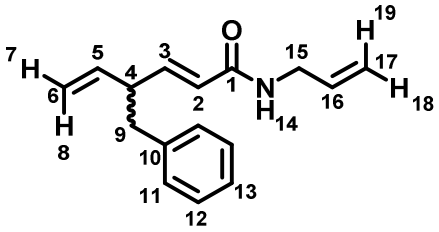

[1,5]-Isomers: Orange oil (6 mg, 0.03 mmol, 6%).

^{1}H NMR (400 MHz, Chloroform-*d*): δ 7.36-7.09 (5H, m, H11-H13), 6.83 (1H, dd, *J* = 15.5, 7.1 Hz, H3), 5.91-5.72 (2H, m, H5, H16), 5.68 (1H, dd, *J* = 15.5, 1.3 Hz, H2), 5.51 (1H, br s, H14), 5.17 (1H, dd, *J* = 18.0, 1.3 Hz, H19), 5.13 (1H, dd, *J* = 10.1, 1.3 Hz, H18), 5.05 (1H, dd, *J* = 10.3, 1.3 Hz, H7), 4.99 (1H, dd, *J* = 17.9, 1.3 Hz, H8), 3.99-3.89 (2H, m, H15), 3.15 (1H, quint, *J* = 7.1 Hz, H4), 2.79 (2H, d, *J* = 7.1 Hz, H9).

^{13}C NMR (101 MHz, Chloroform-*d*): δ 165.6 (C1), 146.0 (C3), 139.2 (C10), 138.8 (C11), 134.2 (C12), 129.4 (C5), 128.4 (C13), 126.3 (C16), 123.7 (C2), 116.6 (C17), 116.3 (C16), 48.0 (C15), 42.0 (C4), 40.9 (C9).

HRMS (ESI$^+$) *m/z* calculated for $C_{16}H_{20}NO$ $[M+H]^+$ 242.1539, found 242.1532.

IR: ν_{max} = 3286 (N-H), 2922 (C-H), 1710 (C=O), 1665 (C=C), 1627 (C=C), 1537 (C=C), 1258, 985, 698.

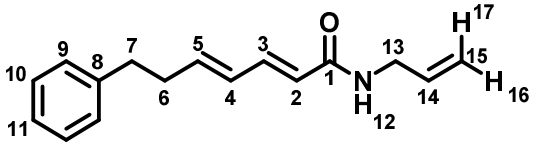

[1,7]-Isomer: White crystalline solid (14 mg, 0.06 mmol, 14%).

^{1}H NMR (400 MHz, Chloroform-*d*): δ 7.32-7.12 (6H, m, H3, H9-H11), 6.19-6.04 (2H, m, H4, H5), 5.86 (1H, ddt, *J* = 16.9, 10.1, 5.9 Hz, H14), 5.76 (1H, d, *J* = 15.3 Hz, H2), 5.62 (1H, br s, H12), 5.19 (1H, dd, *J*

= 16.9, 1.3 Hz, H17), 5.13 (1H, dd, *J* = 10.1, 1.3 Hz, H16), 3.96 (2H, tt, *J* = 5.9, 1.5 Hz, H13), 2.74 (2H, t, *J* = 7.6 Hz, H7), 2.47 (1H, q, *J* = 7.6 Hz, H6).

^{13}C NMR (101 MHz, Chloroform-*d*): δ 166.3 (C1), 142.5 (C3), 141.5 (C5), 141.3 (C8), 134.3 (C14), 128.9 (C4), 128.5 (C9), 128.4 (C11), 126.1 (C12), 122.0 (C2), 116.6 (C15), 42.1 (C13), 35.3 (C7), 34.9 (C6).

HRMS (ESI$^+$) *m/z* calculated for $C_{16}H_{20}NO$ $[M+H]^+$ 242.1539, found 242.1533.

MP: 91-92 °C.

IR: ν_{max} = 3298 (N-H), 2919 (C-H), 1652 (C=O), 1625 (C=C), 1610 (C=C), 1538 (C=C), 1260, 989, 697.

(*E*)-*N*-Benzyl-*N*-methylhexa-3,5-dienamide (187)

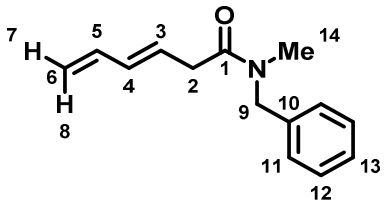

The title compound was synthesised according to General Procedure 1a using (*E*)-hexa-3,5-dienoic acid (**125**) (1.00 g, 8.92 mmol, 1.0 eq.) and *N*-methyl-1-phenylmethanamine (1.27 mL, 9.81 mmol, 1.1 eq.). Purification by flash column chromatography (10% EtOAc / petroleum ether) afforded the amide as a colourless liquid (1.60 g, 7.40 mmol, 83%). Broad NMR peaks and ^{13}C signal duplication noted due to rotameric structure.

^{1}H NMR (400 MHz, Chloroform-*d*): δ 7.41-7.14 (5H, m, H11-H13), 6.43-6.29 (1H, m, H5), 6.20-6.05 (1H, m, H4), 5.94-5.84 (1H, m, H3), 5.14 (1H, d, *J* = 17.0, H8), 5.05 (1H, d, *J* = 10.5 Hz, H7), 4.60 (1.20H, s, H9), 4.55 (0.80H, s, H9), 3.24 (2H, t, *J* = 6.9 Hz, H2), 2.96 (1.20H, s, H14), 2.93 (1.80H, s, H14).

^{13}C NMR (101 MHz, Chloroform-*d*): δ 171.4 (C1), 171.0 (C1), 137.4 (C10), 136.7 (C10), 136.6 (C5), 136.6 (C5), 133.9 (C4), 133.8 (C4), 129.0 (C11), 128.7 (C11), 128.2 (C13), 127.7 (C13), 127.5 (C12), 127.3 (C3), 127.0 (C3), 126.4 (C12), 116.6 (C6), 116.5 (C6), 53.6 (C9), 51.0 (C9), 37.7 (C2), 37.4 (C2), 35.0 (C14), 34.1 (C14).

HRMS (ESI$^+$) *m/z* calculated for $C_{14}H_{18}NO$ $[M+H]^+$ 216.1383, found 216.1379.

IR: ν_{max} = 2922 (C-H), 1634 (C=O and C=C broad), 1451 (C=C), 1398, 1003.

2-Benzyl-*N*-methylhexa-3,5-dienamide, (*E*)-4-Benzyl-*N*-methylhexa-2,5-dienamide and (2*E*,4*E*)-*N*-methyl-7-phenylhepta-2,4-dienamide

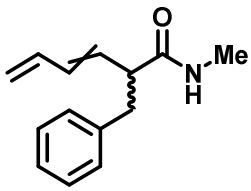
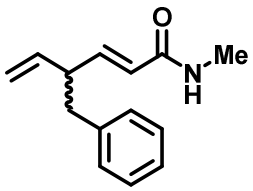
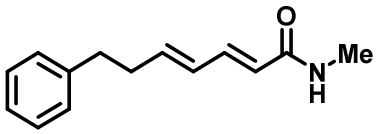

The title compounds were synthesised according to General Procedure 2 using (*E*)-*N*-Benzyl-*N*-methylhexa-3,5-dienamide (**187**) (100 mg, 0.46 mmol, 1.0 eq.). Purification by flash column chromatography (0-5% EtOAc / petroleum ether) afforded the various migration products. Starting material **187** was also isolated from this reaction (15 mg, 0.07 mmol, 15%).

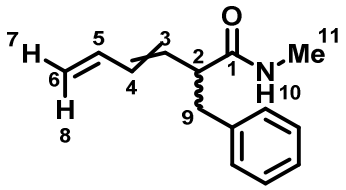

[1,3]-Isomers: Colourless oil (13 mg, 0.06 mmol, 13%). Isolated as a mixture of *E*- and *Z*- isomers, in a ratio of 70:30 respectively. Assignments *E*- and *Z*- in the assignments below relate to the stereoisomer of the molecule, and not the individual atom discussed.

^{1}H NMR (400 MHz, Chloroform-*d*): δ 7.30-7.11 (10H, m, Ar), 6.42 (1H, dt, *J* = 16.9, 10.0 Hz, *Z*-H5), 6.29 (1H, dt, *J* = 16.9, 10.0 Hz, *E*-H5), 6.16-6.03 (2H, m, *E*-H4, *Z*-H4), 5.74 (1H, dd, *J* = 15.5, 7.0 Hz, *E*-H3), 5.51 (1H, t, *J* = 9.5 Hz, *Z*-H3), 5.40 (2H, br s, *E*-H10, *Z*-H10), 5.24 (1H, dd, *J* = 16.9, 1.1 Hz, *Z*-H8), 5.18-5.10 (2H, m, *E*-H8, *Z*-H7), 5.06 (1H, dd, *J* = 10.0, 1.1 Hz, *E*-H7), 3.52 (1H, dt, *J* = 9.5, 7.2 Hz, *Z*-H2), 3.24 (1H, dd, *J* = 13.7, 7.2 Hz, *Z*-H9), 3.19 (1H, dd, *J* = 13.0, 7.0 Hz, *E*-H9), 3.05 (1H, q, *J* = 7.0 Hz, *E*-H2), 2.87-2.78 (2H, m, *Z*-H9, *E*-H9), 2.73 (3H, d, *J* = 4.9 Hz, *Z*-H11), 2.72 (3H, d, *J* = 4.9 Hz, *E*-H11).

^{13}C NMR (101 MHz, Chloroform-*d*): δ 173.2 (*E*-C1), 173.1 (*Z*-C1), 139.4 (Ar), 139.3 (Ar), 136.4 (*E*/*Z*-C5), 136.4 (*E*/*Z*-C5) 133.9 (*E*-C4), 132.3 (*Z*-C4), 132.1 (*E*-C3), 131.2 (*Z*-C3), 129.6 (Ar), 129.3 (Ar), 128.5 (Ar), 126.4 (Ar), 120.0 (*Z*-C6), 117.5 (*E*-C6), 53.0 (*E*-C2), 47.9 (*Z*-C2), 38.8 (*E*/*Z*-C9), 38.8 (*E*/*Z*-C9), 26.6 (*Z*-C11), 26.5 (*E*-C11).

HRMS (ESI^{+}) *m/z* calculated for $C_{14}H_{18}NO$ $[M+H]^{+}$ 216.1383, found 216.1378.

IR: ν_{max} = 3380 (N-H), 2922 (C-H), 1641 (C=O and C=C), 1451 (C=C), 1400, 1117.

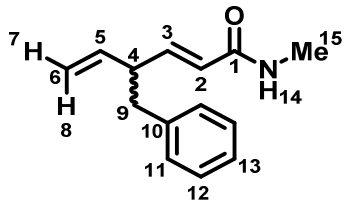

[1,5]-Isomers: Colourless oil (10 mg, 0.05 mmol, 10%).

^{1}H NMR (400 MHz, Chloroform-*d*): δ 7.30-7.10 (5H, m, H11-H13), 6.80 (1H, dd, *J* = 15.1, 7.4 Hz, H3), 5.75 (1H, ddd, *J* = 17.6, 10.5, 7.4 Hz, H5), 5.66 (1H, dd, *J* = 15.1, 1.0 Hz, H2), 5.47 (1H, br s, H14), 5.04 (1H, dd, *J* = 10.5, 1.0 Hz, H7), 4.99 (1H, dd, *J* = 17.6, 1.0 Hz, H8), 3.14 (1H, quint, *J* = 7.4 Hz, H4), 2.84 (3H, d, *J* = 5.0 Hz, H15), 2.79 (2H, d, *J* = 7.4 Hz, H9).

^{13}C NMR (101 MHz, Chloroform-*d*): δ 166.5 (C1), 145.4 (C3), 139.2 (C10), 138.9 (C5), 129.4 (C12), 128.4 (C11), 126.3 (C13), 123.8 (C2), 116.2 (C6), 47.9 (C4), 41.0 (C9), 26.4 (C15).

HRMS (ESI^{+}) *m/z* calculated for $C_{14}H_{18}NO$ $[M+H]^{+}$ 216.1383, found 216.1378.

IR: ν_{max} = 3291 (N-H), 3084 (C-H), 2923 (C-H), 1664 (C=O), 1623 (C=C), 1550 (C=C), 1272, 1158, 698.

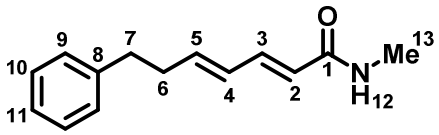

[1,7]-Isomer: White solid (13 mg, 0.06 mmol, 13%).

^{1}H NMR (400 MHz, Chloroform-*d*): δ 7.37-7.19 (6H, m, H3, H9-H11), 6.23-6.09 (2H, m, H4, H5), 5.81 (1H, d, *J* = 14.9 Hz, H2), 5.72 (1H, br s, H12), 2.93 (3H, d, *J* = 4.9 Hz, H13), 2.79 (2H, t, *J* = 6.9 Hz, H7), 2.52 (1H, q, *J* = 6.9 Hz, H6).

^{13}C NMR (101 MHz, Chloroform-*d*): δ 167.1 (C1), 141.8 (C4), 141.4 (C8), 141.0 (C3), 129.0 (C5), 128.5 (C10), 128.4 (C9), 126.1 (C11), 122.1 (C2), 35.3 (C7), 34.8 (C6), 26.5 (C9).

HRMS (ESI^{+}) *m/z* calculated for $C_{14}H_{18}NO$ $[M+H]^{+}$ 216.1383, found 216.1378.

MP: 82-83 °C.

IR: ν_{max} = 3302 (N-H), 2955 (C-H), 2923 (C-H), 2853 (C-H), 1654 (C=O), 1628 (C=C), 1454 (C=C), 1262, 996, 695.

(*E*)-*N*-Benzyl-*N*-cyclopropylhexa-3,5-dienamide (188)

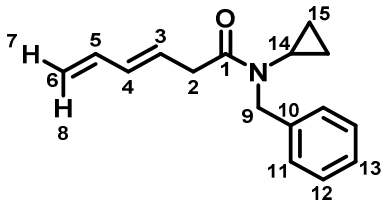

The title compound was synthesised according to General Procedure 1a using (*E*)-hexa-3,5-dienoic acid (**125**) (1.00 g, 8.92 mmol, 1.0 eq.) and *N*-benzylcyclopropylamine (1.44 g, 9.81 mmol, 1.1 eq.). Purification by flash column chromatography (5% EtOAc / petroleum ether) afforded the amide as a colourless oil (1.09 g, 4.55 mmol, 51%).

^{1}H NMR (400 MHz, Chloroform-*d*): δ 7.34-7.19 (5H, m, H11-H13), 6.36 (1H, dt, *J* = 17.1, 10.2 Hz, H5), 6.14 (1H, dd, *J* = 15.4, 10.2 Hz, H4), 5.97-5.87 (1H, m, H3), 5.12 (1H, d, *J* = 17.1 Hz, H8), 5.02 (1H, d, *J* = 10.2 Hz, H7), 4.60 (2H, s, H9), 3.43 (2H, d, *J* = 6.9 Hz, H2), 2.60-2.52 (1H, m, H14), 0.91-0.72 (4H, m, H15).

^{13}C NMR (101 MHz, Chloroform-*d*): δ 173.9 (C1), 138.3 (C10), 136.8 (C5), 133.7 (C4), 128.5 (C11), 127.9 (C13), 127.7 (C3), 127.1 (C12), 116.3 (C6), 49.9 (C9), 38.2 (C2), 30.1 (C14), 9.3 (C15).

HRMS (ESI^{+}) *m/z* calculated for $C_{16}H_{20}NO$ $[M+H]^{+}$ 242.1539, found 242.1536.

IR: ν_{max} = 3302 (N-H), 2925 (C-H), 1651 (C=O and C=C broad), 1397, 1253, 1002, 698.

2-Benzyl-*N*-cyclopropylhexa-3,5-dienamide, (*E*)-4-benzyl-*N*-cyclopropylhexa-2,5-dienamide and (2*E*,4*E*)-*N*-cyclopropyl-7-phenylhepta-2,4-dienamide

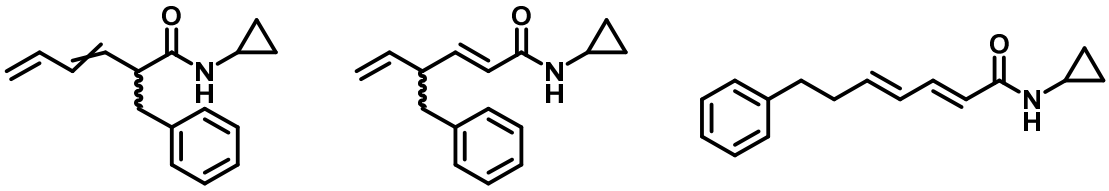

The title compounds were synthesised according to General Procedure 2 using (*E*)-*N*-benzyl-*N*-cyclopropylhexa-3,5-dienamide (**188**) (100 mg, 0.41 mmol, 1.0 eq.). Purification by flash column chromatography (5-30% EtOAc / petroleum ether) afforded the various migration products.

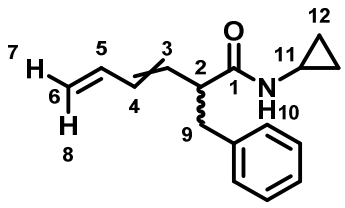

[1,3]-Isomers: Colourless oil (27 mg, 0.11 mmol, 27%). Isolated as a mixture of *E*- and *Z*- isomers, in a ratio of 81:19 respectively. Assignments *E*- and *Z*- in the assignments below relate to the stereoisomer of the molecule, and not the individual atom discussed.

^{1}H NMR (400 MHz, Chloroform-*d*): δ 7.34-7.09 (5H, m, Ar), 6.43 (1H, dt, *J* = 16.8, 10.8 Hz, *Z*-H5), 6.30 (1H, dt, *J* = 17.2, 10.0 Hz, *E*-H5), 6.16-6.02 (2H, 2 × dd, *J* = 15.0, 9.8 Hz, *E*-H4, *Z*-H4), 5.76 (1H, dd, *J* = 15.0, 7.4 Hz, *E*-H3), 5.64-5.48 (3H, br m, *Z*-H3, *E*-H10, *Z*-H10), 5.24 (1H, dd, *J* = 16.8, 1.0 Hz, *Z*-H8), 5.19-5.10 (2H, m, *Z*-H7, *E*-H8), 5.07 (1H, d, *J* = 10.0 Hz, *E*-H7), 3.48 (1H, dt, *J* = 9.6, 6.9 Hz, *Z*-H2), 3.23-3.11 (2H, 2 × dd, *J* = 13.7, 8.5 Hz, *E*-H9, *Z*-H9), 3.01 (1H, q, *J* = 7.4 Hz, *E*-H2), 2.87-2.74 (2H, 2 × dd, *J* = 13.7, 6.9 Hz, *E*-H9, *Z*-H9), 2.65-2.57 (2H, m, *E*-H11, *Z*-H11), 0.73-0.64 (4H, m, *E*-H12, *Z*-H12), 0.37-0.30 (4H, m, *E*-H12, *Z*-H12).

^{13}C NMR (101 MHz, Chloroform-*d*): δ 174.0 (*E*-C1), 173.9 (*Z*-C1), 139.3 (Ar), 139.2 (Ar), 136.5 (*E*-C5), 133.6 (*E*-C4), 132.0 (*E*-C3), 132.0 (*Z*-C4), 131.2 (*Z*-C5), 129.5 (*Z*-C3), 129.3 (Ar), 129.2 (Ar), 129.0 (Ar), 128.5 (Ar), 128.4 (Ar), 126.4 (Ar), 119.8 (*Z*-C6), 117.2 (*E*-C6), 52.9 (*E*-C2), 47.8 (*Z*-C2), 38.9 (*E*-C9), 38.9 (*Z*-C9), 22.7 (*Z*-C11), 22.7 (*E*-C11), 6.7 (*E*-C12), 6.7 (*Z*-C12), 6.6 (*Z*-C12), 6.6 (*E*-C12).

HRMS (ESI^{+}) *m/z* calculated for $C_{16}H_{20}NO$ $[M+H]^{+}$ 242.1539, found 242.1535.

IR: ν_{max} = 3279 (N-H), 2980 (C-H), 2922 (C-H), 1646 (C=O and C=C), 1453 (C=C), 1399.

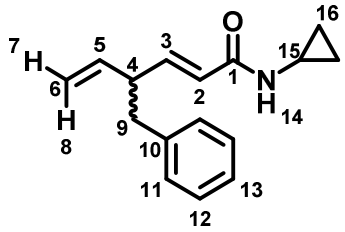

[1,5]-Isomers: Colourless oil (16 mg, 0.07 mmol, 16%).

^{1}H NMR (400 MHz, Chloroform-*d*): δ 7.30-7.08 (5H, m, H11-H13), 6.82 (1H, dd, *J* = 15.4, 7.3 Hz, H3), 5.73 (1H, ddd, *J* = 17.3, 10.1, 7.5 Hz, H5), 5.65-5.56 (2H, m, H2, H14), 5.04 (1H, d, *J* = 10.1 Hz, H7), 4.97 (1H, d, *J* = 17.3 Hz, H8), 3.18-3.07 (1H, m, H4), 2.82-2.75 (3H, m, H9, H15), 0.81-0.71 (2H, m, H16), 0.55-0.46 (2H, m, H16).

^{13}C NMR (101 MHz, Chloroform-*d*): δ 167.1 (C1), 145.7 (C3), 139.2 (C10), 138.8 (C5), 129.4 (C11), 128.4 (C13), 126.3 (C12), 123.7 (C2), 116.2 (C6), 48.0 (C4), 40.9 (C9), 22.8 (C15), 6.8 (C16), 6.7 (C16).

HRMS (ESI$^+$) *m/z* calculated for $C_{16}H_{20}NO$ $[M+H]^+$ 242.1539, found 242.1537.

IR: ν_{max} = 3251 (N-H), 2955 (C-H), 2921 (C-H), 2852 (C-H), 1701 (C=O), 1634 (C=C), 1454 (C=C), 975.

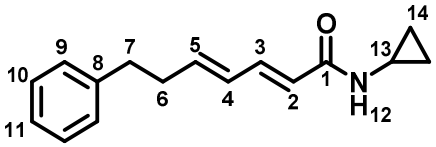

[1,7]-Isomer: White solid (43 mg, 0.18 mmol, 43%).

^{1}H NMR (400 MHz, Chloroform-*d*): δ 7.31-7.13 (6H, m, H3, H9-H11), 6.16-6.04 (2H, m, H4, H5), 5.68 (1H, d, *J* = 15.0 Hz, H2), 5.62 (1H, br s, H12), 2.86-2.76 (1H, m, H13), 2.73 (2H, t, *J* = 7.4 Hz, H7), 2.52-2.42 (2H, m, H6), 0.82-0.76 (2H, m, H14), 0.55-0.50 (2H, m, H14).

^{13}C NMR (101 MHz, Chloroform-*d*): δ 167.7 (C1), 142.0 (C4), 141.4 (C8), 141.3 (C3), 128.9 (C5), 128.6 (C9), 128.5 (C11), 126.2 (C10), 122.0 (C2), 35.3 (C7), 34.9 (C6), 22.9 (C13), 6.9 (C14).

HRMS (ESI$^+$) *m/z* calculated for $C_{16}H_{20}NO$ $[M+H]^+$ 242.1539, found 242.1538.

MP: 140-141 °C.

IR: ν_{max} = 3292 (N-H), 2980 (C-H), 2924 (C-H), 1628 (C=O), 1381 (C=C), 1152.

N-Benzhydrylpropan-2-amine (189)

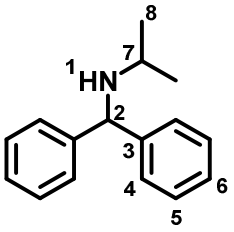

Synthesised according to a modified procedure from Hampton *et al.*[149]

To a solution of benzophenone (**19**) (1.00 g, 5.49 mmol, 1.0 eq.) in anhydrous CH_2Cl_2 (6 mL) was added $TiCl_4$ (6.10 mL, 6.10 mmol, 1.1 eq., 1 M in CH_2Cl_2) in an ice bath. After 10 minutes stirring at rt, a solution of isopropylamine (1.00 mL, 12.80 mmol, 2.3 eq.) in anhydrous THF (6 mL) was added slowly and the mixture left to stir for 3 h. A solution of $NaBH_3CN$ (0.41 g, 6.52 mmol, 1.2 eq.) in anhydrous THF (7 mL) was added and the mixture left to stir for 16 h. The reaction was quenched with $NaOH_{(aq.)}$

(50 mL, 1 M) and left to stir for 30 minutes before the mixture was filtered through celite. The aqueous layer was extracted with EtOAc (3 × 30 mL). The combined organics were washed with brine (60 mL), dried over $MgSO_4$, filtered and concentrated *in vacuo*. Purification by flash column chromatography (5% EtOAc / petroleum ether) afforded the title compound as a colourless oil (0.89 g, 3.95 mmol, 72%).

^{1}H NMR (400 MHz, Chloroform-*d*): δ 7.45-7.40 (4H, m, H4), 7.36-7.30 (4H, m, H5), 7.26-7.20 (2H, m, H6), 5.02 (1H, s, H2), 2.80 (1H, sept, *J* = 6.6 Hz, H7), 1.13 (6H, d, *J* = 6.6 Hz, H8).

^{13}C NMR (101 MHz, Chloroform-*d*): δ 144.7 (C3), 128.5 (C4), 127.5 (C5), 126.9 (C6), 64.3 (C2), 46.2 (C7), 23.3 (C8).

Data consistent with literature.[149]

(*E*)-*N*-Benzhydryl-*N*-isopropylhexa-3,5-dienamide (190)

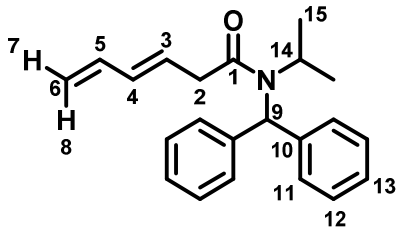

The title compound was synthesised according to General Procedure 1b using (*E*)-hexa-3,5-dienoic acid (**125**) (0.33 g, 2.95 mmol, 1.0 eq.) and *N*-benzhydrylpropan-2-amine (**189**) (0.60 g, 3.25 mmol, 1.1 eq.). Purification by flash column chromatography (0-10% EtOAc / petroleum ether) to afford the amide as a yellow oil (0.33 g, 0.96 mmol, 36%). Broad NMR peaks noted due to rotameric structure.

^{1}H NMR (500 MHz, Chloroform-*d*, 50 °C): δ 7.40-7.25 (10H, m, H11-H13), 6.31 (1H, dt, *J* = 16.7, 10.2 Hz, H5), 6.13-6.03 (1H, br s, H9), 6.03-5.90 (1H, br m, H4), 5.81 (1H, br dt, *J* = 14.8, 6.7 Hz, H3), 5.09 (1H, d, *J* = 16.7 Hz, H8), 5.01 (1H, d, *J* = 10.2 Hz, H7), 4.25-4.05 (1H, br m, H14), 3.17-2.95 (1H, br m, H2), 1.23 (6H, d, *J* = 6.5 Hz, H15).

^{13}C NMR (101 MHz, Chloroform-*d*, 50°C): δ 167.6 (C1), 140.3 (C10), 136.9 (C5), 133.6 (C4), 130.5 (C9), 129.0 (C11), 128.9 (C13), 128.5 (C12), 128.0 (C3), 116.2 (C6), 49.0 (C14), 40.2 (C2), 21.8 (C15).

HRMS (ESI^+) *m/z* calculated for $C_{22}H_{26}NO$ $[M+H]^+$ 320.2009, found 320.2013.

IR: ν_{max} = 2980 (C-H), 2971 (C-H), 1650 (C=O), 1634 (C=C), 1599 (C=C), 1430 (C=C), 1002.

(*E*)-2-Benzhydryl-*N*-isopropylhexa-3,5-dienamide, 4-benzhydryl-*N*-isopropylhexa-2,5-dienamide and (2*E*,4*E*)-*N*-Isopropyl-7,7-diphenylhepta-2,4-dienamide

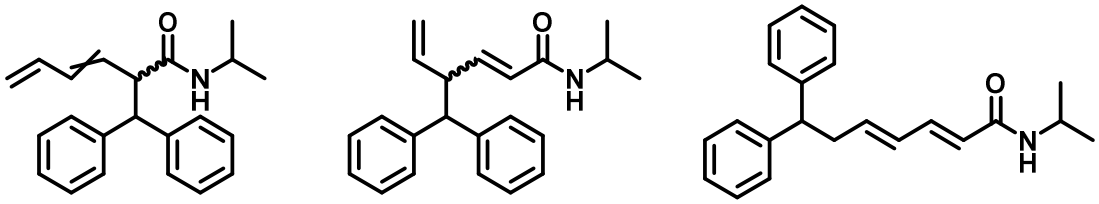

The title compounds were synthesised according to General Procedure 2 using (*E*)-*N*-benzhydryl-*N*-isopropylhexa-3,5-dienamide (**190**) (100 mg, 0.31 mmol, 1.0 eq.). Purification by flash column chromatography (5-10% EtOAc / petroleum ether) afforded the various migration products.

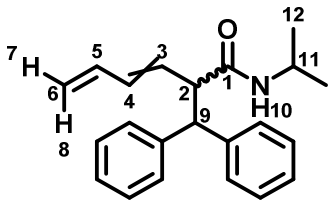

[1,3]-Isomers: White solid (7 mg, 0.02 mmol, 7%). Isolated as a mixture of *E*- and *Z*- isomers, in a ratio of 89:11 respectively. Assignments *E*- and *Z*- in the assignments below relate to the stereoisomer of the molecule, and not the individual atom discussed. Peaks corresponding to the *Z*-isomer were not seen in the ^{13}C NMR spectra, due to low concentration of this isomer in the sample. Reported ^{13}C signals are for the *E*-isomer of the title compound.

^{1}H NMR (400 MHz, Chloroform-*d*): δ 7.32-7.11 (20H, m, Ar), 6.63 (1H, dt, *J* = 16.6, 10.1 Hz, *Z*-H5), 6.17 (1H, dt, *J* = 16.1, 10.6 Hz, *E*-H5), 6.05 (2H, 2 × dd, *J* = 15.5, 10.6 Hz, *E*-H4, *Z*-H4), 5.67 (1H, dd, *J* = 15.5, 8.5 Hz, *E*-H3), 5.47 (1H, t, *J* = 10.6 Hz, *Z*-H3), 5.23 (1H, d, *J* = 16.6 Hz, *Z*-H8), 5.19 (1H, d, *J* = 10.1 Hz, *Z*-H7), 5.06 (1H, dd, *J* = 16.1, 1.8 Hz, *E*-H8), 5.06 (2H, br s, *E*-H10, *Z*-H10), 4.96 (1H, dd, *J* = 10.6, 1.8 Hz, *E*-H7), 4.54 (1H, d, *J* = 10.1 Hz, *Z*-H9), 4.44 (1H, d, *J* = 10.9 Hz, *E*-H9), 3.94 (1H, t, *J* = 10.1 Hz, *Z*-H2), 3.84 (2H, sept, *J* = 6.8 Hz, *E*-H11, *Z*-H11), 3.52 (1H, dd, *J* = 10.9, 8.5 Hz, *E*-H2), 0.98 (3H, d, *J* = 6.8 Hz, *E*-H12), 0.97 (3H, d, *J* = 6.8 Hz, *Z*-H12), 0.75 (3H, d, *J* = 6.8 Hz, *Z*-H12), 0.71 (3H, d, *J* = 6.8 Hz, *E*-H12).

^{13}C NMR (101 MHz, Chloroform-*d*): δ 171.2 (C1), 143.1 (Ar), 141.8 (Ar), 136.7 (C5), 134.0 (C4), 131.7 (C3), 128.8 (Ar), 128.6 (Ar), 128.5 (Ar), 128.2 (Ar), 126.7 (Ar), 126.6 (Ar), 116.9 (C6), 56.6 (C2), 54.0 (C9), 41.2 (C11), 22.6 (C12), 22.5 (C12).

HRMS (ESI^{+}) *m/z* calculated for $C_{22}H_{26}NO$ $[M+H]^{+}$ 320.2009, found 320.2009.

MP: 86-87 °C.

IR: ν_{max} = 3293 (N-H), 2980 (C-H), 2888 (C-H), 1633 (C=O and C=C broad), 1382, 1153.

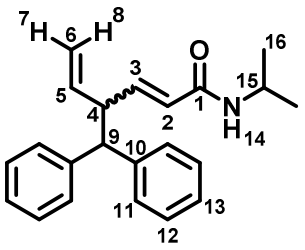

[1,5]-Isomers and [1,7]-Isomer: Yellow oil (29 mg, 0.09 mmol, 29%). Isolated as a mixture of this isomer and below isomer in a ratio of 79:21, giving a 6% yield for this isomer and 23% yield for the below isomer.

^{1}H NMR (400 MHz, Chloroform-*d*): δ 7.29-7.11 (10H, m, H11-H13), 6.69 (1H, dd, *J* = 15.6, 7.7 Hz, H3), 5.67-5.61 (1H, m, H5), 5.61-5.59 (1H, d, *J* = 15.6 Hz, H2), 5.20 (1H, br s, H14), 5.00 (1H, dd, *J* = 16.2, 1.3 Hz, H8), 4.98 (1H, d, *J* = 10.7, 1.3 Hz, H7), 4.06 (1H, sept, *J* = 6.6 Hz, H15), 3.95 (1H, d, *J* = 10.5 Hz, H9), 3.77-3.69 (1H, m, H4), 1.10 (3H, d, *J* = 6.6 Hz, H16), 1.09 (3H, d, *J* = 6.6 Hz, H16).

^{13}C NMR (101 MHz, Chloroform-*d*): δ 164.8 (C1), 144.3 (C10), 138.3 (C5), 128.7 (C11), 128.5 (C12), 128.5 (C3), 126.6 (C13), 125.2 (C2), 117.3 (C6), 56.2 (C9), 41.4 (C15), 50.4 (C4), 22.9 (C16).

HRMS (ESI^{+}) *m/z* calculated for $C_{22}H_{26}NO$ $[M+H]^{+}$ 320.2009, found 320.2010.

IR: ν_{max} = 3280 (N-H), 2980 (C-H), 1657 (C=O), 1626 (C=C), 1539 (C=C), 1382, 1251, 1154.

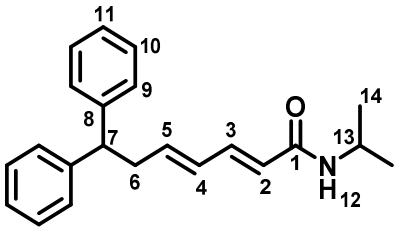

^{1}H NMR (400 MHz, Chloroform-*d*): δ 7.28-7.11 (10H, m, H9-H11), 7.04 (1H, dd, *J* = 15.7, 10.9 Hz, H3), 6.09 (1H, dd, *J* = 15.5, 10.9 Hz, H4), 5.93 (1H, dt, *J* = 15.5, 7.3 Hz, H5), 5.65 (1H, d, *J* = 15.7 Hz, H2), 5.37 (1H, br s, H12), 4.12 (1H, sept, *J* = 7.8 Hz, H13), 4.01 (1H, t, *J* = 7.3 Hz, H7), 2.89 (2H, t, *J* = 7.3 Hz, H6), 1.14 (6H, d, *J* = 6.6 Hz, H14).

^{13}C NMR (101 MHz, Chloroform-*d*): δ 165.5 (C1), 144.2 (C8), 140.7 (C3), 140.3 (C5), 130.0 (C4), 128.6 (C9), 128.0 (C10), 126.5 (C11), 122.8 (C2), 51.2 (C7), 41.5 (C9), 39.2 (C6), 22.9 (C10).

HRMS (ESI^{+}) *m/z* calculated for $C_{22}H_{26}NO$ $[M+H]^{+}$ 320.2009, found 320.2010.

IR: ν_{max} = 3280 (N-H), 2980 (C-H), 1657 (C=O), 1626 (C=C), 1539 (C=C), 1382, 1251, 1154.

(*E*)-*N*-Allyl-*N*-(*tert*-butyl)hexa-3,5-dienamide (192)

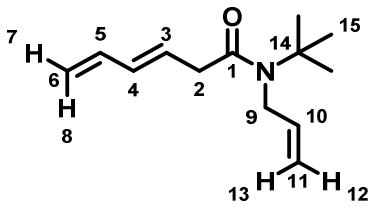

The title compound was synthesised according to General Procedure 1b using (*E*)-hexa-3,5-dienoic acid (**125**) (1.00 g, 8.92 mmol, 1.0 eq.) and *N*-(*tert*-butyl)prop-2-en-1-amine (**191**) (1.20 mL, 9.81 mmol, 1.1 eq.). Purification by flash column chromatography (0-1% MeOH / CH_2Cl_2) to afford the amide as an orange oil (0.39 g, 1.95 mmol, 24%).

^{1}H NMR (400 MHz, Chloroform-*d*): δ 6.32 (1H, dt, *J* = 17.3, 10.4 Hz, H5), 6.05 (1H, dd, *J* = 15.7, 10.4 Hz, H4), 5.88-5.78 (2H, m, H3, H10), 5.23-5.16 (2H, m, H12, H13), 5.09 (1H, d, *J* = 17.3 Hz, H8), 4.99 (1H, d, *J* = 10.4 Hz, H7), 3.94-3.91 (2H, m, H9), 3.10 (2H, d, *J* = 7.0 Hz, H2), 1.42 (9H, s, H15).

^{13}C NMR (101 MHz, Chloroform-*d*): δ 172.2 (C1), 136.9 (C5), 136.1 (C10), 133.2 (C4), 128.5 (C3), 116.2 (C6), 116.0 (C11), 57.7 (C14), 47.4 (C9), 40.0 (C2), 28.8 (C15).

HRMS (ESI^+) *m/z* calculated for $C_{13}H_{22}NO$ $[M+H]^+$ 208.1696, found 208.1690.

IR: ν_{max} = 2963 (C-H), 2925 (C-H), 1715 (C=O), 1625 (C=C), 1393 (C=C), 1361, 1194.

(*E*)-2-Allyl-*N*-(*tert*-butyl)hexa-3,5-dienamide, (*E*)-*N*-(*tert*-utyl)-4-vinylhepta-2,6-dienamide and (2*E*,4*E*)-*N*-(*tert*-butyl)nona-2,4,8-trienamide

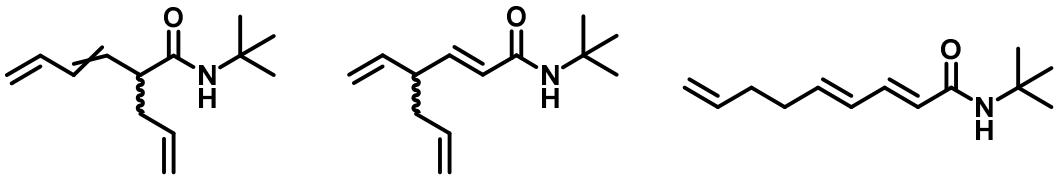

The title compounds were synthesised according to General Procedure 2 using (*E*)-*N*-allyl-*N*-(*tert*-butyl)hexa-3,5-dienamide (**192**) (100 mg, 0.48 mmol, 1.0 eq.). Purification by flash column chromatography (0-10% EtOAc / petroleum ether) afforded the various migration products.

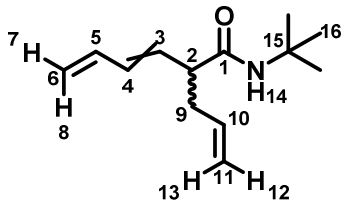

[1,3]-Isomers: Colourless oil (14 mg, 0.07 mmol, 14%). Isolated as a mixture of *E*- and *Z*- isomers, in a ratio of 69:31 respectively. Assignments *E*- and *Z*- in the assignments below relate to the stereoisomer of the molecule, and not the individual atom discussed.

^{1}H NMR (400 MHz, Chloroform-*d*): δ 6.55 (1H, dt, *J* = 17.9, 9.3 Hz, *Z*-H5), 6.32 (1H, dd, *J* = 17.8, 10.0, 8.3 Hz, *E*-H5), 6.21-6.08 (2H, m, *E*-H4, *Z*-H4), 5.78-5.64 (3H, m, *E*-H3, *E*-H10, *Z*-H10), 5.45 (1H, t, *J* = 10.3 Hz, *Z*-H3), 5.35-5.21 (3H, m, *Z*-H13, *Z*-H7, *Z*-H8), 5.17 (1H, dd, *J* = 17.8, 1.8 Hz, *E*-H8), 5.09-5.04 (2H, m, *Z*-H12, *E*-H7), 5.04-4.99 (2H, m, *E*-H12, *E*-H13), 3.27-3.20 (1H, m, *Z*-H2), 2.77 (1H, q, *J* = 7.9 Hz, *E*-H2), 2.59-2.49 (2H, m, *E*-H9, *Z*-H9), 2.33-2.24 (2H, m, *E*-H6, *Z*-H6), 1.32 (9H, s, *E*-H16), 1.30 (9H, s, *Z*-H16).

^{13}C NMR (101 MHz, Chloroform-*d*): δ 171.9 (*E*-C1), 171.6 (*Z*-C1), 136.6 (*E*-C5), 135.7 (*E*-C10), 135.7 (*Z*-C10), 133.5 (*E*-C4), 132.6 (*E*-C3), 132.0 (*Z*-C4), 131.6 (*Z*-C5), 130.3 (*Z*-C3), 119.8 (*Z*-C6), 117.2 (*E*-C6), 117.0 (*Z*-11), 116.9 (*E*-C11), 54.1 (*E*-C15), 54.0 (*Z*-C15), 51.4 (*E*-C2), 46.3 (*Z*-C2), 36.9 (*Z*-C9), 36.8 (*E*-C9), 28.9 (*E*-C16), 28.8 (*Z*-C16).

HRMS (ESI^{+}) *m/z* calculated for $C_{13}H_{22}NO$ $[M+H]^{+}$ 208.1696, found 208.1689.

IR: ν_{max} = 3319 (N-H), 2961 (C-H), 2923 (C-H), 1643 (C=O), 1538 (C=C), 1365, 1221.

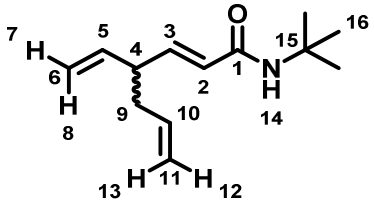

[1,5]-Isomers: Colourless oil (6 mg, 0.03 mmol, 6%).

^{1}H NMR (400 MHz, Chloroform-*d*): δ 6.73 (1H, dd, *J* = 15.3, 7.3 Hz, H3), 5.79-5.64 (3H, m, H2, H5, H10), 5.27 (1H, br s, H14), 5.09-5.00 (4H, m, H7, H8, H12, H13), 2.91 (1H, quint, *J* = 7.6 Hz, H4), 2.24 (2H, t, *J* = 7.6 Hz, H9), 1.38 (9H, s, H16).

^{13}C NMR (101 MHz, Chloroform-*d*): δ 165.2 (C1), 145.0 (C3), 139.1 (C5), 135.8 (C10), 124.8 (C2), 116.9 (C11), 115.9 (C6), 51.4 (C15), 46.0 (C4), 38.6 (C9), 29.0 (C16).

HRMS (ESI^{+}) *m/z* calculated for $C_{13}H_{22}NO$ $[M+H]^{+}$ 208.1696, found 208.1689.

IR: ν_{max} = 3287 (N-H), 3077 (C-H), 2967 (C-H), 2925 (C-H), 1664 (C=O), 1627 (C=C), 1547 (C=C), 1360, 1224, 986, 912.

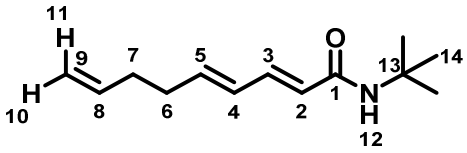

[1,7]-Isomer: White crystalline solid (9 mg, 0.04 mmol, 9%).

^{1}H NMR (400 MHz, Chloroform-*d*): δ 7.12 (1H, dd, *J* = 15.0, 10.6 Hz, H3), 6.12 (1H, dd, *J* = 15.2, 10.6 Hz, H4), 6.06-5.97 (1H, m, H5), 5.78 (1H, ddt, *J* = 17.1, 10.6, 6.9 Hz, H8), 5.69 (1H, d, *J* = 15.0 Hz, H2), 5.31 (1H, br s, H12), 5.01 (1H, dd, *J* = 17.1, 1.6 Hz, H11), 4.97 (1H, dd, *J* = 10.6, 1.6 Hz, H10), 2.27-2.12 (4H, m, H6, H7), 1.38 (9H, s, H14).

^{13}C NMR (101 MHz, Chloroform-*d*): δ 165.8 (C1), 141.6 (C5), 140.5 (C3), 137.8 (C8), 128.8 (C4), 123.4 (C2), 115.8 (C9), 51.4 (C13), 33.8 (C7), 32.4 (C6), 29.0 (C14).

HRMS (ESI^+) *m/z* calculated for $C_{13}H_{22}NO$ $[M+H]^+$ 208.1696, found 208.1689.

MP: 82-83 °C.

IR: ν_{max} = 3261 (N-H), 3074 (C-H), 2954 (C-H), 2923 (C-H), 1715 (C=O), 1611 (C=C), 1652 (C=C), 1626 (C=C), 1550 (C=C), 1361, 1223, 1005.

Benzyl (*E*)-hexa-3,5-dienoate (194)

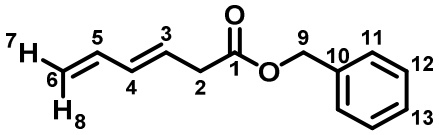

(*E*)-Hexa-3,5-dienoic acid (**125**) (1.00 g, 8.92 mmol, 1.1 eq.) was dissolved in CH_2Cl_2 (10 mL) before addition of benzyl alcohol (**193**) (0.83 mL, 8.11 mmol, 1.0 eq.). A solution of DCC (1.84 g, 8.92 mmol, 1.0 eq.) and DMAP (0.10 g, 0.81 mmol, 0.1 eq.) in CH_2Cl_2 (10 mL) was added to the reaction flask slowly to give a grey slurry. The mixture was left to stir for 16 h before being filtered through a pad of celite and solvent removed *in vacuo* to give the title compound as a yellow oil (1.57 g, 8.18 mmol, 92%).

^{1}H NMR (400 MHz, Chloroform-*d*): δ 7.40-7.32 (5H, m, H11-H13), 6.35 (1H, dt, *J* = 17.2, 10.2 Hz, H5), 6.16 (1H, dd, *J* = 15.2, 10.2 Hz, H4), 5.82 (1H, dt, *J* = 15.2, 7.3 Hz, H3), 5.17 (1H, dd, *J* = 17.2, 1.7 Hz, H8), 5.14 (2H, s, H9), 5.07 (1H, dd, *J* = 10.2, 1.7 Hz, H7), 3.18 (2H, d, *J* = 7.3 Hz, H2).

^{13}C NMR (101 MHz, Chloroform-*d*): δ 170.4 (C1), 136.4 (C5), 135.5 (C10), 134.6 (C4), 129.2 (C12), 128.4 (C13), 128.4 (C11), 125.1 (C3), 117.1 (C6), 66.6 (C9), 36.9 (C2).

HRMS (EI^+) *m/z* calculated for $C_{13}H_{14}O_2$ $[M]^+$ 202.0988, found 202.0986.

IR: ν_{max} = 2931 (C-H), 2875 (C-H), 2116 (C=C), 1734 (C=O), 1260, 1165, 1142, 735, 696 cm^{-1}.

2-Benzylhexa-3,5-dienoic acid (*E*/*Z*-195), (*E*)-4-benzylhexa-2,5-dienoic acid (196) and (2*E*,4*E*)-7-phenylhepta-2,4-dienoic acid (197)

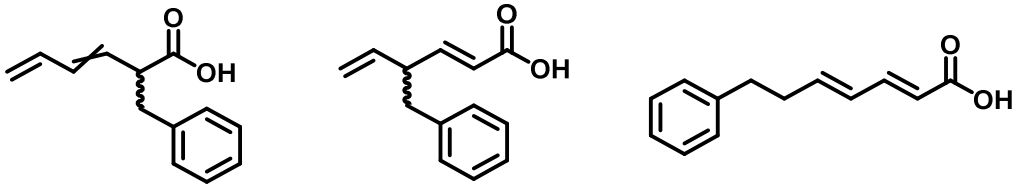

The title compounds were synthesised according to General Procedure 2 using Benzyl (*E*)-hexa-3,5-dienoate (**194**) (100 mg, 0.49 mmol, 1.0 eq.). Acidification of the crude mixture (pH 2) with $HCl_{(aq.)}$ (1 M) before purification by flash column chromatography (0-30% EtOAc / petroleum ether) afforded the various migration products.

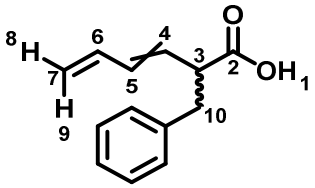

[1,3]-Isomers *E*/*Z*-195: Colourless oil (10 mg, 0.05 mmol, 10%). Isolated as a mixture of *E*- and *Z*-isomers, in a ratio of 57:43 respectively. Assignments *E*- and *Z*- in the assignments below relate to the stereoisomer of the molecule, and not the individual atom discussed.

^{1}H NMR (400 MHz, Chloroform-*d*): δ 7.37 (1H, dd, *J* = 9.7, 9.0 Hz, *Z*-H5), 7.29-7.24 (4H, m, Ar), 7.22-7.14 (6H, m, Ar), 6.46 (1H, dt, *J* = 16.5, 9.0 Hz, *Z*-H6), 6.29 (1H, dt, *J* = 16.5, 10.1 Hz, *E*-H6), 6.11 (1H, dt, *J* = 16.0, 10.1 Hz, *E*-H5), 5.78 (1H, dd, *J* = 16.0, 8.8 Hz, *E*-H4), 5.55 (1H, t, *J* = 10.3 Hz, *Z*-H4), 5.27-5.05 (6H, m, *E*-H1, *Z*-H1, *E*-H8, *Z*-H8, *E*-H8, *E*-H9), 3.42 (1H, dt, *J* = 9.8, 7.9 Hz, *Z*-H3), 3.18-3.13 (2H, m, *E*-H10, *Z*-H10), 2.94 (1H, td, *J* = 7.9, 7.1 Hz, *E*-H3), 2.76-2.84 (2H, m, *E*-H10, *Z*-H10), 1.25 (9H, s, *Z*-H16), 1.23 (9H, s, *E*-H16).

^{13}C NMR, HRMS and IR not possible to obtain due to poor sample quality arising from polymerisation of the substrate.

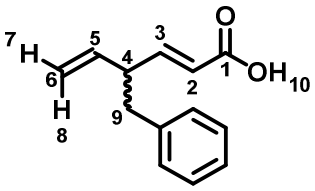

[1,5]-Isomers 196 and [1,7]-Isomer 197: Orange oil (13 mg, 0.06 mmol, 13%). Isolated as a mixture of this **196** and **197** in a ratio of 62:38, giving a 5% yield for **196** and 8% yield **197**.

^{1}H NMR (400 MHz, Chloroform-*d*): δ 10.02 (1H, br s, H10), 7.32-7.11 (5H, m, Ar), 7.04 (1H, dd, *J* = 15.8, 7.7 Hz, H3), 5.77-5.69 (2H, m, H2, H5), 5.09 (1H, dd, *J* = 10.5, 1.2 Hz, H7), 5.03 (1H, dd, *J* = 17.1, 1.2 Hz, H8), 3.27-3.14 (1H, m, H4), 2.82 (1H, d, *J* = 7.1 Hz, H9), 2.78 (1H, d, *J* = 7.1 Hz, H9).

^{13}C NMR, HRMS and IR not possible to obtain due to poor sample quality arising from polymerisation of the substrate.

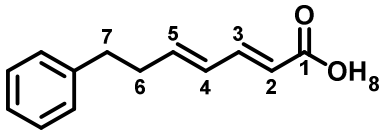

^{1}H NMR (400 MHz, Chloroform-*d*): δ 10.02 (1H, br s, H8), 7.35 (1H, dd, *J* = 15.2, 10.1 Hz, H3), 7.31-7.11 (5H, m, Ar), 6.24-6.19 (2H, m, H4, H5), 5.79 (1H, d, *J* = 15.2 Hz, H2), 2.76 (2H, t, *J* = 7.5 Hz, H7), 2.55-2.49 (2H, m, H6).

^{13}C NMR, HRMS and IR not possible to obtain due to poor sample quality arising from polymerisation of the substrate.

(*E*)-1-(2-Phenylpyrrolidin-1-yl)hexa-3,5-dien-1-one (198)

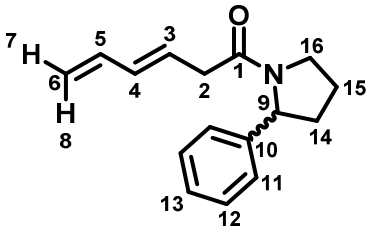

The title compound was synthesised according to General Procedure 1a using (*E*)-hexa-3,5-dienoic acid (**125**) (0.50 g, 4.46 mmol, 1.0 eq.) and 2-phenylpyrrolidine (0.73 mL, 4.91 mmol, 1.1 eq.). Purification by flash column chromatography (0-1% MeOH / CH_2Cl_2) afforded the amide as an orange oil (0.84 g, 3.48 mmol, 78%). Broad NMR peaks noted due to rotameric structure.

^{1}H NMR (400 MHz, Chloroform-*d*): δ 7.32-7.0 (5H, m, H11-H13), 6.32-6.04 (1H, m, H5), 5.84-5.60 (2H, m, H3, H4), 5.16-4.85 (2H, m, H7, H8), 4.92 (1H, d, *J* = 7.5 Hz, H9), 3.74-3.57 (2H, m, H16), 2.87 (1H, dd, *J* = 7.3 Hz, H2), 2.70 (1H, dd, *J* = 7.2 Hz, H2), 2.35-2.11 (2H, m, H14), 1.96-1.71 (2H, m, H15).

^{13}C NMR (101 MHz, Chloroform-*d*): δ 170.4 (C1), 143.3 (C10), 136.7 (C5), 133.5 (C4), 128.9 (C13), 128.5 (C12), 128.4 (C11), 127.3 (C3), 116.4 (C6), 61.6 (C9), 47.2 (C16), 39.0 (C2), 36.4 (C14), 21.7 (C15).

HRMS (EI^{+}) *m/z* calculated for $C_{16}H_{19}NO$ $[M]^{+}$ 241.1461, found 241.1462.

IR: ν_{max} = 2980 (C-H), 2889 (C-H), 1641 (C=O and C=C broad), 1393, 1251, 1153.

(*E*)-1-(2,5-Dihydro-1*H*-pyrrol-1-yl)hexa-3,5-dien-1-one (199)

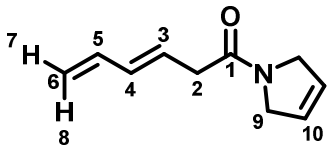

The title compound was synthesised according to General Procedure 1a using (*E*)-hexa-3,5-dienoic acid (**125**) (1.00 g, 8.92 mmol, 1.0 eq.) and 3-pyrroline (0.75 mL, 9.81 mmol, 1.1 eq.). Purification by flash column chromatography (10-30% EtOAc / petroleum ether) afforded the amide as a yellow liquid (1.13 g, 6.96 mmol, 78%).

^{1}H NMR (400 MHz, Chloroform-*d*): δ 6.30 (1H, dt, *J* = 17.2, 10.1 Hz, H5), 6.10 (1H, dd, *J* = 10.1, 9.2 Hz, H4), 5.86-5.77 (2H, m, H3, H10), 5.76-5.72 (1H, m, H10), 5.09 (1H, dd, *J* = 17.2, 1.0 Hz, H8), 4.99 (1H, dd, *J* = 10.1, 1.0 Hz, H7), 4.24-4.16 (4H, m, H9), 3.08 (2H, d, *J* = 7.2 Hz, H2).

^{13}C NMR (101 MHz, Chloroform-*d*): δ 169.1 (C1), 136.6 (C5), 133.9 (C4), 126.7 (C10), 126.4 (C3), 116.5 (C6), 53.4 (C9), 38.6 (C2).

HRMS (EI^{+}) *m/z* calculated for $C_{10}H_{14}NO$ $[M]^{+}$ 164.1070, found 164.1067.

IR: ν_{max} = 2971 (C-H), 2859 (C-H), 1637 (C=O), 1617 (C=C), 1428, 1199, 1001.

(*E*)-1-(3,4-Dihydroisoquinolin-2(1*H*)-yl)hexa-3,5-dien-1-one (200)

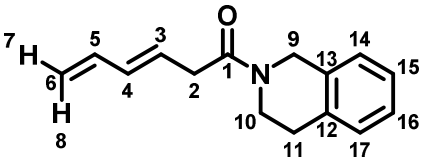

The title compound was synthesised according to General Procedure 1a using (*E*)-hexa-3,5-dienoic acid (**125**) (0.50 g, 4.46 mmol, 1.0 eq.) and tetrahydroisoquinoline (0.62 mL, 4.91 mmol, 1.1 eq.). Purification by flash column chromatography (0-10% EtOAc / petroleum ether) afforded the amide as a yellow oil (0.80 g, 3.52 mmol, 79%). Broad NMR peaks and doubling of C^{13} signals noted due to rotameric structure.

^{1}H NMR (400 MHz, Chloroform-*d*): δ 7.23-7.02 (4H, m, H14-H17), 6.40-6.25 (1H, m, H5), 6.16 (1H, dd, *J* = 15.3, 10.0 Hz, H4), 5.86 (1H, dt, *J* = 15.3, 6.7 Hz, H3), 5.17-5.10 (1H, m, H8), 5.03 (1H, dd, *J* = 10.1, 1.0 Hz, H7), 4.72 (1.25H, s, H9), 4.61 (0.75H, s, H9), 3.82 (0.90H, t, *J* = 5.9 Hz, H10), 3.66 (1.10H, t, *J* = 5.9 Hz, H10), 3.26 (2H, br d, *J* = 6.7 Hz, H2), 2.91-2.81 (2H, m, H11).

^{13}C NMR (101 MHz, Chloroform-*d*): δ 169.8 (C1), 169.7 (C1), 136.6 (C5), 136.5 (C5), 135.1 (C12), 134.0 (C12), 133.9 (C4), 133.4 (C13), 132.6 (C13), 133.8 (C4), 128.9 (C16), 128.3 (C16), 127.0 (C3), 126.9 (C3), 126.8 (C14), 126.7 (C14), 126.6 (C17), 126.5 (C17), 126.4 (C15), 126.1 (C15), 116.7 (C6), 116.6 (C6), 47.5 (C9), 44.4 (C9), 43.5 (C10), 39.9 (C10), 38.0 (C2), 37.9 (C2), 29.5 (C11), 28.5 (C11).

HRMS (EI$^+$) *m/z* calculated for $C_{15}H_{17}NO$ $[M]^+$ 226.1226, found 226.1226.

IR: ν_{max} = 2980 (C-H), 2889 (C-H), 1633 (C=O and C=C broad), 1428, 1381, 1154, 967.

(*E*)-*N*-Benzyl-*N*-(*tert*-butyl)hex-2-enamide (210)

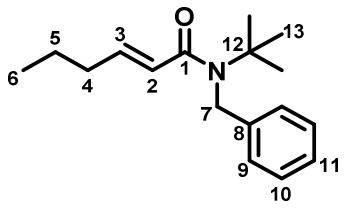

The title compound was synthesised according to General Procedure 1a using (*E*)-2-hexenoic acid (**209**) (0.80 g, 7.00 mmol, 1.0 eq.) and *N*-benzyl-2-methylpropan-2-amine (**121**) (1.26 g, 7.70 mmol, 1.1 eq.). Purification by flash column chromatography (5-10% EtOAc / petroleum ether) afforded the amide as a white solid (0.40 g, 1.54 mmol, 22%).

^{1}H NMR (400 MHz, Chloroform-*d*): δ 7.38-7.34 (2H, m, H10), 7.28-7.23 (3H, m, H9, H11), 6.86 (1H, dt, *J* = 15.0, 7.4 Hz, H3), 6.03 (1H, dt, *J* = 15.0, 1.5 Hz, H2), 4.62 (2H, s, H7), 2.06 (2H, tdd, *J* = 7.4, 7.1, 1.5 Hz, H4), 1.44 (9H, s, H13), 1.39 (2H, qt, *J* = 7.4, 7.1 Hz, H5), 0.86 (3H, t, *J* = 7.4 Hz, H6).

^{13}C NMR (101 MHz, Chloroform-*d*): δ 169.1 (C1), 145.7 (C3), 139.9 (C8), 128.7 (C10), 127.0 (C11), 125.8 (C9), 124.2 (C2), 57.6 (C12), 49.1 (C7), 34.4 (C4), 28.7 (C13), 21.7 (C5), 13.7 (C6).

HRMS (ESI$^+$) *m/z* calculated for $C_{17}H_{26}NO$ $[M+H]^+$ 260.2009, found 260.2013.

MP: 80-81 °C.

IR: ν_{max} = 2961 (C-H), 2930 (C-H), 2873 (C-H), 1655 (C=O), 1621 (C=C), 1393, 1354, 1192, 705 cm^{-1}.

(*E*)-*N*-Benzyl-*N*-(*tert*-butyl)hex-3-enamide (213)

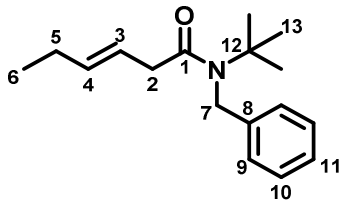

The title compound was synthesised according to General Procedure 1a using (*E*)-hex-3-enoic acid (**212**) (2.0 g, 17.52 mmol, 1.0 eq.) and *N*-benzyl-2-methylpropan-2-amine (**121**) (3.14 g, 19.27 mmol, 1.1 eq.). Purification by flash column chromatography (5% EtOAc / petroleum ether) afforded the amide as a colourless oil (1.16 g, 4.47 mmol, 26%).

^{1}H NMR (400 MHz, Chloroform-*d*): δ 7.39-7.34 (2H, m, H10), 7.29-7.21 (3H, m, H9, H11), 5.59 (1H, dtt, *J* = 16.2, 7.2, 1.5 Hz, H3), 5.46 (1H, dtt, *J* = 16.2, 7.5, 1.6 Hz, H4), 4.60 (2H, s, H7), 3.03 (2H, dd, *J* = 7.2, 1.7 Hz, H2), 2.09-2.01 (2H, m, H5), 1.45 (9H, s, H13), 0.98 (3H, t, *J* = 7.2 Hz, H6).

^{13}C NMR (101 MHz, Chloroform-*d*): δ 173.3 (C1), 139.6 (Ar), 135.0 (H4), 129.5 (Ar), 127.1 (Ar), 125.7 (Ar), 121.5 (C3), 57.1 (C12), 48.4 (C7), 40.4 (C2), 28.8 (C13), 25.7 (C5), 13.6 (C6).

HRMS (ESI$^+$) *m/z* calculated for $C_{17}H_{26}NO$ $[M+H]^+$ 260.2009, found 260.2012.

IR: ν_{max} = 2963 (C-H), 2931 (C-H), 1644 (C=O), 1605 (C=C), 1393, 1357, 1192, 968 cm^{-1}.

Section 5 Experimental

Methyl 4-oxo-4-phenylbutanoate (240)

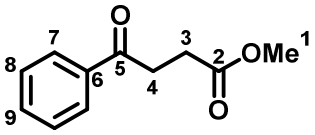

To a solution of 3-benzoylpropionic acid **(239)** (10.00 g, 56.16 mmol, 1.0 eq.) in MeOH (200 mL) was added conc. H_2SO_4 (4 mL) and the mixture heated to reflux for 16 h. The solvent was removed *in vacuo* before addition of saturated $NaHCO_{3(aq.)}$ (50 mL). The aqueous layer was extracted with CH_2Cl_2 (3 × 30 mL) before the combined organics were washed with saturated $NaHCO_{3(aq.)}$ (50 mL), dried over $MgSO_4$, filtered and concentrated *in vacuo* to afford the title compound as an orange liquid (10.36 g, 53.91 mmol, 96%) which was used without further purification.

^{1}H NMR (400 MHz, Chloroform-*d*): δ 8.00-7.95 (2H, m, H7), 7.56 (1H, tt, *J* = 7.4, 1.3 Hz, H9), 7.48-7.42 (2H, m, H8), 3.69 (3H, s, H1), 3.31 (2H, t, *J* = 6.2 Hz, H4), 2.76 (2H, t, *J* = 6.2 Hz, H3).

^{13}C NMR (101 MHz, Chloroform-*d*): δ 198.1 (C5), 173.4 (C2), 136.6 (C6), 133.3 (C9), 128.7 (C8), 128.1 (C7), 51.9 (C1), 33.5 (C4), 28.1 (C3).

Data consistent with literature.[150]

Methyl 4-(*tert*-butylamino)-4-phenylbutanoate (242a)

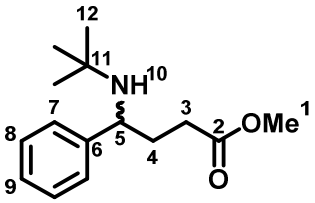

To a solution of methyl 4-oxo-4-phenylbutanoate (**240**) (5.00 g, 26.03 mmol, 1.0 eq.) in anhydrous Et_2O (50 mL) was added *tert*-butylamine (**101**) (6.00 mL, 52.06 mmol, 2.0 eq.) and Et_3N (**107**) (11.00 mL, 78.09 mmol, 3.0 eq.). At −15 °C, $TiCl_4$ (18.20 mL, 18.20 mmol, 0.7 eq., 1 M in CH_2Cl_2) was added slowly. The mixture was allowed to warm to rt and left to stir for 16 h. The mixture was then poured into saturated $NaHCO_{3(aq.)}$ (150 mL) and stirred for 10 minutes to precipitate the titanium salts. The slurry was filtered under reduced pressure before the aqueous layer was extracted with EtOAc (3 × 40

mL) before the combined organics were washed with brine (3 × 50 mL), dried over $MgSO_4$, filtered and concentrated *in vacuo* to give a mixture of the *E*- and *Z*-isomers of the respective imine.

This imine was dissolved in MeOH (150 mL) before addition of $NaBH_4$ (1.18 g, 31.24 mmol, 1.2 eq.) portion-wise in an ice bath. The mixture was left to stir for 2 h at rt before solvent was removed *in vacuo*. Water (100 mL) was added and the aqueous layer was extracted with CH_2Cl_2 (3 × 50 mL). The combined organics were washed with brine (50 mL), dried over $MgSO_4$, filtered and concentrated *in vacuo* to afford the title compound as an orange oil (6.01 g, 24.10 mmol, 93%) which was used without further purification.

^{1}H NMR (400 MHz, Chloroform-*d*): δ 7.33-7.27 (4H, m, H7, H8), 7.25-7.19 (1H, m, H9), 3.77 (1H, t, *J* = 7.2 Hz, H5), 3.65 (3H, s, H1), 2.25 (2H, td, *J* = 7.6, 1.0 Hz, H3), 2.00-1.86 (2H, m, H4), 1.00 (9H, s, H12).

^{13}C NMR (101 MHz, Chloroform-*d*): δ 174.2 (C2), 146.6 (C6), 128.5 (C8), 127.0 (C7), 126.3 (C9), 57.0 (C5), 52.2 (C11), 51.6 (C1), 35.2 (C4), 31.4 (C3), 30.2 (C12).

HRMS (ESI^+) *m/z* calculated for $C_{15}H_{24}NO_2$ $[M+H]^+$ 250.1802, found 250.1799.

IR: ν_{max} = 3440 (N-H), 2979 (C-H), 1725 (C=O), 1390, 1365, 1145.

1-(*tert*-Butyl)-5-phenylpyrrolidin-2-one (243a)

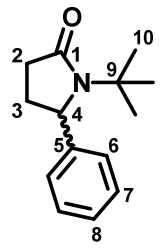

To a solution of methyl 4-(*tert*-butylamino)-4-phenylbutanoate (**242a**) (0.90 g, 4.01 mmol, 1.0 eq.) in DMF (10 mL) was added DMAP (0.98 g, 8.02 mmol, 2.0 eq.) and the mixture heated to reflux for 3 days before cooling to rt and addition of water (30 mL). The aqueous layer was extracted with Et_2O (3 × 30 mL) before the combined organics were washed with water (30 mL), brine (30 mL), dried over $MgSO_4$, filtered and concentrated *in vacuo*. Purification by flash column chromatography (0-5% EtOAc / petroleum ether) afforded the title compound as a white crystalline solid (0.41 g, 2.09 mmol, 52%).

^{1}H NMR (400 MHz, Chloroform-*d*): δ 7.34 (2H, t, *J* = 7.2 Hz, H6), 7.27 (1H, tt, *J* = 7.4, 1.5 Hz, H8), 7.24-7.19 (2H, m, H7), 4.89 (1H, d, *J* = 8.6 Hz, H4), 2.65 (1H, ddd, *J* = 15.9, 8.6, 7.1 Hz, H2), 2.46-2.34 (1H, m, H3), 2.27 (1H, ddd, *J* = 15.9, 9.6, 7.1 Hz, H2), 1.75-1.68 (1H, m, H3), 1.34 (9H, s, H10).

^{13}C NMR (101 MHz, Chloroform-*d*): δ 176.6 (C1), 145.2 (C5), 129.0 (C6), 127.5 (C8), 125.5 (C7), 62.6 (C4), 55.6 (C9), 31.0 (C2), 29.5 (C3), 28.3 (C10).

HRMS (ESI^+) *m/z* calculated for $C_{14}H_{20}NO$ $[M+H]^+$ 218.1539, found 218.1536.

MP: 99-100 °C.

IR: ν_{max} = 2890 (C-H), 1661 (C=O), 1393, 1142, 1073.

Methyl 4-(isopropylamino)-4-phenylbutanoate (242b)

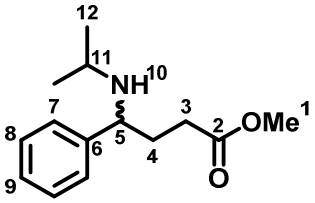

To a solution of methyl 4-oxo-4-phenylbutanoate (**240**) (5.00 g, 26.03 mmol, 1.0 eq.) in anhydrous Et_2O (50 mL) was added isopropylamine (4.50 mL, 52.06 mmol, 2.0 eq.) and Et_3N (11.00 mL, 78.09 mmol, 3.0 eq.). At −15 °C, $TiCl_4$ (18.20 mL, 18.20 mmol, 0.7 eq., 1 M in CH_2Cl_2) was added slowly. The mixture was allowed to warm to rt and left to stir for 16 h. The mixture was then poured into saturated $NaHCO_{3(aq.)}$ (150 mL) and stirred for 10 minutes to precipitate the titanium salts. The slurry was filtered under reduced pressure before the aqueous layer was extracted with EtOAc (3 × 40 mL) before the combined organics were washed with brine (3 × 50 mL), dried over $MgSO_4$, filtered and concentrated *in vacuo* to give a mixture of the *E*- and *Z*-isomers of the respective imine.

This imine was dissolved in MeOH (150 mL) before addition of $NaBH_4$ (1.18 g, 31.24 mmol, 1.2 eq.) portion-wise in an ice bath. The mixture was left to stir for 2 h at rt before solvent was removed *in vacuo*. Water (100 mL) was added and the aqueous layer was extracted with CH_2Cl_2 (3 × 50 mL). The combined organics were washed with brine (50 mL), dried over $MgSO_4$, filtered and concentrated *in vacuo* to afford the title compound as an orange oil (5.01 g, 22.65 mmol, 87%) which was used without further purification.

^{1}H NMR (400 MHz, Chloroform-*d*): δ 7.28-7.21 (2H, m, H7), 7.19-7.14 (3H, m, H8, H9), 3.62 (1H, t, *J* = 7.3 Hz, H5), 3.55 (3H, s, H1), 2.52 (1H, sept, *J* = 6.5 Hz, H11), 2.20 (1H, d, *J* = 7.6 Hz, H3), 2.16 (1H, d, *J* = 7.6 Hz, H3), 1.98-1.88 (1H, m, H4), 1.87-1.76 (1H, m, H4), 0.92 (3H, d, *J* = 6.5 Hz, H12), 0.88 (3H, d, *J* = 6.5 Hz, H12).

^{13}C NMR (101 MHz, Chloroform-*d*): δ 174.1 (C2), 143.9 (C6), 128.5 (C8), 127.1 (C9), 127.1 (C7), 59.6 (C5), 51.9 (C1), 45.4 (C11), 33.4 (C4), 31.2 (C3), 24.2 (C12), 22.2 (C12).

HRMS (ESI$^+$) *m/z* calculated for $C_{14}H_{22}NO_2$ $[M+H]^+$ 236.1651, found 236.1659.

IR: ν_{max} = 3411 (N-H), 2965 (C-H), 1776 (C=O), 1340, 1274.

1-Isopropyl-5-phenylpyrrolidin-2-one (243b)

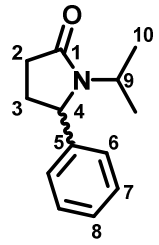

To a solution of methyl 4-(isopropylamino)-4-phenylbutanoate (**242b**) (0.50 g, 21.26 mmol, 1.0 eq.) in DMF (20 mL) was added DMAP (0.52 g, 42.52 mmol, 2.0 eq.) and the mixture heated to reflux for 16 h before addition of water (50 mL). The aqueous layer was extracted with Et_2O (5 × 30 mL) before the combined organics were washed with water (50 mL), brine (50 mL), dried over $MgSO_4$, filtered and concentrated *in vacuo*. Purification by flash column chromatography (15% EtOAc / petroleum ether) afforded the title compound as an orange crystalline solid (0.32 g, 15.73 mmol, 74%).

^{1}H NMR (400 MHz, Chloroform-*d*): δ 7.38-7.32 (2H, m, H6), 7.31-7.28 (1H, m, H8), 7.28-7.23 (2H, m, H7), 4.69 (1H, dd, *J* = 8.3, 8.1 Hz, H4), 4.09 (1H, sept, *J* = 7.0 Hz, H9), 2.70-2.60 (1H, m, H2), 2.49-2.33 (2H, m, H2, H3), 1.90-1.82 (1H, m, H3), 1.22 (3H, d, *J* = 7.0 Hz, H10), 0.89 (3H, d, *J* = 7.0 Hz, H10).

^{13}C NMR (101 MHz, Chloroform-*d*): δ 175.5 (C1), 143.6 (C5), 128.9 (C6), 127.9 (C8), 126.4 (C7), 61.2 (C4), 45.0 (C9), 30.6 (C2), 29.4 (C3), 20.9 (C10), 20.0 (C10).

HRMS (ESI$^+$) *m/z* calculated for $C_{13}H_{18}NO$ $[M+H]^+$ 204.1388, found 204.1394.

MP: 61-62 °C.

IR: ν_{max} = 2789 (C-H), 1667 (C=O), 1393, 1135.

Physical form difference noted to that reported in literature (solid here rather than oil in literature).[151]

(*Z*)-3-((*E*)-But-2-en-1-ylidene)-1-isopropyl-5-phenylpyrrolidin-2-one (245) and (*E*)-3-(buta-1,3-dien-1-yl)-1-isopropyl-5-phenylpyrrolidin-2-one (246)

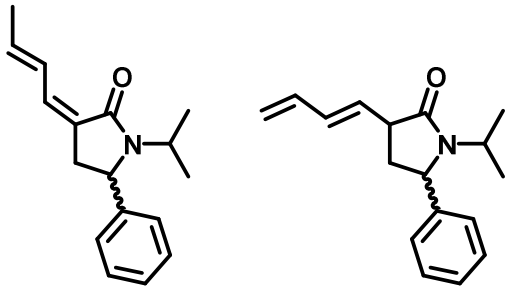

Two main isomers of the conjugated lactam were isolated according to General Procedure 4a using 1-isopropyl-5-phenylpyrrolidin-2-one **(243b)** (1.50 g, 7.38 mmol, 1.0 eq.) as the lactam and crotonaldehyde (**16**) (0.73 mL, 8.86 mmol, 1.2 eq.) as the aldehyde component. Purification was carried out using flash column chromatography (0-10% EtOAc / petroleum ether) to separate the isomers. The minor isomers could not be isolated with good purity, and their stereochemistry could not be determined and hence they are not included here. Assignment was carried out by analogy to lactone **260**. Machine learning was not able to accurately predict each isomer here and NOE experiments were inconclusive.

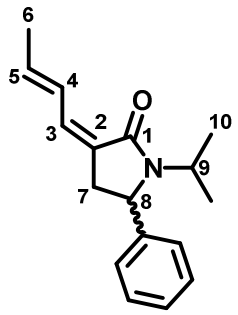

Isomer 245: Colourless oil (0.41 g, 1.62 mmol, 22%).

^{1}H NMR (400 MHz, Chloroform-*d*): δ 7.64 (1H, ddd, *J* = 15.3, 10.5, 1.5 Hz, H4), 7.31-7.10 (5H, m, Ar), 6.20 (1H, d, *J* = 10.5 Hz, H3), 5.82-5.69 (1H, m, H5), 4.56 (1H, dd, *J* = 8.8, 3.0 Hz, H8), 4.00 (1H, sept, *J* = 7.3 Hz, H9), 3.11 (1H, dd, *J* = 17.4, 8.8 Hz, H7), 2.45 (1H, dd, *J* = 17.4, 3.0 Hz, H7), 1.79 (3H, d, *J* = 6.5 Hz, H6), 1.17 (3H, d, *J* = 7.3 Hz, H10), 0.84 (3H, d, *J* = 7.3 Hz, H10).

^{13}C NMR (101 MHz, Chloroform-*d*): δ 168.9 (C1), 144.2 (Ar), 135.6 (C5), 133.8 (C3), 128.9 (Ar), 128.1 (Ar), 127.6 (C4), 127.0 (C2), 126.6 (Ar), 58.5 (C8), 45.5 (C9), 37.4 (C7), 20.8 (C10), 19.9 (C10), 18.6 (C6).

HRMS (ESI^{+}) *m/z* calculated for $C_{17}H_{22}NO$ $[M+H]^{+}$ 256.1696, found 256.1691.

IR: ν_{max} = 2986 (C-H), 1666 (C=O and C=C broad), 1381, 1251, 1153.

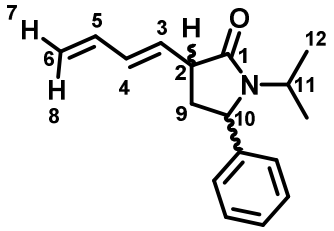

Isomers 246: Yellow oil (0.66 g, 2.58 mmol, 35%). Note that this isomer could not be isolated cleanly and contains another diastereomer which could not be assigned (with approximate dr 75:25). NOESY analysis was inconclusive due to the complex mixture.

^{1}H NMR (400 MHz, Chloroform-*d*): δ 7.31-7.12 (5H, m, Ar), 6.28 (1H, dt, *J* = 17.0, 10.1 Hz, H5), 6.08 (1H, dd, *J* = 15.5, 10.1 Hz, H4), 5.79-5.67 (1H, m, H3), 5.08 (1H, d, *J* = 17.0 Hz, H8), 4.98 (1H, d, *J* = 10.1 Hz, H7), 4.64 (1H, dd, *J* = 9.3, 2.8 Hz, H10), 4.02 (1H, sept, *J* = 6.8 Hz, H11), 2.66-2.62 (1H, m, H9), 1.90-1.83 (1H, m, H9), 1.61 (1H, dd, *J* = 6.2, 1.4 Hz, H2), 1.16 (3H, d, *J* = 6.8 Hz, H12), 0.83 (3H, d, *J* = 6.8 Hz, H12).

^{13}C NMR (101 MHz, Chloroform-*d*): δ 173.2 (C1), 144.3 (Ar), 137.3 (C5), 133.6 (C4), 131.3 (C3), 128.9 (Ar), 127.9 (Ar), 126.3 (Ar), 116.8 (C6), 59.7 (C10), 45.6 (C11), 30.4 (C9), 20.6 (C12), 20.1 (C12), 17.6 (C2).

HRMS (ESI^{+}) *m/z* calculated for $C_{17}H_{22}NO$ $[M+H]^{+}$ 256.1696, found 256.1699.

IR: ν_{max} = 2677 (C-H), 1673 (C=O and C=C broad), 1455, 1380, 1219.

(*E*)-1-(Buta-1,3-dien-1-yl)-*N*-methyl-2-phenylcyclopropane-1-carboxamide (247)

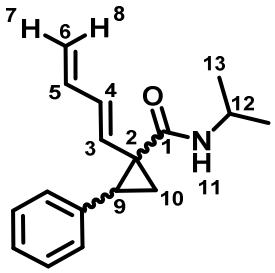

The title compound was synthesised according to General procedure 6a using (*E*)-3-(buta-1,3-dien-1-yl)-1-isopropyl-5-phenylpyrrolidin-2-one (**245**) 80 mg, 0.39 mmol, 1.0 eq.). Purification with flash column chromatography (20-50% EtOAc / petroleum ether) afforded a mixture of 2 diastereomers with dr (51:49) as a colourless oil (11 mg, 0.05 mmol, 14%). D1 and D2 refer to the diastereomer of product.

^{1}H NMR (400 MHz, Chloroform-*d*): δ 7.21-7.05 (8H, m, Ar), 7.03-6.96 (2H, m, Ar), 6.29 (1H, dt, *J* = 16.8, 10.3 Hz, H5 D1), 6.22-6.07 (3H, m, H4 D1, H4 D2, H5 D2), 5.80 (1H, d, *J* = 15.1 Hz, H3 D1), 5.59 (1H, br s, H11 D1/D2), 5.35 (1H, d, *J* = 15.1 Hz, H3 D2), 5.17-4.96 (5H, m, H7 D1, H7 D2, H8 D1, H8 D2, H11 D1/D2), 4.00 (1H, sept, *J* = 6.5 Hz, H12 D1), 3.70 (1H, sept, *J* = 6.5 Hz, H12 D2), 2.93 (1H, dd, *J* = 9.0, 7.2 Hz, H9 D1), 2.46 (1H, t, *J* = 8.1 Hz, H9 D2), 2.08 (1H, dd, *J* = 8.1, 5.3 Hz, H10 D2), 1.75 (1H, dd, *J* = 9.0, 4.8 Hz, H10 D1), 1.40 (1H, dd, *J* = 7.2, 4.8 Hz, H10 D1), 1.23 (1H, dd, *J* = 8.1, 5.3 Hz, H10 D2), 1.08 (3H, d, *J* = 6.5 Hz, H13 D1), 1.06 (3H, d, *J* = 6.5 Hz, H13 D1), 0.90 (3H, d, *J* = 6.5 Hz, H13 D2), 0.53 (3H, d, *J* = 6.5 Hz, H13 D2).

^{13}C NMR (101 MHz, Chloroform-*d*): δ 171.4 (C1 D1), 167.6 (C1 D2), 138.9 (C4 D1), 136.9 (Ar), 136.7 (Ar), 136.4 (C5 D1), 136.0 (C5 D2), 134.9 (C3 D1), 131.2 (C4 D2), 128.9 (Ar), 128.4 (Ar), 128.3 (C3 D2), 128.3 (Ar), 128.0 (Ar), 126.7 (Ar), 126.4 (Ar), 118.4 (C6 D1), 117.2 (C6 D2), 42.1 (C12 D1), 41.6 (C12 D2), 37.7 (C2 D2), 34.5 (C2 D1), 32.9 (C9 D2), 31.2 (C9 D1), 23.0 (C13 D1), 22.9 (C13 D1), 22.6 (C13 D2), 22.4 (C13 D2), 19.3 (C10 D1), 17.9 (C10 D2).

HRMS (ESI^{+}) *m/z* calculated for $C_{17}H_{22}NO$ $[M+H]^{+}$ 256.1696, found 256.1690.

IR: ν_{max} = 3434 (N-H), 2666 (C-H), 1676 (C=O), 1472, 1382, 1156.

5-Phenyldihydrofuran-2(3*H*)-one (248)

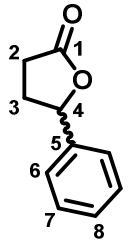

Synthesised according to the procedure by Clerici *et al.*[88]

To a solution of 4-oxo-4-phenylbutanoic acid (**239**) (5.00 g, 28.08 mmol, 1.0 eq.) in MeOH (100 mL) and 30% $NH_{3(aq.)}$ (95 mL) was added $TiCl_3$ (95 mL, 112.32 mmol, 4.0 eq., 15% in HCl) in an ice bath to give a pale-blue slurry (pH 10/11). The mixture was allowed to warm to rt and stirred for 4 h before being quenched and neutralised with conc. HCl until pH 2. Water (150 mL) was added, and the aqueous layer extracted with EtOAc (3 × 100 mL) before the combined organics were washed with brine (100 mL), dried over $MgSO_4$, filtered and concentrated *in vacuo*. Purification by flash column chromatography (20% EtOAc / petroleum ether) afforded the title compound as a colourless oil (3.92 g, 24.15 mmol, 86%).[88]

^{1}H NMR (400 MHz, Chloroform-*d*): δ 7.34-7.21 (5H, m, H6-H8), 5.42 (1H, dd, *J* = 7.8, 6.3 Hz, H4), 2.62-2.53 (3H, m, H2, H3), 2.15-2.05 (1H, m, H3).

^{13}C NMR (101 MHz, Chloroform-*d*): δ 177.0 (C1), 139.5 (C5), 128.8 (C6), 128.5 (C8), 125.3 (C7), 81.3 (C4), 31.0 (C3), 29.0 (C2).

Data consistent with literature.[88]

(*Z*)-3-((*E*)-But-2-en-1-ylidene)-5-phenyldihydrofuran-2(3*H*)-one (250) and (*E*)-3-((*E*)-But-2-en-1-ylidene)-5-phenyldihydrofuran-2(3*H*)-one (251)

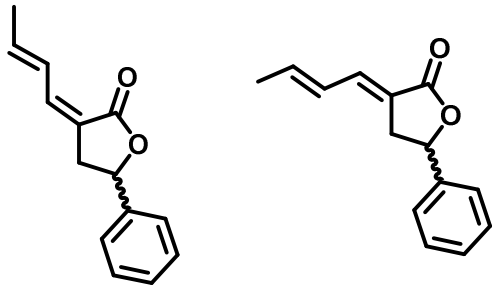

Two isomers of the conjugated lactone were synthesised according to General Procedure 4a using 5-phenyldihydrofuran-2(3*H*)-one (**248**) (1.50 g, 9.26 mmol, 1.0 eq.) as the lactone and crotonaldehyde (**16**) (0.89 mL, 11.11 mmol, 1.2 eq.) as the aldehyde component. Purification was carried out using flash column chromatography (10-30% EtOAc / petroleum ether) to separate the isomers. Isomer stereochemistry was assigned according to the predicted NMR spectra from the IMPRESSION machine learning algorithm.

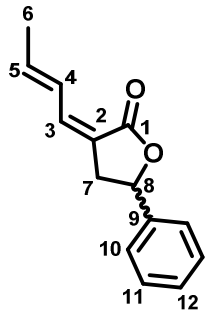

Isomer 250: Yellow oil (0.22 g, 1.02 mmol, 11%).

^{1}H NMR (400 MHz, Chloroform-*d*): δ 7.42 (1H, ddd, *J* = 14.9, 11.3, 1.3 Hz, H4), 7.34-7.18 (5H, m, H10-H12), 6.50 (1H, d, *J* = 11.3 Hz, H3), 6.04-5.91 (1H, m, H5), 5.39 (1H, t, *J* = 7.5 Hz, H8), 3.27 (1H, dd, *J* = 17.2, 7.5 Hz, H7), 2.81 (1H, dd, *J* = 17.2, 7.5 Hz, H7), 1.82 (3H, dd, *J* = 6.9, 1.1 Hz, H6).

^{13}C NMR (101 MHz, Chloroform-*d*): δ 169.6 (C1), 140.2 (C9), 139.8 (C3), 139.5 (C5), 128.7 (C10), 128.3 (C12), 127.0 (C4), 125.4 (C11), 120.4 (C2), 77.9 (C8), 37.7 (C7), 18.6 (C6).

HRMS (EI$^+$) *m/z* calculated for $C_{14}H_{14}O_2$ $[M]^+$ 214.0988, found 214.0985.

IR: ν_{max} = 2976 (C-H), 1744 (C=O), 1644 (C=C), 1365, 1190.

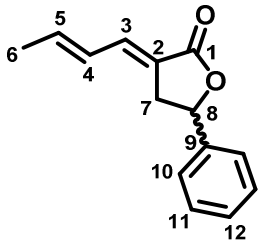

Isomer 251: Peach-coloured oil (0.38 g, 1.76 mmol, 19%).

^{1}H NMR (400 MHz, Chloroform-*d*): δ 7.41-7.28 (5H, m, H10-H12), 7.13 (1H, dt, *J* = 11.0, 2.7 Hz, H3), 6.24 (1H, dq, *J* = 14.9, 6.9 Hz, H5), 6.13 (1H, ddd, *J* = 14.9, 11.0, 1.2 Hz, H4), 5.54 (1H, dd, *J* = 8.4, 6.1 Hz, H8), 3.41 (1H, dd, *J* = 17.5, 8.4 Hz, H7), 2.87 (1H, dd, *J* = 17.5, 8.4 Hz, H7), 1.89 (3H, d, *J* = 6.9 Hz, H6).

^{13}C NMR (101 MHz, Chloroform-*d*): δ 171.8 (C1), 141.3 (C5), 140.6 (C9), 136.6 (C3), 128.9 (C10), 128.5 (C12), 127.7 (C4), 125.5 (C11), 122.6 (C2), 78.2 (C8), 34.5 (C7), 19.1 (C6).

HRMS (EI$^+$) *m/z* calculated for $C_{14}H_{14}O_2$ $[M]^+$ 214.0988, found 214.0985.

IR: ν_{max} = 2876 (C-H), 1734 (C=O), 1646 (C=C), 1459, 1380, 1189.

1-Methyl-5-phenylpyrrolidin-2-one (254)

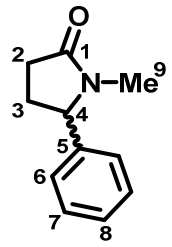

The title compound was synthesised according to General Procedure 3 using 4-oxo-4-phenylbutanoic acid (**239**) (0.50 g, 2.80 mmol, 1.0 g) and *N*-methyl formamide (**255**) (3.30 mL, 56.00 mmol, 20.0 eq.). Purification by flash column chromatography (20-50% EtOAc / petroleum ether) afforded the title compound as a yellow oil (0.40 g, 2.27 mmol, 81%).

^{1}H NMR (400 MHz, Chloroform-*d*): δ 7.35-2.23 (3H, m, H6, H8), 7.16-7.10 (2H, m, H7), 4.46 (1H, dd, *J* = 7.7, 6.2 Hz, H4), 2.61 (3H, s, H9), 2.55-2.33 (3H, m, H2, H3), 1.86-1.77 (1H, m, H3).

^{13}C NMR (101 MHz, Chloroform-*d*): δ 175.5 (C1), 141.1 (C5), 129.0 (C6), 128.1 (C8), 126.3 (C7), 64.6 (C4), 30.2 (C2), 28.5 (C3), 28.2 (C9).

HRMS (ESI$^+$) *m/z* calculated for $C_{13}H_{16}NO$ $[M+H]^+$ 176.1070, found 176.1066.

IR: ν_{max} = 3459 (C-H), 2953 (C-H), 1666 (C=O), 1454, 1395, 1278, 1114.

N-Methyl-2-phenylcyclopropane-1-carboxamide (258 and 259)

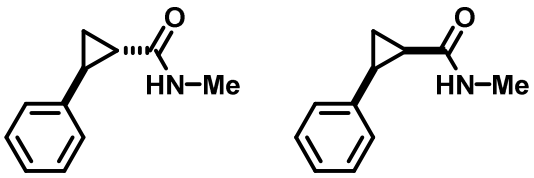

Isomers of the title compound were synthesised according to General Procedure 6c using 1-methyl-5-phenylpyrrolidin-2-one (**254**) (100 mg, 0.57 mmol, 1.0 eq.). Purification by flash column chromatography (30-50% EtOAc / petroleum ether) afforded two diastereomers of ring-contracted product.

The stereochemistry of the minor diastereomer was assigned by NOESY analysis. Therefore, the stereochemistry of the major diastereomer was inferred. Starting material **254** (25%) remained in this process and was inseparable from the (minor) *cis*-isomers **259**.

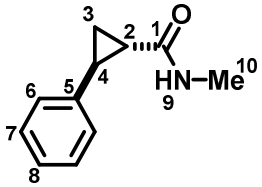

***Trans*-Isomers 258**: Brown solid (15 mg, 0.09 mmol, 15%).

^{1}H NMR (400 MHz, Chloroform-*d*): δ 7.28-7.21 (2H, m, H6), 7.19-7.13 (1H, m, H8), 7.08 (2H, m, H7), 5.74 (1H, br s, H9), 2.82 (3H, d, *J* = 4.8 Hz, H10), 2.50-2.43 (1H, m, H4), 1.62-1.53 (2H, m, H2, H3), 1.24-1.18 (1H, m, H3).

^{13}C NMR (101 MHz, Chloroform-*d*): δ 172.6 (C1), 141.0 (C5), 128.6 (C6), 126.3 (C7), 126.1 (C8), 26.8 (C2), 26.7 (C10), 25.1 (C4), 15.9 (C3).

HRMS (ESI$^+$) *m/z* calculated for $C_{11}H_{14}NO$ $[M+H]^+$ 176.1070, found 176.1067.

MP: 92-93 °C.

IR: ν_{max} = 3267 (N-H), 2936 (C-H), 1635 (C=O), 1574 (C=C), 1404, 1250.

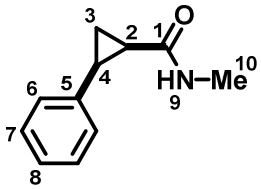

***Cis*-Isomers 259 mixed with starting material 254**: Orange oil (10 mg, 0.06 mmol, 10%) with 25% starting material.

^{1}H NMR (400 MHz, Chloroform-*d*): δ 7.4-7.15 (5H, m, H6-H8), 5.55 (1H, br s, H9), 2.59 (3H, d, *J* = 4.5 Hz, H10), 2.49-2.38 (1H, m, H4), 1.92-1.82 (1H, m, H2), 1.67 (1H, ddd, *J* = 11.0, 7.3, 5.3 Hz, H3), 1.29-1.23 (2H, m, H2, H3).

^{13}C NMR (101 MHz, Chloroform-*d*): δ 170.3 (C1), 137.2 (C5), 128.9 (C6), 128.2 (C8), 126.5 (C7), 26.5 (C10), 24.5 (C4), 24.0 (C2), 10.4 (C3).

HRMS (ESI$^+$) *m/z* calculated for $C_{11}H_{14}NO$ $[M+H]^+$ 176.1070, found 176.1067.

IR: ν_{max} = 3274 (N-H), 2930 (C-H), 1629 (C=O), 1566 (C=C), 1456, 1325.

NOESY for the mixture containing 259 and starting material:

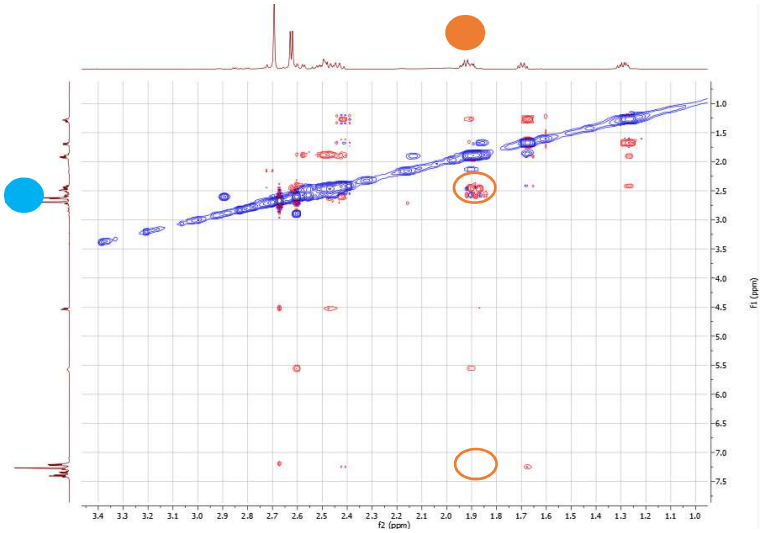

Note that for the minor diastereomer from the reaction (**259**), the proton adjacent to the carbonyl H2 sees the adjacent benzylic proton H4 but does not see the aromatic protons.

*Figure 30: NOESY of minor diastereomer **259**, showing a key correlation.*

(*Z*)- and (*E*)-3-Ethylidene-1-methyl-5-phenylpyrrolidin-2-one (263 and 262)

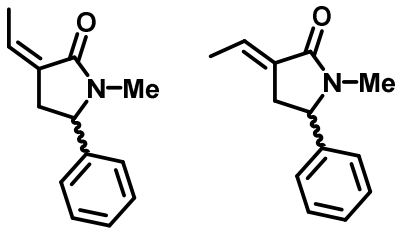

The *E*- and *Z*-isomers of the unsaturated lactam were isolated according to General Procedure 4b and 5 using 1-methyl-5-phenylpyrrolidin-2-one (**254**) (1.00 g, 5.71 mmol, 1.0 eq.) as the lactam and acetaldehyde (**13**) (0.38 mL, 6.85 mmol, 1.2 eq.) as the electrophile. Purification was carried out using flash column chromatography (20% EtOAc / petroleum ether) to separate the isomers.

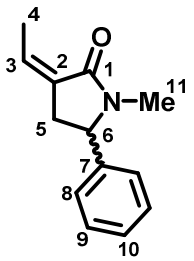

***Z*-Isomers 263**: Orange liquid (0.26 g, 1.27 mmol, 22%).

^{1}H NMR (400 MHz, Chloroform-*d*): δ 7.35-7.23 (3H, m, H8, H10), 7.17-7.12 (2H, m, H7), 5.94-5.85 (1H, m, H3), 4.41 (1H, dd, *J* = 8.5, 4.5 Hz, H6), 3.13-3.02 (1H, m, H5), 2.67 (3H, s, H11), 2.53-2.43 (1H, m, H5), 2.20 (3H, dt, *J* = 7.4, 2.3 Hz, H4).

^{13}C NMR (101 MHz, Chloroform-*d*): δ 169.4 (C1), 141.4 (C7), 131.5 (C3), 129.1 (C2), 129.0 (C8), 128.0 (C10), 126.3 (C9), 61.6 (C6), 36.4 (C5), 28.2 (C11), 13.2 (C4).

HRMS (ESI^{+}) *m/z* calculated for $C_{13}H_{16}NO$ $[M+H]^{+}$ 202.1226, found 202.1220.

IR: ν_{max} = 2921 (C-H), 1685 (C=O), 1663 (C=C), 1392, 1265.

NOESY for this stereoisomer:

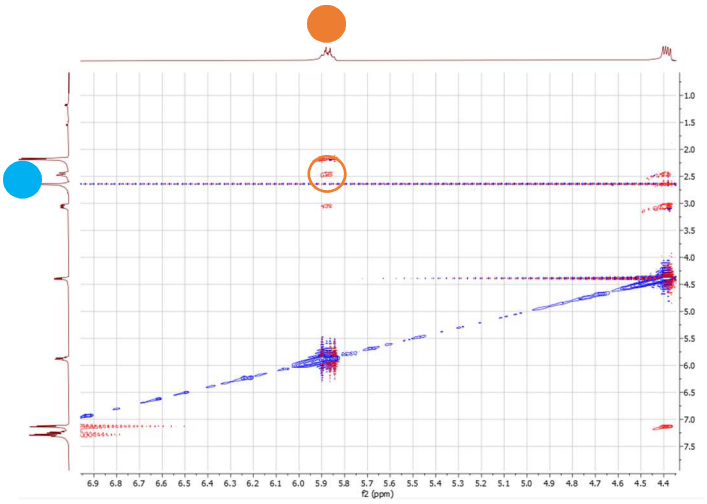

Note that for *cis*-isomers **263** reported here, the alkene proton H3 sees the adjacent lactam alkyl protons H5.

Figure 31: NOESY for cis*-isomers **263**, showing a key correlation.*

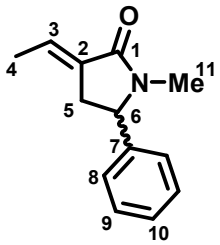

***E*-Isomers 262**: Brown solid (0.59 g, 2.95 mmol, 52%).

^{1}H NMR (400 MHz, Chloroform-*d*): δ 7.37-7.26 (3H, m, H8, H10), 7.19-7.13 (2H, m, H9), 6.60-6.52 (1H, m, H3), 4.49 (1H, dd, *J* = 8.9, 4.2 Hz, H6), 3.16-3.06 (1H, m, H5), 2.72 (3H, s, H11), 2.53-2.45 (1H, m, H5), 1.84 (1H, dt, *J* = 7.1, 1.9 Hz, H4).

^{13}C NMR (101 MHz, Chloroform-*d*): δ 169.0 (C1), 141.6 (C7), 131.5 (C2), 129.1 (C8), 128.2 (C10), 127.9 (C2), 126.4 (C9), 61.8 (C6), 32.7 (C5), 28.5 (C11), 14.7 (C4).

HRMS (ESI^{+}) *m/z* calculated for $C_{13}H_{16}NO$ $[M+H]^{+}$ 202.1226, found 202.1219.

MP: 61-62 °C.

IR: ν_{max} = 2936 (C-H), 1665 (C=O), 1627 (C=C), 1393, 1270.

N-Methyl-2-phenyl-1-vinylcyclopropane-1-carboxamide (264)

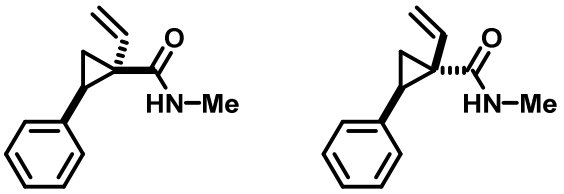

The title compound was synthesised according to General procedure 6b using (*E*)-3-ethylidene-1-methyl-5phenylpyrrolidin-2-one (**262**) (100 mg, 0.52 mmol, 1.0 eq.). Purification with flash column chromatography (0-30% EtOAc / petroleum ether) afforded an orange oil as a mixture of both diastereomers of ring-contraction product with a crude dr of 52:48 (66 mg, 0.34 mmol, 66%). Stereochemistry assigned by NOESY analysis (see below).

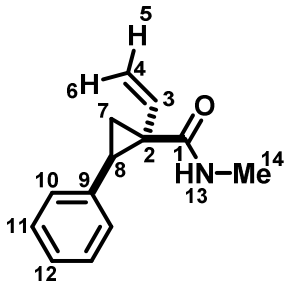

Major Diastereomers

^{1}H NMR (400 MHz, Chloroform-*d*): δ 7.27-7.06 (5H, m, H10-H12), 6.09 (1H, dd, *J* = 17.0, 10.5 Hz, H3), 5.49 (1H, br s, H13), 5.34-5.26 (1H, m, H6), 5.21 (1H, d, *J* = 10.5 Hz, H5), 2.54 (4H, m, H14, H8), 2.10 (1H, dd, *J* = 7.3, 5.1 Hz, H7), 1.29 (1H, dd, *J* = 9.0, 5.1 Hz, H7).

^{13}C NMR (101 MHz, Chloroform-*d*): δ 169.4 (C1), 138.7 (C3), 136.9 (C9), 128.3 (C10), 128.0 (C12), 126.6 (C11), 116.0 (C4), 38.0 (C2), 32.2 (C8), 26.6 (C14), 17.7 (C7).

HRMS (LCMS) (ESI^{+}) *m/z* calculated for $C_{13}H_{16}NO$ $[M+H]^{+}$ 202.1226, found 202.1218.

IR: ν_{max} = 3331 (N-H), 2938 (C-H), 2844 (C-H), 1634 (C=O), 1525 (C=C), 1409, 1283.

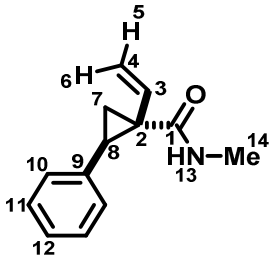

Minor Diastereomers

^{1}H NMR (400 MHz, Chloroform-*d*): δ 7.27-7.06 (5H, m, H10-H12), 6.00 (1H, br s, H13), 5.64 (1H, dd, *J* = 17.3, 10.5 Hz, H3), 5.34-5.26 (2H, m, H5, H6), 3.03 (1H, dd, *J* = 9.1, 7.2 Hz, H8), 2.83 (3H, d, *J* = 4.8 Hz, H14), 1.77 (1H, ddd, *J* = 9.1, 4.6, 0.8 Hz, H7), 1.49 (1H, dd, *J* = 7.2, 4.6 Hz, H7).

^{13}C NMR (101 MHz, Chloroform-*d*): δ 172.9 (C1), 136.7 (C9), 133.3 (C3), 128.3 (C10), 128.1 (C12), 126.4 (C11), 123.4 (C4), 35.1 (C2), 30.6 (C8), 27.0 (C10), 18.3 (C7).

HRMS (LCMS) (ESI^{+}) *m/z* calculated for $C_{13}H_{16}NO$ $[M+H]^{+}$ 202.1226, found 202.1222.

IR: ν_{max} = 3331 (N-H), 2938 (C-H), 2844 (C-H), 1634 (C=O), 1525 (C=C), 1409, 1283.

NOESY for both diastereomers:

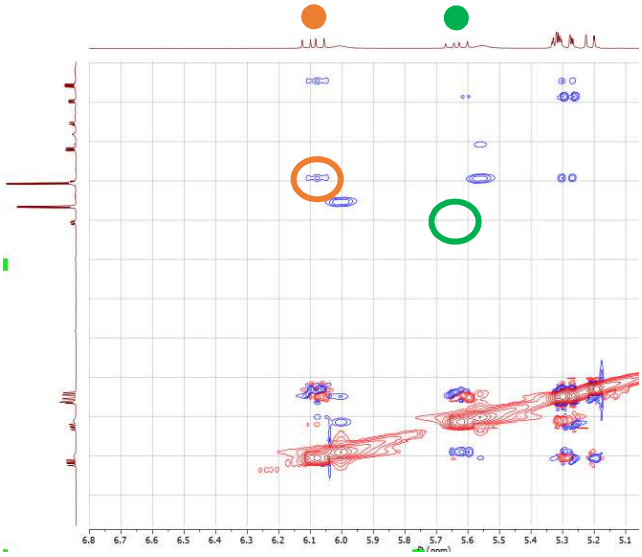

Note that for the major diastereomer, the alkene proton H3 sees the adjacent benzylic proton; whilst for the minor diastereomer, the alkene proton H3 doesn't.

*Figure 32: NOESY of the mixture of diastereomers of **264**.*

5-(4-Chlorophenyl)-1-methylpyrrolidin-2-one (271)

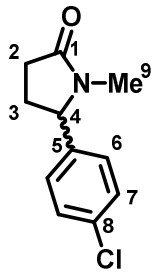

The title compound was synthesised according to General Procedure 3 using 4-(4-chlorophenyl)-4-oxobutanoic acid (**268**) (0.50 g, 2.36 mmol, 1.0 eq.) and *N*-methyl formamide (**255**) (2.76 mL, 47.20 mmol, 20.0 eq.). Purification by flash column chromatography (CH_2Cl_2) afforded the title compound as an orange oil (0.25 g, 1.18 mmol, 50%).

^{1}H NMR (400 MHz, Chloroform-*d*): δ 7.29 (2H, d, *J* = 8.5 Hz, H7), 7.09 (2H, d, *J* = 8.5 Hz, H6), 4.45 (1H, dd, *J* = 7.4, 5.3 Hz, H4), 2.60 (3H, s, H9), 2.54-2.28 (3H, m, H2, H3), 1.83-1.72 (1H, m, H3).

^{13}C NMR (101 MHz, Chloroform-*d*): δ 175.3 (C1), 139.6 (C5), 133.7 (C8), 129.1 (C7), 127.7 (C6), 63.8 (C4), 29.9 (C2), 28.3 (C3), 28.1 (C9).

HRMS (ESI^+) *m/z* calculated for $C_{11}H_{13}ClNO$ $[M+H]^+$ 210.0680, found 210.0672.

IR: ν_{max} = 2981 (C-H), 2922 (C-H), 1673 (C=O), 1596 (C=C), 1393, 1012.

(*Z*)- and (*E*)-5-(4-Chlorophenyl)-3-ethylidene-1-methylpyrrolidin-2-one (277 and 274)

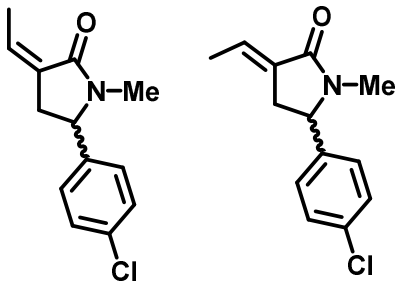

The *E*- and *Z*-isomers of the unsaturated lactam were isolated according to General Procedure 4b and 5 using 5-(4-chlorophenyl)-1-methylpyrrolidin-2-one (**271**) (0.50 g, 2.39 mmol, 1.0 eq.) as the lactam and acetaldehyde (**13**) (0.16 mL, 2.87 mmol, 1.2 eq.) as the electrophile. Purification was carried out using flash column chromatography (20% EtOAc / petroleum ether) to separate the isomers.

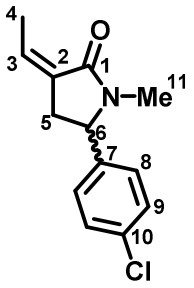

***Z*-Isomers 277**: Orange oil (92 mg, 0.38 mmol, 16%).

^{1}H NMR (400 MHz, Chloroform-*d*): δ 7.30 (2H, d, *J* = 8.3 Hz, H9), 7.10 (2H, d, *J* = 8.3 Hz, H8), 5.92 (1H, q, *J* = 7.1 Hz, H3), 4.40 (1H, dd, *J* = 9.2, 4.3 Hz, H6), 3.09 (1H, dd, *J* = 16.4, 9.2 Hz, H5), 2.66 (3H, s, H11), 2.44 (1H, dd, *J* = 16.4, 4.3 Hz, H5), 2.20 (3H, d, *J* = 7.1 Hz, H4).

^{13}C NMR (101 MHz, Chloroform-*d*): δ 169.4 (C1), 140.0 (C7), 133.9 (C10), 132.1 (C3), 129.2 (C9), 128.7 (C2), 127.8 (C8), 61.0 (C6), 36.3 (C5), 28.2 (C11), 13.3 (C4).

HRMS (ESI^{+}) *m/z* calculated for $C_{13}H_{15}ClNO$ $[M+H]^{+}$ 236.0837, found 236.0829.

IR: ν_{max} = 2981 (C-H), 2937 (C-H), 1687 (C=O), 1664 (C=C), 1489 (C=C), 1392, 1087.

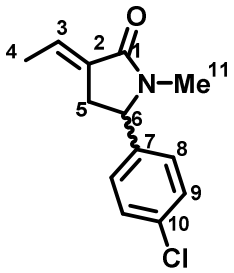

***E*-Isomers 274**: Orange oil (0.21 g, 0.79 mmol, 37%).

^{1}H NMR (400 MHz, Chloroform-*d*): δ 7.30 (2H, d, *J* = 8.3 Hz, H9), 7.09 (2H, d, *J* = 8.3 Hz, H8), 6.60-6.51 (1H, m, H3), 4.47 (1H, dd, *J* = 8.6, 4.1 Hz, H6), 3.10 (1H, dd, *J* = 17.4, 8.6 Hz, H5), 2.69 (3H, s, H11), 2.47-2.38 (1H, m, H5), 1.72 (3H, d, *J* = 7.1 Hz, H4).

^{13}C NMR (101 MHz, Chloroform-*d*): δ 168.9 (C1), 140.2 (C7), 134.0 (C10), 131.1 (C2), 129.3 (C9), 128.3 (C3), 127.8 (C8), 61.1 (C6), 32.6 (C5), 28.5 (C11), 14.7 (C4).

HRMS (ESI^{+}) *m/z* calculated for $C_{13}H_{15}ClNO$ $[M+H]^{+}$ 236.0837, found 236.0828.

IR: ν_{max} = 2981 (C-H), 2923 (C-H), 1688 (C=O), 1666 (C=C), 1394, 1087.

5-(4-Methoxyphenyl)-1-methylpyrrolidin-2-one (272)

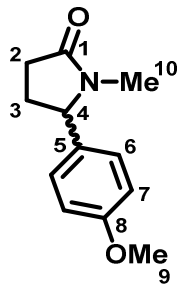

The title compound was synthesised according to General Procedure 3 using 4-(4-methoxyphenyl)-4-oxobutanoic acid (**269**) (0.50 g, 2.40 mmol, 1.0 eq.) and *N*-methyl formamide (**255**) (2.80 mL, 48.00 mmol, 20.0 eq.). Purification by flash column chromatography (CH_2Cl_2) afforded the title compound as an orange solid (0.38 g, 1.85 mmol, 77%).

^{1}H NMR (400 MHz, Chloroform-*d*): δ 7.07 (2H, d, *J* = 8.8 Hz, H6), 6.85 (2H, d, *J* = 8.8 Hz, H7), 4.41 (1H, dd, *J* = 7.2, 6.1 Hz, H4), 3.75 (3H, s, H9), 2.58 (3H, s, H10), 2.55-2.31 (3H, m, H2, H3), 1.86-1.74 (1H, m, H3).

^{13}C NMR (101 MHz, Chloroform-*d*): δ 175.4 (C1), 159.4 (C8), 133.0 (C5), 127.6 (C6), 114.3 (C7), 64.1 (C4), 55.3 (C9), 30.2 (C2), 28.5 (C3), 28.0 (C10).

HRMS (ESI^+) *m/z* calculated for $C_{12}H_{16}NO_2$ $[M+H]^+$ 206.1176, found 206.1167.

MP: 62-63 °C.

IR: ν_{max} = 2981 (C-H), 2938 (C-H), 2865 (C-H), 1645 (C=O), 1611 (C=C), 1512 (C=C), 1246, 1051.

(*Z*)- and (*E*)-3-Ethylidene-5-(4-methoxyphenyl)-1-methylpyrrolidin-2-one (278 and 275)

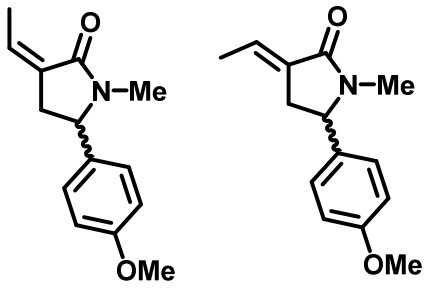

The *E*- and *Z*-isomers of the unsaturated lactam were isolated according to General Procedure 4b and 5 using 5-(4-methoxyphenyl)-1-methylpyrrolidin-2-one (**272**) (1.00 g, 4.88 mmol, 1.0 eq.) as the lactam

and acetaldehyde (**13**) (0.33 mL, 5.86 mmol, 1.2 eq.) as the electrophile. Purification was carried out using flash column chromatography (20% EtOAc / petroleum ether) to separate the isomers.

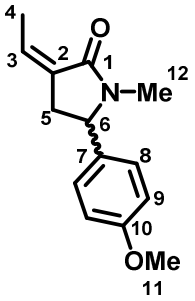

***Z*-Isomers 278**: Orange oil (0.14 g, 0.59 mmol, 12%).

^{1}H NMR (400 MHz, Chloroform-*d*): δ 7.08 (2H, d, *J* = 8.0 Hz, H8), 6.85 (2H, d, *J* = 8.0 Hz, H9), 5.94-5.85 (1H, m, H3), 4.36 (1H, dd, *J* = 8.6, 4.8 Hz, H6), 3.77 (3H, s, H11), 3.1-2.99 (1H, m, H5), 2.64 (3H, s, H12), 2.51-2.42 (1H, m, H5), 2.19 (3H, d, *J* = 7.3 Hz, H4).

^{13}C NMR (101 MHz, Chloroform-*d*): δ 169.3 (C1), 159.4 (C10), 133.4 (C7), 131.4 (C3), 129.4 (C2), 127.6 (C8), 114.3 (C9), 61.1 (C6), 55.3 (C11), 36.5 (C5), 28.0 (C12), 13.2 (C4).

HRMS (ESI^{+}) *m/z* calculated for $C_{14}H_{18}NO_2$ $[M+H]^+$ 232.1332, found 232.1323.

IR: ν_{max} = 2966 (C-H), 2865 (C-H), 1662 (C=O), 1611 (C=C), 1511 (C=C), 1245.

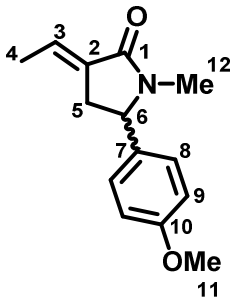

***E*-Isomers 275**: Orange solid (0.39 g, 1.66 mmol, 34%).

^{1}H NMR (400 MHz, Chloroform-*d*): δ 7.09 (2H, d, *J* = 8.6 Hz, H8), 6.87 (2H, d, *J* = 8.6 Hz, H9), 6.59-6.52 (1H, m, H3), 4.44 (1H, dd, *J* = 8.5, 3.9 Hz, H6), 3.79 (3H, s, H11), 3.08 (1H, dd, *J* = 17.0, 8.5 Hz, H5), 2.69 (3H, s, H12), 2.52-2.43 (1H, m, H5), 1.74 (3H, dt, *J* = 7.1, 1.6 Hz, H4).

^{13}C NMR (101 MHz, Chloroform-*d*): δ 169.0 (C1), 159.5 (C10), 134.5 (C7), 131.7 (C2), 127.7 (C3), 127.7 (C8), 114.5 (C9), 61.3 (C6), 55.4 (C11), 33.6 (C5), 28.4 (C12), 14.7 (C4).

HRMS (ESI^{+}) *m/z* calculated for $C_{14}H_{18}NO_2$ $[M+H]^+$ 232.1332, found 232.1321.

MP: 57-58 °C.

IR: ν_{max} = 2937 (C-H), 2922 (C-H), 1694 (C=O), 1667 (C=C), 1511 (C=C), 1389, 1245.

2-(4-Methoxyphenyl)-*N*-methyl-1-vinylcyclopropane-1-carboxamide (281)

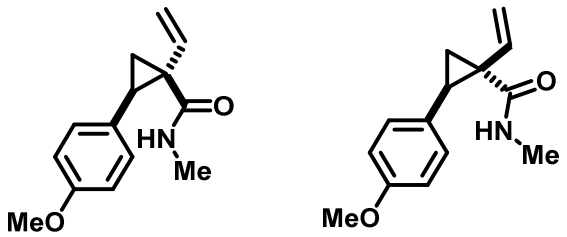

The title compound was synthesised according to General procedure 6b using (*E*)-3-ethylidene-5-(4-methoxyphenyl)-1-methylpyrrolidin-2-one (**275**) (100 mg, 0.43 mmol, 1.0 eq.). Purification with flash column chromatography (30% EtOAc / petroleum ether) afforded a colourless oil as a mixture of isomers of the title compound with a crude dr of 51:49 (67 mg, 0.29 mmol, 67%).

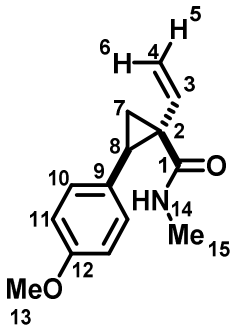

Major Diastereomers

^{1}H NMR (400 MHz, Chloroform-*d*): δ 7.09 (2H, d, *J* = 8.6 Hz, H10), 6.78 (2H, d, *J* = 8.6 Hz, H11), 6.09 (1H, dd, *J* = 17.3, 10.3 Hz, H3), 5.61 (1H, br s, H14), 5.26 (1H, d, *J* = 17.3 Hz, H6), 5.19 (1H, d, *J* = 10.3 Hz, H5), 3.74 (3H, s, H13), 2.55 (1H, d, *J* = 5.0 Hz, H15), 2.46 (1H, dd, *J* = 8.5, 7.2 Hz, H8), 2.04 (1H, dd, *J* = 7.2, 4.9 Hz, H7), 1.25 (1H, dd, *J* = 8.5, 4.9 Hz, H7).

^{13}C NMR (101 MHz, Chloroform-*d*): δ 173.1 (C1), 158.2 (C12), 133.4 (C3), 129.9 (C10), 128.6 (C9), 123.2 (C4), 113.5 (C11), 55.2 (C13), 34.8 (C2), 30.1 (C8), 27.0 (C15), 18.3 (C7).

HRMS (ESI$^+$) *m/z* calculated for $C_{14}H_{18}NO_2$ $[M+H]^+$ 232.1332, found 232.1327.

IR: ν_{max} = 3320 (N-H), 2981 (C-H), 2923 (C-H), 1628 (C=O), 1612 (C=C), 1513 (C=C), 1244, 1033.

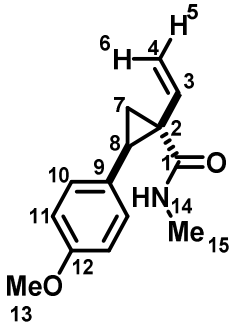

Minor Diastereomers

^{1}H NMR (400 MHz, Chloroform-*d*): δ 7.00 (2H, d, *J* = 8.6 Hz, H10), 6.78 (2H, d, *J* = 8.6 Hz, H11), 6.00 (1H, br s, H14), 5.63 (1H, dd, *J* = 17.5, 11.0 Hz, H3), 5.30 (1H, dd, *J* = 11.0, 1.0 Hz, H5), 5.26 (1H, dd, *J* = 17.5, 1.0 Hz, H6), 3.75 (3H, s, H13), 2.96 (1H, dd, *J* = 9.0, 7.1 Hz, H8), 2.82 (3H, d, *J* = 4.8 Hz, H15), 1.73 (1H, dd, *J* = 9.0, 4.4 Hz, H7), 1.41 (1H, dd, *J* = 7.1, 4.4 Hz, H7).

^{13}C NMR (101 MHz, Chloroform-*d*): δ 169.6 (C1), 158.3 (C12), 138.8 (C3), 129.3 (C10), 128.8 (C9), 115.8 (C4), 113.5 (C11), 55.2 (C13), 37.6 (C2), 31.7 (C8), 26.6 (C15), 17.7 (C7).

HRMS (ESI^+) *m/z* calculated for $C_{14}H_{18}NO_2$ $[M+H]^+$ 232.1332, found 232.1326.

IR: ν_{max} = 3320 (N-H), 2981 (C-H), 2923 (C-H), 1628 (C=O), 1612 (C=C), 1513 (C=C), 1244, 1033.

1-Methyl-5-(thiophen-2-yl)pyrrolidin-2-one (273)

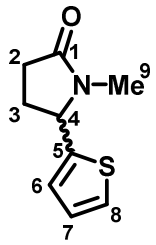

The title compound was synthesised according to General Procedure 3 using 4-oxo-4-(thiophen-2-l)butanoic acid (**270**) (0.50 g, 2.72 mmol, 1.0 eq.) and *N*-methyl formamide (**255**) (3.18 mL, 54.40 mmol, 20.0 eq.). Purification by flash column chromatography (20-50% EtOAc / petroleum ether) afforded the title compound as a yellow oil (0.26 g, 1.44 mmol, 53%).

^{1}H NMR (400 MHz, Chloroform-*d*): δ 7.26 (1H, dd, *J* = 4.3, 3.0 Hz, H8), 6.96-6.93 (2H, m, H6, H7), 4.78 (1H, dd, *J* = 7.5, 5.7 Hz, H4), 2.68 (3H, s, H9), 2.63-2.36 (3H, m, H2, H3), 2.06-1.97 (1H, m, H3).

^{13}C NMR (101 MHz, Chloroform-*d*): δ 174.8 (C1), 144.9 (C5), 126.9 (C7), 125.6 (C6), 125.5 (C8), 60.0 (C4), 30.0 (C2), 29.0 (C3), 28.1 (C9).

HRMS (ESI$^+$) *m/z* calculated for $C_9H_{12}NOS$ $[M+H]^+$ 182.0634, found 182.0629.

IR: ν_{max} = 2981 (C-H), 2973 (C-H), 1724 (C=O), 1660 (C=C), 1416, 1395, 1033, 704.

(*Z*)- and (*E*)-3-Ethylidene-1-methyl-5-(thiophen-2-yl)pyrrolidin-2-one (279 and 276)

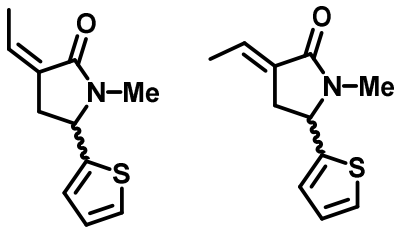

The *E*- and *Z*-isomers of the unsaturated lactam were isolated according to General Procedure 4b and 5 using 1-methyl-5-(thiophen-2-yl)pyrrolidin-2-one (**273**) (1.00 g, 5.52 mmol, 1.0 eq.) as the lactam and acetaldehyde (**13**) (0.37 mL, 6.62 mmol, 1.2 eq.) as the electrophile. Purification was carried out using flash column chromatography (20-60% EtOAc / petroleum ether) to separate the isomers.

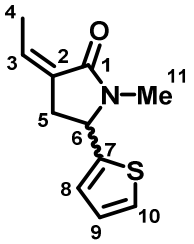

***Z*-Isomers 279**: Orange oil (55 mg, 0.28 mmol, 5%).

^{1}H NMR (400 MHz, Chloroform-*d*): δ 7.27 (1H, dd, *J* = 5.4, 1.7 Hz, H10), 6.98-6.94 (2H, m, H8, H9), 5.97 (1H, qt, *J* = 7.4, 2.2 Hz, H3), 4.75 (1H, dd, *J* = 8.2, 4.6 Hz, H6), 3.15 (1H, ddt, *J* = 16.1, 8.2, 2.2 Hz, H5), 2.75 (3H, s, H11), 2.72-2.64 (1H, m, H5), 2.22 (1H, dt, *J* = 7.4, 2.2 Hz, H4).

^{13}C NMR (101 MHz, Chloroform-*d*): δ 168.8 (C1), 145.3 (C7), 132.1 (C3), 128.7 (C2), 126.8 (C9), 125.6 (C8), 125.5 (C10), 57.3 (C6), 37.1 (C5), 28.1 (C11), 13.4 (C4).

HRMS (ESI$^+$) *m/z* calculated for $C_{11}H_{14}NOS$ $[M+H]^+$ 208.0791, found 208.0789.

IR: ν_{max} = 2981 (C-H), 2936 (C-H), 1690 (C=O), 1663 (C=C), 1393, 1055.

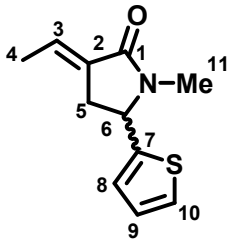

***E*-Isomers 276**: Orange oil (0.24 g, 1.16 mmol, 21%).

^{1}H NMR (400 MHz, Chloroform-*d*): δ 7.27 (1H, ddd, *J* = 4.8, 1.7, 0.7 Hz, H10), 6.98-6.95 (2H, m, H8, H9), 6.62-6.55 (1H, m, H3), 4.80 (1H, dd, *J* = 8.6, 4.3 Hz, H6), 3.20-3.11 (1H, m, H5), 2.78 (3H, s, H11), 2.70-2.62 (1H, m, H5), 1.77 (1H, dt, *J* = 7.0, 1.9 Hz, H4).

^{13}C NMR (101 MHz, Chloroform-*d*): δ 168.4 (C1), 145.4 (C7), 131.0 (C2), 128.5 (C3), 127.0 (C9), 126.9 (C8), 125.7 (C10), 57.4 (C6), 33.4 (C5), 28.5 (C11), 14.8 (C4).

HRMS (ESI^{+}) *m/z* calculated for $C_{11}H_{14}NOS$ $[M+H]^{+}$ 208.0791, found 208.0786.

IR: ν_{max} = 2980 (C-H), 2930 (C-H), 1693 (C=O), 1660 (C=C), 1394, 1050.

(1*S*,2*S*)-*N*-Methyl-2-(thiophen-2-yl)-1-vinylcyclopropane-1-carboxamide (282)

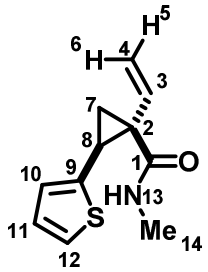

The title compound was synthesised according to General procedure 6b using (*E*)-3-ethylidene-1-methyl-5-(thiophen-2-yl)pyrrolidin-2-one (**276**) (100 mg, 0.48 mmol, 1.0 eq.). Purification with flash column chromatography (30% EtOAc / petroleum ether) afforded the title compound as a colourless oil as a single diastereomer of the title compound with a crude dr of 58:42 (35 mg, 0.17 mmol, 35%). Note the minor diastereomer could not be isolated in good purity and is not included here.

^{1}H NMR (400 MHz, Chloroform-*d*): δ 7.10 (1H, dd, *J* = 5.2, 1.2 Hz, H12), 6.89 (1H, dd, *J* = 5.2, 3.4 Hz, H11), 6.81 (1H, dt, *J* = 3.4, 1.2 Hz, H10), 6.06 (1H, dd, *J* = 17.2, 10.4 Hz, H3), 5.60 (1H, br s, H13), 5.30 (1H, dd, *J* = 17.2, 0.7 Hz, H6), 5.23 (1H, dd, *J* = 10.4, 0.7 Hz, H5), 2.63 (3H, d, *J* = 5.1 Hz, H14), 2.61 (1H, dd, *J* = 7.5, 7.1 Hz, H8), 2.09 (1H, dd, *J* = 7.1, 5.2 Hz, H7), 1.38 (1H, dd, *J* = 7.5, 5.2 Hz, H7).

^{13}C NMR (101 MHz, Chloroform-*d*): δ 169.1 (C1), 140.6 (C9), 137.9 (C3), 126.9 (C11), 125.5 (C10), 124.0 (C12), 116.7 (C4), 38.4 (C2), 26.8 (C8), 26.7 (C14), 19.6 (C7).

HRMS (ESI$^+$) *m/z* calculated for $C_{11}H_{14}NOS$ $[M+H]^+$ 208.0791, found 208.0786.

IR: ν_{max} = 3332 (N-H), 2981 (C-H), 2923 (C-H), 1626 (C=O), 1553 (C=C), 1539 (C=C), 1033.

5-(4-Fluorophenyl)pyrrolidin-2-one (285)

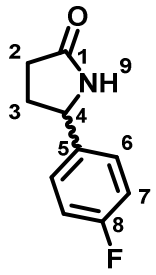

The title compound was synthesised according to General Procedure 3 using 4-(4-fluorophenyl)-4-oxobutanoic acid (**283**) (0.50 g, 2.55 mmol, 1.0 eq.) and formamide (**284**) (2.00 mL, 51.00 mmol, 20.0 eq.). Purification by flash column chromatography (0-5% MeOH / CH_2Cl_2) afforded the title compound as an orange oil (0.24 g, 1.25 mmol, 49%).

^{1}H NMR (400 MHz, Chloroform-*d*): δ 7.30-7.23 (2H, m, H6), 7.10-7.02 (2H, m, H7), 6.54 (1H, br s, H9), 4.74 (1H, t, *J* = 7.0 Hz, H4), 2.61-2.49 (1H, m, H3), 2.48-2.35 (2H, m, H2), 1.98-1.87 (1H, m, H3).

^{13}C NMR (101 MHz, Chloroform-*d*): δ 178.6 (C1), 162.49 (d, *J* = 246.0 Hz, C8), 138.4 (d, *J* = 3.1 Hz, C5), 127.4 (d, *J* = 8.2 Hz, C6), 115.9 (d, *J* = 21.6 Hz, C7), 57.6 (C4), 31.6 (C3), 30.4 (C2).

^{19}F NMR (377 MHz, Chloroform-*d*): δ −114.4

HRMS (ESI$^+$) *m/z* calculated for $C_{10}H_{11}FNO$ $[M+H]^+$ 180.0819, found 180.0823.

IR: ν_{max} = 3174 (N-H), 2981 (C-H), 2949 (C-H), 1683 (C=O), 1033.

5-(4-Fluorophenyl)-1-methylpyrrolidin-2-one (286)

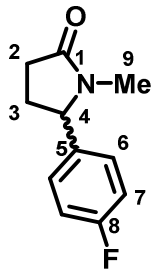

To a slurry of NaH (0.19 g, 4.69 mmol, 1.2 eq., 60% in mineral oil) in anhydrous THF (10 mL) was slowly added a solution of 5-(4-fluorophenyl)pyrrolidine-2-one (**285**) (0.70 g, 3.91 mmol, 1.0 eq.) in anhydrous THF (15 mL) in an ice bath. After warming to rt and leaving to stir for 1 h, MeI (0.30 mL, 4.69 mmol, 1.2 eq.) was added slowly and the mixture left to stir for a further 2 h at rt. Water (50 mL) was added carefully, and the aqueous layer was extracted with EtOAc (3 × 50 mL). The combined organics were washed with brine (50 mL), dried over $MgSO_4$, filtered and concentrated *in vacuo*. Purification by flash column chromatography (20-70% EtOAc / petroleum ether) afforded the title compound as a yellow oil (0.66 g, 3.40 mmol, 87%).

^{1}H NMR (400 MHz, Chloroform-*d*): δ 7.19-7.14 (2H, m, H6), 7.07 (2H, t, *J* = 8.7 Hz, H7), 4.50 (1H, t, *J* = 6.6 Hz, H4), 2.65 (3H, s, H9), 2.60-2.40 (3H, m, H2, H3), 1.89-1.81 (1H, m, H3).

^{13}C NMR (101 MHz, Chloroform-*d*): δ 175.6 (C1), 162.6 (d, *J* = 246.9 Hz, C8), 137.0 (d, *J* = 3.0 Hz, C5), 128.2 (d, *J* = 8.3 Hz, C6), 116.1 (d, *J* = 21.6 Hz, C7), 64.1 (C4), 30.2 (C2), 28.7 (C3), 28.3 (C9).

^{19}F NMR (377 MHz, Chloroform-*d*): δ –114.0

HRMS (ESI$^+$) *m/z* calculated for $C_{11}H_{13}FNO$ $[M+H]^+$ 194.0976, found 194.0970.

IR: ν_{max} = 2981 (C-H), 2949 (C-H), 2932 (C-H), 1683 (C=O), 1033.

(*Z*)- and (*E*)-3-Ethylidene-5-(4-fluorophenyl)-1-methylpyrrolidin-2-one (287 and 288)

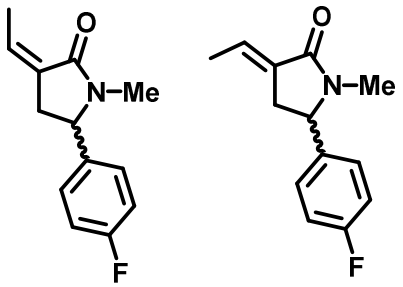

The *E*- and *Z*-isomers of the unsaturated lactam were isolated according to General Procedure 4b and 5 using 5-(4-fluorophenyl)-1-methylpyrrolidin-2-one (**286**) (0.50 g, 2.59 mmol, 1.0 eq.) as the lactam and acetaldehyde (**13**) (0.17 mL, 3.11 mmol, 1.2 eq.) as the electrophile. Purification was carried out using flash column chromatography (15-30% EtOAc / petroleum ether) to separate the isomers.

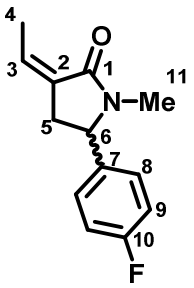

***Z*-Isomers 287**: Orange oil (0.11 g, 0.52 mmol, 20%).

^{1}H NMR (400 MHz, Chloroform-*d*): δ 7.15 (2H, dd, *J* = 8.6, 5.3 Hz, H8), 7.02 (2H, t, *J* = 8.6 Hz, H9), 5.93 (1H, qt, *J* = 7.3, 2.1 Hz, H3), 4.42 (1H, dd, *J* = 8.7, 4.5 Hz, H6), 3.09 (ddq, *J* = 16.4, 8.7, 2.1 Hz, H5), 2.67 (3H, s, H11), 2.50-2.43 (1H, m, H5), 2.21 (3H, dt, *J* = 7.3, 2.3 Hz, H4).

^{13}C NMR (101 MHz, Chloroform-*d*): δ 169.4 (C1), 162.5 (d, *J* = 245.3 Hz, C10), 137.3 (d, *J* = 2.9 Hz, C7), 131.9 (C3), 128.9 (C2), 128.1 (d, *J* = 7.7 Hz, C8), 116.0 (d, *J* = 22.1 Hz, C9), 61.0 (C6), 36.5 (C5), 28.2 (C11), 13.3 (C4).

^{19}F NMR (377 MHz, Chloroform-*d*): δ –114.1

HRMS (ESI^{+}) *m/z* calculated for $C_{13}H_{15}FNO$ $[M+H]^{+}$ 220.1132, found 220.1125.

IR: ν_{max} = 2922 (C-H), 2858 (C-H), 1686 (C=O), 1664 (C=C), 1508 (C=C), 1392, 1221.

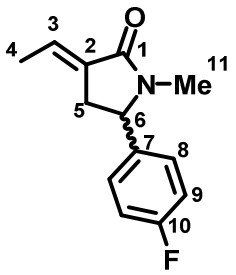

***E*-Isomers 288**: Orange oil (0.24 g, 1.06 mmol, 41%).

^{1}H NMR (400 MHz, Chloroform-*d*): δ 7.14 (2H, dd, *J* = 8.7, 5.5 Hz, H8), 7.03 (2H, t, *J* = 8.7 Hz, H9), 6.60-6.54 (1H, m, H3), 4.48 (1H, dd, *J* = 8.8, 4.2 Hz, H6), 3.11 (1H, ddq, *J* = 18.0, 8.8, 2.1 Hz, H5), 2.70 (3H, s, H11), 2.49-2.42 (1H, m, H5), 1.74 (3H, dt, *J* = 7.2, 2.1 Hz, H4).

^{13}C NMR (101 MHz, Chloroform-*d*): δ 169.0 (C1), 162.5 (d, *J* = 246.1 Hz, C10), 137.4 (d, *J* = 3.3 Hz, C7), 131.2 (C2), 128.3 (C3), 128.1 (d, *J* = 8.2 Hz, C8), 116.1 (d, *J* = 21.6 Hz, C9), 61.1 (C6), 32.7 (C5), 28.5 (C11), 14.7 (C4).

^{19}F NMR (377 MHz, Chloroform-*d*): δ –114.0

HRMS (ESI$^+$) *m/z* calculated for $C_{13}H_{15}FNO$ $[M+H]^+$ 220.1132, found 220.1126.

IR: ν_{max} = 2921 (C-H), 2861 (C-H), 1692 (C=C), 1666 (C=O), 1509 (C=C), 1394, 1220.

2-(4-Fluorophenyl)-*N*-methyl-1-vinylcyclopropane-1-carboxamide (289)

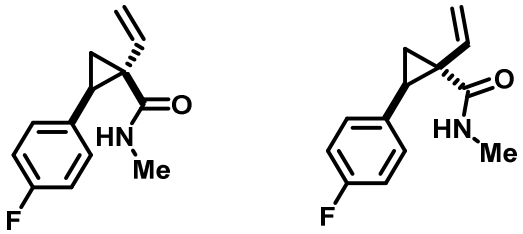

The title compound was synthesised according to General procedure 6b using (*E*)-3-ethylidene-5-(4-fluorophenyl)-1-methylpyrrolidin-2-one (**288**) (100 mg, 0.46 mmol, 1.0 eq.). Purification with flash column chromatography (20% EtOAc / petroleum ether) afforded a colourless oil as a mixture of isomers of the title compound with a crude dr of 52:48 (45 mg, 0.21 mmol, 45%).

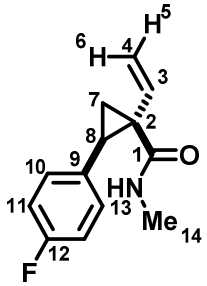

Major Diastereomers

^{1}H NMR (400 MHz, Chloroform-*d*): δ 7.15 (2H, dd, *J* = 8.1, 5.3 Hz, H10), 6.93 (2H, t, *J* = 8.1 Hz, H11), 6.11 (1H, dd, *J* = 17.0, 10.3 Hz, H3), 5.62 (1H, br s, H13), 5.32 (1H, d, *J* = 17.0 Hz, H6), 5.24 (1H, d, *J* = 10.3 Hz, H5), 2.57 (3H, d, *J* = 4.8 Hz, H14), 2.51 (1H, t, *J* = 8.3 Hz, H8), 2.08 (1H, dd, *J* = 8.3, 4.9 Hz, H7), 1.27 (1H, dd, *J* = 8.3, 4.9 Hz, H7).

^{13}C NMR (101 MHz, Chloroform-*d*): δ 169.3 (C1), 161.6 (d, *J* = 244.1 Hz, C12), 138.3 (C3), 132.7 (d, *J* = 3.2 Hz, C9), 130.0 (d, *J* = 7.5 Hz, C10), 116.8 (C4), 114.8 (d, *J* = 21.1 Hz, C11), 37.6 (C2), 31.4 (C8), 26.7 (C14), 17.9 (C7).

^{19}F NMR (377 MHz, Chloroform-*d*): δ −116.4

HRMS (ESI$^+$) *m/z* calculated for $C_{13}H_{15}FNO$ $[M+H]^+$ 220.1132, found 220.1133.

IR: ν_{max} = 3335 (N-H), 2936 (C-H), 1635 (C=O), 1606 (C=C), 1510 (C=C), 1222, 1158.

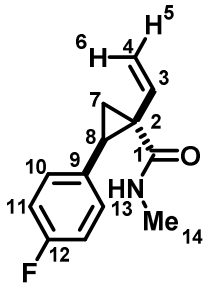

Minor Diastereomers

^{1}H NMR (400 MHz, Chloroform-*d*): δ 7.04 (2H, dd, *J* = 8.2, 5.3 Hz, H10), 6.93 (2H, t, *J* = 8.2 Hz, H11), 5.97 (1H, br s, H13), 5.62 (1H, dd, *J* = 17.0, 10.3 Hz, H3), 5.32 (1H, d, *J* = 17.0 Hz, H6), 5.24 (1H, d, *J* = 10.3 Hz, H5), 3.01 (1H, t, *J* = 8.4 Hz, H8), 2.83 (3H, d, *J* = 4.9 Hz, H14), 1.76 (1H, dd, *J* = 8.4, 4.6 Hz, H7), 1.43 (1H, dd, *J* = 8.4 Hz, 4.6 Hz, H7).

^{13}C NMR (101 MHz, Chloroform-*d*): δ 172.8 (C1), 161.6 (d, *J* = 244.2 Hz, C12), 133.1 (C3), 132.4 (d, *J* = 3.2 Hz, C9), 130.3 (d, *J* = 8.0 Hz, C10), 123.7 (C4), 115.0 (d, *J* = 21.7 Hz, C11), 35.0 (C2), 29.8 (C8), 27.1 (C14), 18.4 (C7).

^{19}F NMR (377 MHz, Chloroform-*d*): δ −116.6

HRMS (ESI$^+$) *m/z* calculated for $C_{13}H_{15}FNO$ $[M+H]^+$ 220.1132, found 220.1135.

IR: ν_{max} = 3335 (N-H), 2936 (C-H), 1635 (C=O), 1606 (C=C), 1510 (C=C), 1222, 1158.

1-Methyl-5-phenyl-3-(propan-2-ylidene)pyrrolidin-2-one (290) and (3*R*,5*S*)-1-Methyl-5-phenyl-3-(prop-1-en-2-yl)pyrrolidine-2-one (291)

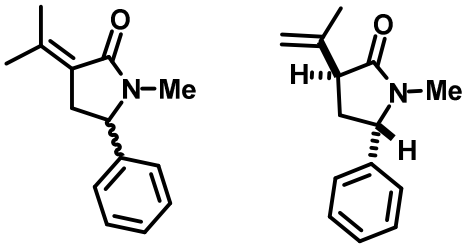

Two main isomers of the unsaturated lactam were isolated according to General Procedure 4b and 5 using 1-methyl-5-phenylpyrrolidin-2-one (**254**) (1.00 g, 5.71 mmol, 1.0 eq.) as the lactam and acetone (**1**) (0.50 mL, 6.85 mmol, 1.2 eq.) as the electrophile. Purification was carried out using flash column chromatography (15% EtOAc / petroleum ether) to separate the isomers.

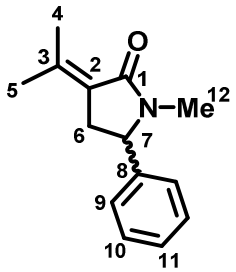

Conjugated Isomers 290: Yellow solid (0.55 g, 2.57 mmol, 45%).

^{1}H NMR (400 MHz, Chloroform-*d*): δ 7.37-7.24 (3H, m, H9, H11), 7.17 (2H, d, *J* = 7.2 Hz, H10), 4.41 (1H, dd, *J* = 8.8, 4.3 Hz, H7), 3.10 (1H, dd, *J* = 16.3, 8.8 Hz, H6), 2.68 (3H, s, H12), 2.47 (1H, dd, *J* = 16.3, 4.3 Hz, H6), 2.31 (3H, s, H5), 1.73 (3H, s, H4).

^{13}C NMR (101 MHz, Chloroform-*d*): δ 169.7 (C1), 142.2 (C8), 141.7 (C3), 129.1 (C9), 128.0 (C11), 126.4 (C10), 123.2 (C2), 60.9 (C7), 35.0 (C6), 28.4 (C12), 23.6 (C5), 19.0 (C4).

HRMS (ESI^{+}) *m/z* calculated for $C_{14}H_{18}NO$ $[M+H]^{+}$ 216.1383, found 216.1375.

MP: 71-72 °C.

IR: ν_{max} = 2980 (C-H), 2922 (C-H), 1677 (C=O), 1646 (C=C), 1053, 1032, 1012.

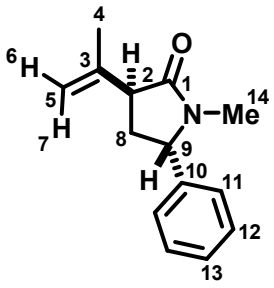

Unconjugated *trans*-Isomers 291: Yellow oil (0.32 g, 1.48 mmol, 26%).

^{1}H NMR (400 MHz, Chloroform-*d*): δ 7.38-7.24 (3H, m, Ar), 7.15 (2H, d, *J* = 7.6 Hz, Ar), 4.91 (1H, s, H7), 4.87 (1H, s, H6), 4.51 (1H, dd, *J* = 7.9, 4.4 Hz, H9), 3.31 (1H, t, *J* = 7.6 Hz, H2), 2.70 (3H, s, H14), 2.46-2.35 (1H, m, H8), 2.10-2.00 (1H, m, H8), 1.78 (3H, s, H4).

^{13}C NMR (101 MHz, Chloroform-*d*): δ 175.0 (C1), 142.4 (C3), 140.9 (C10), 129.1 (C11), 128.0 (C13), 126.2 (C12), 113.8 (C5), 62.8 (C9), 48.6 (C2), 34.5 (C8), 28.5 (C14), 20.1 (C4).

HRMS (ESI^{+}) *m/z* calculated for $C_{14}H_{18}NO$ $[M+H]^{+}$ 216.1383, found 216.1374.

IR: ν_{max} = 2980 (C-H), 2921 (C-H), 1681 (C=O), 1603 (C=C), 1394, 1032.

NOESY for this isomer:

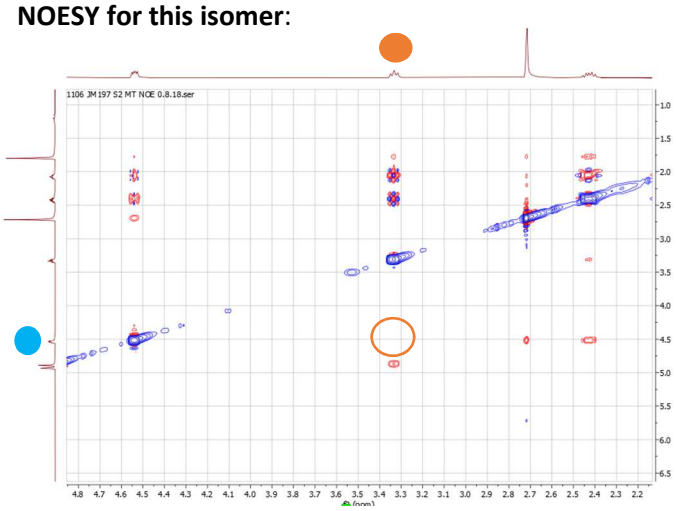

Note that for this isomer, H2 does not correlate with H9, positioning them *trans*- in the stereochemical assignment.

Figure 33: NOESY for trans*-stereoisomer* ***291****.*

N-Methyl-2-phenyl-1-(prop-1-en-2-yl)cyclopropane-1-carboxamide (292)

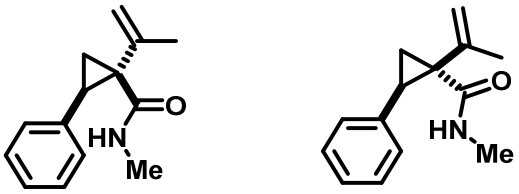

The title compound was synthesised according to General procedure 6b using 1-methyl-5-phenyl-3-(propan-2-ylidene)pyrrolidin-2-one (**290**) (100 mg, 0.46 mmol, 1.0 eq.). Purification with flash column chromatography (20% EtOAc / petroleum ether) afforded a colourless oil as a mixture of isomers of the title compound with a crude dr of 58:42 (67 mg, 0.31 mmol, 67%).

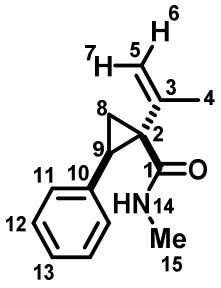

Major Diastereomers

^{1}H NMR (400 MHz, Chloroform-*d*): δ 7.32-7.17 (5H, m, H11-H13), 5.87 (1H, br s, H14), 5.30 (1H, s, H7), 5.18 (1H, s, H6), 2.68 (1H, t, *J* = 9.0 Hz, H9), 2.59 (3H, d, *J* = 4.9 Hz, H15), 2.14 (1H, dd, *J* = 9.0, 4.6 Hz, H8), 1.90 (3H, s, H4), 1.12 (1H, dd, *J* = 9.0, 4.6 Hz, H8).

^{13}C NMR (101 MHz, Chloroform-*d*): δ 169.1 (C1), 146.2 (C3), 137.2 (C10), 128.6 (C11), 128.0 (C13), 126.4 (C12), 115.8 (C5), 41.5 (C2), 31.1 (C9), 26.7 (C15), 21.5 (C4), 15.9 (C8).

HRMS (ESI^{+}) *m/z* calculated for $C_{14}H_{18}NO$ $[M+H]^{+}$ 216.1383, found 216.1373.

IR: ν_{max} = 3351 (N-H), 2980 (C-H), 2922 (C-H), 1641 (C=O), 1519 (C=C), 1032.

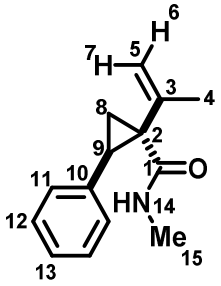

Minor Diastereomers

^{1}H NMR (400 MHz, Chloroform-*d*): δ 7.32-7.17 (3H, m, H12, H13), 7.13 (2H, d, *J* = 7.2 Hz, H11), 6.14 (1H, br s, H14), 5.22 (1H, s, H7), 5.08 (1H, s, H6), 3.16 (1H, dd, *J* = 8.7, 7.7 Hz, H9), 2.86 (3H, d, *J* = 4.9 Hz, H15), 1.67 (1H, dd, *J* = 8.7, 4.7 Hz, H8), 1.55 (1H, dd, *J* = 7.7, 4.7 Hz, H8), 1.43 (3H, s, H4).

^{13}C NMR (101 MHz, Chloroform-*d*): δ 127.3 (C1), 141.0 (C3), 137.5 (C10), 127.9 (C11), 127.9 (C13), 126.2 (C12), 120.8 (C5), 40.4 (C2), 29.2 (C9), 27.0 (C15), 21.9 (C4), 19.4 (C8).

HRMS (ESI^{+}) *m/z* calculated for $C_{14}H_{18}NO$ $[M+H]^{+}$ 216.1383, found 216.1373.

IR: ν_{max} = 3351 (N-H), 2980 (C-H), 2922 (C-H), 1641 (C=O), 1519 (C=C), 1032.

(*Z*)- and (*E*)-3-(3,3-Dimethylbutylidene)-1-methyl-5-phenylpyrrolidin-2-one (294 and 293)

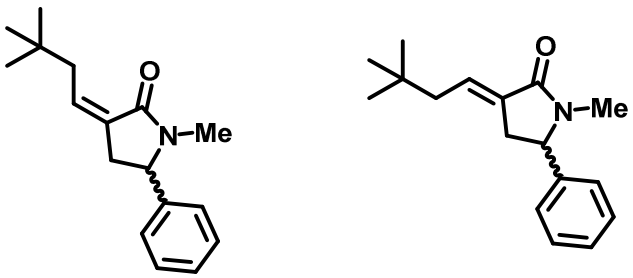

The *E*- and *Z*-isomers of the unsaturated lactam were isolated according to General Procedure 4b and 5 using 1-methyl-5-phenylpyrrolidin-2-one (**254**) (1.00 g, 5.71 mmol, 1.0 eq.) as the lactam and 3,3-dimethylbutyraldehyde (0.86 mL, 6.85 mmol, 1.2 eq.) as the electrophile. Purification was carried out using flash column chromatography (20% EtOAc / petroleum ether) to separate the isomers.

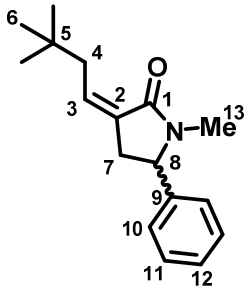

***Z*-Isomers 294**: Orange oil (0.23 g, 0.91 mmol, 16%).

^{1}H NMR (400 MHz, Chloroform-*d*): δ 7.42-7.23 (3H, m, H11, H12), 7.15 (2H, d, *J* = 7.1 Hz, H10), 5.91 (1H, tt, *J* = 8.0, 2.0 Hz, H3), 4.42 (1H, dd, *J* = 8.7, 4.3 Hz, H8), 3.12 (1H, ddd, *J* = 16.4, 8.7, 2.1 Hz, H7), 2.79 (1H, ddt, *J* = 14.5, 8.0, 2.0 Hz, H4), 2.69 (1H, ddt, *J* = 14.5, 8.0, 2.0 Hz, H4), 2.66 (3H, s, H13), 2.51 (1H, dd, *J* = 16.4, 4.3 Hz, H7), 0.92 (9H, s, H6).

^{13}C NMR (101 MHz, Chloroform-*d*): δ 169.2 (C1), 141.5 (C9), 134.6 (C3), 129.7 (C2), 129.0 (C11), 128.1 (C12), 126.4 (C10), 61.6 (C8), 39.9 (C4), 36.7 (C7), 31.5 (C5), 29.3 (C6), 28.2 (C13).

HRMS (ESI^{+}) *m/z* calculated for $C_{17}H_{24}NO$ $[M+H]^{+}$ 258.1852, found 258.1841.

IR: ν_{max} = 2950 (C-H), 2864 (C-H), 1681 (C=O), 1660 (C=C), 1389, 1363, 1067, 1033.

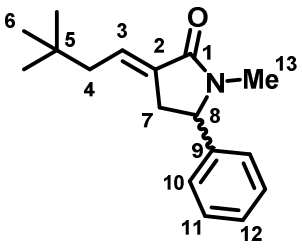

***E*-Isomers 293**: Orange solid (0.93 g, 3.60 mmol, 63%).

^{1}H NMR (400 MHz, Chloroform-*d*): δ 7.39-7.27 (3H, m, H11, H12), 7.17 (2H, d, *J* = 8.2 Hz, H10), 6.62 (1H, tt, *J* = 8.1, 2.8 Hz, H3), 4.49 (1H, dd, *J* = 8.7, 4.1 Hz, H8), 3.11 (1H, ddd, *J* = 17.3, 8.7, 1.5 Hz, H7), 2.74 (3H, s, H13), 2.50 (1H, dd, *J* = 17.3, 4.1 Hz, H7), 1.99 (2H, d, *J* = 8.1 Hz, H4), 0.93 (9H, s, H6).

^{13}C NMR (101 MHz, Chloroform-*d*): δ 169.1 (C1), 141.7 (C9), 131.9 (C2), 130.9 (C3), 129.2 (C11), 128.2 (C12), 126.4 (C10), 61.8 (C8), 43.6 (C4), 33.1 (C7), 32.1 (C5), 29.5 (C6), 28.6 (C13).

HRMS (ESI^{+}) *m/z* calculated for $C_{17}H_{24}NO$ $[M+H]^{+}$ 258.1852, found 258.1840.

MP: 50-51 °C.

IR: ν_{max} = 2953 (C-H), 2865 (C-H), 1685 (C=C), 1663 (C=O), 1392, 1033.

(*E*)-1-Methyl-3-(2-methylpropylidene)-5-phenylpyrrolidin-2-one (296)

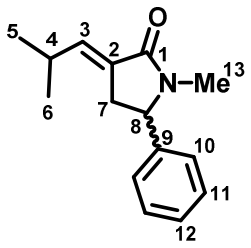

One main isomer of the unsaturated lactam was isolated according to General Procedure 4b and 5 using 1-methyl-5-phenylpyrrolidin-2-one (**254**) (1.00 g, 5.71 mmol, 1.0 eq.) as the lactam and isobutyraldehyde (0.52 mL, 6.85 mmol, 1.2 eq.) as the electrophile. Purification was carried out using flash column chromatography (20% EtOAc / petroleum ether) to afford the title compound as a yellow-orange solid (0.73 g, 3.20 mmol, 56%).

^{1}H NMR (400 MHz, Chloroform-*d*): δ 7.39-7.28 (3H, m, H11, H12), 7.18 (2H, d, *J* = 7.6 Hz, H10), 6.38 (1H, dt, *J* = 9.8, 2.7 Hz, H3), 4.49 (1H, dd, *J* = 8.6, 4.2 Hz, H8), 3.14 (1H, ddd, *J* = 17.0, 8.6, 2.7 Hz, H7), 2.73 (3H, s, H13), 2.52 (1H, ddd, *J* = 17.0, 4.2, 2.7 Hz, H7), 2.47-2.36 (1H, m, H4), 1.03 (3H, d, *J* = 6.9 Hz, H5), 1.01 (3H, d, *J* = 6.9 Hz, H6).

^{13}C NMR (101 MHz, Chloroform-*d*): δ 169.5 (C1), 141.7 (C9), 139.9 (C3), 129.2 (C10), 128.3 (C12), 126.4 (C11), 61.9 (C8), 32.6 (C7), 29.0 (C4), 28.6 (C13), 22.1 (C5), 22.0 (C6).

HRMS (ESI^{+}) *m/z* calculated for $C_{15}H_{20}NO$ $[M+H]^{+}$ 230.1539, found 230.1536.

MP: 48-49 °C.

IR: ν_{max} = 2958 (C-H), 2922 (C-H), 1689 (C=O), 1665 (C=C), 1393, 1032.

1-Methyl-3-(2-methylallyl)-5-phenylpyrrolidin-2-one (300 and 301)

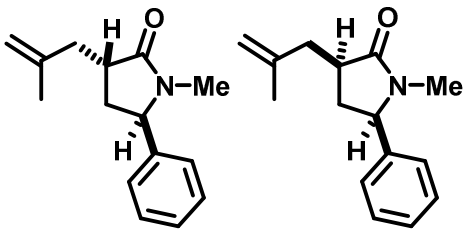

Two main isomers of the unsaturated lactam were isolated according to General Procedure 4b using 1-methyl-5-phenylpyrrolidin-2-one (**254**) (1.00 g, 5.71 mmol, 1.0 eq.) as the lactam and 3-bromo-2-

methylpropene (**299**) (0.69 mL, 6.85 mmol, 1.2 eq.) as the electrophile. Purification was carried out using flash column chromatography (20% EtOAc / petroleum ether) to separate the isomers.

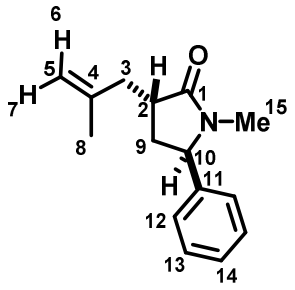

***Trans*-Isomers 300**: Yellow oil (0.33 g, 1.43 mmol, 25%).

^{1}H NMR (400 MHz, Chloroform-*d*): δ 7.38-7.32 (2H, m, H13), 7.31-7.25 (1H, m, H14), 7.20-7.14 (2H, m, H12), 4.75 (1H, br s, H7), 4.68 (1H, br s, H6), 4.47 (1H, dd, *J* = 8.7, 3.8 Hz, H10), 2.83-2.74 (1H, m, H2), 2.71 (3H, s, H15), 2.70-2.65 (1H, m, H3), 2.17 (1H, dt, *J* = 16.4, 8.7 Hz, H9), 2.07-1.96 (2H, m, H3, H9), 1.69 (3H, s, H8).

^{13}C NMR (101 MHz, Chloroform-*d*): δ 177.0 (C1), 143.2 (C4), 141.3 (C11), 129.1 (C12), 128.0 (C14), 126.2 (C13), 112.1 (C5), 62.7 (C10), 39.8 (C3), 38.7 (C2), 34.7 (C9), 28.5 (C15), 22.2 (C8).

HRMS (ESI^{+}) *m/z* calculated for $C_{15}H_{20}NO$ $[M+H]^{+}$ 230.1539, found 230.1529.

IR: ν_{max} = 2980 (C-H), 2966 (C-H), 1687 (C=O), 1642 (C=C), 1393, 1054, 1033.

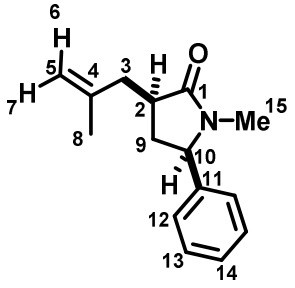

***Cis*-Isomers 301**: Yellow oil (0.25 g, 1.08 mmol, 19%).

^{1}H NMR (400 MHz, Chloroform-*d*): δ 7.40-7.34 (2H, m, H13), 7.32-7.28 (1H, m, H14), 7.20-7.17 (2H, m, H12), 4.72 (1H, br s, H7), 4.65 (1H, br s, H6), 4.39 (1H, dd, *J* = 8.6, 7.6 Hz, H10), 2.84-2.76 (1H, dd, *J* = 14.6, 4.0 Hz, H3), 2.72-2.64 (1H, m, H2), 2.63 (3H, s, H15), 2.61-2.53 (1H, m, H9), 2.05 (1H, dd, *J* = 14.6, 10.9 Hz, H3), 1.72 (3H, s, H8), 1.56-1.47 (1H, m, H9).

^{13}C NMR (101 MHz, Chloroform-*d*): δ 177.7 (C1), 143.3 (C4), 141.1 (C11), 129.1 (C12), 128.2 (C14), 126.8 (C13), 111.3 (C5), 63.2 (C10), 40.4 (C2), 40.2 (C3), 36.4 (C9), 28.6 (C15), 22.8 (C8).

HRMS (ESI$^+$) *m/z* calculated for $C_{15}H_{20}NO$ $[M+H]^+$ 230.1539, found 230.1529.

IR: ν_{max} = 2981 (C-H), 2972 (C-H), 1668 (C=O), 1605 (C=C), 1454, 1055.

NOESY for diastereomers 301:

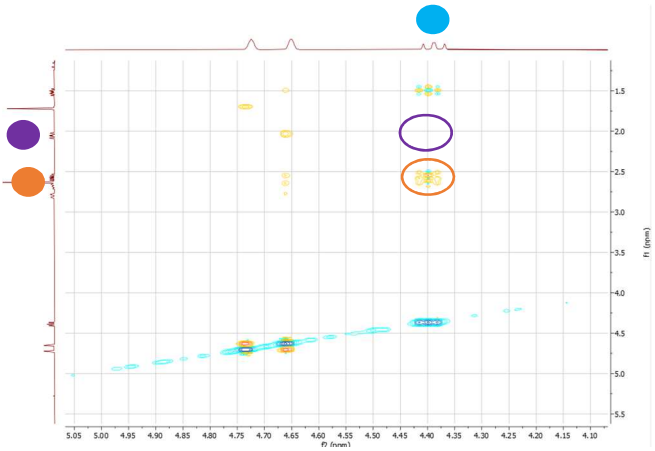

Note that for diastereomers **301**, H2 has a correlation to H10, and no correlation between H10 and H3, indicating a *cis*-relationship.

Figure 34: NOESY for cis*-diastereomers* ***301****.*

(3*R*,5*R*)-1-Methyl-3-(2-methylprop-1-en-1-yl)-5-phenylpyrrolidin-2-one (302)

To a stirred solution of *trans*-1-methyl-3-(2-methylallyl)-5-phenylpyrrolidin-2-one (**300**) (100 mg, 0.44 mmol, 1.0 eq.) in $CHCl_3$ (2 mL) was added a few crystals of *p*-toluenesulfonic acid monohydrate. The mixture was heated to 60 °C for 4 h before being cooled to rt. Water (10 mL) was added, and the aqueous layer extracted with CH_2Cl_2 (3 × 10 mL). Combined organics were washed with brine (10 mL), dried over $MgSO_4$, filtered and concentrated *in vacuo*. Purification by flash column chromatography (10% EtOAc / petroleum ether) afforded the title compound as a colourless oil (55 mg, 0.24 mmol, 55%).

^{1}H NMR (400 MHz, Chloroform-*d*): δ 7.43-7.31 (3H, m, H11, H12), 7.22-7.15 (2H, m, H10), 5.18 (1H, dsept, *J* = 8.7, 1.4 Hz, H3), 4.55 (1H, dd, *J* = 8.4, 3.7 Hz, H8), 3.52 (1H, q, *J* = 8.7 Hz, H2), 2.76 (3H, s, H13), 2.26-2.14 (2H, m, H7), 1.78 (3H, s, H6), 1.70 (3H, s, H5).

^{13}C NMR (101 MHz, Chloroform-*d*): δ 176.6 (C1), 141.2 (C8), 136.5 (C4), 129.2 (C11), 128.0 (C12), 126.2 (C10), 122.2 (C3), 62.8 (C8), 40.3 (C2), 36.6 (C7), 28.8 (C13), 25.9 (C6), 18.5 (C5).

HRMS (ESI$^+$) *m/z* calculated for $C_{15}H_{20}NO$ $[M+H]^+$ 230.1539, found 230.1546.

IR: ν_{max} = 2987 (C-H), 2981 (C-H), 1675 (C=O), 1600 (C=C), 1460, 1070.

N-Methyl-1-(2-methylprop-1-en-1-yl)-2-phenylcyclopropane-1-carboxamide (297)

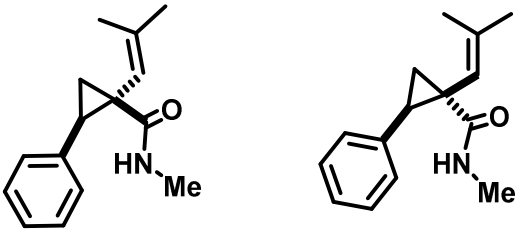

The title compound was synthesised according to General procedure 6b using (3*R*,5*R*)-1-methyl-3-(2-methylprop-1-en-1-yl)-5-phenylpyrrolidin-2-one (**302**) (100 mg, 0.44 mmol, 1.0 eq.). Purification with flash column chromatography (20% EtOAc / petroleum ether) afforded a colourless oil as a mixture of isomers of the title compound with a crude dr of 57:43 (63 mg, 0.27 mmol, 63%).

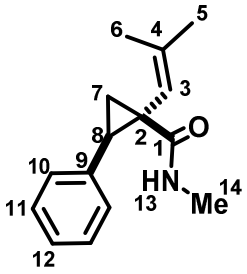

Major Diastereomers

^{1}H NMR (400 MHz, Chloroform-*d*): δ 7.32-7.17 (4H, m, H10, H11), 7.07 (1H, d, *J* = 7.5 Hz, H12), 6.22 (1H, br s, H13), 4.96 (1H, s, H3), 2.91 (1H, dd, *J* = 9.1, 7.0 Hz, H8), 2.85 (3H, d, *J* = 4.8 Hz, H14), 2.02 (1H, dd, *J* = 9.1, 4.1 Hz, H7), 1.67 (3H, s, H5), 1.56 (3H, s, H6), 1.27-1.22 (1H, m, H7).

^{13}C NMR (101 MHz, Chloroform-*d*): δ 173.6 (C1), 144.02 (C9), 137.6 (C10), 129.1 (C11), 128.5 (C12), 127.8 (C4), 119.8 (C3), 34.7 (C2), 31.9 (C8), 27.0 (C14), 25.2 (C5), 21.5 (C7), 19.5 (C6).

HRMS (ESI$^+$) *m/z* calculated for $C_{15}H_{20}NO$ $[M+H]^+$ 230.1539, found 230.1531.

IR: ν_{max} = 3350 (N-H), 2982 (C-H), 2980 (C-H), 1664 (C=O), 1623 (C=C), 1235, 1160.

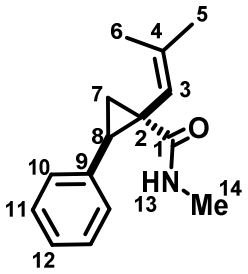

Minor Diastereomers

^{1}H NMR (400 MHz, Chloroform-*d*): δ 7.32-7.17 (4H, m, H10, H11), 7.07 (1H, d, *J* = 7.5 Hz, H12), 5.93 (1H, br s, H9), 5.55 (1H, br s, H3), 2.63 (3H, d, *J* = 4.9 Hz, H14), 2.43 (1H, t, *J* = 8.1 Hz, H8), 2.25 (1H, dd, *J* = 8.1, 4.5 Hz, H7), 1.85 (3H, s, H5), 1.82 (3H, s, H6), 1.27-1.22 (1H, m, H7).

^{13}C NMR (101 MHz, Chloroform-*d*): δ 170.7 (C1), 141.2 (C9), 137.4 (C10), 127.9 (C11), 126.4 (C12), 126.2 (C4), 125.1 (C3), 33.2 (C2), 31.7 (C8), 26.8 (C14), 25.5 (C5), 20.0 (C7), 19.6 (C6).

HRMS (ESI^{+}) *m/z* calculated for $C_{15}H_{20}NO$ $[M+H]^{+}$ 230.1539, found 230.1533.

IR: ν_{max} = 3350 (N-H), 2982 (C-H), 2980 (C-H), 1664 (C=O), 1623 (C=C), 1235, 1160.

(3*R*,5*S*)-3-(Cyclohex-1-en-1-yl)-1-methyl-5-phenylpyrrolidin-2-one (304)

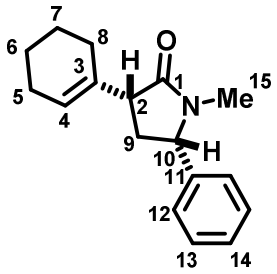

The title isomer of the unsaturated lactam was isolated according to General Procedure 4b and 5 using 1-methyl-5-phenylpyrrolidin-2-one (**254**) (1.00 g, 5.71 mmol, 1.0 eq.) as the lactam and cyclohexanone (0.71 mL, 6.85 mmol, 1.2 eq.) as the electrophile, with an extended elimination (GP5) reaction time of 3 days to push conversion. This gave a mixture of eliminated product with some unreacted alcohol intermediate. To purify via isomerisation, the mixture was subjected to General Procedure 6b, without LED irradiation. This converted all eliminated product into the title compound. Purification was carried out using flash column chromatography (15% EtOAc / petroleum ether) to afford the title compound as a yellow oil (0.84 g, 3.31 mmol, 58%).

^{1}H NMR (400 MHz, Chloroform-*d*): δ 7.40-7.28 (3H, m, H13, H14), 7.22 (2H, d, *J* = 8.0 Hz, H12), 5.68-5.64 (1H, br m, H4), 4.36 (1H, t, *J* = 8.9 Hz, H10), 3.16 (1H, t, *J* = 10.1 Hz, H2), 2.62 (3H, s, H11), 2.54 (1H, ddd, *J* = 13.3, 10.1, 8.9 Hz, H9), 2.15-1.93 (4H, m, H5, H8), 1.80 (1H, ddd, *J* = 13.3, 10.1, 8.9 Hz, H9), 1.71-1.50 (4H, m, H6, H7).

^{13}C NMR (101 MHz, Chloroform-*d*): δ 175.8 (C1), 141.0 (C11), 134.5 (C3), 129.0 (C13), 128.1 (C14), 126.8 (C12), 125.9 (C4), 62.8 (C10), 50.4 (C2), 35.2 (C9), 28.7 (C15), 25.4 (C8), 25.3 (C5), 22.7 (C7), 22.2 (C6).

HRMS (ESI^{+}) *m/z* calculated for $C_{17}H_{22}NO$ $[M+H]^{+}$ 256.1696, found 256.1684.

IR: ν_{max} = 2924 (C-H), 2864 (C-H), 1667 (C=O), 1665 (C=C), 1454, 1032.

NOESY for diastereomers 254:

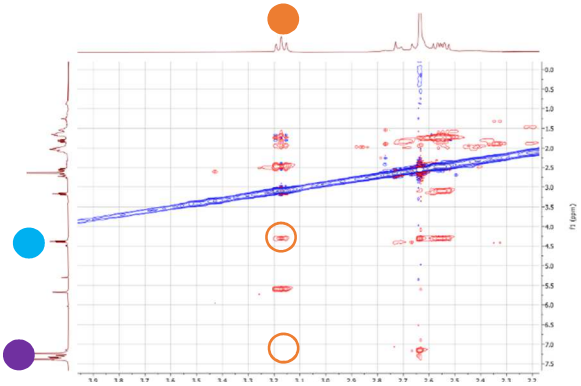

Note that for diastereomers **304**, H2 correlates with H10 but not to the aromatic ring, confirming the relative stereochemistry.

*Figure 35: NOESY for **304**, showing a* cis*-relationship across the lactam.*

1-(Cyclohex-1-en-1-yl)-*N*-methyl-2-phenylcyclopropane-1-carboxamide (305)

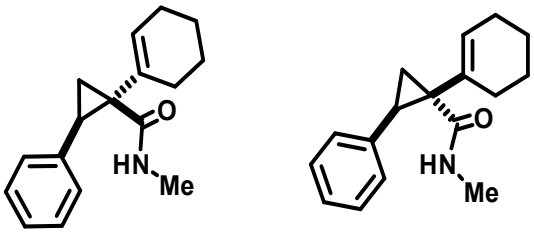

The title compound was synthesised according to General procedure 6b using 1-methyl-5-phenyl-3-(propan-2-ylidene)pyrrolidin-2-one (**304**) (100 mg, 0.39 mmol, 1.0 eq.). Purification with flash column chromatography (20% EtOAc / petroleum ether) afforded a colourless oil as a mixture of isomers of the title compound with a crude dr of 58:42 (60 mg, 0.23 mmol, 60%).

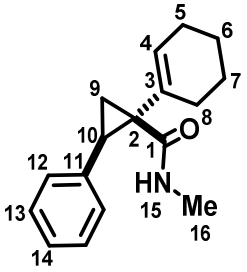

Major Diastereomers

^{1}H NMR (400 MHz, Chloroform-*d*): δ 7.33-7.14 (5H, m, H12-H14), 6.07-6.02 (1H, br m, H4), 5.87 (1H, br s, H15), 2.63 (1H, dd, *J* = 9.0, 6.9 Hz, H10), 2.59 (3H, d, *J* = 4.9 Hz, H16), 2.24-1.97 (5H, m, H5, H8, H9), 1.75-1.57 (4H, m, H6, H7), 1.07 (1H, dd, *J* = 9.0, 4.9 Hz, H9).

^{13}C NMR (101 MHz, Chloroform-*d*): δ 169.9 (C1), 138.8 (C3), 137.5 (C11), 128.7 (C12), 127.7 (C4), 127.7 (C13), 126.3 (C14), 41.5 (C2), 30.7 (C10), 27.7 (C5), 26.8 (C16), 25.5 (C8), 23.0 (C7), 22.3 (C6), 15.7 (C9).

HRMS (ESI^{+}) *m/z* calculated for $C_{17}H_{22}NO$ $[M+H]^{+}$ 256.1696, found 256.1684.

IR: ν_{max} = 3348 (N-H), 2924 (C-H), 2861 (C-H), 1649 (C=O), 1516 (C=C), 1053, 1033.

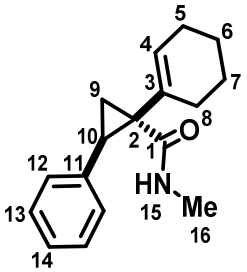

Minor Diastereomers

^{1}H NMR (400 MHz, Chloroform-*d*): δ 7.33-7.14 (3H, m, H13, H14), 7.09 (2H, d, *J* = 7.7 Hz, H12), 6.08 (1H, br s, H15), 5.84-5.79 (1H, br m, H4), 3.11 (1H, dd, *J* = 9.2, 7.3 Hz, H10), 2.86 (3H, d, *J* = 4.9 Hz, H16), 2.24-1.97 (4H, m, H5, H8), 1.75-1.57 (3H, m, H7, H9), 1.51 (1H, dd, *J* = 7.3, 4.3 Hz, H9), 1.46-1.35 (2H, m, H6).

^{13}C NMR (101 MHz, Chloroform-*d*): δ 173.2 (C1), 138.0 (C11), 133.3 (C3), 132.7 (C4), 127.9 (C12), 127.8 (C13), 126.0 (C14), 40.5 (C2) 28.8 (C10), 28.2 (C5), 27.1 (C16), 25.6 (C8), 22.8 (C7), 22.0 (C6), 19.5 (C9).

HRMS (ESI^{+}) *m/z* calculated for $C_{17}H_{22}NO$ $[M+H]^{+}$ 256.1696, found 256.1684.

IR: ν_{max} = 3348 (N-H), 2924 (C-H), 2861 (C-H), 1649 (C=O), 1516 (C=C), 1053, 1033.

(*R*)-1-(1-Phenylethyl)pyrrolidine-2,5-dione (308)

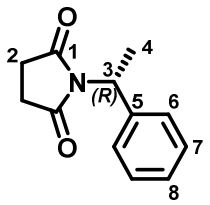

Synthesised according to modified procedure by Butters *et al.*[100]

To a solution of succinic anhydride (**307**) (5.35 g, 53.49 mmol, 1.0 eq.) in toluene (125 mL) was added (*R*)-α-methylbenzylamine (**306**) (6.90 mL, 53.49 mmol, 1.0 eq.) and the mixture heated to reflux for 16 h. The solvent was removed *in vacuo* and the resulting residue was redissolved in acetic anhydride (50 mL) and heated to reflux for 2 h. The solution was carefully poured onto ice and extracted with CH_2Cl_2 (3 × 30 mL). The combined organics were washed with saturated $NaHCO_3$ (3 × 50 mL), dried over $MgSO_4$, filtered and concentrated *in vacuo*. Purification by flash column chromatography (20% EtOAc / petroleum ether) afforded the title compound as an orange oil (7.82 g, 38.51 mmol, 72%).

^{1}H NMR (400 MHz, Chloroform-*d*): δ 7.45 (2H, d, *J* = 7.1 Hz, H6), 7.35-7.24 (3H, m, H7, H8), 5.42 (1H, q, *J* = 7.4 Hz, H3), 2.64 (4H, s, H2), 1.81 (3H, d, *J* = 7.4 Hz, H4).

^{13}C NMR (101 MHz, Chloroform-*d*): δ 177.1 (C1), 139.7 (C5), 128.6 (C7), 128.0 (C8), 127.8 (C6), 50.5 (C3), 28.2 (C2), 16.7 (C4).

Data consistent with literature.[100]

(*R*)-5-Phenyl-1-(1-phenylethyl)pyrrolidine-2-one (310)

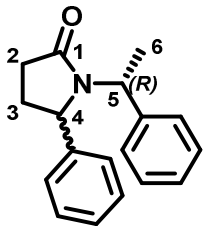

Synthesised according to modified procedures by Butters *et al.*[100] and Zhang *et* al.[101]

To a solution of (*R*)-1-(1-Phenylethyl)pyrrolidine-2,5-dione (**308**) (4.00 g, 19.70 mmol, 1.0 eq.) in anhydrous THF (50 mL) was added $LiEt_3BH$ (28.00 mL, 27.58 mmol, 1.4 eq., 1 M in THF) at −78 °C slowly. After 1 h at −78 °C, the reaction was quenched in an ice bath with saturated $NaHCO_{3(aq.)}$ until effervescence ceased. The mixture was extracted with CH_2Cl_2 (3 × 30 mL) before combined organics

were washed with saturated $NaHCO_{3(aq.)}$ (30 mL), brine (30 mL), dried over $MgSO_4$, filtered and concentrated *in vacuo*. This gave a white wax as the alcohol intermediate product (**309**).

To triflic acid (17.00 mL, 197.00 mmol, 10 eq.) was added a solution of alcohol (**309**) in benzene (35 mL) slowly before being heated to 80 °C for 2 h. The reaction mixture was cooled to rt and water was added cautiously until effervescence ceased. The mixture was extracted with EtOAc (3 × 30 mL) before organics were washed with brine (30 mL), dried over $MgSO_4$, filtered and concentrated *in vacuo*. Purification by flash column chromatography (20% EtOAc / petroleum ether) afforded the title compound as a yellow liquid (0.76 g, 2.96 mmol, 15%) with a dr of 68:32 for D1:D2. D1 and D2 refer to the diastereomer of product.

^{1}H NMR (400 MHz, Chloroform-*d*): δ 7.36-7.28 (4H, m, Ar), 7.20-7.08 (13H, m, Ar), 7.03-6.99 (3H, m, Ar), 5.54 (1H, q, *J* = 7.6 Hz, H5 D2), 4.83 (1H, q, *J* = 7.3 Hz, H5 D1), 4.63 (1H, dd, *J* = 7.9, 5.3 Hz, H4 D1), 4.26 (1H, dd, *J* = 8.7, 3.2 Hz, H4 D2), 2.73 (1H, dt, *J* = 16.9, 7.9 Hz, H2 D2), 2.67-2.57 (1H, m, H2 D1), 2.47-2.36 (3H, m, H2 D1, H2 D2, H3 D1), 2.35-2.23 (1H, m, H3 D2), 1.91-1.76 (2H, m, H3 D1, H3 D2), 1.69 (3H, d, *J* = 7.6 Hz, H6 D1), 1.13 (3H, d, *J* = 7.3 Hz, H6 D2).

^{13}C NMR (101 MHz, Chloroform-*d*): δ 176.0 (C1 D1), 175.6 (C1 D2), 143.6 (Ar), 141.8 (Ar), 141.3 (Ar), 140.2 (Ar), 128.8 (Ar), 128.6 (Ar), 128.5 (Ar), 128.1 (Ar), 127.9 (Ar), 127.7 (Ar), 127.7 (Ar), 127.6 (Ar), 127.6 (Ar), 127.1 (Ar), 126.8 (Ar), 126.6 (Ar), 62.6 (C4 D1), 60.5 (C4 D2), 52.5 (C5 D1), 50.9 (C5 D2), 31.1 (C2 D1), 30.1 (C2 D2), 29.3 (C3 D1), 29.1 (C3 D2), 17.9 (C6 D2), 17.7 (C6 D1).

HRMS (ESI^+) *m/z* calculated for $C_{18}H_{20}NO$ $[M+H]^+$ 266.1539, found 266.1533.

IR: ν_{max} = 2973 (C-H), 2866 (C-H), 1677 (C=O), 1603 (C=C), 1493 (C=C), 1054, 697.

(*Z,R*) and (*E,R*)-3-Ethylidene-5-phenyl-1-(1-phenylethyl)pyrrolidin-2-one (311 and 312)

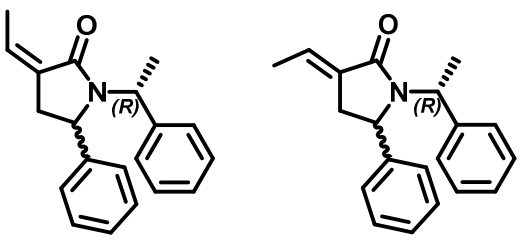

The *E*- and *Z*-isomers of the unsaturated lactam were isolated as mixtures of diastereomers according to General Procedure 4b and 5 using (*R*)-5-phenyl-1-(1-phenylethyl)pyrrolidine-2-one (**310**) (0.56 g, 2.11 mmol, 1.0 eq.) as the lactam and acetaldehyde (**13**) (0.14 mL, 2.53 mmol, 1.2 eq.) as the

electrophile. Purification was carried out using flash column chromatography (0-20% EtOAc / petroleum ether) to separate the isomers.

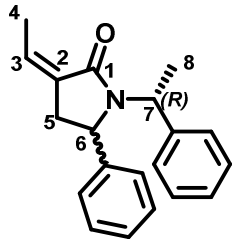

***Z*-Isomers 311**: Orange oil (59 mg, 0.21 mmol, 10%). Isolated with a dr of 63:37 for D1:D2 where D1 and D2 refer to the diastereomer of product.

^{1}H NMR (400 MHz, Chloroform-*d*): δ 7.36-7.27 (4H, m, Ar), 7.18-7.07 (13H, m, Ar), 7.04-7.00 (3H, m, Ar), 5.98-5.89 (2H, m, H3 D1, H3 D2), 5.58 (1H, q, *J* = 7.4 Hz, H7 D2), 4.90 (1H, q, *J* = 7.3 Hz, H7 D1), 4.58 (1H, dd, *J* = 8.8, 4.2 Hz, H6 D1), 4.18 (1H, dd, *J* = 9.1, 2.5 Hz, H6 D2), 3.07 (1H, ddt, *J* = 16.2, 8.6, 2.5 Hz, H5 D1), 3.02-2.95 (1H, m, H5 D2), 2.52-2.46 (1H, m, H5 D1), 2.44-2.38 (1H, m, H5 D2), 2.29 (3H, ddd, *J* = 7.2, 1.6, 1.0 Hz, H4 D2), 2.25 (3H, dt, *J* = 7.3, 2.3 Hz, H4 D1), 1.70 (3H, d, *J* = 7.3 Hz, H8 D1), 1.10 (3H, d, *J* = 7.4 Hz, H8 D2).

^{13}C NMR (101 MHz, Chloroform-*d*): δ 169.7 (C1 D1), 169.2 (C1 D2), 143.9 (Ar), 142.1 (Ar), 141.3 (Ar), 140.2 (Ar), 132.2 (C3 D2), 131.8 (C3 D1), 129.9 (C2 D1), 129.5 (C2 D2), 128.7 (Ar), 128.6 (Ar), 128.5 (Ar), 128.1 (Ar), 127.9 (Ar), 127.9 (Ar), 127.7 (Ar), 127.6 (Ar), 127.6 (Ar), 127.0 (Ar), 126.7 (Ar), 126.6 (Ar), 59.4 (C6 D1), 57.4 (C6 D2), 52.6 (C7 D1), 50.7 (C7 D2), 37.4 (C5 D2), 37.3 (C5 D1), 17.7 (C8 D2), 17.6 (C8 D1), 13.5 (C4 D2), 13.5 (C4 D1).

HRMS (ESI^{+}) *m/z* calculated for $C_{20}H_{22}NO$ $[M+H]^{+}$ 291.1618, found 291.1612 and 291.1612 for each diastereomer.

IR: ν_{max} = 2973 (C-H), 2923 (C-H), 2865 (C-H), 1683 (C=O), 1662 (C=C), 1603 (C=C), 1402, 1054.

$[\boldsymbol{\alpha}]_{\boldsymbol{D}}^{\mathbf{21}}$**:** +43 (*c* 1.2, $CHCl_3$).

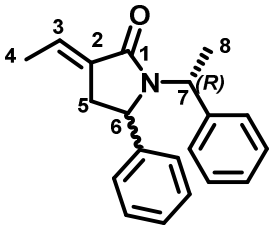

***E*-Isomers 312**: Orange oil (0.30 g, 1.06 mmol, 50%). Isolated with a dr of 60:40 for D1:D2 where D1 and D2 refer to the diastereomer of product.

^{1}H NMR (400 MHz, Chloroform-*d*): δ 7.35-7.27 (4H, m, Ar), 7.21-7.02 (16H, m, Ar), 6.69-6.63 (1H, m, H3 D2), 6.63-6.57 (1H, m, H3 D1), 5.60 (1H, q, *J* = 7.2 Hz, H7 D2), 4.83 (1H, q, *J* = 7.4 Hz, H7 D1), 4.62 (1H, dd, *J* = 9.0, 4.2 Hz, H6 D1), 4.23 (1H, dd, *J* = 9.0, 2.8 Hz, H6 D2), 3.07 (1H, ddd, *J* = 17.4, 8.3, 2.1 Hz, H5 D1), 2.94 (1H, ddd, *J* = 17.0, 9.0, 2.3 Hz, H5 D2), 2.53-2.44 (2H, m, H5 D1, H5 D2), 1.76-1.71 (3H, m, H4 D1, H4 D2, H8 D1), 1.10 (3H, d, *J* = 7.4 Hz, H8 D2).

^{13}C NMR (101 MHz, Chloroform-*d*): δ 169.3 (C1 D1), 168.9 (C1 D2), 144.2 (Ar), 142.4 (Ar), 141.5 (Ar), 140.0 (Ar), 132.3 (C2 D1), 131.8 (C2 D2), 128.8 (Ar), 128.7 (Ar), 128.7 (C3 D2), 128.5 (C3 D1), 128.2 (Ar), 128.1 (Ar), 128.1 (Ar), 128.0 (Ar), 127.8 (Ar), 127.7 (Ar), 127.6 (Ar), 127.1 (Ar), 126.8 (Ar), 126.8 (Ar), 59.7 (C6 D1), 57.7 (C6 D2), 53.1 (C7 D1), 51.3 (C7 D2), 33.6 (C5 D2), 33.5 (C5 D1), 17.8 (C8 D1), 17.7 (C8 D2), 14.8 (C4 D2), 14.7 (C4 D1).

HRMS (ESI$^+$) *m/z* calculated for $C_{20}H_{22}NO$ $[M+H]^+$ 291.1618, found 291.1612 and 291.1612 for each diastereomer.

IR: ν_{max} = 2937 (C-H), 2865 (C-H), 1691 (C=O), 1667 (C=C), 1603 (C=C), 1335, 1055.

$[\alpha]_D^{21}$: +43 (*c* 1.2, $CHCl_3$).

2-(4-Methoxyphenyl)-*N*-methyl-1-vinylcyclopropane-1-carboxamide (313, 314, 315 and 316)

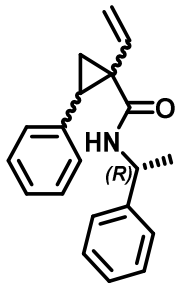

The title compound was synthesised according to General procedure 6b using a mixture of diastereomers of (*E,R*)-3-ethylidene-5-phenyl-1-(1-phenylethyl)pyrrolidin-2-one (**312**) (100 mg, 0.34 mmol, 1.0 eq.). Purification with flash column chromatography (15% EtOAc / petroleum ether) afforded a colourless oil as a mixture of four isomers of the title compound with a crude dr of approximately 36:27:19:18 (60 mg, 0.20 mmol, 60%). The two major diastereomers were the *S*,*R* and the *R*,*S* isomers (**313** and **314**) assigned by NOESY analysis. However, distinguishing between the two are not possible and are reported together here. D1 and D2 refer to the diastereomer of product.

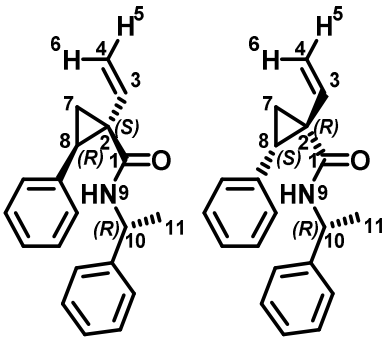

Major Diastereomers 313 and 314

^{1}H NMR (400 MHz, Chloroform-*d*): δ 7.43-7.09 (16H, m, Ar), 6.81-6.75 (4H, m, Ar), 6.12 (1H, dd, *J* = 17.2, 10.5 Hz, H3 D1), 6.05 (1H, dd, *J* = 16.8, 10.1 Hz, H3 D2), 5.69 (2H, br s, H9 D1, H9 D2), 5.40-5.14 (4H, m, H5 D1, H5 D2, H6 D1, H6 D2), 4.96-4.84 (2H, m, H10 D1, H10 D2), 2.63-2.56 (2H, m, H8 D1, H8 D2), 2.23-2.17 (2H, m, H7 D1, H7 D2), 1.39 (3H, d, *J* = 7.0 Hz, H11 D1), 1.35-1.29 (2H, m, H7 D1, H7 D2), 0.99 (3H, d, *J* = 7.0 Hz, H11 D2).

^{13}C NMR (101 MHz, Chloroform-*d*): δ 167.7 (C1 D1), 167.6 (C1 D2), 143.1 (Ar), 142.6 (Ar), 139.0 (C3 D1), 138.8 (C3 D2), 136.7 (Ar), 136.4 (Ar), 128.9 (Ar), 128.7 (Ar), 128.4 (Ar), 128.4 (Ar), 128.3 (Ar), 128.3 (Ar), 127.3 (Ar), 126.9 (Ar), 126.7 (Ar), 126.2 (Ar), 126.1 (Ar), 126.0 (Ar), 115.6 (C4 D1), 115.6 (C4 D2), 48.8 (C10 D1/D2), 48.6 (C10 D1/D2), 38.3 (C2 D1/D2), 38.1 (C2 D1/D2), 32.5 (C8 D1/D2), 32.2 (C8 D1/D2), 21.1 (C11 D2), 21.0 (C11 D1), 17.4 (C7 D1/D2), 17.3 (C7 D1/D2).

HRMS (ESI^{+}) *m/z* calculated for $C_{20}H_{22}NO$ $[M+H]^{+}$ 291.1618, found 291.1614 and 291.1614 for each diastereomer.

IR: ν_{max} = 3283 (N-H), 2950 (C-H), 2937 (C-H), 2866 (C-H), 1645 (C=O), 1634 (C=C), 1495 (C=C), 1453, 1054, 695.

$[\alpha]_D^{24}$**:** +65 (*c* 1.1, $CHCl_3$).

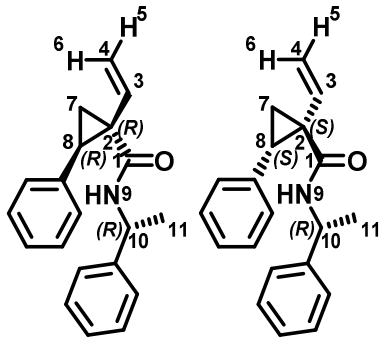

Minor Diastereomers 315 and 316

^{1}H NMR (400 MHz, Chloroform-*d*): δ 7.42-7.09 (20H, m, Ar), 6.26 (2H, br s, H9 D1, H9 D2), 5.76-5.62 (2H, m, H3 D1, H3 D2), 5.40-5.14 (6H, m, H5 D1, H5 D2, H6 D1, H6 D2, H10 D1, H10 D2), 3.09 (2H, q, *J* = 7.8 Hz, H8 D1, H8 D2), 1.87-1.77 (2H, m, H7 D1, H7 D2), 1.58-1.49 (8H, m, H7 D1, H7 D2, H11 D1, H11 D2).

^{13}C NMR (101 MHz, Chloroform-*d*): δ 171.3 (C1 D1), 171.3 (C1 D2), 143.5 (Ar), 143.5 (Ar), 136.7 (Ar), 136.7 (Ar), 133.3 (C3 D1/D2), 133.3 (C3 D1/D2), 128.8 (Ar), 128.8 (Ar), 128.3 (Ar), 128.0 (Ar), 128.0 (Ar), 127.4 (Ar), 127.4 (Ar), 127.3 (Ar), 126.5 (Ar), 126.4 (Ar), 126.1 (Ar), 126.0 (Ar), 123.6 (C4 D1/D2), 123.5 (C4 D1/D2), 49.4 (C10 D1/D2), 49.4 (C10 D1/D2), 35.2 (C2 D1/D2), 35.1 (C2 D1/D2), 30.7 (C8 D1/D2), 30.7 (C8 D1/D2), 22.3 (C11 D1/D2), 22.2 (C11 D1/D2), 18.5 (C7 D1/D2), 18.5 (C7 D1/D2).

HRMS (ESI^{+}) *m/z* calculated for $C_{20}H_{22}NO$ $[M+H]^{+}$ 291.1618, found 291.1615 and 291.1615 for each diastereomer.

IR: ν_{max} = 3283 (N-H), 2950 (C-H), 2937 (C-H), 2866 (C-H), 1645 (C=O), 1634 (C=C), 1495 (C=C), 1453, 1054, 695.

$[\alpha]_D^{24}$**:** +65 (*c* 1.1, $CHCl_3$).

NOESY for the mixture:

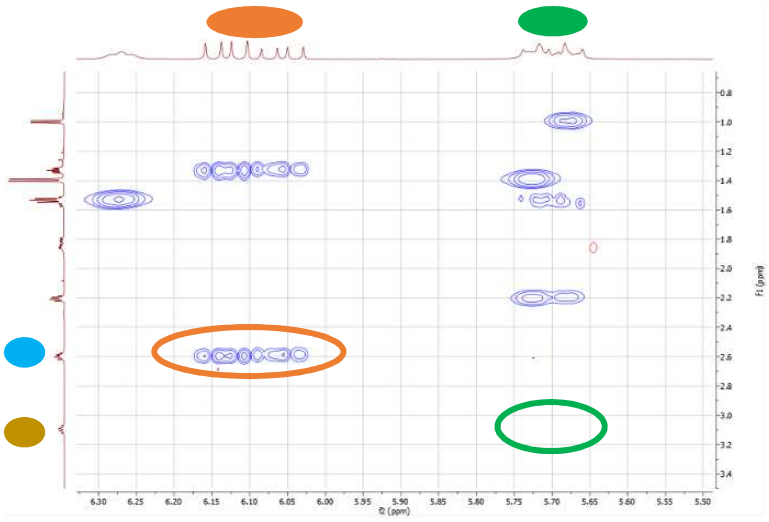

Note that for the major two diastereomers, their alkene protons H3 correlates to the adjacent benzylic proton H8; whilst for the minor diastereomers, the alkene protons H3 doesn't see its' adjacent benzylic proton H8.

*Figure 36: NOESY of the mixture of diastereomers **313**, **314**, **315** and **316**.*

1-Methyl-5-oxo-2-phenylpyrrolidine-3-carboxylic acid (319)

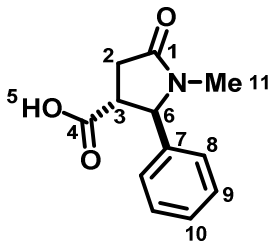

Synthesised according to the procedure by Piwowarczyk *et al*.[102]

To a solution of *N*-methyl-1-phenylmethanimine (**318**) (5.20 mL, 42.00 mmol, 1.0 eq.) in toluene (200 mL) was added succinic anhydride (**307**) (4.20 g, 42.00 mmol, 1.0 eq.) and the mixture heated to reflux for 16 h. After cooling to rt, solvent was removed *in vacuo*. CH_2Cl_2 (30 mL) was added and the mixture basified with saturated $NaHCO_{3(aq.)}$ until pH 10. The aqueous layer was extracted with CH_2Cl_2 (3 × 30 mL) before the aqueous layer was acidified with $HCl_{(aq.)}$ (3 M) until pH 2. The mixture was extracted with CH_2Cl_2 (3 × 30 mL), dried over $MgSO_4$, filtered and concentrated *in vacuo* to afford the title compound as a white solid (3.26 g, 14.70 mmol, 35%). Only the *trans*-isomer **319** was observed, as in literature.[102]

^{1}H NMR (400 MHz, Chloroform-*d*): δ 9.68 (1H, br s, H5), 7.42-7.32 (3H, m, H9, H10), 7.26-7.21 (2H, m, H8), 4.85 (1H, d, *J* = 5.8 Hz, H6), 3.12-3.04 (1H, m, H3), 3.00-2.80 (2H, m, H2), 2.68 (3H, s, H11).

^{13}C NMR (101 MHz, Chloroform-*d*): δ 175.6 (C4), 174.0 (C1), 139.1 (C7), 129.4 (C9), 128.8 (C10), 126.7 (C8), 66.8 (C6), 46.0 (C3), 33.6 (C2), 28.6 (C11).

Data consistent with literature.[102]

4-(Hydroxymethyl)-1-methyl-5-phenylpyrrolidin-2-one (320)

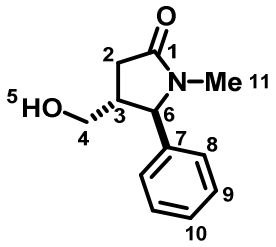

To a solution of 1-methyl-5-oxo-2-phenylpyrrolidine-3-carboxylic acid (**319**) (2.55 g, 11.64 mmol, 1.0 eq.) in MeOH (150 mL) was added conc. H_2SO_4 (2 mL) and the mixture heated to reflux for 16 h. The solvent was removed *in vacuo* before careful addition of saturated $NaHCO_{3(aq.)}$ until effervescence

ceased. The mixture was extracted with CH_2Cl_2 (3 × 30 mL) before the combined organics were washed with saturated $NaHCO_{3(aq.)}$ (30 mL), dried over $MgSO_4$, filtered and concentrated *in vacuo* to give the corresponding methyl ester which was used directly in the next step.

The residue was dissolved in MeOH (100 mL) before slow addition of $LiBH_4$ (0.50 g, 23.28 mmol, 2.0 eq.). The mixture was heated to reflux for 1 h and stirred at rt for 16 h before solvent was removed *in vacuo*. Water (30 mL) was added and the aqueous layer extracted with CH_2Cl_2 (3 × 30 mL). The combined organics were washed with brine (30 mL), dried over $MgSO_4$, filtered and concentrated *in vacuo* to afford the title alcohol as a yellow oil (2.10 g, 10.13 mmol, 87%) which was used without further purification.

^{1}H NMR (400 MHz, Chloroform-*d*): δ 7.40-7.27 (3H, m, H9, H10), 7.19 (2H, d, *J* = 7.5 Hz, H8), 4.41 (1H, d, *J* = 5.1 Hz, H6), 3.66 (2H, t, *J* = 5.3 Hz, H4), 3.08 (1H, br s, H5), 2.67-2.61 (1H, m, H2), 2.65 (3H, s, H11), 2.37-2.30 (2H, m, H2, H3).

^{13}C NMR (101 MHz, Chloroform-*d*): δ 175.0 (C1), 140.5 (C7), 129.2 (C9), 128.2 (C10), 126.6 (C8), 67.0 (C6), 63.3 (C4), 43.9 (C3), 33.2 (C2), 28.4 (C11).

HRMS (ESI^+) *m/z* calculated for $C_{12}H_{16}NO_2$ $[M+H]^+$ 205.1103, found 205.1105.

IR: ν_{max} = 2980 (C-H), 2971 (C-H), 2939 (C-H), 2870 (C-H), 1677 (C=O), 1600 (C=C), 1110.

4-((Benzyloxy)methyl)-1-methyl-5-phenylpyrrolidin-2-one (321)

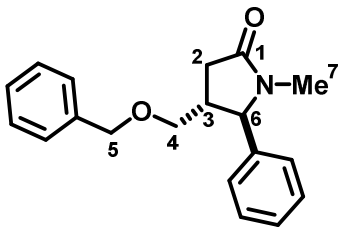

To a solution of 4-(hydroxymethyl)-1-methyl-5-phenylpyrrolidin-2-one (**320**) (1.98 g, 9.65 mmol, 1.0 eq.) in anhydrous THF (50 mL) was added NaH (0.77 g, 19.31 mmol, 2.0 eq., 60% in mineral oil) portion-wise. Benzyl bromide (1.80 mL, 14.48 mmol, 1.5 eq.) was added and the mixture allowed to stir for 16 h. The mixture was quenched slowly with saturated $NH_4Cl_{(aq.)}$ (30 mL) before the aqueous layer was extracted with EtOAc (3 × 30 mL). The combined organics were washed with brine (30 mL), dried over $MgSO_4$, filtered and concentrated *in vacuo*. Purification by flash column chromatography (0-80% EtOAc / petroleum ether) afforded the title compound as a yellow liquid (2.04 g, 6.95 mmol, 72%).

^{1}H NMR (400 MHz, Chloroform-*d*): δ 7.39-7.27 (8H, m, Ar), 7.16 (2H, d, *J* = 7.1 Hz, Ar), 4.54 (1H, d, *J* = 11.9 Hz, H5), 4.50 (1H, d, *J* = 11.9 Hz, H5), 4.37 (1H, d, *J* = 5.2 Hz, H6), 3.53-3.44 (2H, m, H4), 2.71-2.62 (1H, m, H2), 2.66 (3H, s, H7), 2.46-2.32 (2H, m, H2, H3).

^{13}C NMR (101 MHz, Chloroform-*d*): δ 174.6 (C1), 140.5 (Ar), 138.0 (Ar), 129.1 (Ar), 128.5 (Ar), 128.1 (Ar), 127.9 (Ar), 127.8 (Ar), 126.7 (Ar), 73.2 (C5), 70.6 (C4), 67.1 (C6), 41.9 (C3), 33.5 (C2), 28.4 (C7).

HRMS (ESI$^+$) *m/z* calculated for $C_{19}H_{22}NO_2$ $[M+H]^+$ 296.1645, found 296.1636.

IR: ν_{max} = 2981 (C-H), 2973 (C-H), 2938 (C-H), 2865 (C-H), 1673 (C=O), 1603 (C=C), 1454 (C=C), 1101, 1013.

(*Z*)- and (*E*)-4-((Benzyloxy)methyl)-3-ethylidene-1-methyl-5-phenylpyrrolidin-2-one (322 and 317)

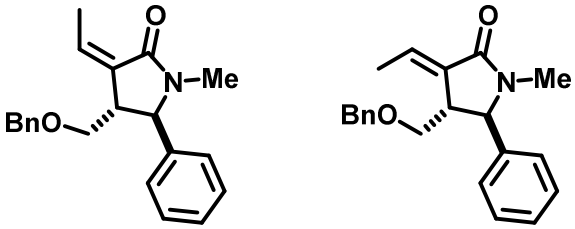

The *E*- and *Z*-isomers of the unsaturated lactam were isolated according to General Procedure 4b and 5 using 4-((benzyloxy)methyl)-1-methyl-5-phenylpyrrolidin-2-one (**321**) (1.50 g, 5.08 mmol, 1.0 eq.) as the lactam and acetaldehyde (**13**) (0.34 mL, 6.10 mmol, 1.2 eq.) as the electrophile. Purification was carried out using flash column chromatography (0-20% EtOAc / petroleum ether) to separate the isomers.

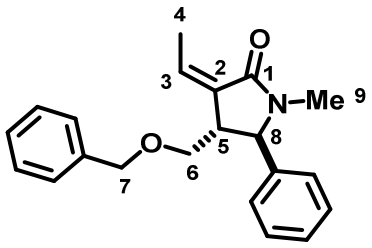

***Z*-Isomers 322**: Orange oil (0.24 g, 0.76 mmol, 15%).

^{1}H NMR (400 MHz, Chloroform-*d*): δ 7.38-7.26 (8H, m, Ar), 7.16 (2H, d, *J* = 7.1 Hz, Ar), 5.97 (1H, qd, *J* = 7.3, 1.9 Hz, H3), 4.55 (1H, d, *J* = 11.9 Hz, H7), 4.51 (1H, d, *J* = 11.9 Hz, H7), 4.37 (1H, d, *J* = 3.1 Hz, H8), 3.55-3.48 (2H, m, H6), 2.89-2.83 (1H, m, H5), 2.73 (3H, s, H9), 2.25 (3H, dd, *J* = 7.3, 1.7 Hz, H4).

^{13}C NMR (101 MHz, Chloroform-*d*): δ 168.9 (C1), 141.1 (Ar), 138.1 (Ar), 133.8 (C3), 130.4 (C2), 129.1 (Ar), 128.6 (Ar), 128.0 (Ar), 127.9 (Ar), 127.8 (Ar), 126.5 (Ar), 73.1 (C7), 73.0 (C6), 65.0 (C8), 47.7 (C5), 28.4 (C9), 13.5 (C4).

HRMS (ESI$^+$) *m/z* calculated for $C_{21}H_{24}NO_2$ $[M+H]^+$ 322.1802, found 322.1791.

IR: ν_{max} = 2910 (C-H), 2856 (C-H), 1685 (C=O), 1664 (C=C), 1495 (C=C), 1394, 1088.

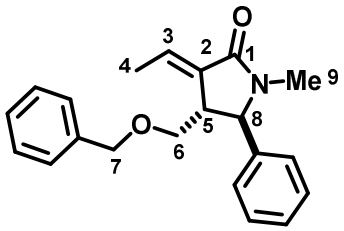

***E*-Isomers 317**: Orange oil (0.85 g, 2.64 mmol, 52%).

^{1}H NMR (400 MHz, Chloroform-*d*): δ 7.39-7.27 (8H, m, Ar), 7.13 (2H, d, *J* = 7.8 Hz, Ar), 6.66 (1H, qd, *J* = 7.3, 2.1 Hz, H3), 4.60 (1H, d, *J* = 12.0 Hz, H7), 4.52 (1H, d, *J* = 12.0 Hz, H7), 4.51 (1H, d, *J* = 2.1 Hz, H8), 3.60 (1H, dd, *J* = 9.7, 4.7 Hz, H6), 3.44 (1H, t, *J* = 9.7 Hz, H6), 3.11-3.06 (1H, m, H5), 2.78 (3H, s, H9), 1.75 (3H, dd, *J* = 7.3, 1.2 Hz, H4).

^{13}C NMR (101 MHz, Chloroform-*d*): δ 168.5 (C1), 141.1 (Ar), 138.1 (Ar), 132.0 (C2), 130.8 (C3), 129.1 (Ar), 128.6 (Ar), 128.0 (Ar), 127.9 (Ar), 127.7 (Ar), 126.2 (Ar), 73.1 (C7), 71.2 (C6), 65.4 (C8), 45.2 (C5), 28.7 (C9), 14.6 (C4).

HRMS (ESI$^+$) *m/z* calculated for $C_{21}H_{24}NO_2$ $[M+H]^+$ 322.1802, found 322.1796.

IR: ν_{max} = 2916 (C-H), 2856 (C-H), 1693 (C=O), 1668 (C=C), 1396, 1103, 697.

2-((Benzyloxy)methyl)-*N*-methyl-3-phenyl-1-vinylcyclopropane-1-carboxamide (323 and 324)

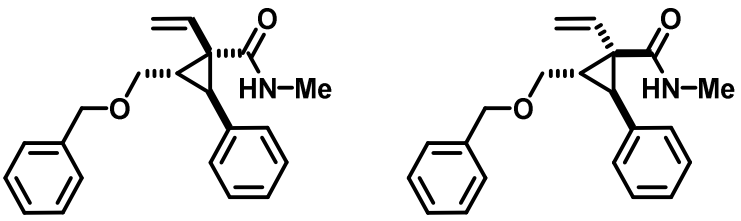

The title compound was synthesised according to General procedure 6b using 4-((benzyloxy)methyl)-3-ethylidene-1-methyl-5-phenylpyrrolidin-2-one (**317**) (100 mg, 0.31 mmol, 1.0 eq.). Purification with flash column chromatography (0-20% EtOAc / petroleum ether) afforded the title compound as a yellow oil with a dr of 89:11 (71 mg, 0.22 mmol, 71%). Only the major diastereomers are reported here.

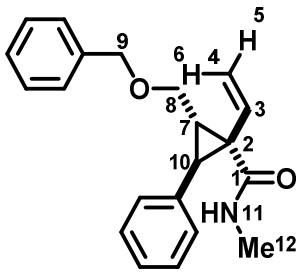

Major Diastereomers 323

^{1}H NMR (400 MHz, Chloroform-*d*): δ 7.30-7.04 (10H, m, Ar), 6.08 (1H, br s, H11), 5.49 (1H, dd, *J* = 17.1, 10.4 Hz, H3), 5.27 (1H, dd, *J* = 17.1, 1.0 Hz, H6), 5.19 (1H, dd, *J* = 10.4, 1.0 Hz, H5), 4.47 (1H, d, *J* = 12.1 Hz, H9), 4.44 (1H, d, *J* = 12.1 Hz, H9), 3.89 (1H, dd, *J* = 10.8, 5.2 Hz, H8), 3.58 (1H, dd, *J* = 10.8, 8.0 Hz, H8), 3.08 (1H, d, *J* = 7.3 Hz, H10), 2.74 (3H, d, *J* = 5.2 Hz, H12), 2.18-2.12 (1H, m, H7).

^{13}C NMR (101 MHz, Chloroform-*d*): δ 170.3 (C1), 138.5 (Ar), 136.1 (Ar), 134.9 (C3), 128.9 (Ar), 128.4 (Ar), 128.1 (Ar), 127.7 (Ar), 127.7 (Ar), 126.5 (Ar), 121.6 (C4), 73.0 (C9), 68.5 (C8), 40.4 (C2), 32.6 (C10), 30.3 (C7), 26.9 (C12).

HRMS (ESI^{+}) *m/z* calculated for $C_{21}H_{24}NO_2$ $[M+H]^+$ 322.1802, found 322.1792.

IR: ν_{max} = 3353 (N-H), 2933 (C-H), 2858 (C-H), 1651 (C=O), 1520 (C=C), 1498, 1972.

NOESY for major diastereomers 323:

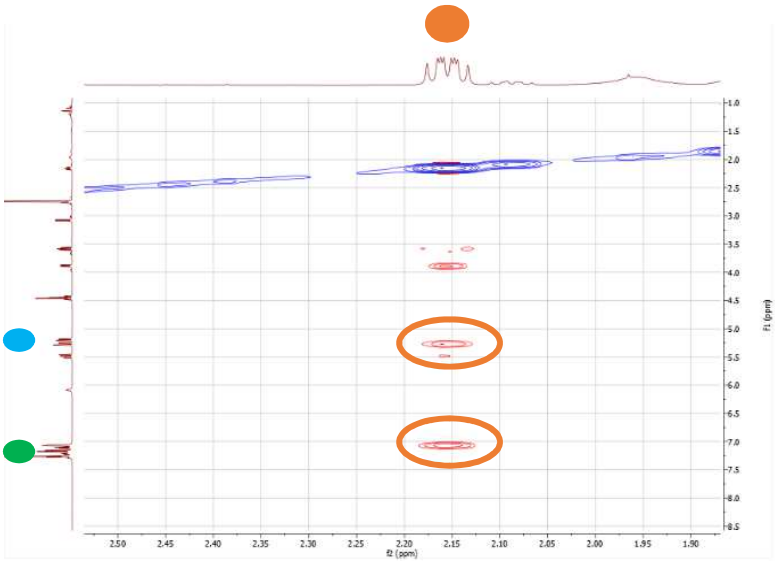

Note that for major diastereomers **323**, H7 correlates to adjacent alkenyl protons H3 and aromatic protons.

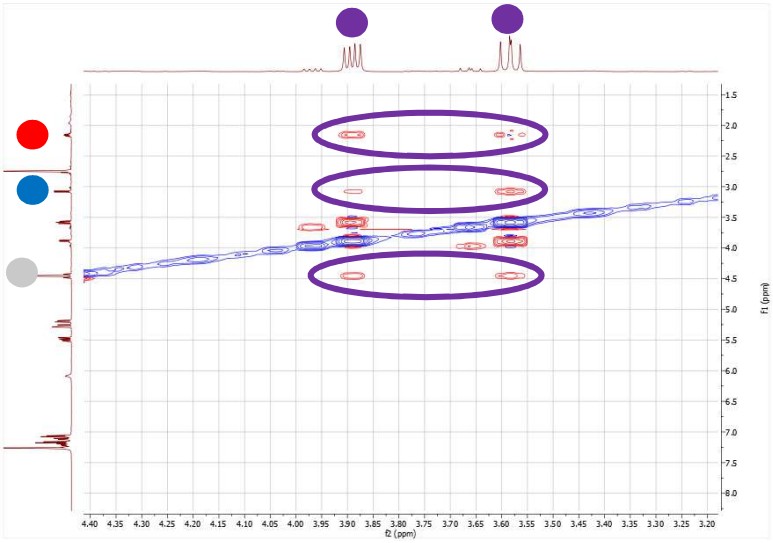

Further evidence for the shown stereochemistry arises from NOE correlations from H8. We see correlations to H7, H10 and H9 as expected for this stereoisomer.

*Figure 37: Two NOESY spectra for **323**, detailing important correlations.*

1-Methyl-6-phenylpiperidin-2-one (329)

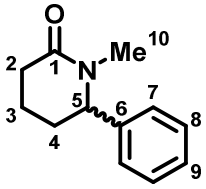

The title compound was synthesised according to General Procedure 3 using 5-oxo-5-phenylpentanoic acid (**328**) (0.50 g, 2.60 mmol, 1.0 eq.) and *N*-methyl formamide (**255**) (3.04 mL, 52.00 mmol, 20.0 eq.).

Purification by flash column chromatography (20-50% EtOAc / petroleum ether) afforded a yellow oil (0.38 g, 2.03 mmol, 78%).

^{1}H NMR (400 MHz, Chloroform-*d*): δ 7.45 (2H, t, *J* = 7.3 Hz, H8), 7.37 (1H, tt, *J* = 7.3, 1.0 Hz, H9), 7.25 (2H, d, *J* = 7.3 Hz, H7), 4.60 (1H, t, *J* = 5.5 Hz, H5), 2.89 (3H, s, H10), 2.66-2.51 (2H, m, H2), 2.32-2.21 (1H, m, H4), 1.96-1.68 (3H, m, H3, H4).

^{13}C NMR (101 MHz, Chloroform-*d*): δ 171.0 (C1), 131.5 (C6), 128.8 (C8), 127.6 (C9), 126.5 (C7), 63.7 (C5), 34.0 (C10), 32.3 (C2), 32.3 (C4), 17.6 (C3).

HRMS (ESI^{+}) *m/z* calculated for $C_{12}H_{16}NO$ $[M+H]^{+}$ 190.1226, found 190.1228.

MP: 68-69 °C.

IR: ν_{max} = 2980 (C-H), 1626 (C=O), 1601 (C=C), 1392, 1155, 1074.

3-(But-2-en-1-ylidene)-1-methyl-6-phenylpiperidin-2-one (332)

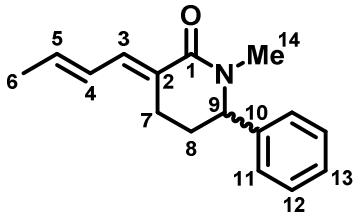

Various isomers of the conjugated lactam were synthesised according to General Procedure 4a using 1-methyl-6-phenylpiperidin-2-one (**329**) (1.00 g, 5.29 mmol, 1.0 eq.) as the lactam and crotonaldehyde (**16**) (0.53 mL, 6.35 mmol, 1.2 eq.) as the aldehyde component. Purification was carried out using flash column chromatography (15% EtOAc / petroleum ether) to separate the isomers. The main isomer is reported here, isolated as an orange oil (0.42 g, 1.75 mmol, 33%). The minor isomers could not be isolated with good purity, and their stereochemistry could not be determined and are therefore not included here.

^{1}H NMR (400 MHz, Chloroform-*d*): δ 7.41-7.22 (5H, m, H3, H12, H13), 7.13 (2H, d, *J* = 7.6 Hz, H11), 6.29-6.20 (1H, m, H4), 6.10 (1H, dq, *J* = 15.1, 6.5 Hz, H5), 4.59 (1H, t, *J* = 4.7 Hz, H9), 3.13 (3H, s, H14), 2.59-2.50 (1H, m, H7), 2.35-2.26 (1H, m, H7), 2.26-2.19 (1H, m, H8), 1.95-1.88 (1H, m, H8), 1.83 (3H, d, *J* = 6.5 Hz, H6).

^{13}C NMR (101 MHz, Chloroform-*d*): δ 166.4 (C1), 140.7 (C10), 137.3 (C5), 135.1 (C3), 128.8 (C11), 127.6 (C13), 126.9 (C4), 126.5 (C12), 125.8 (C2), 63.2 (C9), 31.7 (C14), 30.4 (C8), 20.5 (C7), 19.0 (C6).

HRMS (ESI$^+$) *m/z* calculated for $C_{16}H_{20}NO$ $[M+H]^+$ 242.1539, found 242.1537.

IR: ν_{max} = 2989 (C-H), 1648 (C=O), 1616 (C=C), 1393, 1311, 1170.

NOESY for this isomer:

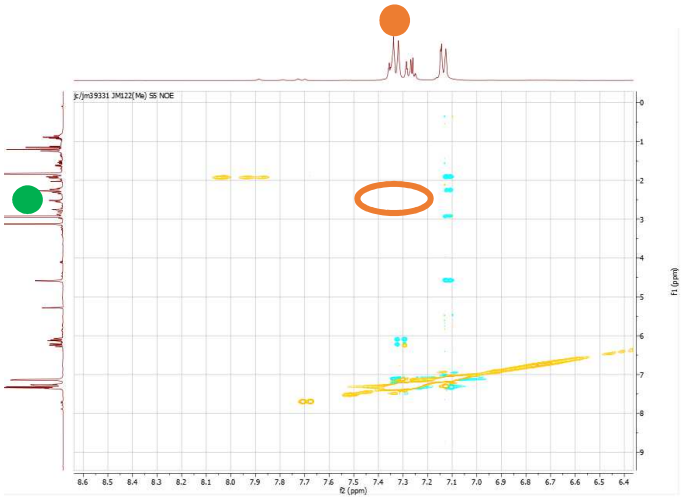

This isomer structure was confirmed by the lack of correlation between H3 and H7.

*Figure 38: NOESY for isomer **332**, detailing the important lack of correlation.*

(*E*)-1-(Buta-1,3-dien-1-yl)-*N*-methyl-2-phenylcyclobutane-1-carboxamide (333) and *N*-Methyl-6-vinyl-1,2,3,6-tetrahydro-[1,1'-biphenyl]-4-carboxamide (334)

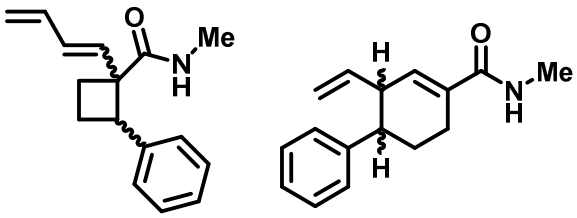

The title compound was synthesised according to General procedure 6a using 3-(but-2-en-1-ylidene)-1-methyl-6-phenylpiperidin-2-one (**332**) (100 mg, 0.41 mmol, 1.0 eq.). Purification with flash column chromatography (20-50% EtOAc / petroleum ether) afforded the photochemical products.

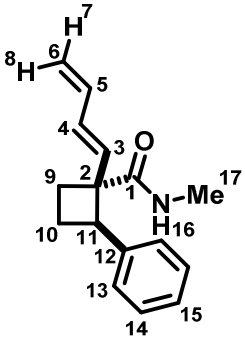

Ring-Contraction Isomers 333: Colourless oil (16 mg, 0.06 mmol, 16%). Only the major diastereoisomers were isolated clean from purification and hence are the only diastereomers reported here. The reaction afforded a crude dr of 80:20.

^{1}H NMR (400 MHz, Chloroform-*d*): δ 7.36-7.31 (2H, m, H14), 7.25-7.20 (3H, m, H13, H15), 6.33-6.22 (2H, m, H4, H5), 5.46 (1H, br s, H16), 5.43 (1H, d, *J* = 14.5 Hz, H3), 5.24 (1H, dd, *J* = 16.5, 1.0 Hz, H8), 5.11 (1H, dd, *J* = 10.7, 1.0 Hz, H7), 4.39 (1H, dd, *J* = 10.2, 7.8 Hz, H11), 2.86 (3H, d, *J* = 4.8 Hz, H17), 2.56-2.48 (1H, m, H9), 2.36-2.28 (1H, m, H10), 2.27-2.20 (1H, m, H9), 2.19-2.11 (1H, m, H10).

^{13}C NMR (101 MHz, Chloroform-*d*): δ 175.1 (C1), 139.5 (C12), 136.6 (C4), 133.1 (C5), 132.3 (C3), 128.4 (C13), 128.2 (C14), 126.6 (C15), 117.6 (C6), 55.8 (C2), 46.3 (C11), 27.1 (C9), 26.8 (C17), 21.3 (C10).

HRMS (ESI^{+}) *m/z* calculated for $C_{16}H_{20}NO$ $[M+H]^{+}$ 242.1539, found 242.1531.

IR: ν_{max} = 3187 (N-H), 2921 (C-H), 1647 (C=O), 1601 (C=C), 1462, 1367, 1011.

NOESY for major diastereomers of 333:

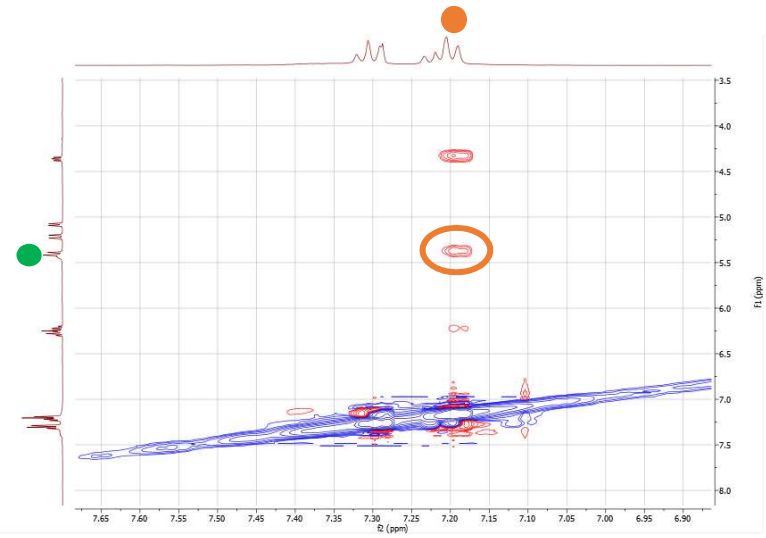

Note that for these diastereomers, the aromatic protons H13 sees the adjacent alkenyl proton H3, indicating a *cis*-relationship between the two groups.

*Figure 39: NOESY for diastereomers **333**.*

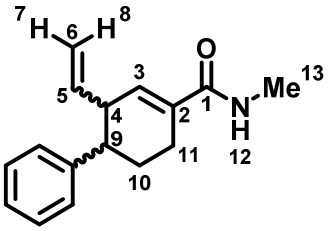

"**Ring-Swing**" **Isomers 334**: Yellow oil (17 mg, 0.07 mmol, 17%) with a crude dr of 66:33 for D1:D2 where D1 and D2 refer to the diastereomer of product. NOE was inconclusive due to a complex mixture arising from compound polymerisation.

^{1}H NMR (400 MHz, Chloroform-*d*): δ 7.37-7.15 (10H, m, Ar), 6.63 (1H, br d, *J* = 5.2 Hz, H3 D1), 6.59-6.55 (1H, m, H3 D2), 5.83 (2H, br s, H12 D1, H12 D2), 5.68 (1H, ddd, *J* = 17.1, 10.2, 7.6 Hz, H5 D2), 5.45 (1H, ddd, *J* = 17.3, 10.2, 7.1 Hz, H5 D1), 5.05 (1H, d, *J* = 10.2 Hz, H7 D1), 4.99 (1H, dd, *J* = 10.2, 0.9 Hz, H7 D2), 4.93 (1H, dd, *J* = 17.1, 0.9 Hz, H8 D2), 4.88 (1H, d, *J* = 17.3 Hz, H8 D1), 3.30-3.23 (1H, m, H4 D1), 3.17-3.05 (2H, m, H4 D2, H9 D1), 2.95 (3H, d, *J* = 4.9 Hz, H13 D1), 2.94 (3H, d, *J* = 4.9 Hz, H13 D2), 2.63-2.53 (1H, m, H9 D2), 2.51-2.33 (4H, m, H11 D1, H11 D2), 2.09-1.84 (4H, m, H10 D1, H10 D2).

^{13}C NMR (101 MHz, Chloroform-*d*): δ 169.0 (C1 D1), 169.0 (C1 D2), 144.7 (Ar), 143.3 (Ar), 139.6 (C5 D2), 136.4 (C5 D1), 134.9 (C3 D2), 134.3 (C3 D1), 134.0 (C2 D1), 133.9 (C2 D2), 128.5 (Ar), 128.3 (Ar), 127.9 (Ar), 127.6 (Ar), 126.5 (Ar), 126.4 (Ar), 118.0 (C6 D1), 116.2 (C6 D2), 46.5 (C4 D2), 46.0 (C9 D2), 44.7 (C4 D1), 42.6 (C9 D1), 30.0 (C10 D2), 26.6 (C13 D2), 25.6 (C13 D1), 24.9 (C11 D2), 24.0 (C11 D1), 22.5 (C10 D1).

HRMS (ESI^{+}) *m/z* calculated for $C_{16}H_{20}NO$ $[M+H]^{+}$ 242.1539, found 242.1530.

IR: ν_{max} = 3330 (N-H), 2982 (C-H), 1658 (C=O), 1614 (C=C), 1393, 1154, 966.

6-(Phenylsulfonyl)piperidin-2-one (338)

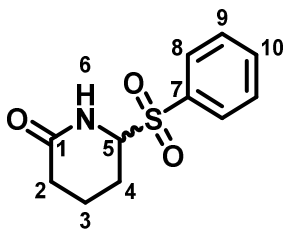

Synthesised according to a procedure by Neipp *et al*.[152]

Glutarimide (**337**) (6.00 g, 53.07 mmol, 1.0 eq.) was slurried in EtOH (200 mL) before addition of $NaBH_4$ (4.92 g, 0.13 mol, 2.5 eq.) in an ice bath. Using a syringe pump (1.41 mL/h), a solution of HCl (5.50 mL,

2 M in EtOH) was added over 4 h at this temperature. HCl (90 mL, 2 M in EtOH) was then added cautiously to the mixture in the ice bath before the mixture was allowed to stir at rt for 16 h. To this mixture, $NaOH_{(aq.)}$ (5 M) was added until pH 8/9 and the mixture was filtered before the filtrate was concentrated *in vacuo* to remove EtOH. The aqueous layer was extracted with CH_2Cl_2 (3 × 40 mL) and then to this crude solution was added $PhSO_2Na$ (18.06 g, 0.11 mol, 2.0 eq.) and formic acid (5.10 mL, 0.12 mol, 2.2 eq., 88%). The mixture was left to stir for 16 h before addition of brine (100 mL) and the aqueous layer extracted with CH_2Cl_2 (3 × 50 mL). The combined organics were washed with brine (2 × 60 mL), dried over $MgSO_4$, filtered and concentrated *in vacuo* to give the title compound as a white solid (9.39 g, 39.27 mmol, 74%).

^{1}H NMR (400 MHz, Chloroform-*d*): δ 7.90 (2H, d, *J* = 7.2 Hz, H8), 7.74-7.68 (1H, m, H10), 7.60 (2H, t, *J* = 7.2 Hz, H9), 6.91 (1H, br s, H6), 4.53 (1H, dt, *J* = 7.9, 6.1 Hz, H5), 2.29 (1H, t, *J* = 7.1 Hz, H2), 2.22 (1H, t, *J* = 7.1 Hz, H2), 2.18-2.08 (2H, m, H4), 1.99-1.87 (1H, m, H3), 1.74-1.62 (1H, m, H3).

^{13}C NMR (101 MHz, Chloroform-*d*): δ 173.0 (C1), 135.0 (C7), 134.9 (C10), 129.8 (C9), 129.7 (C8), 72.4 (C5), 30.8 (C2), 21.9 (C4), 17.5 (C3).

Data consistent with literature.[152]

6-Vinylpiperidin-2-one (339)

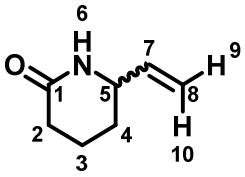

Synthesised according to a procedure by Neipp *et al*.[152]

To a slurry of 6-(phenylsulfonyl)piperidin-2-one (**338**) (3.00 g, 12.55 mmol, 1.0 eq.) in anhydrous THF (45 mL) was added vinyl magnesium bromide (38.00 mL, 37.65 mmol, 3.0 eq., 1 M in THF) via cannula transfer at −78 °C. After 15 minutes at this temperature, the mixture was placed in a NaCl/ice/water bath for 20 minutes, with the temperature kept below −10 °C. The ice bath was removed, and the mixture stirred at rt for 30 minutes. Saturated $NaHCO_{3(aq.)}$ (50 mL) was added and the mixture was left to stir for 30 min. The slurry was filtered under vacuum, washing with $CHCl_3$ before the filtrate was concentrated *in vacuo*. The aqueous layer was extracted with $CHCl_3$ (3 × 30 mL) before the combined organics were washed with water (30 mL), brine (30 mL), dried over $MgSO_4$, filtered and concentrated

in vacuo. Purification by flash column chromatography (0-1% MeOH / CH_2Cl_2) afforded the title compound as a yellow crystalline solid (1.06 g, 8.53 mmol, 68%).

^{1}H NMR (400 MHz, Chloroform-*d*): δ 6.60 (1H, br s, H6), 5.73 (1H, ddd, *J* = 17.2, 10.3, 6.2 Hz, H7), 5.17 (1H, dt, *J* = 17.2, 1.1 Hz, H10), 5.10 (1H, dt, *J* = 10.3, 1.1 Hz, H9), 3.94-3.86 (1H, m, H5), 2.35-2.19 (2H, m, H2), 1.92-1.83 (1H, m, H4), 1.82-1.75 (1H, m, H3), 1.71-1.58 (1H, m, H3), 1.52-1.42 (1H, m, H4).

^{13}C NMR (101 MHz, Chloroform-*d*): δ 172.5 (C1), 139.0 (C7), 116.5 (C8), 55.3 (C5), 31.7 (C2), 28.5 (C4), 18.9 (C3).

Data consistent with literature.[152]

1-Methyl-6-vinylpiperidin-2-one (340)

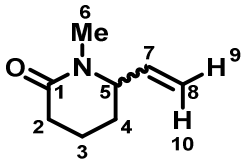

A solution of 6-vinylpiperidin-2-one (**339**) (1.50 g, 12.00 mmol, 1.0 eq.) in anhydrous THF (20 mL) was cooled to −78 °C before addition of ^{n}BuLi (5.70 mL, 14.39 mmol, 1.2 eq., 2.5 M in hexanes) at this temperature to give a thick orange slurry. After 30 minutes, MeI (1.50 mL, 24.00 mmol, 2.0 eq.) was added slowly before the mixture was allowed to warm to rt. After stirring at rt for 3.5 h, saturated $NH_4Cl_{(aq.)}$ (30 mL) and H_2O (30 mL) were added, and the layers separated. The aqueous layer was extracted with EtOAc (3 × 30 mL) before the organics were washed with brine (30 mL), dried over Mg_2SO_4, filtered and concentrated *in vacuo* to give an orange liquid (1.45 g, 10.42 mmol, 87%) which was used without further purification.

^{1}H NMR (400 MHz, Chloroform-*d*): δ 5.62 (1H, ddd, *J* = 17.2, 10.2, 6.3 Hz, H7), 5.11 (1H, d, *J* = 10.2 Hz, H9), 5.01 (1H, d, *J* = 17.2 Hz, H10), 3.76 (1H, q, *J* = 6.3 Hz, H5), 2.76 (3H, s, H6), 2.33-2.18 (2H, m, H2), 1.88-1.78 (1H, m, H4), 1.76-1.66 (1H, m, H3), 1.65-1.52 (2H, m, H3, H4).

^{13}C NMR (101 MHz, Chloroform-*d*): δ 170.5 (C1), 137.7 (C7), 116.8 (C8), 61.8 (C5), 33.6 (C6), 32.2 (C2), 28.8 (C4), 17.7 (C3).

HRMS (ESI^+) *m/z* calculated for $C_8H_{14}NO$ $[M+H]^+$ 140.1070, found 140.1066.

IR: ν_{max} = 2975 (C-H), 1620 (C=O and C=C broad), 1396, 1243, 1044.

(*E*)-3-((*E*)-But-2-en-1-ylidene)-1-methyl-6-vinylpiperidin-2-one (342)

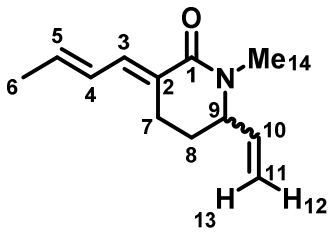

Various isomers of the conjugated lactam were synthesised according to General Procedure 4a using 1-methyl-6-vinylpiperidin-2-one **(340)** (1.20 g, 8.63 mmol, 1.0 eq.) as the lactam and crotonaldehyde (**16**) (0.86 mL, 10.36 mmol, 1.2 eq.) as the aldehyde component. Purification was carried out using flash column chromatography (0-20% EtOAc / petroleum ether) to separate the isomers. The main isomer is reported here, isolated as a yellow liquid (0.19 g, 0.95 mmol, 11%). The minor isomers could not be isolated with good purity, and their stereochemistry could not be determined and hence they are not included here.

^{1}H NMR (400 MHz, Chloroform-*d*): δ 7.13 (1H, d, *J* = 11.6 Hz, H3), 6.17 (1H, ddd, *J* = 16.1, 11.6, 1.2 Hz, H4), 6.01-5.90 (1H, m, H5), 5.65 (1H, ddd, *J* = 17.4, 10.3, 5.9 Hz, H10), 5.11 (1H, dd, *J* = 10.3, 1.4 Hz, H12), 4.99 (1H, dd, *J* = 17.4, 1.4 Hz, H13), 3.84 (1H, t, *J* = 5.9 Hz, H9), 2.87 (3H, s, H14), 2.50 (1H, dt, *J* = 7.5, 4.2 Hz, H7), 2.42-2.29 (1H, m, H7), 1.95-1.83 (1H, m, H8), 1.74 (3H, dd, *J* = 6.4, 1.2 Hz, H6), 1.73-1.67 (1H, m, H8).

^{13}C NMR (101 MHz, Chloroform-*d*): δ 165.5 (C1), 136.6 (C5), 136.3 (C10), 134.4 (C3), 126.7 (C4), 125.6 (C2), 116.4 (C11), 61.0 (C9), 34.3 (C14), 27.0 (C8), 20.6 (C7), 18.7 (C6).

HRMS (ESI^+) *m/z* calculated for $C_{12}H_{18}NO$ $[M+H]^+$ 192.1383, found 192.1383.

IR: ν_{max} = 2887 (C-H), 1644 (C=O), 1606 (C=C), 1475, 1395, 1314.

1-(Buta-1,3-dien-1-yl)-*N*-methyl-2-vinylcyclobutane-1-carboxamide (343) and *N*-Methyl-3,4-divinylcyclohex-1-ene-1-carboxamide (344)

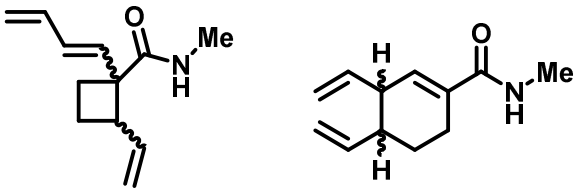

The title compounds were synthesised according to General procedure 6a using (*E*)-3-((*E*)-but-2-en-1-ylidene)-1-methyl-6-vinylpiperidin-2-one (**342**) (100 mg, 0.52 mmol, 1.0 eq.). Purification with flash column chromatography (10-30% EtOAc / petroleum ether) afforded the photochemical products.

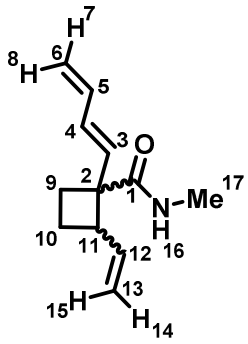

Ring-Contraction Isomers 343: Colourless oil (2 mg, 0.01 mmol, 2%). Only one diastereomer of ring-contracted product was isolated. Not enough material was isolated for a clear ^{13}C NMR spectra or IR spectra and hence it is not reported here. Similarly, a confident NOESY analysis could not be conducted, and therefore the stereochemistry cannot be confirmed.

^{1}H NMR (400 MHz, Chloroform-*d*): δ 6.36 (1H, dt, *J* = 16.7, 10.0 Hz, H5), 6.23-6.16 (1H, m, H4), 5.93-5.78 (2H, m, H3, H12), 5.48 (1H, br s, H16), 5.25 (1H, dd, *J* = 16.7, 1.3 Hz, H8), 5.13 (1H, dd, *J* = 10.0, 1.3 Hz, H7), 5.08 (1H, dd, *J* = 17.1, 1.1 Hz, H15), 5.02 (1H, dd, *J* = 10.3, 1.1 Hz, H14), 3.20 (1H, q, *J* = 8.9 Hz, H11), 2.78 (3H, d, *J* = 4.9 Hz, H17), 2.65-2.57 (1H, m, H9), 2.21-2.10 (1H, m, H10), 2.07-1.96 (1H, m, H10), 1.93-1.85 (1H, m, H9).

HRMS (ESI$^+$) *m/z* calculated for $C_{12}H_{18}NO$ $[M+H]^+$ 192.1383, found 192.1383.

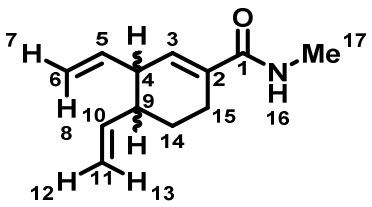

"**Ring-Swing**" **Isomers 344**: Colourless oil (39%, 0.20 mmol, 39%) with a crude dr of 50:50 where D1 and D2 refer to the diastereomer of product.

^{1}H NMR (400 MHz, Chloroform-*d*): δ 6.47-6.42 (1H, m, H3 D1), 6.40-6.35 (1H, m, H3 D2), 5.93 (2H, br s, H16 D1, H16 D2), 5.81-5.69 (3H, m, H5 D1/D2, H10 D1, H10 D2), 5.66 (1H, ddd, *J* = 17.2, 10.0, 7.6 Hz, H5 D1/D2), 5.11-4.94 (8H, m, H7 D1, H7 D2, H8 D1, H8 D2, H12 D1, H12 D2, H13 D1, H13 D2), 2.99 (1H, br q, *J* = 6.3 Hz, H4 D1), 2.84 (6H, d, *J* = 4.8 Hz, H17 D1, H17 D2), 2.72-2.63 (1H, m, H4 D2), 2.44-2.30 (3H, m, H9 D1, H14 D1), 2.28-2.16 (2H, m, H14 D2), 2.07-1.96 (1H, m, H9 D2), 1.90-1.82 (1H, m, H15 D2), 1.76-1.67 (1H, m, H15 D1), 1.64-1.54 (1H, m, H15 D1), 1.54-1.43 (1H, m, H15 D2).

^{13}C NMR (101 MHz, Chloroform-*d*): δ 169.0 (C1 D1), 168.9 (C1 D2), 141.3 (C10 D1/D2), 140.3 (C10 D1/D2), 139.9 (C5 D1), 137.1 (C5 D2), 134.0 (C3 D2), 133.9 (C3 D1), 133.8 (C2 D1), 133.7 (C2 D2), 117.3 (C6 D2), 116.1 (C11 D1), 114.7 (C6 D1), 114.6 (C11 D2), 45.3 (C4 D2), 43.5 (C4 D1), 42.7 (C9 D1), 41.0 (C9 D2), 27.1 (C15 D2), 26.5 (C17 D1), 26.4 (C17 D2), 24.0 (C14 D1/D2), 23.9 (C14 D1/D2), 23.7 (C15 D1).

HRMS (ESI$^+$) *m/z* calculated for $C_{12}H_{18}NO$ $[M+H]^+$ 192.1383, found 192.1382.

IR: ν_{max} = 3328 (N-H), 2976 (C-H), 1656 (C=O), 1635 (C=C), 1536, 1407, 1155.

(*E*)- and (*Z*)-3-Ethylidene-1-methyl-6-phenylpiperidin-2-one (352 and 351)

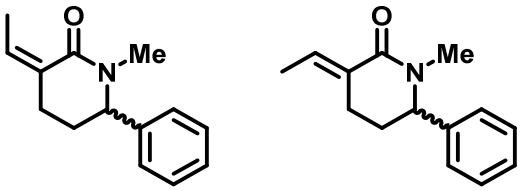

The *E*- and *Z*-isomers of the unsaturated lactam were isolated according to General Procedure 4b and 5 using methyl 1-methyl-6-phenylpiperidin-2-one (**329**) (1.00 g, 5.29 mmol, 1.0 eq.) as the lactam and acetaldehyde (**13**) (0.36 mL, 6.35 mmol, 1.2 eq.) as the electrophile. Purification was carried out using flash column chromatography (0-50% EtOAc / petroleum ether) to separate the isomers.

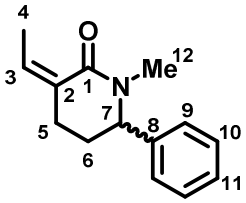

***Z*-Isomers 352**: Brown oil (0.24 g, 1.11 mmol, 21%).

^{1}H NMR (400 MHz, Chloroform-*d*): δ 7.29-7.15 (3H, m, H10, H11), 7.10-7.06 (2H, m, H9), 5.82 (1H, qt, *J* = 7.3, 1.3 Hz, H3), 4.44 (1H, t, *J* = 5.5 Hz, H7), 2.75 (3H, s, H12), 2.38-2.27 (1H, m, H5), 2.23-2.13 (2H, m, H5, H6), 2.12 (3H, d, *J* = 7.3 Hz, H4), 1.81-1.72 (1H, m, H6).

^{13}C NMR (101 MHz, Chloroform-*d*): δ 166.2 (C1), 141.4 (C8), 135.9 (C3), 128.7 (C2), 128.5 (C10), 127.3 (C11), 126.2 (C9), 63.5 (C7), 33.6 (C12), 32.3 (C6), 28.6 (C5), 15.6 (C4).

HRMS (ESI$^+$) *m/z* calculated for $C_{14}H_{18}NO$ $[M+H]^+$ 216.1383, found 216.1372.

IR: ν_{max} = 2937 (C-H), 2922 (C-H), 1660 (C=O), 1615 (C=C), 1444, 1393.

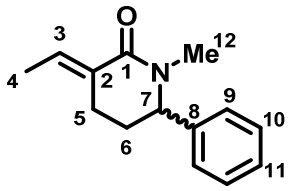

***E*-Isomers 351**: Brown solid (0.52 g, 2.43 mmol, 46%).

^{1}H NMR (400 MHz, Chloroform-*d*): δ 7.37-7.23 (3H, m, H10, H11), 7.13 (2H, d, *J* = 7.4 Hz, H9), 7.00 (1H, q, *J* = 7.4 Hz, H3), 4.59-4.55 (1H, br m, H7), 2.92 (3H, s, H12), 2.47-2.36 (1H, m, H5), 2.28-2.13 (2H, m, H5, H6), 1.97-1.87 (1H, m, H6), 1.71 (3H, d, *J* = 7.4 Hz, H4).

^{13}C NMR (101 MHz, Chloroform-*d*): δ 165.9 (C1), 140.7 (C8), 133.4 (C3), 129.3 (C2), 128.8 (C10), 127.6 (C11), 126.5 (C9), 63.2 (C7), 34.8 (C12), 30.5 (C6), 20.1 (C5), 13.7 (C4).

HRMS (ESI^{+}) *m/z* calculated for $C_{14}H_{18}NO$ $[M+H]^{+}$ 216.1383, found 216.1373.

MP: 59-60 °C.

IR: ν_{max} = 2936 (C-H), 2922 (C-H), 1660 (C=O), 1606 (C=C), 1477, 1433.

N-Methyl-2-phenyl-1-vinylcyclobutane-1-carboxamide (353) and *N*-Methyl-1,2,3,6-tetrahydro-[1,1'-biphenyl]-4-carboxamide (354)

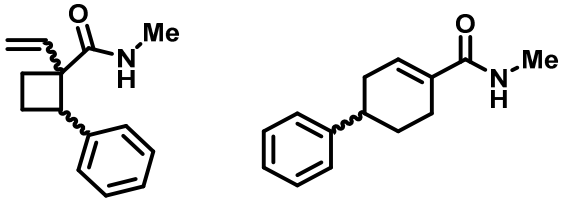

The title compounds were synthesised according to General procedure 6b using (*E*)-3-ethylidene-1-methyl-6-phenylpiperidin-2-one (**351**) (100 mg, 0.46 mmol, 1.0 eq.). Purification with flash column chromatography (10-40% EtOAc / petroleum ether) afforded the photochemical products.

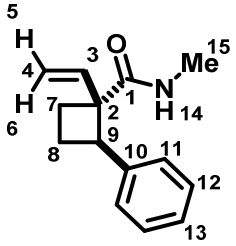

Ring-Contraction Major Diastereomers 353: White crystalline solid (30 mg, 0.14 mmol, 30%). Stereochemistry of the major diastereomer of ring-contraction product (with crude dr 83:17) was confirmed by X-Ray crystallography.

^{1}H NMR (400 MHz, Chloroform-*d*): δ 7.31-7.11 (5H, m, H11-H13), 5.53 (1H, dd, *J* = 17.4, 10.5 Hz, H3), 5.46 (1H, br s, H14), 5.30-5.23 (2H, m, H5, H6), 4.34 (1H, dd, *J* = 9.3, 7.9 Hz, H9), 2.79 (3H, d, *J* = 4.8 Hz, H15), 2.43-2.33 (1H, m, H7), 2.29-2.14 (2H, m, H7, H8), 2.12-2.02 (1H, m, H8).

^{13}C NMR (101 MHz, Chloroform-*d*): δ 175.0 (C1), 139.6 (C10), 136.6 (C3), 128.3 (C12), 128.2 (C13), 126.4 (C11), 117.2 (C4), 56.2 (C2), 45.5 (C9), 26.7 (C15), 26.2 (C7), 20.9 (C8).

HRMS (ESI^{+}) *m/z* calculated for $C_{14}H_{18}NO$ $[M+H]^{+}$ 216.1383, found 216.1377.

MP: 62-63 °C.

IR: ν_{max} = 3354 (C-N), 2966 (C-H), 2922 (C-H), 1659 (C=O), 1614 (C=C), 1527, 1454.

X-Ray Crystallography:

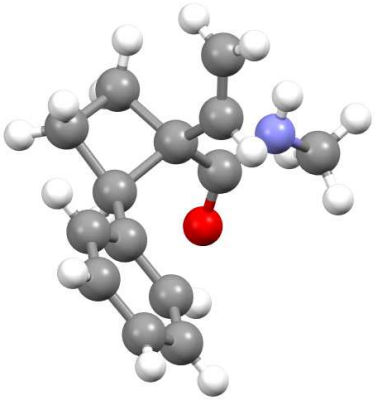

Empirical formula	$C_{14}H_{17}NO$
Formula weight	215.28
Temperature/K	100(2)
Crystal system	orthorhombic
Space group	Pbca
a/Å	9.2148(3)
b/Å	8.6567(3)
c/Å	30.1947(11)
α/°	90
β/°	90
γ/°	90
Volume/Å^3	2408.62(14)
Z	8
ρ_{calc}g/cm^3	1.187
μ/mm^{-1}	0.074

F(000)	928.0
Crystal size/mm^3	0.36 × 0.32 × 0.26
Radiation	MoKα (λ = 0.71073)
2Θ range for data collection/°	5.18 to 55.766
Index ranges	-12 ≤ h ≤ 12, -11 ≤ k ≤ 10, -39 ≤ l ≤ 39
Reflections collected	34453
Independent reflections	2878 [R_{int} = 0.0737, R_{sigma} = 0.0400]
Data/restraints/parameters	2878/0/148
Goodness-of-fit on F^2	1.068
Final R indexes [I>=2σ (I)]	R_1 = 0.0511, wR_2 = 0.1067
Final R indexes [all data]	R_1 = 0.0742, wR_2 = 0.1163
Largest diff. peak/hole / e Å^{-3}	0.27/-0.20

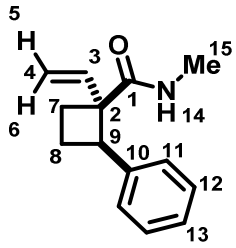

Ring-Contraction Minor Diastereomers: Yellow oil (2 mg, 0.01 mmol, 2%). Not enough sample isolated to obtain a clear ^{13}C NMR or IR spectra.

^{1}H NMR (400 MHz, Chloroform-*d*): δ 7.33-7.14 (5H, m, H11-H13), 6.10 (1H, dd, *J* = 17.3, 10.5 Hz, H3), 5.40 (1H, dd, *J* = 17.3, 1.0 Hz, H6), 5.27 (1H, dd, *J* = 10.5, 1.0 Hz, H5), 4.94 (1H, br s, H14), 3.89 (1H, dd, *J* = 10.2, 9.0 Hz, H9), 2.60 (1H, ddt, *J* = 10.2, 9.0, 7.0 Hz, H8), 2.38 (3H, d, *J* = 5.0 Hz, H15), 2.14-2.07 (1H, m, H8), 2.0-1.91 (2H, m, H7).

HRMS (ESI$^+$) *m/z* calculated for $C_{14}H_{18}NO$ $[M+H]^+$ 216.1383, found 216.1376.

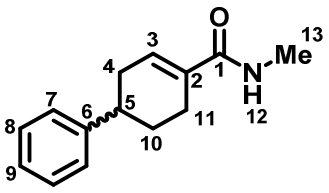

"**Ring-Swing**" **Isomers 354**: Yellow oil (21 mg, 0.10 mmol, 21%).

^{1}H NMR (400 MHz, Chloroform-*d*): δ 7.35-7.16 (5H, m, H7-H9), 6.71 (1H, br s, H3), 5.75 (1H, br s, H12), 2.89 (3H, d, *J* = 4.8 Hz, H13), 2.84-2.74 (1H, m, H5), 2.53-2.41 (2H, m, H4, H11), 2.40-2.22 (2H, m, H4, H11), 2.09-2.00 (1H, m, H10), 1.85-1.73 (1H, m, H10).

^{13}C NMR (101 MHz, Chloroform-*d*): δ 169.1 (C1), 146.1 (C6), 133.1 (C2), 132.9 (C3), 128.6 (C8), 126.9 (C9), 126.5 (C7), 39.3 (C5), 33.5 (C4), 29.5 (C10), 26.6 (C13), 25.1 (C11).

HRMS (ESI$^+$) *m/z* calculated for $C_{14}H_{18}NO$ $[M+H]^+$ 216.1383, found 216.1375.

IR: ν_{max} = 3356 (N-H), 2967 (C-H), 2938 (C-H), 1660 (C=O), 1615 (C=C), 1527, 1454.

1-Methyl-5-phenyl-3-(trimethylsilyl)pyrrolidine-2-one (364)

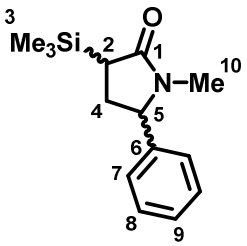

To an oven-dried flask was added anhydrous THF (3 mL), DIPA (0.48 mL, 3.43 mmol, 2.0 eq.) and ^{n}BuLi (1.51 mL, 3.60 mmol, 2.1 eq. 2.5 M in hexanes) in an ice bath before addition of a solution of 1-methyl-5-phenylpyrrolidin-2-one (**254**) (0.30 g, 1.71 mmol, 1.0 eq.) in anhydrous THF (10 mL) in an ice bath. After 30 min, TMSCl (0.25 mL, 1.88 mmol, 1.1 eq.) was added dropwise and the mixture allowed to warm to rt. After 1 h, the reaction was quenched with saturated $NH_4Cl_{(aq.)}$ (10 mL) and water (10 mL). The aqueous layer was extracted with EtOAc (3 × 10 mL) before the combined organics were washed with brine (10 mL), dried over $MgSO_4$, filtered and concentrated *in vacuo*. Purification by flash column chromatography (15% EtOAc / petroleum ether) afforded two diastereomers of C-silylated product.

Diastereomer 1: Colourless oil (0.15 g, 0.60 mmol, 35%).

^{1}H NMR (400 MHz, Chloroform-*d*): δ 7.35-7.20 (3H, m, H8, H9), 7.16 (2H, d, *J* = 7.8 Hz, H7), 4.35 (1H, t, *J* = 7.5 Hz, H5), 2.59 (3H, s, H10), 2.36-2.27 (1H, m, H4), 2.11 (1H, dd, *J* = 10.0, 4.7 Hz, H2), 2.04-1.94 (1H, m, H4), 0.11 (9H, s, H3).

^{13}C NMR (101 MHz, Chloroform-*d*): δ 177.5 (C1), 141.7 (C6), 128.9 (C8), 127.9 (C9), 126.3 (C7), 64.2 (C5), 32.0 (C2), 31.2 (C4), 28.1 (C10), −2.6 (C3).

HRMS (ESI$^+$) *m/z* calculated for $C_{14}H_{22}NOSi$ $[M+H]^+$ 248.1465, found 248.1457.

IR: ν_{max} = 3400 (C-H), 2953 (C-H), 2290 (Si-H), 1659 (C=O), 1450, 1395, 1000.

Diastereomer 2: Colourless oil (0.14 g, 0.58 mmol, 34%).

^{1}H NMR (400 MHz, Chloroform-*d*): δ 7.36-7.22 (3H, m, H8, H9), 7.18-7.13 (2H, m, H7), 4.40 (1H, t, *J* = 8.5 Hz, H5), 2.56 (3H, s, H10), 2.52-2.42 (1H, m, H4), 2.01 (1H, t, *J* = 9.7 Hz, H2), 1.67-1.55 (1H, m, H4)

^{13}C NMR (101 MHz, Chloroform-*d*): δ 178.2 (C1), 141.9 (C6), 129.0 (C8), 127.9 (C9), 126.5 (C7), 65.1 (C5), 31.9 (C2), 31.7 (C4), 28.4 (C10), −2.9 (C3).

HRMS (ESI^+) *m/z* calculated for $C_{14}H_{22}NOSi$ $[M+H]^+$ 248.1465, found 248.1459.

IR: ν_{max} = 3465 (C-H), 2945 (C-H), 2281 (Si-H), 1660 (C=O), 1435, 1278, 1065.

1-Methyl-6-phenyl-3,6-dihydropyridin-2(1*H*)-one (366)

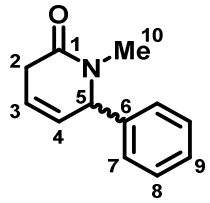

Synthesised according to the procedure by L. Huang *et al*.[118]

To a solution of $Fe(acac)_3$ (0.16 g, 0.46 mmol, 5 mol%) in anhydrous THF (40 mL) was added *N*-methyl-2-pyridone (**375**) (0.90 mL, 9.17 mmol, 1.0 eq.). At – 20 °C, PhMgBr (**376**) (9.20 mL, 27.51 mmol, 3.0 eq.) was added to give a dark red solution and the mixture was left at this temperature for 90 min. The reaction was then quenched with saturated $NH_4Cl_{(aq.)}$ (30 mL) and extracted with EtOAc (3 × 30 mL) before organics were washed with brine (30 mL), dried over $MgSO_4$, filtered and concentrated *in vacuo*. Purification by flash column chromatography (10-40% EtOAc / petroleum ether) afforded the title compound as a yellow oil (0.86 g, 4.59 mmol, 50%).

^{1}H NMR (400 MHz, Chloroform-*d*): δ 7.31-7.18 (3H, m, H8, H9), 7.15-7.08 (2H, m, H7), 5.69-5.60 (2H, m, H3, H4), 4.79 (1H, td, *J* = 7.8, 4.0 Hz, H5), 3.11-2.95 (2H, m, H2), 2.74 (3H, s, H10).

^{13}C NMR (101 MHz, Chloroform-*d*): δ 167.5 (C1), 140.2 (C6), 129.0 (C8), 128.1 (C9), 126.8 (C7), 126.1 (C4), 120.7 (C3), 66.5 (C5), 32.6 (C10), 31.8 (C2).

Data consistent with literature.[118]

N-Methyl-5-phenylpenta-2,4-dienamide (377, 378, 379 and 380)

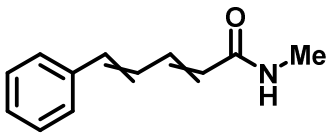

To a solution of DIPA (0.14 mL, 1.07 mmol, 2.0 eq.) in anhydrous THF (5 mL) was added ^{n}BuLi (0.46 mL, 1.12 mmol, 2.1 eq., 2.5 M in hexanes) at −78 °C. To this basic solution was added 1-methyl-6-phenyl-3,6-dihydropyridin-2(1*H*)-one (**366**) (100 mg, 0.53 mmol, 1.0 eq.) in anhydrous THF (10 mL) at –78 °C. The orange-red solution was irradiated at 365 nm (Thorlabs M365LP1) for 2.5 h before being quenched with saturated $NH_4Cl_{(aq.)}$ (10 mL). The aqueous layer was extracted with EtOAc (3 × 10 mL) before the combined organics were washed with brine (10 mL), dried over Na_2SO_4, filtered and concentrated *in vacuo*. Purification by flash column chromatography (15-30% EtOAc / petroleum ether) afforded two separate mixtures, each containing two isomers of ring-opened product (see below).

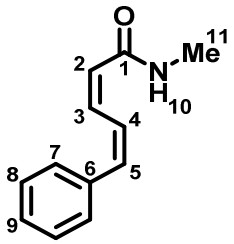

Isomers 377 and 378: White solid (70 mg, 0.37 mmol, 70%). Isolated as a mixture of isomers **377** and **378** in a ratio of 77:23 respectively, giving 54% yield of **377** and 16% yield of **378**.

^{1}H NMR (400 MHz, Chloroform-*d*): δ 7.52 (1H, t, *J* = 11.9 Hz, H4), 7.30-7.18 (5H, m, H7-H9), 6.80 (1H, t, *J* = 11.9 Hz, H3), 6.72 (1H, d, *J* = 11.9 Hz, H5), 6.09 (1H, br s, H10), 5.68 (1H, d, *J* = 11.9 Hz, H2), 2.82 (3H, d, *J* = 4.5 Hz, H11).

^{13}C NMR (101 MHz, Chloroform-*d*): δ 167.2 (C1), 136.6 (C6), 136.2 (C3), 136.1 (C5), 129.4 (C7), 128.3 (C8), 127.7 (C9), 125.9 (C4), 122.5 (C2), 26.2 (C11).

HRMS (ESI^{+}) *m/z* calculated for $C_{12}H_{14}NO$ $[M+H]^{+}$ 188.1070, found 188.1077.

IR: ν_{max} = 3295 (N-H), 2981 (C-H), 2922 (C-H), 2865 (C-H), 1640 (C=O), 1548 (C=C), 1454, 1407.

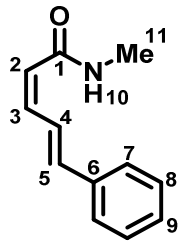

^{1}H NMR (400 MHz, Chloroform-*d*): δ 8.24 (1H, dd, *J* = 16.0, 11.6 Hz, H4), 7.31-7.17 (5H, m, H7-H9), 6.65 (1H, d, *J* = 16.0 Hz, H5), 6.48 (1H, t, *J* = 11.6 Hz, H3), 6.09 (1H, br s, H10), 5.62 (1H, d, *J* = 11.6 Hz, H2), 2.80 (3H, d, *J* = 4.5 Hz, H11).

^{13}C NMR (101 MHz, Chloroform-*d*): δ 167.4 (C1), 141.1 (C3), 139.5 (C5), 136.7 (C6), 128.7 (C9), 128.6 (C8), 127.3 (C7), 125.4 (C4), 120.3 (C2), 26.2 (C11).

HRMS (ESI^{+}) *m/z* calculated for $C_{12}H_{14}NO$ $[M+H]^{+}$ 188.1070, found 188.1074.

IR: ν_{max} = 3295 (N-H), 2981 (C-H), 2922 (C-H), 2865 (C-H), 1640 (C=O), 1548 (C=C), 1454, 1407.

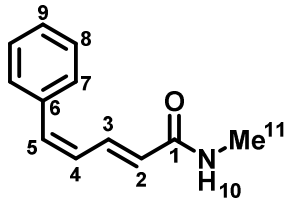

Isomers 379 and 380: Yellow oil (16 mg, 0.08 mmol, 16%). Isolated as a mixture of isomers **379** and **380** in a ratio of 55:45 respectively, giving a 9% yield of **379** and 7% yield of **380**.

^{1}H NMR (400 MHz, Chloroform-*d*): δ 7.71 (1H, dd, *J* = 15.0, 11.5 Hz, H3), 7.46-7.27 (5H, m, H7-H9), 6.74 (1H, d, *J* = 11.5 Hz, H5), 6.32 (1H, t, *J* = 11.5 Hz, H4), 6.00 (1H, d, *J* = 15.0 Hz, H2), 5.65 (1H, br s, H10), 2.89 (3H, d, *J* = 4.1 Hz, H11).

^{13}C NMR (101 MHz, Chloroform-*d*): δ 166.9 (C1), 136.7 (C3), 136.6 (C6), 136.4 (C5), 129.3 (C7), 128.6 (C8), 128.1 (C9), 127.6 (C4), 126.2 (C2), 26.6 (C11).

HRMS (ESI^{+}) *m/z* calculated for $C_{12}H_{14}NO$ $[M+H]^{+}$ 188.1068, found 188.1077.

IR: ν_{max} = 3305 (N-H), 2995 (C-H), 2865 (C-H), 1642 (C=O), 1603 (C=C), 1548 (C=C), 1450, 1386.

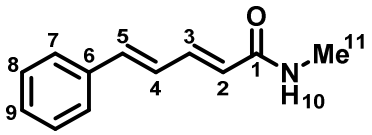

^{1}H NMR (400 MHz, Chloroform-*d*): δ 7.47-7.27 (6H, m, H3, H7-H9), 6.89-6.79 (2H, m, H4, H5), 5.96 (1H, d, *J* = 15.1 Hz, H2), 5.67 (1H, br s, H10), 2.91 (3H, d, *J* = 5.1 Hz, H11).

^{13}C NMR (101 MHz, Chloroform-*d*): δ 167.3 (C1), 141.0 (C3), 139.3 (C5), 136.4 (C6), 128.9 (C7), 128.8 (C8), 127.1 (C9), 126.5 (C4), 123.8 (C2), 26.6 (C11).

HRMS (ESI^{+}) *m/z* calculated for $C_{12}H_{14}NO$ $[M+H]^{+}$ 188.1070, found 188.1065.

IR: ν_{max} = 3305 (N-H), 2995 (C-H), 2865 (C-H), 1642 (C=O), 1603 (C=C), 1548 (C=C), 1450, 1386.

1-Methyl-6-vinyl-3,6-dihydropyridin-1(1*H*)-one (381)

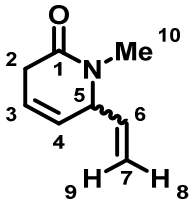

Synthesised according to the procedure by Sošnicki *et al.*[119]

To a solution of vinyl magnesium chloride (8.00 mL, 12.84 mmol, 1.6 eq.) in anhydrous THF (15 mL) in an ice bath was added MeLi (16.00 mL, 25.68 mmol, 2.8 eq.). After 5 min stirring in an ice bath, the mixture was cooled to −78 °C before addition of a solution of *N*-methyl-2-pyridone (**375**) (0.90 mL, 9.17 mmol, 1.0 eq.) in anhydrous THF (40 mL) slowly. After 1 h stirring at −78 °C, the mixture was left to stir for 45 min in an ice bath. The reaction was carefully quenched with saturated $NH_4Cl_{(aq.)}$ (30 mL) and water (20 mL) and the aqueous layer extracted with EtOAc (3 × 30 mL). The combined organics were washed with brine (30 mL), dried over $MgSO_4$, filtered and concentrated *in vacuo*. The crude mixture was filtered through a silica plug, washing with EtOAc to afford the title compound as an orange liquid (0.81 g, 5.96 mmol, 65%).

^{1}H NMR (400 MHz, Chloroform-*d*): δ 5.76-5.70 (1H, m, H3), 5.63-5.58 (1H, m, H4), 5.55 (1H, ddd, *J* = 15.1, 10.0, 8.1 Hz, H6), 5.19 (1H, dt, *J* = 15.1, 1.0 Hz, H9), 5.16 (1H, dt, *J* = 10.0, 1.0 Hz, H8), 4.23 (1H, dq, *J* = 8.1, 3.5 Hz, H5), 2.95-2.87 (5H, m, H2, H10).

^{13}C NMR (101 MHz, Chloroform-*d*): δ 167.5 (C1), 136.8 (C6), 124.5 (C4), 122.3 (C3), 117.2 (C7), 64.3 (C5), 32.4 (C10), 31.9 (C2).

Data consistent with literature.[119]

N-Methylhepta-2,4,6-trienamide (383, 384 and 385)

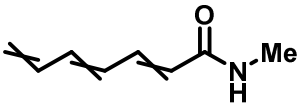

To a solution of DIPA (0.20 mL, 1.46 mmol, 2.0 eq.) in anhydrous THF (5 mL) was added ^{n}BuLi (0.64 mL, 1.53 mmol, 2.1 eq., 2.5 M in hexanes) at −78 °C. To this basic solution was added 1-methyl-6-vinyl-3,6-dihydropyridin-1(1*H*)-one (**381**) (100 mg, 0.73 mmol, 1.0 eq.) in anhydrous THF (10 mL) at –78 °C. The orange-red solution was irradiated at 365 nm (Thorlabs M365LP1) for 2.5 h before being quenched with saturated $NH_4Cl_{(aq.)}$ (10 mL). The aqueous layer was extracted with EtOAc (3 × 10 mL) before the combined organics were washed with brine (10 mL), dried over Na_2SO_4, filtered and concentrated *in vacuo*. Purification by flash column chromatography (15%-30% EtOAc / petroleum ether) afforded two separate mixtures, each containing two isomers of ring-opened product (see below).

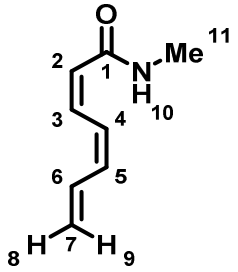

Isomers 383 and 384: White solid (68 mg, 0.42 mmol, 68%). Isolated as a mixture of isomers **383** and **384** in a ratio of 77:23 respectively, giving a 51% yield for **383** and 17% yield for **384**.

^{1}H NMR (400 MHz, Chloroform-*d*): δ 7.34 (1H, tt, *J* = 11.0, 0.9 Hz, H5), 6.89-6.78 (2H, m, H3, H6), 6.24 (1H, t, *J* = 11.0 Hz, H4), 6.08 (1H, br s, H10), 5.67 (1H, d, *J* = 11.4 Hz, H2), 5.34 (1H, d, *J* = 16.6 Hz, H9), 5.26 (1H, d, *J* = 10.0 Hz, H8), 2.82 (3H, d, *J* = 5.0 Hz, H11).

^{13}C NMR (101 MHz, Chloroform-*d*): δ 167.2 (C1), 135.8 (C4), 134.3 (C3), 131.1 (C6), 125.2 (C5), 121.5 (C2), 121.0 (C7), 26.2 (C11).

HRMS (ESI^+) *m/z* calculated for $C_8H_{12}NO$ $[M+H]^+$ 138.0913, found 138.0905.

IR: ν_{max} = 3290 (N-H), 2987 (C-H), 2845 (C-H), 1650 (C=O), 1656 (C=C), 1543 (C=C), 1475, 1460, 1386.

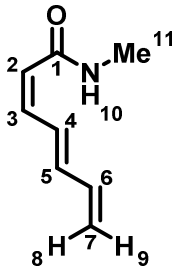

^{1}H NMR (400 MHz, Chloroform-*d*): δ 7.62 (1H, dd, *J* = 14.6, 11.4 Hz, H5), 6.50-6.32 (3H, m, H3, H4, H6), 6.08 (1H, br s, H10), 5.60 (1H, d, *J* = 11.1 Hz, H2), 5.32 (1H, d, *J* = 16.1 Hz, H8), 5.21 (1H, d, *J* = 9.9 Hz, H9), 2.82 (3H, d, *J* = 5.0 Hz, H11).

^{13}C NMR (101 MHz, Chloroform-*d*): δ 167.2 (C1), 140.5 (C3), 140.1 (C6), 136.9 (C4), 129.5 (C5), 120.7 (C2), 120.5 (C7), 26.2 (C11).

HRMS (ESI^{+}) *m/z* calculated for $C_8H_{12}NO$ $[M+H]^+$ 138.0913, found 138.0906.

IR: ν_{max} = 3290 (N-H), 2987 (C-H), 2845 (C-H), 1650 (C=O), 1656 (C=C), 1543 (C=C), 1475, 1460, 1386.

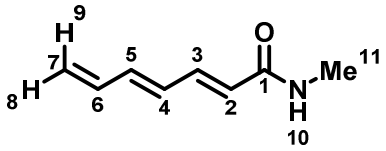

Isomer 385: White solid (25 mg, 0.18 mmol, 25%).

^{1}H NMR (400 MHz, Chloroform-*d*): δ 7.23 (1H, dd, *J* = 15.0, 11.7 Hz, H3), 6.49 (1H, dd, *J* = 14.8, 10.9 Hz, H5), 6.44-6.32 (1H, m, H6), 6.27 (1H, dd, *J* = 14.8, 11.7 Hz, H4), 5.89 (1H, d, *J* = 15.0 Hz, H2), 5.85 (1H, br s, H10), 5.36 (1H, d, *J* = 16.6 Hz, H9), 5.25 (1H, d, *J* = 9.8 Hz, H8), 2.88 (3H, d, *J* = 5.0 Hz, H11).

^{13}C NMR (101 MHz, Chloroform-*d*): δ 166.9 (C1), 140.4 (C3), 139.7 (C5), 136.4 (C6), 130.7 (C4), 124.2 (C2), 120.8 (C7), 26.5 (C11).

HRMS (ESI^{+}) *m/z* calculated for $C_8H_{12}NO$ $[M+H]^+$ 138.0913, found 138.0907.

IR: ν_{max} = 3287 (N-H), 2967 (C-H), 2832 (C-H), 1666 (C=O), 1650 (C=C), 1620 (C=C), 1467, 1452, 1365.

Section 6 Experimental

N-Benzyl-*N*-(*tert*-butyl)quinoline-3-carboxamide (428)

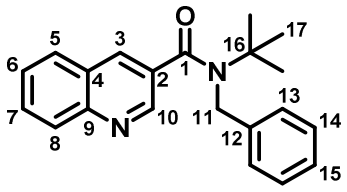

To a solution of 3-quinoline carboxylic acid (0.50 g, 2.89 mmol, 1.0 eq.) in anhydrous CH_2Cl_2 (30 mL) was added a few drops of anhydrous DMF. Thionyl chloride (1.25 mL, 17.34 mmol, 6.0 eq.) was added, and the mixture refluxed for 16 h. Excess volatiles were removed *in vacuo* before the grey residue was dissolved in anhydrous CH_2Cl_2 (20 mL). Et_3N (**107**) (1.20 mL, 3.48 mmol, 3.0 eq.) was added before addition of *N*-benzyl-2-methylpropan-2-amine (**121**) (0.70 g, 4.33 mmol, 1.5 eq.) and the mixture left to stir for 3 h. The reaction was quenched with $HCl_{(aq.)}$ (20 mL, 3 M) and the aqueous layer was extracted with CH_2Cl_2 (3 × 20 mL). The combined organics were washed with water (2 × 20 mL), brine (2 × 20 mL), dried over $MgSO_4$, filtered and concentrated *in vacuo*. Purification by flash column chromatography (10-20% EtOAc / petroleum ether) afforded the title compound as an oil which solidified to a white solid (0.72 g, 2.28 mmol, 79%).

^{1}H NMR (400 MHz, Chloroform-*d*): δ 8.94 (1H, d, *J* = 2.1 Hz, H3), 8.15 (1H, d, *J* = 2.1 Hz, H10), 8.05 (1H, dd, *J* = 8.5, 0.8 Hz, H5), 7.73-7.67 (2H, m, H6, H7), 7.52 (1H, td, *J* = 7.7, 1.0 Hz, H8), 7.35-7.29 (2H, m, H14), 7.26-7.19 (3H, m, H13, H15), 4.66 (2H, s, H11), 1.57 (9H, s, H13).

^{13}C NMR (101 MHz, Chloroform-*d*): δ 171.4 (C1), 148.3 (C3), 148.1 (C9), 139.5 (C12), 133.6 (C10), 132.2 (C4), 130.4 (C6), 129.4 (C5), 128.9 (C14), 128.3 (C7), 127.4 (C2), 127.3 (C15), 127.1 (C8), 126.3 (C14), 58.8 (C16), 51.8 (C11), 28.8 (C17).

HRMS (ESI^+) *m/z* calculated for $C_{21}H_{23}N_2O$ $[M+H]^+$ 319.1805, found 319.1795.

IR: ν_{max} = 2977 (C-H), 1628 (C=O), 1392 (C=C), 1250, 942.

2-(*tert*-Butyl)-3-phenyl-2,3,3a,4-tetrahydro-1*H*-pyrrolo[3,4-*b*]quinoline-1-one (443) and 2-(*t*ert-Butyl)-3-phenyl-2,3-dihydro-1*H*-pyrrolo[3,4-*b*]quinolin-1-one (444)

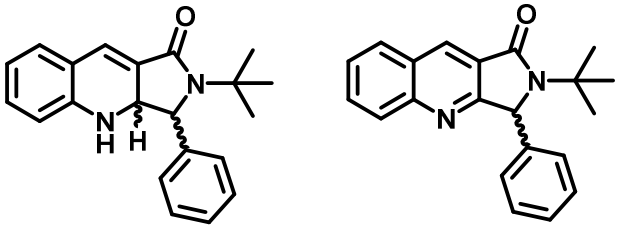

Synthesised according to the procedure by Clayden *et al.*[34]

To a solution of DIPA (0.13 mL, 0.94 mmol, 3.0 eq.) in anhydrous THF (5 mL) was added ^{n}BuLi (0.41 mL, 1.04 mmol, 3.3 eq., 2.5 M in hexanes) at −40 °C. After 15 min at this temperature, a solution of *N*-benzyl-*N*-(*tert*-butyl)quinoline-3-carboxamide (**428**) (100 mg, 0.31 mmol, 1.0 eq.) in anhydrous THF (10 mL) was added to give a deep purple colour. After 15 minutes at this temperature, the reaction was quenched with saturated $NH_4Cl_{(aq.)}$ (10 mL) and water (10 mL) as the mixture became a light fluorescent green/yellow colour. The aqueous layer was extracted with EtOAc (3 × 10 mL) before the combined organics were washed with brine (10 mL), dried over $MgSO_4$, filtered and concentrated *in vacuo*. Purification by flash column chromatography (10-30% EtOAc / petroleum ether) afforded a fluorescent green/yellow solid as a mixture of the title compounds in an approximate ratio of 66:33 (**443**:**444**). The dearomatised compound **443** is only observed if the purification is carried out without delay, due to rearomatisation in air to give **444**.

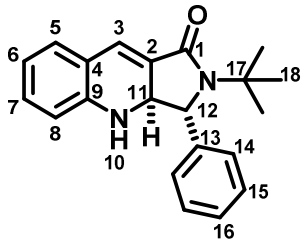

Dearomatised Product (443): Yellow fluorescent solid (40 mg, 0.12 mmol, 40%) before full rearomatisation to **444**. Relative stereochemistry assigned based on analogy to the dearomatising cyclisation of benzyl benzamide studied in the Clayden group. IR characterisation or melting point analysis not possible due to rapid oxidation in air.

^{1}H NMR (400 MHz, Chloroform-*d*): δ 7.35-7.17 (5H, m, H14-H16), 7.01 (1H, s, H3), 7.00 (1H, dd, *J* = 7.8, 1.5 Hz, H5), 6.89 (1H, td, *J* = 7.8, 1.5 Hz, H7), 6.58 (1H, td, *J* = 7.8, 1.1 Hz, H6), 6.24 (1H, d, *J* = 7.8 Hz,

H8), 5.06 (1H, d, *J* = 7.7 Hz, H12), 4.96 (1H, dq, *J* = 7.7, 1.7 Hz, H11), 3.24 (1H, br s, H10), 1.36 (9H, s, H18).

^{13}C NMR (101 MHz, Chloroform-*d*): δ 167.4 (C1), 145.1 (C9), 138.0 (C13), 130.1 (C7), 129.1 (C14), 128.7 (C3), 128.4 (C15), 128.2 (C16), 127.0 (C2), 125.9 (C5), 120.7 (C4), 118.9 (C6), 114.0 (C8), 65.8 (C12), 55.7 (C17), 53.8 (C11), 28.3 (C18).

HRMS (ESI$^+$) *m/z* calculated for $C_{21}H_{23}N_2O$ $[M+H]^+$ 319.1805, found 319.1799.

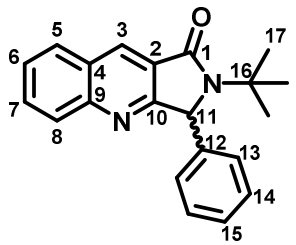

Rearomatised Product (444): White crystalline solid obtained after rearomatisation of **443** in solution (59 mg, 0.19 mmol, 60%). The structure of this molecule is confirmed by single crystal X-ray crystallography.

^{1}H NMR (400 MHz, Chloroform-*d*): δ 8.49 (1H, s, H3), 7.93 (1H, d, *J* = 7.0 Hz, H5), 7.86 (1H, d, *J* = 7.0 Hz, H8), 7.62 (1H, td, *J* = 7.0, 1.6 Hz, H6), 7.45 (1H, td, *J* = 7.0, 1.2 Hz, H7), 7.29-7.12 (5H, m, H13-H15), 5.78 (1H, s, H11), 1.45 (9H, s, H17).

^{13}C NMR (101 MHz, Chloroform-*d*): δ 167.8 (C1), 164.2 (C10), 150.3 (C9), 139.6 (C12), 132.3 (C3), 131.0 (C6), 129.5 (C5), 129.4 (C8), 129.1 (C13), 128.2 (C14), 127.8 (C15), 127.0 (C2), 126.8 (C7), 124.1 (C4), 66.6 (C11), 56.6 (C16), 28.7 (C17).

HRMS (ESI$^+$) *m/z* calculated for $C_{21}H_{21}N_2O$ $[M+H]^+$ 317.1648, found 317.1643.

IR: ν_{max} = 2979 (C-H), 1635 (C=O), 1380 (C=C), 1267, 943.

X-Ray Crystallography:

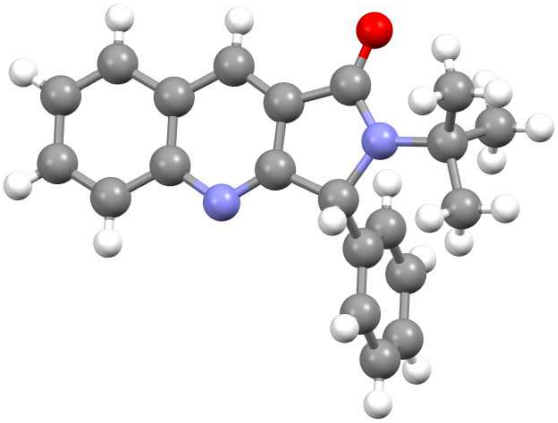

Empirical formula	$C_{21}H_{20}N_2O$
Formula weight	316.39
Temperature/K	100.00
Crystal system	triclinic
Space group	P-1
a/Å	6.3357(6)
b/Å	10.9143(11)
c/Å	11.9768(11)
α/°	85.975(3)
β/°	84.488(3)
γ/°	77.816(3)
Volume/Å^3	804.73(13)
Z	2
ρ_{calc}g/cm^3	1.306
μ/mm^{-1}	0.081
F(000)	336.0
Crystal size/mm^3	0.353 × 0.308 × 0.06
Radiation	MoKα (λ = 0.71073)
2Θ range for data collection/°	3.42 to 54.184
Index ranges	$-8 \leq h \leq 8$, $-13 \leq k \leq 13$, $-15 \leq l \leq 15$
Reflections collected	18364
Independent reflections	3536 [R_{int} = 0.0600, R_{sigma} = 0.0620]
Data/restraints/parameters	3536/0/220
Goodness-of-fit on F^2	1.037
Final R indexes [I>=2σ (I)]	R_1 = 0.0466, wR_2 = 0.0966
Final R indexes [all data]	R_1 = 0.0841, wR_2 = 0.1073
Largest diff. peak/hole / e Å^{-3}	0.19/-0.25

N-Benzyl-*N*-(*tert*-butyl)quinoline-2-carboxamide (435)

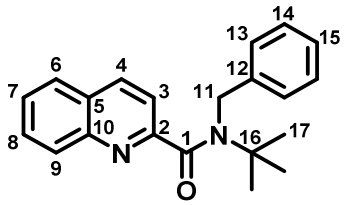

To a solution of quinaldic acid (1.00 g, 5.78 mmol, 1.0 eq.) in anhydrous CH_2Cl_2 (50 mL) was added a few drops of anhydrous DMF. Thionyl chloride (2.50 mL, 34.67 mmol, 6.0 eq.) was added, and the mixture refluxed for 4 h. Excess volatiles were removed *in vacuo* before the grey residue was dissolved in anhydrous CH_2Cl_2 (30 mL). Et_3N (**107**) (2.40 mL, 17.34 mmol, 3.0 eq.) was added before addition of *N*-benzyl-2-methylpropan-2-amine (**121**) (1.40 g, 8.67 mmol, 1.5 eq.) and the mixture left to stir for 16 h. The reaction was quenched with $HCl_{(aq.)}$ (40 mL, 3 M) and the aqueous layer was extracted with CH_2Cl_2 (3 × 30 mL). The combined organics were washed with water (2 × 20 mL), brine (2 × 20 mL), dried over $MgSO_4$, filtered and concentrated *in vacuo*. Purification by flash column chromatography (0-20% EtOAc / petroleum ether) afforded the title compound as an off-white solid (1.59 g, 4.97 mmol, 86%).

^{1}H NMR (400 MHz, Chloroform-*d*): δ 8.13 (1H, d, *J* = 8.3 Hz, H4), 7.96 (1H, d, *J* = 6.9 Hz, H9), 7.75 (1H, d, *J* = 6.9 Hz, H6), 7.66 (1H, td, *J* = 6.9, 1.6 Hz, H8), 7.60 (1H, d, *J* = 8.3 Hz, H3), 7.51 (1H, td, *J* = 6.9 Hz, 1.2 Hz, H7), 7.35-7.24 (4H, m, H13-H14), 7.22-7.16 (1H, m, H15), 4.78 (2H, s, H11), 1.57 (9H, s, H17).

^{13}C NMR (101 MHz, Chloroform-*d*): δ 171.3 (C1), 156.3 (C2), 146.7 (C10), 140.0 (C12), 137.0 (C4), 129.9 (C8), 129.8 (C9), 128.4 (C14), 127.8 (C5), 127.6 (C6), 127.2 (C7), 126.9 (C15), 126.8 (C13), 120.2 (C3), 58.7 (C16), 50.8 (C11), 28.8 (C17).

HRMS (ESI^+) *m/z* calculated for $C_{21}H_{23}N_2O$ $[M+H]^+$ 319.1805, found 319.1798.

IR: ν_{max} = 2967 (C-H), 1646 (C=O), 1462 (C=C), 1382, 1251, 1151.

2-(*tert*-Butyl)-1-phenyl-1,2-dihydro-3*H*-pyrrolo[3,4-*b*]quinolin-3-one (437)

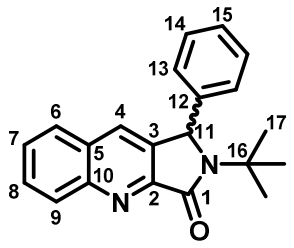

Synthesised according to the procedure by Clayden *et al.*[34]

To a solution of DIPA (0.13 mL, 0.94 mmol, 3.0 eq.) in anhydrous THF (5 mL) was added ^{n}BuLi (0.41 mL, 1.04 mmol, 3.3 eq., 2.5 M in hexanes) at −40 °C. After 15 min at this temperature, a solution of *N*-benzyl-*N*-(*tert*-butyl)quinoline-2-carboxamide (**435**) (100 mg, 0.31 mmol, 1.0 eq.) in anhydrous THF (10 mL) was added to give a deep blue-green solution. After 3 h at this temperature, the reaction was quenched with saturated $NH_4Cl_{(aq.)}$ (10 mL) and water (10 mL). The aqueous layer was extracted with EtOAc (3 × 10 mL) before the combined organics were washed with brine (10 mL), dried over $MgSO_4$, filtered and concentrated *in vacuo*. Purification by flash column chromatography (0-20% EtOAc / petroleum ether) afforded the title compound as a white solid (23 mg, 0.07 mmol, 23%).

^{1}H NMR (400 MHz, Chloroform-*d*): δ 8.34 (1H, d, *J* = 8.9 Hz, H9), 7.80 (1H, s, H4), 7.75-7.69 (2H, m, H6, H8), 7.54 (1H, ddd, *J* = 9.0, 6.6, 1.3 Hz, H7), 7.37-7.25 (5H, m, H13-H15), 5.86 (1H, s, H11), 1.53 (9H, s, H17).

^{13}C NMR (101 MHz, Chloroform-*d*): δ 167.4 (C1), 150.9 (C2), 149.3 (C10), 140.9 (C12), 135.9 (C13), 131.0 (C9), 130.5 (C4), 130.0 (C6), 129.4 (C5), 129.1 (C3), 128.4 (C14), 128.0 (C8), 127.8 (C7), 126.3 (C15), 62.6 (C11), 57.1 (C16), 28.5 (C17).

Data consistent with literature.[34]

1-(*tert*-Butyl)-4-phenyl-1'*H*-spiro[azetidine-3,2'-quinolin]-2-one (447)

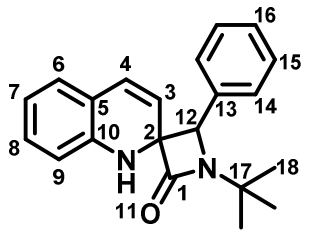

To a solution of DIPA (0.13 mL, 0.94 mmol, 3.0 eq.) in anhydrous THF (5 mL) was added ^{n}BuLi (0.41 mL, 1.04 mmol, 3.3 eq., 2.5 M in hexanes) at −78 °C. After 15 min at this temperature, a solution of *N*-benzyl-*N*-(*tert*-butyl)quinoline-2-carboxamide (**435**) (100 mg, 0.31 mmol, 1.0 eq.) in anhydrous THF (10 mL) was added to give a deep green solution. After 1 h at this temperature, the reaction was quenched with saturated $NH_4Cl_{(aq.)}$ (10 mL) and water (10 mL). The aqueous layer was extracted with EtOAc (3 × 10 mL) before the combined organics were washed with brine (10 mL), dried over $MgSO_4$, filtered and concentrated *in vacuo*. This afforded the title compound as a white solid (66 mg, 0.21 mmol, 68%) which overnight degraded to a black goo. Melting point and IR data not reported due to degradation of sample following NMR analysis. Similarly, the relative stereochemistry of the diastereomer has not been determined.

^{1}H NMR (400 MHz, Chloroform-*d*): δ 7.28-7.13 (5H, m, H14-H16), 6.90 (1H, ddd, *J* = 7.9, 7.7, 1.0 Hz, H7), 6.68 (1H, dd, *J* = 7.7, 1.0 Hz, H6), 6.49 (1H, td, *J* = 7.9, 1.3 Hz, H8), 6.44 (1H, d, *J* = 7.9 Hz, H9), 6.19 (1H, d, *J* = 9.9 Hz, H4), 5.22 (1H, dd, *J* = 9.9, 1.0 Hz, H3), 4.57 (1H, br s, H11), 4.42 (1H, s, H12), 1.28 (9H, s, H18).

^{13}C NMR (101 MHz, Chloroform-*d*): δ 171.7 (C1), 141.0 (C5), 137.0 (C13), 129.0 (C7), 128.4 (C4), 128.3 (C16), 127.8 (C15), 127.1 (C14), 127.0 (C6), 118.6 (C10), 117.9 (C8), 117.0 (C3), 112.4 (C9), 76.7 (C12), 74.7 (C2), 54.5 (C17), 28.3 (C18).

HRMS (ESI^{+}) *m/z* calculated for $C_{21}H_{23}N_2O$ $[M+H]^{+}$ 319.1805, found 319.1797.

Section 7 Experimental

N-Benzyl-*N*-(*tert*-butyl)acrylamide (469)

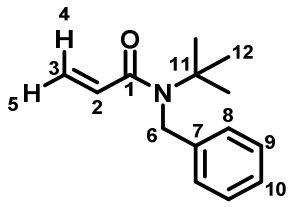

Synthesised according to the procedure by Clayden *et al.*[137]

To a solution of *N*-benzyl-2-methylpropan-2-amine (**121**) (4.00 g, 24.51 mmol, 2.2 eq.) in anhydrous CH_2Cl_2 (20 mL) was added Et_3N (**107**) (3.10 mL, 22.28 mmol, 2.0 eq.) and DMAP (0.14 g, 1.11 mmol, 0.1 eq.). In an ice bath, a solution of acryloyl chloride (0.90 mL, 11.14 mmol, 1.0 eq.) in anhydrous CH_2Cl_2 (10 mL) was added slowly and the mixture left to stir at rt for 16 h. The reaction was quenched with $HCl_{(aq.)}$ (30 mL, 1 M) and the layers separated. The aqueous layer was extracted with CH_2Cl_2 (20 mL) before the combined organics were washed with $HCl_{(aq.)}$ (10 mL, 3 M), dried over $MgSO_4$, filtered and concentrated *in vacuo*. Purification by flash column chromatography (0-5% EtOAc / petroleum ether) afforded the title compound as a white crystalline solid (2.21 g, 10.25 mmol, 92%).

^{1}H NMR (400 MHz, Chloroform-*d*): δ 7.39-7.33 (2H, m, H8), 7.29-7.21 (3H, m, H9, H10), 6.38 (1H, dd, *J* = 16.7, 9.9 Hz, H2), 6.30 (1H, dd, *J* = 16.7, 3.0 Hz, H4), 5.53 (1H, dd, *J* = 9.9, 3.0 Hz, H5), 4.63 (2H, s, H6), 1.45 (9H, s, H12).

^{13}C NMR (101 MHz, Chloroform-*d*): δ 168.7 (C1), 139.6 (C7), 131.7 (C2), 128.9 (C8), 127.3 (C3), 127.2 (C10), 125.8 (C9), 57.9 (C11), 49.1 (C6), 28.7 (C12).

Data consistent with literature.[137]

N-Benzyl-*N*-(*tert*-butyl)-1*H*-pyrrole-3-carboxamide (471)

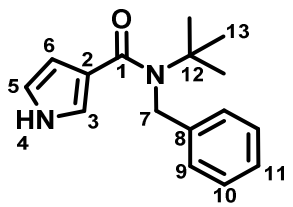

Synthesised according to the procedure by Clayden *et al.*[137]

A solution of *N*-benzyl-*N*-(*tert*-butyl)acrylamide (**469**) (2.00 g, 9.17 mmol, 1.0 eq.) and tosylmethylisocyanide (**470**) (1.80 g, 9.17 mmol, 1.0 eq.) in DMSO (22 mL) and Et_2O (28 mL) was added slowly to a stirred suspension of NaH (1.11 g, 11.92 mmol, 1.3 eq., 60% in mineral oil) in Et_2O (50 mL) in an ice bath. The reaction was stirred at rt for 16 h before being quenched with water (30 mL) and $NaOH_{(aq.)}$ (30 mL, 1 M). The aqueous layer was extracted with Et_2O (3 × 40 mL) before the combined organics were washed with water (3 × 30 mL), dried over $MgSO_4$, filtered and concentrated *in vacuo*. Trituration with CH_2Cl_2 afforded the title compound as an off-white solid (1.10 g, 4.31 mmol, 47%).

^{1}H NMR (400 MHz, Chloroform-*d*): δ 9.02 (1H, br s, H4), 7.43-7.23 (5H, m, H9-H11), 7.02 (1H, br s, H3), 6.56 (br q, *J* = 2.4 Hz, H5), 6.31 (1H, br q, *J* = 2.4 Hz, H6), 4.90 (2H, s, H7), 1.49 (9H, s, H13).

^{13}C NMR (101 MHz, Chloroform-*d*): δ 170.2 (C1), 141.6 (C8), 128.7 (C10), 126.8 (C11), 126.3 (C9), 121.6 (C2), 121.0 (C3), 117.9 (C5), 110.0 (C6), 58.1 (C12), 51.7 (C7), 28.8 (C13).

Data consistent with literature.[137]

tert-Butyl 3-(benzyl(*tert*-butyl)carbamoyl)-1*H*-pyrrole-1-carboxylate (464)

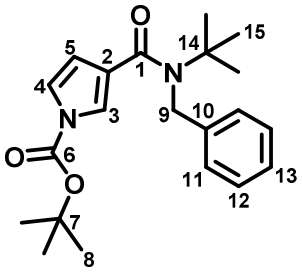

Synthesised according to the procedure by Clayden *et al.*[137]

A solution of *N*-benzyl-*N*-(*tert*-butyl)-1*H*-pyrrole-3-carboxamide (**471**) (0.50 g, 1.95 mmol, 1.1 eq.) in anhydrous THF (20 mL) was added slowly to a slurry of NaH (0.16 g, 3.90 mmol, 2.2 eq., 60% in mineral oil) in anhydrous THF (20 mL). After 30 minutes, di-*tert*-butyl dicarbonate (0.45 mL, 1.85 mmol, 1.0 eq.) was added slowly and the reaction heated to 50 °C for 16 h. The reaction was quenched with water (20 mL) and the aqueous layer extracted with EtOAc (3 × 30 mL). The combined organics were washed with water (60 mL), dried over $MgSO_4$, filtered and concentrated *in vacuo*. Purification by flash column chromatography (5% EtOAc / petroleum ether) afforded the title compound as a white solid (0.62 g, 1.65 mmol, 89%).

^{1}H NMR (400 MHz, Chloroform-*d*): δ 7.41 (1H, t, *J* = 1.7 Hz, H3), 7.39-7.22 (5H, m, H11-H13), 7.06 (1H, dd, *J* = 3.3, 1.7 Hz, H4), 6.29 (1H, dd, *J* = 3.3, 1.7, H5), 4.79 (2H, s, H9), 1.49 (9H, s, H8), 1.47 (9H, s, H15).

^{13}C NMR (101 MHz, Chloroform-*d*): δ 168.6 (C1), 148.4 (C6), 140.9 (C10), 128.8 (C12), 127.0 (C13), 126.2 (C11), 124.9 (C2), 121.9 (C3), 119.7 (C4), 112.0 (C5), 84.3 (C7), 58.3 (C14), 51.4 (C9), 28.7 (C15), 27.9 (C8).

Data constsistent with literature.[137]

tert-Butyl (*Z*)-(2-(1-(*tert*-butyl)-2-oxo-5-phenyl-2,5-dihydro-1*H*-pyrrol-3-yl)vinyl)carbamate (466)

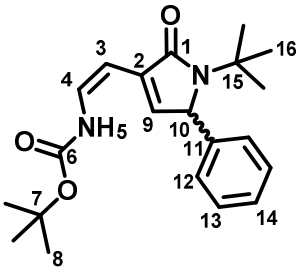

Synthesised according to the procedure by Clayden *et al.*[137]

To a solution of DIPA (0.12 mL, 0.84 mmol, 3.0 eq.) in anhydrous THF (5 mL) was added ^{n}BuLi (0.36 mL, 0.84 mmol, 3.0 eq., 2.5 M in hexanes) dropwise in an ice bath. After stirring in the ice bath for 20 minutes, a solution of *tert*-butyl 3-(benzyl(*tert*-butyl)carbamoyl)-1*H*-pyrrole-1-carboxylate (**464**) (0.10 g, 0.28 mmol, 1.0 eq.) in anhydrous THF (10 mL) was added slowly. After stirring at this temperature for 7 h, the reaction was quenched with saturated $NH_4Cl_{(aq.)}$ (10 mL) and water (10 mL) and the layers separated. The aqueous layer was extracted with EtOAc (3 × 10 mL) before the combined organics were washed with brine (10 mL), dried over $MgSO_4$, filtered and concentrated *in vacuo*. Purification by flash column chromatography (5% EtOAc / petroleum ether) afforded the title compound as a white solid (39 mg, 0.11 mmol, 39%). Remaining starting material **464** was also isolated (29 mg, 0.08 mmol, 29%).

^{1}H NMR (400 MHz, Chloroform-*d*): δ 11.07 (1H, br d, *J* = 9.7 Hz, H5), 7.36-7.12 (5H, m, H12-H14), 6.62 (1H, t, *J* = 9.7 Hz, H4), 6.40 (1H, d, *J* = 2.5 Hz, H9), 5.25 (1H, d, *J* = 2.5 Hz, H10), 4.93 (1H, d, *J* = 9.7 Hz, H3), 1.52 (9H, s, H8), 1.38 (9H, s, H16).

^{13}C NMR (101 MHz, Chloroform-*d*): δ 172.7 (C1), 153.6 (C6), 141.1 (C9), 138.4 (C11), 134.5 (C2), 129.2 (C13), 128.1 (C14), 127.2 (C4), 126.5 (C12), 96.4 (C3), 80.3 (C7), 65.9 (C10), 55.9 (C15), 28.5 (C8), 28.4 (C16).

HRMS (ESI^{+}) *m/z* calculated for $C_{21}H_{29}N_2O_3$ $[M+H]^{+}$ 357.2173, found 357.2175.

MP: 159-160 °C.

IR: ν_{max} = 3185 (N-H), 2965 (C-H), 1725 (C=O), 1659 (C=O), 1640 (C=C), 1464, 1384, 1156, 957.

8.9. Recorded and Predicted UV-Visible Spectra for Relevant Enolates

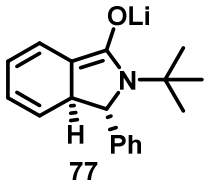

77

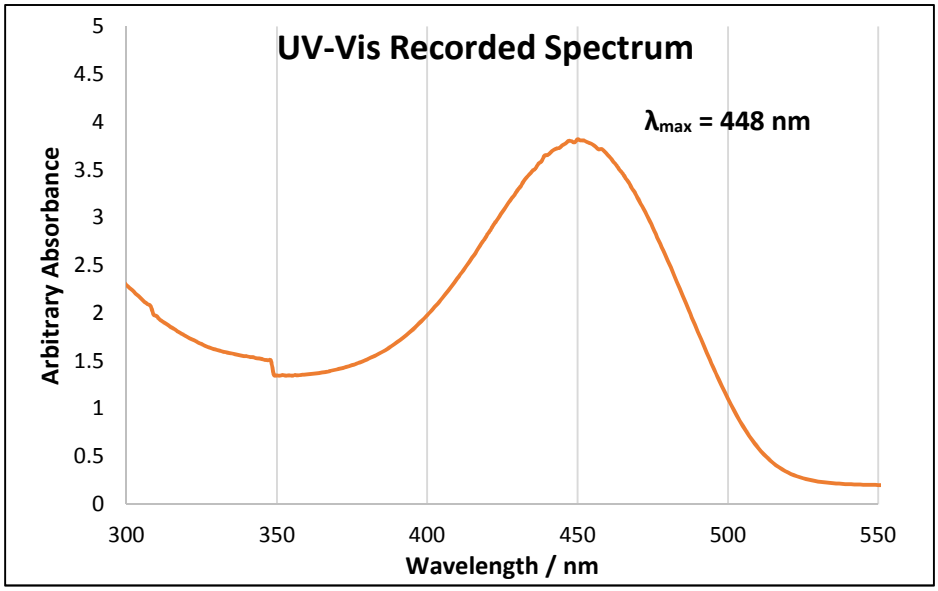

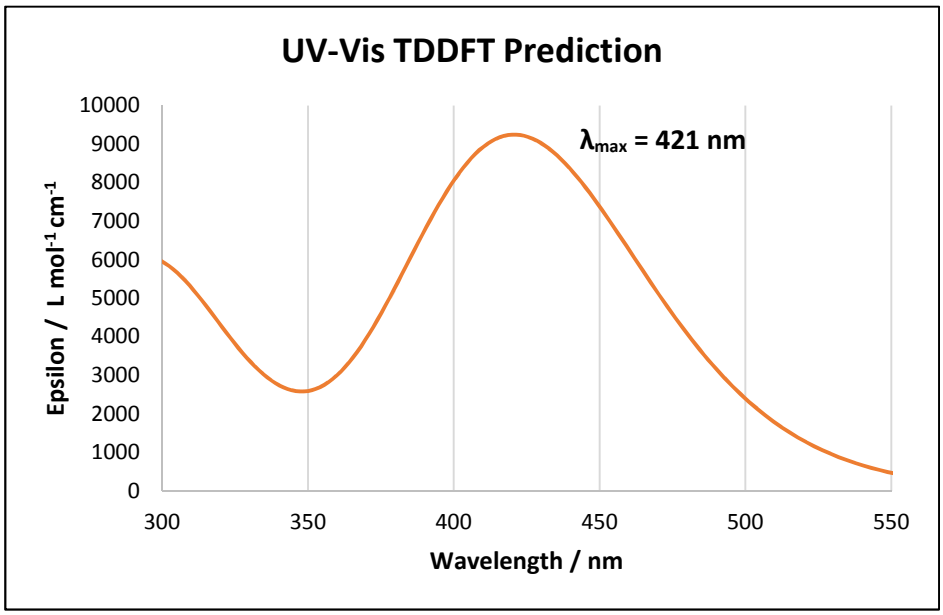

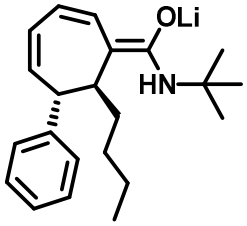
OLi
HN

86

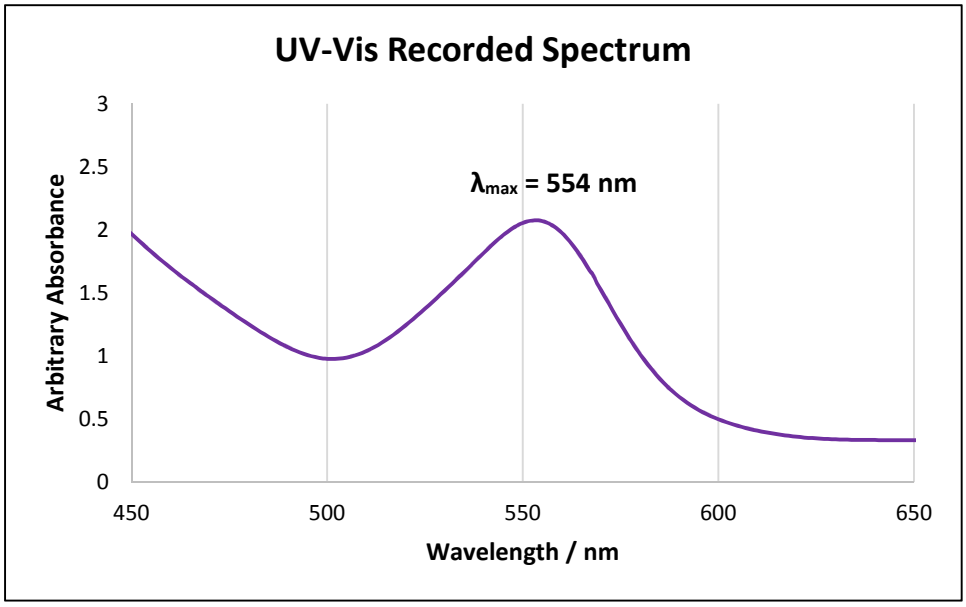
UV-Vis Recorded Spectrum
λmax = 554 nm
Arbitrary Absorbance
3
2.5
2
1.5
1
0.5
0
450
500
550
600
650
Wavelength / nm

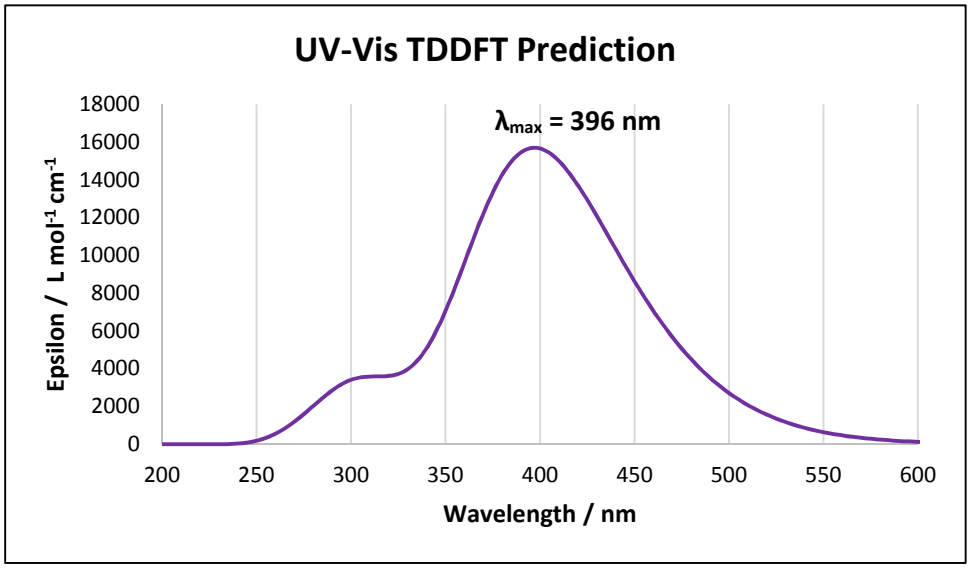
UV-Vis TDDFT Prediction
λmax = 396 nm
Epsilon / L mol-1 cm-1
18000
16000
14000
12000
10000
8000
6000
4000
2000
0
200
250
300
350
400
450
500
550
600
Wavelength / nm

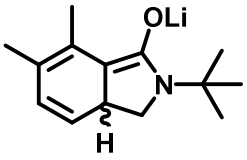
OLi
N
H

87

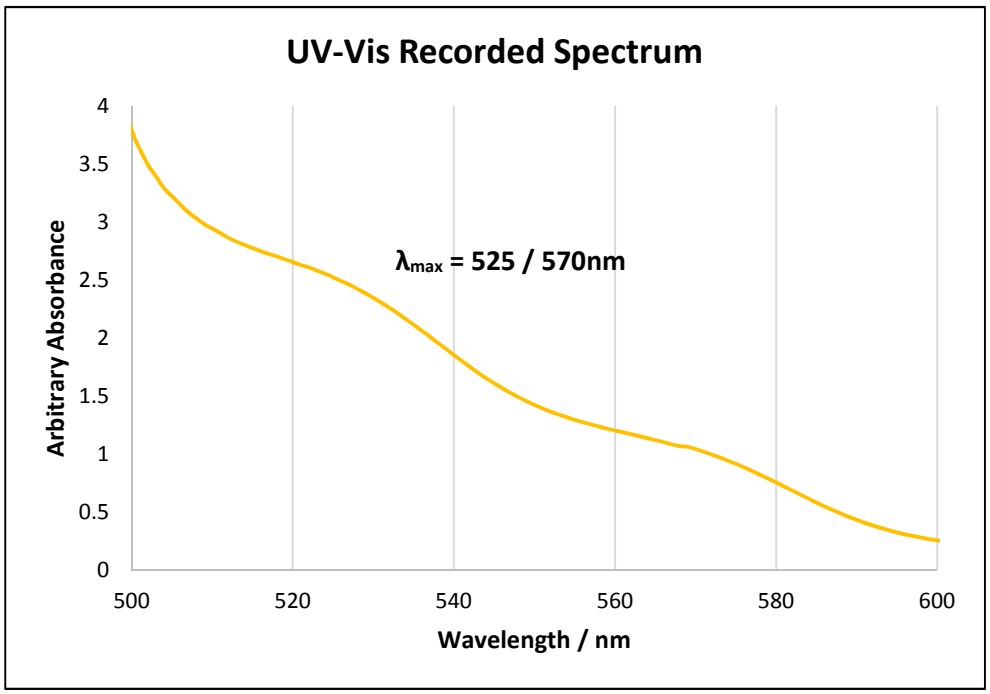
UV-Vis Recorded Spectrum
Arbitrary Absorbance
4
3.5
3
2.5
2
1.5
1
0.5
0
500
520
540
560
580
600
Wavelength / nm
λmax = 525 / 570nm

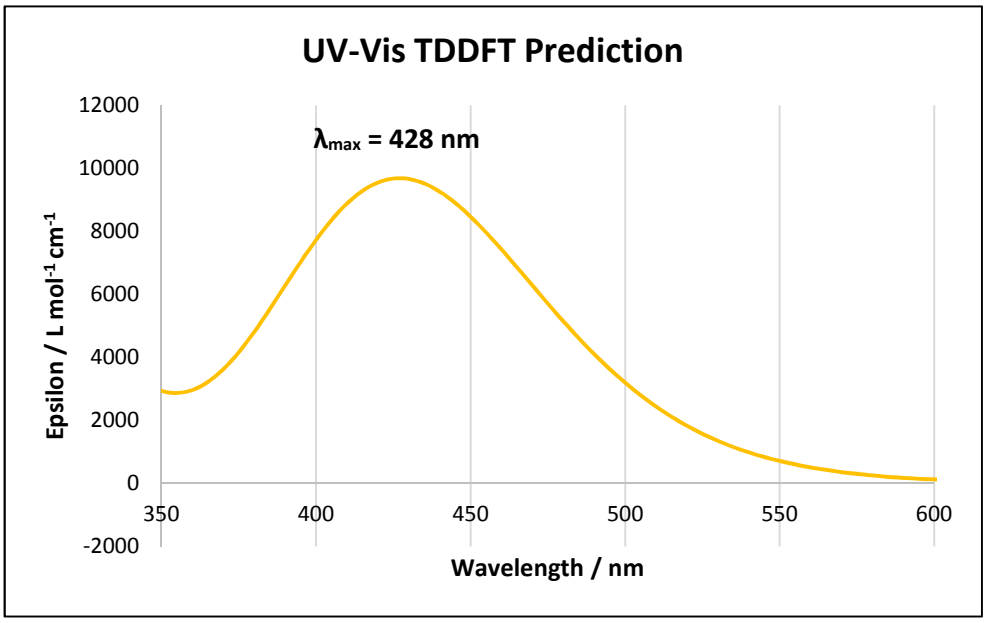
UV-Vis TDDFT Prediction
Epsilon / L mol-1 cm-1
12000
10000
8000
6000
4000
2000
0
-2000
350
400
450
500
550
600
Wavelength / nm
λmax = 428 nm

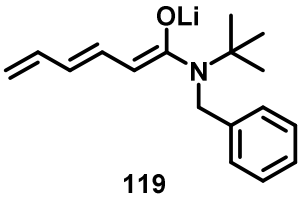

119

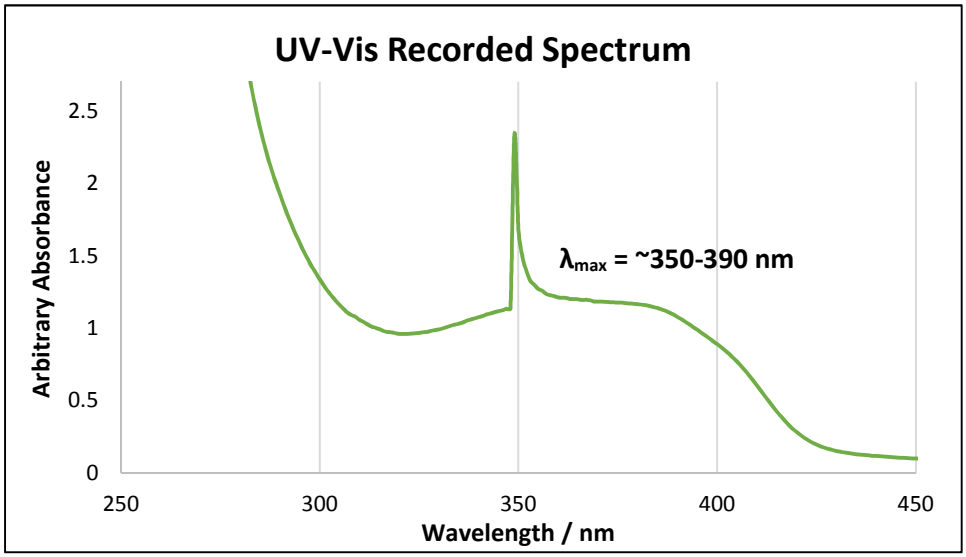

Note: The sharp increase in absorbance at 350 nm is an instrument artifact, arising from the bulb switching from visible to UV.

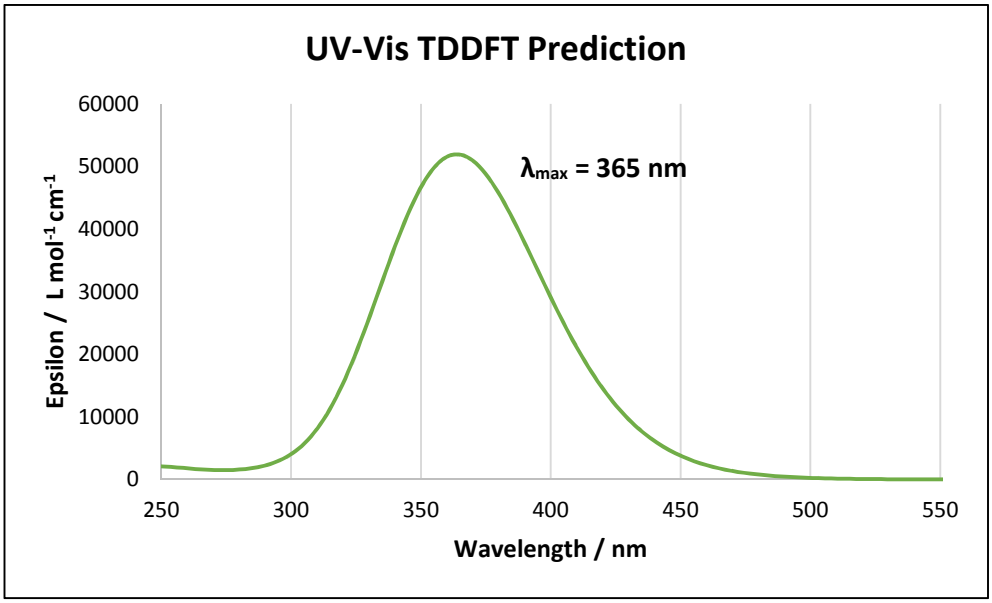

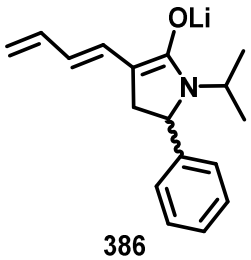
OLi
N

386

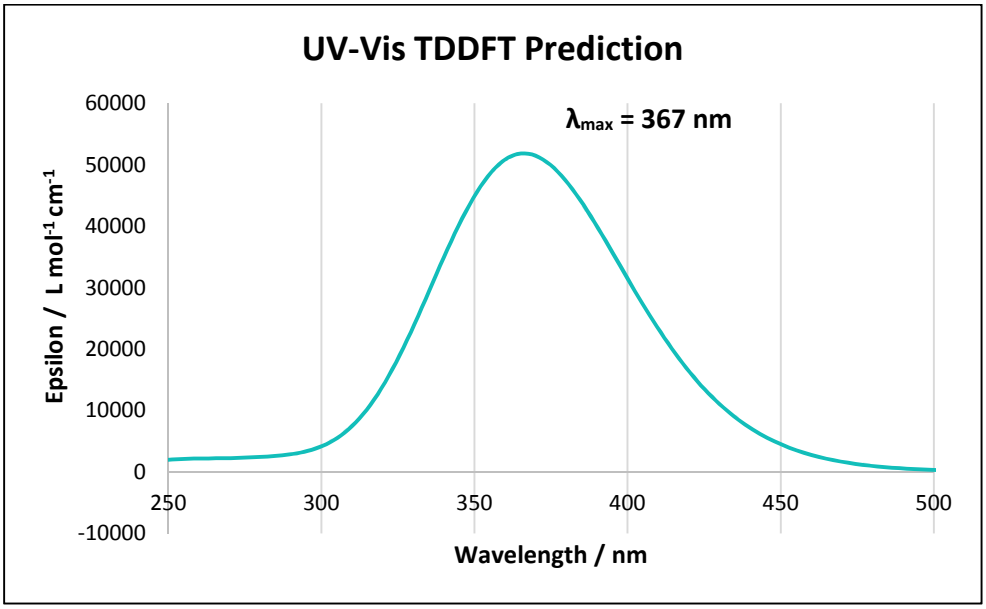
UV-Vis TDDFT Prediction
λmax = 367 nm
Epsilon / L mol-1 cm-1
60000
50000
40000
30000
20000
10000
0
-10000
250
300
350
400
450
500
Wavelength / nm

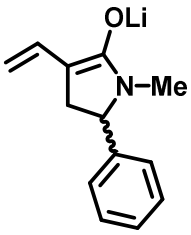
OLi
N–Me

348

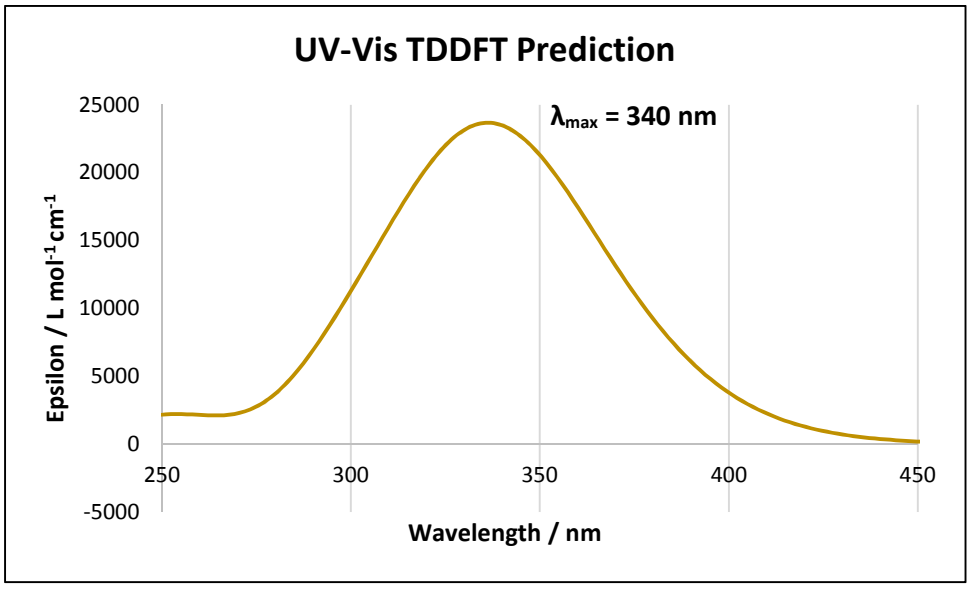
UV-Vis TDDFT Prediction
λmax = 340 nm
Epsilon / L mol-1 cm-1
25000
20000
15000
10000
5000
0
-5000
250
300
350
400
450
Wavelength / nm

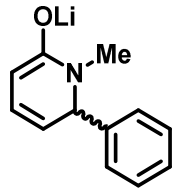
OLi
Me
N

367

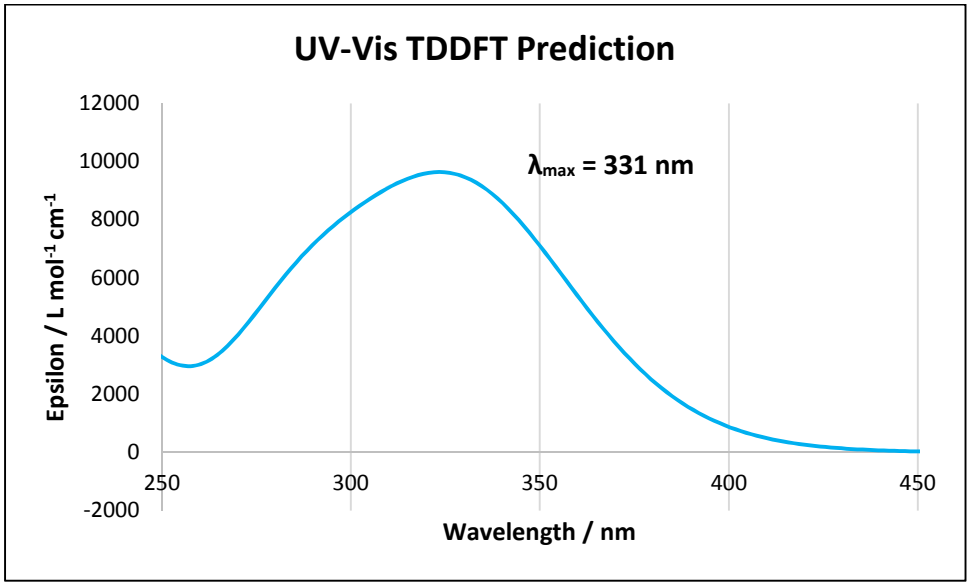
UV-Vis TDDFT Prediction
12000
10000
8000
6000
4000
2000
0
-2000
250
300
350
400
450
λmax = 331 nm
Epsilon / L mol-1 cm-1
Wavelength / nm

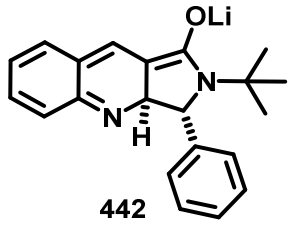
OLi
N
N
H

442

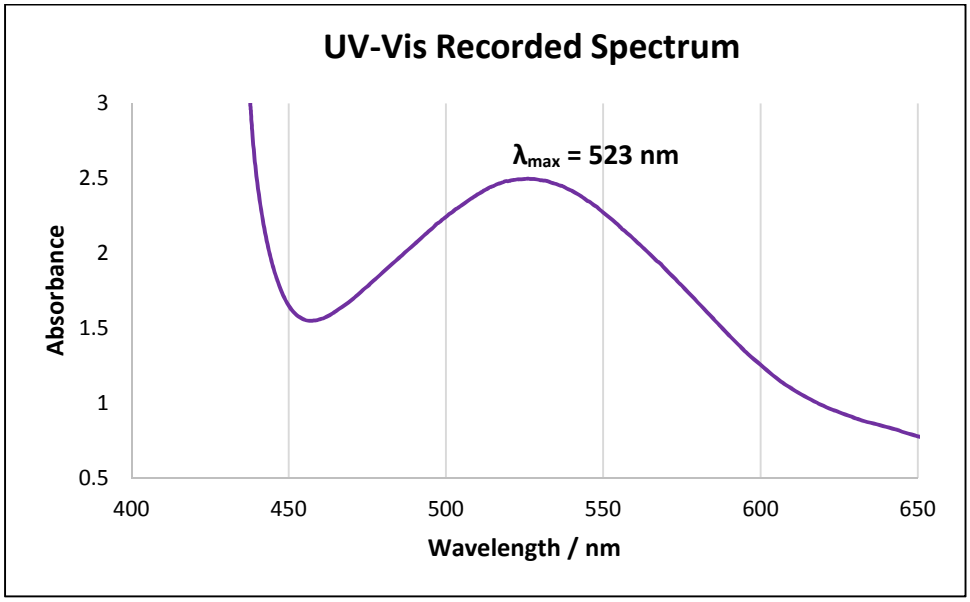
UV-Vis Recorded Spectrum
λmax = 523 nm
Absorbance
3
2.5
2
1.5
1
0.5
400
450
500
550
600
650
Wavelength / nm

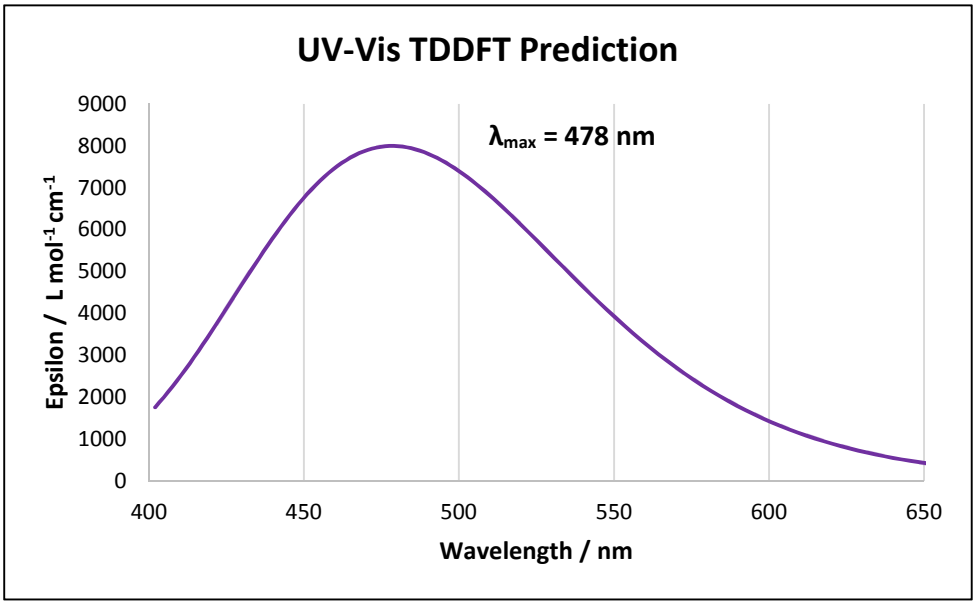
UV-Vis TDDFT Prediction
λmax = 478 nm
Epsilon / L mol-1 cm-1
9000
8000
7000
6000
5000
4000
3000
2000
1000
0
400
450
500
550
600
650
Wavelength / nm

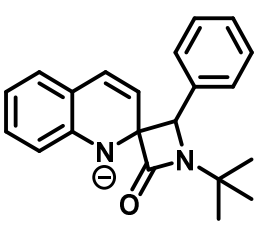

448

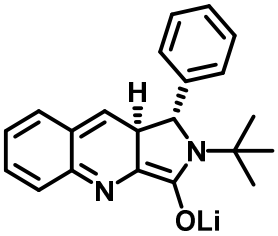

436

Note that the UV-Vis spectra were ran at room temperature, but the sample was taken either from a reaction mixture at −78 or −40 °C. The right-hand peak appears initially larger in intensity with the colder mixture, giving indication that the spiro-product is responsible for the longer wavelength absorbance.

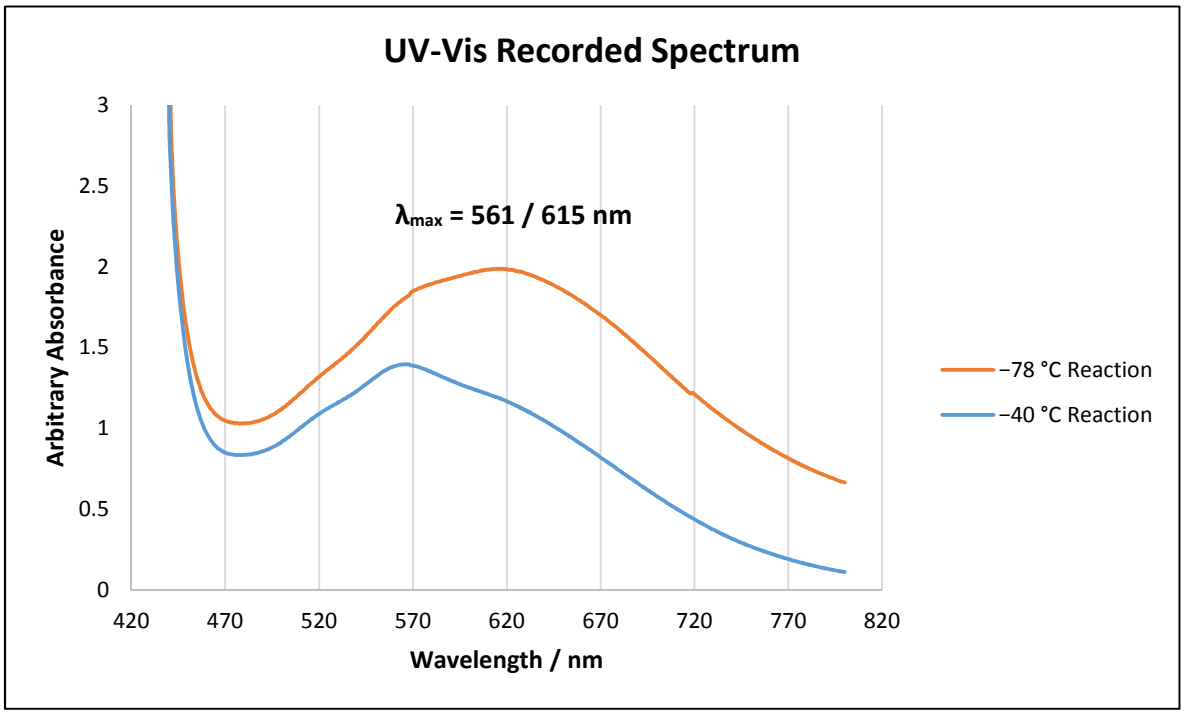

References

1 R. K. Saunthwal, J. Mortimer, A. J. Orr-Ewing and J. Clayden, *Chem. Sci.*, 2022, **13**, 2079–2085.

2 B. P. Straughan and S. Walker, *Spectroscopy*, 1976, 103–119.

3 N. F. Eisele, R. Rahrt, L. Giachanou, F. Shikho and K. Koszinowski, *Chem. Eur. J.*, 2023, **29**, e202302540.

4 R. J. Rapf and V. Vaida, *Phys. Chem. Chem. Phys.*, 2016, **18**, 20067–20084.

5 M. Oelgemöller, *Chem. Rev.*, 2016, **116**, 9664–9682.

6 D. Cambie and T. Noel, *Top. Curr. Chem*., 2018, **376**, 45.

7 A. Doty, *Microwaves & Rf*, 1987, **26**, 133–134.

8 J. Fritzsche, *J. Prakt. Chem.*, 1867, **101**, 333–343.

9 G. Papeo and M. Pulici, *Molecules,* 2013, **18**, 10870–10900.

10 D. Ravelli, S. Protti and M. Fagnoni, *Applied Photochemistry*, 2016, **92**, 281–342.

11 M. Oelgemöller, N. Healy, L. de Oliveira, C. Jung and J. Mattay, *Green Chem.*, 2006, **8**, 831–834.

12 P. E. da Silva, H. I. M. Amin, A. M. Nauth, F. D. Emery, S. Protti and T. Opatz, *ChemPhotoChem.*, 2018, **2**, 878–883.

13 C. Sambiagio and T. Noel, *Trends Chem.*, 2020, **2**, 92–106.

14 J. P. Menzel, B. B. Noble, J. P. Blinco and C. Barner-Kowollik, *Nat. Commun.*, 2021, **12**(1), 1–12.

15 S. Protti, D. Ravelli and M. Fagnoni, *Photochem. Photobiol. Sci.*, 2019, **18**, 2094–2101.

16 S. L. Walden, H. Frisch, B. V. Unterreiner, A.-N. Unterreiner and C. Barner-Kowollik, *J. Chem. Educ.*, 2019, **97**, 543–548.

17 S. Ishikawa, Y. Uchimura, K. Baba, Y. Eguchi and K. Kido, *Bull. Environ. Contam. Toxicol.*, 1992, **49**, 368-374.

18 F. Knowles, *Photochemical Rearrangement of Amide Enolates and the Total Synthesis of (-)-Isodomoic Acid C,* PhD Thesis, University of Manchester, 2005.

19 J. D. Williams and C. O. Kappe, *Curr. Opin. Green Sustain. Chem.*, 2020, **25**, 100351.

20 K. Hö Lz, J. Lietard and M. M. Somoza, *ACS Sustainable Chem. Eng.,* 2017, **5**(1), 828-834.

21 F. Diaba and J. Bonjoch, *Chem. Commun.*, 2011, **47**, 3251–3253.

22 T. D. Svejstrup, A. Chatterjee, D. Schekin, T. Wagner, J. Zach, M. J. Johansson, G. Bergonzini and B. König, *ChemPhotoChem.*, 2021, **5**, 808–814.

23 L. Ruiz Espelt, E. M. Wiensch and T. P. Yoon, *J. Org. Chem.*, 2013, **78**, 4107–4114.

24 D. Frackowiak, *J. Photochem. Photobiol.*, 1988, **2**(3), 399.

25 V. Ramamurthy and N. J. Turro, *Chem. Rev.*, 1993, **93**, 1–2.

26 T. Förster, *Ann. Phys.*, 1948, **437**(1), 55-75.

27 M. J. Oddy, D. A. Kusza and W. F. Petersen, *Org. Lett.*, 2021, **23**, 45.

28 R. A. Bragg and J. Clayden, *Tetrahedron Lett.*, 1999, **40**, 8323–8326.

29 A. Ahmed, J. Clayden and S. A. Yasin, *Chem. Commun*., 1999, 231-232.

30 A. Ahmed, J. Clayden and M. Rowley, *Chem. Commun.*, 1998, 297–298.

31 J. Clayden and C. J. Menet, *Tetrahedron Lett.*, 2003, **44**, 3059–3062.

32 J. Clayden, R. Turnbull and I. Pinto, *Org. Lett.*, 2004, **6**, 609–611.

33 J. Senczyszyn, H. Brice and J. Clayden, *Bioorg. Med. Chem. Lett.*, 2008, **112**, 5.

34 J. Clayden, S. D. Hamilton and R. T. Mohammed, *Org. Lett.*, 2005, **7**, 3673–3676.

35 J. Clayden, C. J. Menet and D. J. Mansfield, *Chem. Commun.*, 2002, 38-39.

36 J. Clayden, S. Purewal, M. Helliwell and S. J. Mantell, *Angew. Chem. Int. Ed*., 2002, **41**(6), 1049-1051.

37 J. Clayden, K. Tchabanenko, S. A. Yasin and M. D. Turnbull, *Synlett*, 2001, **2001**, 302–304.

38 A. Yogev, M. Gorodetsky and Y. Mazur, *J. Am. Chem. Soc.*, 1964, **86**, 5208–5213.

39 P. De Mayo, *Acc. Chem. Res.*, 1971, **4**, 41–47.

40 D. E. Minter and C. D. Winslow, *J. Org. Chem.*, 2004, **69**, 1603–1606.

41 J. P. Lopes, G. Tarozzo, A. Reggiani, D. Piomelli and A. Cavalli, *Brain Behav.*, 2013, **3**, 67.

42 N. Salaverri, J. Alemán and L. Marzo, *Adv. Synth. Catal.*, 2024, **366**, 156–167.

43 L. Marzo, S. K. Pagire, O. Reiser and B. König, *Angew. Chem. Int. Ed.*, 2018, **57**, 10034–10072.

44 C. R. J. Stephenson, T. P. Yoon and D. W. C. MacMillan, *Visible Light Photocatalysis in Organic Chemistry*, 2017, 1–444.

45 E. E. Van Tamelen, J. Schwartz and J. I. Brauman, *J. Am. Chem. Soc.*, 1970, **92**, 5798–5799.

46 J. Clayden, F. E. Knowles and C. J. Menet, *J. Am. Chem. Soc.*, 2003, **125**, 9278–9279.

47 E. Runge and E. K. U. Gross, *Phys. Rev. Lett.*, 1984, **52**, 997.

48 H. Louis, O. C. Enudi, J. O. Odey, I. B. Onyebuenyi, A. T. Igbalagh, T. O. Unimuke and T. N. Ntui, *SN Appl. Sci.*, 2021, **3**, 1–14.

49 A. D. Laurent, A. Blondel and D. Jacquemin, *Theor. Chem. Acc.*, 2015, **134**, 1–11.

50 D. Escudero, A. D. Laurent and D. Jacquemin, *Handbook of Computational Chemistry*, 2017, 927–961.

51 J. Shen and S. H. Li, *Sci. China Chem.*, 2010, **53**, 289–296.

52 C. A. Ullrich and Z. hui Yang, *Braz. J. Phys.*, 2014, **44**, 154–188.

53 Y. Paz, *J. Phys. Condens. Matter*, 2019, **31**, 503004.

54 R. Berera, A. E. Rienk, G. Ae and J. T. M. Kennis, *Photosynth. Res.*, 2009, **101**, 105-118.

55 Y. Zhu and J. X. Cheng, *J. Chem. Phys.*, 2020, **152**, 20901.

56 L. Wang, J. R. Pyle, K. A. Cimatu and J. Chen, *J. Photochem. Photobiol. Chem.*, 2018, **367**, 411–419.

57 J. C. Worch, C. J. Stubbs, M. J. Price and A. P. Dove, *Chem. Rev.*, 2021, **121**, 6744.

58 A. W. McCulloch and A. G. McInnes, *Can. J. Chem.*, 2011, **52**, 3569–3576.

59 A. Saito, T. Ono and Y. Hanzawa, *J. Org. Chem.*, 2006, **71**, 6437–6443.

60 P. Ballester, A. Costa, A. García-Raso, A. Gómez-Solivellas and R. Mestres, *Tetrahedron Lett.*, 1985, **26**, 3625–3628.

61 D. M. Smith, A. Nicolaides, B. T. Golding and L. Radom, *J. Am. Chem. Soc.*, 1998, **120**, 10223.

62 J. Clayden, J. Ré, M. Dufour, D. M. Grainger and M. Helliwell, *J. Am. Chem. Soc.*, **129**(24), 7488-7489.

63 D. A. Cogan and J. A. Ellman, *J. Chem. Soc., Perkin Trans. 1*, 1998, **37**, 341–343.

64 D. A. Cogan, G. Liu and J. Ellman, *Tetrahedron*, 1999, **55**, 8883–8904.

65 J. A. Ciaccio and C. E. Aman, *Synth. Commun.*, 2006, **36**, 1333–1341.

66 J. E. Baldwin, *J. Chem. Soc. Chem. Commun.*, 1976, 734–736.

67 R. D. Taylor, M. Maccoss and A. D. G. Lawson, *J. Med. Chem.*, 2014, **57**, 5845–5859.

68 T. T. Talele, *J. Med. Chem.*, 2016, **59**, 8712–8756.

69 M. R. Bauer, P. Di Fruscia, S. C. C. Lucas, I. N. Michaelides, J. E. Nelson, R. I. Storer and B. C. Whitehurst, *RSC Med. Chem.*, 2021, **12**, 448.

70 S. J. Chawner, M. J. Cases-Thomas and J. A. Bull, *Eur. J. Org. Chem.*, 2017, 5015-5024.

71 Z. Chen, E. Sakurai, W. Hu, C. Jin, Y. Kiso, M. Kato, T. Watanabe, E. Wei and K. Yanai, *Br. J. Pharmacol.*, 2004, **143**, 573–580.

72 M. S. Alavijeh, M. Chishty, M. Z. Qaiser and A. M. Palmer, *NeuroRx*, 2005, **2**(4), 554-571.

73 C. Jin, A. M. Decker, D. L. Harris and B. E. Blough, *ACS Chem. Neurosci.*, 2016, **7**, 1418–1432.

74 S. Zhang, M. E. W. Collier, D. J. Heyes, F. Giorgini and N. S. Scrutton, *Arch. Biochem. Biophys.*, 2021, **697**, 108702.

75 J. Tyrrell, V. M. Kolb and C. Y. Meyers, *J. Am. Chem. Soc.*, 1979, **101**, 3497–3500.

76 M. J. S. ; M. J. S. Dewar and R. C. Dougherty, *J. Am. Chem. Soc.*, 1984, **106**, 669–682.

77 E. Richmond, J. Yi, V. D. Vuković, F. Sajadi, C. N. Rowley and J. Moran, *Chem. Sci.*, 2018, **9**, 6411-6416.

78 C. Ebner and E. M. Carreira, *Chem. Rev.*, 2017, **117**, 11651–11679.

79 W. Wu, Z. Lin and H. Jiang, *Org. Biomol. Chem.*, 2018, **16**, 7315–7329.

80 X. Zhong, J. Lv and S. Luo, *Org. Lett.*, 2017, **19**, 3331–3334.

81 A. Homs, M. E. Muratore and A. M. Echavarren, *Org. Lett.*, 2015, **17**, 461–463.

82 C. Pei, C. Empel and R. M. Koenigs, *Org. Lett.*, 2023, **25**, 169–173.

83 P. Cauliez, B. Rigo, D. Fasseur and D. Couturier, *J. Heterocycl. Chem.*, 1991, **28**, 1143–1146.

84 D. Fasseur, B. Rigo, C. Leduc, P. Cauliez and D. Couturier, *J. Heterocycl. Chem.*, 1992, **29**, 1285–1291.

85 P. Stanetty, M. Turner and M. D. Mihovilovic, *Molecules,* 2005, **10**, 367–375.

86 T. -Y Lin, C. A. Kingsbury and N. H. Cromwell, *J. Heterocycl. Chem.*, 1984, **21**, 1871–1875.

87 L. S. Santos and R. A. Pilli, *J. Braz. Chem. Soc*, 2003, **14**, 982–993.

88 A. Clerici, N. Pastori and O. Porta, *Eur. J. Org. Chem.*, 2001, 2235-2243.

89 W. Gerrard, L. A. Bratholm, M. J. Packer, A. J. Mulholland, D. R. Glowacki and C. P. Butts, *Chem. Sci.*, 2020, **11**, 508–515.

90 H. Li, H. Wu, H. Zhang, Y. Su, S. Yang and E. J. M. Hensen, *ChemSusChem.*, 2019, **12**, 3778–3784.

91 R. Porta, M. Benaglia and A. Puglisi, *Org. Process. Res. Dev.*, 2016, **20**, 2-25.

92 P. Heretsch, *Beilstein J. Org. Chem.*, 2023, **19**, 33–35.

93 M. Baumann, T. S. Moody, M. Smyth and S. Wharry, *Org. Process. Res. Dev.*, 2020, **24**, 1802–1813.

94 F. Gomollón-Bel, *Chem. Int.*, 2019, **41**, 12–17.

95 T. H. Rehm, *Chem. Eur. J.*, 2020, **26**, 16952–16974.

96 G. W. Stutte, *HortScience*, 2015, **50**(9), 1297-1300.

97 T. von Keutz, F. J. Strauss, D. Cantillo and C. O. Kappe, *Tetrahedron*, 2018, **74**, 3113–3117.

98 E. Cooper, E. Alcock, M. Power and G. Mcglacken, *React. Chem. Eng*, 2023, **8**, 1839.

99 D. O'hagan, *Chem. Soc. Rev.*, 2008, **37**, 308–319.

100 M. Butters, C. D. Davies, M. C. Elliott, J. Hill-Cousins, B. M. Kariuki, L.-L. Ooi, J. L. Wood and S. V Wordingham, *Org. Biomol. Chem.*, 2009, **7**, 5001-5009.

101 Y. Zhang, D. J. Deschepper, T. M. Gilbert, K. Kumar, S. Sai and D. A. Klumpp, *Chem. Commun.*, 2007, 4032-4034.

102 K. Piwowarczyk, A. Zawadzka, P. Roszkowski, J. Szawkało, A. Leniewski, J. K. Maurin, D. Kranz and Z. Czarnocki, *Tetrahedron Asymmetry*, 2008, **19**, 309–317.

103 J. Kaneti, A. J. Kirby, A. H. Koedjikov and I. G. Pojarlieff, *Org. Biomol. Chem.*, 2004, **2**, 1098–1103.

104 M. R. van der Kolk, M. A. C. H. Janssen, F. P. J. T. Rutjes and D. Blanco-Ania, *ChemMedChem.*, 2022, **17**(9), e202200020.

105 A. Gohier, C. Mannoury la Cour, M. J. Millan and S. Hanessian, *Bioorg. Med. Chem.*, 2017, **25**, 38–52.

106 S. Ahmad, W. N. Washburn, A. S. Hernandez, S. Bisaha, K. Ngu, W. Wang, M. A. Pelleymounter, D. Longhi, N. Flynn, A. V. Azzara, K. Rohrbach, J. Devenny, S. Rooney, M. Thomas, S. Glick, H. Godonis, S. Harvey, H. Zhang, B. Gemzik, E. B. Janovitz, C. Huang, L. Zhang, J. A. Robl and B. J. Murphy, *J. Med. Chem.*, 2016, **59**, 8848–8858.

107 I. A. Mayer and C. L. Arteaga, *Annu. Rev. Med.*, 2016, **67**, 11–28.

108 J. Li, K. Gao, M. Bian and H. Ding, *Org. Chem. Front.*, 2019, **7**, 136–154.

109 W. Cui, G. Guo, Y. Wang, X. Song, J. Lv and D. Yang, *Chem. Commun.*, 2023, **59**, 6367–6370.

110 W. P. Weber, *Silicon Reagents for Organic Synthesis, Reactivity and Structure Concepts in Organic Chemistry,* 1983, 206–227.

111 R. P. Woodbury and M. W. Rathke, *J. Org. Chem.*, 1978, **43**, 881–884.

112 A. Song, J. C. Lee, K. A. Parker and N. S. Sampson, *J. Am. Chem. Soc.*, 2010, **132**, 10513-10520.

113 L. Shen, K. Zhao, K. Doitomi, R. Ganguly, Y. X. Li, Z. L. Shen, H. Hirao and T. P. Loh, *J. Am. Chem. Soc.*, 2017, **139**, 13570–13578.

114 G. Hilt, A. Paul and J. Treutwein, *Org. Lett.*, 2010, **12**, 1536–1539.

115 Y. Bin Bai, Z. Luo, Y. Wang, J. M. Gao and L. Zhang, *J. Am. Chem. Soc.*, 2018, **140**, 5860–5865.

116 X. Ning, Y. Chen, F. Hu and Y. Xia, *Org. Lett.*, 2021, **23**, 8348–8352.

117 W. Ouyang, J. Huo and J. Wang, *Synlett*, 2022, **34**, 1507–1511.

118 L. Huang, Y. Gu and A. Fürstner, *Chem. Asian. J.*, 2019, **14**, 4017–4023.

119 J. G. Sośnicki, P. Dzitkowski and Ł. Struk, *Eur. J. Org. Chem.*, 2015, **2015**, 5189–5198.

120 J. G. Parmentier, B. Portevin, R. M. Golsteyn, A. Pierré, J. Hickman, P. Gloanec and G. De Nanteuil, *Bioorg Med. Chem. Lett.*, 2009, **19**, 841–844.

121 E. E. Schultz, V. N. G. Lindsay and P. R. Sarpong, *Angew. Chem. Int. Ed.*, 2014, **53**(37), 9904-9908.

122 C. Kunick, C. Bleeker, C. Prühs, F. Totzke, C. Schächtele, M. H. G. Kubbutat and A. Link, *Bioorg. Med. Chem. Lett.*, 2006, **16**, 2148–2153.

123 B. E. Blass, *ACS Med. Chem. Lett.*, 2019, **10**(9), 1243-1244.

124 R. Koliqi, C. Polidori and H. Islami, *Mater. Sociomed.*, 2015, **27**, 167–171.

125 R. Fayez and V. Gupta, *xPharm: The Comprehensive Pharmacology Reference*, 2023, 1–5.

126 S. K. Maddili, R. Chowrasia, V. K. Kannekanti and H. Gandham, *J. Photochem. Photobiol. B*, 2018, **178**, 101–107.

127 Y. Zhang, J. Tan and Y. Chen, *Chem. Commun.*, 2023, **59**, 2413.

128 K. Lamara and R. K. Smalley, *Tetrahedron*, 1991, **47**, 2277–2290.

129 B. R. Nagaraj Ayyangar, R. B. Bambal and A. G. Lugade, *J. Chem. Soc., Chem. Commun.*, 1981, 790-791.

130 H. Yang, Z. Ning, S. Wang, J. Li, Z. L. Wang, W. L. Wang and X. M. Xu, *Tetrahedron Lett.*, 2021, **74**, 153174.

131 William Terry-Wright, *Photochemical Ring Expansion of Pyridines to Azepines*, MSci Thesis, University of Bristol, 2023.

132 G. E. Zhussupova and A. I. Zhussupova, *Procedia. Soc. Behav. Sci.*, 2015, **191**, 1247–1254.

133 Callum Trent, *Photochemical Ring-Expansion of Pyridines to Azepines*, MSci Thesis, University of Bristol, 2024.

134 N. Ritter, P. Disse, B. Wünsch, G. Seebohm and N. Strutz-Seebohm, *Biomedicines,* 2023, **11**, 1367.

135 J. M. Serrano-Rodríguez, M. Gómez-Díez, M. Esgueva, C. Castejón-Riber, A. Mena-Bravo, F. Priego-Capote, N. Ayala, J. M. S. Caballero and A. Muñoz, *Res. Vet. Sci.*, 2017, **114**, 117–122.

136 G. Golor, H. McElwaine-Johnn, R. Handy, C. Yea and J. Lambert, *J. Urol.*, 2013, **189**, e930–e931.

137 J. Clayden, R. Turnbull and I. Pinto, *Org. Lett.*, 2004, **6**, 609–611.

138 M. J. Frisch, G. W. Trucks, H. B. Schlegel, G. E. Scuseria, M. A. Robb, J. R. Cheeseman, G. Scalmani, V. Barone, G. A. Petersson, H. Nakatsuji, X. Li, M. Caricato, A. V Marenich, J. Bloino, B. G. Janesko, R. Gomperts, B. Mennucci, H. P. Hratchian, J. V Ortiz, A. F. Izmaylov, J. L. Sonnenberg, Williams, F. Ding, F. Lipparini, F. Egidi, J. Goings, B. Peng, A. Petrone, T. Henderson, D. Ranasinghe, V. G. Zakrzewski, J. Gao, N. Rega, G. Zheng, W. Liang, M. Hada, M. Ehara, K. Toyota, R. Fukuda, J. Hasegawa, M. Ishida, T. Nakajima, Y. Honda, O. Kitao, H. Nakai, T. Vreven, K. Throssell, J. A. Montgomery Jr., J. E. Peralta, F. Ogliaro, M. J. Bearpark, J. J. Heyd, E. N. Brothers, K. N. Kudin, V. N. Staroverov, T. A. Keith, R. Kobayashi, J. Normand, K. Raghavachari, A. P. Rendell, J. C. Burant, S. S. Iyengar, J. Tomasi, M. Cossi, J. M. Millam, M. Klene, C. Adamo, R. Cammi, J. W. Ochterski, R. L. Martin, K. Morokuma, O. Farkas, J. B. Foresman and D. J. Fox, *Gaussian 16*, 2016.

139 Thorlabs - M530L4 530 nm, 370 mW (Min) Mounted LED, 1000 mA, https://www.thorlabs.com/thorproduct.cfm?partnumber=M530L4, (accessed 12 September 2024).

140 Thorlabs - MINTL5 554 nm, 650 mW (Min) Mounted LED, 1225 mA, https://www.thorlabs.com/thorproduct.cfm?partnumber=MINTL5, (accessed 12 September 2024).

141 D. M. Mercea, M. G. Howlett, A. D. Piascik, D. J. Scott, A. Steven, A. E. Ashley and M. J. Fuchter, *Chem. Commun.*, 2019, **55**, 7077–7080.

142 A. F. Abdelmagid, C. A. Maryanoff and K. G. Carson, *Tetrahedron Lett.*, 1990, **31**, 5595–5598.

143 P. L. Lagueux-Tremblay, A. Fabrikant and B. A. Arndtsen, *ACS Catal.*, 2018, **8**, 5350–5354.

144 E. Pini, V. Bertacche, F. Molinari, D. Romano and R. Gandolfi, *Tetrahedron*, 2008, **64**, 8638–8641.

145 P. Vinczer, L. Novak and C. Szantay, *Org. Prep. Proced. Int.*, 1992, **24**, 349–351.

146 D. H. Birtwistle, J. M. Brown and M. W. Foxton, *Tetrahedron*, 1988, **44**, 7309–7318.

147 A. L. Reznichenko, F. Hampel and K. C. Hultzsch, *Chem. Eur. J.*, 2009, **15**, 12819–12827.

148 J. A. Ciaccio and C. E. Aman, *Synth. Commun.*, 2006, **36**, 1333–1341.

149 S. E. Hampton, B. Baragaña, A. Schipani, C. Bosch-Navarrete, J. A. Musso-Buendía, E. Recio, M. Kaiser, J. L. Whittingham, S. M. Roberts, M. Shevtsov, J. A. Brannigan, P. Kahnberg, R. Brun, K. S. Wilson, D. González-Pacanowska, N. G. Johansson and I. H. Gilbert, *ChemMedChem.*, 2011, **6**, 1816–1831.

150 E.-A. Jo and C.-H. Jun, *Eur. J. Org. Chem.*, 2006, 2504-2507.

151 F. Machrouhi and J. L. Namy, *Tetrahedron*, 1998, **54**, 11111–11122.

152 C. E. Neipp and S. F. Martin, *J. Org. Chem.*, 2003, **68**(23), 8867-8878.